

UC Berkeley

UC Berkeley Electronic Theses and Dissertations

Title

The Total Synthesis of Cycloprodigiosin and Synthetic Efforts Toward the Pentacyclic Ambiguine Class of Natural Products

Permalink

<https://escholarship.org/uc/item/2pt771kg>

Author

Johnson, Rebecca Elizabeth

Publication Date

2018

Peer reviewed|Thesis/dissertation

**The Total Synthesis of Cycloprodigiosin and Synthetic Efforts Toward the Pentacyclic
Ambiguine Class of Natural Products**

by

Rebecca Elizabeth Johnson

A dissertation submitted in partial satisfaction of the

requirements for the degree of

Doctor of Philosophy

in

Chemistry

in the

Graduate Division

of the

University of California, Berkeley

Committee in charge:

Professor Richmond Sarpong, Chair

Professor Thomas Maimone

Assistant Professor Markita Landry

Summer 2018

The Total Synthesis of Cycloprodigiosin and Synthetic Efforts Toward the Pentacyclic Ambiguine Class of Natural Products

Copyright 2018
by
Rebecca Elizabeth Johnson

Abstract

The Total Synthesis of Cycloprodigiosin and Synthetic Efforts Toward the Pentacyclic Ambiguine Class of Natural Products

by

Rebecca Elizabeth Johnson

Doctor of Philosophy in Chemistry

University of California, Berkeley

Professor Richmond Sarpong, Chair

The synthesis and absolute stereochemical determination of cycloprodigiosin has been completed. Chapter 1 discusses the historical, synthetic, and biological background of prodiginine natural products, specifically of prodigiosin and cycloprodigiosin. Chapter 2 details our synthetic attempts for the synthesis of cycloprodigiosin and the strategy used to determine the absolute stereochemistry at the C4' position of this prodiginine. The syntheses of both enantiomers of cycloprodigiosin were completed in an efficient five step sequence utilizing a Barton-Schöllkopf-Zard pyrrole synthesis. Cycloprodigiosin was isolated from its parent bacterial source, *Pseudoalteromonas rubra*, by Tristan de Rond in a collaboration with the Keasling group at UC Berkeley. The natural isolate was determined to exist as a scalemic mixture in a ratio of 83:17 (*R*):(*S*) at C4'. The enzyme responsible for the final oxidative cyclization event from prodigiosin to cycloprodigiosin was identified as the alkylglycerol monooxygenase-like enzyme PRUB680.

The second topic of this thesis details the first total synthesis of ambiguityne P in 19 steps from (*S*)-carvone. The isolation, biosynthetic, and synthetic background of the ambiguityne family of natural products is discussed in Chapter 3. The challenges associated with the synthesis of pentacyclic ambiguitynes are described in Chapter 4 and focus on the formation of the pentacyclic core in addition to the installation of the C12 quaternary center. The 1st generation synthetic approach to access the ambiguityne pentacyclic core involves a key γ -enolate cross-coupling reaction to form the tetracyclic precursor. The intermediates in this approach were synthesized from indole and (*S*)-carvone using an intermolecular Nicholas alkylation. The 2nd generation synthetic route to access the key pentacyclic core involves an intramolecular Nicholas alkylation at C2 of indole, followed by Friedel-Crafts cyclization at C4 to successfully generate the pentacyclic core.

Chapter 5 describes the completion of ambiguityne P; many strategies were explored to install the C12 quaternary center, and eventually a directed C–C bond construction utilizing formates was found that successfully formed the C–C bond on the desired α -face. The requisite vinyl group at C12 and the amide functionality at C11 were installed using an interrupted Peterson olefination strategy. Attempts are described to access ambiguityne L from these late-stage intermediates using benzylic oxidation and hydration methodologies.

*To my family for their unwavering
love and support.*

List of Abbreviations

9-BBN	9-borabicyclo[3.3.1]octane
Ac	acetyl
AIBN	azobis(iso-butyronitrile)
b	broad
Boc	<i>tert</i> -butyloxycarbonyl
Bu	butyl
cat.	catalytic
CuTc	copper(I)-thiophene-2-carboxylate
d	doublet
DBU	1,8-diazabicyclo[5.4.0]undec-7-ene
DCE	1,2-dichloroethane
DCM	dichloromethane
DEAD	diethyl azodicarboxylate
DEF	diethylformamide
DIBAL-H	diisobutyl aluminum hydride
DMAP	(4-dimethylamino)pyridine
DMF	dimethylformamide
DMP	Dess-Martin periodinane
DMSO	dimethylsulfoxide
DNPH	2,4-dinitrophenylhydrazine
DTBP	2,6-di- <i>tert</i> -butylpyridine

EI	electron impact ionization
equiv	equivalent
ESI	electrospray ionization
HPLC	high-pressure liquid chromatography
HRMS	high-resolution mass spectrometry
IR	infrared
L-selectride	lithium tri-(<i>sec</i> -butyl)borohydride
LAH	lithium aluminum hydride
LCMS	liquid chromatography mass spectrometry
LDA	lithium diisopropylamide
LHMDS	Lithium hexamethyldisilazane
LHMDS	lithium hexamethyldisilazide
m	multiplet
Me	methyl
mp	melting point
MTBD	7-methyl-1,5,7-triazabicyclo[4.4.0]dec-5-ene
n	normal
NaHMDS	sodium hexamethyldisilazide
NBS	N-bromosuccinimide
NCS	<i>N</i> -chlorosuccinimide
NMR	nuclear magnetic resonance
PDC	pyridinium dichromate
Ph	phenyl
PIDA	phenyliododiacetate
PIFA	[bis(trifluoroacetoxy)iodo]benzene
prenyl	3,3-dimethylallyl
PSMS	zinc bis[(phenylsulfonyl)methanesulfinate]

pyr.	pyridine
q	quartet
reverse prenyl	1,1-dimethylallyl
rt	room temperature
s	singlet
sec	secondary
SEM	2-(trimethylsilyl)ethoxymethyl
t	triplet
TBAF	tetrabutylammonium fluoride
TBHP	<i>tert</i> -butylhydroperoxide
TBS	<i>tert</i> -butyldimethylsilyl
tert	tertiary
THF	tetrahydrofuran
TLC	thin-layer chromatography
TMS	trimethylsilyl
Ts	<i>para</i> -toluenesulfonyl

Contents

Acknowledgments	vii
1 Chapter 1 : Background to the Tripyrrole Natural Products Prodigiosin and Cycloprodigiosin	1
1.1 History of the Prodiginine Family of Natural Products	1
1.2 Total Syntheses of Prodigiosin and Structural Confirmation	3
1.3 Total Syntheses of Cycloprodigiosin and Structural Confirmation	7
1.4 Biosynthesis of Prodigiosin Natural Products and Their Biological Activity	9
1.5 Conclusion and Outlook	12
1.6 References	13
2 Chapter 2 : Synthesis of Cycloprodigiosin Identifies the Natural Isolate as a Scalemic Mixture	15
2.1 Motivations for Pursuing the Synthesis of Cycloprodigiosin	15
2.2 1 st Generation Synthesis of Cycloprodigiosin Derived from Established Chemistry . .	16
2.3 A Concise and Efficient 2 nd Generation Approach for the Synthesis of Cycloprodigiosin	17
2.4 Biosynthetic Investigations Into the Late-Stage Oxidative Cyclization from Prodi- giosin to Cycloprodigiosin	22
2.5 Conclusion and Outlook	23
2.6 Experimental Contributors	23
2.7 Materials and Methods	24
2.8 Experimental Methods and Procedures	25
2.9 References	39
Appendix 2.a : NMR Spectra Relevant to Chapter 2	41
Appendix 2.b : X-ray Crystallographic Data Relevant to Chapter 2	68
3 The Isolation, Bioactivity, and Synthetic Background of the Pentacyclic Ambiguine Natural Products	74
3.1 The Isolation and Bioactivity of Ambiguine Natural Products	74
3.2 Biosynthetic Investigations of Hapalindole and Ambiguine Natural Products	78
3.3 Previous Attempts to Synthesize Ambiguine Natural Products	84
3.4 Conclusion and Outlook	93
3.5 References	93

4 Chapter 4 : Synthetic Approaches to the Pentacyclic Class of Ambiguine Natural Products	95
4.1 Challenges Associated with the Synthesis of Pentacyclic Ambiguines	95
4.2 1 st Generation Route Toward the Synthesis of the Pentacyclic Ambiguines	99
4.3 2 nd Generation Route Toward the Synthesis of the Pentacyclic Ambiguines	103
4.4 Experimental Contributors	110
4.5 Materials and Methods	111
4.6 Experimental Methods and Procedures	111
4.7 References	119
Appendix 4.a NMR Spectra Relevant to Chapter 4	120
Appendix 4.b X-ray Crystallographic Data Relevant to Chapter 4	137
5 Chapter 5 : Late-Stage Strategies for the Synthesis of Pentacyclic Ambiguine Natural Products	155
5.1 Installation of the C12 Quaternary Center	155
5.2 Late-Stage Manipulations to Install the Vinyl Group and the Isonitrile Functionality .	163
5.3 Synthesis of Ambiguine P	167
5.4 Conclusion and Outlook	172
5.5 Experimental Contributors	175
5.6 Materials and Methods	175
5.7 Experimental Methods and Procedures	176
5.8 References	190
Appendix 5.a NMR Spectra Relevant to Chapter 5	192
Appendix 5.b X-ray Crystallographic Data Relevant to Chapter 5	235

Acknowledgments

First I would like to thank my mentor, Professor Richmond Sarpong. Richmond gave me the opportunity to work in his lab which has been a truly meaningful experience from both a chemistry and personal development perspective. I have learned that excellence should always be the ultimate goal and that hard work is always worth the effort. He is a tremendous mentor in chemistry and I am lucky to have had the opportunity to learn from his expertise.

I have to thank all of the Sarpong group members and specifically those who have helped edit this document, Magnus Pfaffenbach, Ian Bakanas, Shelby McCowen, Brian Wang, Melissa Hardy, and Nick O'Connor. I appreciate your thoughtful and constructive comments.

I would also like to thank my lab mates who have worked in 832 these past few years. Kyle Owens, you may be shocked but I have actually learned a tremendous amount from you. You have an incredible way of performing chemistry and I am honored to have overlapped for 5 years with you. Also, this thesis would not have been written without your LaTeX expertise. Shelby McCowen, you are a fantastic friend and I wish we had overlapped for a longer time but I am thankful to have had the opportunity to work next to you for 2 years. Hwisoo Ree, your patience and grace with chemistry and life has been inspirational to me and I am so thankful to have had the opportunity to work with you.

I am indebted to my coworkers who have contributed to my projects in the group. Erica Schultz, Tristan de Rond, Vincent Lindsay, Marco Hartmann, Laura Lang, Shota Sawano, and Hwisoo Ree. I have learned from each of you and thank you for your hard work and dedication to the projects.

I am also grateful to my qualifying exam and thesis committee, Prof. Thomas Maimone, Prof. Dean Toste, Prof. Carolyn Bertozzi, Prof. Michi Taga, and Prof. Markita Landry. I sincerely appreciate your help and mentorship with fulfilling the degree requirements.

Others in the group have provided support and friendship over the years. Jason Pflueger, I will always be in awe of your command of chemistry and your dedication as a teacher. Paul Leger, you were always a source of positivity and encouragement to myself and also to the group.

I am thankful to my undergraduate research advisor, Professor Christian Rojas who has provided recommendation letters and continued support throughout my graduate career. Your mentorship over the years has continued to influence me in a positive way.

Finally, I have to thank those who have been closest to me throughout my entire graduate career. Patrick Smith, through the best and worst of times your love and support has meant the world to me and has motivated me to finish this degree. Harvest, my Border Collie is my best friend, everything I have done has been in pursuit to give you the biggest yard you could imagine so that we can throw the ball until you get so tired that you can't run anymore. I love you both and can't wait to experience a new chapter of life with you.

Thank you to the music that has kept me focused on these rainbows in life even in the darkest of moments:

*I've found a rainbow, rainbow, baby
Trust me, I know, life is scary
But just put those colors on, girl
Come and paint the world with me tonight
—Kesha (Rainbow)*

Chapter 1

Chapter 1 : Background to the Tripyrrole Natural Products Prodigiosin and Cycloprodigiosin

1.1 History of the Prodiginine Family of Natural Products

The prodiginines are a family of natural products characterized by their unique highly conjugated tripyrrolic core typified by the members shown in Figure 1.1. These molecules exist as either linear congeners as in undecylprodigiosin (**1.1**), and prodigiosin (**1.2**) or as cyclized structures such as streptorubin B (**1.3**), metacycloprodigiosin (**1.4**), cycloprodigiosin (**1.5**), and nonylprodigiosin (**1.6**). This family of natural products has captivated the chemistry community because of their unique bioactivities, unusual biosynthesis, and the impressive total syntheses that have been developed for their preparation.¹⁻³ In addition, their highly conjugated core leads to a captivating blood-red or pink hue. Such a recognizable appearance has given these molecules a place in history that can be traced back to Alexander the Great's Siege of Tyre in 322 B.C.³

Reviews have been published on the prodiginines in the last few decades that have communicated these historical accounts stemming from the B.C. era.^{2,3} The rich historical background of the prodiginines largely has to do with their native bacterial source (i.e., *Streptomyces* and *Serratia* genera), which also happens to thrive on bread and other foods. There have been many reports of "bleeding" bread in history and although these stories have not been proven to be a direct result of prodiginines, there are few other molecules that when produced naturally, appear blood red (Figure 1.2). One of the most popular stories goes back to the night before the Siege of Tyre in 322 B.C. when Macedonian soldiers observed "bleeding" bread and interpreted this as a good omen for the battle about to ensue. The Macedonian army proceeded to conquer the city of Tyre in a brutal and bloody fashion.

Prodiginines make another appearance in history, in the conception of the festival of the Corpus Christi in 1263. The story begins with a German priest who, having doubts about the idea of transubstantiation, observed "blood" dripping from his communion wafer (Figure 1.3b). Such an event erased all doubt from his mind and the occurrence was commemorated as "The Miracle of Bolsena." To celebrate this historical event, the Italian painter and architect, Raphael, illustrated the moment in his fresco-style painting completed in the year 1514 (Figure 1.3b). Pope Urban

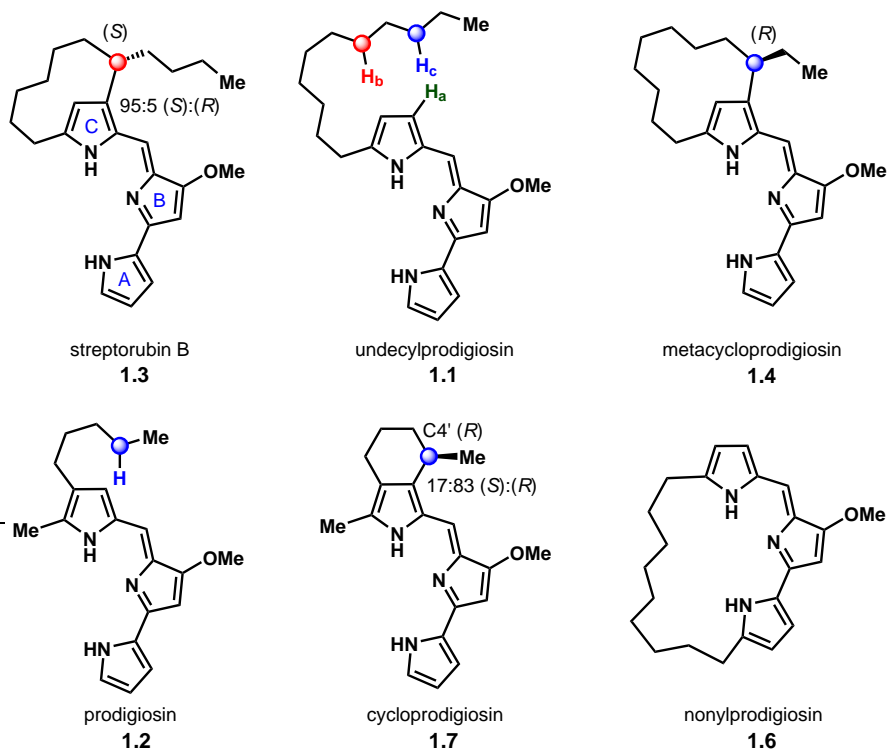


Figure 1.1: Selected members of the prodiginosin family of natural products

IV also recognized the significance of the priest's experience and initiated the festival of Corpus Christi in celebration of such a reconstitution of faith.

The alleged impact that these molecules have had on history is breathtaking and is a beautiful example of how chemistry weaves its threads into world culture. Despite having a deep-seated impact on history, the existence of the prodiginine producing bacteria was not acknowledged until a group of scientists dispelled rumors of witchcraft being responsible for "bleeding" food in a village near Padova in the year 1819. If it was not for the work of Pietro Melo (a botanist), Bartolomeo Bizio (a pharmacist), and Vincenzo Sette (a physician), who identified the "bleeding" as a biological entity originally assumed to be a fungus, the small village would have erupted in witchcraft hysteria. Later, the blood-red "fungus" was identified as a bacterium and given the name "*Serratia marcescens*," which has continued to be used to the present day.



Figure 1.2: Agar plate containing *Serratia marcescens*, the strain of bacteria that produces prodiginosin (1.2).

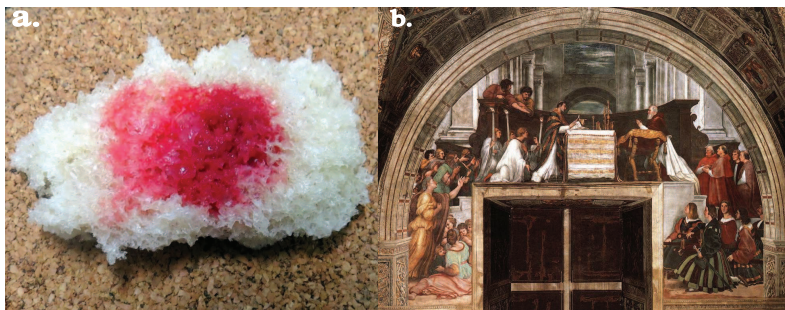


Figure 1.3: a. Bread hosting the growth of *Serratia marcescens*. b. "The Miracle of Bolsena" by Raphael (1512), Fresco, Apostolic Palace, Vatican City.

The pathogenic nature of the bacterial strain *Serratia marcescens* was largely assumed to be non-existent until the early 1950's when it was typical for the bacteria to be used in classroom demonstrations. The infectious character of *Serratia marcescens* became of greater importance to the community after the fatal consequence of the covert military operation known as "Operation Sea Spray." Taking place in the San Francisco Bay Area during the Cold War era, the U.S. military made the decision to use *S. marcescens* as an experimental bacterial substitute for the bacteria known to cause the disease tularemia, already being weaponized at the time. On September 26th and 27th 1950, the U.S navy released balloons containing *S. marcescens* into the air a couple of miles off the coast of San Francisco. The navy purposefully burst the balloons over the Bay Area, exposing the population to the previously assumed innocuous *Serratia marcescens*. However, as a result of this incident, *S. marcescens* is now known to cause serious urinary and respiratory tract infections. The repercussions were realized when there was a rise of infection in the local population leading to the death of Edward J. Nevin who, around the time of this bacterial release, suffered from a fatal urinary tract infection. Remarkably, the details of this operation were not made public until 1976 after which there was much backlash from citizens including a lawsuit against the federal government undertaken by Nevin's family.⁴

1.2 Total Syntheses of Prodigiosin and Structural Confirmation

It wasn't until 1962, 12 years after Operation Sea Spray when the molecule responsible for the characteristic blood-red color of *Serratia marcescens* was identified. Speculation as to the tripyrrolic core of the natural product prodigiosin had been made in 1933 by Wrede and Rothhaas with proposed structures **1.2**, **1.8**, and **1.9**.⁵ There were many conflicting reports of spectroscopic data that supported more than one structure, which led to the proposal of the pyridyl-containing structure **1.10** by Treihe and Galler in 1958.⁶ In 1959, through NMR, UV, and degradation analyses, Wasserman ruled out structures **1.8**, **1.9**, and **1.10**.⁷ The favored structure at this time was **1.2**, however, as shown in Scheme 1.1, the location of the methoxy group was still in question. It was just four years later in 1962 when a total synthesis by Rapoport and Willson of prodigiosin confirmed the structure of prodigiosin as **1.2**.^{8,9}

In this case, Rapoport narrowed the synthesis down to two bispyrrole precursors (Scheme 1.2, **1.14** and **1.15**). Since pyrrole **1.16** was a known compound, **1.15** was synthesized first (Scheme 1.2a). Starting with 4-substituted methoxy pyrrole **1.16**, condensation with 1-pyrroline in methanol led

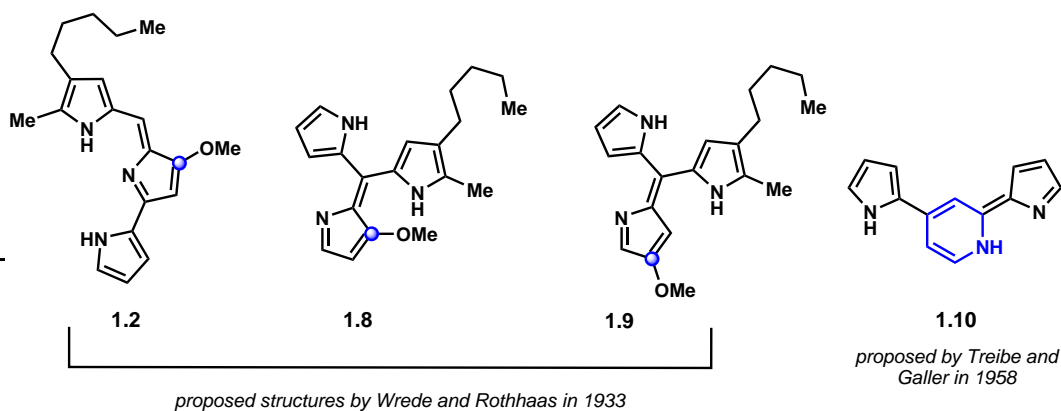
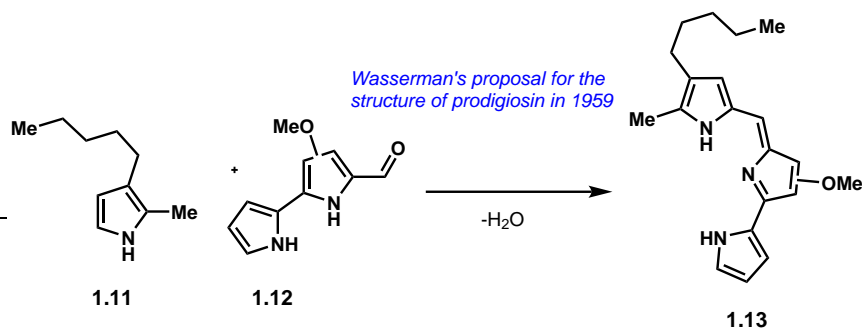


Figure 1.4: Structural isomers that were proposed for the natural product prodigiosin (**1.2**) before the structure was confirmed in 1962 as **1.2**



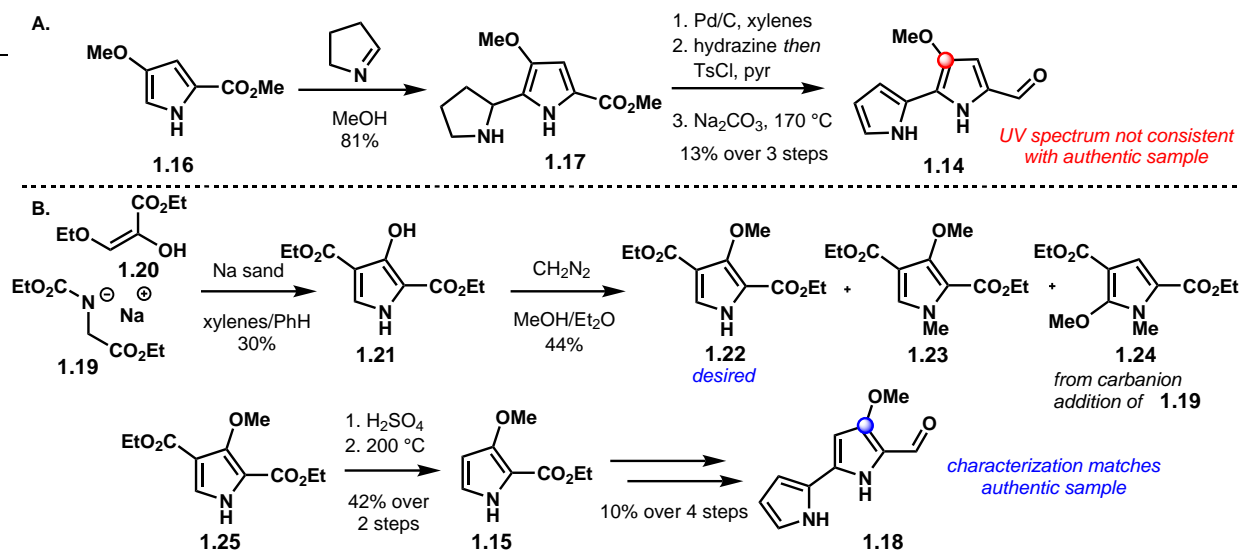
Scheme 1.1: Wasserman proposed two possible congeners for the structure of prodigiosin as **1.13**. The group set out to synthesize both congeners of the bispyrrole intermediate(**1.12**)

to C2, C4, C5-substituted pyrrole **1.17** in 81% yield. Heating **1.17** in xylenes in the presence of Pd/C led to dehydrogenation of the pyrrolidine scaffold generating a bispyrrole, which was then subjected to standard McFayden-Stevens conditions to form the aldehyde (**1.14**) from the corresponding tosyl hydrazone. Treatment of the hydrazone with sodium carbonate at high temperatures generated Rapoport's desired methoxy-substituted aldehyde **1.14** in low yield over the three steps. Unfortunately, the UV spectrum of **1.14** did not match that of an authentic sample from *Serratia marcescens*, and as a result, the focus was shifted to the synthesis of the other methoxy pyrrole congener (**1.18**). This intermediate (**1.18**), however, proved to be more challenging to synthesize.

The synthesis of **1.18** began with the addition of sodium amide **1.19** into the Michael acceptor **1.20** utilizing sodium sand (Scheme 1.2b) leading to a pyrrole intermediate which was assumed to be **1.21**. Submitting this crude reaction mixture to methylation conditions using diazomethane generated three congeners identified as desired pyrrole **1.22**, and undesired pyrroles **1.23** and **1.24** in a 12:1:15 ratio. The synthesis of the 5-methoxy substituted pyrrole (**1.24**) was rationalized to result from carbanion addition of amide **1.19** into alkene **1.20** as opposed to the desired nitrogen nucleophilic attack.

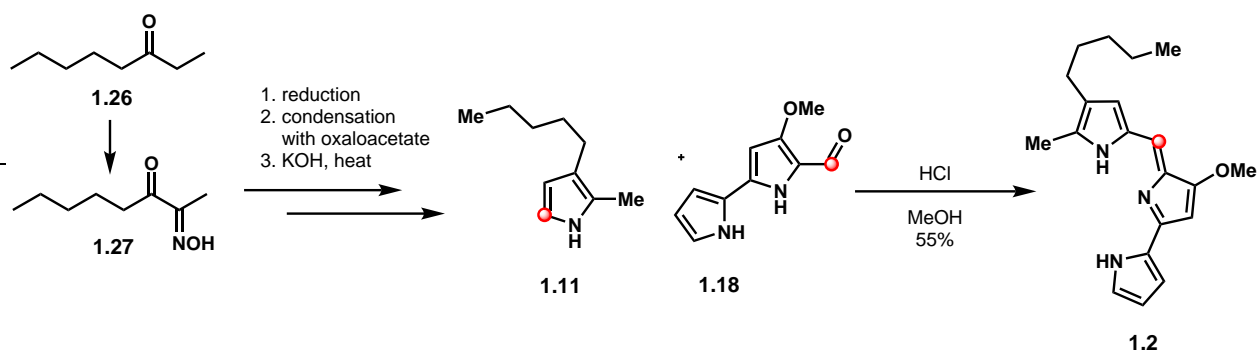
Nevertheless, desired pyrrole **1.22** was purified using alumina column chromatography and subsequently selectively saponified and decarboxylated to generate 2, 3-substituted pyrrole **1.15** in 42% yield over the two steps. The desired bispyrrole aldehyde (**1.18**) was produced in 10%

yield over a four-step sequence identical to the synthesis of the alternative congener **1.14**. The UV spectrum of **1.18** matched that of the authentic sample, confirming the structure as bispyrrole **1.18**.



Scheme 1.2: The first synthesis of prodigiosin (**1.2**) by Rapoport and Holden in 1962.⁹ A. Synthesis of the proposed bispyrrole condensation partners **1.14**. B. Synthesis of the correct bispyrrole condensation precursor **1.18**.

With condensation precursor **1.18** in hand, the Rapoport group investigated the construction of the pyrrole C-ring of prodigiosin that had been previously identified as 2-methyl, 3-amyl pyrrole **1.11** through degradation and synthesis studies performed by Wrede and Rothhaas.¹⁰ For the synthesis of pyrrole **1.11**, a slightly modified procedure from that of Wrede and Rothhaas was employed beginning with the oximation of ketone **1.26** to yield oxime **1.27** (Scheme 1.3). Following condensation with oxaloacetate, cyclization to the pyrrole generated the desired 2-methyl-3-amyl pyrrole **1.11**. The condensation of **1.11** and **1.18** had already been established previously⁷ and in this way, prodigiosin was formed upon treatment with methanolic HCl in 55% yield. Rapoport and Holden's synthesis represents the first total synthesis of prodigiosin and also confirmed prodigiosin's structure as the tripyrrollic system **1.2**.

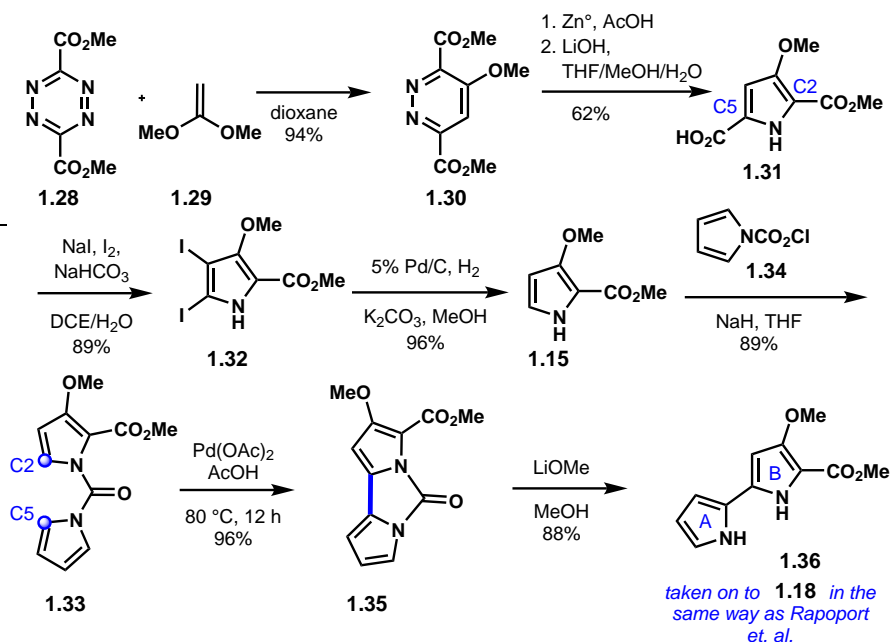


Scheme 1.3: The first synthesis of prodigiosin by Rapoport and Holden. Completion of prodigiosin **1.2** through an acid-mediated condensation between pyrrole **1.11** and bispyrrole **1.18**.

There was continued interest in the synthesis of prodigiosin through the late 20th century where new methodologies for generating key bispyrrole intermediate **1.18** were still being developed. One of these syntheses was carried out by Boger and Patel in 1987.¹¹

In the Boger synthesis, a tetrazine inverse-demand cycloaddition was the first key reaction used to form the B-ring pyrrole present in **1.18** (Scheme 1.4). A cycloaddition between bis-methylester tetrazine **1.28** and electron-rich alkene **1.29** formed the corresponding 1,2-diazene (**1.30**) in high yield. A reductive ring-contraction was then performed using zinc and acetic acid to generate the pyrrole species which was immediately saponified selectively at C5 to generate the corresponding carboxylic acid (**1.31**). Boger argued that the C5 ester is less electron-rich and more sterically available for nucleophilic attack by hydroxide anion compared to the C2 ester moiety. Iodination decarboxylation of **1.31** generated bis-iodo pyrrole **1.32** in high yield and subjecting **1.32** to hydrogenation conditions using Pd/C and H₂ efficiently reduced the bis-iodo species to 3-methoxypyrrole-2-carboxylate **1.15**.

Boger and Patel also envisioned forming the requisite C5–C2 pyrrole linkage through a palladium catalyzed C–H functionalization reaction (**1.33** to **1.18**). With this idea in mind, the sodium salt of methoxy pyrrole **1.15** was added to a solution of acid chloride **1.34**, which generated the carbonyldipyrrole compound **1.33**. The authors went on to screen a wide variety of coupling conditions using both Pd(OAc)₂ and polymer-supported Pd(OAc)₂ and found that polymer-supported Pd(OAc)₂ in AcOH at 80 °C for 12 h provided excellent conversion to the desired coupled pyrrole **1.35** in 96% yield. A straightforward methanolysis of **1.35** provided access to the intermediate **1.36** which they carried forward to **1.18** using the same methods as described previously by Rapoport et. al.⁹



Scheme 1.4: The synthesis of bispyrrole intermediate **1.18** by Patel and Boger in 1987. A key inverse-demand cycloaddition using tetrazine **1.28** and dienophile **1.29** was employed to form the B-ring pyrrole. A Pd-catalyzed coupling reaction was employed to stitch together the A and B-ring pyrroles.

1.3 Total Syntheses of Cycloprodigiosin and Structural Confirmation

In the early 1980's, a cyclic variety of prodigiosin had also been isolated from the marine bacterial species *Alteromonas rubra* and *Beneckeia gazogenes*. However, the structure of this compound was not firmly established until Wasserman and Fukuyama reported the first total synthesis in 1984.¹² In 1979 Gerber and Gauthier originally mis-characterized what was eventually known as cycloprodigiosin as the 5-membered ring-annulated compound **1.37** due to the presence of an aliphatic impurity in the proton NMR spectrum.¹³ Once cycloprodigiosin had been reassigned to the 6-membered ring-annulated congener **1.38** by Laatsch and Thompson in 1983,¹⁴ Wasserman and Fukuyama completed the first total synthesis of racemic cycloprodigiosin **1.7**.

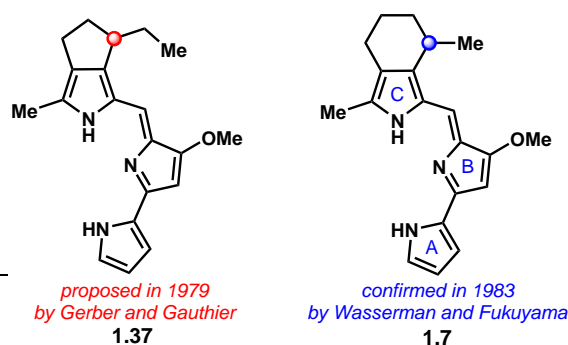
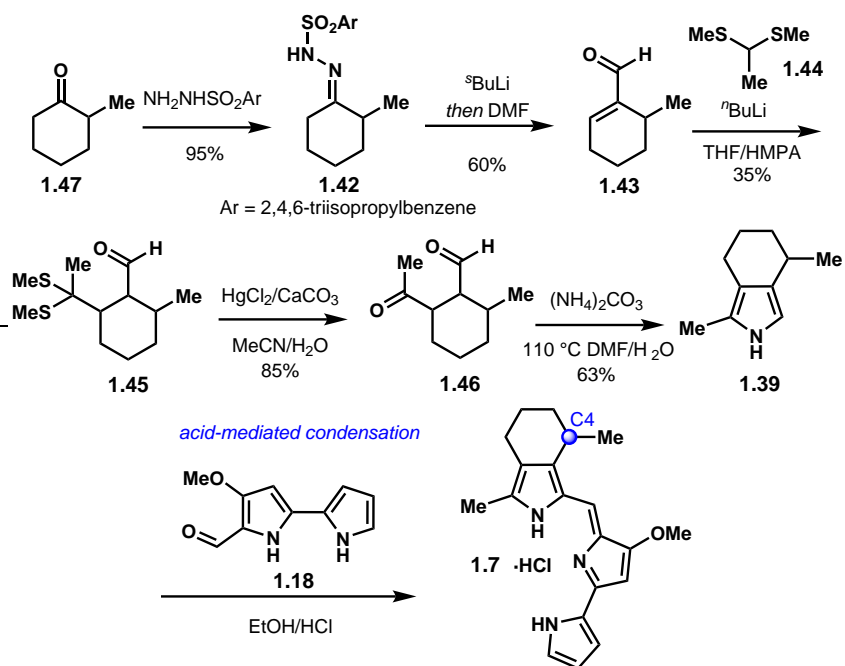


Figure 1.5: The structure originally proposed in 1979 by Gerber and Gauthier for the natural product cycloprodigiosin due to an aliphatic impurity present in the ^1H NMR spectrum. The correct structure for cycloprodigiosin is **1.38** confirmed through total synthesis by Wasserman and Fukuyama in 1984.

In Wasserman's synthesis, the annulated pyrrole C-ring (**1.39**, Scheme 1.5) and bispyrrole **1.18** are constructed separately. While the synthesis of **1.18** was already well-established, C-ring pyrrole **1.40** was not a known compound. The synthesis of **1.39** commenced with condensation of methylcyclohexanone **1.41** and aryl hydrazide, yielding hydrazone **1.42**. A Shapiro reaction was employed using *sec*-butyllithium and quenching with dimethylformamide to generate α , β -unsaturated aldehyde **1.43**. A formyl group at the β -position of this unsaturated aldehyde was installed using the conjugate addition of the lithium salt of **1.44** to form adduct **1.45**. Conversion to the corresponding aldehyde (**1.46**) proceeded smoothly and in high yield. Wasserman planned a final condensation of bisaldehyde **1.46** with ammonium carbonate in order to generate the desired annulated pyrrole C-ring (**1.39**). This final condensation worked well to give **1.39** and upon acid-mediated condensation with known **1.18**, racemic cycloprodigiosin was produced in an unspecified yield. Through NMR comparison, Wasserman confirmed the structure of cycloprodigiosin as the 6-membered ring annulated pyrrole congener (**1.5**). While Wasserman did indeed complete the first racemic total synthesis of cycloprodigiosin, the absolute stereochemistry at C4 was still undetermined.

Surprisingly, it took another 40 years until the first enantioselective route to cycloprodigiosin was reported by the Sarpong group in 2013.¹⁵ Sarpong's synthesis featured a Rh-catalyzed pyrrole annulation strategy to generate the enantiopure C-ring of cycloprodigiosin (Scheme 1.6).



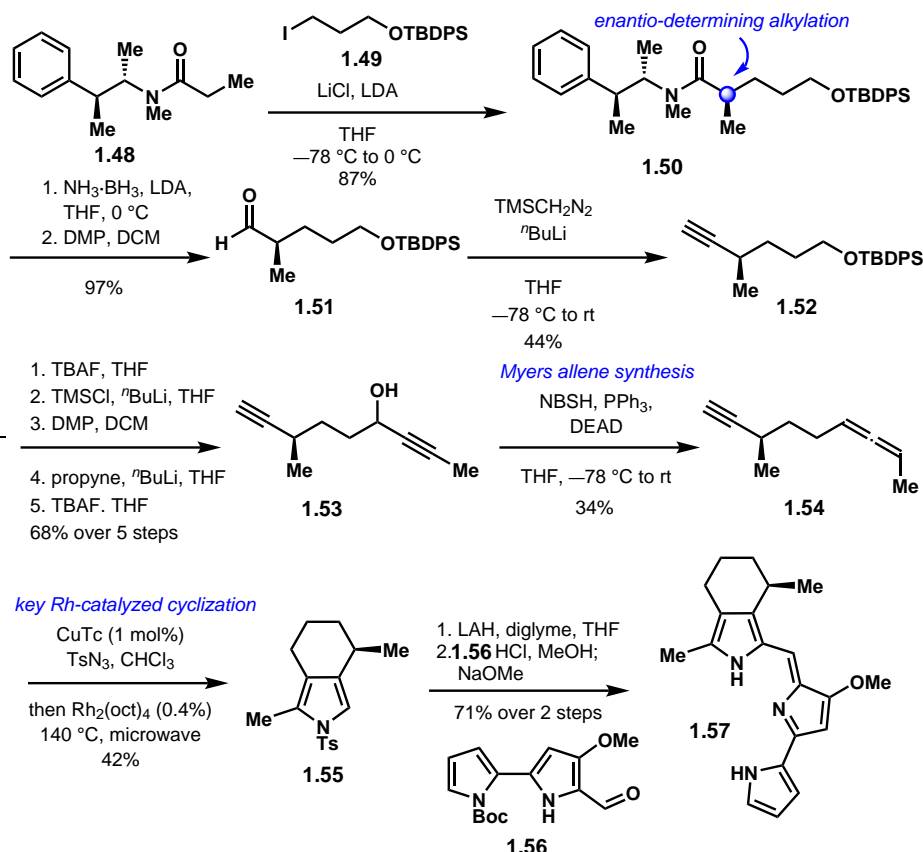
Scheme 1.5: The first synthesis of cycloprodigiosin **1.7** by Wasserman and Fukuyama in 1984.

The first step in this synthesis involved an enantioselective alkylation reaction using the chiral pseudoephedrine derivative **1.48**. Alkylation proceeded in high yield using alkyl iodide **1.49** as the electrophile to generate enantiopure intermediate **1.50**. With the desired chiral methyl-bearing stereocenter in place, the remainder of the synthesis focused on incorporating the allene and alkyne units required for a Rh-catalyzed pyrrole annulation reaction.

The synthesis proceeded with reductive removal of the chiral auxiliary using $\text{NH}_3 \cdot \text{BH}_3$ and LDA, followed by oxidation of the primary hydroxyl to furnish aldehyde **1.51**. Following alkylation using TMS diazomethane to generate compound **1.52**, a five-step protocol was performed in high yield (68% over five steps) to access **1.53**. This five-step procedure began with deprotection of the alcohol group using TBAF followed by silylation at the terminal alkyne position using TMSCl and *n*-butyl lithium. Oxidation of the primary hydroxyl using DMP furnished the corresponding aldehyde, which, upon addition of lithiated propyne in a 1,2-fashion and final deprotection of the alkyne, provided bisalkyne **1.53**.

With the alkyne unit successfully installed, the allene functionality was incorporated using a Myers allene synthesis involving NBSH, PPh_3 , and DEAD, to produce the chiral allene compound **1.54**.¹⁶ At this point in the synthesis, a one-pot two-component pyrrole annulation could be effected. First, the corresponding triazole of **1.54** was formed *in situ* through reaction with CuTc and tosyl azide. With the addition of the Rh(II) catalyst ($\text{Rh}_2(\text{oct})_4$) and heating to 140 °C in the microwave, the desired tosylated pyrrole (**1.55**) was isolated in moderate yield. Pyrrole precursor **1.55** was deprotected using LAH and then immediately subjected to condensation with Boc-protected bispyrrole **1.56**¹⁷ forming the enantiopure natural product cycloprodigiosin **1.57** in 71% yield over the two steps.

While this sequence is quite long to access annulated pyrrole C-ring **1.55**, the Rh(II) methodology is broadly applicable and provides access to a wide-variety of novel pyrrole derivatives in moderate to good yields.



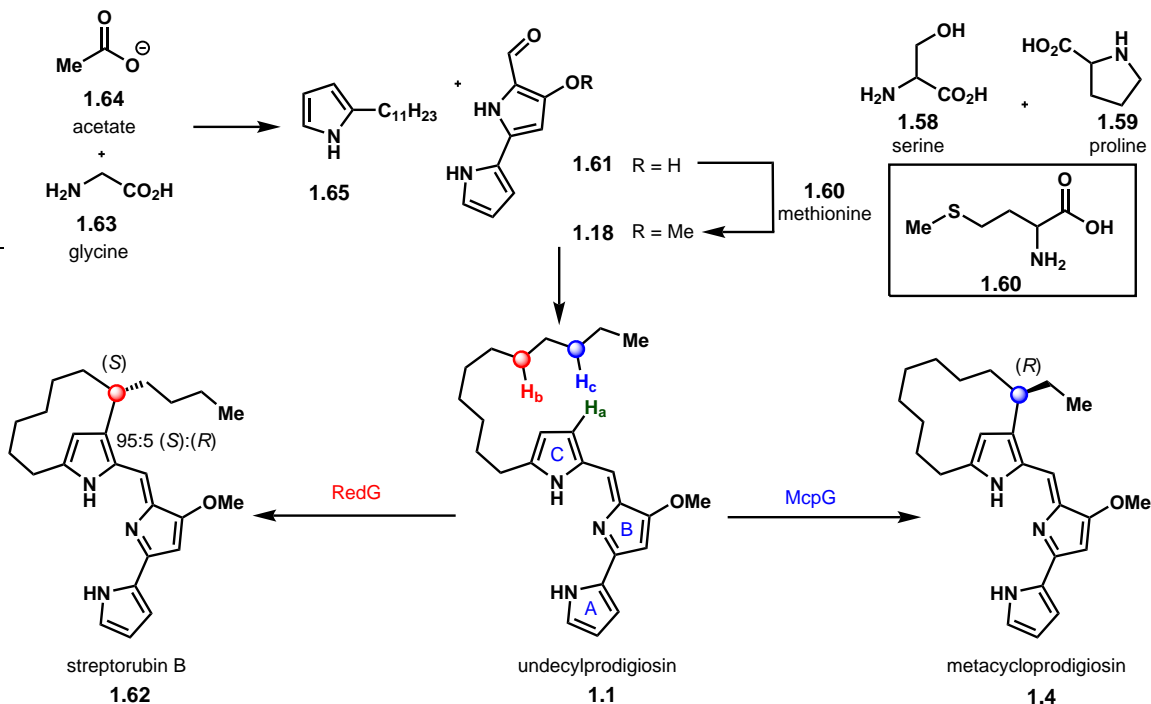
Scheme 1.6: Synthesis of cycloprodiginin **1.7** by Sarpong and Schultz in 2013 featuring a Rh-catalyzed pyrrole annulation to form the 3, 4-substituted pyrrole condensation precursor **1.39**

1.4 Biosynthesis of Prodigiosin Natural Products and Their Biological Activity

The biosynthesis of the A and B-rings (see **1.18**, Scheme 1.7) for all four classes of the prodiginines begins from the same components. That is, the bispyrrole **1.18** foundation is derived from amino acids serine **1.58** and proline **1.59**. Interestingly, the methoxy group is derived from methionine (**1.60**) through a final methylation of norbispyrrole **1.61**. The synthesis of the C-ring pyrrole is the defining feature for each family member where the linear alkyl chain is derived from acetate building blocks. Upon non-enzymatic condensation of the A/B-ring portion with the C-ring pyrrole to yield **1.1**, a late-stage enzyme-catalyzed oxidative cyclization event is believed to ensue from the linear precursor generating cyclized prodiginines.¹

It has been established that the cyclization event for streptorubin B (**1.62**) is catalyzed by Rieske-oxygenase RedG while the cyclization to metacycloprodiginosin (**1.4**) is catalyzed by McpG,

an enzyme also characterized from the same Rieske-oxygenase family. RedG was identified from the Red gene cluster of the bacterial strain *S. coelicolor* by Challis and coworkers in 2011. In the same paper, Challis identified the McpG gene cluster from *S. longispororuber* which is homologous to the RedG gene sequence.¹⁸



Scheme 1.7: The components of the biosynthesis of undecylprodigiosin as elucidated through feeding studies, and genome sequencing of *S. coelicolor* and *S. longispororuber*.

Besides their blood-red appearance, perhaps the most notable property of the prodigiosin family of molecules is their wide-ranging biological activities including immunosuppressant¹⁹ and antiparasitic activity.²⁰ The focus, however, has largely been shifted towards their ability to induce apoptosis in cancer cells as a result of the popular prodigiosin-like experimental anticancer agent Obatoclax® (1.66).²¹ This anticancer agent was advanced to Phase III clinical trials in 2012 but was soon after withdrawn by the sponsoring company Cephalon (acquired by Teva Pharmaceuticals).^{22,23}

It was originally established that Obatoclax® induces apoptosis through inhibition of the Bcl-2 family of proteins. However, its anticancer potency is much higher than that of molecules that are known to only inhibit Bcl-2 proteins, suggesting other modes of action are at hand.²⁴ Indeed, in addition to Bcl-2 protein inhibition, prodigiosin natural products and analogues have been proposed to induce apoptosis through two other major pathways including double-stranded DNA (dsDNA) cleavage and chloride anion transport.

Apoptosis is controlled by the Bcl-2 and Bax families of proteins and for this reason their interactions have been studied extensively. The Bcl-2 family of proteins are anti-apoptotic proteins while the Bax family of proteins are pro-apoptotic proteins that induce apoptosis through dimerization at the mitochondrial membrane (Figure 1.6).²⁵ The Bcl-2 family of proteins bind to Bax proteins and prevents their dimerization, which subsequently also halts apoptosis. Molecules in the

prodigiosin family are small-molecule inhibitors (SMI) that bind to and inhibit the anti-apoptotic set of Bcl-2 proteins, allowing the Bax pro-apoptotic proteins to dimerize and initiate the apoptotic pathway as illustrated in Figure 1.6. This overall pathway has been assumed to contribute to the anticancer activity exhibited by prodiginine natural products and their analogues.

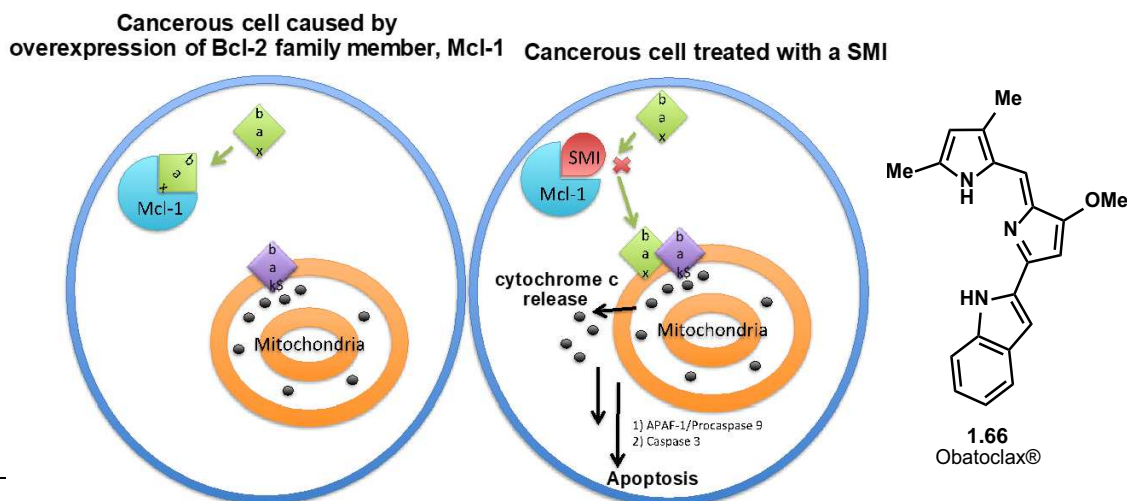
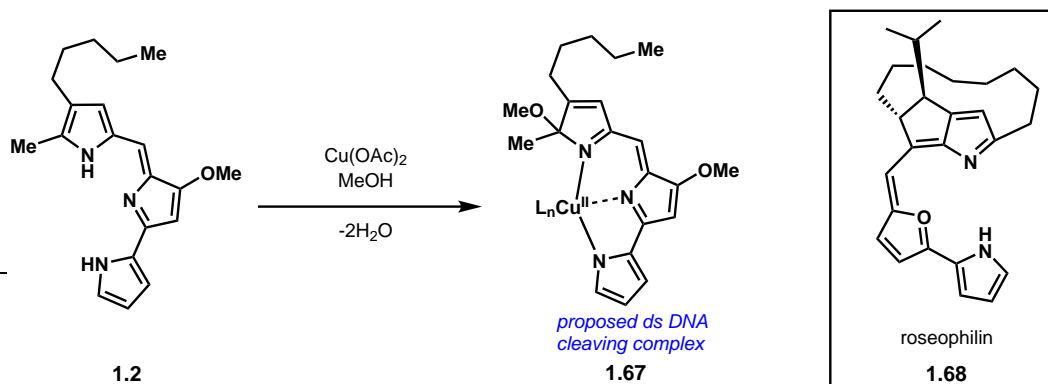


Figure 1.6: The proposed mechanism for apoptosis through Mcl-1 protein inhibition by prodiginin-like molecules. The anticancer activity exhibited by Obatoclax **1.66** is likely due to inhibition of the related Bcl-1 protein target (graphic adapted from Weinberg et. al.).²⁵

Prodiginine anticancer activity is also presumed to arise through dsDNA cleavage initiation. There are two proposed theories for how the prodiginins effect dsDNA cleavage. The first is through DNA intercalation followed by topoisomerase I/II poisoning.²⁶ The second is through oxidative cleavage by production of hydrogen peroxide from oxygen, which was found to be produced by prodiginin Cu(II) complex **1.67** (Scheme 1.8).²⁷ The exact mechanism for the conversion of oxygen to hydrogen peroxide by this complex is unknown, however, it is believed to be required for dsDNA cleavage. Notably, it was found by Fürstner and Grabowski in 2001 that roseophilin (**1.68**) in the presence of Cu(OAc)₂ led to no double-stranded DNA cleavage.²⁸ Roseophilin (**1.68**) is a natural product related to the prodiginines in that the middle B-ring has been replaced with a furan moiety. It was speculated that this furan moiety in roseophilin does not allow for the binding of copper in the same manner as in the tripyrrolic prodiginines, which led to reduced dsDNA cleavage activity.

A final proposed mechanism of action for the prodiginines is anion transport, specifically, chloride anion transport. When protonated, prodiginin and related molecules bind chloride anions and transport them through lipid bilayers while allowing internal anions to exit through a process known as antiport.^{29,30} For example, when prodiginin analogues are introduced into cells, bicarbonate anions are effluxed, which disrupts cell polarity and ultimately leads to apoptosis. Additionally, the prodiginines likely acidify the intracellular environment through transport of HCl out of acidic organelles and into the intracellular environment, thus triggering apoptosis. This mechanism of action is also believed to be operative in a closely related class of molecules known as the tambjamines (Figure 1.7, **1.69**).²⁹

Since anion transport by prodiginines relies on the protonated form of prodiginins, the pK_a



Scheme 1.8: Proposed structure of the double-strand DNA cleaving derivative **1.67**.

of the positively charged nitrogen is an important property for anion-transport efficiency. This hypothesis is supported by pK_a investigations conducted on prodiginosin analogue **1.70**.³¹ Anion-transport efficiency decreased for the electron-depleted analogue **1.70**, which bears an ester group on the C-ring as illustrated in Figure 1.7. This pK_a property may be exploited in developing prodiginosin analogues with potent apoptotic activity.

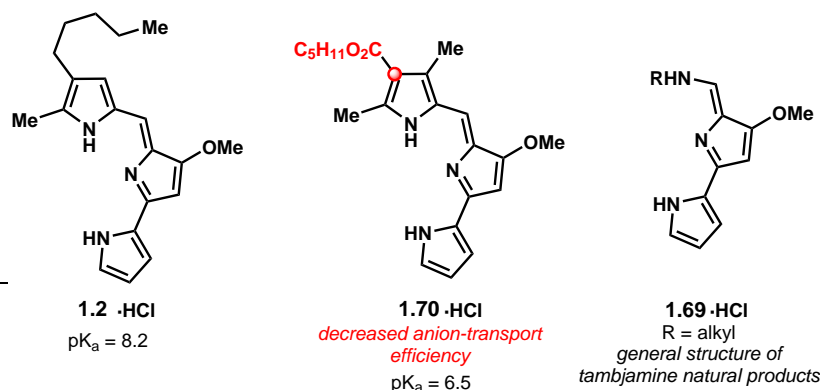


Figure 1.7: A comparison of pK_a 's for the natural product **1.2** and the esterified derivative **1.70**. Anion-transport activity is decreased for the electron-withdrawn derivative **1.70**.

1.5 Conclusion and Outlook

The prodiginines represent a novel and fascinating class of natural products, the existence of which dates back to the B.C. era when they first left their colorful impact on history. It wasn't until the 20th century that prodiginosin's structure was elucidated and the mystery surrounding *Serratia marcescens*' blood-red color was solved. Indeed, the characteristic red color of this bacterium is a result of the highly conjugated tripyrrolic core of prodiginines.

Synthetic chemists have been particularly captivated by the prodiginines and as a result, many total syntheses have been developed over the last 50 years. Total synthesis of prodiginines has allowed for their structural elucidation and further exploration into the mechanisms of action for their pronounced biological activity.

There were still several unanswered questions surrounding the prodiginines, specifically, cycloprodigiosin (**1.5**). The absolute stereochemistry of the single stereocenter at C4' had not been determined prior to our work and the enzyme responsible for the oxidative cyclization of prodigiosin to cycloprodigiosin had not been identified. The answers to these questions will form a more complete picture of the prodiginines and are discussed in Chapter 2.

1.6 References

1. Fürstner Alois, *Angew. Chem. Int. Ed.* **2003**, *42*, 3582–3603.
2. Hu, D. X.; Withall, D. M.; Challis, G. L.; Thomson, R. J. *Chem. Rev.* **2016**, *116*, 7818–7853.
3. Bennett, J.; Bentley, R. *Adv. Appl. Microbiol.*; Elsevier, 2000; Vol. 47; pp 1–32.
4. Thompson, H.
5. Wrede, F.; Rothhaas, A. *Hoppe-Seyler's Z. Physiol. Chem.* **1933**, *219*, 267.
6. Treihls, A.; Zimmer-Galler, R. *Hoppe-Seyler's Z. Physiol. Chem.* **1960**, *318*, 12.
7. Wasserman, H. H.; McKeon, J. E.; Smith, L.; Forgione, P. *J. Am. Chem. Soc.* **1960**, *82*, 506–507.
8. Rapoport, H.; Willson, C. D. *J. Am. Chem. Soc.* **1962**, *84*, 630–635.
9. Rapoport, H.; Holden, K. G. *J. Am. Chem. Soc.* **1962**, *84*, 635–642.
10. Wrede, F.; Rothhaas, A. *Hoppe-Seyler's Z. Physiol. Chem.* **1934**, *226*, 95.
11. Boger, D. L.; Patel, M. *J. Org. Chem.* **1988**, *53*, 1405–1415.
12. Wasserman, H. H.; Fukuyama, J. M. *Tetrahedron Lett.* **1984**, *25*, 1387–1388.
13. Gerber, N.; Gauthier, M. *Appl. Environ. Microbiol.* **1979**, *37*, 1176–1179.
14. Lattasch, H.; Thomson, R. H. *Tetrahedron Lett.* **1983**, *24*, 2701–2704.
15. Schultz, E. E.; Sarpong, R. *J. Am. Chem. Soc.* **2013**, *135*, 4696–4699.
16. Myers, A. G.; Zheng, B. *J. Am. Chem. Soc.* **1996**, *118*, 4492–4493.
17. Dairi, K.; Tripathy, S.; Attardo, G.; Lavallée, J.-F. *Tetrahedron Lett.* **2006**, *47*, 2605–2606.
18. Sydor, P. K.; Barry, S. M.; Odulate, O. M.; Barona-Gomez, F.; Haynes, S. W.; Corre, C.; Song, L.; Challis, G. L. *Nat. Chem.* **2011**, *3*, 388–392.
19. Azuma, T.; Watanabe, N.; Yagisawa, H.; Hirata, H.; Iwamura, M.; Kobayashi, Y. *Immunopharmacology* **2000**, *46*, 29–37.
20. Kim, H. S.; Hayashi, M.; Shibata, Y.; Wataya, Y.; Mitamura, T.; Horii, T.; Kawauchi, K.; Hirata, H.; Tsuboi, S.; Moriyama, Y. *Biol. Pharm. Bull.* **1999**, *22*, 532–534.
21. Nguyen, M. *et al. Proc. Natl. Acad. Sci. U.S.A.* **2007**, *104*, 19512–19517.
22. Schimmer, A. D. *et al. Clin. Cancer Res.* **2008**, *14*, 8295–8301.
23. Paik, P. K.; Rudin, C. M.; Pietanza, M. C.; Brown, A.; Rizvi, N. A.; Takebe, N.; Travis, W.; James, L.; Ginsberg, M. S.; Juergens, R.; Markus, S.; Tyson, L.; Subzwari, S.; Kris, M. G.; Krug, L. M. *Lung Cancer* **2011**, *74*, 481–485.
24. Tse, C. *et al. Cancer Res.* **2008**, *68*, 3421–3428.
25. Weinberg, R. A. *The Biology of Cancer*, 2nd ed.; Garland Science: New York, 2014; p 366.
26. Montaner, B.; Castillo-Ávila, W.; Martinell, M.; Öllinger, R.; Aymami, J.; Giralt, E.; Pérez-Tomás, R. *Toxicol. Sci.* **2005**, *85*, 870–879.
27. Park, G.; Tomlinson, J. T.; Melvin, M. S.; Wright, M. W.; Day, C. S.; Manderville, R. A. *Org. Lett.* **2003**, *5*, 113–116.
28. Fürstner, A.; Grabowski, E. J. *ChemBioChem* **2001**, *2*, 706–709.

29. Gale, P. A.; Pérez-Tomás, R.; Quesada, R. *Acc. Chem. Res.* **2013**, *46*, 2801–2813.
30. Yamamoto, C.; Takemoto, H.; Kuno, K.; Yamamoto, D.; Tsubura, A.; Kamata, K.; Hirata, H.; Yamamoto, A.; Kano, H.; Seki, T.; Inoue, K. *Hepatology* **1999**, *30*, 894–902.
31. Rastogi, S.; Marchal, E.; Uddin, I.; Groves, B.; Colpitts, J.; McFarland, S. A.; Davis, J. T.; Thompson, A. *Org. Biomol. Chem.* **2013**, *11*, 3834.

Chapter 2

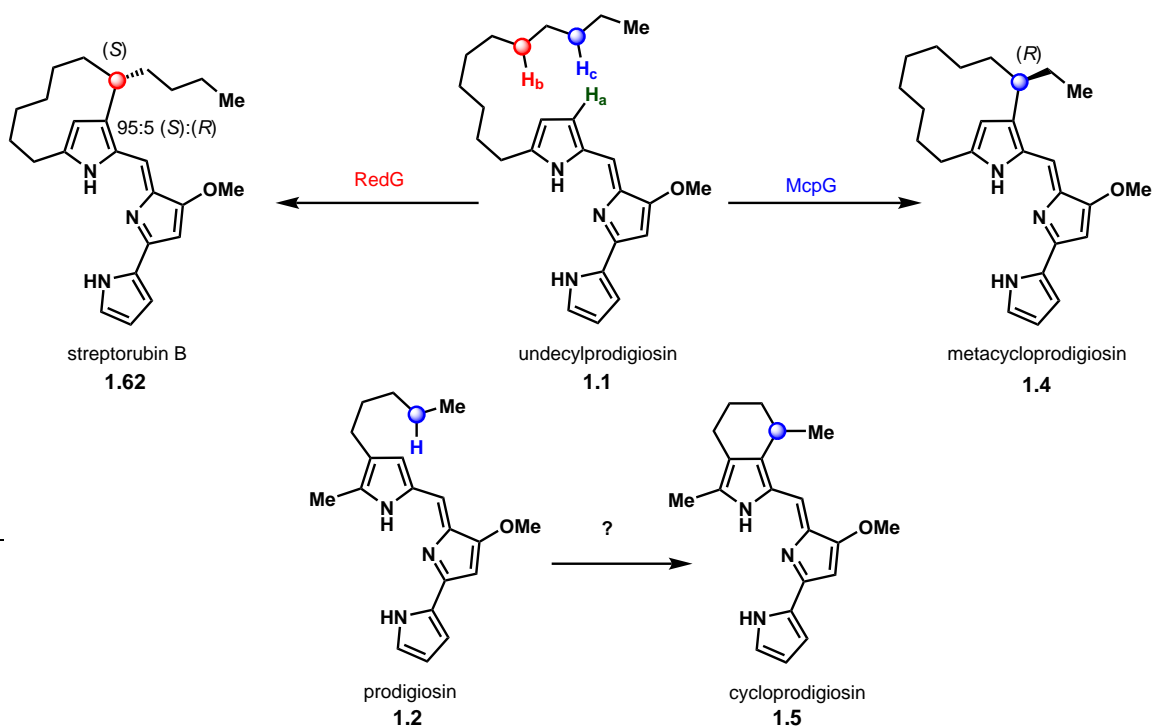
Chapter 2 : Synthesis of Cycloprodigiosin Identifies the Natural Isolate as a Scalemic Mixture

2.1 Motivations for Pursuing the Synthesis of Cycloprodigiosin

In the last decade, total synthesis and analysis has led to the absolute stereodetermination of two prodiginine natural products, streptorubin B¹ and metacycloprodigiosin.² These two natural products arise from the oxidative cyclization of a linear precursor, undecylprodigiosin (**1.1**), in a stereoselective manner (Scheme 2.1) to provide streptorubin B (**1.62**) as the *S*-enantiomer and metacycloprodigiosin (**1.4**) as the *R*-enantiomer. Surprisingly, in 2011, Challis and Thomson determined that streptorubin B (**1.62**) exists as a scalemic mixture in nature with a 95:5 ratio of (*S*) to (*R*) enantiomers.^{1,3,4}

As discussed in Chapter 1, the biosynthesis of these cyclic prodigiosins from a linear congener (i.e., **1.1** to **1.4** and **1.62**) has been shown to be mediated by a notable class of Rieske non-heme iron dependent oxygenases in *Streptomyces* sp.^{2,5,6} The biosynthesis of cycloprodigiosin (**1.5**, Scheme 2.1) – first isolated from the marine bacterium *Pseudoalteromonas rubra* – presumably proceeds by oxidative cyclization of the linear congener prodigiosin (**1.2**), however, this hypothesis remains unsubstantiated. Additionally, while the constitution of cycloprodigiosin has been secured through careful analysis and total synthesis^{7,8} it remains unknown whether cycloprodigiosin occurs in nature as a racemic, scalemic, or enantiopure form.

Additionally, whether **1.4** also occurs as a scalemic mixture has not been rigorously established.² As a result, the stereochemistry at C4' of cycloprodigiosin (**1.5**) cannot be presumed by analogy to the other existing cyclic prodiginines. We envisioned that an efficient and enantiodivergent total synthesis of cycloprodigiosin would allow us to determine the absolute stereochemistry of the single stereocenter in the molecule through a comparison of synthetic material with the natural isolate.



Scheme 2.1: The late-stage enzymatic oxidative cyclization reactions of undecylprodigiosin leading to either streptorubin B (**1.62**) catalyzed by Rieske-oxygenase RedG, or metacycloprodigiosin (**1.4**) by McpG. The enzyme catalyzing the final oxidative cyclization event in the biosynthesis of cycloprodigiosin (**1.5**) from prodigiosin (**1.2**) has not been determined. The stereochemistry of the single stereocenter in cycloprodigiosin has not been determined.

2.2 1st Generation Synthesis of Cycloprodigiosin Derived from Established Chemistry

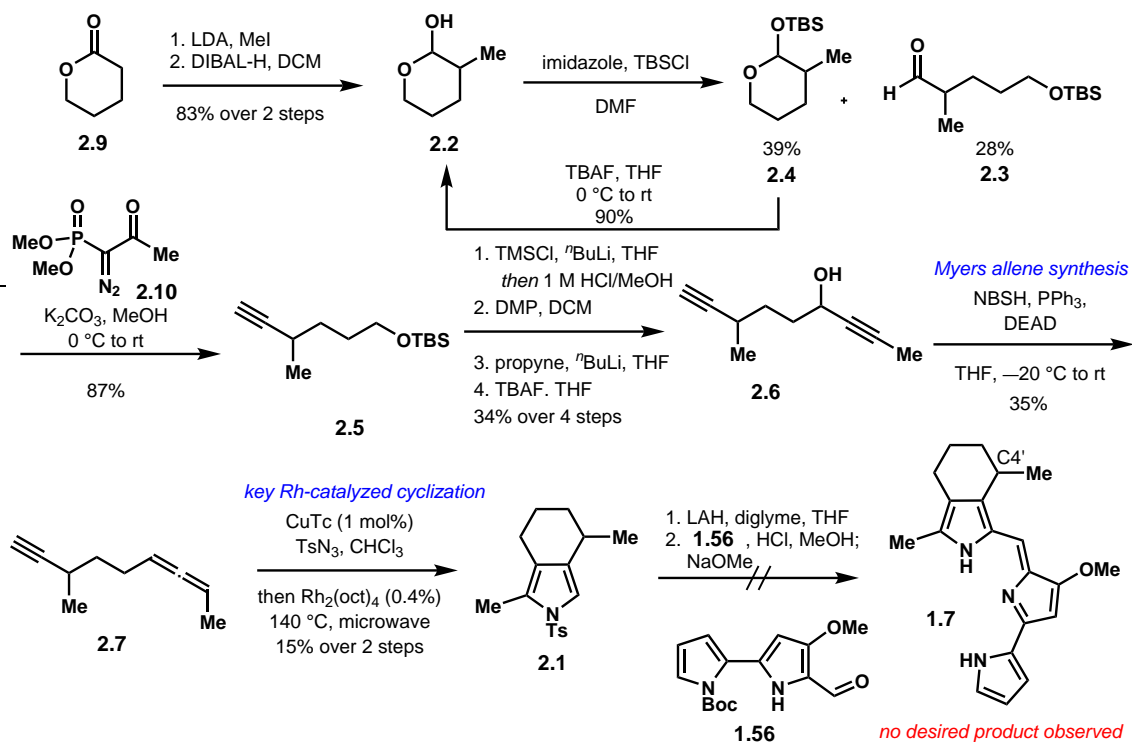
In our group, a synthesis of cycloprodigiosin (**1.57**, Chapter 1)⁹ had already been developed. However, the route was quite long and low-yielding, leading to small isolated quantities of the natural product.⁹ In an effort to improve the efficiency of this synthesis, we set out to conduct a racemic synthesis of key pyrrole precursor **2.1** using a more scalable route. We envisioned that by having access to larger quantities of the natural product, it would allow us to use X-ray crystallography to determine the absolute stereochemistry at C4' of the natural product.

The racemic synthesis commenced with the methylation of δ -valerolactone using LDA and MeI (Scheme 2.2). Subsequent reduction to the lactol with DIBAL-H provided compound **2.2** in 83% over two steps. Ring-opening of the lactol and subsequent trapping with TBSCl delivered linear aldehyde **2.3**. However, TBS-protected lactol **2.4** was also isolated in substantial quantities leading to only 28% yield of desired compound **2.3**. The undesired silylated lactol **2.4** could be recycled back to **2.2** through treatment with TBAF, and the same sequence could be performed again (i.e., **2.2** to **2.3**).

With aldehyde **2.3** in hand, productive alkynylation conditions were found using the Ohira-Bestmann protocol^{10,11} providing the alkynylated product **2.5** in 87% yield. In an analogous se-

quence to our previously established enantiospecific route,⁹ a series of protecting group and redox manipulations provided bisalkyne **2.6** in 34% yield over four steps. A Myers allene synthesis was performed on **2.6** using NBSH, PPh₃, and DEAD, yielding the highly volatile allene intermediate **2.7**.¹² The low yield of 35% was likely due to the volatility of this species (**2.7**) and its loss throughout the work-up process. Nevertheless, the racemic version of pyrrole precursor **2.8** was synthesized through a Rh(II)-catalyzed pyrrole annulation, albeit in a poor 15% yield. Unfortunately, due to a lack of material at this stage, we were not able to successfully complete the synthesis of racemic cycloprodigiosin **1.7**.

It was clear at this stage that a more robust synthesis would have to be employed to pursue our ultimate goal of determining the absolute stereochemistry of cycloprodigiosin (**1.5**).

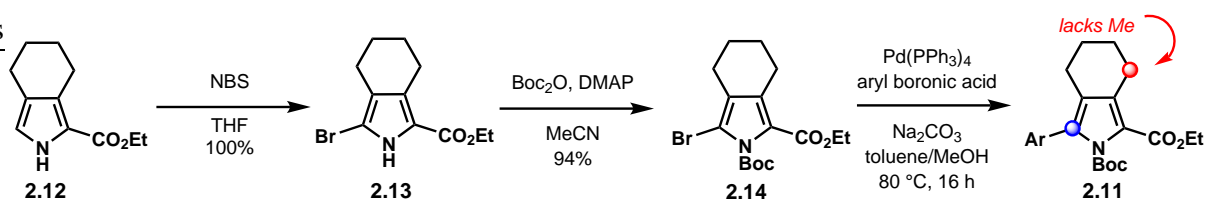


Scheme 2.2: Our initial synthesis for racemic cycloprodigiosin **1.7**.

2.3 A Concise and Efficient 2nd Generation Approach for the Synthesis of Cycloprodigiosin

We eventually found a protocol developed by Neumann and coworkers that provided access to 3, 4-annulated pyrrole derivatives (see **2.11**, Scheme 2.3) through a Barton-Schöllkopf-Zard (SBZ) pyrrole annulation.¹³ Notably, the pyrrole analogues that the Neumann group reported, lack the pseudo-benzylic methyl group present in cycloprodigiosin as highlighted in compound **2.11**.

It was our immediate goal to use the precedent by Neumann and coworkers as inspiration for the synthesis of the A-ring of cycloprodigiosin. In this way, we designed a retrosynthetic route



Scheme 2.3: Neumann's reported route to access C5-arylated pyrrole derivatives (**2.11**) through a SBZ pyrrole annulation and Suzuki cross-coupling strategy.

(Figure 2.1) that would provide access to the racemate as well as each enantiomer of the natural product.

As shown in Figure 2.1, we envisioned **1.7** arising from condensation of fused pyrrole **2.15** with bis-pyrrole aldehyde **1.18** following the well-established precedent of Wasserman using anhydrous HCl.¹⁴ Key to this coupling would be an initial saponification/decarboxylation sequence of the ester group in **2.15**. Fused pyrrole **2.15** could in turn be prepared from the two-component coupling of cyclic nitroalkene **2.16** and isocynoacetate **2.17** using a SBZ pyrrole synthesis.¹⁵ While this retrosynthetic plan only leads to racemic **1.7**, we planned to use a chiral auxiliary in place of the ethyl substituent, on the carboxy group of **2.17** to facilitate an enantiodivergent synthesis of cycloprodiginosin.

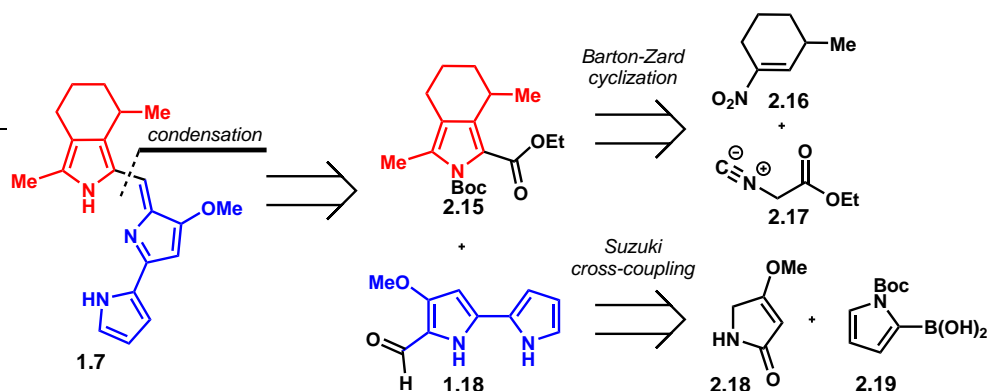
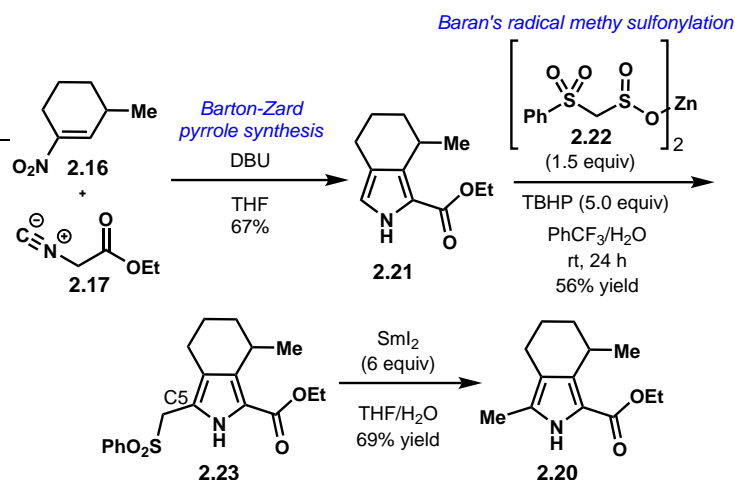


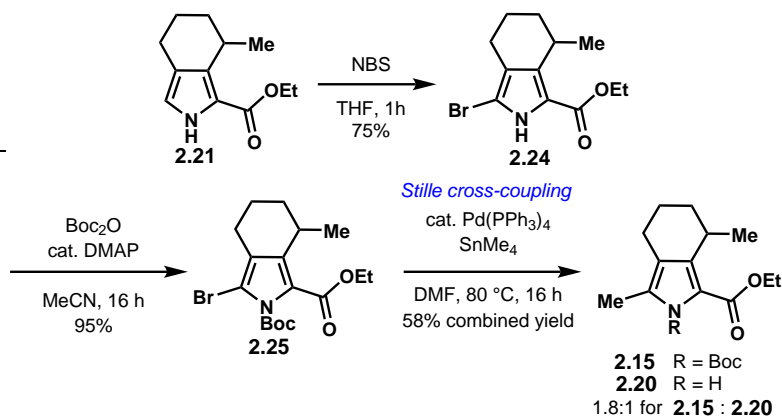
Figure 2.1: Retrosynthetic plan highlighting a two-component SBZ pyrrole annulation

The synthesis of esterified pyrrole **2.20** commenced with the preparation of 3-methyl-1-nitrocyclohexene (**2.16**, see Scheme 2.4), which was obtained from 3-methylcyclohexene in one step according to the procedure by Estreicher and Corey.¹⁶ Subjecting **2.16** to ethyl isocynoacetate (**2.17**) in the presence of DBU effected a SBZ pyrrole annulation¹⁵ to afford **2.21** in 67% yield. Several methods were then explored for installation of a methyl group at the pyrrole C5 position. Envisioning rapid access to methylated pyrrole **2.20**, we first investigated a method recently developed by Baran and coworkers.¹⁷ Thus, treatment of pyrrole **2.21** with zinc bis[(phenylsulfonyl) methanesulfonate] (PSMS; **2.22**) and *tert*-butylhydroperoxide (TBHP) afforded methylenesulfone adduct **2.23** (56% yield), which upon treatment with freshly prepared samarium iodide was reduced to the desired C5 methylated pyrrole (**2.20**) in 69% yield. While this method provided efficient access to **2.20**, in our hands, an alternative approach proved to be more serviceable and cost-effective.



Scheme 2.4: The methylation sequence using Baran's PSMS reagent.

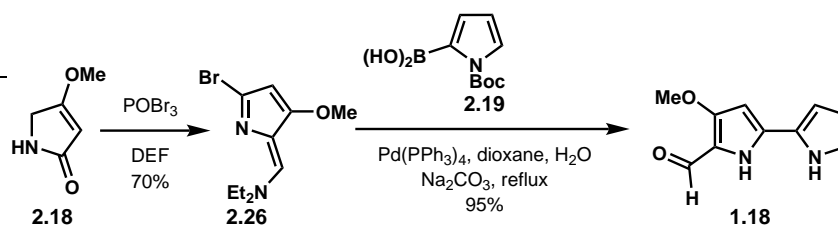
In this more practical sequence (Scheme 2.5), we installed a cross-coupling handle on pyrrole **2.21** through bromination at C5 using NBS, which provided **2.24** in 75% yield. As reported by Neumann and coworkers,¹³ the coupling efficiency was significantly higher upon Boc-protection of the pyrrole nitrogen (to give **2.25**). A survey of Pd-catalyzed cross-coupling partners revealed that tetramethyltin served as the most reliable coupling partner to provide a mixture of **2.15** and the deprotected analogue (**2.20**) in a combined 58% yield from **2.25**. Notably, the formation of both **2.15** and **2.20** was inconsequential as each compound served as a substrate in the final condensation to form cycloprodigiosin.



Scheme 2.5: An alternative and more practical methylation sequence utilizing brominated pyrrole (**2.24**) as a coupling partner.

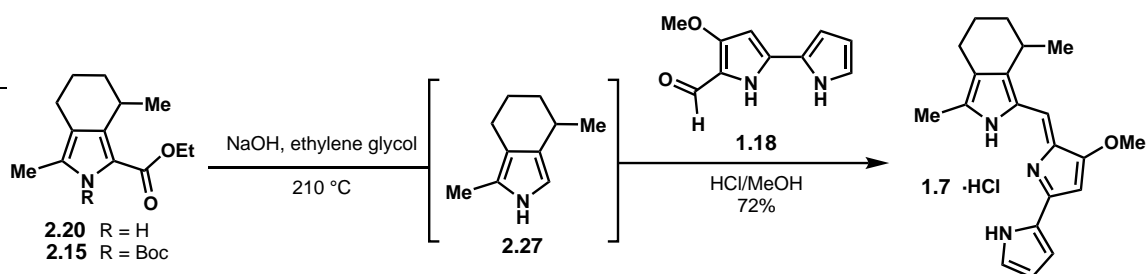
We followed an established synthetic procedure developed by Lavalée and coworkers in which they reported the synthesis of **1.18** in a two-step cross-coupling sequence as shown in Scheme 2.6.¹⁸ Starting from pyrrolidinone **2.18**, treatment with POBr_3 in the presence of DEF promoted a Vilsmeier-Haack reaction to produce intermediate **2.26**. A Suzuki cross-coupling utilizing boronic acid **2.19** was effected followed by hydrolysis to form the desired bispyrrole partner **1.18** in 95% yield.

Subjection of the mixture of compounds **2.20** and **2.15** to NaOH in ethylene glycol at 210 °C



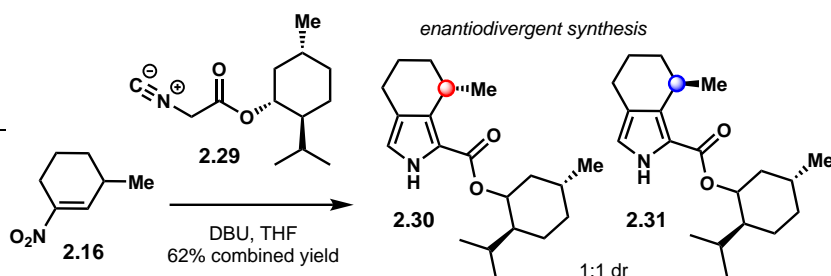
Scheme 2.6: Synthesis of the bispyrrole coupling partner **1.18**.¹⁸

effected a saponification/decarboxylation sequence yielding the highly unstable N-H pyrrole intermediate **2.27**. Immediate subjection of this crude compound to **1.18** in MeOH in the presence of freshly prepared anhydrous HCl, yielded racemic cycloprodigiosin·HCl (**2.28**·HCl) in 72% yield.



Scheme 2.7: Synthesis of the racemic version of cycloprodigiosin **1.7** through a biomimetic condensation reaction.

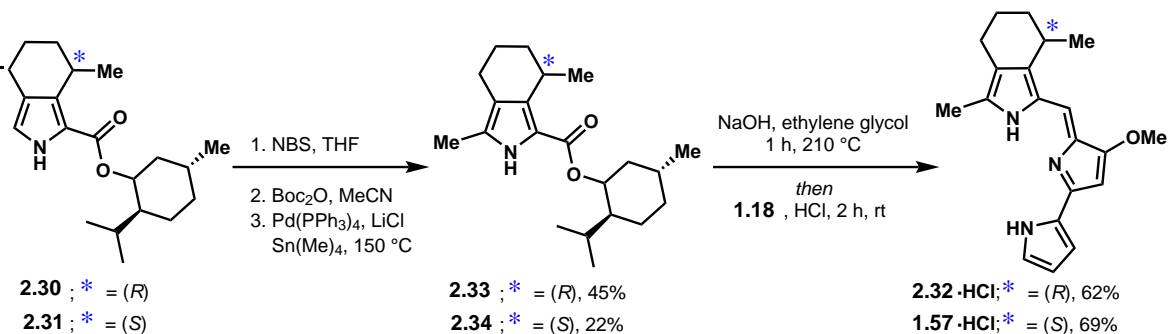
This synthetic sequence also provided the basis for the preparation of enantioenriched cycloprodigiosin using (–)-menthol-derived isocyanoacetate **2.29** (Scheme 2.8; prepared according to the procedure of Verkade)¹⁹ in place of ethyl isocyanoacetate in the SBZ pyrrole annulation. This annulation reaction worked in comparable yield as with the non-chiral isocyanoacetate (**2.17**) and delivered a 1:1 ratio of fused pyrrole diastereomers (**2.30** and **2.31**). Consistent with our plan, these diastereomers were indeed isolable through SiO₂ chromatography and were carried forward separately in the synthesis.



Scheme 2.8: Synthesis of diastereomeric pyrrole intermediates **2.30** and **2.31** through a SBZ pyrrole annulation using chiral isocyanoacetate **2.29**.

The enantiomers of cycloprodigiosin ((*S*)-**2.32**·HCl and (*R*)-**1.57**·HCl) were prepared with similar efficiencies using the same protocol as described for the racemic case by advancing diastereomers **2.30** and **2.31** separately as shown in Scheme 2.9.

X-ray crystallographic analysis of the HCl salt of enantiomer (*R*)-**1.57** enabled absolute stereochemical characterization of the materials that we prepared, which set the stage for comparison to the natural isolate. The crystal structure of cycloprodigiosin that we obtained, illustrating the absolute stereochemistry of the (*R*)-enantiomer, is shown in Figure 2.2.



Scheme 2.9: Synthesis of both enantiomers of cycloprodigiosin as **2.32** and **1.57**.

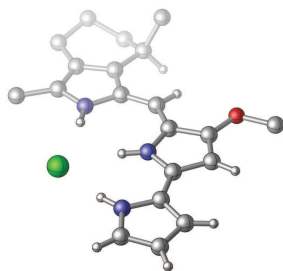
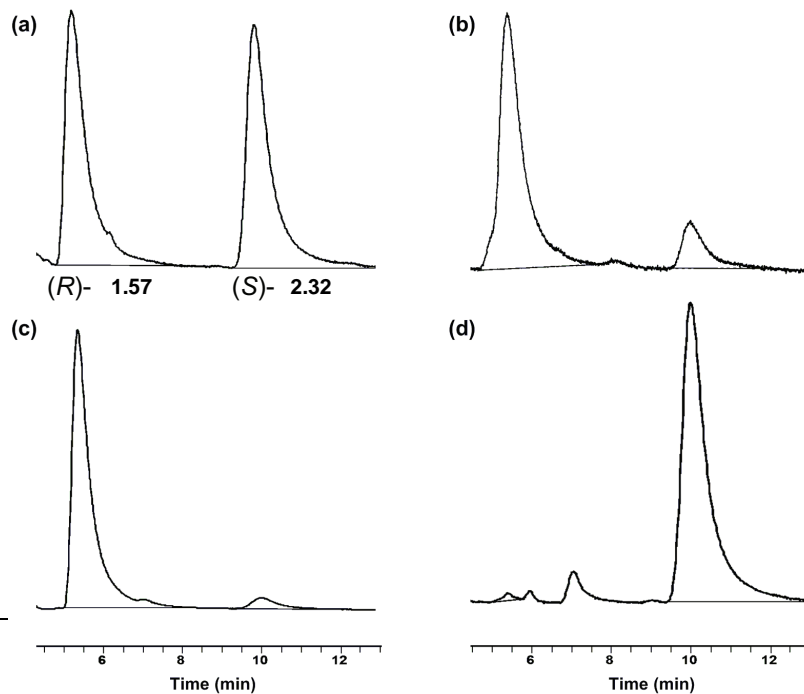


Figure 2.2: Crystal structure for the determination of the absolute stereochemistry of **1.57·HCl**.

This project also featured a collaboration with Tristan de Rond of the Keasling group at UC Berkeley who contributed the natural isolate of cycloprodigiosin. A sample of naturally occurring cycloprodigiosin was obtained from *P. rubra* (Gauthier 1976, ATCC 29570)²⁰ and purified by sequential normal and reversed-phase chromatography. In total, 0.2 mg of the natural product was obtained from 1 L of culture. With the natural isolate of cycloprodigiosin (from *P. rubra*) as well as our synthetic material in hand, we analyzed these materials using HPLC (Chiralpak IA) monitoring the absorbance at 500 nm.^{8,21} Comparison of the HPLC trace of the natural isolate to those of the racemic and enantiopure ((*S*)-**2.32** and (*R*)-**1.57**) material prepared by us is shown in Scheme 2.10.

(*R*)-**1.57** has a retention time of 5.43 min (Scheme 2.10C) whereas (*S*)-**2.32** has a retention time of 10.02 min (Figure Scheme 2.10D). These observations are corroborated by our observations for racemic cycloprodigiosin (Scheme 2.10A). The natural isolate displays two peaks that correspond to the two enantiomers in the ratio of 83:17 for (*R*)-**1.57**:(*S*)-**2.32** (Scheme 2.10B). Two independent production experiments gave identical enantiomeric ratios. Thus, it would appear that naturally occurring **1.7** is scalemic. These observations are consistent with those of Challis et al. for streptorubin B, albeit occurring with markedly lower enantiopurity in the case of cycloprodigiosin.

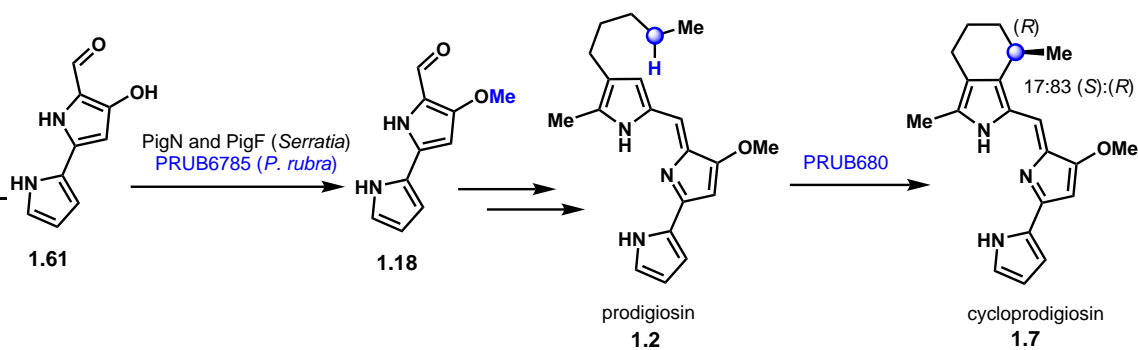


Scheme 2.10: Chiral HPLC traces of (A) racemic cycloprodigiosin **1.7**, (B) natural cycloprodigiosin, (C) synthetic (*R*)-cycloprodigiosin, (D) synthetic (*S*)-cycloprodigiosin.

2.4 Biosynthetic Investigations Into the Late-Stage Oxidative Cyclization from Prodigiosin to Cycloprodigiosin

As discussed in Chapter 1, the cyclase enzyme responsible for the oxidative cyclization of prodigiosin (**1.2**) to cycloprodigiosin (**1.5**) had not been identified previously. The collaboration with the Keasling group led to the identification and initial characterization of the enzyme responsible for the final oxidative cyclization producing cycloprodigiosin. This discovery began with the identification of the gene sequence for the enzyme PRUB675 which is responsible for converting bispyrrole precursor **1.61** to the methylated intermediate **1.18** (Scheme 2.11). Within the same gene transcriptional unit was the sequence for PRUB680 which was recognized as a relative of other iron-dioxygenase enzymes. Performing a gene knockout of PRUB680 with *P. rubra* confirmed that the absence of PRUB680 led to no production of cycloprodigiosin.

PRUB680 was characterized as a di-iron containing member of the fatty-acid hydroxylase family of enzymes that are found in the transmembrane space. Notably, PRUB680 shares no homology to the Rieske enzymes (RedG and McpG) responsible for the oxidative cyclization of undecylprodigiosin to streptorubin B and metacycloprodigiosin respectively. Therefore, PRUB680 represents a new class of enzymes capable of performing oxidative cyclizations and may be further explored as a potential biocatalyst for non-native molecular scaffolds. Along these lines, the promiscuity of PRUB680 has yet to be explored. With the synthesis of non-natural prodigiosin analogs, such exploration could be conducted as a future investigation for our group or others.



Scheme 2.11: The identification of PRUB675 led to the discovery PRUB680 as the enzyme responsible for the late-stage oxidative cyclization.

2.5 Conclusion and Outlook

In this chapter, a rapid and novel synthesis of cycloprodigiosin was reported that was easily modified to afford both enantiomers of the natural product. In collaboration with the Keasling group, the growth and isolation of cycloprodigiosin from *P. rubra* was also achieved. Analyses of these materials using a combination of X-ray crystallography and chiral HPLC have revealed that naturally occurring cycloprodigiosin obtained from *P. rubra* occurs as a scalemic mixture, which is analogous to observations made previously for streptorubin B. These observations initiated an exploration into the final oxidative cyclization event of cycloprodigiosin in *P. rubra*. Through a collaboration with the Keasling group, the di-iron oxygenase PRUB680 was identified as the enzyme responsible for the final oxidative cyclization from prodigiosin to cycloprodigiosin. The promiscuity of PRUB680 in addition to its potential as a biocatalyst for late-stage oxidations has yet to be examined.

2.6 Experimental Contributors

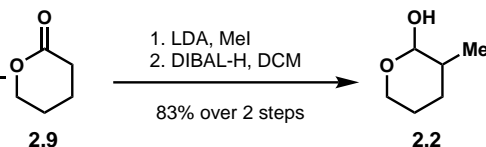
The work presented in Section 2.2 (1st Generation Synthesis of Cycloprodigiosin Derived from Previously Established Chemistry) was conducted by both Rebecca E. Johnson (R.J.) and Dr. Erica Schultz (E.S.) and is unpublished. Partial characterization is reported in Section 2.8 (Experimental Methods and Procedures). All work presented in Section 2.3 (A Concise and Efficient 2nd Generation Approach for the Synthesis of Cycloprodigiosin) was conducted by R.J. Ideas and strategy were developed by R.J. with the assistance of Prof. Richmond Sarpong (R.S.). Tristan de Rond (T.d.R.) optimized the production of cycloprodigiosin in *P. rubra* and isolated natural cycloprodigiosin from *P. rubra*. Vincent N. G. Lindsay (V.N.G.L.) performed all chiral HPLC analysis. This work was published in 2015 (Synthesis of Cycloprodigiosin Identifies the Natural Isolate as a Scalemic Mixture, Johnson, R. E.; de Rond, T.; Lindsay, V. N. G.; Keasling, J. D.; Sarpong, R. *Org. Lett.*, **2015**, *17*, 3474.) and full characterization is provided in Section 2.8 (Experimental Methods and Procedures). The work presented in Section 2.4 (Biosynthetic Investigations Into the Late-Stage Oxidative Cyclization from Prodigiosin to Cycloprodigiosin) was conceived by Dr. Tristan de Rond (T.d.R.), (R.J.), (R.S.), and Prof. Jay D. Keasling (J.D.K.). T.d.R., Parker Stow (P.S.) and Ian Eigl (I.E.) constructed plasmids and performed microbiological manipulations and

extractions, R.J. performed synthetic organic chemistry. T.d.R., Edward E K Baidoo (E.E.K.B.), and Christopher J. Petzold (C.J.P.) performed analytical chemistry, Leanne Jade G Chan (L.J.G.C.) and C.J.P. performed proteomic analysis, and Garima Goyal (G.G.) and Nathan J. Hillson (N.J.H.) PCR amplified and purified DNA fragments. T.d.R. performed bioinformatic analysis. All authors contributed to the manuscript published in 2017 (Oxidative cyclization of prodigiosin by an alkyl-glycerol monooxygenase-like enzyme, de Rond, T.; Stow, P.; Eigl, I.; Johnson, R. E.; Chan, L. J. G.; Goyal, G.; Baidoo, E, EK.; Hillson, N. J.; Petzold, C. J.; Sarpong, R.; Keasling, J. D. *Nature Chemical Biology*, **2017**, *13*, 1155.)

2.7 Materials and Methods

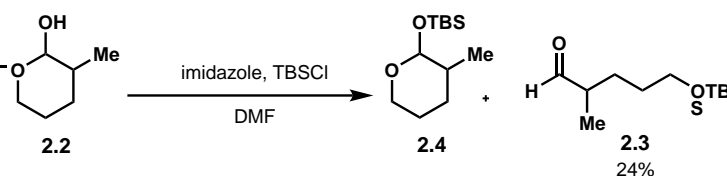
Unless stated otherwise, reactions were performed in oven-dried glassware with sealed with rubber septa under a nitrogen atmosphere and were stirred with Teflon®-coated magnetic stir bars. Liquid reagents and solvents were transferred by syringe using standard Schlenk techniques. Tetrahydrofuran (THF), toluene, acetonitrile (MeCN), and methanol (MeOH) were dried by passage over a column of activated alumina; Dichloromethane (DCM) was distilled over calcium hydride. Samarium iodide (SmI₂) was freshly prepared before use. N-bromosuccinimide (NBS) was recrystallized from water (approx. 1 g/mL) before use. All other solvents and reagents were used as received unless otherwise noted. Solutions were degassed using three cycles of freeze/pump/thaw (freezing the solution contained within a Schlenk flask in liquid nitrogen, opening the flask to vacuum for 5 min, then allowing the solution to thaw under vacuum). Thin layer chromatography was performed using SiliCycle SiO₂ 60 F-254 precoated plates (0.25 mm) and visualized by UV irradiation, anisaldehyde, cerium ammonium molybdenate (CAM), potassium permanganate, or iodine stain. Melting points were recorded on a Mel-Temp II by Laboratory Devices Inc., USA. Optical rotation was recorded on a Perkin Elmer Polarimeter 241 at the D line (1.0 dm path length), c = mg/mL, in CHCl₃ unless otherwise stated. ¹H and ¹³C-NMR NMR experiments were performed on Bruker spectrometers operating at 300, 400, 500 or 600 MHz for ¹H and 75, 100, 125, or 150 MHz for ¹³C experiments. Chemical shifts (δ) are reported in ppm relative to the residual solvent signal (CDCl₃ δ = 7.26 for ¹H NMR and δ = 77.16 for ¹³C NMR; Data are reported as follows: chemical shift (multiplicity, coupling constants where applicable, number of hydrogens). Abbreviations are as follows: s (singlet), d (doublet), t (triplet), q (quartet), dd (doublet of doublet), dt (doublet of triplet), ddq (doublet of doublets of quartets), m (multiplet), bs (broad singlet). IR spectra were recorded on a Bruker ALPHA Platinum ATR FT-IR spectrometer. Low and high-resolution mass spectral data were obtained from the University of California, Berkeley Mass Spectral Facility, on a VG 70-Se Micromass spectrometer for FAB, and a VG Prospec Micromass spectrometer for EI.

2.8 Experimental Methods and Procedures



3-Methyltetrahydro-2H-pyran-2-ol (2.2). To a solution of diisopropylamine (3.5 mL, 25 mmol, 1.3 equiv) in THF (40 mL) was added *n*-BuLi dropwise (10 mL of a 2.5 M solution in hexanes, 25 mmol, 1.25 equiv). The solution was warmed to 0 °C for 20 minutes then cooled back down to -78 °C. δ -valerolactone **2.9** (1.83 mL, 20 mmol, 1.0 equiv) was added as a solution in THF (10 mL) dropwise via syringe. The solution was allowed to stir at -78 °C for 1 hour and at that time methyl iodide (5.0 mL, 80 mmol, 4.0 equiv) was added dropwise via syringe. The solution was allowed to stir at -78 °C for 18 hours and then quenched with saturated aqueous ammonium chloride (50 mL). The layers were separated and the aqueous layers were extracted with diethyl ether (2 x 60 mL). The combined organic layers were washed with water (50 mL) and brine (50 mL), dried over sodium sulfate, filtered, and concentrated *in vacuo* to yield the methylated lactone that was used immediately in the next step without further purification.

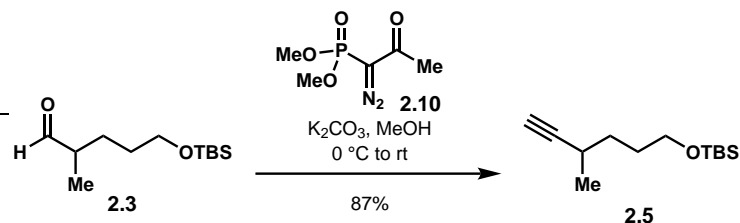
To a solution of lactone (2.05 g, 18.0 mmol, 1.0 equiv) in dichloromethane (60 mL) at -78 °C was added diisobutyl aluminum hydride (3.52 mL, 19.8 mmol, 1.1 equiv) dropwise over 7 minutes. The resulting solution was stirred at -78 °C for 30 minutes and was then quenched by the addition of ethyl acetate (8.2 mL). The solution was warmed to ambient temperature and added to a solution of sodium potassium tartrate (Rochelle's salt) (400 mL, 0.045 M). The layers were separated and the aqueous layer was extracted with dichloromethane (4 x 50 mL). The combined organic layers were dried over sodium sulfate, filtered, concentrated *in vacuo*, then purified via SiO₂ gel column chromatography eluting with 2:1 diethyl ether:hexanes. The resulting lactol (**2.35**) was isolated as a colorless oil (1.93 g, 83% yield over 2 steps). ¹H NMR (400 MHz, CDCl₃) δ 4.34 - 4.31 (m, 1H), 3.58 - 3.46 (m, 2H), 2.89 (bs, 1H), 1.87 - 1.77 (m, 1H), 1.64 - 1.43 (m, 4H), 0.98 (d, *J* = 8 Hz, 3H). All physical properties are in accordance with those reported by Grunanger and Breit.²²



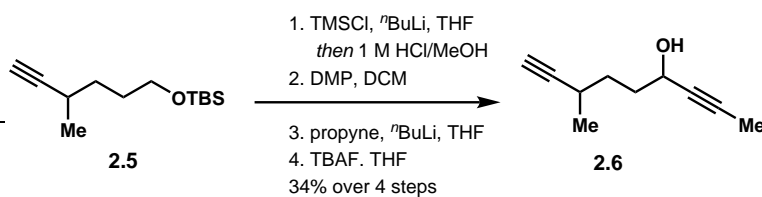
5-((Tert-butyldimethylsilyl)oxy)-2-methylpentanal (2.3). To a solution of lactol **2.2** (3.02 g, 26.0 mmol, 1.0 equiv) in dimethyl formamide (30 mL) at 0 °C was added imidazole (2.65 g, 39.0 mmol, 1.5 equiv) followed by tertbutyldimethylsilyl chloride (5.88 g, 39.0 mmol, 1.5 equiv). The solution was allowed to stir at 0 °C for 30 minutes then warmed to ambient temperature for 1 hour. The reaction mixture was diluted with ethyl acetate (30 mL), washed with water (1 x 20 mL), then brine (1 x 20 mL) and dried over sodium sulfate. The solution was filtered, concentrated *in vacuo* and purified via SiO₂ column chromatography (eluting with 5% ether in petroleum ether) to afford aldehyde **2.3** (1.42 g, 24% yield) as a colorless oil. ¹H NMR (400 MHz, CDCl₃) δ 9.60 (d, *J* = 1.9 Hz, 1H), 3.60 (t, *J* = 6.2 Hz, 2H), 2.35 (m, 1H), 1.80 - 1.67 (m, 1H), 1.61 - 1.49 (m, 2H), 1.48 -

1.36 (m, 1H), 1.08 (d, $J = 7.0$ Hz, 3H), 0.87 (s, 9H), 0.03 (s, 6H). ^{13}C NMR (100 MHz, CDCl_3) δ 205.3, 62.9, 46.2, 30.2, 27.0, 26.1, 18.4, 13.5, -5.2.

***tert*-butyldimethyl((3-methyltetrahydro-2H-pyran-2-yl)oxy)silane (2.4).** ^1H NMR (300 MHz, CDCl_3) δ 4.25 (d, $J = 7.1$ Hz, 1H), 3.95 (dddd, $J = 11.5, 4.6, 3.2, 1.9$ Hz, 1H), 3.40 (ddd, $J = 11.5, 10.3, 3.3$ Hz, 1H), 1.80 (dq, $J = 13.2, 3.9, 1.8$ Hz, 1H), 1.61 - 1.40 (m, 2H), 1.31 - 1.04 (m, 2H), 0.94 - 0.83 (m, 12H), 0.09 (d, $J = 6.0$ Hz, 6H).



***Tert*-butyldimethyl((4-methylhex-5-yn-1-yl)oxy)silane (2.5).** To a solution of aldehyde **2.5** (1.42 g, 6.17 mmol, 1.0 equiv) in methanol (30 mL) at 0°C was added potassium carbonate (2.55 g, 18.5 mmol, 3.0 equiv). To this mixture was added the Ohira-Bestmann reagent (**2.10**, 2.13 mL, 14.2 mmol, 2.3 equiv) and the reaction was allowed to warm to ambient temperature and stir for 20 hours. The reaction mixture was diluted with diethyl ether (30 mL) and quenched with 5% aqueous sodium bicarbonate (20 mL). The layers were separated and the aqueous layer was extracted with diethyl ether (2 x 30 mL). The combined organic layers were washed with brine, dried over sodium sulfate, filtered, concentrated *in vacuo* and purified via SiO_2 column chromatography (eluting with 4:1 hexanes:ethyl acetate) to provide terminal alkyne **2.5** (1.22 g, 87% yield) as a light yellow oil. ^1H NMR (400 MHz, CDCl_3) δ 3.63 (t, $J = 6.4$ Hz, 2H), 2.51 - 2.39 (m, 1H), 2.03 (d, $J = 2.4$ Hz, 1H), 1.78 - 1.40 (m, 4H), 1.19 (d, $J = 6.9$ Hz, 3H), 0.89 (s, 9H), 0.05 (s, 6H). ^{13}C NMR (100 MHz, CDCl_3) δ 68.4, 63.1, 33.2, 31.8, 30.6, 26.1, 25.6, 21.2, -5.1.

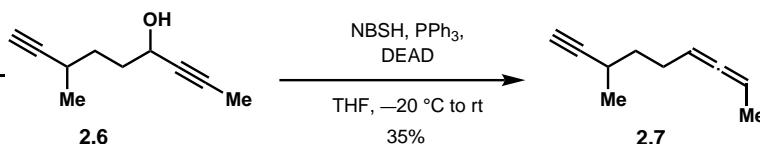


Bis-alkyne (2.6): To a solution of terminal alkyne **2.5** (344 mg, 3.07 mmol, 1.0 equiv) in THF (10 mL) at -78°C was added *n*-BuLi (3.68 mL of a 2.5 M solution in hexanes, 3.0 equiv) dropwise via syringe. The reaction mixture was allowed to stir for 30 minutes at -78°C at which time trimethylsilyl chloride (1.36 mL, 10.8 mmol, 3.5 equiv) was added dropwise by syringe. The solution was allowed to stir at -78°C for 15 minutes then at ambient temperature for 1 hour. The reaction mixture was quenched with H_2O (10 mL) and HCl (10 mL of a 1 M solution in MeOH, 0.33 M) was added dropwise via pipette. The solution was allowed to stir at ambient temperature for 20 hours upon which it was quenched with saturated aqueous sodium bicarbonate (10 mL). The layers were separated and the aqueous layer was extracted with diethyl ether (3 x 30 mL). The combined organic layers were washed with brine, dried over sodium sulfate, and concentrated *in vacuo* and used immediately in the next reaction. To a solution of alcohol (3.53 g, 19.0 mmol, 1.0 equiv) in dichloromethane (100 mL) at ambient temperature was added Dess-Martin periodinane

(13.1 g, 31.0 mmol, 1.63 equiv) portionwise over 30 minutes. The reaction mixture was allowed to stir for 1.5 hours at which time it was quenched with saturated aqueous sodium bicarbonate (50 mL) and saturated aqueous sodium thiosulfate (50 mL). The layers were separated and the aqueous layer was extracted with diethyl ether (3 x 50 mL). The combined organic layers were dried over sodium sulfate, filtered, concentrated *in vacuo* and used in the next step without purification.

Propyne (0.27 mL, 4.8 mmol, 6.0 equiv) was condensed into a flask at $-78\text{ }^{\circ}\text{C}$ and diluted with THF (1.2 mL). To the reaction mixture was added *n*-BuLi (0.96 mL of a 2.5 M solution in hexanes, 2.4 mmol, 3.0 equiv) dropwise via syringe. The reaction mixture was allowed to stir at $-78\text{ }^{\circ}\text{C}$ for 2 hours and at that time aldehyde (146 mg, 0.80 mmol, 1.0 equiv) was added dropwise via syringe as a solution in THF (2 mL). The dry ice bath was filled with dry ice, insulated, and allowed to slowly warm to ambient temperature over 20 hours upon which the reaction mixture was quenched with a saturated solution of aqueous ammonium chloride (5 mL) and extracted with diethyl ether (3 x 5 mL). The combined organic layers were washed with brine (5 mL), dried over sodium sulfate, filtered, concentrated *in vacuo* and used in the next step without purification.

To a solution of propargylic alcohol (104 mg, 0.470 mmol, 1.0 equiv) in THF (2.5 mL) at $0\text{ }^{\circ}\text{C}$ was added tetrabutylammonium fluoride (1 mL of a 1.0 M solution in THF, 2.0 equiv). The solution was allowed to stir at $0\text{ }^{\circ}\text{C}$ for 30 minutes and then at ambient temperature for 2 hours upon which TLC indicated complete consumption of starting material. The reaction mixture was quenched with a saturated solution of aqueous ammonium chloride (3 mL) and extracted with pentane (3 x 3 mL). The combined organic layers were dried over sodium sulfate, filtered, concentrated *in vacuo* and purified by SiO₂ column chromatography (eluting with 6:1 hexanes:ethyl acetate) affording terminal alkyne **2.6** (55 mg, 34% yield over 4 steps) as a colorless oil. ¹H NMR (500 MHz, CDCl₃) δ 4.38 - 4.32 (m, 1H), 2.53 - 2.39 (m, 1H), 2.04 (dd, *J* = 2.4, 1.3 Hz, 1H), 2.00 - 1.93 (bs, 1H), 1.89 - 1.84 (m, 1H), 1.83 (d, *J* = 2.2 Hz, 3H), 1.80 - 1.70 (m, 1H), 1.65 - 1.51 (m, 2H), 1.19 (dd, *J* = 7.1, 1.0 Hz, 3H). ¹³C NMR (126 MHz, CDCl₃) δ 88.6, 88.6, 81.2, 81.2, 80.2, 80.2, 68.7, 68.7, 62.5, 62.3, 35.8, 35.7, 32.2, 32.1, 25.5, 25.4, 21.0, 21.0, 3.6, 3.6. All data (MS, IR) is fully consistent with those reported by Schultz and Sarpong.⁹



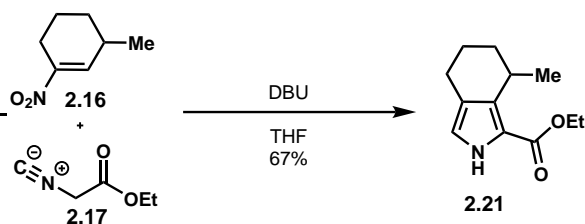
3-Methylnona-6,7-dien-1-yne (2.7). To a solution of triphenylphosphine (144 mg, 0.55 mmol, 1.5 equiv) in THF (0.50 mL) at $-20\text{ }^{\circ}\text{C}$ was added diethyl azodicarboxylate (86 μL , 0.55 mmol, 1.5 equiv) dropwise over 1 minute. The reaction mixture was allowed to stir at $-20\text{ }^{\circ}\text{C}$ for 10 minutes and then charged with propargylic alcohol **2.6** (55 mg, 0.37 mmol, 1.0 equiv) as a solution in THF (0.75 mL). After 30 minutes at $-20\text{ }^{\circ}\text{C}$, 2-nitrobenzylsulfonylhydrazine (NBSH) (119 mg, 0.55 mmol, 1.5 equiv) as a solution in THF (0.50 mL) was added dropwise by syringe. The reaction mixture was held at $-20\text{ }^{\circ}\text{C}$ for an additional 2 hours, then allowed to warm to ambient temperature. After stirring for 10 hours at ambient temperature, the reaction mixture was diluted with pentane (5 mL) and washed 10 times with cold deionized water. The organic layer was dried over sodium sulfate, filtered, mixed with SiO₂, concentrated *in vacuo* using an iced water bath, and immediately purified by SiO₂ column chromatography eluting with pentanes. **2.7** (17 mg, 35% yield) was isolated as a colorless oil. ¹H NMR (600 MHz, CDCl₃) δ 5.11 - 5.00 (m, 2H), 2.53 -

2.46 (m, 2H), 2.22 - 2.12 (m, 2H), 2.12 - 2.05 (m, 1H), 2.05- 2.03 (m, 1H), 1.64 (dt, $J = 6.6$, 3.3 Hz, 3H), 1.61 - 1.48 (m, 2H), 1.19 (d, $J = 6.9$ Hz, 3H). ^{13}C NMR (150 MHz, CDCl_3) δ 204.7, 204.7, 89.6, 89.6, 88.8, 88.8, 85.9, 85.8, 68.3, 35.9, 35.9, 26.5, 26.4, 25.0, 25.0, 20.8, 20.8, 14.5. All physical properties are in accordance with those reported by Schultz and Sarpong.⁹



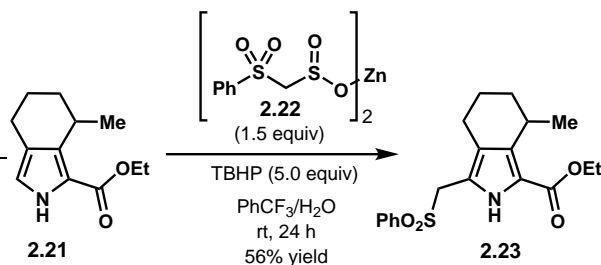
1,4-Dimethyl-2-tosyl-4,5,6,7-tetrahydro-2H-isoindole (2.1). A flask filled with copper(II) thiophene carboxylate (13 mg, 6.8 μmol , 5.0 mol%) was evacuated and backfilled with N_2 (3 x) and then allene **2.36** (181 mg, 1.4 mmol, 1.0 equiv) in chloroform (6.8 mL, 0.2 M) was added, followed by p-toluensulfonyl azide (0.22 mL, 1.4 mmol, 1.0 equiv). The reaction mixture was allowed to stir at ambient temperature for 20 hours and then it was quenched with a saturated aqueous solution of ammonium chloride (10 mL), and extracted with dichloromethane (3 x 10 mL). The combined organic layers were washed with brine (30 mL), dried over sodium sulfate, filtered, concentrated *in vacuo*, and used immediately in the next step.

To a flame-dried microwave vial charged with triazole (260 mg, 0.77 mmol, 1.0 equiv) and chloroform (4.0 mL) was added dirhodium tetraoctanoate (3.0 mg, 3.9 μmol , 0.50 mol%). The resulting mixture was heated to 140 $^\circ\text{C}$ under microwave irradiation and held at this temperature for 15 minutes. After cooling the reaction mixture, SiO_2 was added and the solvent was removed *in vacuo*. The resulting residue was purified by column chromatography (eluting with 6:1 hexanes:ethyl acetate) to afford pyrrole **2.1** (35 mg, 15% yield) as a light yellow oil. ^1H NMR (500 MHz, CDCl_3) δ 7.66 (d, $J = 8.3$ Hz, 2H), 7.28 (d, $J = 8.2$ Hz, 2H), 7.01 (d, $J = 1.6$ Hz, 1H), 2.63 - 2.54 (m, 1H), 2.40 (s, 3H), 2.39 - 2.36 (m, 1H), 2.26 - 2.18 (m, 2H), 2.15 (s, 3H), 1.90 - 1.77 (m, 2H), 1.54 - 1.46 (m, 1H), 1.18 (d, $J = 6.7$ Hz, 3H). ^{13}C NMR (150 MHz, CDCl_3) δ 144.2, 136.9, 129.8, 129.8, 126.8, 124.3, 122.5, 115.9, 32.5, 28.5, 22.7, 21.6, 21.5, 21.3, 11.0. All physical properties are in accordance with those reported by Schultz and Sarpong.⁹

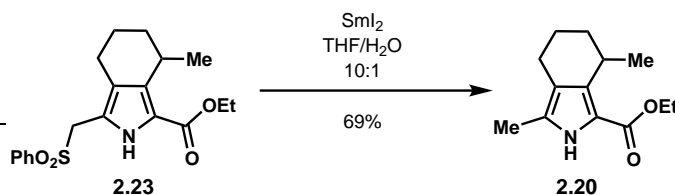


Ethyl 7-methyl-4,5,6,7-tetrahydro-2H-isoindole-1-carboxylate (2.21): To a solution of 3-methyl-1-nitrocyclohex-1-ene (**2.16**) (0.35 mmol, 50 mg, 1.0 equiv) in THF (0.8 M) was added ethyl isocyanoacetate (**2.17**) (0.35 mmol, 38 μL , 1.0 equiv) followed by DBU (0.35 mmol, 51 μL , 1.0 equiv). The reaction mixture was allowed to stir for 16 h at room temperature at which time it was partitioned with dichloromethane followed by brine. The organic layer was dried over sodium sulfate, filtered, and concentrated *in vacuo*. The crude oil was purified using SiO_2 column chromatography eluting with dichloromethane to afford pyrrole **2.21** as a white solid (49 mg, 67%): IR (neat) 3302, 2980, 2934, 2849, 1660 cm^{-1} ; ^1H NMR (400 MHz, CDCl_3) δ 8.94 (bs, 1H), 6.62

(d, $J = 2.8$ Hz, 1H), 4.37 - 4.28 (m, 2H), 3.30-3.26 (m, 1H), 2.62 - 2.58 (m, 1H), 2.46 - 2.41 (m, 1H), 1.81 - 1.63 (m, 4H), 1.35 (t, $J = 7.1$ Hz, 3H), 1.26 (d, $J = 6.9$ Hz, 3H). ^{13}C NMR (101 MHz, CDCl_3) δ 161.4, 133.7, 121.5, 118.6, 117.7, 59.9, 30.9, 26.8, 22.1, 21.9, 18.7, 14.6. HRMS (ESI): Exact mass calc'd for $\text{C}_{12}\text{H}_{18}\text{O}_2\text{N}_1$ [$\text{M}+\text{H}$] $^+$, 208.1332. Found 208.1330. MP: 53-57 °C.

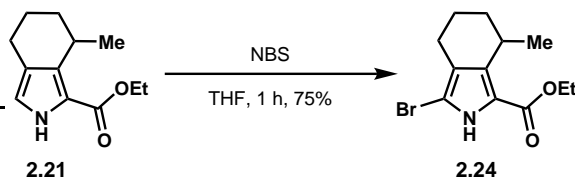


Ethyl 7-methyl-3-((phenylsulfonyl)methyl)-4,5,6,7-tetrahydro-2H-isoindole-1-carboxylate (2.23): To a solution of pyrrole **2.21** (0.048 mmol, 10.0 mg, 1.0 equiv) and zinc bis[(phenylsulfonyl)methanesulfinate] (PSMS) $_2$ (**2.22**) (0.072 mmol, 36 mg, 1.5 equiv) in a mixture of trifluorotoluene and water (2.5:1, 0.14 M) was added *tert*-butyl hydroperoxide (70% wt% in water) (0.24 mmol, 31 μL , 5.0 equiv) at 0 °C. After stirring for 5 min at 0 °C, the solution was warmed to room temperature and allowed to stir for 24 h. The reaction mixture was quenched with 5% sodium bicarbonate (sat. aq.) and 5% EDTA - 2Na solution, and the aqueous layer was extracted with dichloromethane (3 x 10 mL). The combined organic layers were washed with brine (30 mL) and dried over sodium sulfate. The solution was filtered, and concentrated *in vacuo*. The crude reaction mixture was purified using SiO_2 column chromatography eluting with 2:1 hexanes:ethyl acetate to afford pyrrole **2.23** as a light pink gum (9.5 mg, 56%): IR (neat) 3292, 2928, 1664, 1449 cm^{-1} ; ^1H NMR (400 MHz, CDCl_3) δ 9.75 (bs, 1H), 7.64 - 7.50 (m, 3H), 7.39 (t, $J = 7.7$ Hz, 2H), 4.58 - 4.11 (m, 4H), 3.31 - 2.94 (m, 1H), 1.78 (dt, $J = 15.5, 4.0$ Hz, 1H), 1.63 - 1.55 (m, 1H), 1.51 - 1.37 (m, 4H), 1.31 (t, $J = 7.1$ Hz, 3H), 1.12 (d, $J = 6.9$ Hz, 3H). ^{13}C NMR (101 MHz, CDCl_3) δ 161.1, 137.7, 133.8, 133.5, 128.8, 128.4, 122.5, 118.8, 118.0, 60.0, 54.0, 30.3, 26.4, 21.5, 20.4, 17.9, 14.3. HRMS (ESI): Exact mass calc'd for $\text{C}_{19}\text{H}_{23}\text{O}_4\text{NNaS}$ [$\text{M}+\text{Na}$] $^+$, 384.1240. Found 384.1242.

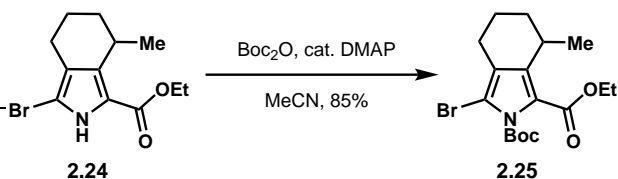


Ethyl 3,7-dimethyl-4,5,6,7-tetrahydro-2H-isoindole-1-carboxylate (2.20): A solution of methylene sulfone **2.23** (0.21 mmol, 75 mg, 1.0 equiv) in a mixture of THF and water (10:1) (4.1 mL, 0.05 M) was degassed using 3 cycles of freeze/pump/thaw. A solution of freshly prepared SmI_2 (0.1 M in THF) (1.2 mmol, 12 mL, 6.0 equiv) was added to the reaction mixture by syringe and the resulting dark purple solution was stirred at room temperature for 30 min, (it turns yellow after approximately 2 min). The reaction mixture was quenched with sodium bicarbonate (sat. aq.) solution and extracted with ethyl acetate (3 x 20 mL). The combined organic layers were washed with brine (60 mL) and dried over sodium sulfate. The suspension was filtered and concentrated *in vacuo* to afford pyrrole **2.20** as a white solid (31.7 mg, 69%): IR (neat) 3303, 2982, 2926, 2852,

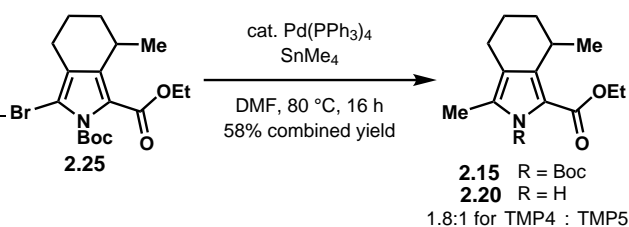
1660 cm^{-1} ; $^1\text{H NMR}$ (600 MHz, CDCl_3) δ 9.58 - 8.76 (m, 1H), 4.45 - 4.14 (m, 2H), 3.26 (dt, J = 7.2, 3.7 Hz, 1H), 2.48 (dt, J = 15.3, 3.2 Hz, 1H), 2.36 - 2.24 (m, 1H), 2.17 (s, 3H), 1.85 - 1.59 (m, 5H), 1.36 (t, J = 7.1 Hz, 3H), 1.25 (d, J = 6.9 Hz, 3H). $^{13}\text{C NMR}$ (151 MHz, CDCl_3) δ 161.4, 134.5, 128.6, 118.1, 115.3, 59.5, 30.7, 26.8, 21.7, 21.3, 18.4, 14.5, 11.1. **HRMS** (ESI): Exact mass calc'd for $\text{C}_{13}\text{H}_{20}\text{O}_2\text{N}$ $[\text{M}+\text{H}]^+$, 222.1486. Found 222.1489. MP 80-84 $^\circ\text{C}$.



Ethyl 3-bromo-7-methyl-4,5,6,7-tetrahydro-2H-indole-1-carboxylate (2.24): A flame-dried flask immersed in a room temperature water bath was charged with pyrrole **2.21** (1.6 mmol, 0.30 g, 1.0 equiv) and THF (11 mL, 0.2 M). To the solution was added NBS (1.6 mmol, 0.28 g, 1.1 equiv) portionwise over approximately 10 min. The reaction mixture was allowed to stir for 1 h at which time it was diluted with dichloromethane (10 mL) and washed with water (3 x 10 mL) followed by brine (1 x 30 mL). The organic layer was dried over sodium sulfate, filtered, concentrated, and purified by SiO_2 column chromatography eluting with 4:1 hexanes:ethyl acetate to afford brominated pyrrole **2.24** as a light yellow gum (0.33 g, 75%): **IR** (neat) 3247, 2980, 2940, 2862, 1658 cm^{-1} ; $^1\text{H NMR}$ (600 MHz, CDCl_3) δ 9.10 (s, 1H), 4.40 - 4.21 (m, 2H), 3.32 - 3.14 (m, 1H), 2.46 (dt, J = 16.2, 3.8 Hz, 1H), 2.27 (dt, J = 16.0, 8.6 Hz, 1H), 1.88 - 1.58 (m, 4H), 1.36 (t, J = 7.1, 3H), 1.28 - 1.16 (m, 3H). $^{13}\text{C NMR}$ (151 MHz, CDCl_3) δ 160.6, 135.1, 121.4, 118.8, 102.2, 60.3, 30.6, 27.0, 21.9, 21.6, 18.1, 14.6. **HRMS** (ESI): Exact mass calc'd for $\text{C}_{13}\text{H}_{20}\text{O}_2\text{NBr}$ $[\text{M}+\text{OH}]$, 302.0386. Found 302.0383.

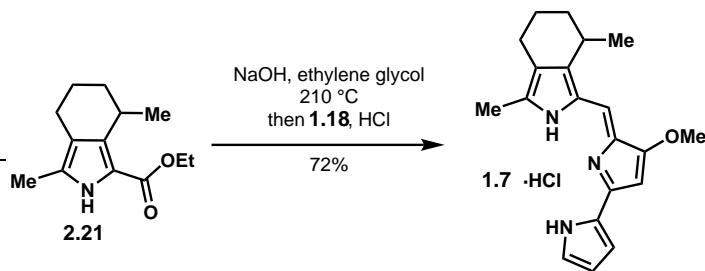


2-(Tert-butyl) 1-ethyl 3-bromo-7-methyl-4,5,6,7-tetrahydro-2H-indole-1,2-dicarboxylate (2.25): A flame-dried flask was charged with brominated pyrrole **2.24** (1.2 mmol, 0.35 g, 1.0 equiv) followed by MeCN (0.15 M, 8.2 mL). To the suspension was added 4-dimethylaminopyridine (0.19 mmol, 23 mg, 0.15 equiv) followed by di-tert-butyl-dicarbonate (1.2 mmol, 0.28 mL, 1.0 equiv) and the suspension was allowed to stir for 12 h at room temperature. The reaction mixture was diluted with dichloromethane (10 mL), washed with sodium hydrogensulfate (sat. aq.) (2 x 20 mL), then sodium bicarbonate (sat. aq.) (2 x 20 mL) and finally water (1 x 20 mL). The organic layer was dried over sodium sulfate, filtered, and concentrated. The crude mixture was purified using SiO_2 column chromatography eluting with 4:1 hexanes:ethyl acetate to yield a colorless viscous oil (404 mg, 85%): **IR** (neat) 2982, 2939, 1812, 1796, 1701 cm^{-1} ; $^1\text{H NMR}$ (600 MHz, CDCl_3) δ 4.45 - 4.10 (m, 2H), 3.22 - 3.18 (m, 1H), 2.44 - 2.40 (m, 1H), 2.23 - 2.18 (m, 1H), 1.77 - 1.59 (m, 4H), 1.57 (s, 9H), 1.31 (t, J = 7.1, 3H), 1.16 (d, J = 7.1, 3H). $^{13}\text{C NMR}$ (151 MHz, CDCl_3) δ 160.0, 148.6, 136.5, 122.1, 120.8, 104.3, 85.4, 60.4, 30.3, 27.5, 26.7, 22.0, 21.4, 17.6, 14.3. **HRMS** (ESI): Exact mass calc'd for $\text{C}_{17}\text{H}_{25}\text{O}_4\text{NBr}$ $[\text{M}+\text{H}]^+$, 386.0961. Found 386.0959.



2-(*Tert*-butyl) 1-ethyl 3,7-dimethyl-4,5,6,7-tetrahydro-2H-isoindole-1,2-dicarboxylate (2.20):

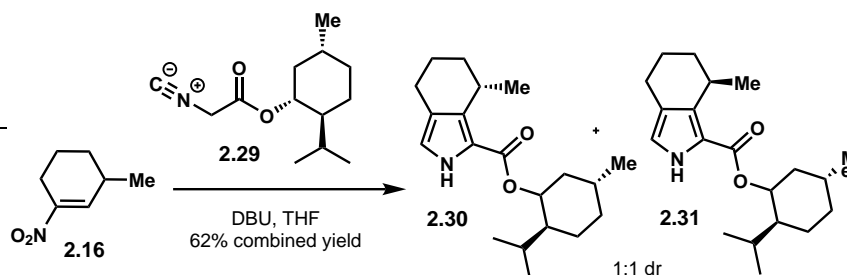
A flame-dried Schlenk flask was charged with Boc-protected pyrrole **2.25** (0.26 mmol, 100 mg, 1.0 equiv). The flask was then brought into the glovebox where it was charged with Pd(PPh₃)₄ (0.026 mmol, 30 mg, 0.1 equiv) and anhydrous lithium chloride (1.3 mmol, 55 mg, 5.0 equiv). The flask was brought out of the glovebox and degassed dimethylformamide was added by cannula (1.0 mL), followed by tetramethyltin (1.3 mmol, 0.18 mL, 5.0 equiv). The Schlenk flask was sealed and heated to 80 °C and held at this temperature for 16 h. The reaction mixture was allowed to cool to room temperature and diluted with ethyl acetate (10 mL). The organic layer was washed with water (1 x 10 mL) followed by brine (1 x 10 mL). The organic layer was dried over sodium sulfate, filtered, and concentrated *in vacuo*. The crude reaction mixture was purified by SiO₂ chromatography eluting with 9:1 hexanes:ethyl acetate to yield the deprotected methylated pyrrole **2.20** as a white solid (0.053 mmol, 7.2 mg) (*analytical data matched that for 2.20, reported above*) and the Boc-protected methylated pyrrole **2.15** as a colorless oil (0.10 mmol, 17 mg, 58% overall): **IR** (neat) 2981, 2936, 1803, 1758, 1703 cm⁻¹; **¹H NMR** (600 MHz, CDCl₃) δ 4.29 (q, *J* = 7.3 Hz, 2H), 3.20 - 3.17 (m, 1H), 2.53 - 2.42 (m, 1H), 2.28 - 2.24 (m, 1H), 2.22 (s, 3H), 1.79 - 1.58 (m, 4H), 1.56 (s, 9H), 1.34 (t, *J* = 6.9 Hz, 2H), 1.19 (d, *J* = 7.0 Hz, 3H). **¹³C NMR** (151 MHz, CDCl₃) δ 161.5, 150.2, 137.0, 130.9, 128.9, 128.7, 128.6, 128.6, 119.0, 118.9, 84.1, 60.3, 30.7, 27.9, 27.8, 26.7, 21.8, 21.4, 18.4, 14.5, 11.6. **HRMS** (ESI): Exact mass calc'd for C₁₈H₂₈O₄N [M+H]⁺, 322.2013. Found 322.2014. *N*-Boc pyrrole **2.15** was isolated along with a co-eluting impurity believed to be triphenylphosphine oxide.



(*R/S*)-cycloprodigosin hydrochloride (1.7·HCl): A suspension of pyrrole **2.20** (0.034 mmol, 7.5 mg, 1.0 equiv) and sodium hydroxide (0.31 mmol, 12 mg, 9.0 equiv) in ethylene glycol (1.0 mL) was degassed using three cycles of freeze/pump/thaw. The Schlenk flask was sealed and placed in a sand bath where it was heated to 210 °C and held at this temperature for 2 h. The resulting suspension was diluted with hexanes and the organic layer was washed with water (5 x 10 mL), followed by brine (1 x 10 mL). The organic layer was dried over sodium sulfate, filtered, concentrated *in vacuo* and submitted immediately to the next step.

To the isolated crude product was added anhydrous methanol (1.0 mL) followed by **1.18** and anhydrous HCl (0.02 mmol, 34 μL from a freshly prepared 1.0 M solution of acetyl chloride in

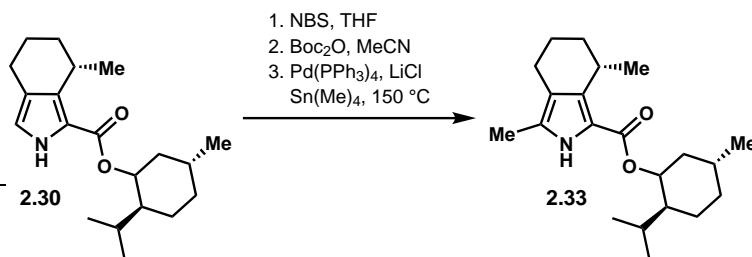
anhydrous methanol, 1.0 equiv). The mixture turned a vibrant red to purple over a period of 1 h at which time the solvent was removed and the mixture was immediately purified by SiO₂ column chromatography, eluting with 1% methanol in chloroform followed by a second column eluting with 2% methanol in chloroform to yield the HCl salt of the natural product as a purple-black microcrystalline solid (7.9 mg, 72%). **IR** (neat) 3357, 3151, 3099, 2919, 2850, 1599 cm⁻¹; **¹H NMR** (600 MHz, CDCl₃) δ 12.59 (bs, 2H), 12.47 (bs, 1H), 7.18 (s, 1H), 7.00 (s, 1H), 6.86 (s, 1H), 6.33 (s, 1H), 6.08 (s, 1H), 4.00 (s, 3H), 3.12 (s, 1H), 2.67 - 2.04 (m, 5H), 1.95 - 1.66 (m, 4H), 1.28 (d, *J* = 7.2 Hz, 3H). **¹³C NMR** (151 MHz, CDCl₃) δ 165.0, 147.2, 146.4, 145.8, 126.2, 123.9, 123.1, 122.7, 119.2, 115.9, 113.1, 111.5, 92.7, 58.7, 30.6, 26.3, 24.0, 21.0, 18.5, 12.4. **HRMS** (ESI): Exact mass calc'd for C₂₀H₂₄ON₃ [M+H]⁺, 322.1914. Found 322.1912. MP >220 °C (decomposes at >220 °C). The pure product was subject to chiral HPLC analysis: Chiralpak IA column, flow rate of 1.0 mL/min, 50% isopropanol in hexanes, 0.1% diethylamine, 500 nm. Retention times: 5.43 min (*R*)/10.02 min (*S*), 49:51 er. *N-H* peaks for cycloprodigosin are only visible in the ¹H NMR for the HCl salt.



(*S*)-2-((1*S*,2*R*,4*R*)-4-methyl-2-(((*S*)-7-methyl-4,5,6,7-tetrahydro-2H-indole-1-carbonyl)oxy)cyclohexyl)propan-1-yl (2.30): To a solution of 3-methyl-1-nitrocyclohex-1-ene (**2.16**) (2.2 mmol, 0.32 g, 1.0 equiv) was added menthyl isocyanoacetate (0.91 mmol, 0.20 g, 1.0 equiv) followed by DBU (2.24 mmol, 0.5 g, 1.0 equiv) and the reaction mixture was allowed to stir for 16 h at room temperature. The resulting mixture was partitioned with dichloromethane followed by brine. The organic layer was dried over sodium sulfate, filtered, and concentrated *in vacuo*. The crude mixture was purified by SiO₂ column chromatography eluting with dichloromethane to yield a colorless, viscous oil (0.44 g, 62%). The diastereomeric mixture was separated by multiple fractionations using a Yamazen® automated column eluting with a gradient of 3% ethyl acetate in hexanes over a period of 50 min. Diastereomer **2.30** is lower in polarity: **IR** (neat) 3311, 2954, 2927, 2866, 1661 cm⁻¹; **¹H NMR** (500 MHz, CDCl₃) δ 8.94 (bs, 1H), 6.62 (s, 1H), 4.95 (td, *J* = 10.8, 4.4 Hz, 1H), 3.29 (m, 1H), 2.63 - 2.59 (m, 1H), 2.51 - 2.35 (m, 1H), 2.07 - 2.05 (m, 1H), 2.00 - 1.95 (m, 1H), 1.86 - 1.61 (m, 6H), 1.61 - 1.40 (m, 2H), 1.26 (d, *J* = 6.9 Hz, 3H), 1.18 - 1.01 (m, 2H), 0.90 (dd, *J* = 11.4, 6.7 Hz, 7H), 0.80 (d, *J* = 6.9 Hz, 3H). **¹³C NMR** (126 MHz, CDCl₃) δ 160.9, 133.5, 121.5, 118.4, 117.9, 73.3, 47.5, 41.7, 34.4, 31.6, 30.9, 26.8, 26.2, 23.2, 22.2, 22.1, 21.9, 21.1, 18.6, 16.2. **HRMS** (ESI): Exact mass calc'd for C₂₀H₃₁O₂NNa [M+Na]⁺, 340.2247. Found 340.2247. [α]_D = -7.6 (*c* = 1.19 g/100 mL, CH₂Cl₂). Isolated with 86% purity.

(1*R*,2*S*,5*R*)-2-isopropyl-5-methylcyclohexyl (*R*)-7-methyl-4,5,6,7-tetrahydro-2H-indole-1-carboxylate (2.31): Diastereomer **2.31** is higher in polarity: **IR** (neat) 3312, 2955, 2927, 2866, 1664 cm⁻¹; **¹H NMR** (500 MHz, CDCl₃) δ 9.06 (bs, 1H), 6.63 (d, *J* = 2.8 Hz, 1H), 4.90 (td, *J* = 10.9, 4.4 Hz, 1H), 3.36 - 3.15 (m, 1H), 2.64 - 2.59 (m, 1H), 2.48 - 2.41 (m, 1H), 2.14 - 2.10 (m, 1H), 2.02 - 1.96 (m, 1H), 1.84 - 1.63 (m, 6H), 1.61 - 1.42 (m, 2H), 1.27 (d, *J* = 6.9 Hz, 3H), 1.17 - 1.02

(m, 2H), 0.92 (t, $J = 7.0$ Hz, 7H), 0.79 (d, $J = 6.9$ Hz, 3H). ^{13}C NMR (126 MHz, CDCl_3) δ 161.5, 133.5, 121.8, 118.8, 118.4, 77.8, 77.5, 77.3, 74.0, 48.0, 41.6, 34.8, 31.9, 31.3, 27.2, 26.7, 23.9, 22.5, 22.5, 22.4, 21.4, 19.1, 16.8. HRMS(ESI): Exact mass calc'd for $\text{C}_{20}\text{H}_{31}\text{O}_2\text{NNa}$ [$\text{M}+\text{Na}$] $^+$, 340.2247. Found 340.2247. $[\alpha]_{\text{D}} = -32.1$ ($c = 0.24$ g/100 mL, CH_2Cl_2).

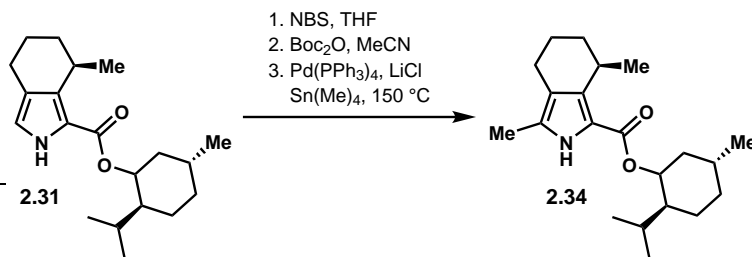


(1*R*,2*S*,5*R*)-2-isopropyl-5-methylcyclohexyl (S)-3,7-dimethyl-4,5,6,7-tetrahydro-2H-isindole-1-carboxylate (2.33): A flame-dried flask immersed in a room temperature water bath was charged with pyrrole menthyl ester **2.30** (0.13 mmol, 42 mg, 1.0 equiv) and tetrahydrofuran (0.8 mL, 0.2 M). To the solution was added NBS (0.14 mmol, 25 mg, 1.1 equiv) portionwise over a period of 5 min. The reaction mixture was allowed to stir for 1 h at which time it was diluted with dichloromethane and washed with water (3 x 10 mL) followed by brine (1 x 30 mL). The organic layer was dried over sodium sulfate, filtered, concentrated, and purified using SiO_2 column chromatography eluting with 9:1 hexanes:ethyl acetate to yield a colorless oil that was taken on immediately to the next step.

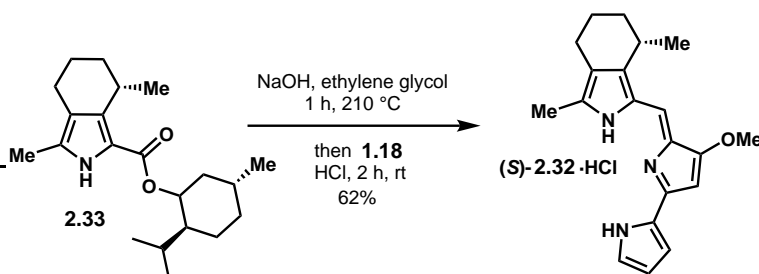
A flame-dried flask was charged with the brominated menthyl ester pyrrole (0.13 mmol, 1.0 equiv) followed by MeCN (0.15 M, 0.87 mL). To the suspension was added DMAP (0.017 mmol, 2.1 mg, 0.15 equiv) followed by di-*tert*-butyl-dicarbonate (0.13 mmol, 30 μL , 1.0 equiv) and the suspension was allowed to stir for 12 h at room temperature. The reaction mixture was diluted with dichloromethane (10 mL), washed with sodium hydrogensulfate (2 x 10 mL), then NaHCO_3 (sat. aq.) (2 x 10 mL) and finally water (1 x 10 mL). The organic layer was dried over sodium sulfate, filtered, and concentrated *in vacuo* and taken on immediately to the next step.

A flame-dried Schlenk flask was charged with Boc-protected pyrrole from the previous step (23 mg, 0.046 mmol, 1.0 equiv) and the flask was then brought into the glovebox where it was charged with $\text{Pd}(\text{PPh}_3)_4$ (0.005 mmol, 5 mg, 0.01 equiv) and anhydrous lithium chloride (0.23 mmol, 9.7 mg, 5.0 equiv). The sealed flask was brought out of the glovebox and degassed dimethylformamide was added using a cannula (1.0 mL). To the flask was then added tetramethyltin (0.23 mmol, 0.032 mL, 5.0 equiv) and the Schlenk flask was sealed and heated to 150 $^\circ\text{C}$ and held at this temperature for 12 h. The reaction mixture was allowed to cool to room temperature and diluted with ethyl acetate (10 mL). The organic layer was washed with water (10 x 10 mL) followed by brine (1 x 10 mL). The organic layer was dried over sodium sulfate, filtered, and concentrated *in vacuo*. The crude reaction mixture was purified by SiO_2 column chromatography eluting with 9:1 hexanes:ethyl acetate to afford methylated pyrrole **2.33** as a colorless oil (9.6 mg, 22% over 3 steps): IR (neat) 3300, 2954, 2924, 2866, 1654 cm^{-1} ; ^1H NMR (400 MHz, CDCl_3) δ 8.63 (s, 1H), 4.93 (td, $J = 10.9, 4.5$ Hz, 1H), 3.24 (td, $J = 7.2, 4.9$ Hz, 1H), 2.48 (dt, $J = 15.7, 3.8$ Hz, 1H), 2.33 - 2.25 (m, 1H), 2.16 (s, 3H), 2.07 - 1.94 (m, 2H), 1.84 - 1.59 (m, 6H), 1.58 - 1.40 (m, 1H), 1.25 (d, $J = 7.0$ Hz, 3H), 1.18 - 0.99 (m, 2H), 0.90 (dd, $J = 8.4, 6.8$ Hz, 6H), 0.79 (d, $J = 6.9$ Hz, 3H). ^{13}C NMR (101 MHz, CDCl_3) δ 160.8, 134.5, 128.1, 118.3, 115.6, 73.0, 47.5, 41.7, 34.5, 31.6,

30.7, 26.8, 26.1, 23.3, 22.2, 21.8, 21.4, 21.1, 18.5, 16.2, 11.3. **HRMS** (ESI): Exact mass calc'd for $C_{21}H_{32}O_2N$ $[M-H]^-$, 330.2428. Found 330.2427. $[\alpha]_D = -2.27$ ($c = 0.66$ g/100 mL, CH_2Cl_2).

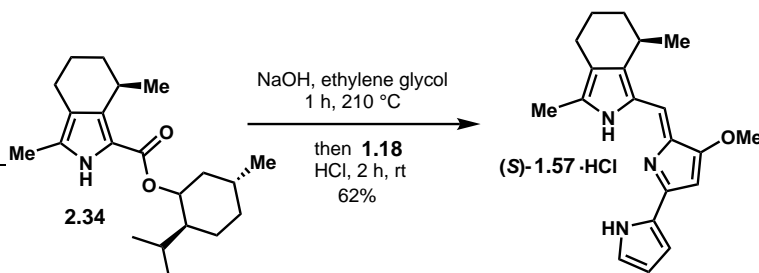


(1*R*,2*S*,5*R*)-2-isopropyl-5-methylcyclohexyl (R)-3,7-dimethyl-4,5,6,7-tetrahydro-2H-indole-1-carboxylate (2.34): Prepared through the same sequence used to prepare diastereomer **2.33**. Isolated as a clear, colorless oil (18 mg, 45% over 3 steps): **IR** (neat) 3296, 2952, 2924, 2864, 1653 cm^{-1} ; 1H NMR (600 MHz, $CDCl_3$) δ 8.72 (bs, 1H), 4.87 (td, $J = 10.9, 4.4$ Hz, 1H), 3.31 - 3.12 (m, 1H), 2.49 - 2.46 (m, 1H), 2.35 - 2.20 (m, 1H), 2.16 (s, 3H), 2.13 - 2.06 (m, 1H), 1.97 (ddq, $J = 9.8, 7.0, 3.5, 2.9$ Hz, 1H), 1.83 - 1.59 (m, 6H), 1.58 - 1.39 (m, 2H), 1.25 (d, $J = 7.1$ Hz, 3H), 1.15 - 0.98 (m, 2H), 0.91 (dd, $J = 9.1, 6.8$ Hz, 7H), 0.77 (d, $J = 6.9$ Hz, 3H). ^{13}C NMR (151 MHz, $CDCl_3$) δ 161.1, 134.2, 128.2, 118.3, 115.9, 73.4, 47.8, 41.4, 34.6, 31.6, 30.9, 27.0, 26.5, 23.7, 22.2, 21.9, 21.5, 21.1, 18.7, 16.5, 11.3. **HRMS** (ESI): Exact mass calc'd for **2.37** $[M+H]^+$, 332.2584. Found 332.2581. $[\alpha]_D = -64.09$ ($c = 0.66$ g/100 mL, CH_2Cl_2).



(S)-cycloprodigosin hydrochloride ((S)-2.32·HCl): A suspension of pyrrole **2.33** (0.015 mmol, 5.0 mg, 1.0 equiv) and sodium hydroxide (0.14 mmol, 5.4 mg, 9.0 equiv) in ethylene glycol (1.0 mL) was degassed using three cycles of freeze/pump/thaw. The Schlenk flask was sealed and placed in a sand bath where it was heated to 210 °C and held at this temperature for 2 h. The suspension was diluted with hexanes and the organic layer was washed with water (5 x 10 mL), followed by brine (1 x 10 mL). The organic layer was dried over sodium sulfate, filtered, concentrated *in vacuo* and submitted immediately to the next step. To the isolated crude product (from the previous step) in a flask immersed in a room temperature water bath was added anhydrous methanol (1.0 mL) followed by 4-methoxy-1*H*,1'*H*-[2,2'-bipyrrole]-5-carbaldehyde (**1.18**) and anhydrous HCl (0.02 mmol, 0.02 mL from a freshly prepared 1.0 M solution of acetyl chloride in anhydrous methanol, 1.0 equiv). The mixture turned a vibrant red to purple over a period of 1 h at which time the solvent was removed *in vacuo* and the mixture was immediately purified by SiO_2 column chromatography, eluting with 1% methanol in chloroform followed by a second column eluting with 2% methanol in chloroform to yield the HCl salt of the natural product as a purple-black microcrystalline solid (3.3 mg, 69%). **IR** (neat) 3357, 3151, 3099, 2919, 2850, 1599

cm⁻¹; ¹H NMR (600 MHz, CDCl₃) δ 12.59 (s, 2H), 12.47 (s, 1H), 7.18 (s, 1H), 7.00 (s, 1H), 6.86 (s, 1H), 6.33 (s, 1H), 6.08 (s, 1H), 4.00 (s, 3H), 3.12 (s, 1H), 2.67 - 2.04 (m, 5H), 1.95 - 1.66 (m, 4H), 1.28 (d, *J* = 7.2 Hz, 3H). ¹³C NMR (151 MHz, CDCl₃) δ 165.0, 147.2, 146.4, 145.8, 126.2, 123.9, 123.1, 122.7, 119.2, 115.9, 113.1, 111.5, 92.7, 58.7, 30.6, 26.3, 24.0, 21.0, 18.5, 12.4. **HRMS** (ESI): Exact mass calc'd for C₂₀H₂₄ON₃ [M+H]⁺, 322.1914. Found 322.1912. MP >220 °C (decomposes at >220 °C). Enantiopurity (95:5 er) was established by chiral HPLC analysis: Chiralpak IA column, flow rate of 1.0 mL/min, 50% isopropanol in hexanes, 0.1% diethylamine, 500 nm. Retention times: 5.31 min (*R*)/10.02 min (*S*). *We attempted to obtain optical rotations, however, at the wavelength we had access to (Na lamp, 584 nm), the transmittance was too low to obtain accurate rotations.*



The same procedures used for the synthesis of (*S*)-cycloprodigiosin were employed in the synthesis of (*R*)-cycloprodigiosin with the exception that diastereomer **2.34** was used instead of diastereomer **2.30** throughout the sequence. Enantiopurity (99:1 er) was established by chiral HPLC analysis: Chiralpak IA column, flow rate of 1.0 mL/min, 50% isopropanol in hexanes, 0.1% diethylamine, 500 nm. Retention times: 5.46 min (*R*)/9.74 min (*S*).

Growth and Isolation of Natural Cycloprodigiosin from *Pseudoalteromonas rubra*

Microbial culture conditions: *Pseudoalteromonas rubra* (Gauthier 1976, ATCC 29570) was obtained from the German Collection of Microorganisms and Cell Cultures (DSMZ 6842) and propagated on Zorbell Marine Agar 2216 (HiMedia Labs) at 25 °C. Production media was MB/5, which contains 8 g Zorbell Marine Broth 2216 (HiMedia Labs) and 29 g Instant Ocean aquarium sea salt (United Pet Group) in 1 L deionized water, sterilized by autoclaving for 30 min.

Microbial cycloprodigiosin production : A two-day old colony of *P. rubra* on Marine Agar was inoculated into 10 mL MB/5 in a glass culture tube and shaken at 25 °C and 200 RPM for 48 h. Two 2 L baffled flasks with 500 mL MB/5 each were inoculated with 5 mL seed culture each and shaken at 25 °C and 200 RPM. After 16 h the cultures were centrifuged at 30,000 x *g* for 15 min and the pellets were combined, frozen, and lyophilized in the dark for 48 h.

Purification of biosynthetic cycloprodigiosin : Lyophilized cell pellets were extracted with 3x20 mL 50:50 chloroform:methanol and filtered, affording a bright purple filtrate. After evaporation of solvents *in vacuo* the crude extract was re-suspended in dichloromethane and chromatographed over SiO₂ (RediSep Rf Gold 24g cartridge) on a Teledyne Isco Combiflash Rf with a dichloromethane:methanol gradient ranging from 0% to 15% methanol.

All colored fractions were analyzed by Nanostructure-Initiator Mass Spectrometry 6 and only those fractions which contained cycloprodigiosin ($M+H = 322.2$ Da) but no prodigiosin ($M+H = 324.2$ Da) were combined and concentrated *in vacuo*. In agreement with Laatsch and Thomson 7 we found that cycloprodigiosin migrates slightly slower than prodigiosin on SiO_2 : prodigiosin eluted with 6% methanol while cycloprodigiosin eluted with 8% methanol in dichloromethane. A slight difference in color was noticeable between prodigiosin and cycloprodigiosin fractions.

The extract was further purified by Reversed-Phase HPLC on an Agilent 1260 infinity series instrument with a ZORBAX SB-C18 semi-prep column (50 mm x 9.4 mm internal diameter, 5 μ M particle size). Separation conditions were as follows: Solvent A = Water, 0.1% formic acid, Solvent B = methanol, 0.1% formic acid. The following gradient was used: 50% B for 2 min, ramp to 95% B in 8 min, wash with 95% B for 4 min, re-equilibrate with 50% B for 4 min. Flow rate was 10 mL/min. Fraction collection was triggered by Abs(540). Retention time for cycloprodigiosin under these conditions was 5 min, corresponding to 65% B. The combined fractions were evaporated under reduced pressure to afford a bright purple solid. Yield: 600 nmol (0.2 mg) as determined by HPLC-MS with racemic prodigiosin as a standard. HRMS (ESI): Exact mass calc'd for $C_{20}H_{24}ON_3$ $[M+H]^+$, 322.1914. Found 322.1912.

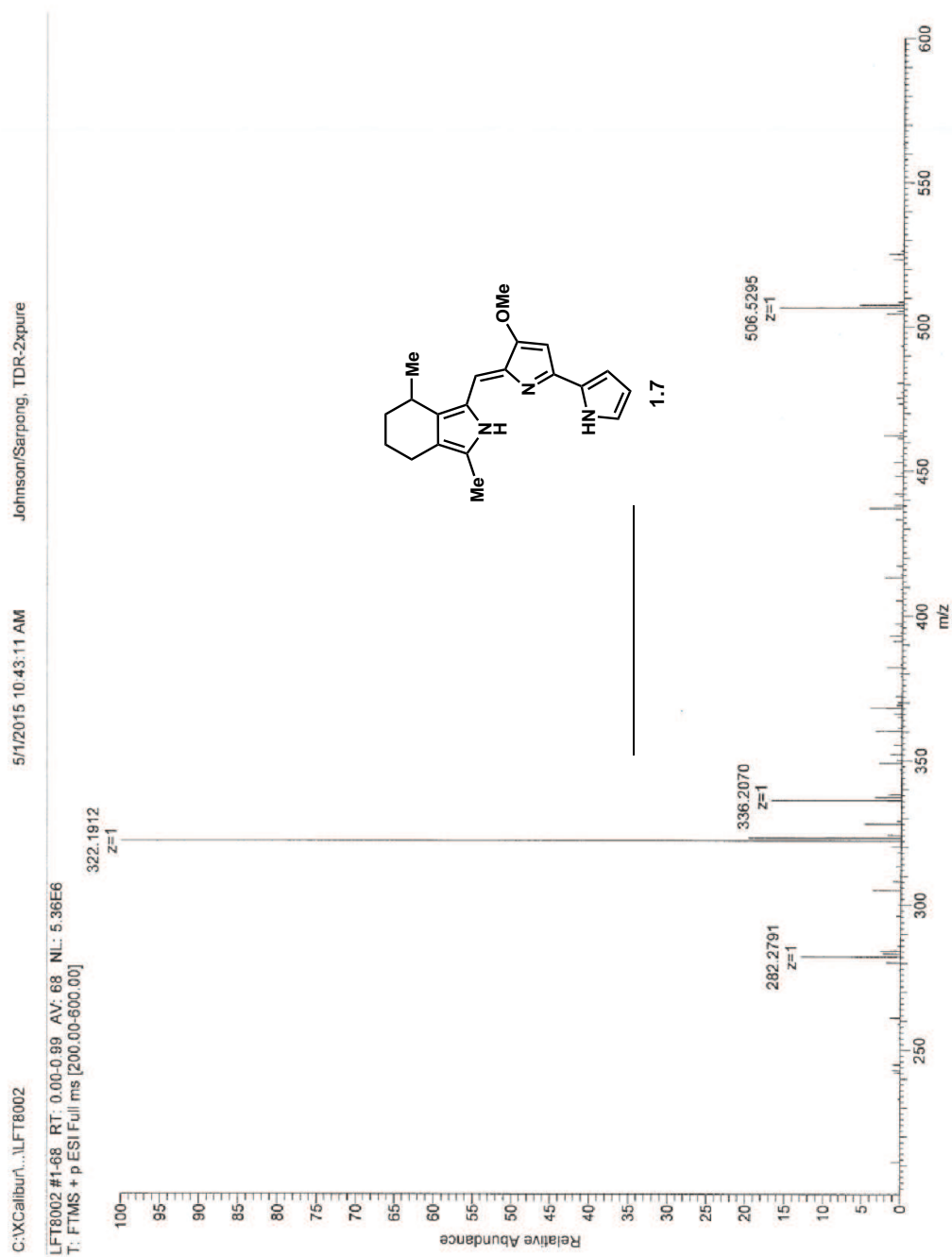


Figure 2.3: The HRMS ESI spectrum of naturally isolated **1.7**

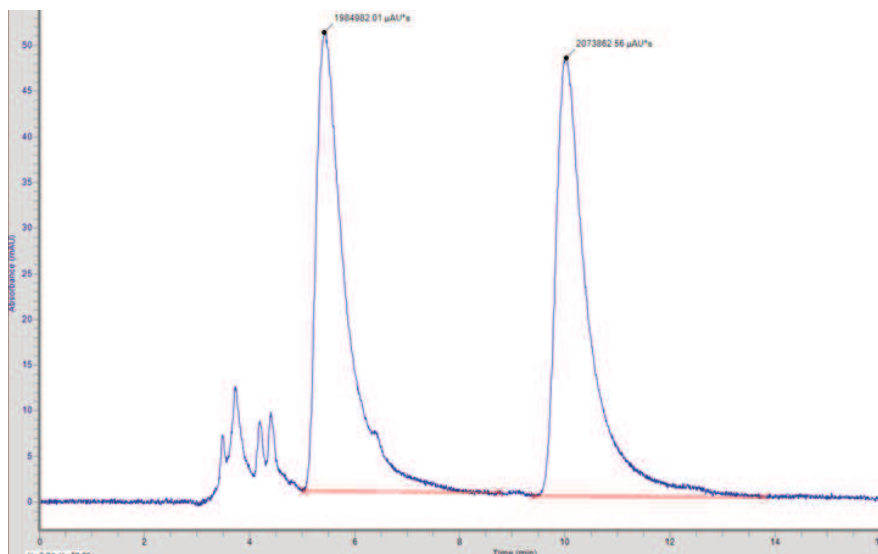


Figure 2.4: Synthetic racemic cycloprodigosin. Retention times: 5.43 min (*R*)/10.02 min (*S*), 49:51 er.

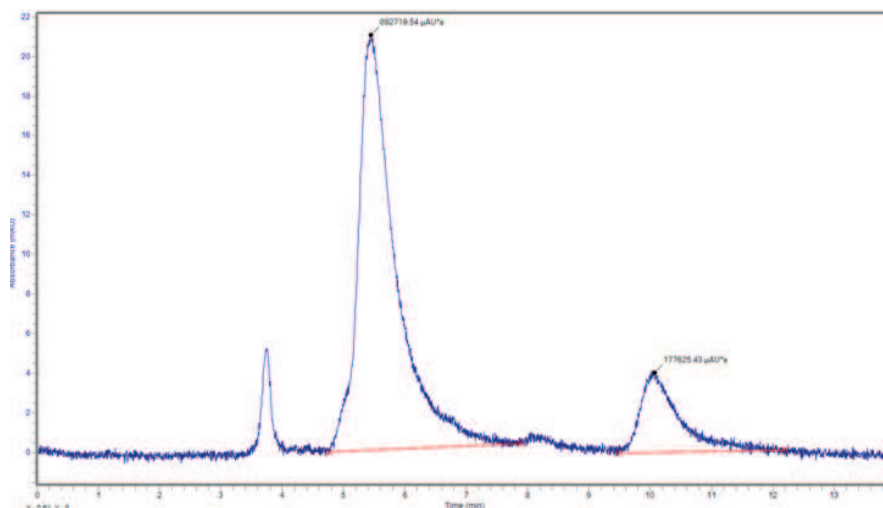


Figure 2.5: Natural cycloprodigosin isolated from *P. rubra*. Retention times: 5.44 min (*R*)/10.07 min (*S*), 83:17 er.

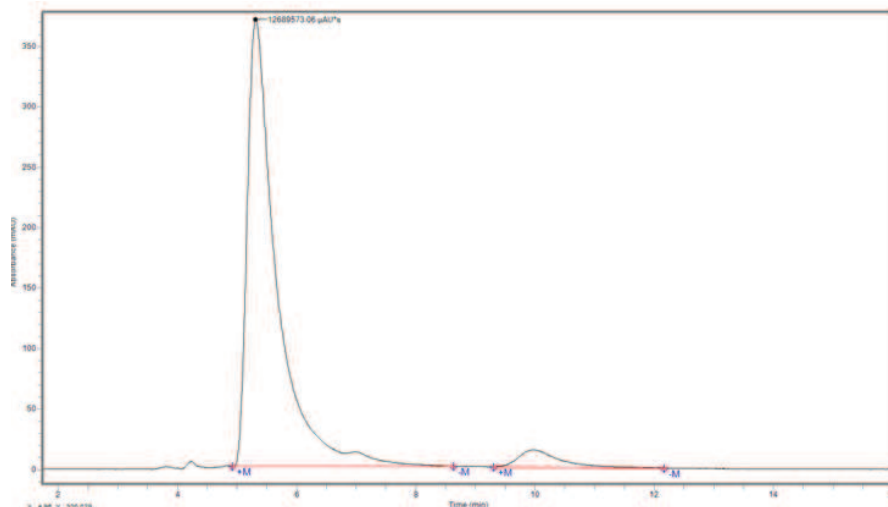


Figure 2.6: Synthetic (*R*)-cycloprodigosin. Retention times: 5.31 min (*R*)/10.02 min (*S*), 95:5 er.

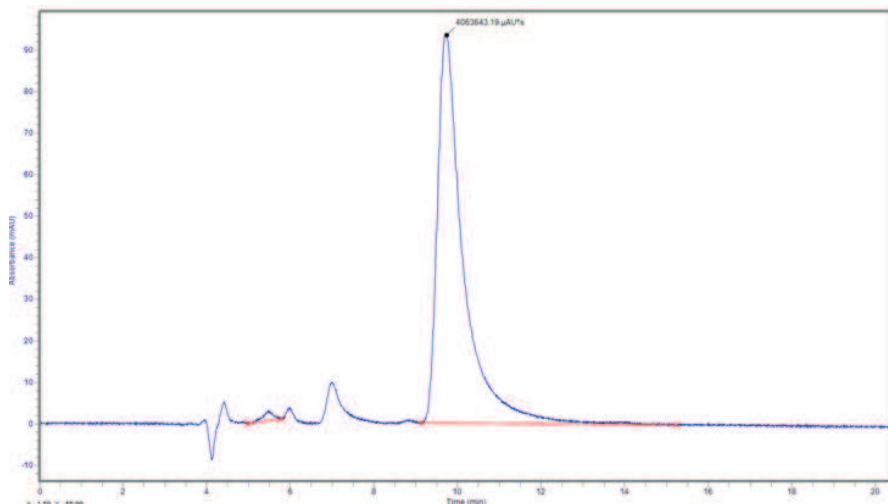


Figure 2.7: Synthetic (*S*)-cycloprodigosin. Retention times: 5.46 min (*R*)/9.74 min (*S*), 99:1 er.

2.9 References

- Haynes, S. W.; Sydor, P. K.; Corre, C.; Song, L.; Challis, G. L. *J. Am. Chem. Soc.* **2011**, *133*, 1793–1798.
- Sydor, P. K.; Barry, S. M.; Odulate, O. M.; Barona-Gomez, F.; Haynes, S. W.; Corre, C.; Song, L.; Challis, G. L. *Nat. Chem.* **2011**, *3*, 388–392.
- Hu, D. X.; Clift, M. D.; Lazarski, K. E.; Thomson, R. J. *J. Am. Chem. Soc.* **2011**, *133*, 1799–1804.
- M., F. J.; H., S. D.; Martin, K.; M., W. R. *Angew. Chem. Int. Ed.* **2012**, *51*, 4802–4836.
- Withall, D. M.; Haynes, S. W.; Challis, G. L. *J. Am. Chem. Soc.* **2015**, *137*, 7889–7897.
- Barry, S. M.; Challis, G. L. *ACS Catal.* **2013**, *3*, 2362–2370.
- Gerber, N.; Gauthier, M. *Appl. Environ. Microbiol.* **1979**, *37*, 1176–1179.
- Lattasch, H.; Thomson, R. H. *Tetrahedron Lett.* **1983**, *24*, 2701–2704.

9. Schultz, E. E.; Sarpong, R. *J. Am. Chem. Soc.* **2013**, *135*, 4696–4699.
10. Ohira, S. *Synth. Commun.* **1989**, *19*, 561–564.
11. Müller, S.; Liepold, B.; Roth, G. J.; Bestmann, H. J. *Synlett* **1996**, *1996*, 521–522.
12. Myers, A. G.; Zheng, B. *J. Am. Chem. Soc.* **1996**, *118*, 4492–4493.
13. Rausaria, S.; Kamadulski, A.; Rath, N. P.; Bryant, L.; Chen, Z.; Salvemini, D.; Neumann, W. L. *J. Am. Chem. Soc.* **2011**, *133*, 4200–4203.
14. Wasserman, H. H.; McKeon, J. E.; Smith, L.; Forgione, P. *J. Am. Chem. Soc.* **1960**, *82*, 506–507.
15. Barton, D. H. R.; Zard, S. Z. *J. Chem. Soc., Chem. Commun.* **1985**, *0*, 1098–1100.
16. Corey, E. J.; Estreicher, H. *J. Am. Chem. Soc.* **1978**, *100*, 6294–6295.
17. Gui, J.; Zhou, Q.; Pan, C.-M.; Yabe, Y.; Burns, A. C.; Collins, M. R.; Ornelas, M. A.; Ishihara, Y.; Baran, P. S. *J. Am. Chem. Soc.* **2014**, *136*, 4853–4856.
18. Dairi, K.; Tripathy, S.; Attardo, G.; Lavallée, J.-F. *Tetrahedron Lett.* **2006**, *47*, 2605–2606.
19. Ilankumaran, P.; Kisanga, P.; Verkade, J. G. *Heteroatom Chem.* **2001**, *12*, 561–562.
20. Gauthier, M. J. *Int. J. of Syst. Evol. Microbiol.* **1976**, *26*, 459–466.
21. Hearn, W.; Medina, J.; Elson, M. *Nature* **1968**, *220*, 170–171.
22. Grünanger, C. U.; Breit, B. *Angew. Chem. Int. Ed.* **2010**, *49*, 967–970.

2.a : NMR Spectra Relevant to Chapter 2

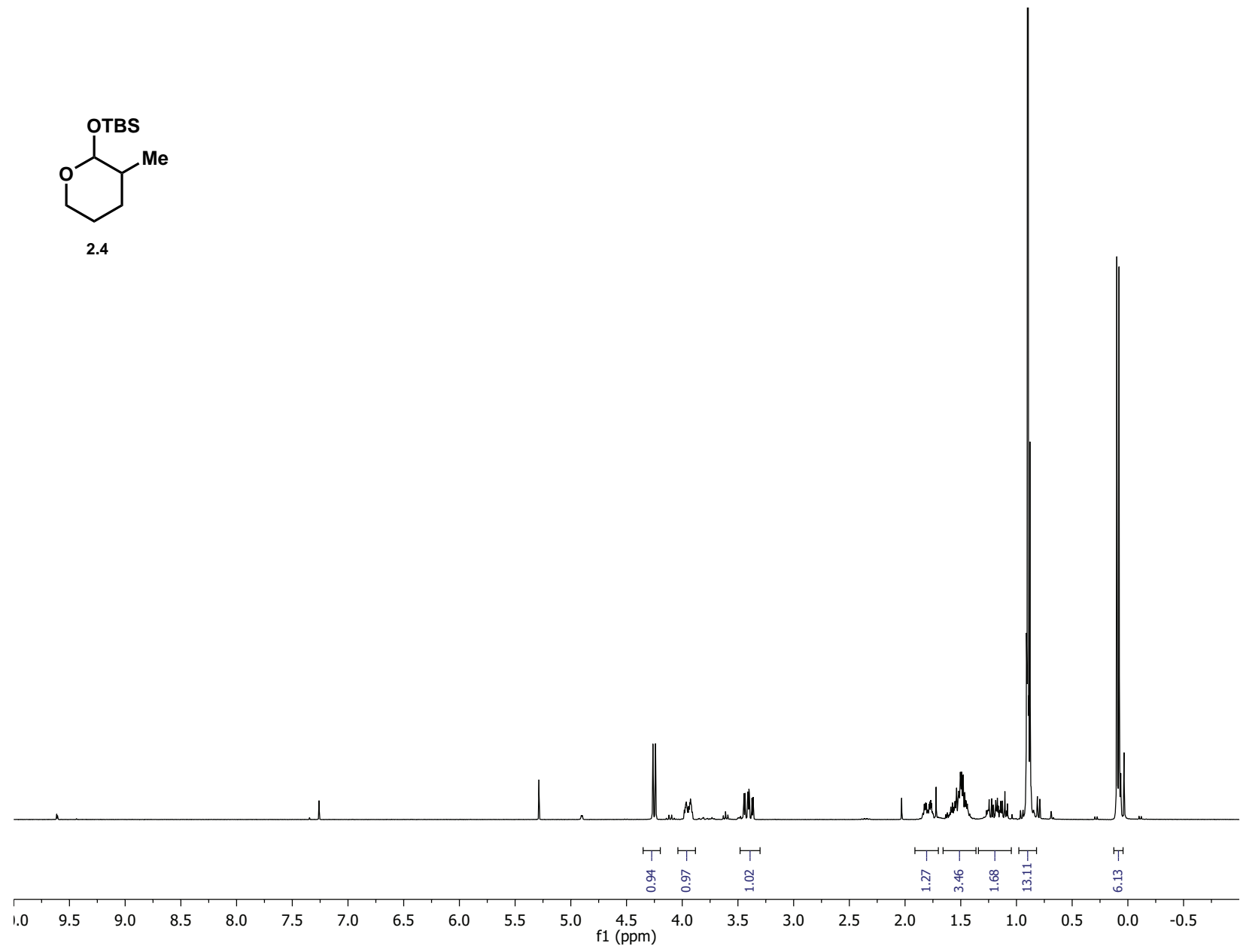
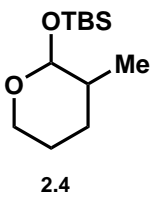
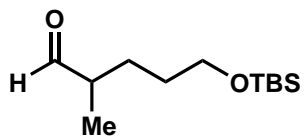


Figure 2.8: ¹H NMR of 2.4 in CDCl₃



2.3

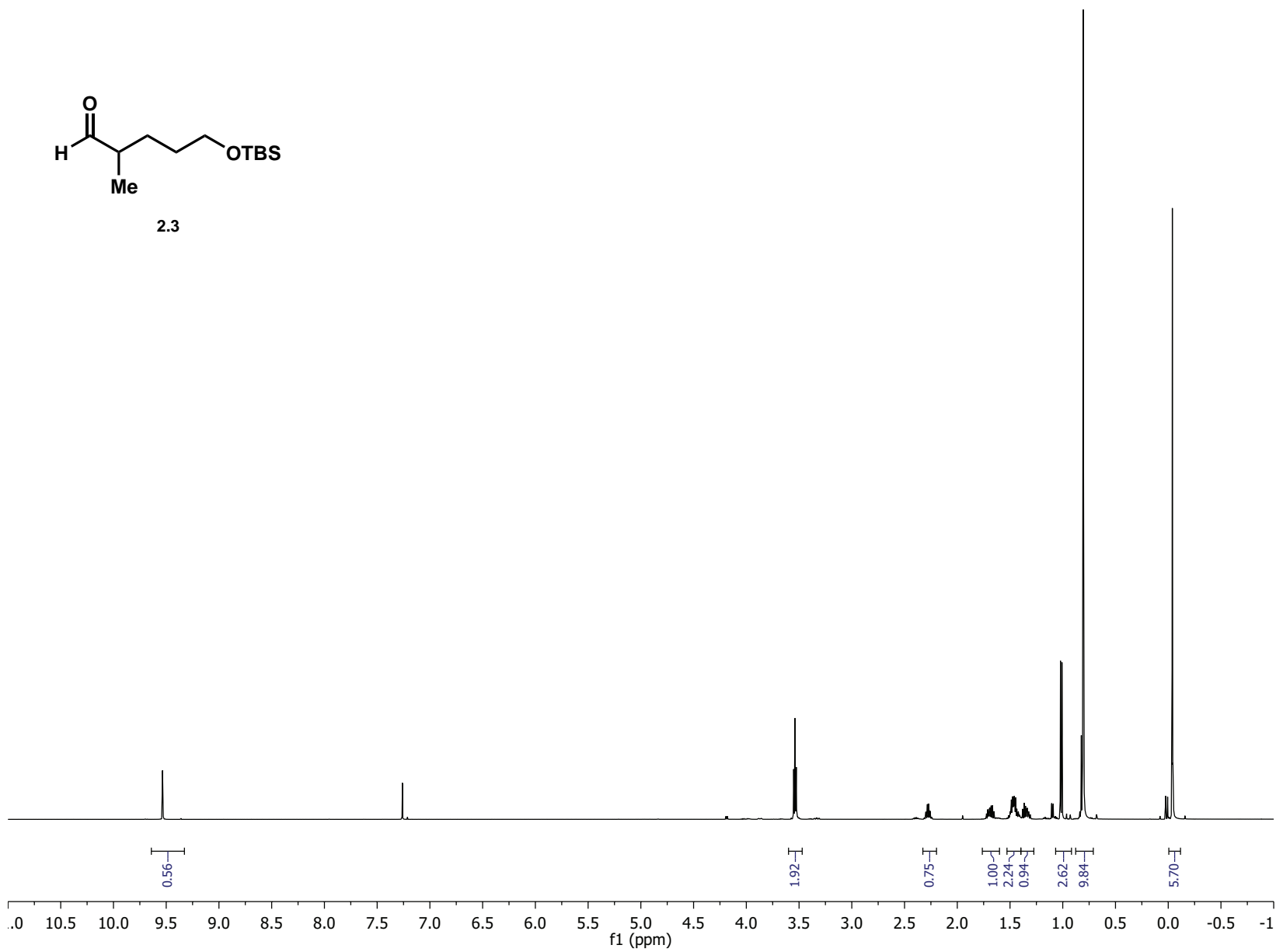
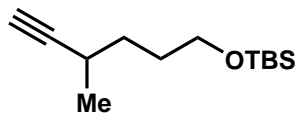


Figure 2.9: ^1H NMR of 2.3 in CDCl_3



2.5

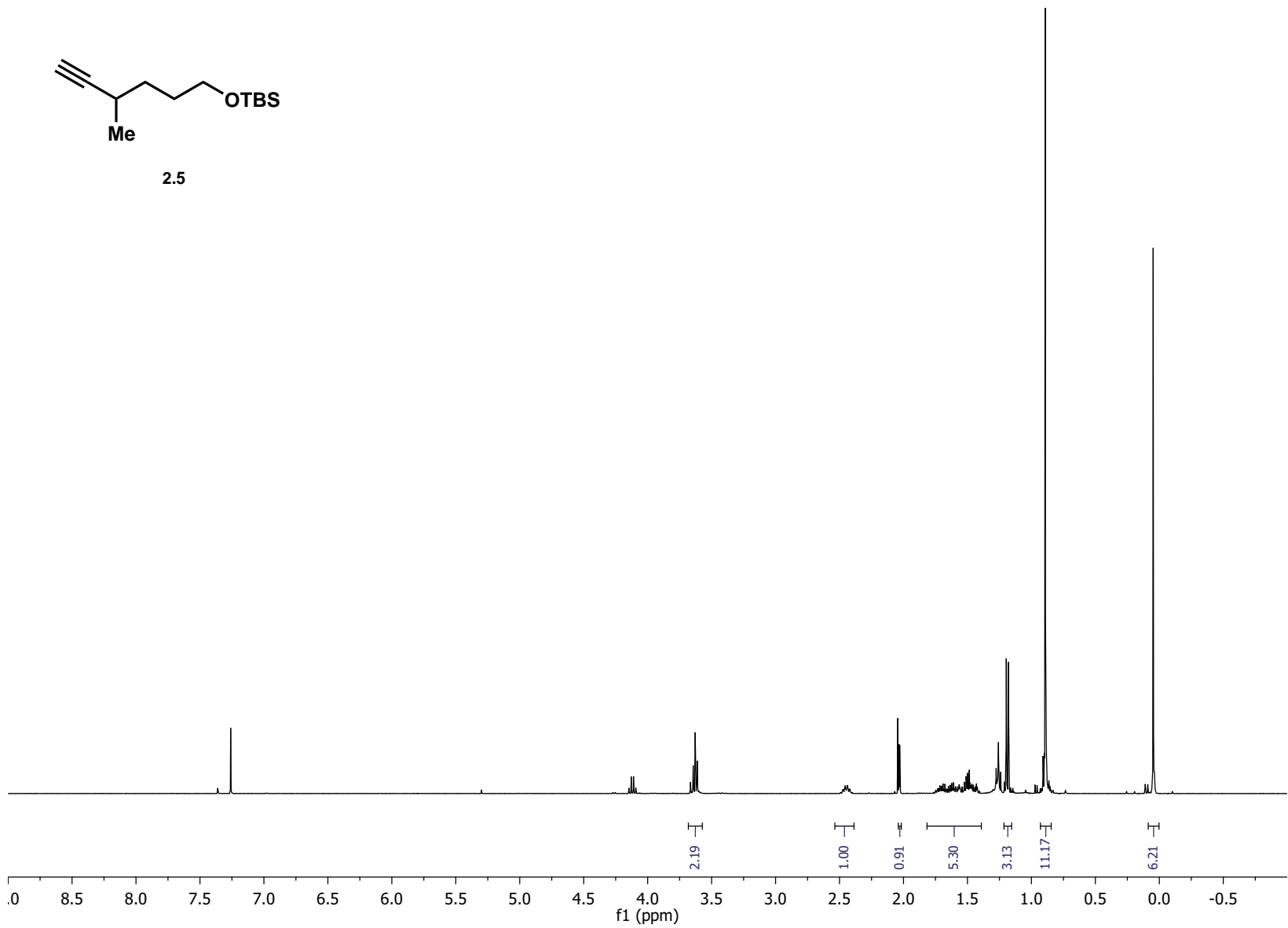


Figure 2.10: ¹H NMR of 2.5 in CDCl₃

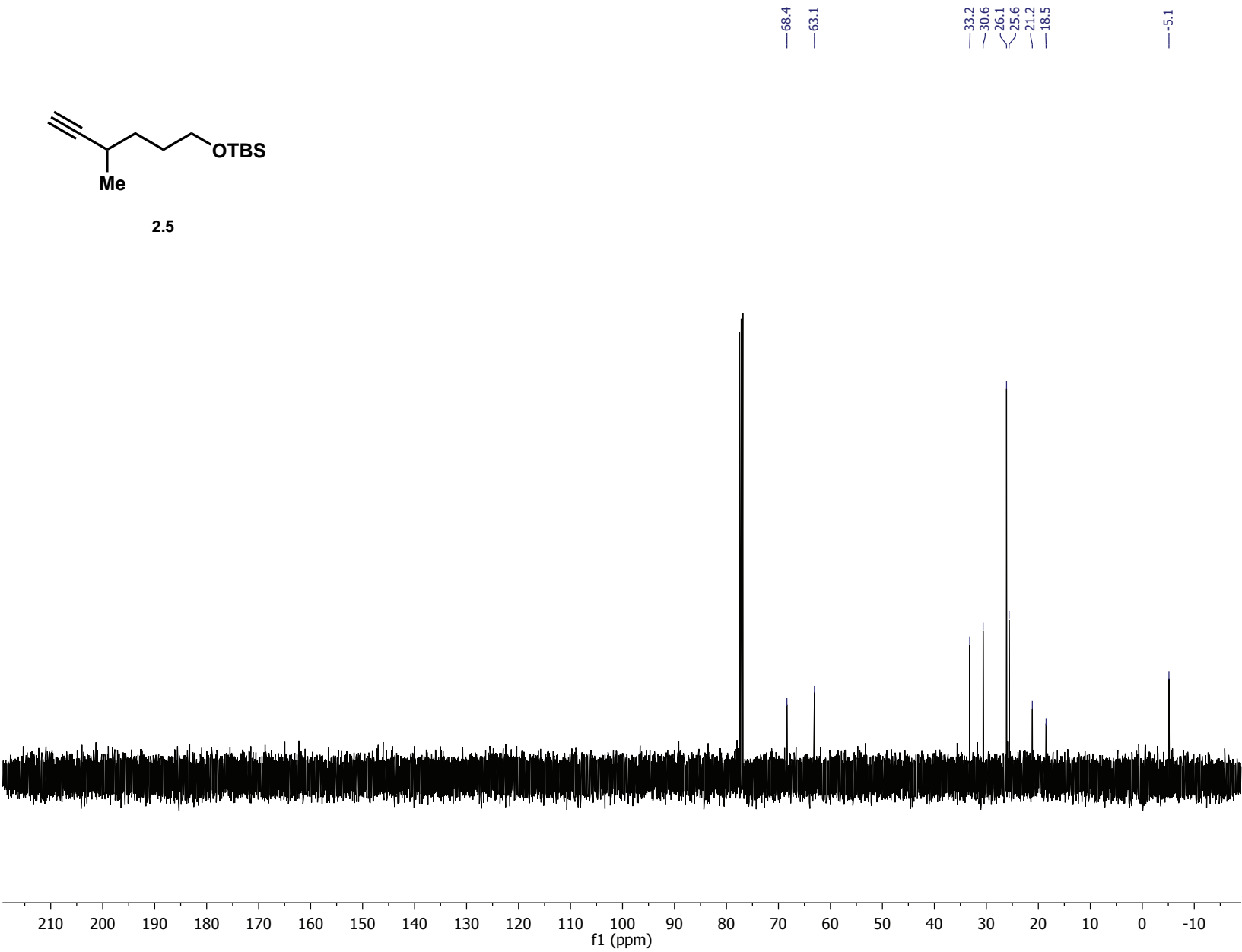


Figure 2.11: ¹³C NMR of 2.5 in CDCl₃

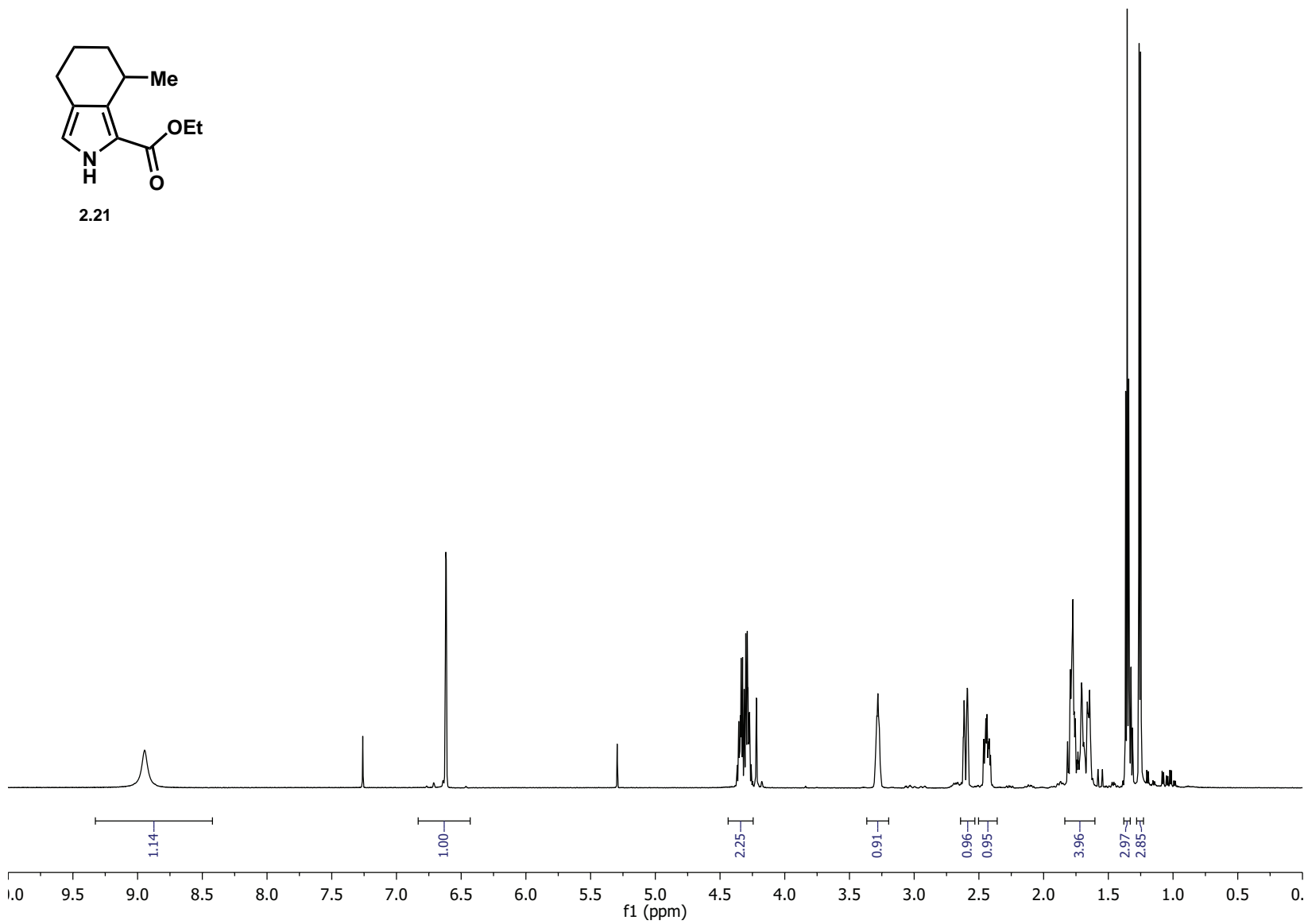
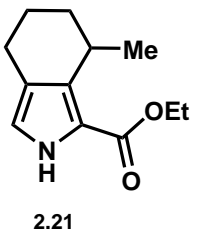


Figure 2.12: ¹H NMR of 2.21 in CDCl₃

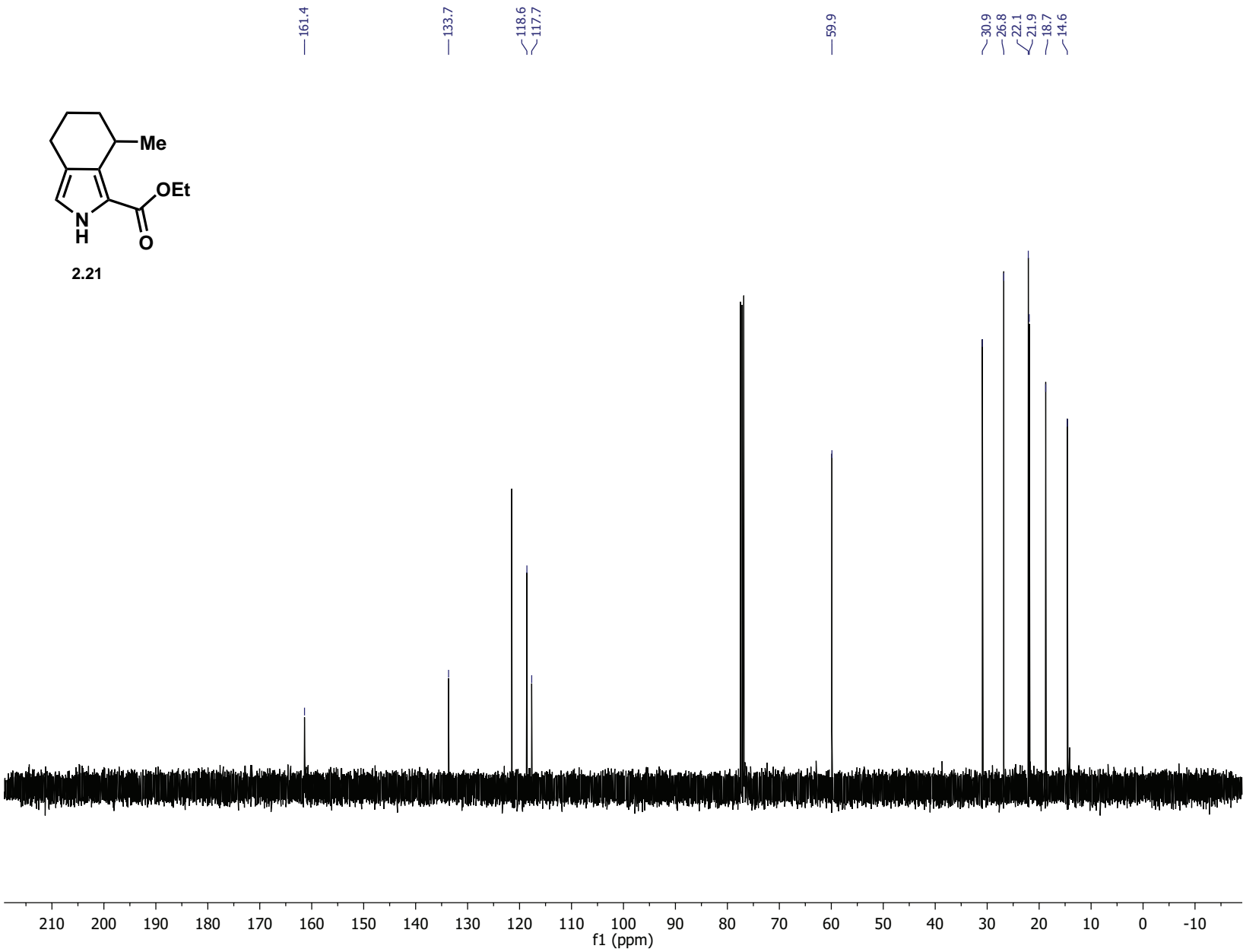


Figure 2.13: ¹³C NMR of 2.21 in CDCl₃

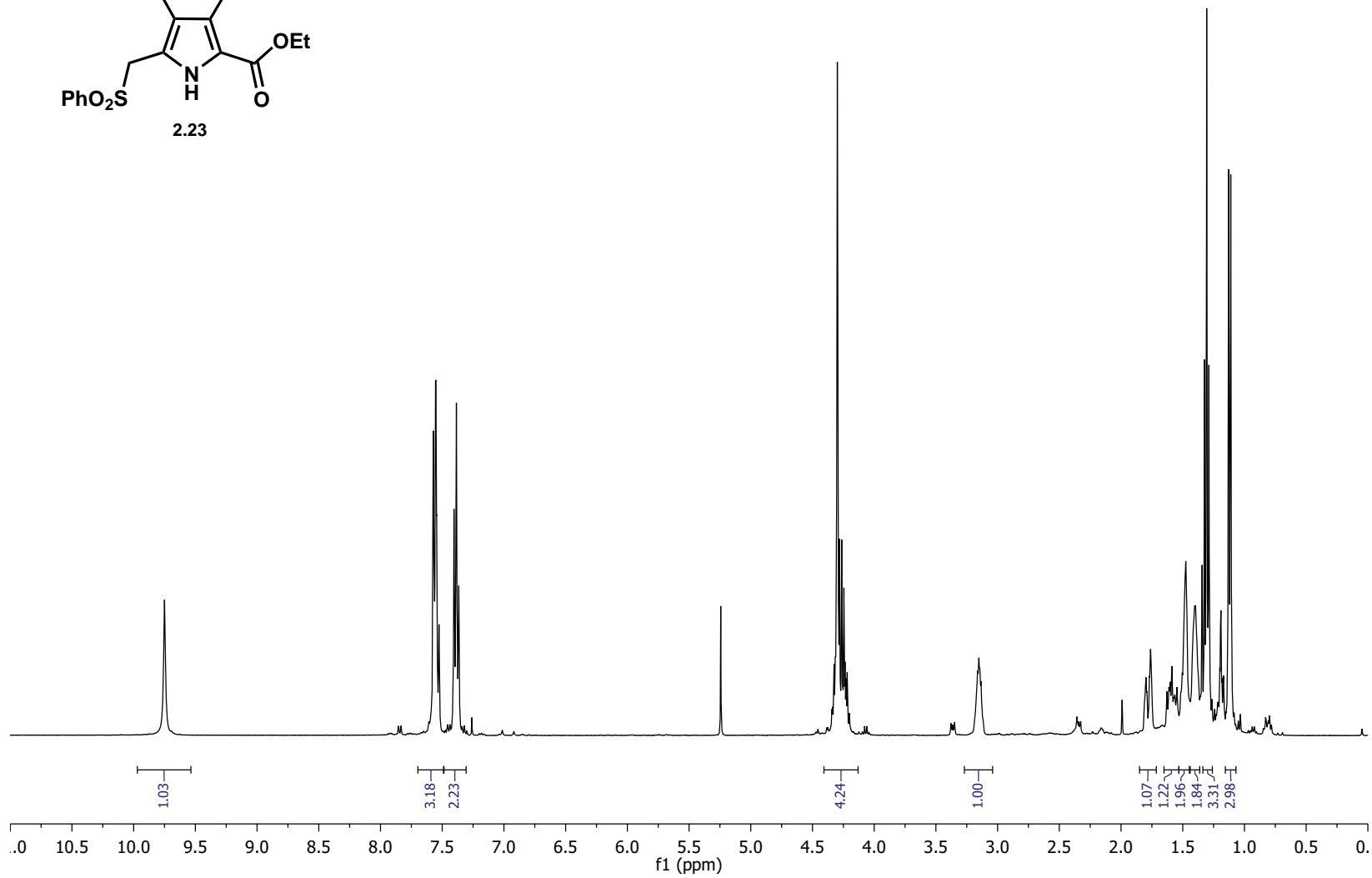
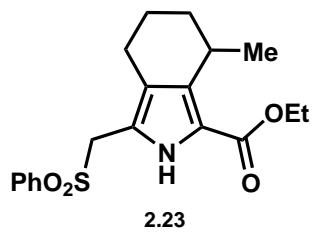


Figure 2.14: ^1H NMR of 2.23 in CDCl_3

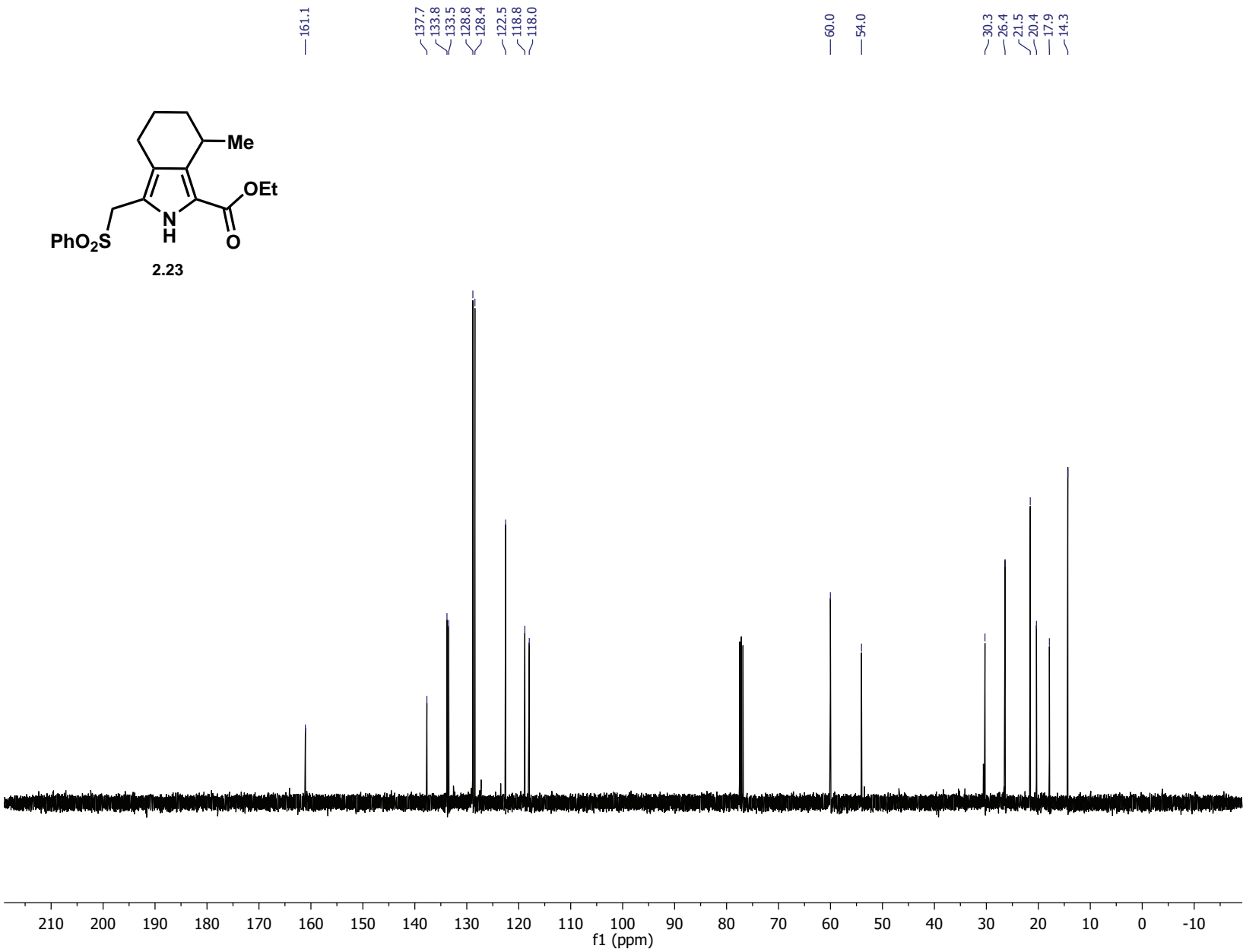


Figure 2.15: ¹³C NMR of 2.23 in CDCl₃

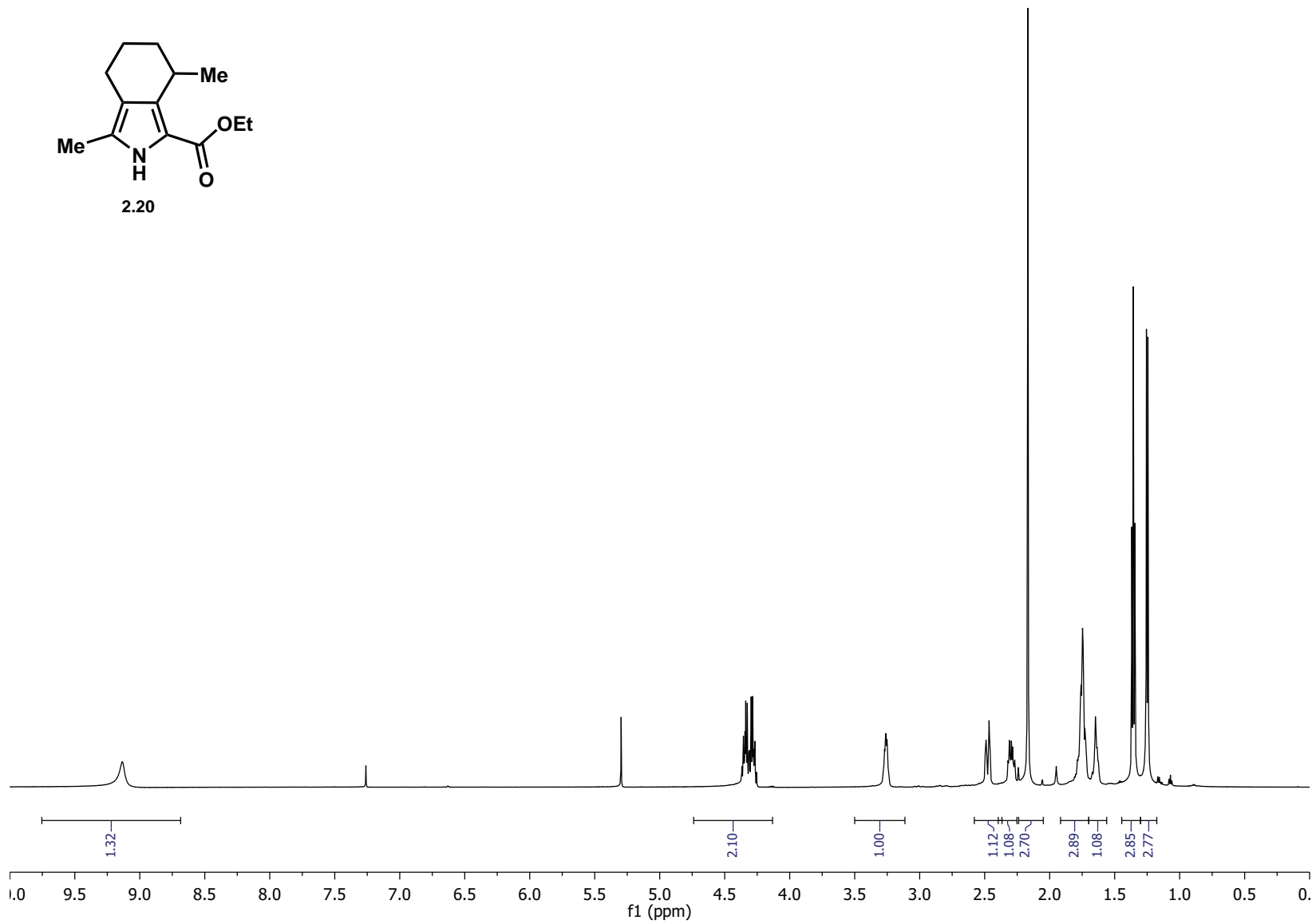
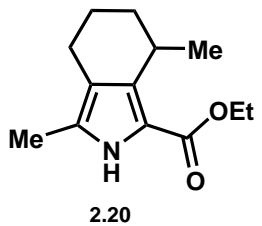


Figure 2.16: ^1H NMR of 2.20 in CDCl_3

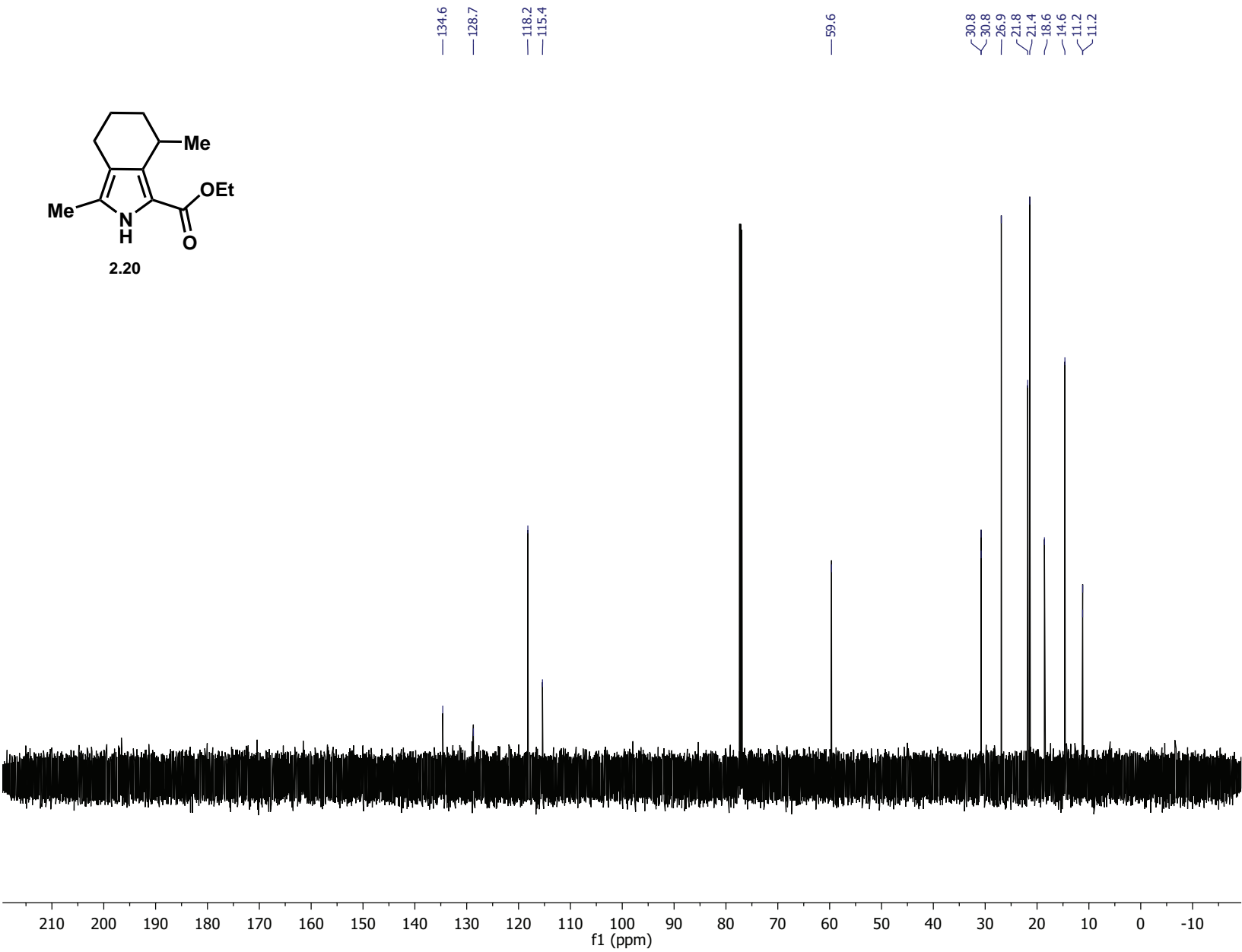


Figure 2.17: ¹³C NMR of 2.20 in CDCl₃

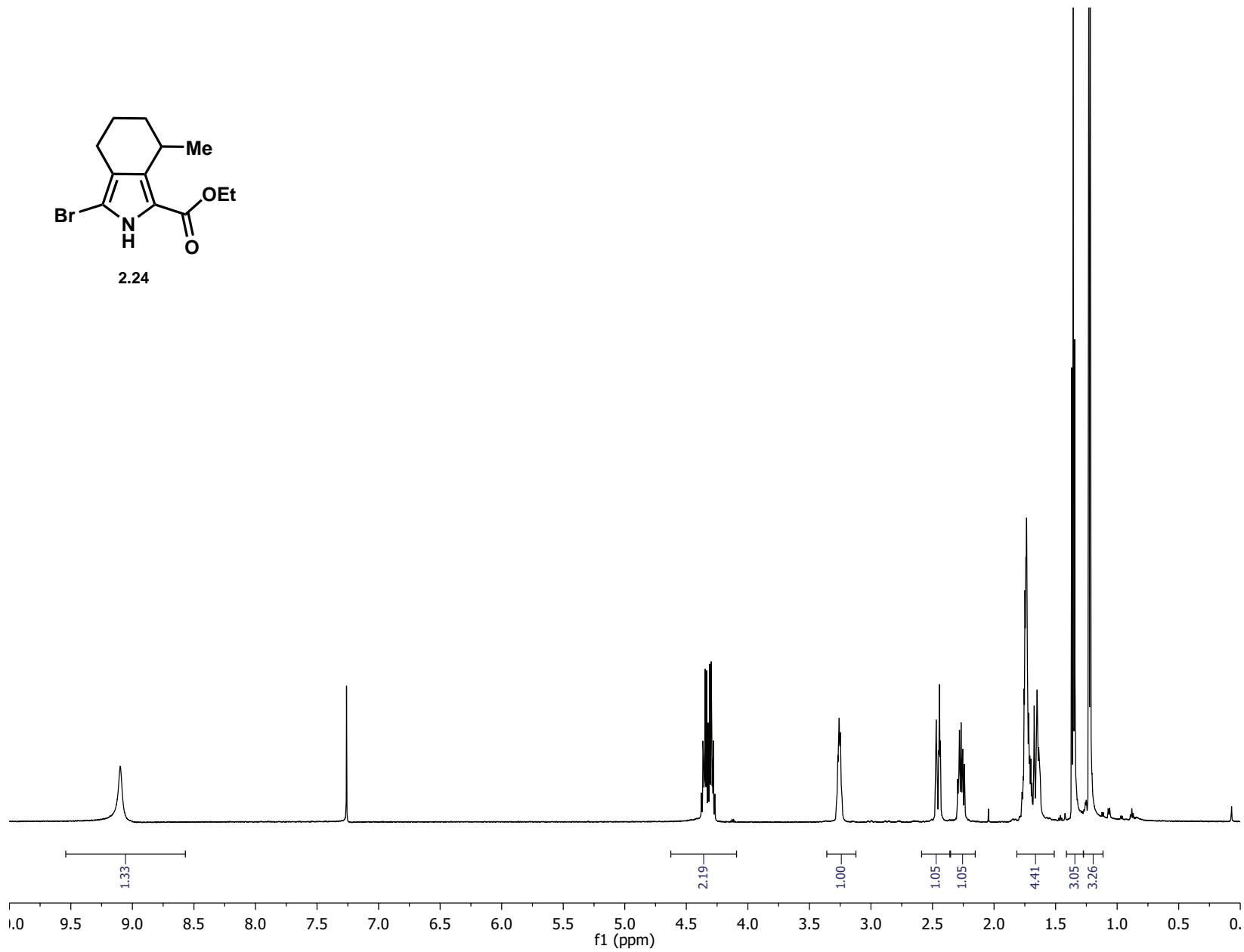
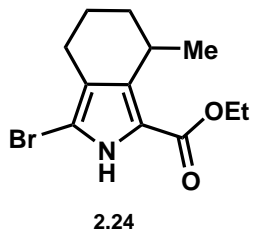


Figure 2.18: ^1H NMR of 2.24 in CDCl_3

EJII-109car/1
3/21/10 CC AV-600 ZBO carbon starting parameters
Q_MOD=DQD

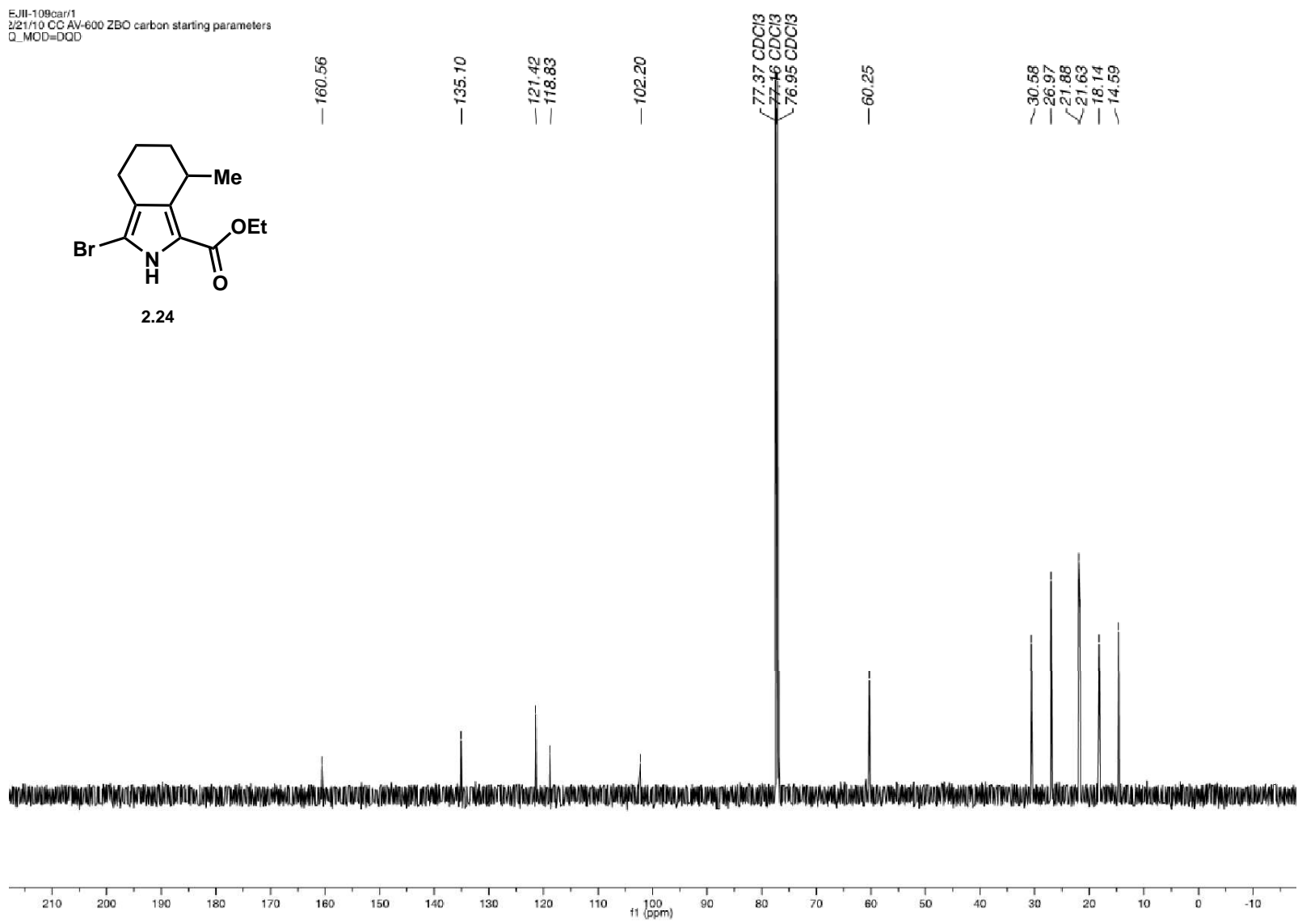
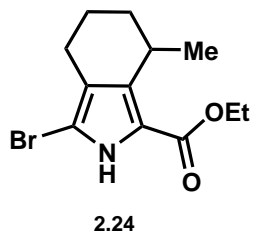


Figure 2.19: ^{13}C NMR of 2.24 in CDCl_3

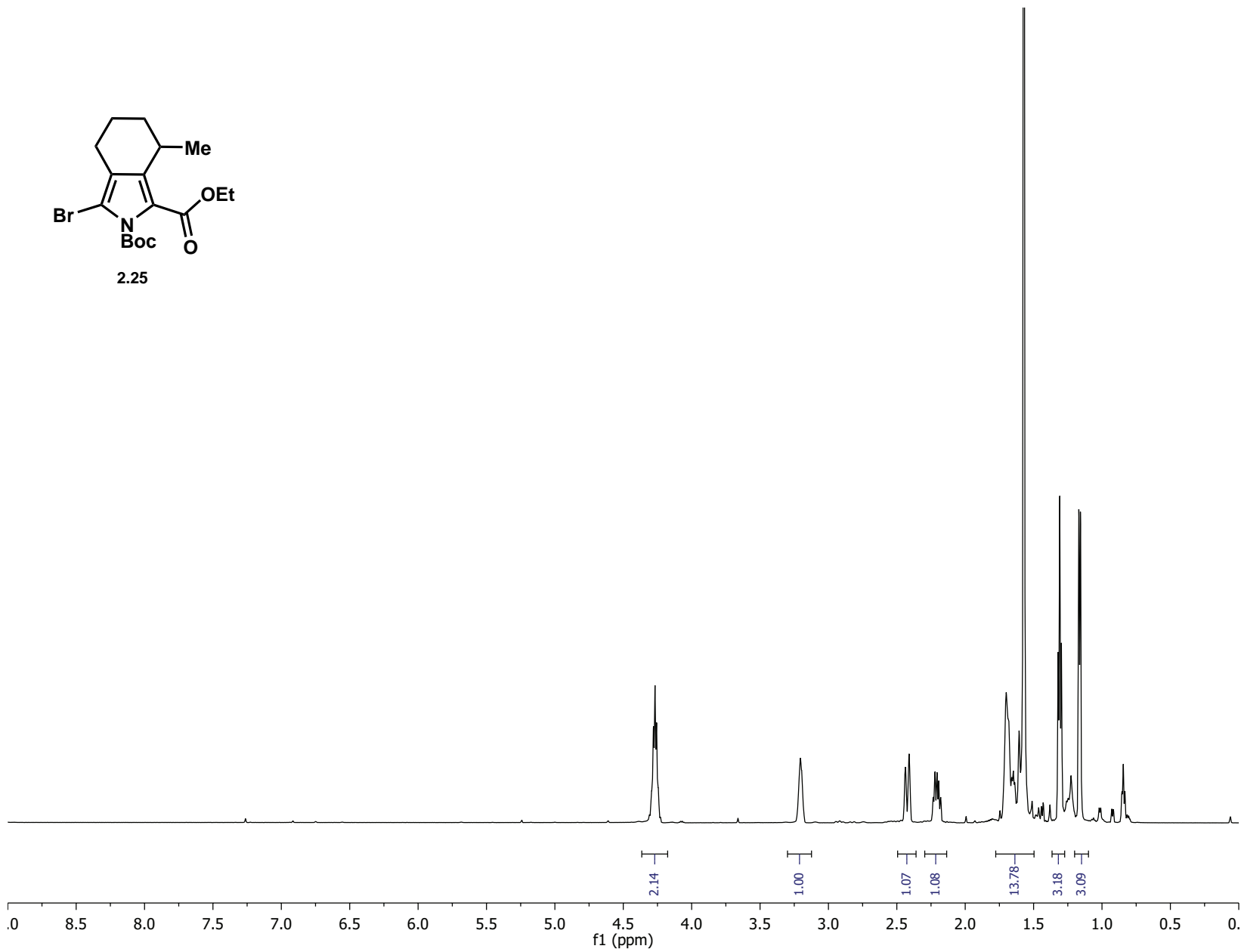
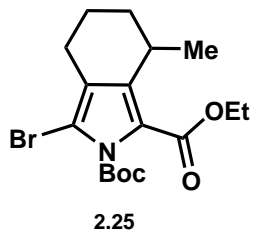


Figure 2.20: ¹H NMR of 2.25 in CDCl₃

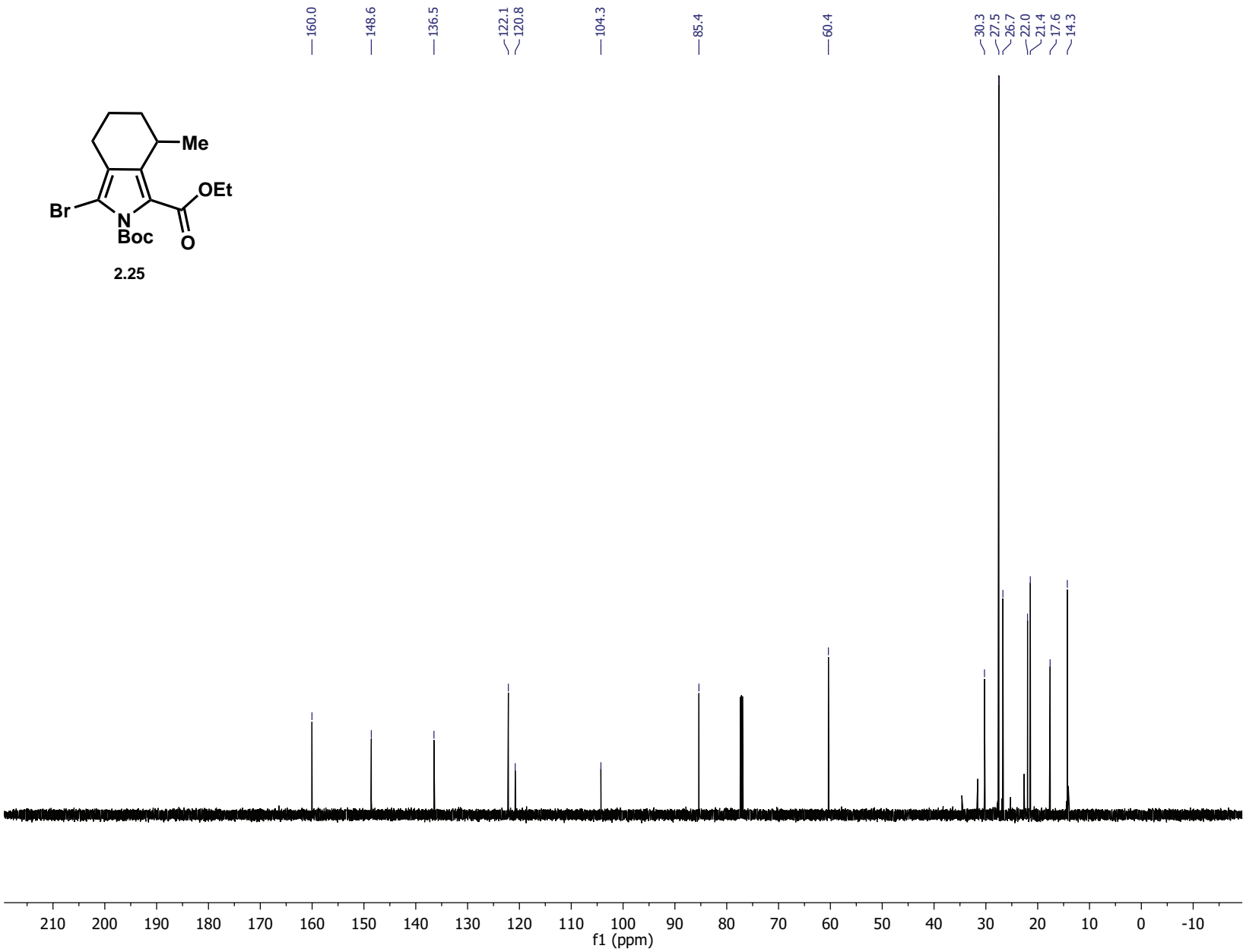


Figure 2.21: ^{13}C NMR of 2.25 in CDCl_3

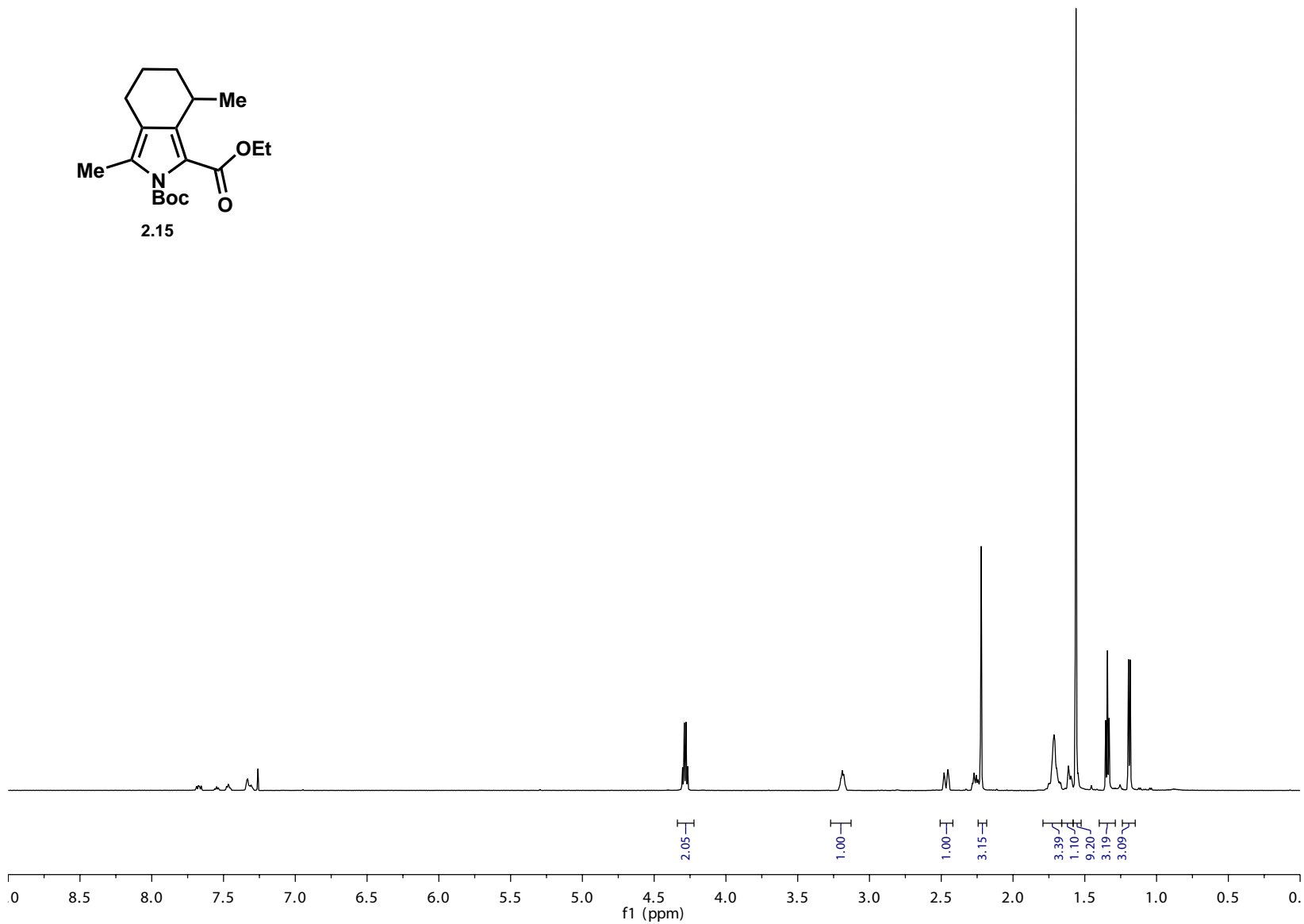
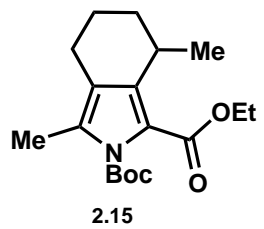


Figure 2.22: ¹H NMR of 2.15 in CDCl₃

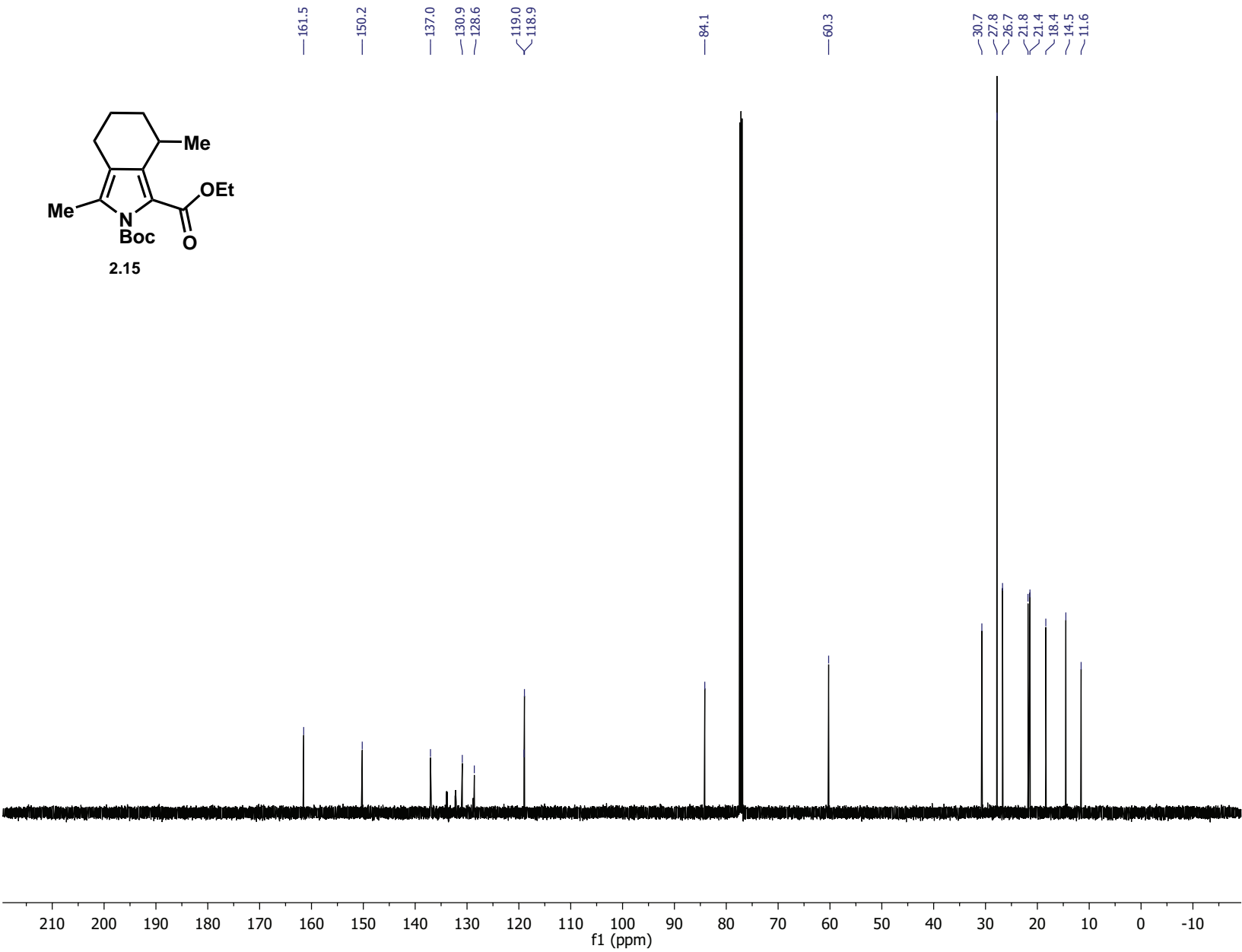


Figure 2.23: ¹³C NMR of 2.15 in CDCl₃

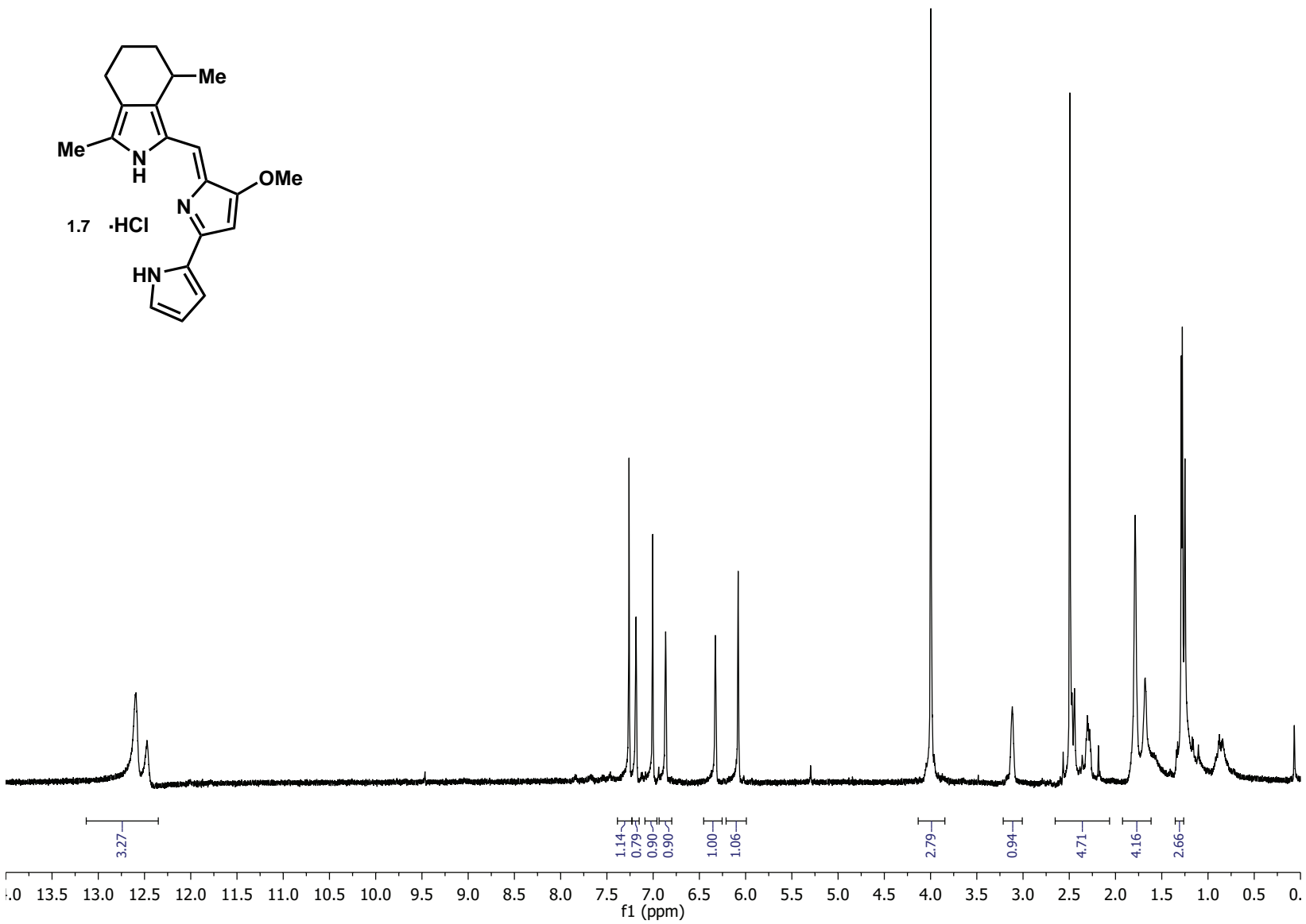


Figure 2.24: ¹H NMR of 1.7 in CDCl₃

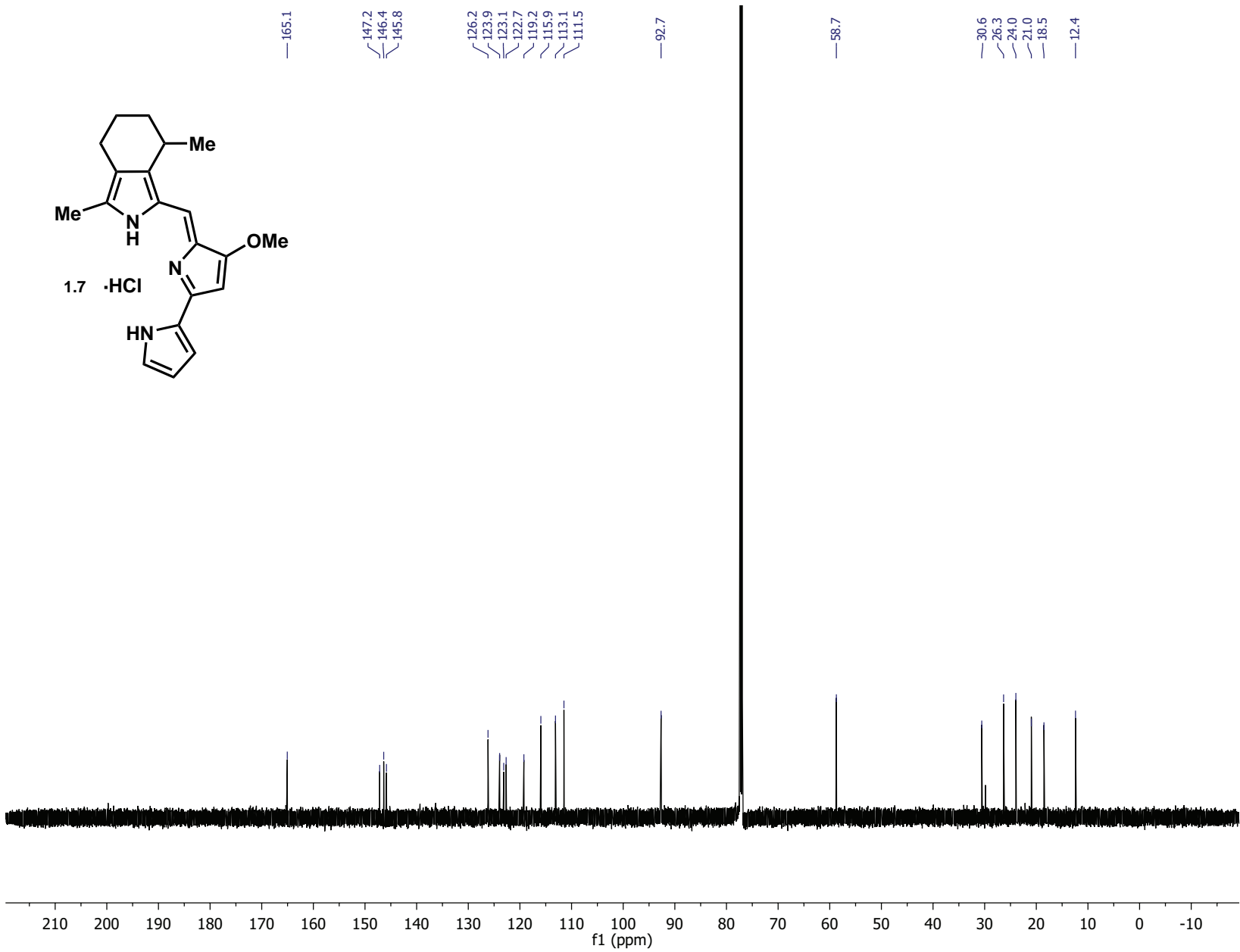


Figure 2.25: ^{13}C NMR of 1.7 in CDCl_3

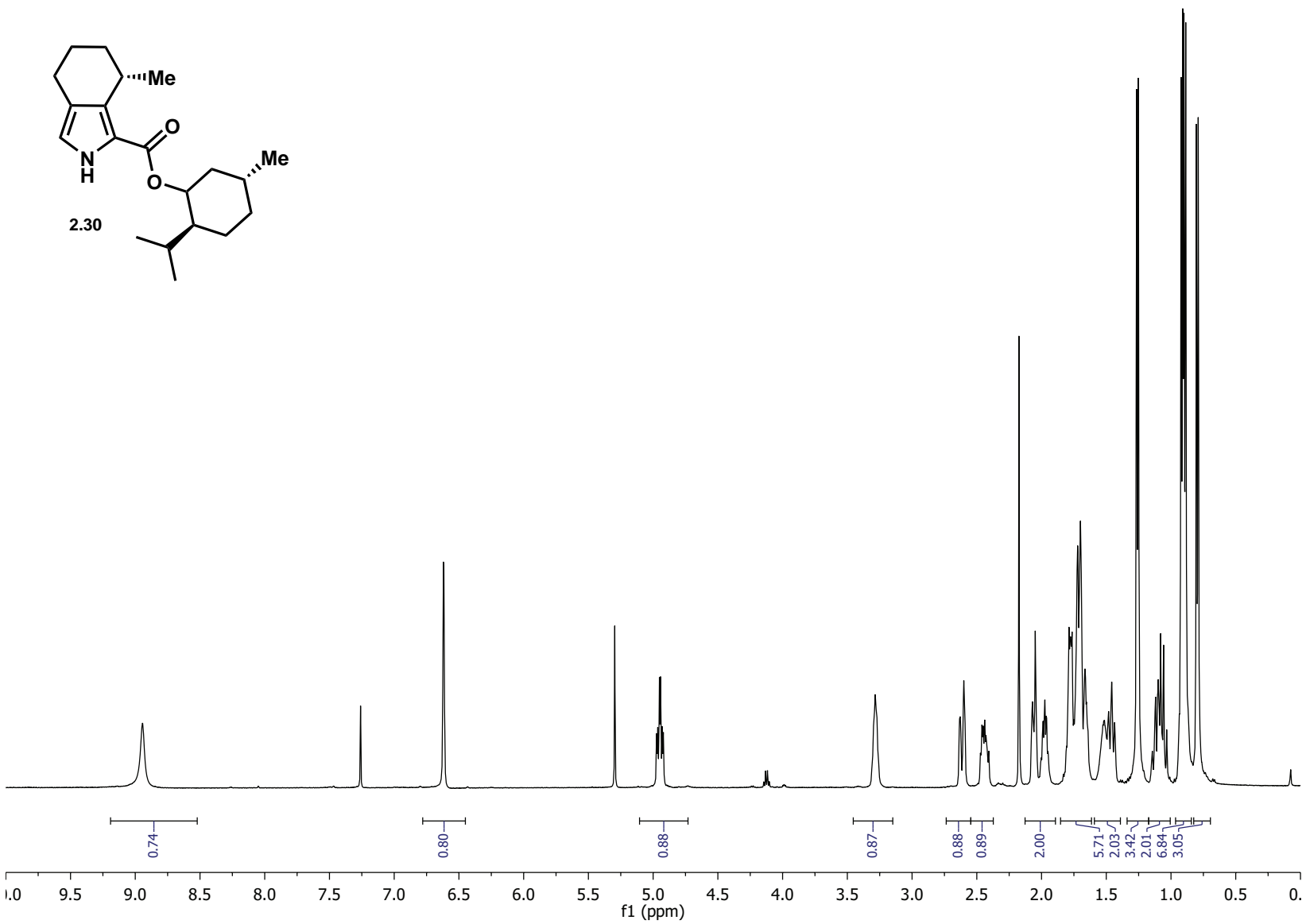


Figure 2.26: ^1H NMR of 2.30 in CDCl_3

1EJIL-147.diastr1 car/1
V-600 TBIP probe
2/18/12 CC

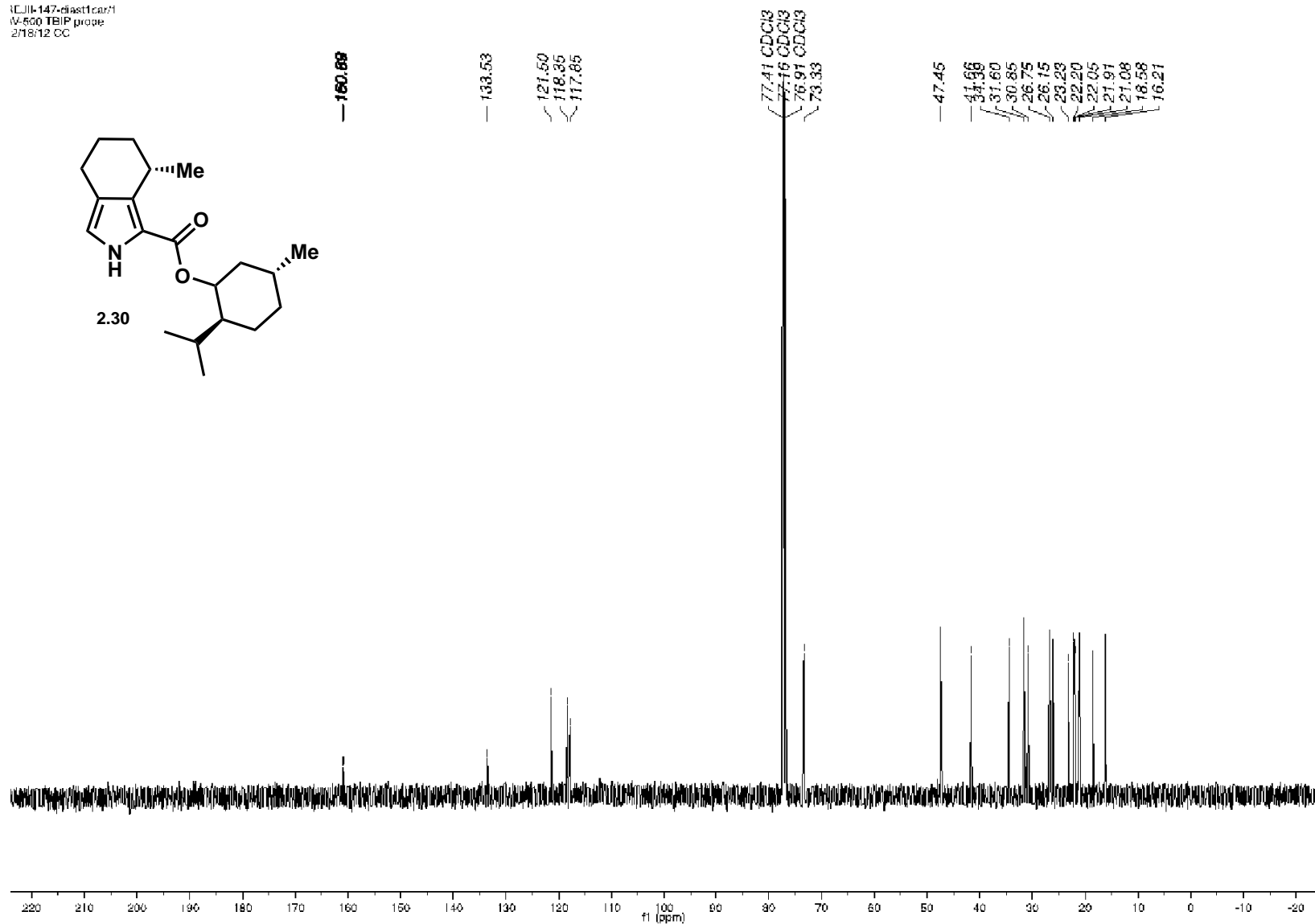


Figure 2.27: ^{13}C NMR of 2.30 in CDCl_3

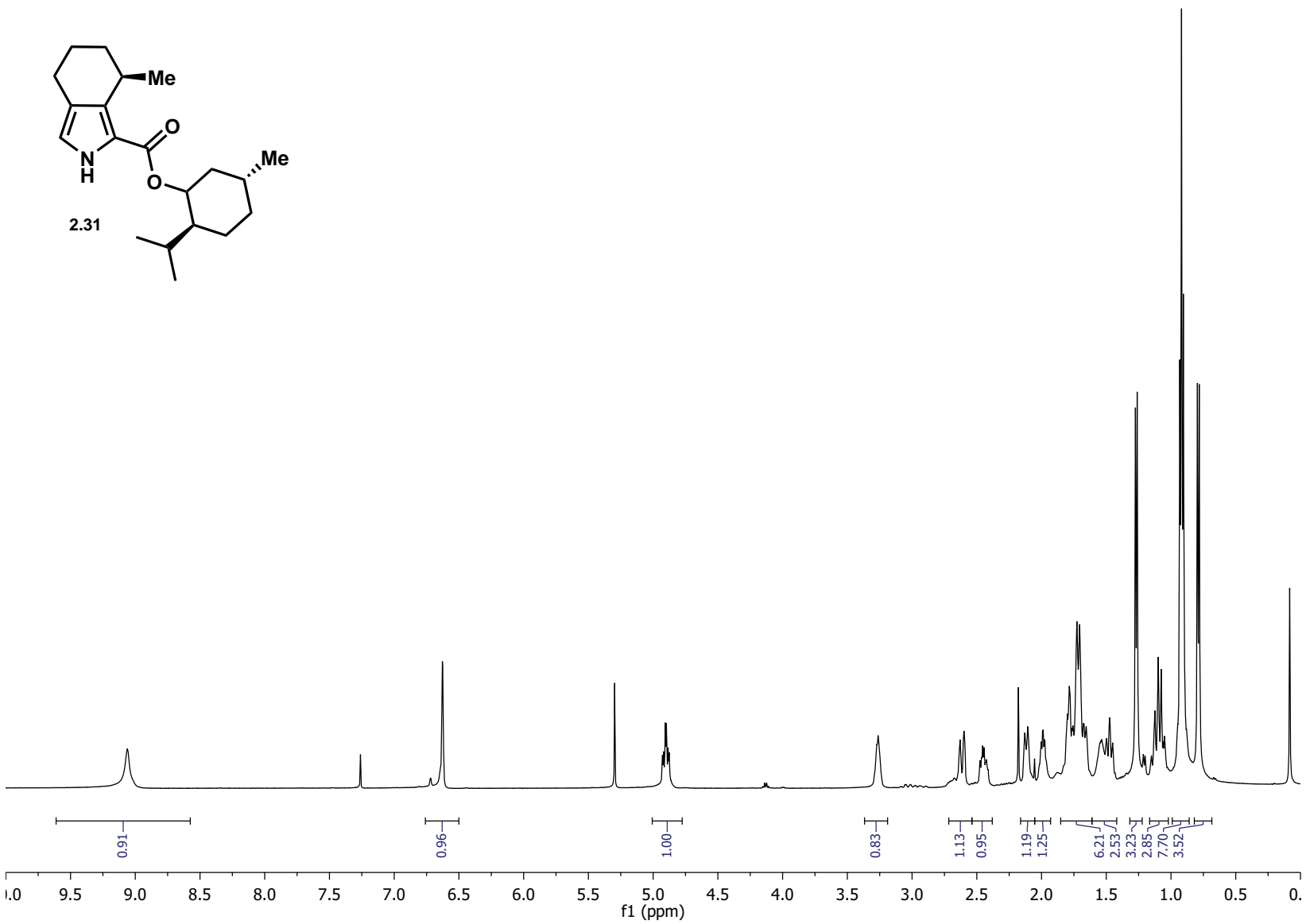


Figure 2.28: ¹H NMR of 2.31 in CDCl₃

IEJH147-elast2ca.r1
C: 12182012 AV-500 TBIP proba
H 1D NMR

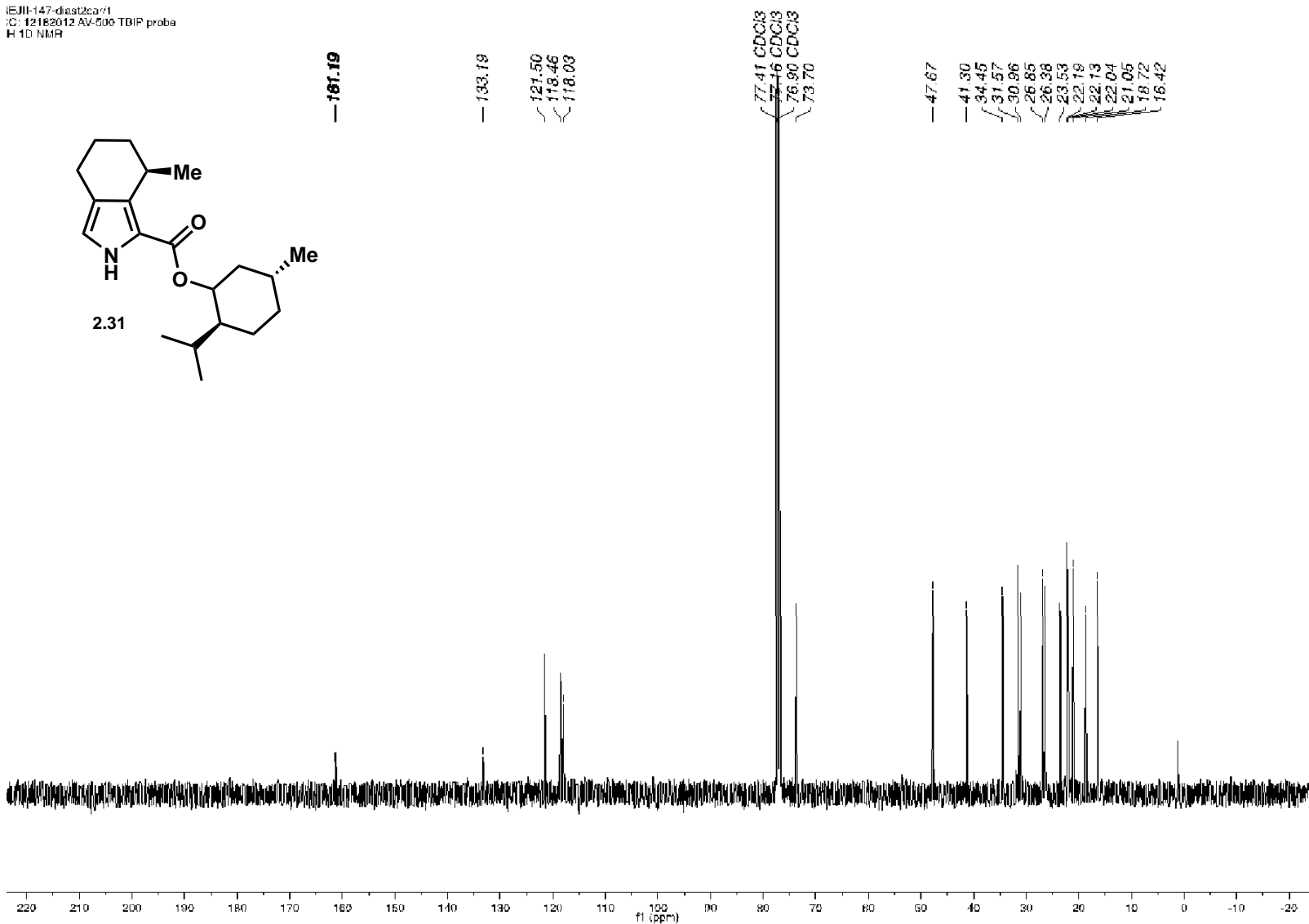
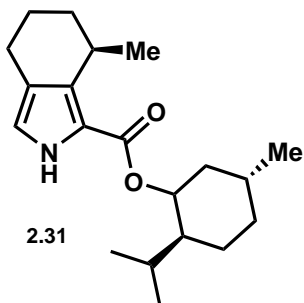
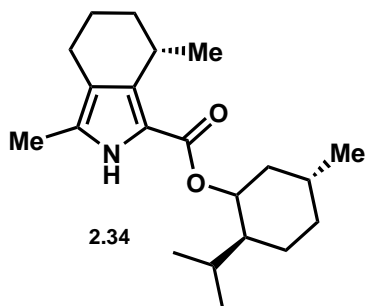


Figure 2.29: ^{13}C NMR of 2.31 in CDCl_3



2.34

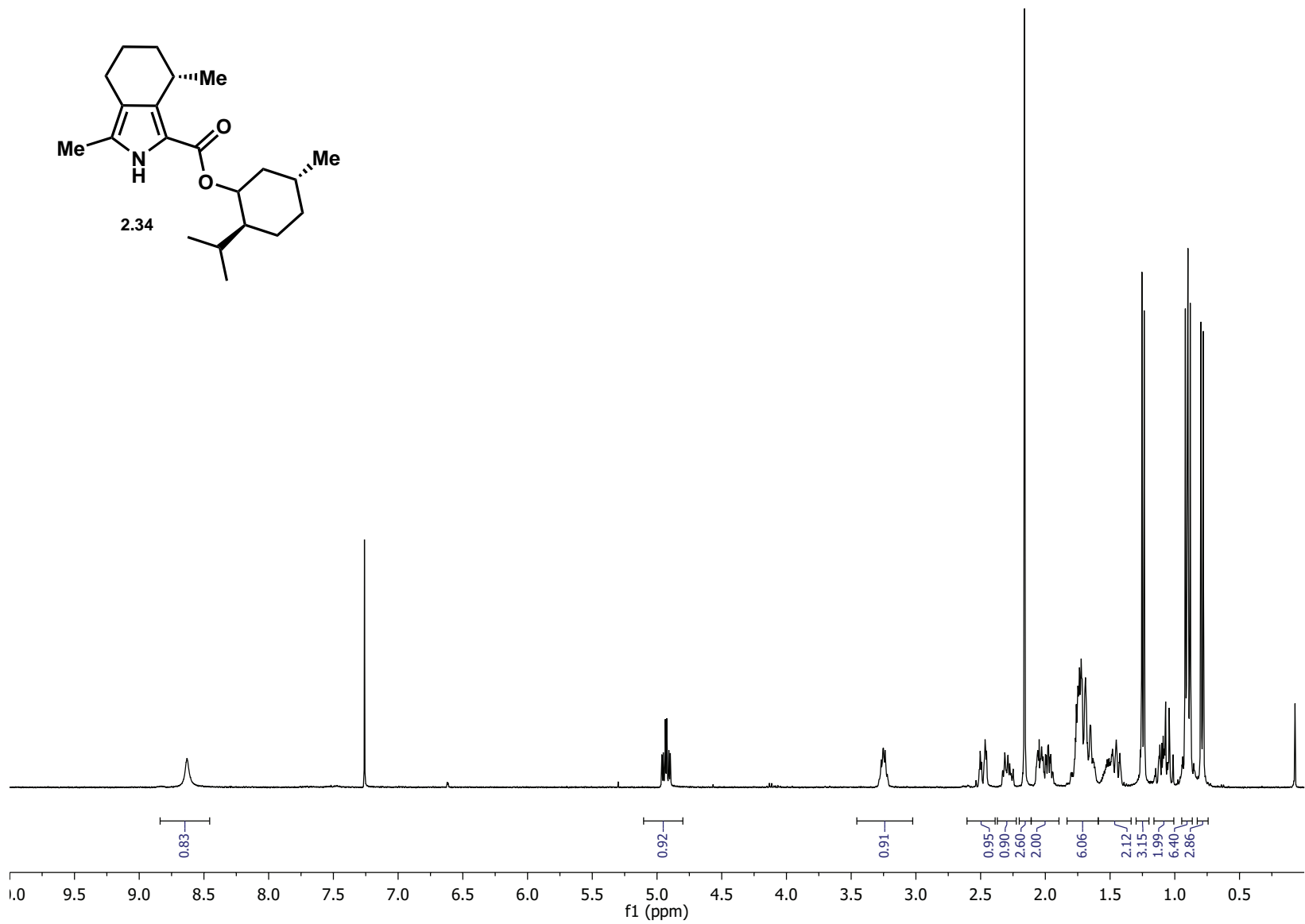


Figure 2.30: ¹H NMR of 2.34 in CDCl₃

1C_111-032dest1 car1
WB-00 ZBO Carbon Shifting parameters 6/11/03 RM

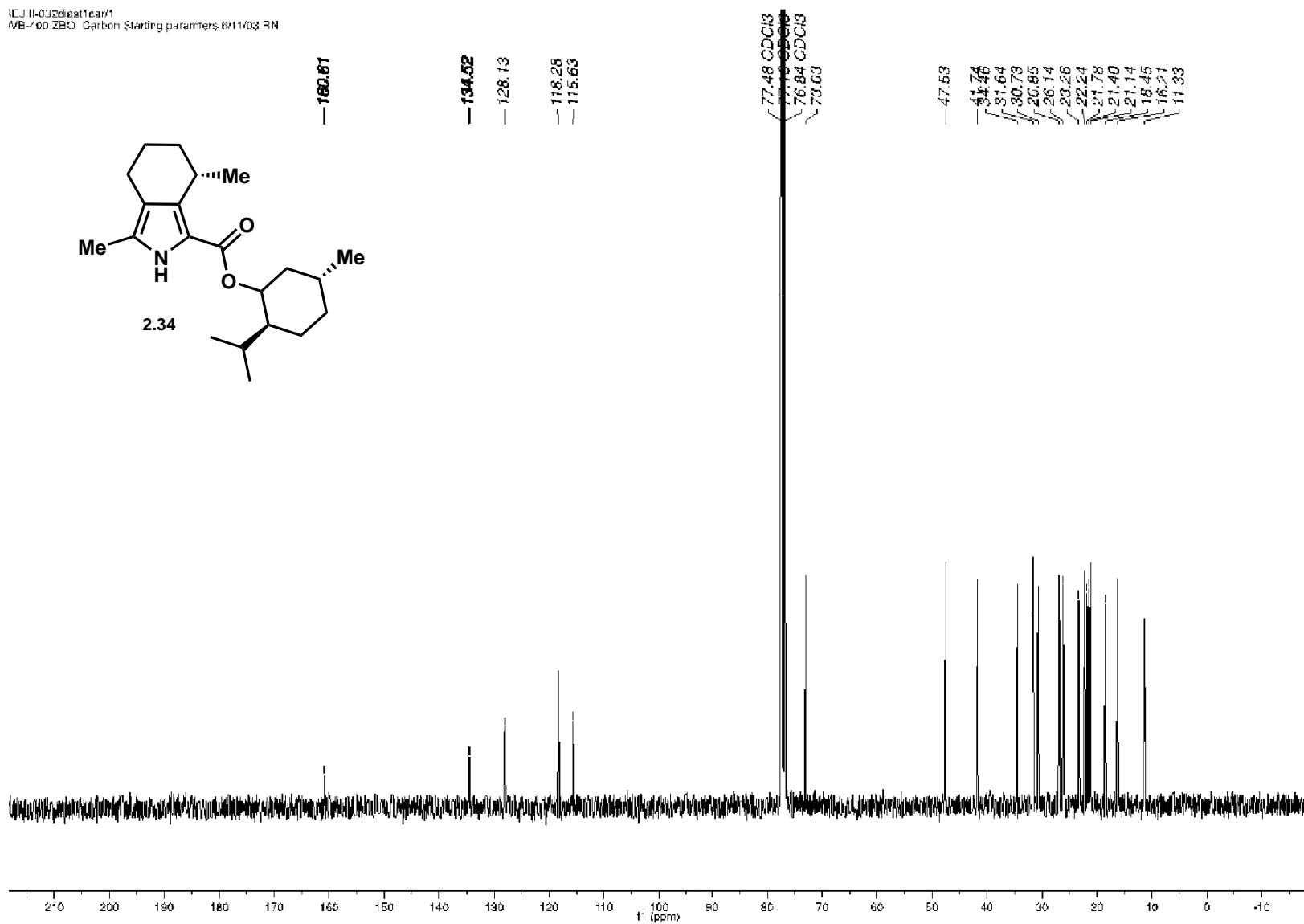


Figure 2.31: ¹³C NMR of 2.34 in CDCl₃

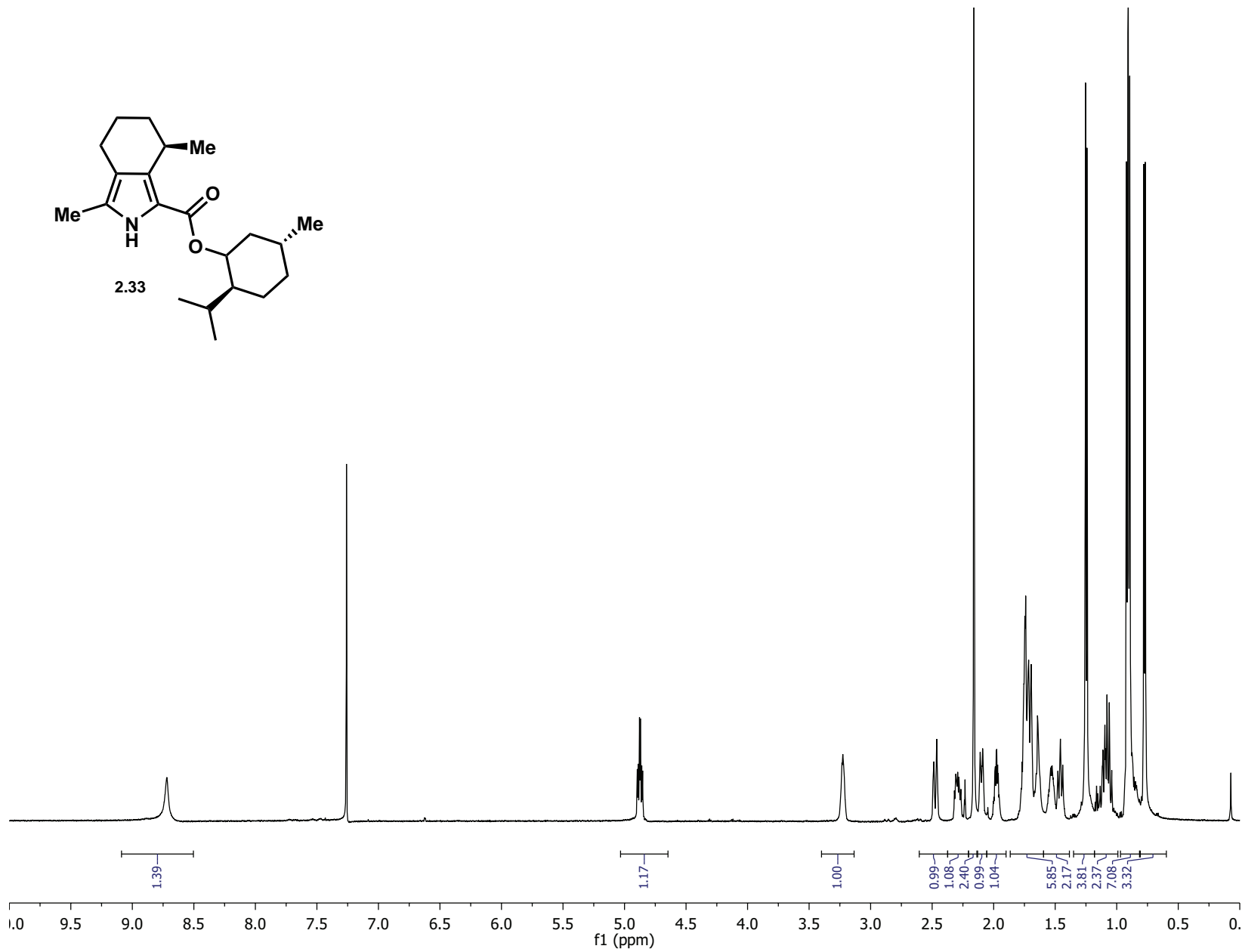
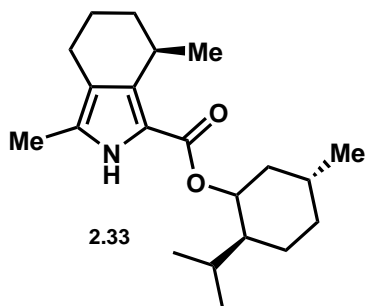


Figure 2.32: ^1H NMR of 2.33 in CDCl_3

2.b : X-ray Crystallographic Data Relevant to Chapter 2

X-ray Crystallography Data

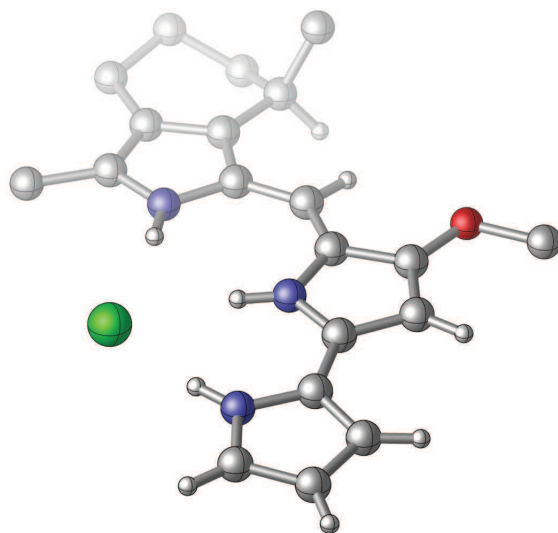


Figure 2.34: X-ray crystal structure of **1.57**

A purple plate 0.050 x 0.040 x 0.020 mm in size was mounted on a Cryoloop with Paratone oil. Data were collected in a nitrogen gas stream at 100(2) K using phi and omega scans. Crystal-to-detector distance was 60 mm and exposure time was 10 seconds per frame using a scan width of 2.0°. Data collection was 100.0% complete to 67.000° in θ . A total of 27626 reflections were collected covering the indices, $-13 \leq h \leq 13$, $-8 \leq k \leq 8$, $-15 \leq l \leq 15$. 3342 reflections were found to be symmetry independent, with an R_{int} of 0.0503. Indexing and unit cell refinement indicated a primitive, monoclinic lattice. The space group was found to be P 21 (No. 4). The data were integrated using the Bruker SAINT software program and scaled using the SADABS software program. Solution by iterative methods (SHELXT) produced a complete heavy-atom phasing model consistent with the proposed structure. All non-hydrogen atoms were refined anisotropically by full-matrix least-squares (SHELXL-2014). All hydrogen atoms were placed using a riding model. Their positions were constrained relative to their parent atom using the appropriate HFIX command in SHELXL-2014. Absolute stereochemistry was unambiguously determined to be *R* at C6.

Table 2.1: Crystal data and structure refinement for **1.57**.

X-ray ID	sarpong111	
Sample/notebook ID	REJIII-035E2	
Empirical formula	C ₂₀ H ₂₄ Cl N ₃ O	
Formula weight	357.87	
Temperature	100(2) K	
Wavelength	1.54178 Å	
Crystal system	Monoclinic	
Space group	P 21	
Unit cell dimensions	a = 10.8680(8) Å b = 6.8325(6) Å c = 12.6102(10) Å	a = 90°. b = 103.793(5)°. g = 90°.
Volume	909.38(13) Å ³	
Z	2	
Density (calculated)	1.307 Mg/m ³	
Absorption coefficient	1.952 mm ⁻¹	
F(000)	380	
Crystal size	0.050 x 0.040 x 0.020 mm ³	
Theta range for data collection	3.609 to 69.145°.	
Index ranges	-13<=h<=13, -8<=k<=8, -15<=l<=15	
Reflections collected	27626	
Independent reflections	3342 [R(int) = 0.0503]	
Completeness to theta = 67.000°	100.00%	
Absorption correction	Semi-empirical from equivalents	
Max. and min. transmission	0.929 and 0.809	
Refinement method	Full-matrix least-squares on F ²	
Data / restraints / parameters	3342 / 1 / 229	
Goodness-of-fit on F ²	1.047	
Final R indices [I>2sigma(I)]	R1 = 0.0467, wR2 = 0.1104	
R indices (all data)	R1 = 0.0562, wR2 = 0.1169	
Absolute structure parameter	0.054(12)	
Extinction coefficient	n/a	
Largest diff. peak and hole	0.521 and -0.166 e.Å ⁻³	

Table 2.2: Atomic coordinates ($\times 10^4$) and equivalent isotropic displacement parameters ($\text{\AA}^2 \times 10^3$) for sarpong111. $U(\text{eq})$ is defined as one third of the trace of the orthogonalized U^{ij} tensor.

	x	y	z	$U(\text{eq})$
C(1)	5116(3)	4446(8)	321(3)	27(1)
C(2)	6354(3)	4400(8)	174(3)	27(1)
C(3)	6765(4)	4333(9)	-886(3)	33(1)
C(4)	8198(4)	4627(11)	-671(3)	41(1)
C(5)	8919(4)	3536(7)	346(4)	38(1)
C(6)	8585(3)	4312(8)	1392(3)	31(1)
C(7)	7169(3)	4397(7)	1201(3)	27(1)
C(8)	6432(3)	4486(8)	1990(3)	25(1)
C(9)	3889(3)	4436(9)	-520(3)	31(1)
C(10)	9212(4)	6271(8)	1746(4)	42(1)
C(11)	6898(3)	4557(8)	3115(3)	27(1)
C(12)	6362(3)	4676(8)	3995(3)	26(1)
C(13)	7045(3)	4765(7)	5109(3)	29(1)
C(14)	6217(4)	4801(7)	5778(3)	31(1)
C(15)	5003(3)	4730(7)	5080(3)	28(1)
C(16)	8870(4)	4950(11)	6519(4)	53(2)
C(17)	3825(3)	4732(7)	5419(3)	30(1)
C(18)	3664(4)	4710(8)	6472(3)	32(1)
C(19)	2354(4)	4723(8)	6398(3)	35(1)
C(20)	1760(4)	4765(8)	5312(4)	38(1)
N(1)	5177(3)	4494(7)	1404(2)	26(1)
N(2)	5087(3)	4672(6)	4031(2)	26(1)
N(3)	2656(3)	4750(7)	4723(3)	35(1)
O(1)	8314(2)	4847(6)	5363(2)	38(1)
Cl(1)	2599(1)	4457(2)	2184(1)	37(1)

Table 2.3: Bond lengths [\AA] for sarpong111.

C(1)-N(1)	1.352(4)	C(4)-C(5)-C(6)	111.8(4)
C(1)-C(2)	1.401(5)	C(4)-C(5)-H(5A)	109.2
C(1)-C(9)	1.492(5)	C(6)-C(5)-H(5A)	109.2
C(2)-C(7)	1.383(5)	C(4)-C(5)-H(5B)	109.2
C(2)-C(3)	1.508(5)	C(6)-C(5)-H(5B)	109.2
C(3)-C(4)	1.530(5)	H(5A)-C(5)-H(5B)	107.9
C(3)-H(3A)	0.99	C(7)-C(6)-C(10)	112.6(4)
C(3)-H(3B)	0.99	C(7)-C(6)-C(5)	108.5(3)
C(4)-C(5)	1.528(7)	C(10)-C(6)-C(5)	111.9(4)
C(4)-H(4A)	0.99	C(7)-C(6)-H(6)	107.9

C(4)-H(4B)	0.99	C(10)-C(6)-H(6)	107.9
C(5)-C(6)	1.542(6)	C(5)-C(6)-H(6)	107.9
C(5)-H(5A)	0.99	C(2)-C(7)-C(8)	108.3(3)
C(5)-H(5B)	0.99	C(2)-C(7)-C(6)	123.6(3)
C(6)-C(7)	1.501(5)	C(8)-C(7)-C(6)	128.1(3)
C(6)-C(10)	1.520(7)	N(1)-C(8)-C(11)	128.1(3)
C(6)-H(6)	1	N(1)-C(8)-C(7)	105.9(3)
C(7)-C(8)	1.420(5)	C(11)-C(8)-C(7)	126.0(3)
C(8)-N(1)	1.388(4)	C(1)-C(9)-H(9A)	109.5
C(8)-C(11)	1.388(5)	C(1)-C(9)-H(9B)	109.5
C(9)-H(9A)	0.98	H(9A)-C(9)-H(9B)	109.5
C(9)-H(9B)	0.98	C(1)-C(9)-H(9C)	109.5
C(9)-H(9C)	0.98	H(9A)-C(9)-H(9C)	109.5
C(10)-H(10A)	0.98	H(9B)-C(9)-H(9C)	109.5
C(10)-H(10B)	0.98	C(6)-C(10)-H(10A)	109.5
C(10)-H(10C)	0.98	C(6)-C(10)-H(10B)	109.5
C(11)-C(12)	1.374(5)	H(10A)-C(10)-H(10B)	109.5
C(11)-H(11)	0.95	C(6)-C(10)-H(10C)	109.5
C(12)-N(2)	1.397(4)	H(10A)-C(10)-H(10C)	109.5
C(12)-C(13)	1.425(5)	H(10B)-C(10)-H(10C)	109.5
C(13)-O(1)	1.341(4)	C(12)-C(11)-C(8)	134.9(3)
C(13)-C(14)	1.372(5)	C(12)-C(11)-H(11)	112.6
C(14)-C(15)	1.401(5)	C(8)-C(11)-H(11)	112.6
C(14)-H(14)	0.95	C(11)-C(12)-N(2)	129.9(3)
C(15)-N(2)	1.348(4)	C(11)-C(12)-C(13)	125.3(3)
C(15)-C(17)	1.443(5)	N(2)-C(12)-C(13)	104.8(3)
C(16)-O(1)	1.440(5)	O(1)-C(13)-C(14)	129.8(4)
C(16)-H(16A)	0.98	O(1)-C(13)-C(12)	120.1(3)
C(16)-H(16B)	0.98	C(14)-C(13)-C(12)	110.0(3)
C(16)-H(16C)	0.98	C(13)-C(14)-C(15)	105.7(3)
C(17)-N(3)	1.362(5)	C(13)-C(14)-H(14)	127.1
C(17)-C(18)	1.381(5)	C(15)-C(14)-H(14)	127.1
C(18)-C(19)	1.404(5)	N(2)-C(15)-C(14)	110.1(3)
C(18)-H(18)	0.95	N(2)-C(15)-C(17)	124.2(3)
C(19)-C(20)	1.368(6)	C(14)-C(15)-C(17)	125.7(3)
C(19)-H(19)	0.95	O(1)-C(16)-H(16A)	109.5
C(20)-N(3)	1.358(5)	O(1)-C(16)-H(16B)	109.5
C(20)-H(20)	0.95	H(16A)-C(16)-H(16B)	109.5
N(1)-H(1)	0.88	O(1)-C(16)-H(16C)	109.5
N(2)-H(2)	0.88	H(16A)-C(16)-H(16C)	109.5
N(3)-H(3)	0.88	H(16B)-C(16)-H(16C)	109.5
N(1)-C(1)-C(2)	108.5(3)	N(3)-C(17)-C(18)	107.9(3)
N(1)-C(1)-C(9)	122.5(3)	N(3)-C(17)-C(15)	124.5(3)
C(2)-C(1)-C(9)	129.0(3)	C(18)-C(17)-C(15)	127.6(4)
C(7)-C(2)-C(1)	107.3(3)	C(17)-C(18)-C(19)	107.2(3)

C(7)-C(2)-C(3)	124.8(3)	C(17)-C(18)-H(18)	126.4
C(1)-C(2)-C(3)	127.9(3)	C(19)-C(18)-H(18)	126.4
C(2)-C(3)-C(4)	110.1(3)	C(20)-C(19)-C(18)	107.2(3)
C(2)-C(3)-H(3A)	109.6	C(20)-C(19)-H(19)	126.4
C(4)-C(3)-H(3A)	109.6	C(18)-C(19)-H(19)	126.4
C(2)-C(3)-H(3B)	109.6	N(3)-C(20)-C(19)	108.6(3)
C(4)-C(3)-H(3B)	109.6	N(3)-C(20)-H(20)	125.7
H(3A)-C(3)-H(3B)	108.2	C(19)-C(20)-H(20)	125.7
C(5)-C(4)-C(3)	112.4(4)	C(1)-N(1)-C(8)	110.1(3)
C(5)-C(4)-H(4A)	109.1	C(1)-N(1)-H(1)	125
C(3)-C(4)-H(4A)	109.1	C(8)-N(1)-H(1)	125
C(5)-C(4)-H(4B)	109.1	C(15)-N(2)-C(12)	109.3(3)
C(3)-C(4)-H(4B)	109.1	C(15)-N(2)-H(2)	125.3
H(4A)-C(4)-H(4B)	107.9	C(12)-N(2)-H(2)	125.3
		C(20)-N(3)-C(17)	109.1(3)
		C(20)-N(3)-H(3)	125.4
		C(17)-N(3)-H(3)	125.4
		C(13)-O(1)-C(16)	113.8(3)

Symmetry transformations used to generate equivalent atoms:

Table 2.4: Anisotropic displacement parameters ($\text{\AA}^2 \times 10^3$) for sarpong111. The anisotropic displacement factor exponent takes the form: $-2\pi^2 [h^2 a^{*2} U^{11} + \dots + 2 h k a^* b^* U^{12}]$

	U^{11}	U^{22}	U^{33}	U^{23}	U^{13}	U^{12}
C(1)	27(2)	21(2)	34(2)	-2(2)	10(1)	-4(2)
C(2)	30(2)	21(2)	31(2)	-3(2)	10(1)	-2(2)
C(3)	33(2)	35(2)	32(2)	2(2)	10(2)	0(2)
C(4)	32(2)	58(3)	37(2)	-2(3)	16(2)	-1(3)
C(5)	30(2)	45(3)	44(3)	-1(2)	17(2)	4(2)
C(6)	23(2)	36(2)	36(2)	2(2)	10(1)	1(2)
C(7)	26(2)	20(2)	38(2)	0(2)	13(2)	0(2)
C(8)	23(2)	21(2)	34(2)	0(2)	10(1)	0(2)
C(9)	28(2)	29(2)	36(2)	-3(2)	7(1)	-1(3)
C(10)	24(2)	49(3)	56(3)	-11(2)	14(2)	-2(2)
C(11)	23(2)	24(2)	37(2)	8(2)	11(1)	3(2)
C(12)	23(2)	23(2)	36(2)	1(2)	11(1)	1(2)
C(13)	25(2)	31(3)	35(2)	4(2)	12(2)	4(2)
C(14)	30(2)	34(3)	31(2)	-2(2)	13(2)	3(2)
C(15)	29(2)	22(2)	34(2)	1(2)	13(1)	3(2)
C(16)	28(2)	92(5)	38(2)	0(3)	7(2)	9(3)
C(17)	27(2)	27(2)	37(2)	-2(2)	12(1)	-3(2)
C(18)	29(2)	33(2)	38(2)	-3(2)	13(2)	-3(2)
C(19)	31(2)	37(3)	42(2)	-2(2)	18(2)	-6(2)

Table 2.4: Anisotropic displacement parameters ($\text{\AA}^2 \times 10^3$) for sarpong111. The anisotropic displacement factor exponent takes the form: $-2\pi^2 [h^2 a^{*2} U^{11} + \dots + 2 h k a^* b^* U^{12}]$

	U^{11}	U^{22}	U^{33}	U^{23}	U^{13}	U^{12}
C(20)	24(2)	41(3)	54(2)	-1(3)	19(2)	-3(2)
N(1)	20(1)	25(2)	34(1)	2(2)	11(1)	2(2)
N(2)	20(1)	29(2)	30(1)	2(2)	8(1)	-2(2)
N(3)	27(2)	43(2)	36(2)	1(2)	13(1)	1(2)
O(1)	22(1)	60(3)	32(1)	-4(2)	7(1)	4(2)
Cl(1)	23(1)	52(1)	37(1)	3(1)	9(1)	-1(1)

Table 2.5: Hydrogen coordinates ($\times 10^4$) and isotropic displacement parameters ($\text{\AA}^2 \times 10^3$) for sarpong111.

	x	y	z	U(eq)
H(3A)	6325	5373	-1381	40
H(3B)	6531	3054	-1247	40
H(4A)	8493	4161	-1311	49
H(4B)	8392	6041	-581	49
H(5A)	9841	3683	415	46
H(5B)	8712	2125	265	46
H(6)	8906	3348	1990	37
H(9A)	3185	4458	-157	47
H(9B)	3834	3251	-966	47
H(9C)	3842	5593	-987	47
H(10A)	8897	7251	1179	64
H(10B)	10132	6142	1858	64
H(10C)	9011	6684	2430	64
H(11)	7797	4512	3324	33
H(14)	6424	4862	6552	37
H(16A)	8525	6082	6828	79
H(16B)	9791	5088	6644	79
H(16C)	8672	3751	6871	79
H(18)	4317	4689	7125	39
H(19)	1955	4707	6991	42
H(20)	870	4798	5019	45
H(1)	4517	4525	1694	31
H(2)	4439	4637	3459	31
H(3)	2504	4752	4005	41

Chapter 3

The Isolation, Bioactivity, and Synthetic Background of the Pentacyclic Ambiguine Natural Products

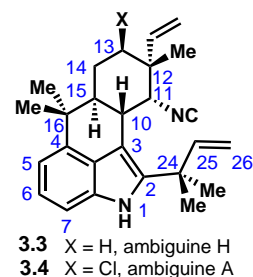
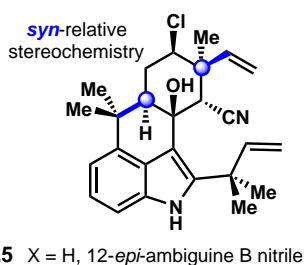
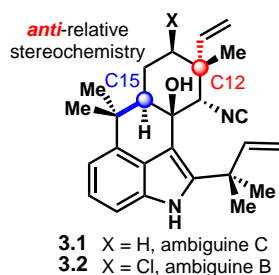
3.1 The Isolation and Bioactivity of Ambiguine Natural Products

The pentacyclic ambiguity family of natural products comprise a highly intriguing class of indole alkaloid secondary metabolites and are a part of the larger hapalindole alkaloid family of natural products. The ambiguines have been of interest to both isolation and synthetic chemists since their first isolation report in 1992.¹ The majority of the tetracyclic and pentacyclic ambiguines have been isolated from the terrestrial strain of cyanobacteria known as *Fischerella ambigua*, from which the name "ambiguine" originates. *Fischerella ambigua* was first discovered in 1895 by Kützing and Flahault in Zurich and has subsequently been recovered from many other continental sources.² It is currently maintained as the purchasable strain UTEX 1903. Ambiguine G has been the only congener to be isolated from the related cyanobacterial freshwater strain known as *Hapalosiphon delicatulus*.³ This strain of cyanobacteria was first reported in 1902 by West and West from the island of Sri Lanka, formerly the British colony Ceylon.⁴ This strain is also maintained by the University of Hawaii as UH isolate BZ-3-1.

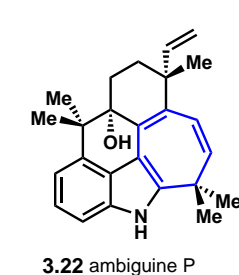
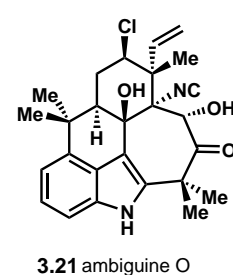
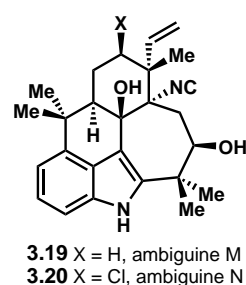
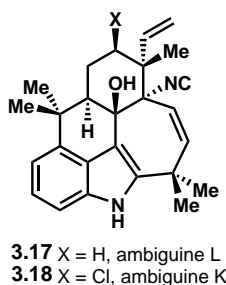
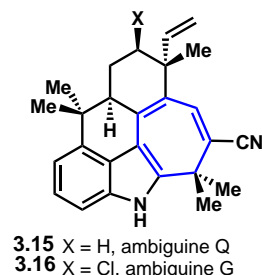
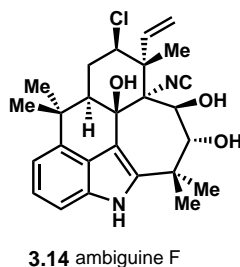
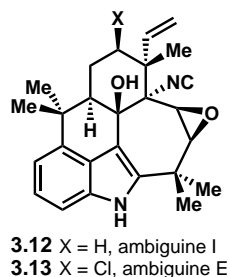
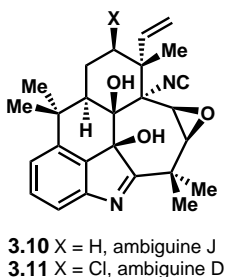
As shown in Figure 3.1, to date there are 13 known pentacyclic ambiguines and 5 known tetracyclic ambiguity natural products. These compounds typically exist with the "anti" relative stereochemistry as shown for ambiguines C (**3.1**) and B (**3.2**). This terminology specifically refers to the relationship between the vinyl group at C12 and the C15 substituent. Pentacyclic ambiguines coexist with their tetracyclic counterparts (e.g. **3.3**, **3.4**, **3.1**, **3.2**, and **3.5**) in which the reverse-prenyl group attached to the C2-position of the indole moiety oxidatively cyclizes to form the characteristic 7-membered E-ring of the pentacyclic congeners. It is presumed that these two classes are related biosynthetically and their relationship will be discussed further in this chapter. In addition to the tetra and pentacyclic ambiguity natural products, there also exists related classes of natural products such as the tricyclic hapalindoles (**3.6**), tetracyclic hapalindoles (**3.7**), fischerindoles (**3.8**), and welwitindolinones (**3.9**). While the focus of this chapter is on the ambiguity class, these other classes will be briefly discussed as well.

The existence of pentacyclic ambiguity natural products was first reported in 1992 by Smitka

a. Tetracyclic ambiguines isolated to date:



b. Pentacyclic ambiguines isolated to date:



c. Related hapalindole family natural product cores:

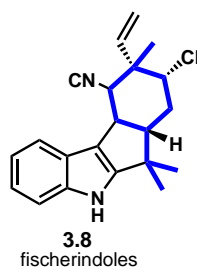
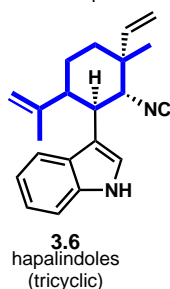


Figure 3.1: Family of ambigaine natural products isolated since 1992.

and coworkers at the University of Hawaii in a collaboration with Eli Lilly, in which they identified a strain of blue-green algae as having moderately potent fungicidal activity.¹ Their initial report detailed the isolation of pentacyclic ambiguines D through F which also included the first isolation of tetracyclic ambigaine natural products A through C. Hapalindole natural products had been known in the literature for at least a decade,⁵ and the ambiguines were clearly related by the addition of a single reverse-prenyl group connected to C2 of the indole foundation.

While ambiguines A (**3.4**) through C (**3.1**) are all tetracyclic in nature, oxidatively cyclized

compounds D (**3.11**), E (**3.23**), and F (**3.24**) are pentacyclic in nature. These pentacyclic ambiguiene natural products vary in their level and pattern of oxygenation throughout the pentacyclic core. Smitka's team also conducted initial bioactivity assays, specifically looking at antifungal activity against three different fungal organisms; the resulting data is tabulated in Table 3.1.

Table 3.1

Fungicide <i>in vitro</i> MIC values ($\mu\text{g/mL}$) adapted from Smitka et. al. 1992			
cmpd	<i>C. albicans</i>	<i>T. Mentagrophytes</i>	<i>A. fumigatus</i>
3.4	2.5 ^{a,b}	10 ^a , >20 ^b	80 ^a
3.2	1.25 ^{a,b}	>80 ^a , 2.5 ^b	20 ^a
3.1	2.5 ^a , 1.25 ^b	>80 ^a , 0.625 ^b	>80 ^a
3.11	1.25 ^{a,b}	>80 ^a , 0.625 ^b	>80 ^a
3.13	5.0 ^a , 2.5 ^b	5 ^a , 2.5 ^b	>80 ^a
3.14	1.25 ^{a,b}	>80 ^a , 1.25 ^b	>80 ^a
amphotericin B	0.312 ^a , 0.156 ^b		1.25 ^a
tolnaftate		<0.02 ^{a,b}	

^aTested in Sabouraud dextrose broth.

^bTested in RPMI broth supplemented with 10% calf serum.

The next isolation report of a pentacyclic ambiguiene was a description by Moore and coworkers in 1998 characterizing ambiguiene G (**3.16**) as the first nitrile containing pentacyclic natural product.³ Ambiguiene G was isolated from the related strain of freshwater cyanobacteria known as *Hapalosiphon delicatulus*. Notably, the isolation chemists identified a conjugated cyano-group located on the seven-membered homoaromatic ring and also concluded the absence of both hydroxyl and isonitrile functionalities typically present in previously isolated pentacyclic ambiguienes.

Carmeli and coworkers in 2007 next reported the isolation of three new pentacyclic ambiguienes H (**3.3**), I (**3.12**), and J (**3.10**) which are the non-chlorinated congeners of ambiguienes A (**3.4**), E (**3.13**), and D (**3.11**) respectively.⁶ Carmeli's group from Tel Aviv University also conducted some preliminary *in vitro* antibacterial and antifungal assays for ambiguienes H (**3.3**) and I (**3.12**) as shown in Table 3.2, demonstrating their moderately potent activity against bacterial and fungal organisms.

In 2009, Orjala and coworkers from the University of Illinois–Chicago identified five new pentacyclic ambiguienes also exhibiting moderate antifungal and antibacterial activity. Orjala's group conducted assays using the 11 ambiguienes they were able to isolate from *Fischerella ambigua* UTEX 1903 and the results are reported in Table 3.3.⁷ They identified ambiguienes K (**3.18**) and M (**3.19**) as having moderately potent MIC values in the μM range against *M. tuberculosis*, with values of 6.6 and 7.5 μM , respectively. In addition, ambiguiene A (**3.4**) showed potent activity against *B. anthracis* with an MIC value of 1.0 μM . Remarkably, the majority of the ambiguienes showed fairly potent activity against the fungus *C. albicans*.

Finally, the last isolation report of ambiguienes was reported in 2010 by Orjala's group in which they disclosed the structures of ambiguienes P (**3.22**) and Q (**3.15**).⁸ They also reported the isolation of the chlorinated congener of ambiguiene Q, already known as ambiguiene G (**3.16**) which was

Table 3.2

<i>In vitro</i> MIC values ($\mu\text{g/mL}$) adapted from Carmeli and Raveh in 2007					
cmpd	<i>E. coli</i> ESS K-12 ^a	<i>S. albus</i> ^a	<i>B. subtilis</i> ^a	<i>S. cerevisiae</i> ^b	<i>C. albicans</i> ATCC 90028 ^b
3.3	10	0.625	1.25	5	6.25 ^c
3.12	2.5	0.078	0.312	0.312	0.39 ^c
streptomycin	0.312	0.156	2.5	--	--
puramycin	--	--	--	0.312	--
amphotericin B	--	--	--	1.56	--

^aTested in LB broth.

^bTested in YPD broth.

^cFungistatic

previously isolated in 1998. Ambiguine P (**3.22**) is unique from the other pentacyclic ambiguines as it is the only compound without an isonitrile or nitrile moiety. The antibacterial and antifungal activity for ambiguines P and G was evaluated (Table 3.3), however, they were not able to isolate Q in enough quantity to acquire bioactivity data. Ambiguine P (**3.22**) was not tested against all fungal and bacterial strains but showed moderate antifungal activity against *C. albicans* with an MIC of 32.9 μM . In addition, ambiguityne G showed fairly potent antibacterial activity against *S. aureus* with an MIC of 6.6 μM .

The most recently isolated ambiguityne in 2014 is 12-*epi*-ambiguine B nitrile **3.5** by Berry and coworkers.⁹ This compound represents an extremely unique ambiguityne as it is currently the only known ambiguityne to possess the "*syn*" relationship between C12 and C15. In addition, **3.5** is the only ambiguityne to contain a nitrile functionality at the C11 position out of the 70+ natural products in the hapalindole family. Given these novel characteristics associated with **3.5**, unambiguous characterization by X-ray crystallography may be required to confirm the structure of **3.5**. In addition, there has been no antifungal or antibacterial bioactivity data reported for this unique structure.

While a mechanism of action has not yet been determined for the antibacterial and antifungal activity demonstrated by the ambiguines, ambiguityne I (**3.12**) has been identified specifically as a potent NF-KB inhibitor with an IC_{50} value of 30 nM leading to antiproliferative effects in the MCF-7 breast cancer cell line.¹⁰ Ambiguine I has also been evaluated for cytotoxic activity against both the HT-29 colon cancer cell line ($\text{EC}_{50} = 4.35 \mu\text{M}$) in addition to the MCF-7 breast cancer cell line ($\text{EC}_{50} = 1.7 \mu\text{M}$). In the report by Carcache de Blanco and coworkers, assay data was presented suggesting that ambiguityne I causes mitochondrial dysfunction leading to non-caspase dependent apoptosis. This information is promising for future studies of these molecules as chemotherapeutic agents that uniquely act through an alternative mechanism as compared to the more standard caspase-dependent cell death pathway.

Another instance of noteworthy bioactivity was reported by the group of Matsumoto from the University of Tsukuba in which they identified ambiguityne D as having plant growth suppression activity.¹¹ The Matsumoto group identified **3.11** through fractionation of the Hapalosiphon species of cyanobacteria guided by a lettuce seedling bioassay. Further exploration into the mechanism of

Table 3.3

<i>In vitro</i> MIC values ($\mu\text{g/mL}$) adapted from Orjala et. al. in 2009 and 2010						
cmpd	<i>M. tuberculosis</i>	<i>B. anthracis</i>	<i>S. aureus</i>	<i>M. smegmatis</i>	<i>C. albicans</i>	Vero cells
3.18	6.6	7.4	4.6	23.7	<0.9	53.2
3.17	11.7	16.2	10.5	19.3	<1.0	44.6
3.19	7.5	28.5	4.7	25.8	1.1	79.8
3.20	27.1	30.9	5.5	48.8	<1.0	118.4
3.21	--	13.8	--	--	--	80.7
3.4	46.7	1.0	1.8	14.8	<1.0	26.0
3.2	--	3.7	10.9	27.8	1.7	58.6
3.1	7.0	16.1	7.4	59.6	<1.0	78.3
3.13	21.0	3.6	1.5	1.4	<0.9	42.6
3.14	61.2	--	--	--	--	57.9
3.12	13.1	>128	8.9	59.7	1.7	>128
3.22	>100	--	>100	--	32.9	--
3.16	53.7	>100	6.6	49.7	>100	--
rifampin	0.1					
ciprofloxacin		0.2				
gentamicin			1.4			
moxifloxacin				0.7		
ketoconazole					0.03	

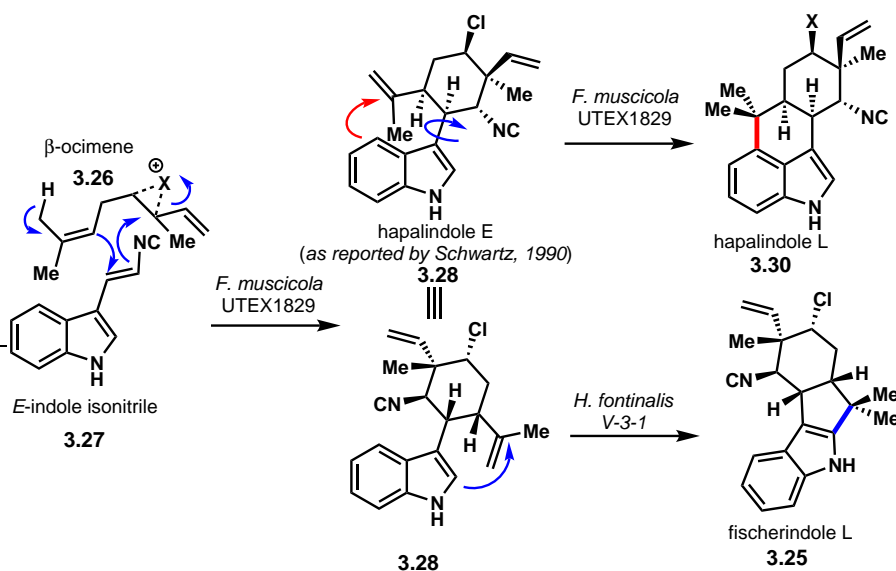
action for the phytotoxic activity led to the discovery that ambigaine D specifically increased the concentration of reactive oxygen species in lettuce root cells leading to peroxidation of lipids. This oxidative stress inhibited mitosis leading to cell death. Interestingly, this is the only known report for phytotoxic activity exhibited by an ambigaine isonitrile and gives promise to their potential use as herbicide agents.

3.2 Biosynthetic Investigations of Hapalindole and Ambigaine Natural Products

In addition to their interesting bioactivity, the biosynthesis of the pentacyclic ambigaines has also been intensely explored. Two groups (Xinyu Liu from the University of Pittsburgh and David Sherman from the University of Michigan) have largely dominated the field of hapalindole/ambigaine biosynthesis and have recently reported some groundbreaking results that have changed the way chemists had previously thought about how these molecules are made in nature.

Initial speculation regarding the biosynthesis of hapalindole natural products began in 1992 when Moore and Patterson isolated a new fischerindole, fischerindole L (**3.25**), and in addition, provided a straightforward biosynthetic proposal leading to **3.25** (Scheme 3.1).¹² In Moore and Patterson's proposal they showed a stepwise synthesis commencing with the cyclization of β -ocimene (**3.26**) and the *E*-indole isonitrile (**3.27**) to generate directly tricyclic hapalindole E (the structure of which is disputed in the literature but was originally reported as **3.28**¹³) using an electrophilic chlorine source as an initiator as shown in Scheme 3.1. It should be noted that while the

Z-isomer of indole isonitrile (**3.29**, Scheme 3.2) was known at the time for its antibiotic properties, there wasn't a reported structure for the *E*-isomer (i.e., **3.27**). However, **3.27** was later confirmed as a natural product in 2004 from an unrelated strain of bacteria.¹⁴ From hapalindole E (**3.28**), Moore and Patterson indicated that depending on the strain of cyanobacteria (i.e. *F. muscicola* or *H. fontinalis*) it could further cyclize to furnish hapalindole L (**3.30**) or fischerindole L (**3.25**) respectively.

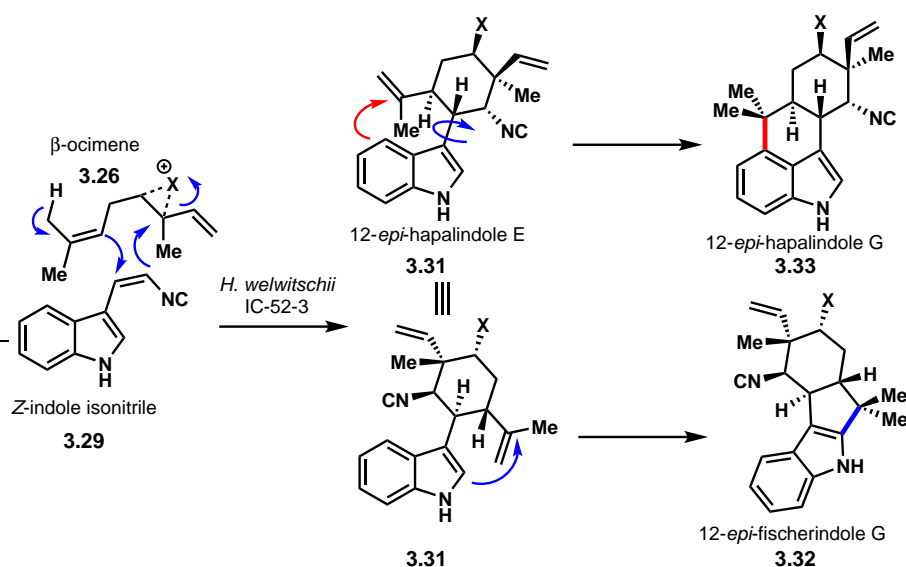


Scheme 3.1: Moore's initial biosynthetic proposal reported in 1992 which commenced with the cyclization of β -ocimene and *E*-indole isonitrile (**3.27**) to form the tricyclic intermediate hapalindole E (**3.28**).

This 1992 proposal was then elaborated upon by Moore with Eli Lilly collaborators in 1994¹⁵ to include the cyclization of *Z*-indole isonitrile **3.29**, which purportedly generated 12-*epi*-hapalindole E (**3.31**) in the related strain of cyanobacteria *H. welwitschii* (Scheme 3.2). Compound **3.31** could further cyclize to furnish 12-*epi*-fischerindole G (**3.32**). While Moore and Smitka did not isolate 12-*epi*-hapalindole G (**3.33**) from the *H. welwitschii* crude material, they proposed that cyclization of **3.31** at C4 (red arrows) could also yield tetracyclic 12-*epi*-hapalindole G (**3.33**).

These proposals by Moore, Patterson, and Smitka went unchallenged until another proposal emerged in 2007 by Carmeli and coworkers.⁶ In Carmeli's proposal, they suggested a concerted one-step cyclization pathway leading directly to the tetracyclic hapalindoles, hapalindole G (**3.34**), U (**3.35**), and 12-*epi*-hapalindole H (**3.36**) as shown in Scheme 3.3. In this case, Carmeli also invoked β -ocimene (**3.26**) as the terpene unit that cyclizes concertedly onto *Z*-indole isonitrile **3.29** to form hapalindoles G (**3.34**) and U (**3.35**) directly. This proposal arose after the Carmeli group isolated only tetra- or pentacyclic ambiguines from the Fischerella source of cyanobacteria IL-199-3-1. This finding suggested that the tricyclic compounds are not necessarily biosynthetic intermediates towards the tetra and pentacyclic hapalindoles/ambiguines as was assumed by Moore in 1992 and 1994.

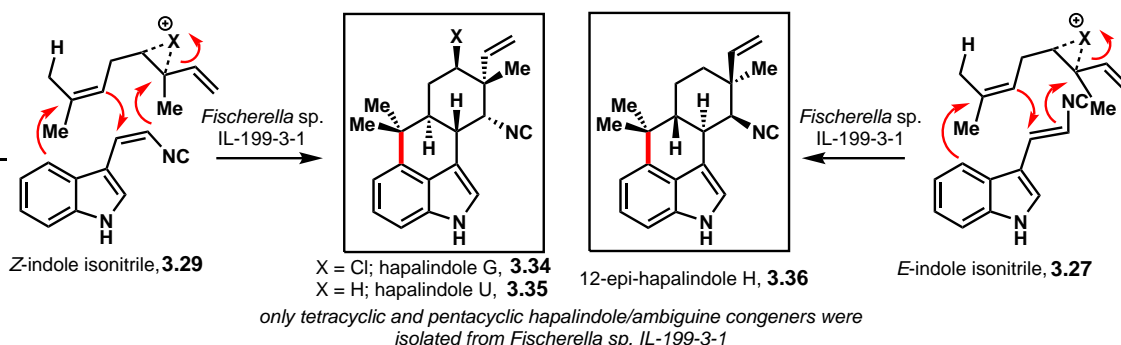
The biosynthetic cyclizations proposed by Moore, Patterson, and Carmeli were generally accepted and recommunicated in other articles published between 1992 and 2013.¹⁶ The first study aimed at identifying gene clusters responsible for the biosynthesis of hapalindole and ambiguine



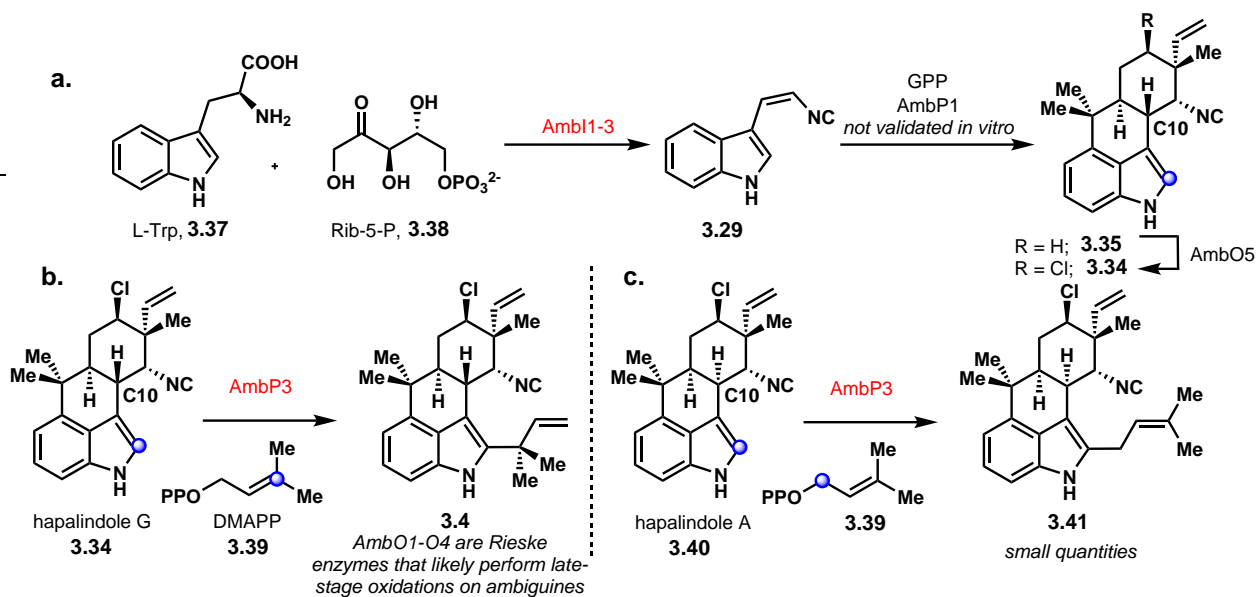
Scheme 3.2: Moore and Smitka's 1994 biosynthetic hypothesis implicating tricycle **3.31** as a precursor to fischerindole and tetracyclic hapalindole cores in the *H. welwitschii* species of cyanobacteria.

natural products was a seminal paper reported by the Liu group in 2014.¹⁷ In this report, Liu disclosed the 42 kbp gene cluster in *Fischerella ambigua* responsible for hapalindole and ambiguine biosynthesis in addition to identifying enzymes for key biosynthetic steps which they named with the precursor "Amb". As shown in Scheme 3.4, AmbI1-3 were determined to be responsible for the formation of the *Z*-indole isonitrile precursor (**3.29**) and the unique mechanism for this process was reported by the same group in 2017.¹⁸ In this 2017 paper, Liu also showed that in support of Moore and Carmeli's proposals, it is possible for AmbI1-3 to produce the *E*-isomer of the indole isonitrile intermediate (**3.27**), however, the production of the *Z*-isomer is far more robust.

Not all of the enzymes identified in the *F. ambigua* gene cluster were validated *in vitro* by the Liu group. This includes AmbP1, which was speculated to be responsible for the cyclization of GPP and **3.29** into hapalindole U (**3.35**) (Scheme 3.4a). Additionally, Liu speculated that AmbO5 is the late-stage chlorinase that transforms hapalindoles and ambiguines into their chlorinated con-



Scheme 3.3: The depiction of Carmeli's concerted one-step proposal to tetracyclic compounds **3.34**, **3.35**, and **3.36** from both **3.29** and **3.27**.



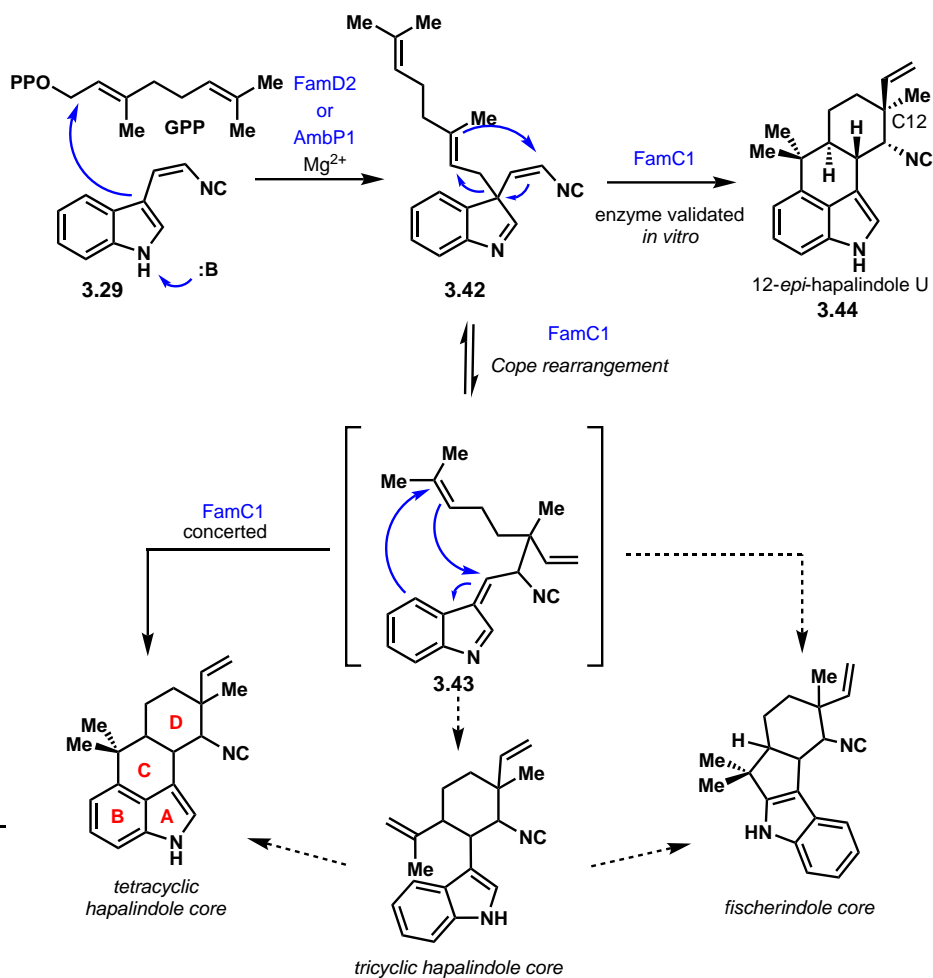
Scheme 3.4: Liu's identification of the enzymes responsible for hapalindole/ambiguine biosynthesis. Enzymes validated *in vitro* are in red. a. Amb1-3 for the formation of **3.29** b. AmbP3 for the reverse prenylation of **3.34**. c. The stereochemical influence at C10 of **3.40** on C2 reverse prenylation.

geners (see Scheme 3.4a, **3.35** to **3.34**). However, Liu identified and validated *in vitro* the function of AmbP3 as a reverse-prenyl transferase to furnish tetracyclic ambiguine A **3.4** (Scheme 3.4b). The enzymatic efficiency was clearly influenced by the stereochemistry at C10 as the epimer of hapalindole G (i.e., hapalindole A, **3.40**) led only to small amounts of the prenylated compound (**3.41**, Scheme 3.4c). Remarkably, the authors also identified four non-heme iron (NHI)-dependent oxygenases, AmbO1-O4. These four NHI-dependent enzymes belong to the Rieske oxygenase family of enzymes,^{19,20} and are likely responsible for the oxidative cyclization reaction to form the pentacyclic ambiguines in addition to performing other late-stage oxygenations to generate all of the ambiguine congeners.

This initial report by Liu in 2014 was followed by two separate publications in 2015 by Sherman²¹ and in 2016 by Liu²² in which both groups detailed an exquisite enzyme-mediated Cope rearrangement, leading to the discovery of a previously unknown biosynthetic intermediate **3.42** as shown in Scheme 3.5. While the Liu group had previously characterized much of the biosynthetic gene sequence from *Fischerella ambigua* with the prefix *Amb*, the Sherman group identified new enzymes within the same gene cluster of *F. ambigua* (UTEX 1903) and renamed the enzymes with the prefix *Fam*.

In both reports by Sherman and Liu, intermediate **3.42** was isolated, which has now led to the complete revision of the previously accepted hapalindole biosynthetic proposals originally presented by Moore and Carmeli. The new data from these groups showed that the *Z*-indole isonitrile (**3.29**) undergoes C3-displacement with geranyl pyrophosphate (GPP) to generate indolenine compound **3.42**, a process shown to be mediated by enzyme FamD2, also known as AmbP1. The Liu group discovered that this process is dependent on the concentration of Mg^{2+} ions and showed

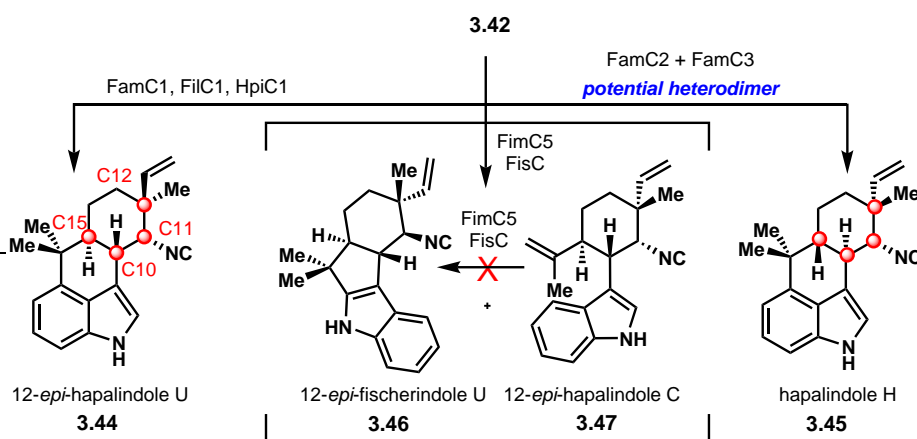
that the enzymatic activity was improved in the presence of $MgCl_2$. From key intermediate **3.42**, it was demonstrated by the Sherman group that FamC1 catalyzes a purported [3,3]-sigmatropic rearrangement leading to intermediate **3.43**, which they did not isolate. In the presence of cell-free lysate containing FamC1, Sherman observed the formation of 12-*epi*-hapalindole U (**3.44**), which is a compound previously unreported by isolation chemists. This finding suggests that the library of hapalindole alkaloids, known to date, is not complete and deserves further isolation efforts. Finally, Sherman proposed that subsequent cyclizations from **3.43** could be stepwise, leading to formation of the tricyclic hapalindole core, or concerted, leading to the fischerindole core (Scheme 3.5).



Scheme 3.5: The compilation of Sherman and Liu’s biosynthetic discoveries of a novel enzyme-mediated Cope rearrangement involving proposed intermediate **3.43** ultimately leading to the tetracyclic hapalindole core and **3.44**.

Two years later in 2017, the Sherman group in collaboration with the Williams group from Colorado State University, analyzed gene clusters from five different hapalindole/ambiguine producing bacteria.²³ In this analysis, Sherman and Williams identified the enzymes responsible for cyclizations from indolenine precursor **3.42** to the tricyclic, tetracyclic, and fischerindole cores (Scheme 3.6). The authors first identified and isolated two FamC1 homologs known as FilC1 and HpiC1 from the IL199-3-1 and ATCC 43239 strains of cyanobacteria respectively. They found

that all of these enzymes (FamC1, FilC1, and HpiC1) catalyze the same cyclization from **3.42** to **3.44**. On the other hand, they observed a different hapalindole isomer, hapalindole H (**3.45**) when **3.42** was treated with cyclases FamC2 and FamC3 in the same pot, but observed no formation of **3.45** when **3.42** was treated separately with FamC2 and FamC3. These data suggest that FamC2 and FamC3 potentially act as a heterodimer to effect the cyclization with a different stereochemical outcome from that of FamC1, FilC1, and HpiC1. In addition, by mining the genomes of two fischerindole producing strains of cyanobacteria (*F. musicola* UTEX 1829 and SAG 46.79) the Sherman group found two cyclases (FimC5 and FisC) that catalyze the cyclization of **3.42** to 12-*epi*-fischerindole U (**3.46**). However, they also isolated tricyclic 12-*epi*-hapalindole C (**3.47**) from this enzymatic reaction which, intriguingly, does not cyclize to **3.46** in the presence of FimC5 or FisC. This finding suggests that tricyclic 12-*epi*-hapalindole C (**3.47**) is not a biosynthetic intermediate towards the tetracyclic fischerindole class of natural products.

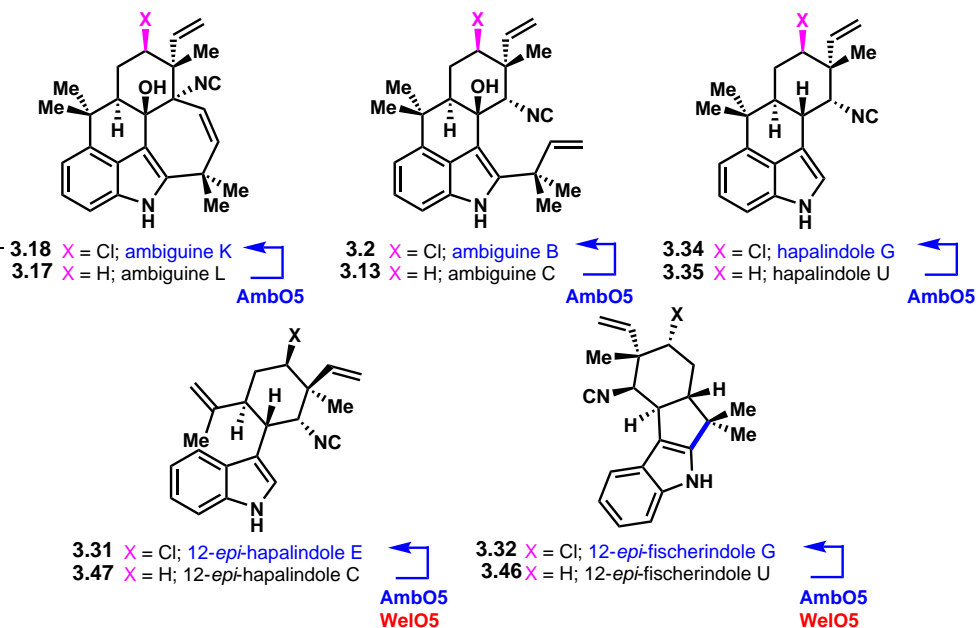


Scheme 3.6: Sherman and Williams' identification of cyclases leading to tetracyclic **3.44**, tricyclic **3.45**, and fischerindole **3.46**. Tricyclic **3.47** does not cyclize to the fischerindole core in the presence of FimC5 and FisC cyclases.

The culmination of Sherman, Liu, and Williams' work suggests that compound **3.43**, which is synthesized through an enzymatic Cope rearrangement, is the biosynthetic precursor to all tri- and tetracyclic hapalindole and fischerindole cores. These groups have also concluded, similar in principle to what Carmeli predicted back in 2007, that the hapalindole core is produced with a certain stereochemical pattern determined by the unique and complex nature of the cyclases present in each respective strain of hapalindole-producing cyanobacteria.

Another aspect of the hapalindole/ambiguine biosynthesis that has been intensely studied is the role of the enzyme AmbO5 in the late-stage chlorination of hapalindole biosynthetic intermediates. In 2016, the Liu group identified the late-stage NHI-dependent C–H halogenase enzyme AmbO5 that is responsible for installing a chlorine atom in a stereospecific manner on ambiguityne substrates as shown in Scheme 3.7.²⁴ Liu was able to identify AmbO5 as the late-stage chlorinase involved in hapalindole/ambiguine biosynthesis having previously identified WelO5 as the late-stage chlorination enzyme involved in welwitindolinone biosynthesis.¹⁷ In addition, Liu and coworkers examined the promiscuity of AmbO5 in comparison to WelO5 and found that AmbO5 had a wider spectrum of activity and catalyzes the functionalization of most hapalindole cores including fischerindole, tri- and tetracyclic hapalindole, and tetra- and pentacyclic ambiguityne cores.

On the other hand, WelO5 was found to only catalyze the conversion of **3.47** and **3.46** to **3.31** and **3.32**. These discoveries are of great importance to the synthetic community as there is potential for these enzymes to serve as engineered biocatalysts for the late-stage chlorination of a broader range of scaffolds.



Scheme 3.7: Liu's examination of the promiscuity of late-stage chlorinating enzyme AmbO5 in comparison to the homologous enzyme WelO5

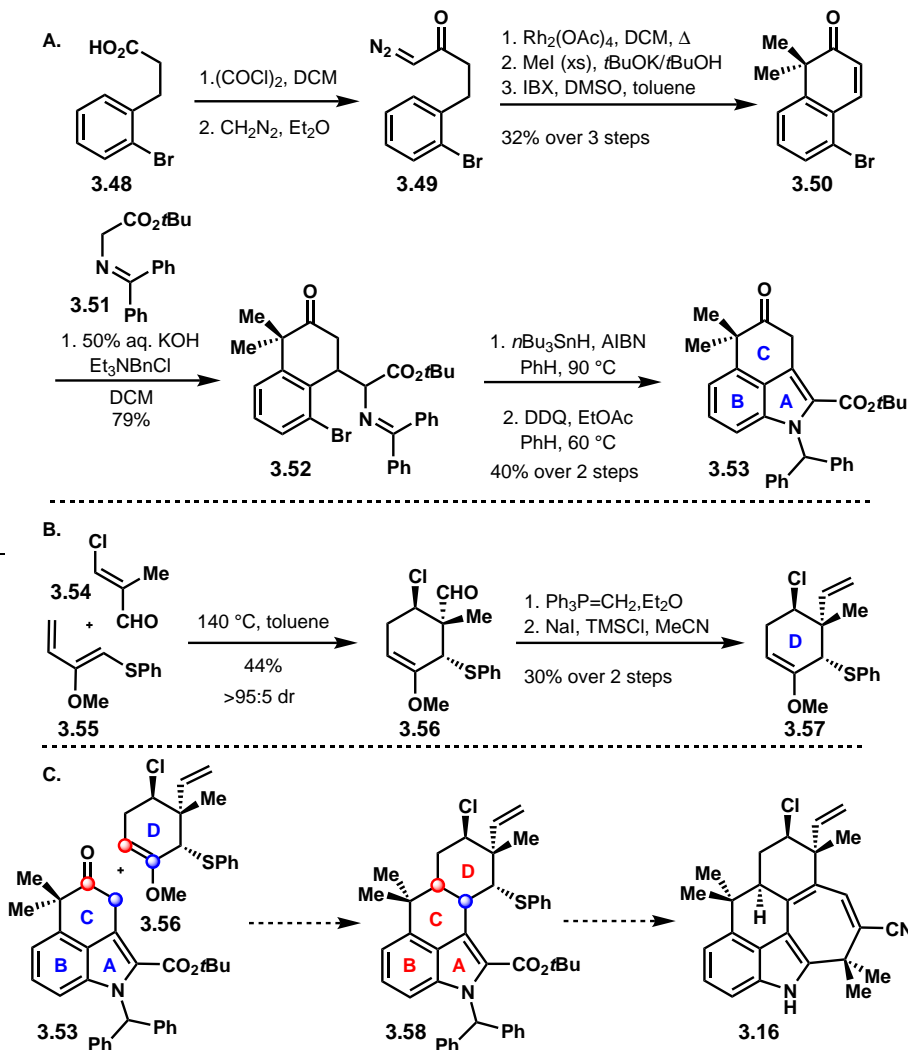
While all of these reports represent groundbreaking discoveries related to the biosynthetic studies of hapalindole natural products, there is still much to be discovered with regard to formation of the vast array of hapalindole-like structures containing highly varied stereochemical patterns and functionalities decorating their cores. These reports also suggest that the collection of hapalindole natural products that have been isolated to date is not complete and further exploration by isolation and synthetic chemists alike is warranted.

Additionally, the later-stage oxidative steps leading to the pentacyclic ambiguines remains largely unexplored, and it is without doubt that discoveries in this realm will be highly intriguing not only to synthetic chemists interested in the hapalindole compounds, but also to the broader biochemical community.

3.3 Previous Attempts to Synthesize Ambiguine Natural Products

Since the report of their initial isolation in 1992, synthetic chemists have been extremely attracted to pentacyclic ambiguine natural products for a number of reasons including their diverse bioactivity, unique biosynthesis, and most importantly the synthetic challenges surrounding formation of their densely functionalized pentacyclic core.

While hapalindoles, fischerindoles, and welwitindolinones are well-represented in the synthetic literature²⁵ with a wide variety of successful approaches having been reported, the pentacyclic ambiguines remain the "holy grail" of the hapalindole family of natural products as no successful syntheses have been reported to date.



Scheme 3.8: A. Johnston's 2007 synthesis of A-, B-, C-ring compound **3.53**. B. The Diels-Alder approach leading to D-ring compound **3.57**. C. Precursors **3.59** and **3.57** map onto the natural product ambiguine G **3.16**.

The Johnston group in 2007 was the first to report an approach to the synthesis of pentacyclic ambiguine-type natural products using a unique Diels-Alder disconnection to address the synthesis of ambiguine G (Scheme 3.8).²⁶ In their approach, the authors synthesized the A-, B-, and C-ring fragment of ambiguine G through a Rh(II) carbenoid-catalyzed C–H bond insertion followed by methylation and subsequent oxidation to access enone intermediate **3.50** (Scheme 3.8a). They next performed a Michael addition with imine fragment **3.60** to form the indole precursor **3.52**. Finally, a radical-mediated indolenine synthesis proceeded in good yield with high diastereoselectivity and upon oxidation with DDQ provided the A-, B-, and C-ring fragment **3.52**. The Johnston group also, separately, formed the D-ring through a [4+2] cycloaddition of vinylogous acyl chloride **3.54** and diene **3.55** (Scheme 3.8b). Interestingly, the authors did not report an attempt to merge the syntheses of the two fragments (**3.57** and **3.53**) together to form the tetracyclic core of ambiguine G (**3.58**) (Scheme 3.8c).

A second attempt towards the pentacyclic ambiguine natural products was reported by the Williams group in two different reports in 2011 and 2012.^{27,28} In their first publication, the Williams group described how they envisioned forming the pentacyclic core (**3.61**) through a key ring-closing metathesis reaction from **3.62** to form the seven-membered E-ring (Figure 3.2). Substrate **3.62** could arise from the tetracyclic ambiguine core (**3.63**) which they envisioned could be pieced together through a coupling reaction between intermediates **3.64** and **3.65**.

Williams applied this approach to the synthesis of tetracyclic hapalindole alkaloids in addition to the ambiguienes; accordingly, before attempting the formation of the tetracyclic ambiguine core, they began with the formation of the tetracyclic hapalindole core (Scheme 3.9).

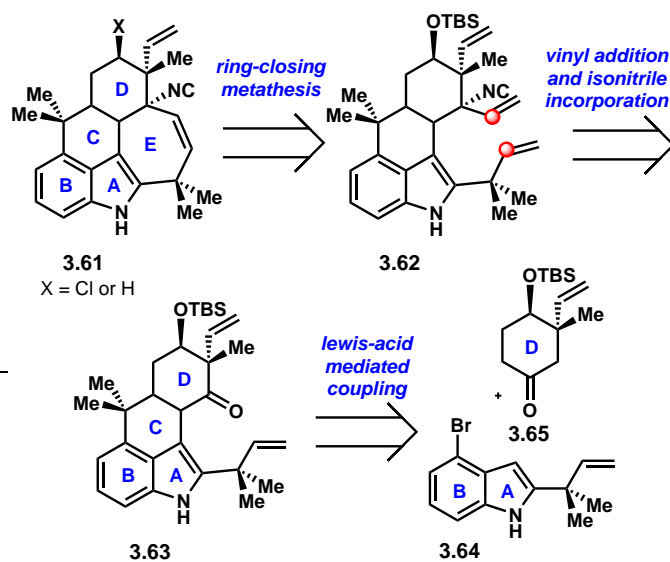
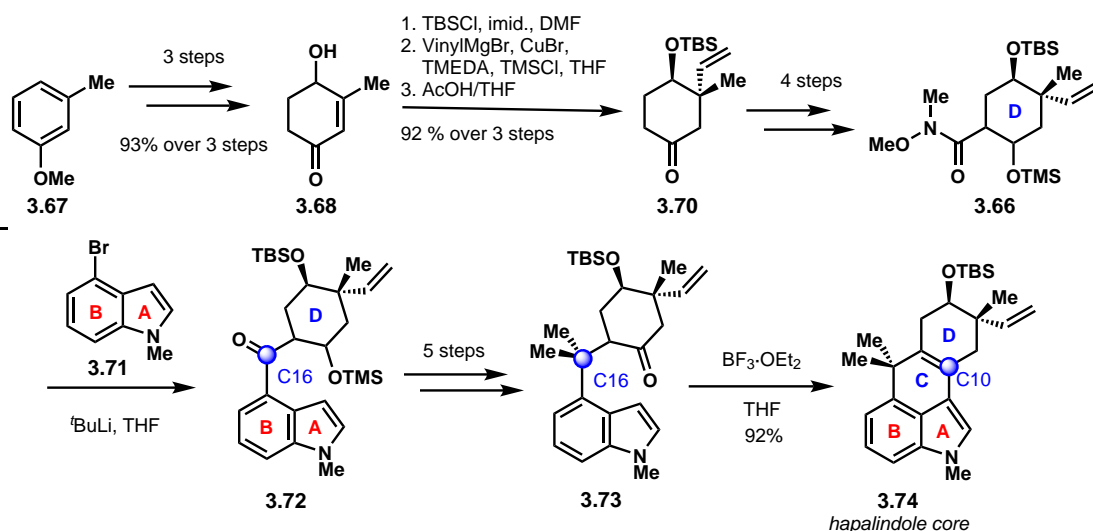


Figure 3.2: Williams' 2011 retrosynthetic plan to access pentacyclic ambiguine natural products highlighting a Grubbs ring-closing metathesis reaction.

In order to form what would be the D-ring coupling partner (**3.66**, Scheme 3.9), Williams envisioned employing a 3-step sequence developed by Rubottom and Gruber in 1977 starting with 3-methyl anisole (**3.67**) to ultimately provide enone **3.68**.²⁹ Subsequent protection of secondary alcohol **3.69** followed by conjugate addition of vinyl Grignard into the enone moiety led to the formation of ketone **3.70** as a single diastereomer. It required four more steps from **3.70** to synthe-

size compound (**3.66**), containing the Weinreb amide that was required in order to couple D-ring fragment **3.66** with the A- and B-ring fragment **3.71**.

In the first generation of the Williams group's synthesis of the hapalindole tetracyclic core, they used a rather lengthy procedure to couple together A- and B-ring indole fragment **3.71** to the D-ring Weinreb amide fragment **3.66** (Scheme 3.9). This initial route began with a lithium halogen exchange of *N*-methyl 4-bromoindole (**3.71**) followed by nucleophilic addition into Weinreb amide partner **3.66** to form tricyclic compound **3.72**. A five step procedure for the installation of a gem-dimethyl group at C16 in addition to oxidizing up to the ketone was employed (**3.72** to **3.73**) followed by treatment of **3.73** with the Lewis acid $\text{BF}_3 \cdot \text{OEt}_2$ to generate tetracycle **3.74**. Notably, although **3.74** contains the tetracyclic core of hapalindoles, it does not bear the functionality at C10 found in hapalindole and ambiguine natural products. The requisite functionality at C10 would have to be installed at a late stage in the Williams group's synthesis.



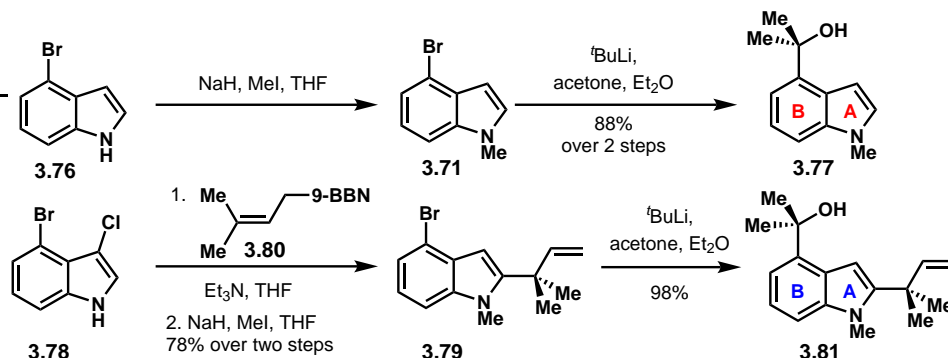
Scheme 3.9: The Williams' group 1st generation approach to access hapalindole core compound **3.74**.

Due to the lengthy protocol required to form the tetracyclic hapalindole core (**3.74**), the Williams group decided to shorten the route by adopting chemistry initially reported by Natsume and Muratake on related hapalindole substrates.³⁰

Using Natsume and Muratake's previously reported chemistry, the Williams group synthesized A- and B-ring indole coupling partner **3.75** starting with the *N*-methylation of commercially available 4-bromoindole (**3.76**, Scheme 3.10). Lithium-halogen exchange of the aryl bromide (**3.71**) using *tert*-butyllithium and subsequent addition into acetone formed the desired tertiary alcohol **3.77** in 88% yield over the two steps.

In order to access the core of the tetracyclic ambiguine natural products, the reverse prenyl group was installed at the C2 position of indole (**3.78** to **3.79**) using established methodology developed by Danishefsky's group in 1999.³¹ The Williams group treated 4-bromo-3-chloro-indole (**3.78**) with freshly prepared prenyl-9-BBN (**3.80**) in the presence of triethylamine to afford the desired reverse-prenylated compound (**3.79**), which subsequently underwent *N*-methylation in an overall 78% yield over the two steps. As previously, lithium-halogen exchange of aryl bromide

3.79 and subsequent addition into acetone furnished tertiary alcohol precursor **3.81**, which would serve as the A- and B-ring coupling partner leading to ambiguline natural products.



Scheme 3.10: The Williams' group synthesis of indole derivatives **3.77** and **3.81**.

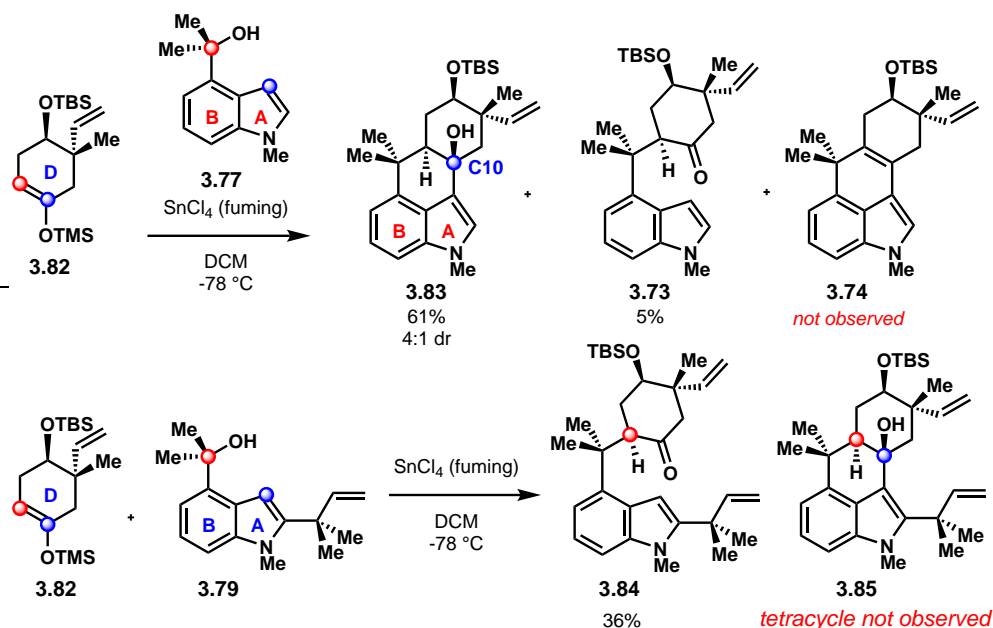
Muratake and Natsume's 1989 strategy involved a Lewis acid-mediated coupling reaction between a silyl enol ether derivative such as **3.82** and a C-4 functionalized indole component such as **3.77**. Applying this strategy to their own synthesis, the Williams group used their previously synthesized ketone compound **3.70** and generated silyl enol ether **3.82** under standard enolizing conditions (Scheme 3.11). With access to the D-ring component (**3.82**) and the A- and B-ring fragment (**3.77**), the authors undertook an extensive screening campaign to access coupled product **3.83** ultimately using fuming SnCl_4 at -78°C . They isolated **3.83** in good yield with a diastereomeric ratio of 4:1 favoring the desired isomer. Remarkably, this is the only instance to date where any group has successfully installed the C10 hydroxyl group in a hapalindole core.

Having developed this route to the hapalindole tetracyclic core bearing the C10 hydroxyl group (**3.83**), the Williams group next investigated forming the tetracyclic ambiguline core which bears a reverse prenyl group attached to the C2 position of the indole. Utilizing the same silyl enol ether compound (**3.82**) as in the previous case, they now employed the C2-reverse prenylated indole derivative **3.81** as the A- and B-ring partner using their previously optimized SnCl_4 -mediated coupling conditions. Unfortunately, they only observed formation of tricyclic compound **3.84** with no sign of desired tetracycle **3.85**.

The Williams group reported no other attempts to improve this coupling reaction. Instead, they returned to this result in their next paper published in 2012, where they also reported a formal synthesis of hapalindole O.³² Curiously, they described a synthetic attempt towards ambiguline A, which they reported as structure **3.86**. However, to the best of our knowledge, this type of ambiguline has never been reported in the literature and the only known structure for ambiguline A is decidedly compound **3.4**.¹

Nevertheless, in their paper, Williams described a protecting group modification from their previous 2011 report that improved the yield of their key SnCl_4 -mediated coupling reaction. Specifically, the use of a TBS-protected reverse-prenylated indole species (**3.87**) instead of *N*-methylated compound **3.79** used in 2011 (Scheme 3.12a). With TBS-protected indole **3.87**, they were able to achieve a Lewis acid-mediated coupling reaction to form tricycle **3.88** in 55% yield, which they then cyclized to the desired tetracycle (**3.89**) using methanolic HCl.

Notably, the C10 hydroxyl group that is present in the majority of ambiguline natural products, eliminated to form alkene compound **3.89**. Indeed, **3.89** would be desired for the synthesis of

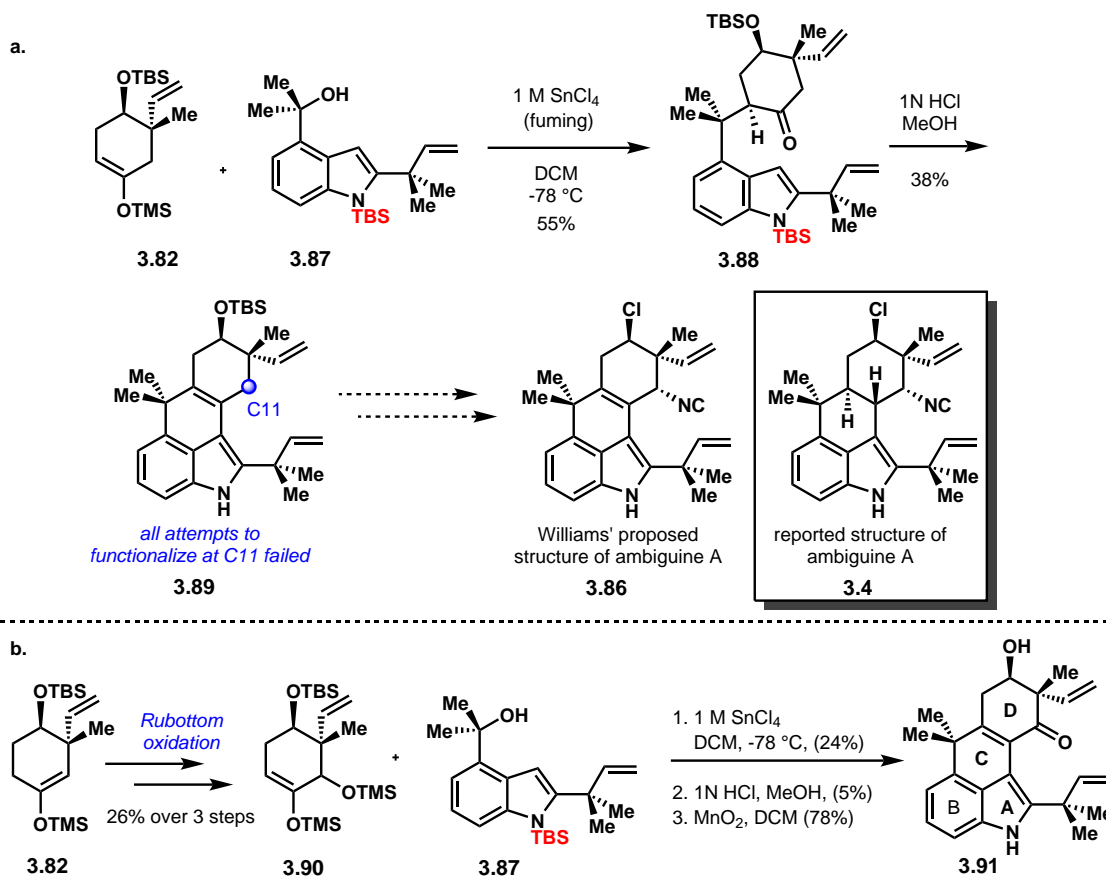


Scheme 3.11: An improved route to access the tetracyclic hapalindole core using Natsume and Muratake's Lewis acid coupling approach. This method was also applied to prenylated indole derivative **3.79** but unfortunately only tricyclic compound **3.84** was isolated.

ambiguine A in the form that the authors reported (**3.86**, Scheme 3.12), however, naturally isolated ambiguine A (**3.4**) bears a β -disposed hydrogen at C10. Nevertheless, the Williams group continued on in their pursuit of proposed structure **3.86**. Unfortunately, all attempts failed to functionalize at C11 of **3.89** in an effort to install the requisite isonitrile functionality present in the natural product.

Considering the challenges associated with functionalizing at C11, Williams and coworkers installed the desired oxygen substituent earlier in the synthesis. They were able to access compound **3.90** through a 3-step protocol beginning with a Rubottom oxidation of silyl enol ether **3.82** (Scheme 3.12b). Subsequent formation of a silyl enol ether from the less-substituted side of the ketone and subsequent hydroxyl protection generated **3.90**. This compound (**3.90**) successfully underwent a Lewis acid-mediated coupling reaction with A- and B-ring partner **3.87** to form a tricyclic intermediate that was cyclized to the corresponding tetracycle using methanolic HCl. The resulting alcohol intermediate was immediately oxidized with MnO_2 to generate ketone **3.91**. In this 3-step sequence (**3.90** to **3.91**), the C-ring cyclization step promoted by methanolic HCl, proceeded in an extremely low 5% yield and is apparently the subject of ongoing study in the Williams group.

The 2012 report was the most recent attempt reported by the Williams group towards the synthesis of ambiguine and hapalindole natural products. To the best of our knowledge, the question of whether or not the structure they propose for ambiguine A corresponds to any natural product has not been addressed in any further context. Nevertheless, Williams provided some thought-provoking methodology to achieve the construction of the tetracyclic core of the ambiguines, in addition to outlining a creative metathesis reaction in their retrosynthetic analysis of the pentacyclic ambiguine natural products.



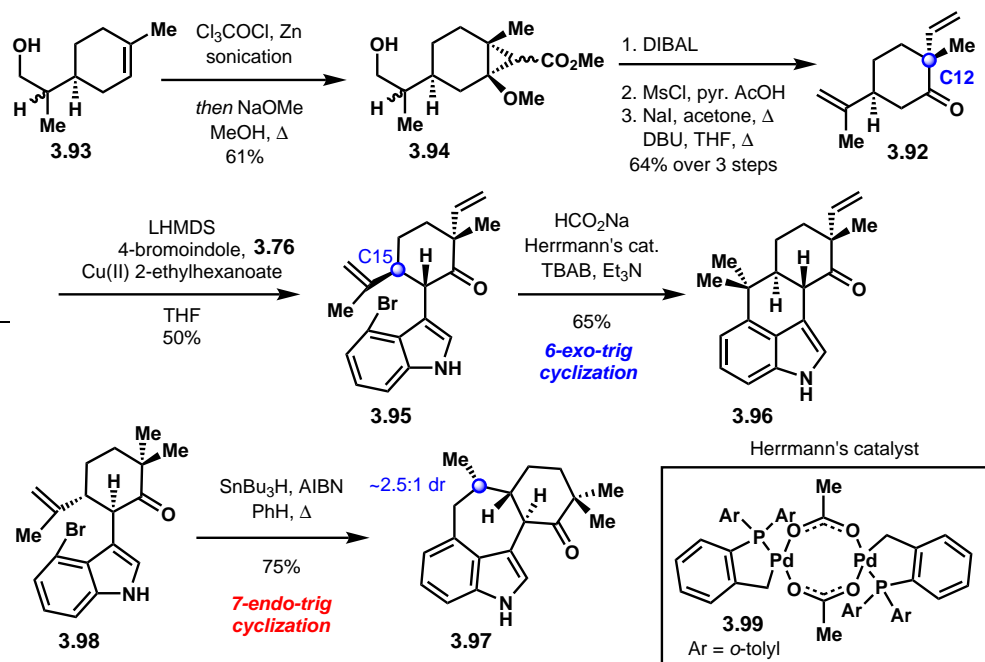
Scheme 3.12: a. A successful cyclization of tricycle **3.88** to the tetracyclic ambigaine core. It is not clear why the authors report the structure of ambigaine A as **3.86** instead of **3.4**. b. Synthesis of the tetracyclic ambigaine core bearing oxygenation at C11.

Although there have been no other formal attempts to access the pentacyclic ambigaine class of natural products, there was one remarkable synthesis of a tetracyclic ambigaine, specifically ambigaine H reported by the Baran group in 2007.³³ The Baran synthesis highlighted the group's previously established copper-mediated oxidative coupling methodology reported in 2004³⁴ and also demonstrated their ability to harness the inherent reactivity of indole in order to abstain entirely from using protecting groups in their synthesis.

The first key step of Baran's 2007 synthesis involved the copper-mediated coupling reaction between 4-bromoindole (**3.76**) and terpene-derived building block **3.92** (Scheme 3.13). The synthesis of this terpene building block began from *p*-menth-1-en-9-ol (**3.93**) in a 4-step sequence previously developed by Mehta in 1994.³⁵ First, dichloroketene (prepared *in situ*) underwent a [2+2] cycloaddition with **3.93**. Base-promoted ring-contraction afforded cyclopropane **3.94** in 61% yield. Subsequent reduction using DIBAL-H followed by mesylation and mesylate elimination gave terpene fragment **3.92** in an excellent 64% yield over three steps. Notably, this compound contains the vinyl methyl quaternary center at C12 with the desired anti relative stereochemistry present in the ambigaine H.

The terpene fragment (**3.92**) was submitted to the copper-mediated oxidative enolate coupling reaction with 4-bromoindole (**3.76**) and the reaction proceeded in a moderate 50% yield to afford

coupled product **3.95** (**3.92** to **3.95**, Scheme 3.13). The use of 4-bromoindole in this synthesis was intended to allow the possibility for a reductive Heck coupling onto the C4 position of indole with the isopropenyl group at C15 to form the tetracyclic core of the hapalindoles in a very efficient sequence. After screening a variety of palladium catalysts, the Baran group found that Herrmann's catalyst provided the best conversion for this reductive Heck reaction leading to tetracycle **3.96**. Importantly, this catalyst minimized reductive de-bromination as a side reaction. The authors also investigated a potential radical-mediated cyclization, but found that in the presence of standard radical-generating conditions (e.g., with Bu_3SnH), only the 7-*endo*-trig product (**3.97**) was obtained.³⁶



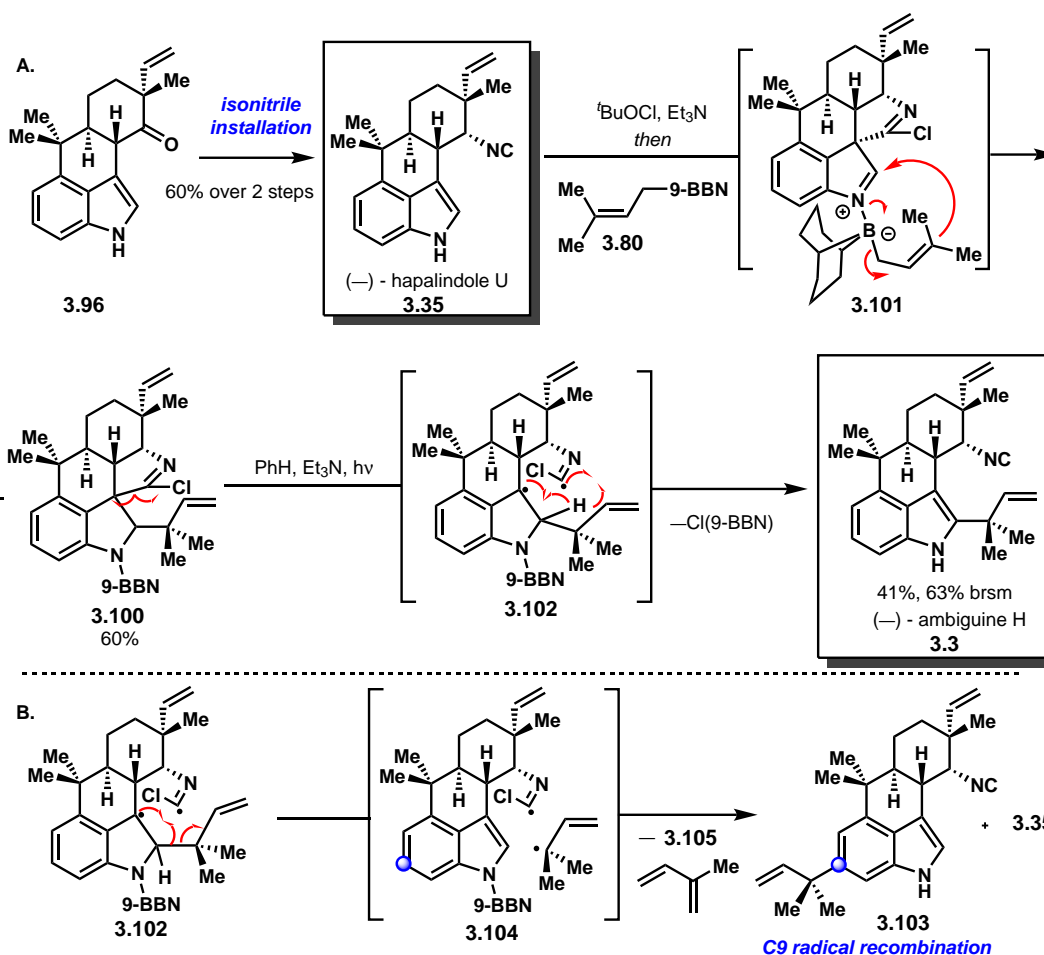
Scheme 3.13: Baran's 2007 synthesis of tetracyclic intermediate **3.96** using a Cu(II)-mediated oxidative enolate coupling reaction to access compound **3.95**. The indole C4 cyclization reaction gives the undesired 7-*endo*-trig product under radical generating conditions.

With the tetracyclic hapalindole core (**3.96**) in hand, Baran et. al. completed the first enantioselective synthesis of (–)-hapalindole U (**3.35**) via a straightforward two step reductive amination, formylation, and dehydration sequence in order to install the C11 isonitrile functionality (Scheme 3.14a). The next challenge in the synthesis toward ambiguine H was to introduce the reverse-prenyl group at the C2 position of the indole moiety, which would provide access to the tetracyclic core of the ambiguienes. The methodology developed by Danishefsky's group in 1999 was used in this case. However, instead of isolating the natural product, C3-functionalized compound **3.100** was instead isolated in 60% yield.

The authors explained that this compound (**3.100**) presumably arose through initial activation of the isonitrile unit with the electrophilic chlorine source $t\text{BuOCl}$ (Scheme 3.14a). The C3 position of the indole fragment could then engage the carbon of the isonitrile moiety to produce an indoline compound such as **3.101** that was subsequently engaged by the prenyl 9-BBN species leading to isolated compound **3.102**. Although compound **3.102** was unexpected, the authors keenly en-

visioned that a Norrish-type fragmentation would initiate a sequence leading to (–)-ambiguine H (**3.3**). A mechanism was proposed where the undesired C–C bond could first be cleaved with UV light, forming diradical species **3.100**. Internal hydrogen atom abstraction and cleavage of the N–B bond would then provide ambiguity H (**3.3**). Indeed, this plan worked as envisioned, and they were able to isolate (–)-ambiguine H in 63% yield. This yield is quite remarkable considering how many transformations took place in this step.

Baran et. al. also reported the isolation of side products (**3.103** and **3.35**) from this light-mediated Norrish C–C bond cleavage reaction (Scheme 3.14b). As presumed by the authors, these two products are formed from C–C bond cleavage of the reverse prenyl group which led to diradical intermediate **3.104**. From **3.104**, radical recombination of the reverse prenyl group onto the C9 position of the indole moiety led to the formation of **3.103** while intermolecular hydrogen atom abstraction of the reverse prenyl radical (generating diene **3.105**) likely produced (–)-hapalindole U (**3.35**).



Scheme 3.14: A. The end-game for Baran’s synthesis of hapalindole U (**3.35**) and ambiguity H (**3.3**). B. Side-products observed in the light-mediated C–C bond cleavage.

Baran and coworkers go on to report the enantiospecific synthesis of (+)-welwitindolinone A and (–)-fischerindole I through expedient means. Although it could also be possible to access the

pentacyclic ambiguine core through an oxidative cyclization of (–)-ambiguine H (**3.3**), no follow-up attempts were reported by the Baran group. This synthesis of (–)-ambiguine H represents not only the first successful synthesis of an ambiguine natural product, but also a highly novel and expedient strategy to access the tetracyclic hapalindole and ambiguine cores without the use of protecting groups.

3.4 Conclusion and Outlook

In summary, the pentacyclic ambiguines are incredibly intriguing secondary metabolites from bioactivity, biosynthetic, and synthetic standpoints. While the majority of isolated ambiguines have been tested in antifungal and antibiotic bioassays, the mechanism of action for these activities has not been investigated. In addition, due to small quantities of material, limited bioactivity data exists for ambiguines P and Q, and the total synthesis of these natural products will likely facilitate a full exploration of their bioactivity.

Synthetic chemists have been attracted to the challenges of preparing pentacyclic ambiguines since their initial isolation in 1992. A seminal report from Johnston in 2007 detailed an attempt to access ambiguine G. Williams reported two papers in 2011 and 2012 that attempted the synthesis of tetracyclic hapalindoles and ambiguines. These have been the only reported attempts to prepare the pentacyclic ambiguines and to date, there have been no successful syntheses of the pentacyclic ambiguines nor of the pentacyclic core. The Baran group reported the first and only total synthesis of an ambiguine natural product, namely, the tetracyclic (–)-ambiguine H in 2007. Nevertheless, it is clear that new methodologies and strategies will have to be developed in order to access the pentacyclic ambiguine natural products using total synthesis. This area is wide open for exploration and will likely lead to the discovery of unexpected and interesting chemistry along the way.

3.5 References

1. Smitka, T. A.; Bonjouklian, R.; Doolin, L.; Jones, N. D.; Deeter, J. B.; Yoshida, W. Y.; Prinsep, M. R.; Moore, R. E.; Patterson, G. M. L. *J. Org. Chem.* **1992**, *57*, 857–861.
2. Gomont, M. M. *Journal de Botanique* **1895**, *9*, 49–52.
3. Huber, U.; Moore, R. E.; Patterson, G. M. L. *J. Nat. Prod.* **1998**, *61*, 1304–1306.
4. West, W.; West, G. S. Hapalosiphon Delicatulus. *Trans. Linn. Soc. Lond.* **1902**, *6*, 123–215.
5. Moore, R. E.; Cheuk, C.; Patterson, G. M. L. *J. Am. Chem. Soc.* **1984**, *106*, 6456–6457.
6. Raveh, A.; Carmeli, S. *J. Nat. Prod.* **2007**, *70*, 196–201.
7. Mo, S.; Krunic, A.; Chlipala, G.; Orjala, J. *J. Nat. Prod.* **2009**, *72*, 894–899.
8. Mo, S.; Krunic, A.; Santarsiero, B. D.; Franzblau, S. G.; Orjala, J. *Phytochemistry* **2010**, *71*, 2116–2123.
9. Walton, K.; Gantar, M.; Gibbs, P. D. L.; Schmale, M. C.; Berry, J. P. *Toxins (Basel)* **2014**, *6*, 3568–3581.
10. AcuÁsa, U. M.; Zi, J.; Orjala, J.; Carcache de Blanco, E. J. *Int J Cancer Res (Tortola)* **2015**, *49*, 1655–1662.
11. Koodkaew, I.; Sunohara, Y.; Matsuyama, S.; Matsumoto, H. *Plant Growth Regulation* **2012**, *68*, 141–150.

12. Park, A.; Moore, R. E.; Patterson, G. M. *Tetrahedron Lett.* **1992**, *33*, 3257–3260.
13. Schwartz, R. E.; Hirsch, C. F.; Sesin, D. F.; Flor, J. E.; Chartrain, M.; Fromtling, R. E.; Harris, G. H.; Salvatore, M. J.; Liesch, J. M.; Yudin, K. *J. Ind. Microbiol.* **1990**, *5*, 113–123.
14. Brady, S. F.; Clardy, J. *Angew. Chem. Int. Ed.* **2005**, *44*, 7063–7065.
15. Stratmann, K.; Moore, R. E.; Bonjouklian, R.; Deeter, J. B.; Patterson, G. M. L.; Shaffer, S.; Smith, C. D.; Smitka, T. A. *J. Am. Chem. Soc.* **1994**, *116*, 9935–9942.
16. Richter, J. M.; Ishihara, Y.; Masuda, T.; Whitefield, B. W.; Llamas, T.; Pohjakallio, A.; Baran, P. S. *J. Am. Chem. Soc.* **2008**, *130*, 17938–17954.
17. Hillwig, M. L.; Zhu, Q.; Liu, X. *ACS Chem. Biol.* **2014**, *9*, 372–377.
18. Chang, W.-c.; Sanyal, D.; Huang, J.-L.; Ittiamornkul, K.; Zhu, Q.; Liu, X. *Org. Lett.* **2017**, *19*, 1208–1211.
19. Barry, S. M.; Challis, G. L. *ACS Catal.* **2013**, *3*, 2362–2370.
20. Sydor, P. K.; Barry, S. M.; Odulate, O. M.; Barona-Gomez, F.; Haynes, S. W.; Corre, C.; Song, L.; Challis, G. L. *Nat. Chem.* **2011**, *3*, 388–392.
21. Li, S.; Lowell, A. N.; Yu, F.; Raveh, A.; Newmister, S. A.; Bair, N.; Schaub, J. M.; Williams, R. M.; Sherman, D. H. *J. Am. Chem. Soc.* **2015**, *137*, 15366–15369.
22. Liu, X.; Hillwig, M. L.; Koharudin, L. M. I.; Gronenborn, A. M. *Chem. Commun.* **2016**, *52*, 1737–1740.
23. Li, S.; Lowell, A. N.; Newmister, S. A.; Yu, F.; Williams, R. M.; Sherman, D. H. *Nat. Chem. Bio.* **2017**, *13*, 467–469.
24. L., H. M.; Qin, Z.; Kuljira, I.; Xinyu, L. *Angew. Chem. Int. Ed.* **2016**, *55*, 5780–5784.
25. Bhat, V.; Dave, A.; MacKay, J. A.; Rawal, V. H. In *The Alkaloids: Chemistry and Biology*; Knölker, H.-J., Ed.; Academic Press, 2014; Vol. 73; pp 65–160.
26. Chandra, A.; Viswanathan, R.; Johnston, J. N. *Org. Lett.* **2007**, *9*, 5027–5029.
27. Rafferty, R. J.; Williams, R. M. *Tetrahedron Lett.* **2011**, *52*, 2037–2040.
28. M. Williams, R.; J. Rafferty, R. *Heterocycles* **2012**, *86*, 219.
29. Rubottom, G. M.; Gruber, J. M. *J. Org. Chem.* **1977**, *42*, 1051–1056.
30. Muratake, H.; Natsume, M. *Tetrahedron Lett.* **1989**, *30*, 1815–1818.
31. Schkeryantz, J. M.; Woo, J. C. G.; Siliphaivanh, P.; Depew, K. M.; Danishefsky, S. J. *J. Am. Chem. Soc.* **1999**, *121*, 11964–11975.
32. Rafferty, R. J.; Williams, R. M. *Tetrahedron Lett* **2011**, *52*, 2037–2040.
33. Baran, P. S.; Maimone, T. J.; Richter, J. M. *Nature* **2007**, *446*, 404–408.
34. Baran, P. S.; Richter, J. M. *J. Am. Chem. Soc.* **2004**, *126*, 7450–7451.
35. Mehta, G.; Acharyulu, P. V. R. *J. Chem. Soc. Chem. Commun.* **1994**, 2759–2760.
36. Maimone, T. J.; Ishihara, Y.; Baran, P. S. *Tetrahedron* **2015**, *71*, 3652–3665.

Chapter 4

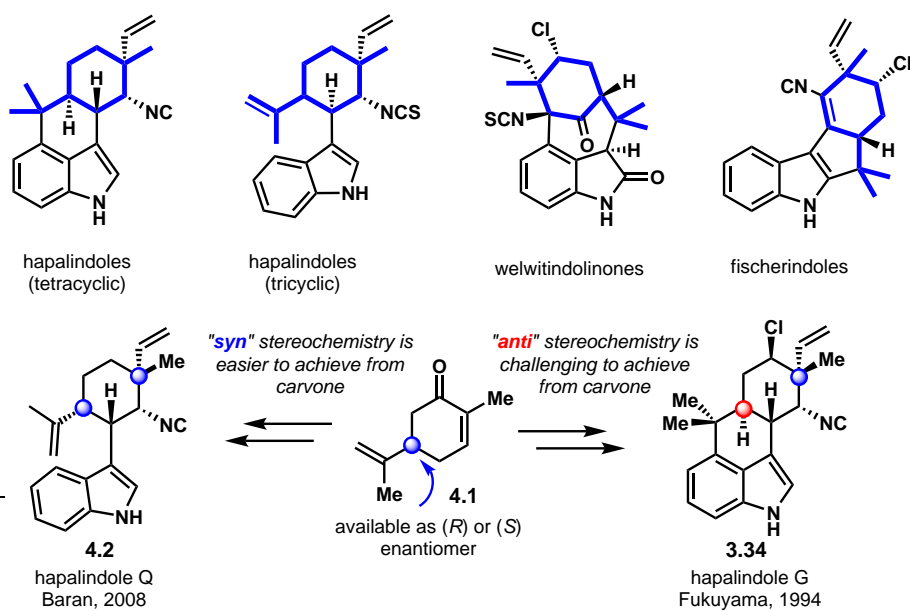
Chapter 4 : Synthetic Approaches to the Pentacyclic Class of Ambiguine Natural Products

4.1 Challenges Associated with the Synthesis of Pentacyclic Ambiguines

The pentacyclic ambiguity natural products present a number of synthetic challenges that have attracted our group, as well as other groups, to these molecules from a synthetic perspective. The first challenge lies in the synthesis of the densely functionalized pentacyclic core that has proven extremely difficult to form and is likely the major reason these molecules have had no previous successful syntheses. Indeed, despite the attempts made by Johnston¹ and Williams^{2,3} discussed in Chapter 3, methods to install the 7-membered ring present in the core have not been established. These challenges, however, present a unique opportunity to develop novel and interesting methods for the formation of the densely functionalized pentacyclic core.

In general, the synthesis of hapalindole alkaloid natural products, which are terpene derived, typically stems from some type of chiral terpene building block that is either commercially available or synthesized at early stages in the route. This piece is usually designed to contain the isopropenyl group at C15 and the vinyl methyl quaternary center at C12 with the desired stereochemistry already set in place.

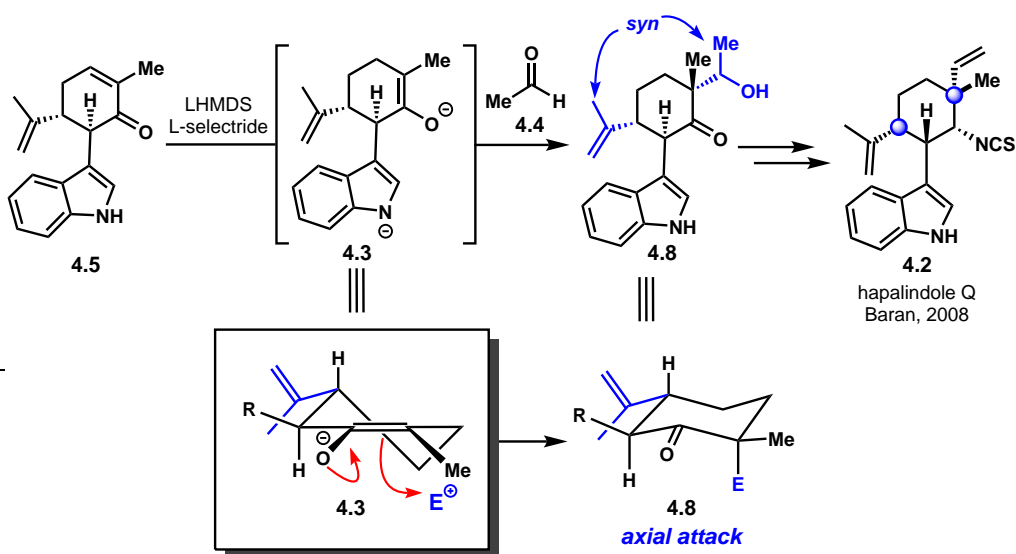
Unsurprisingly, the chiral terpene building block most popular for these syntheses is the readily available and cheap natural product, carvone (**4.1**). Isolated from caraway,⁴ spearmint,⁵ or dill,⁴ carvone is derived from the chiral pool and is beneficial as a building block as it renders the synthesis in which it is used enantiospecific. In addition, carvone contains many of the carbons present in the core skeleton of the hapalindoles since both natural products are terpene derived. Despite its synthetic utility, one challenge associated with using carvone as a starting material in the synthesis of ambiguity natural products arises when installing the C12 quaternary center with the desired *anti* stereochemistry relative to the C15 stereocenter (Scheme 4.1).



Scheme 4.1: Carvone is often used as a building block in the synthesis of hapalindole alkaloids. While carvone is beneficial in many regards, it presents a significant challenge for the installation of the C12 quaternary center with the *anti* relative stereochemistry.

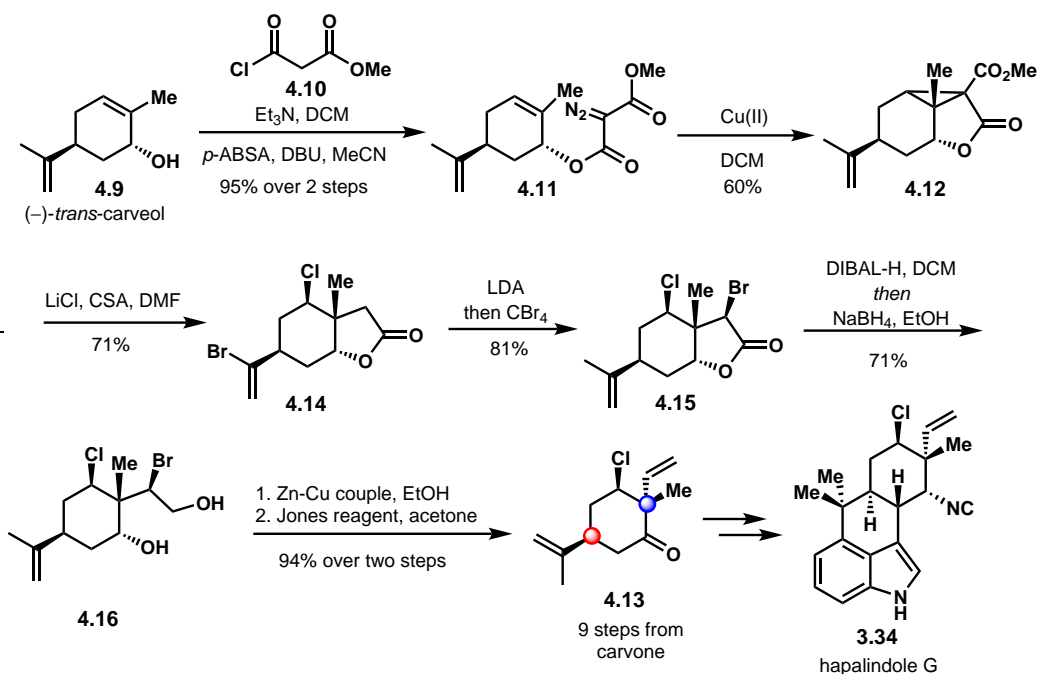
As stated earlier, hapalindole alkaloids contain both *syn* and *anti* relative stereochemistries between the C12 and C15 stereocenters. However, it is far more challenging to install this quaternary center with the *anti* relative stereochemistry when starting with carvone, whereas the *syn* relative stereochemistry is more easily installed. This statement is supported by an examination of two syntheses of hapalindole Q (**4.2**) bearing the *syn* relative stereochemistry, and hapalindole G (**3.34**), which bears the *anti* relationship, by the Baran group in 2008⁶ and the Fukuyama group in 1994,⁷ respectively.

In the Baran group's synthesis of hapalindole Q (**4.2**, Scheme 4.2), they employed a straightforward approach to install the C12 quaternary center using an α -alkylation of enolate intermediate **4.3** with acetaldehyde (**4.4**) as the electrophile. Starting from carvone and indole, they generated product **4.5** using their previously established Cu(II)-mediated oxidative enolate coupling methodology.⁸ From this intermediate (**4.5**), addition of LHMDS fully deprotonates the N–H of the indole in order to prevent the self-quenching of enolate intermediate **4.3**. Enolate species **4.3** was generated through a conjugate hydride delivery using the reductant L-selectride, which was then quenched with acetaldehyde to obtain, with complete selectivity, the desired *syn* isomer **4.6**. This *syn* selectivity can be rationalized by invoking the Fürst-Plattner rule which is applicable for cases involving half-chair intermediates such as enolates and epoxides. In this case, the half-chair enolate (**4.3**) likely proceeds through the lowest energy chair-like transition state leading to axial attack onto acetaldehyde (**4.7**) from the same face as the isopropenyl group. This ultimately leads to compound **4.8** as a single isomer. The Baran group then completed the synthesis of hapalindole Q (**4.2**) in three steps from **4.8**.



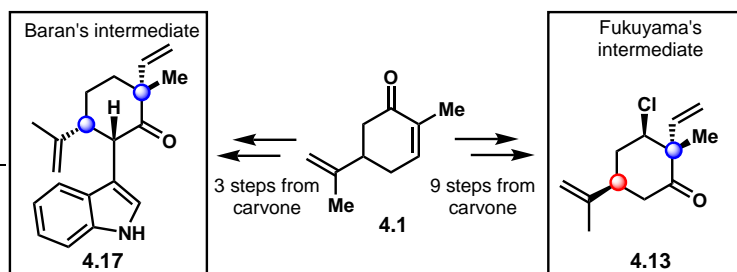
Scheme 4.2: Baran's total synthesis of hapalindole Q (**4.2**) in 2008. The C12 quaternary center was installed by an α -alkylation with acetaldehyde (**4.4**) to form **4.8** with the desired *syn* relative stereochemistry.

On the other hand, the Fukuyama group attempted the synthesis of hapalindole G (**3.34**) which bears the *anti* relative stereochemistry between C12 and C15 (Scheme 4.3). Fukuyama also began the synthesis with carvone, however, as a result of the Fürst-Plattner rule, a simple α -alkylation would lead to the undesired stereocenter at the C12 quaternary center. For this reason, Fukuyama's route was more laborious in regards to step-count but, arguably, still very creative and inspiring as a synthetic strategy. In Fukuyama's synthesis, carvone was reduced to *trans*-carveol (**4.9**) and the resulting secondary alcohol was functionalized with **4.10**. A diazo functional handle was installed between the two carbonyls using Regitz diazo transfer conditions to produce compound **4.11**. With this diazo functionality installed, Fukuyama envisioned using the α -disposed malonyl derived ester to direct a Cu(II)-mediated cyclopropanation reaction from the desired α -face producing cyclopropanated product **4.12**. From cyclopropane **4.12**, an additional five steps was required to transform the cyclopropane ring into the desired vinyl group present in key intermediate **4.13**. By appending the indole moiety to intermediate **4.13**, Fukuyama completed the synthesis of hapalindole G (**3.34**) in a total of 16 steps.



Scheme 4.3: Fukuyama's total synthesis of hapalindole G (**3.34**) in 1994.⁷ The C12 vinyl group, in this case, was installed using the α -disposed hydroxyl group in *trans*-carveol (**4.9**) to direct C–C bond formation in **4.12** from the desired α -face.

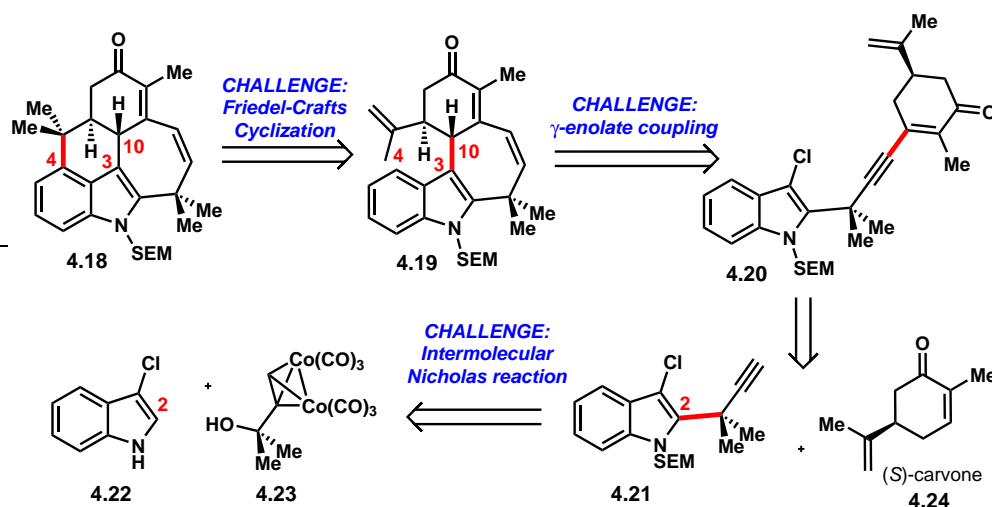
Through a comparison of the two syntheses from the Baran and Fukuyama groups (Scheme 4.4), it can be concluded that while both groups used carveone as their chiral building block, it took only three steps to access Baran's intermediate (**4.17**) bearing the *syn* relative stereochemistry, while it required a total of nine steps to access Fukuyama's intermediate of comparable complexity with the *anti* relative stereochemistry. This vast difference in step-count for the installation of the C12 quaternary center with the requisite stereochemistry, highlights the complexity and challenge associated with the synthesis of ambigine natural products bearing the *anti* relative stereochemistry.



Scheme 4.4: A comparison in step-count for accessing intermediates **4.17** and **4.13** from the Baran group and Fukuyama group respectively.

4.2 1st Generation Route Toward the Synthesis of the Pentacyclic Ambiguines

Keeping the challenges described in Chapter 4.1 in mind, we began thinking about our own strategies for putting together the pentacyclic core of the ambiguityines in our 1st generation retrosynthetic plan as shown in Scheme 4.5. Starting from the proposed dienone-containing pentacyclic core (**4.18**), we envisioned that it could be derived from less-complex tetracycle **4.19**. In the forward direction, a historically challenging indole C4 Friedel-Crafts reaction could be employed to provide pentacycle **4.18**. Tetracycle **4.19** can be taken back to enynone **4.20**. In the forward direction, we envisioned a key palladium-catalyzed γ -enolate coupling would functionalize **4.20** at the indole C3 position after reduction of the alkyne to the corresponding *Z*-alkene. The development of a method of this type to form the indole C3 bond with carvone would represent a novel and unprecedented strategy for the synthesis of hapalindole natural products. Precursor **4.20** can be traced back to (*S*)-carvone and indole derivative **4.21**. In the forward direction, 1,2-addition of the lithium acetylide of **4.21** into (*S*)-carvone followed by an oxidative transposition would lead to **4.20**. Finally, we envisioned that **4.21** could arise from a novel intermolecular Nicholas reaction between 3-chloroindole (**4.22**) and cobalt-complexed alkyne **4.23**.

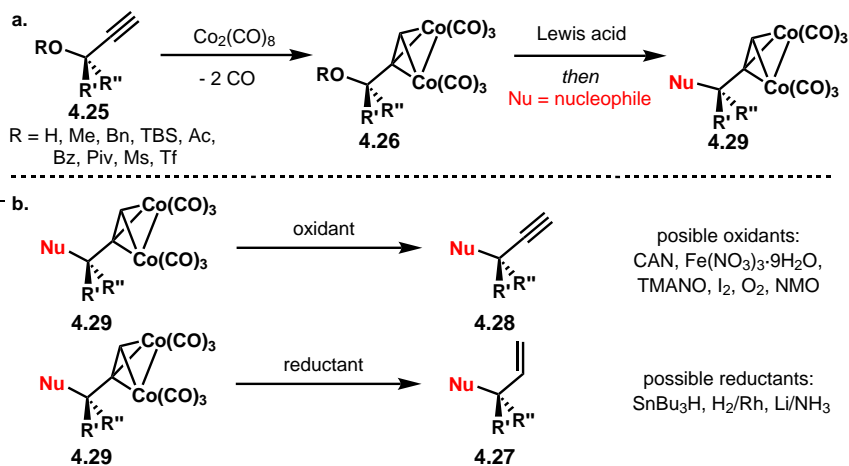


Scheme 4.5: Our first generation approach to access the pentacyclic core (**4.18**) of ambiguityine natural products. This route features a key intermolecular Nicholas reaction between 3-chloroindole (**4.22**) and cobalt-complexed alkyne **4.23**.

This retrosynthetic strategy features a C2 indole functionalization using the Nicholas reaction, which was first reported by Kenneth Nicholas in 1972.⁹ This reaction has been thoroughly explored since its initial discovery, and an overview of its utility is presented in Scheme 4.6.,^{10,11} The Nicholas reaction is a highly versatile methodology that effects substitution of propargylic alcohols with a wide variety of nucleophiles in a regioselective manner. This reaction begins with the complexation of dicobalt octacarbonyl onto propargylic alkynes such as **4.25** to produce derivatives of complex **4.26**. Ionization of the propargylic substituent with a Lewis acid proceeds readily leading to a highly stabilized carbocation where the electron density of the cobalt center stabilizes

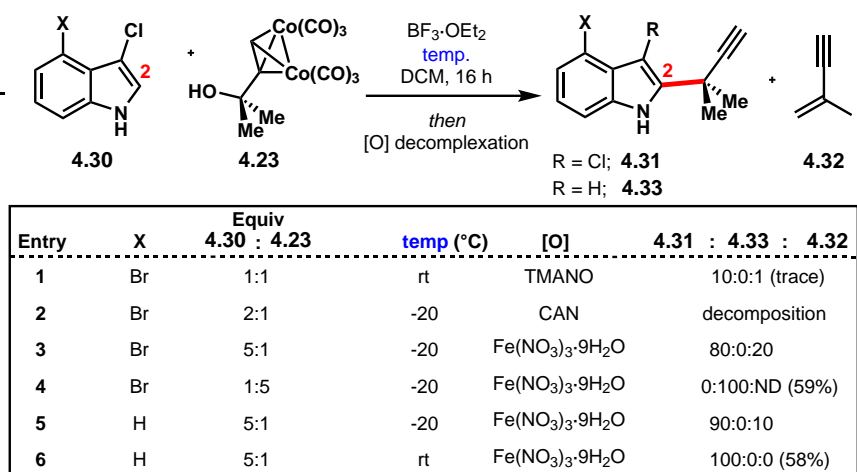
the empty p-orbital of the resulting carbocation. Treatment of this carbocation with a nucleophile leads to functionalization at the propargylic position, providing product in the form of **4.27**.

Typically, the cobalt is decomplexed through one of two ways, an oxidative or a reductive decomplexation. An oxidative process reveals the functionalized alkyne (**4.28**) while a reductive process reveals the corresponding alkene compound, **4.27**. A variety of oxidants and reductants have been reported for these decomplexations ranging from mild to harsh conditions.



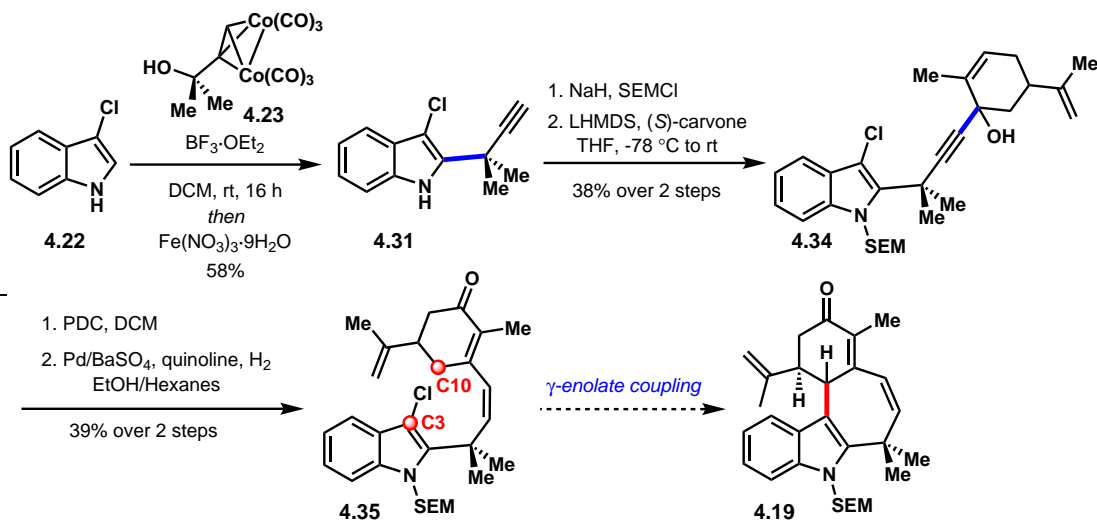
Scheme 4.6: General scheme for the Nicholas reaction originally reported by Nicholas and Pettit in 1972.⁹ a. The Nicholas reaction refers to the nucleophilic substitution of propargylic cobalt-complexed alkynes (**4.26**). b. Cobalt decomplexation occurs under oxidative conditions to reveal the alkyne (**4.28**) or under reductive conditions to reveal the alkene (**4.27**).

The first reaction we decided to pursue in our synthesis was the intermolecular C2 Nicholas alkylation utilizing indole derivative **4.30** and the cobalt-complexed alkyne **4.23**. While Nicholas reactions with indole are known to a limited extent,^{12,13} typically, the C3 position of indole becomes functionalized over the C2 position. In our synthesis, C2 functionalization is desired and as a result, indole was chlorinated at the C3 position to block undesired reactivity. Initial exploration into this reaction using 3-chloro-4-bromoindole and $\text{BF}_3 \cdot \text{OEt}_2$, followed by oxidative decomplexation using TMANO led to trace amounts of the desired product (**4.31**) where X = Br (Scheme 4.7). We also observed formation of a side product (**4.32**) resulting from the elimination of cobalt-complexed alkyne (**4.23**) (Scheme 4.7, entry 1). We explored two other oxidants for oxidative decomplexation and found that $\text{Fe}(\text{NO}_3)_3 \cdot 9\text{H}_2\text{O}$ was suitable for our substrates leading to a 52% yield of desired product **4.31** as shown in entry 3. We found that this intermolecular Nicholas reaction also worked moderately well using 3-chloroindole (**4.22**) at room temperature providing the desired product (**4.31**) in 58% yield (entry 6). As shown in entries 3 and 4, by switching the ratio of **4.30**:**4.23** from 1:5 to 5:1, we observed formation of **4.33** where the chlorine has been replaced with a hydrogen.



Scheme 4.7: Optimization of an intermolecular indole C2 Nicholas reaction.

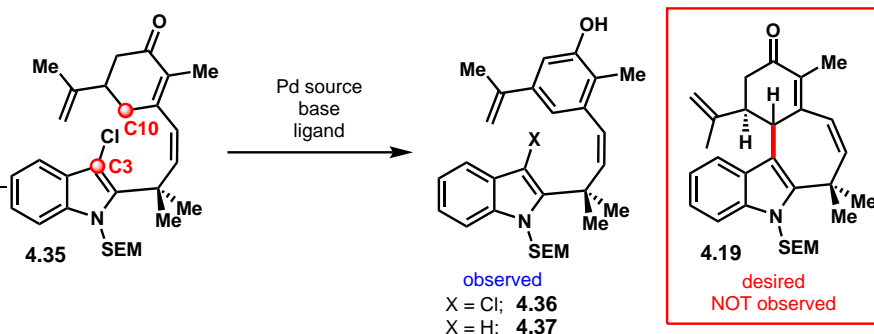
Having optimized this reaction to produce ample quantities of **4.31**, the synthesis was carried forward as shown in Scheme 4.8. Protection of the indole nitrogen using SEMCl and sodium hydride followed by alkyne lithiation and addition into (*S*)-carvone formed allylic alcohol **4.34** in a moderate 38% over 2 steps. Babler-Dauben oxidative transposition^{14,15} using PDC followed by Lindlar reduction of the alkyne provided dienone **4.35** in 39% yield over 2 steps. With the linear alkene (**4.35**) in hand, the next key reaction involved functionalization at the C3 position of indole through development of a γ -enolate coupling reaction to provide tetracyclic compound **4.19**.



Scheme 4.8: The first-generation forward synthesis to access γ -enolate coupling precursor **4.35**.

Indeed, γ -enolate couplings are preceded for cyclohexenone systems such as ours as demonstrated by Buchwald,^{16,17} Maier,¹⁸ and Nomura,¹⁹ thus, we began examining conditions from these reports. A wide variety of combinations of palladium sources, bases, and ligands were explored, but very quickly we discovered that the major pathway for this reaction led to the aromatized phenol compounds **4.36** and **4.37** where the chlorine atom was replaced by a hydrogen atom (Scheme 4.9). The oxidation of carvone by Pd(II) is well preceded and produces the oregano

scented molecule carvacrol.²⁰ Given this highly favorable oxidative aromatization side reaction, our desired transformation would be very challenging to achieve. Additionally, as γ -enolate couplings are typically performed using aryl or vinyl bromides and iodides, we recognized that, in our system, it would be particularly difficult using a vinyl chloride coupling partner.

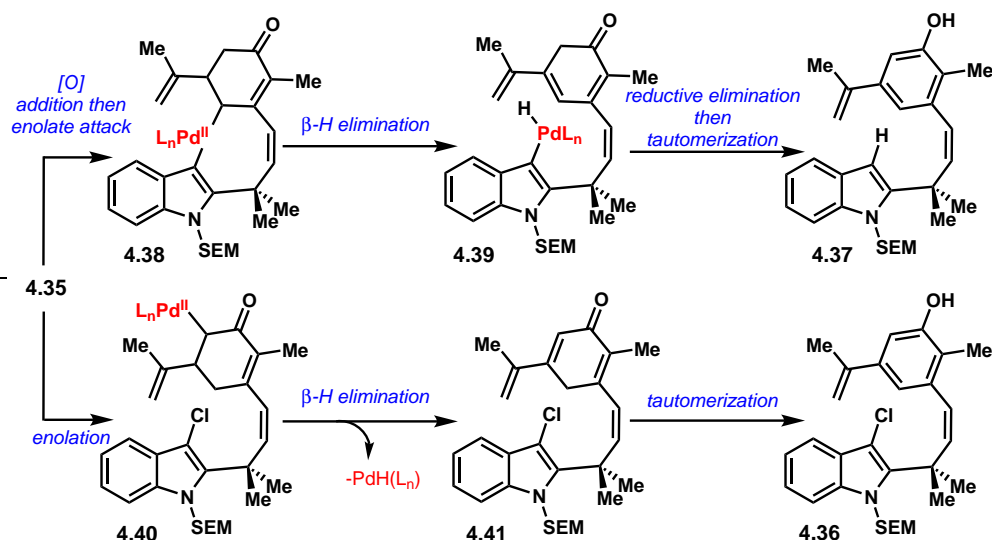


Scheme 4.9: Unsuccessful attempts at generating tetracyclic compound **4.19**. Despite using various combinations of palladium sources, bases, and ligands, the only observed products were **4.36** and **4.37**

Two pathways can be proposed leading to the two major observed products (**4.37** and **4.36**) as shown in Scheme 4.10. From **4.35**, oxidative addition of palladium(0) into the C–Cl bond followed by ligand exchange with the α -enolate, would generate the palladacycle intermediate **4.38**. Reductive elimination of this 8-membered ring palladacycle would lead to our desired tetracycle **4.19**. However, presumably, β -hydride elimination occurs faster than reductive elimination leading to palladium hydride intermediate **4.39**. Reductive elimination of **4.39** followed by tautomerization would lead to the observed phenol side product **4.37**.

Alternatively, oxidation of the carvone unit of **4.35** likely could occur through palladium enolate intermediate **4.40** followed by β -hydride elimination to generate **4.41**. Tautomerization of **4.41** would form the other observed side product **4.36**. While these are not the only possible mechanisms to access the observed products, without extensive mechanistic investigations, these proposals seem reasonable at this time.

Given the lack of success with this key γ -enolate coupling reaction, we searched for alternative ways to form this C3-indole bond and, ultimately, the pentacyclic core. In this 1st generation route, we attempted sequential indole bond functionalizations at C2, C3, and C4 in that order. In our 2nd generation synthesis, we envisioned starting with the functionalization of C3 followed by C2 and C4 for a more robust and successful synthesis.



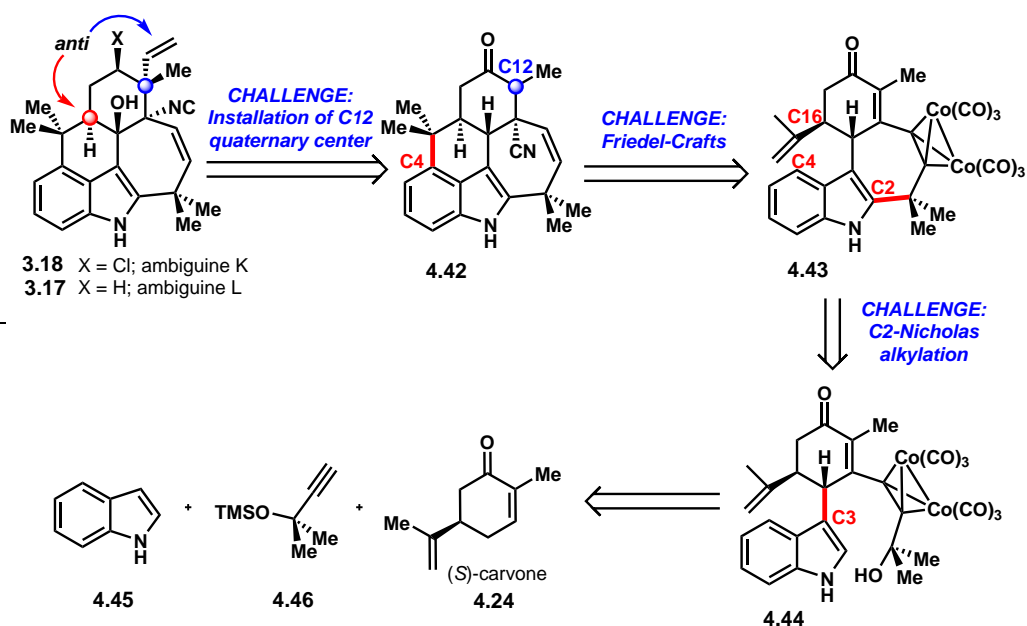
Scheme 4.10: Proposed mechanisms for the formation of isolated products **4.37** and **4.36**.

4.3 2nd Generation Route Toward the Synthesis of the Penta-cyclic Ambiguines

In our 2nd generation retrosynthetic plan (Scheme 4.11) we began from our target natural products, ambiguitynes K (**3.18**) and L (**3.17**) and envisioned them arising from pentacyclic precursor **4.42**. In the forward direction, we would face the challenge of installing the C12 quaternary center with the desired *anti* relative stereochemistry. We believed the C12 quaternary center could be installed through either an α -alkylation of **4.42** or through a novel methodology such as C–H functionalization. Notably, we planned to install this quaternary center at a late-stage in the synthesis, which represents a departure from previous syntheses of hapalindoles containing this *anti* stereochemical relationship. In order to access ambiguitynes L and K (**3.17** and **3.18**) from pentacyclic intermediate **4.42**, the nitrile must be transformed into the isonitrile group, the pseudobenzyl hydroxyl group must be installed, and the ketone must be converted into either a chlorine or hydrogen atom.

Tracing the pentacyclic core back to tetracycle **4.43**, we envisioned performing a historically challenging Friedel-Crafts reaction as originally proposed in our 1st generation retrosynthesis. While previous groups have only observed reactivity from the indole C2 position in this type of Friedel-Crafts reaction, we believed that by having the 7-membered ring already installed, the indole C2 and C3 positions would be unreactive, thus promoting the desired cyclization at C4. Tetracyclic intermediate **4.43** could in turn arise from tricycle **4.44**, and in the forward sense, we expected to use Nicholas chemistry to perform an intramolecular C2-indole Nicholas alkylation to form the 7-membered ring. Rendering this transformation intramolecular was expected to lead to a more robust and reliable reaction. Finally, tricycle **4.44** can be traced back to the readily available and commercial starting materials **4.45**, **4.46**, and **4.24**.

We began the synthesis with the Cu(II)-mediated oxidative enolate coupling reaction between (*S*)-carvone (**4.24**) and indole (**4.45**) (Scheme 4.12). This reaction was developed by the Baran group in 2004 and was applied to their total synthesis of (–)-ambiguine H in 2007.^{8,21} Given our

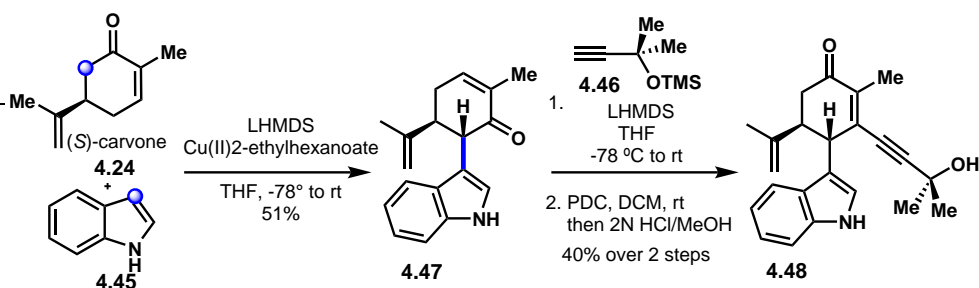


Scheme 4.11: The revised 2nd generation approach for accessing the pentacyclic core (**4.42**) and natural products ambiguines K (**3.18**) and L (**3.17**). This retrosynthetic analysis features an intramolecular C2 Nicholas alkylation in addition to a historically challenging C4 Friedel-Crafts reaction.

unsuccessful attempts in the 1st generation synthesis to forge this indole C3 bond through an alternative γ -enolate coupling, Baran's methodology became the most efficient and reliable way to form this bond early in the synthesis. From known compound **4.47**, we then performed a 1,2-addition of lithium acetylide (**4.46**) into the ketone of **4.47** to produce an allylic alcohol as a mixture of diastereomers. Without purification, the resulting alcohol can be subjected to a Babler-Dauben oxidative transposition using pyridinium dichromate and acidic workup to afford enone **4.48** in 40% yield over two steps.^{14,15} While the 1,2-addition of lithium acetylide **4.49** proceeds cleanly, the Babler-Dauben transformation is likely plagued by a Meyer-Schuster side reaction,²² involving the adjacent alkyne functionality. At this stage, attempts have not been made to prevent this side reaction from occurring.

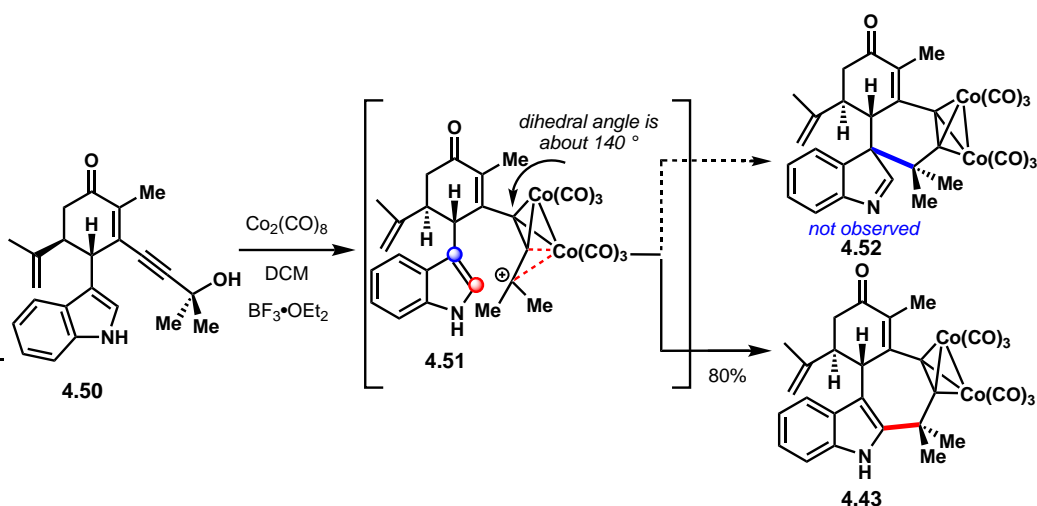
Nevertheless, the formation of tricycle **4.50** on gram-scale set the stage for the C2-Nicholas alkylation, a key reaction that would form the 7-membered ring of the desired tetracycle. As shown in Scheme 4.13, the complexation of dicobalt octacarbonyl to the alkyne proceeded smoothly and upon treatment with the Lewis acid $\text{BF}_3 \cdot \text{OEt}_2$, the complexed intermediate underwent ionization and cyclization to form tetracycle **4.43** in a high 80% yield. This reaction, surprisingly, required no optimization and its success is likely due to the fact that it is intramolecular. In addition, the rehybridization of the alkyne sp carbons to nearly sp^3 carbons, positions the pendant alcohol group in good proximity to the indole C2 carbon for subsequent nucleophilic attack.

While it may be assumed that the C3-position of indole attacks the stabilized carbocation (**4.51**) forming intermediate **4.52**, this scenario is unlikely given the larger dihedral angles associated with cobalt-complexed alkynes. According to crystal structure data from the literature,²³ the dihedral angle of cobalt-complexed alkynes sits around 140° , which is much larger compared to the di-



Scheme 4.12: The 2nd generation synthesis begins with the copper-mediated oxidative coupling reaction as reported by Baran and coworkers in 2004. Lithiate addition of **4.46** followed by Babler-Dauben oxidative transposition leads to compound **4.50**

hedral angles found in cyclohexane (120°). In fact, there is only one reported cobalt-complexed cyclohexane derivative in the literature.²⁴ It is far more typical for cyclic cobalt-complexed alkynes to be used in the synthesis of 8-, 9-, or even 10-membered rings.²⁵

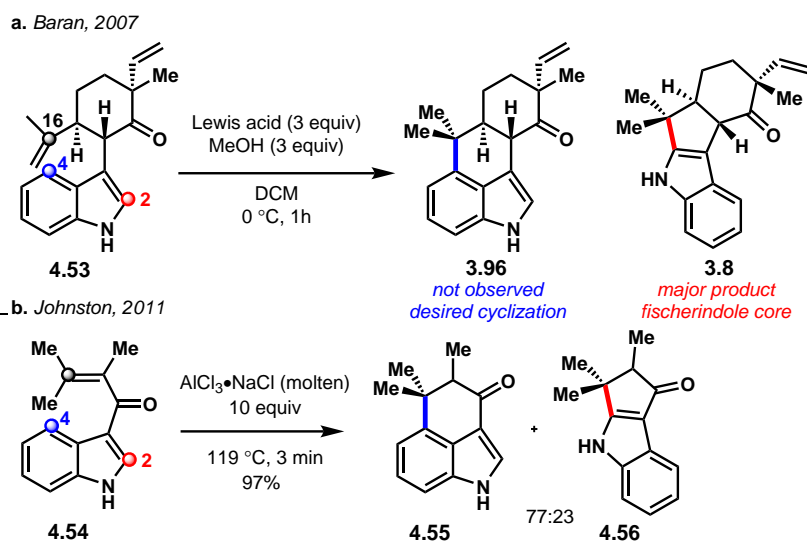


Scheme 4.13: The intramolecular Nicholas reaction proceeds in 80% yield leading to desired tetracycle **4.43**. Formation of **4.52** by C3 attack of the indole moiety is unlikely due to geometric constraints.

With tetracycle **4.43** in hand, we began to look at conditions for performing the historically challenging C4 Friedel-Crafts cyclization reaction. The difficulties associated with this type of cyclization are evident in previous syntheses of hapalindole natural products.

As shown in Scheme 4.14, the Baran group attempted a similar C4 Friedel-Crafts reaction in their synthesis of (-)-ambiguine H in 2007 using substrate **4.53**.²¹ In this case, formation of the fischerindole core (**3.8**) was always observed, presumably generated through C2 attack of the indole unit onto the C16 position of the isopropenyl group. Unfortunately, despite screening a wide variety of Lewis acids and examining different substrates, they never saw productive formation of the desired tetracycle (**3.96**).

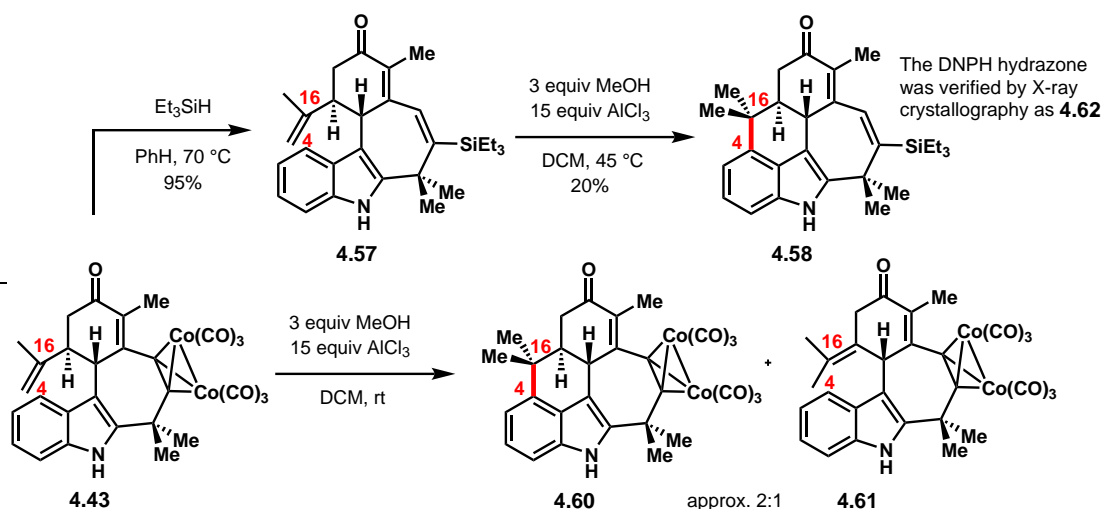
A few years later in 2011, however, the Johnston group reported a remarkable transformation from indole derivative **4.54** to the C4-cyclized product **4.55** (Scheme 4.14). The Johnston group also screened a variety of Lewis acidic conditions and under most reaction conditions, also isolated the major product as the undesired C2-cyclized compound **4.56**. However, using an aluminum trichloride/sodium chloride molten mixture at 119 °C, they observed a more favorable ratio of their desired C4-cyclized product (**4.55**) to the undesired (**4.56**) in about a 3:1 ratio. Despite this incredible result, this reaction still was not completely selective for the desired C4-cyclization.



Scheme 4.14: Previous attempts by Baran in 2007 and Johnston in 2011 for the C4 Friedel-Crafts reaction.

With these unfavorable previous observations in mind, we were anticipating that this cyclization would be challenging to achieve in a selective manner with our substrates. It appears that this cyclization is also highly substrate-dependent, with more complex substrates providing less selective results. As shown in Scheme 4.15, we initially investigated this reaction with decomplexed substrates where the cobalt had been removed through a hydrosilylation reaction to produce the vinyl silane intermediate **4.57** in good yield.²⁶ Using **4.57**, we began screening Lewis and Brønsted acids and eventually found some promising results with a MeOH/ AlCl_3 mixture at slightly elevated temperature. Indeed, we isolated pentacycle **4.58**, which was characterized unambiguously through an X-ray structure of the corresponding DNPH hydrazone compound **4.59**. Unfortunately, the yield of this Friedel-Crafts reaction was quite poor, at only 20%. While screening other tetracyclic substrates, we found that submitting **4.43** to the same conditions at room temperature yielded our desired pentacyclic compound (**4.60**) in a 2:1 ratio with uncyclized, isomerized compound **4.61**. Despite the near quantitative yield of both compounds (**4.60** and **4.61**) this reaction was further optimized using tetracycle **4.43** to provide a more favorable ratio of desired pentacycle **4.60** to **4.61**.

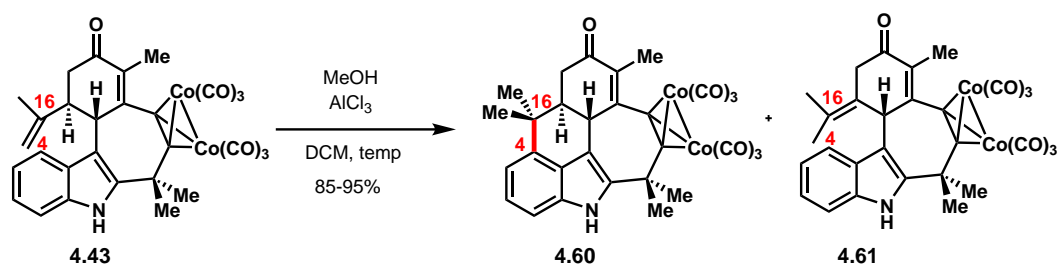
Parameters of optimization included the manipulation of equivalents of MeOH, concentration, temperature, and reaction time. In entry 1 (Scheme 4.16), we found that with 5 equivalents of MeOH and 15 equivalents of AlCl_3 , moderate conversion was achieved to desired pentacycle **4.60** while a significant amount of starting material remained after 30 min. The time of reaction was



Scheme 4.15: The C4 Friedel-Crafts reaction is successful with vinyl silane **4.63** in low yield. An improved Friedel-Crafts reaction was discovered using cobalt-complexed tetracycle **4.43** to generate the pentacycle **4.60** in addition to side product **4.61**.

increased from 30 min to 2 hours (entry 2), and similar conversion to the pentacycle (**4.60**) was observed as well as to the undesired, uncyclized side product **4.61**. On smaller scale (<500 mg) there was excellent conversion to the desired pentacycle using 15 equivalents of MeOH (entry 3), but for reactions run on greater than 1 g scale, formation of side product **4.61** became problematic. Cooling this reaction to 0 °C prior to the addition of MeOH (entry 4) provided excellent conversion, even on large scales (>1 g), to desired **4.60**. Finally, in an effort to reduce the amount of solvent used in this reaction, the concentration was increased to 0.03 M but unfortunately, significant side product formation occurred (entry 5). Given these results, we decided to proceed with the optimized conditions in entry 4 as they worked consistently well with multigram quantities of material at a time.

Throughout the course of optimizing this C4 Friedel-Crafts reaction, an interesting and unexpected cobalt decomplexation pathway was discovered leading to vinyl chloride compound **4.64** (Scheme 4.17). To the best of our knowledge, this type of decomplexation reaction has not been reported in the literature and the mechanism for this transformation is not clear although it may involve a "water-gas shift" process.²⁷ Additionally, given that reductive cobalt decomplexation using SnBu_3H as the reductant is shown to proceed through a radical pathway,²⁶ this decomplexation reaction may also proceed through radical intermediates, though formal mechanistic studies have not yet been pursued.

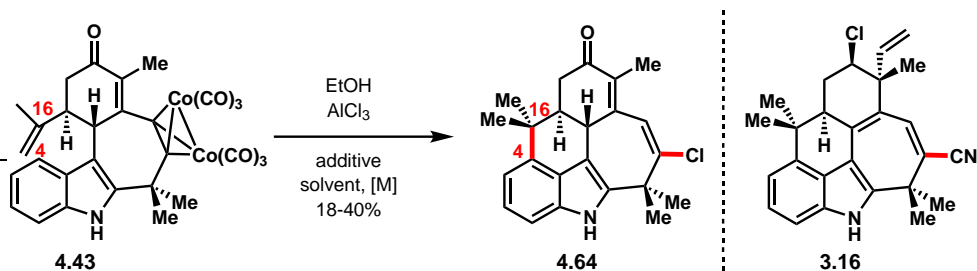


Entry	[M]	Equiv MeOH: AlCl ₃	temp	time	4.60 : 4.61 : 4.43
1	0.01	5:15	rt	30 min	1:0:0.3
2	0.01	5:15	rt	2 h	2:1:1
3	0.01	15:15	rt	2 h	100:0:0
4*	0.01	15:15	0 °C to rt	3 h	100:0:0
5	0.03	15:15	0 °C to rt	2.5 h	1:0.7:0

* Performed on >1 g scale.

Scheme 4.16: A selection of conditions used to optimize the C4 Friedel-Crafts cyclization reaction. Optimal conditions are shown in entry 4 which produced desired pentacycle **4.60** in near quantitative yield.

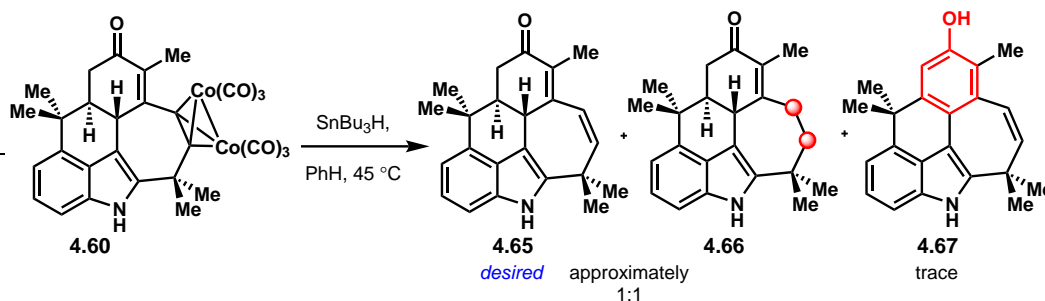
We were quite intrigued by the vinyl chloride (**4.64**) as it maps well onto ambigine G (**3.16**), which bears a vinyl nitrile group at the same position as the chloride. We therefore set out to optimize this reaction. Unfortunately, despite exploring many different conditions including additives, oxidants, halogen sources, salts, the yield of this reaction never rose above 40% on greater than a 10 mg scale. With the lack of promising results for this decomplexation reaction, efforts were shifted away from optimization and back onto the total synthesis of the pentacyclic ambigines using our pentacyclic intermediate **4.60**.



Scheme 4.17: Unexpected conditions found to decomplex tetracycle **4.43** and form the vinyl chloride species **4.64**.

Having developed a robust and scalable route to access the pentacyclic core, the decomplexation of cobalt from **4.60** to reveal the corresponding alkene was attempted as demonstrated in Scheme 4.18. We chose to use the well-precedented and mild conditions developed by Isobe and coworkers in which they use SnBu₃H as the reductant.²⁶ In the initial attempt, treatment of pentacycle **4.60** with SnBu₃H at 45 °C did, in fact, form the desired dienone compound **4.65**. However, we also observed significant formation of side products **4.66** and **4.67**. Side product **4.66** is likely formed through a 1,6-hydride reduction of desired compound **4.65**, while the aromatized

compound, **4.67**, likely forms through exposure of **4.65** to air. In order to prevent formation of these side products, a quaternary center was installed through a second Nicholas reaction at the β -position of enone **4.60**.

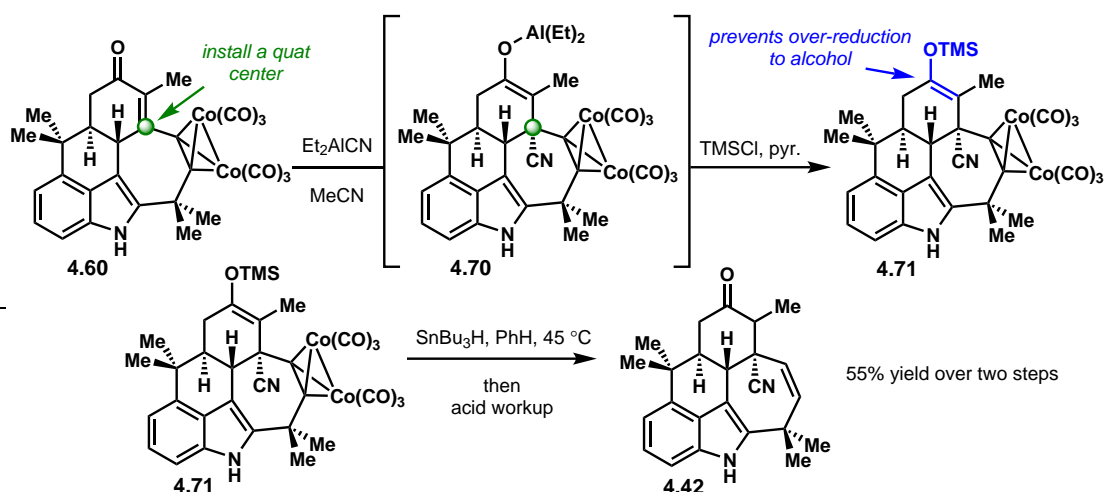


Scheme 4.18: Reductive decomplexation of **4.60** using SnBu_3H leads to desired product **4.68** in addition to undesired side products **4.66** and **4.67**.

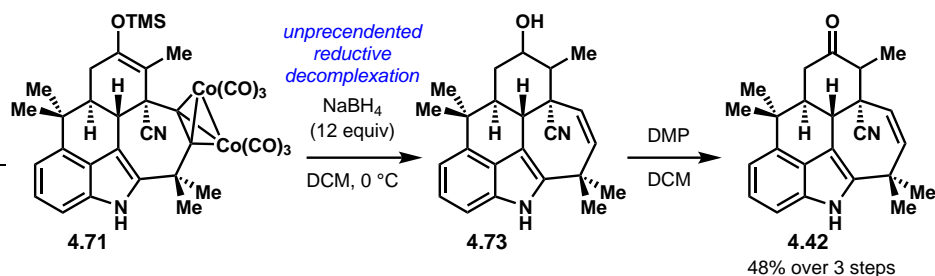
As demonstrated in Scheme 4.19, a nucleophile was installed at the β -position of compound **4.60** through a Nicholas reaction. Ideally, this nucleophile could act as a precursor for the isonitrile that is present in the natural product. This nucleophile also had to be stable enough to withstand subsequent reaction conditions in the synthesis. As such, the nucleophile that was explored for this reaction was the addition of a nitrile. Nitrile additions in the Nicholas reaction are known²⁸ and commonly performed using the reagent Et_2AlCN , also known as Nagata's reagent.²⁹ Indeed, treatment of pentacycle **4.69** with Nagata's reagent delivered cyanide in a 1,4-conjugate fashion forming aluminum enolate **4.70**. Searching through literature reports of 1,4-additions of cyanide using Nagata's reagent, we found conditions reported by the Vandewalle group in 2004 that would trap this aluminum enolate as the silyl enol ether.³⁰ Protecting the ketone in this way should prevent over-reduction to the corresponding alcohol in the reductive decomplexation step. As we expected, quenching the aluminum enolate (**4.70**) with TMSCl provided the silyl enol ether compound **4.71**, and without purification it was submitted to the SnBu_3H reductive decomplexation conditions. In this case, we saw almost exclusive formation of the desired ketone intermediate (**4.42**) in 55% yield over the two steps.

It is also important to report the alternative reductive decomplexation conditions we discovered, that to the best of our knowledge, have not been reported in the literature previously. As shown in Scheme 4.20, we found that a large excess (12 equiv) of NaBH_4 led to a clean reductive decomplexation of **4.71** revealing the alkene. However, during the course of the reaction, the silyl enol ether was removed and the ketone was subsequently reduced to alcohol compound **4.73**. Nevertheless, the alcohol (**4.73**) could be oxidized using DMP to access ketone intermediate **4.42** in 43% yield over the 3 steps. Notably, reductive decomplexation with NaBH_4 is far more environmentally friendly than the more typical SnBu_3H conditions and we expect these reductive decomplexation conditions to be broadly applicable to other cobalt-complexed scaffolds.

At this point in the synthesis, we have developed a robust and scalable route to access key nitrile-containing intermediate **4.42**. The second half of this synthesis involves the manipulation of **4.42** in an attempt to install the C12 quaternary center with the desired *anti* relative stereochemistry and will be discussed in Chapter 5.



Scheme 4.19: Installation of a cyanide followed by enolate trapping with TMSCl led to intermediate **4.71**. The reductive decomplexation of silyl enol ether **4.72** provided nearly exclusive formation of desired compound **4.42**.



Scheme 4.20: A more environmentally friendly reductive decomplexation protocol was discovered using NaBH_4 generating alcohol **4.73**. Oxidation with DMP leads to ketone intermediate **4.42**.

4.4 Experimental Contributors

All of the work presented in Section 4.2 (1st Generation Route Toward the Synthesis of the Pentacyclic Ambiguines) is unpublished and executed solely by Rebecca Johnson (R.J.). Original ideas and strategies were generated by R.J., Prof. Richmond Sarpong (R.S.) and Dr. Svitlana Kulyk (S.K.). The idea of using the Nicholas reaction in the synthesis was originally proposed by Dr. Jason Pfleuger (J.P.). Partial characterization data is reported in Section 4.6 (Experimental Methods and Procedures). The work presented in Section 4.3 (2nd Generation Route Toward the Synthesis of Pentacyclic Ambiguines) was completed by R.J. and Marco Hartmann (M.H.) (visiting student from the ETH, Zürich) and is unpublished. The full characterization is reported in Section 4.6 (Experimental Methods and Procedures). Ideas and strategy were developed with the help of R.S. and M.H.

4.5 Materials and Methods

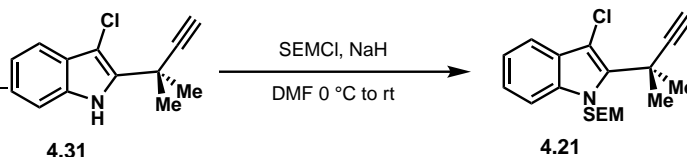
Unless stated otherwise, reactions were performed in oven-dried glassware sealed with rubber septa under a nitrogen atmosphere and were stirred with Teflon®-coated magnetic stir bars. Liquid reagents and solvents were transferred by syringe using standard Schlenk techniques. Tetrahydrofuran (THF), toluene, acetonitrile (MeCN), methanol (MeOH), NEt_3 were dried by passage over a column of activated alumina; Dichloromethane (DCM) was distilled over calcium hydride. All other solvents and reagents were used as received unless otherwise noted. Where stated, solutions were degassed using three cycles of freeze/pump/thaw (freezing the solution contained within a Schlenk flask in liquid nitrogen, opening the flask to vacuum for 5 min, then allowing the solution to thaw under vacuum). Thin layer chromatography was performed using SiliCycle silica gel 60 F-254 precoated plates (0.25 mm) and visualized by UV irradiation, anisaldehyde, cerium ammonium molybdenate (CAM), potassium permanganate, or iodine stain. Optical rotation was recorded on a Perkin Elmer Polarimeter 241 at the D line (1.0 dm path length), $c = \text{mg/mL}$, in CHCl_3 unless otherwise stated. ^1H and ^{13}C -NMR experiments were performed on Bruker spectrometers operating at 300, 400, 500 or 600 MHz for ^1H and 75, 100, 125, or 150 MHz for ^{13}C experiments. Chemical shifts (δ) are reported in ppm relative to the residual solvent signal (CDCl_3 $\delta = 7.26$ for ^1H NMR and $\delta = 77.16$ for ^{13}C NMR; Data are reported as follows: chemical shift (multiplicity, coupling constants where applicable, number of hydrogens). Abbreviations arise as follows: s (singlet), d (doublet), t (triplet), q (quartet), dd (doublet of doublet), dt (doublet of triplet), ddq (doublet of doublets of quartets), m (multiplet), bs (broad singlet). IR spectra were recorded on a Bruker ALPHA Platinum ATR FT-IR spectrometer. Low and high-resolution mass spectral data were obtained from the University of California, Berkeley Mass Spectral Facility, on a VG 70-Se Micromass spectrometer for FAB, and a VG Prospec Micromass spectrometer for EI. Purifications were performed with a Yamazen® automatic purification system and gradients were determined by inputting R_f values and using a Yamazen® generated conditions.

4.6 Experimental Methods and Procedures



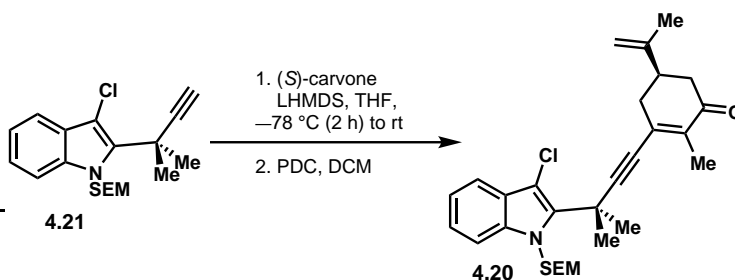
3-Chloro-2-(2-methylbut-3-yn-2-yl)-1H-indole (4.75): To a flame-dried schlenk flask was added DCM (0.10 mL, 0.22 M) and **4.74** (0.20 mmol, 20 μL , 1.0 equiv), followed by $\text{Co}_2(\text{CO})_8$ (0.20 mmol, 75 mg, 1.0 equiv). The reaction mixture was allowed to stir at room temperature for 1 h at which time indole **4.22** (1.1 mmol, 0.17 g, 5.0 equiv) was added and allowed to stir another hour at room temperature. The reaction mixture was quenched with sodium bicarbonate (10 mL) (sat. aq.) and extracted with DCM (3 x 10 mL). The combined organic layers were washed with brine (20 mL), dried over sodium sulfate and concentrated to give a red oil. The crude mixture was purified using SiO_2 column chromatography and immediately carried on to the next step. The red oil was dissolved in 95% EtOH and $\text{Fe}(\text{NO}_3)_3 \cdot 9\text{H}_2\text{O}$ was added, CO evolution

is noticeable. When TLC indicated consumption of starting material, the reaction mixture was partitioned between DCM and H₂O (5 mL) and extracted with DCM (3 x 10 mL). The combined organic layers were washed with brine (30 mL) and dried over sodium sulfate. The crude reaction mixture was purified by SiO₂ column chromatography to provide the product as an off-white oil (40 mg, 58%). ¹H NMR (600 MHz, CDCl₃) δ 8.56 (s, 1H), 7.59 (d, *J* = 7.8 Hz, 1H), 7.35 (d, *J* = 8.0 Hz, 1H), 7.21 (dt, *J* = 24.3, 7.3 Hz, 2H), 2.56 (s, 1H), 1.84 (s, 6H).



3-Chloro-2-(2-methylbut-3-yn-2-yl)-1-((2-(trimethylsilyl)ethoxy)methyl)-1H-indole (4.21):

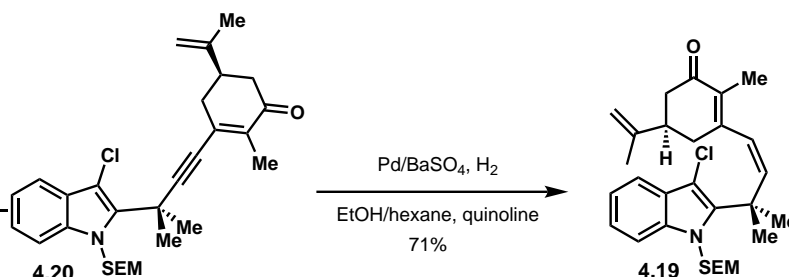
To a flame-dried round-bottomed flask was added indole derivative **4.31** (2.0 mmol, 0.44 g, 1.0 equiv) followed by DMF (10 mL, 0.2 M). After cooling to 0 °C in an ice/water bath, NaH (60% in mineral oil) (2.4 mmol, 97 mg, 1.2 equiv) was added. After stirring at 0 °C for 5 min, SEMCl (2.2 mmol, 0.39 mL, 1.1 equiv) was added and the reaction mixture was allowed to stir at 0 °C until TLC indicated consumption of starting material. The reaction mixture was quenched with ammonium chloride (sat. aq.) (10 mL) and extracted with ethyl acetate (3 x 10 mL). The combined organic layers were washed with brine (2 x 30 mL), dried over sodium sulfate and concentrated *in vacuo* to yield the crude reaction mixture which was taken on immediately to the next step. ¹H NMR (400 MHz, CDCl₃) δ 7.65 - 7.53 (m, 1H), 7.42 (d, *J* = 8.2 Hz, 1H), 7.32 - 7.23 (m, 1H), 7.18 (t, *J* = 7.6 Hz, 1H), 5.92 (s, 2H), 3.73 - 3.53 (m, 2H), 1.95 (s, 6H), 1.04 - 0.87 (m, 2H), -0.02 (s, 9H).



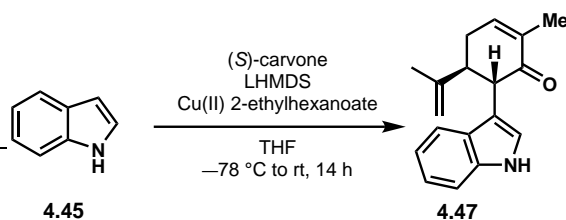
Linear tricyclic (4.20): Alkyne **4.21** (1.9 mmol, 662 mg, 1.0 equiv) was dissolved in THF (9.5 mL, 0.2 M) and cooled to -78 °C. LHMDS (1.0 M in THF) (2.0 mmol, 2.0 mL, 1.1 equiv) was added via syringe and the mixture was allowed to stir at -78 °C for 2 h. At which time (*S*)-carvone (**4.24**) (2.0 mmol, 0.31 mL, 1.1 equiv) was added via syringe and the resulting solution was allowed to warm to room temperature. Once the reaction mixture was fully warmed to room temperature, it was quenched with the addition of ammonium chloride (sat. aq.) (10 mL) and extracted with ethyl acetate (3 x 10 mL). The combined organic layers were washed with brine, dried over sodium sulfate and concentrated *in vacuo*. The crude reaction mixture was subjected to SiO₂ column chromatography to yield the product as an off-white wax (586 mg, 62%)

The pure allylic alcohol (1.0 mmol, 0.50 mg, 1.0 equiv) was then dissolved in DCM (10 mL, 0.10 M) and PDC (1.5 mmol, 0.56 g, 1.5 equiv) was added all at once. This reaction was allowed to stir at room temperature for 14 h at which point it was filtered through a Celite® plug. The

crude reaction mixture was concentrated *in vacuo* and immediately purified via SiO₂ column chromatography to yield compound **4.20** (327 mg, 65% over 3 steps). ¹H NMR (400 MHz, CDCl₃) δ 7.60 (dd, *J* = 7.9, 1.1 Hz, 1H), 7.40 (d, *J* = 8.2 Hz, 1H), 7.32 - 7.26 (m, 1H), 7.20 (td, *J* = 7.5, 7.1, 1.0 Hz, 1H), 5.87 (s, 2H), 4.89 - 4.64 (m, 2H), 3.67 - 3.44 (m, 2H), 2.80 - 2.24 (m, 5H), 2.01 (s, 6H), 1.96 (s, 3H), 1.74 (d, *J* = 1.2 Hz, 3H), 0.95 - 0.89 (m, 2H), -0.04 (s, 9H).

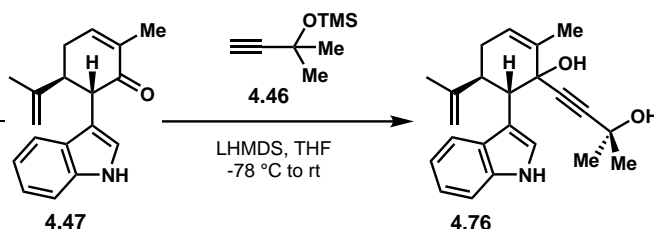


Linear dienone (4.19): Alkyne **4.20** (0.10 mmol, 0.050 g, 1.0 equiv) was dissolved in a 1:1 mixture of EtOH and hexanes (1.0 mL, 0.10 M). Quinoline (0.56 mmol, 67 μL, 5.6 equiv) was added followed by 5% Pd/BaSO₄ (0.010 mmol, 2.0 mg, 0.10 equiv). A balloon of H₂ was fitted in the septum and the flask was evacuated and backfilled with H₂ gas three times. The reaction mixture was allowed to stir for 30 min at which time TLC indicated consumption of starting material and the mixture was filtered through a SiO₂ gel plug to yield the crude reaction mixture. The crude mixture was concentrated *in vacuo* and the crude material was purified via SiO₂ column chromatography to yield the pure material (35 mg, 71%). ¹H NMR (600 MHz, CDCl₃) δ 7.51 (d, *J* = 7.9 Hz, 1H), 7.26 (t, *J* = 7.3 Hz, 1H), 7.21 (t, *J* = 7.6 Hz, 1H), 7.14 (t, *J* = 7.4 Hz, 1H), 6.04 (d, *J* = 12.7 Hz, 1H), 5.90 (d, *J* = 12.6 Hz, 1H), 5.52 - 5.30 (m, 2H), 4.47 (d, *J* = 1.5 Hz, 1H), 4.25 (s, 1H), 3.59 (ddd, *J* = 10.4, 7.1, 3.9 Hz, 2H), 2.23 - 1.98 (m, 2H), 1.83 - 1.68 (m, 10H), 1.64 (t, *J* = 15.0 Hz, 1H), 1.44 (dd, *J* = 17.3, 12.1 Hz, 1H), 1.24 (s, 3H), 0.92 (dd, *J* = 9.3, 7.2 Hz, 2H), 0.07 - -0.11 (m, 9H).

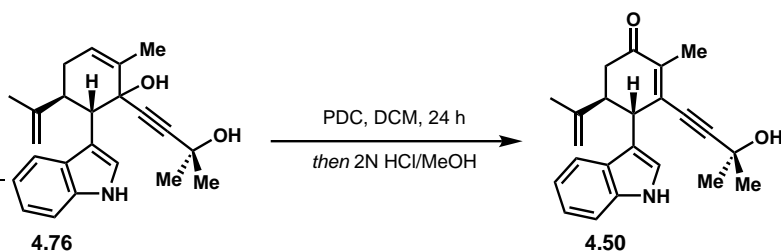


(5*S*,6*S*)-6-(1*H*-indol-3-yl)-2-methyl-5-(prop-1-en-2-yl)cyclohex-2-en-1-one(4.47): An oven-dried 2L round bottomed flask was charged with indole (**4.45**) (15 g, 130 mmol, 2.0 equiv) followed by (*S*)-carvone (10 mL, 65 mmol, 1.0 equiv). To this mixture was added THF (280 mL, 0.23 M) and the resulting solution was cooled in a dry ice/acetone bath to -78 °C. The reaction mixture was held at -78 °C while LHMDS (1.0 M in THF, 210 mL, 210 mmol, 3.3 equiv) was added via cannula transfer dropwise over 30 min. The resulting brownish solution was stirred at -78 °C for 1 h upon which the flask was opened to the atmosphere and Cu(II) 2-ethylhexanoate (34 g, 97 mmol, 1.5 equiv) was added as a solid through a plastic funnel. The reaction mixture was quickly resealed with the septum and allowed to warm to room temperature overnight. The reaction mixture was quenched with ammonium chloride (sat. aq.) (200 mL) and the aqueous layer was extracted

with ethyl acetate (3 x 100 mL). The organic layer was washed with brine (1 x 200 mL), dried over sodium sulfate, and the solvent was removed *in vacuo*. The crude product was purified via SiO₂ column chromatography eluting with 2:1 hexanes:ethyl acetate to afford pure product as an off-white solid. ¹H NMR (CDCl₃, 600 MHz) δ 8.01 (br s, 1H), 7.44 (d, *J* = 7.9 Hz, 1H), 7.33 (d, *J* = 8.1 Hz, 1H), 7.16 (dd, *J* = 7.7, 7.7 Hz, 1H), 7.07 (dd, *J* = 7.6, 7.6 Hz, 1H), 6.91 (d, *J* = 2.3 Hz, 1H), 6.82 - 6.78 (m, 1H), 4.68 (s, 1H), 4.64 (s, 1H), 3.91 (d, *J* = 10.7 Hz, 1H), 3.27 (ddd, *J* = 9.7, 9.7, 5.0 Hz, 1H), 2.61 - 2.53 (m, 1H), 2.50 - 2.43 (m, 1H), 1.87 (s, 3H), 1.63 (s, 3H). ¹³C NMR (CDCl₃, 101 MHz) δ 199.54, 145.85, 143.72, 136.21, 135.37, 126.96, 122.71, 121.62, 119.17, 119.09, 112.79, 112.48, 111.32, 49.05, 48.31, 30.88, 19.30, 16.29. IR (ATIR) 3402, 3349, 3058, 2914, 1678, 1641, 1456, 1421, 1371, 1077, 886, 738 cm⁻¹. C₁₈H₂₀ON [M+H]⁺, 266.1539. Found 266.1540. [α]_D = +34.5

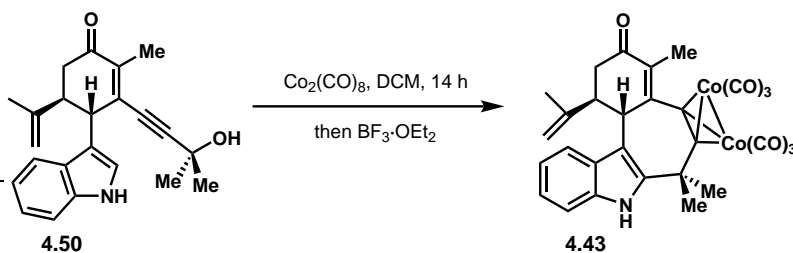


Allylic alcohol (4.76): To a solution of alkyne (4.77) (12 mL, 60 mmol, 2.1 equiv) in THF (230 mL, 0.27 M) at -78°C was added LHMDS (1.0 M in THF, 61 mL, 61 mmol, 2.2 equiv) dropwise over 10 min. This solution was allowed to stir at -78°C for 1 h upon which indole coupled product 4.47 (7.6 g, 29 mmol, 1.0 equiv) was added as a solution in THF (50 mL) dropwise over 5 min. The reaction mixture was immediately taken out of the -78°C bath and allowed to warm fully to room temperature. The reaction mixture was quenched with ammonium chloride (sat. aq.) (200 mL) and the aqueous layer was extracted with ethyl acetate (3 x 100 mL). The organic layers were combined and washed with brine (200 mL), dried over sodium sulfate and the solvent was removed *in vacuo*. The yellowish-red crude reaction mixture was used immediately in the next step.

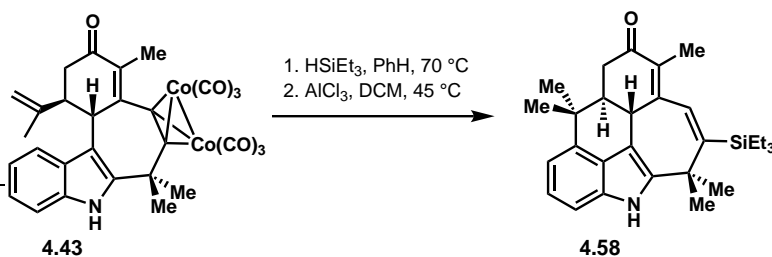


Tricyclic (4.50): The crude product 4.76 was dissolved in DCM (290 mL, 0.10 M) and PDC (16 g, 43 mmol, 1.5 equiv) was added. The reaction mixture was allowed to stir at room temperature overnight. The reaction mixture was then filtered through a plug of Celite® eluting with DCM and to this mixture was added 2N HCl/MeOH (50 mL). Once TLC indicated complete removal of the TMS group (approx. 10 min), the reaction mixture was quenched with sodium bicarbonate (sat. aq.) (200 mL) and the aqueous layer was washed with ethyl acetate (3 x 100 mL). The combined organic layers were washed with brine and dried over sodium sulfate. The solvent was removed *in vacuo* and the crude product was purified via SiO₂ column chromatography eluting with 2:1 hexanes:ethyl acetate then 1:1 hexanes:ethyl acetate to yield pure product as a yellow foam. ¹H

NMR (600 MHz, CDCl₃) δ 8.17 (s, 1H), 7.60 (d, J = 7.9 Hz, 1H), 7.37 (d, J = 8.1 Hz, 1H), 7.20 (t, J = 7.8 Hz, 1H), 7.13 (t, J = 7.5 Hz, 1H), 6.95 (d, J = 2.4 Hz, 1H), 4.75 - 4.64 (m, 2H), 4.12 (dd, J = 7.9, 2.2 Hz, 1H), 3.17 (td, J = 9.0, 4.5 Hz, 1H), 2.75 - 2.49 (m, 2H), 2.01 (d, J = 1.9 Hz, 3H), 1.72 (s, 3H), 1.07 (d, 6H). **¹³C NMR**; (150 MHz, CDCl₃) δ 198.3, 145.2, 139.4, 137.9, 136.3, 127.3, 122.6, 122.1, 119.4, 119.1, 115.85, 112.9, 111.4, 108.8, 81.1, 65.4, 47.6, 41.7, 41.6, 30.5, 30.5, 20.3, 14.1. **IR** (ATIR) 3324, 3260, 2979, 2850, 2220, 1640, 1456, 1340, 1167, 891, 739 cm⁻¹. C₂₃H₂₆O₂N [M+H]⁺, 348.1958. Found 348.1960. [α]_D = +151.3

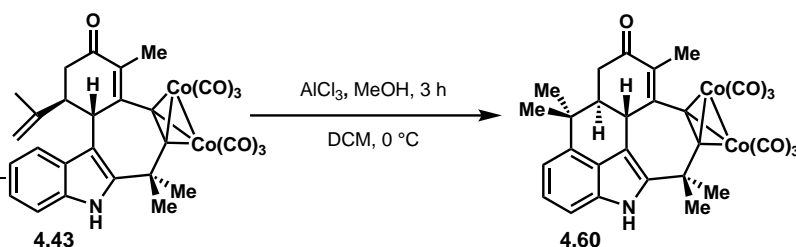


Cobalt-complexed tetracycle (4.43): A 1-L flask was charged with propargylic alcohol (**4.50**) (3.8 g, 11 mmol, 1.0 equiv). To this flask was added DCM (110 mL, 0.10 M) followed by $\text{Co}_2(\text{CO})_8$ (4.5 g, 13 mmol, 1.2 equiv). The reaction mixture was allowed to stir at room temperature overnight. To this reaction mixture was added $\text{BF}_3 \cdot \text{OEt}_2$. After stirring for 5 min the reaction mixture was quenched with sodium bicarbonate (100 mL) and the aqueous layers were extracted with ethyl acetate (3x75 mL). The combined organic layers were washed with brine (sat. aq.) (100 mL), dried over sodium sulfate, and the solvent was removed *in vacuo*. The crude reaction mixture was purified *via* SiO₂ gel column chromatography eluting with hexanes first followed by 2:1 hexanes:ethyl acetate. The pure product was isolated as a dark red solid. **¹H NMR** (500 MHz, CDCl₃) δ 8.27 (s, 1H), 7.67 (d, J = 8.0 Hz, 1H), 7.33 (d, J = 7.9 Hz, 1H), 7.09 (dt, J = 19.6, 7.4 Hz, 2H), 4.82 (d, J = 13.3 Hz, 2H), 4.45 (s, 1H), 3.87 (d, J = 6.2 Hz, 1H), 3.23 (dd, J = 15.9, 5.1 Hz, 1H), 2.77 (dd, J = 15.8, 7.4 Hz, 1H), 2.00 (s, 3H), 1.96 (s, 3H), 1.80 (s, 3H), 1.77 (s, 4H). **¹³C NMR** (125 MHz, CDCl₃) δ 199.3, 198.2, 198.0, 153.9, 146.3, 141.4, 137.8, 134.2, 126.7, 121.3, 120.2, 120.0, 112.1, 111.8, 111.2, 110.6, 85.0, 44.5, 42.1, 42.1, 39.6, 30.2, 29.4, 21.6, 12.4. **IR** (ATIR) 3306, 2974, 2090, 2052, 2012, 1645, 1568, 1437, 1323, 898 cm⁻¹. C₂₉H₂₄O₇NC_o [M+H]⁺, 616.0211. Found 616.0222. We attempted to obtain optical rotations, however, at the wavelength we had access to (Na lamp, 584 nm), the transmittance was too low to obtain accurate rotations.

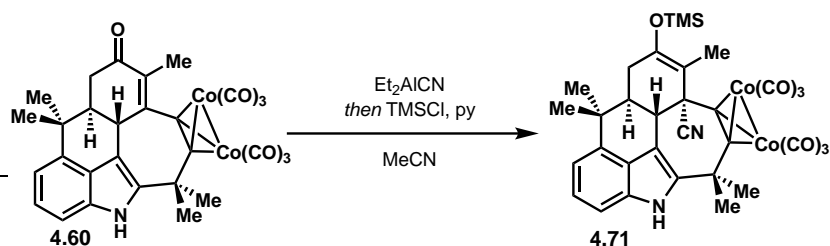


Pentacyclic silane (4.58): The tetracycle (**4.43**) (0.05 mmol, 30 mg, 1 equiv) was dissolved in benzene (0.05 M, 1 mL) in a flame-dried round-bottomed flask. The solution was heated to 70 °C in an oil bath and triethylsilane (0.98 mmol, 15 μL , 20 equiv) was added. After 1.5 h, the

mixture was filtered through a SiO₂ gel plug washing with hexanes (20 mL) to remove excess triethylsilane. ethyl acetate (50 mL) was then flushed through the SiO₂ gel plug and collected in a separate flask. The crude mixture was concentrated *in vacuo* to yield a dark red oil that was carried on immediately to the next step. Crude silane (0.02 mmol, 9 mg, 1.0 equiv) was dissolved in DCM (0.01 M, 2 mL) in a round-bottomed flask and to the solution was added MeOH (0.1 mmol, 4 μ L, 5 equiv) followed by AlCl₃ (0.40 mmol, 54 mg, 20 equiv). The reaction mixture was heated to 45 °C in an oil-bath for 12 h at which time the crude mixture was sent through a SiO₂ gel plug washing with ethyl acetate (20 mL). The crude pentacycle (**4.58**) was unstable and not subjected to further purification (1.3 mg, 14% over 2 steps). ¹H NMR (500 MHz, CDCl₃) δ 7.78 (s, 1H), 7.20 - 7.08 (m, 2H), 7.02 (dd, *J* = 4.9, 3.1 Hz, 1H), 6.74 (s, 1H), 3.97 (d, *J* = 10.3 Hz, 1H), 2.79 (dd, *J* = 15.6, 3.2 Hz, 1H), 2.45 (t, *J* = 15.2 Hz, 1H), 2.21 (ddd, *J* = 14.2, 10.4, 3.1 Hz, 1H), 1.92 (d, *J* = 2.3 Hz, 3H), 1.66 (s, 3H), 1.53 (s, 3H), 1.44 (s, 3H), 1.20 (s, 3H), 0.99 (t, *J* = 7.8 Hz, 9H), 0.81 (q, *J* = 7.5 Hz, 6H).

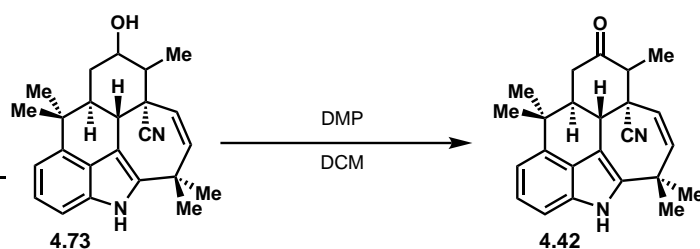


Cobalt-complexed pentacycle (4.60): A flame-dried 1 L round-bottomed flask was brought into the glovebox and charged with AlCl₃ (6.5 g, 49 mmol, 15 equiv). The flask was fitted with a rubber septum and brought out of the glovebox. Fresh-distilled DCM (330 mL, 0.01 M) was added to the flask and the mixture was placed under a stream of N₂. The mixture was cooled to 0 °C and tetracycle **4.43** (2.0 g, 3.3 mmol, 1.0 equiv) was added as a solid immediately followed by the addition of MeOH (2.0 mL, 49 mmol, 15 equiv) via syringe. The reaction mixture was removed from the ice bath and allowed to warm to room temperature. After stirring for 3 h at room temperature, the reaction mixture was quenched by pouring into ice water (100 mL) and the aqueous layer was extracted with DCM (3 x 100 mL). The organic layers were combined, washed with brine (200 mL), dried over sodium sulfate, and the solvent was removed *in vacuo*. The crude product was subjected to the next reaction without purification.

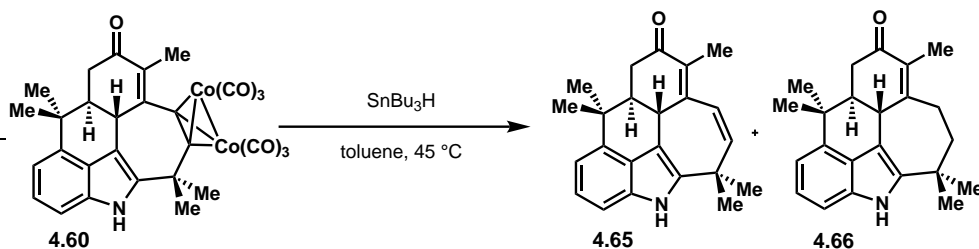


Silyl enol ether (4.71): The cobalt-complexed pentacycle **4.60** (1.0 g, 1.6 mmol, 1.0 equiv) was dissolved in MeCN (16 mL, 0.10 M) in a round bottomed flask. To this solution was added Et₂AlCN (1.0 M in toluene, 4.9 mL, 4.9 mmol, 3.0 equiv) via syringe over 1 min. After 30 min of stirring at room temperature, TMSCl (1.0 mL, 7.9 mmol, 4.8 equiv) followed by pyridine (1.0

and care was taken to add each portion in a controlled manner, approx. 2 min between each addition. Once the addition of sodium borohydride was complete, the reaction mixture was monitored by TLC until cobalt decomplexation was complete (approx. 15 min). At this time, the reaction mixture was quenched with the addition of ammonium chloride (sat. aq.) (100 mL) and the flask was removed from the ice water bath and allowed to warm to room temperature. Ethyl acetate (100 mL) was used to dilute the reaction mixture and the layers were partitioned. The aqueous layer was extracted with ethyl acetate (3 x 100 mL) and the combined organic layers were washed with brine (200 mL) and dried over sodium sulfate. The solution was filtered and concentrated *in vacuo* to deliver the crude mixture containing alcohol **4.73**. The crude mixture was subjected to purification via SiO₂ gel column chromatography on a Yamazen® automatic purification system to yield the alcohol **4.73** as an off-white solid (230 mg, 48%).



Nitrile ketone (4.42): A flame-dried flask was charged with alcohol **4.73** (0.64 mmol, 230 mg, 1.0 equiv) and DCM (1.0 M, 6.4 mL) was added. Dess-Martin periodinane (DMP) (0.83 mmol, 350 mg, 1.3 equiv) was added in one batch and the mixture was allowed to stir for 1 h at room temperature. The reaction mixture was quenched with the addition of sodium thiosulfate (sat. aq.) (50 mL) followed by sodium bicarbonate (sat. aq.) (50 mL) and the biphasic mixture was allowed to stir vigorously for 10 min at room temperature. The mixture was diluted with DCM and the layers were partitioned. The aqueous layer was extracted with DCM (3 x 50 mL) and the combined organic layers were washed with brine (50 mL), dried over sodium sulfate, filtered, and concentrated *in vacuo* to yield crude **4.42**. The crude compound was taken forward in the next step without further purification.



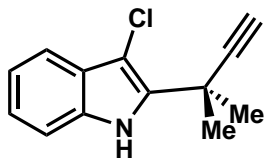
Pentacyclic dienone (4.65): Pentacyclic dicarbonyl (**4.60**) (50 mg, 0.08 mmol) was dissolved in dry benzene (0.032 M, 2.5 mL) and warmed to 45 °C in an oil bath. To this solution was added Bu₃SnH (100 μL, 5 equiv) every 30 min until TLC indicated consumption of starting material (25-40 equiv, 3-4 h). The reaction mixture was then cooled down to room temperature and loaded onto a basic alumina plug. The alumina plug was flushed with hexanes (50 mL) to get rid of apolar tin residues and then the product was washed off with ethyl acetate (50 mL). Purification by SiO₂ gel column chromatography eluting with DCM yielded the product as a yellow/orange solid (6.6 mg, 26%).

Dieneone (**4.65**): $^1\text{H NMR}$ (400 MHz, CDCl_3) δ 7.78 (b, 1H), 7.20 - 7.11 (m, 2H), 7.04 (dd, $J = 6.0, 2.0$ Hz, 1H), 6.43 (d, $J = 13.2$ Hz, 1H), 5.88 (d, $J = 13.3$ Hz, 1H), 4.08 - 3.99 (m, 1H), 2.83 (dd, $J = 15.5, 2.8$ Hz, 1H), 2.43 (t, $J = 15.1$ Hz, 1H), 2.23 (ddd, $J = 14.6, 10.4, 2.7$ Hz, 1H), 1.95 (d, $J = 2.2$ Hz, 3H), 1.56 (s, 3H), 1.50 (s, 3H), 1.47 (s, 3H), 1.17 (s, 3H). Typically, **4.65** was inseparable from the over-reduced side-product **4.66**.

4.7 References

1. Chandra, A.; Viswanathan, R.; Johnston, J. N. *Org. Lett.* **2007**, *9*, 5027–5029.
2. Rafferty, R. J.; Williams, R. M. *Tetrahedron Lett.* **2011**, *52*, 2037–2040.
3. Rafferty, R. J.; Williams, R. M. *Tetrahedron Lett.* **2011**, *52*, 2037–2040.
4. Zheng, G.-q.; Kenney, P. M.; Lam, L. K. T. *Planta Med.* **1992**, *58*, 338–341.
5. Leitereg, T. J.; Guadagni, D. G.; Harris, J.; Mon, T. R.; Teranishi, R. *Nature* **1971**, *230*, 455–456.
6. Richter, J. M.; Ishihara, Y.; Masuda, T.; Whitefield, B. W.; Llamas, T.; Pohjakallio, A.; Baran, P. S. *J. Am. Chem. Soc.* **2008**, *130*, 17938–17954.
7. Fukuyama, T.; Chen, X. *J. Am. Chem. Soc.* **1994**, *116*, 3125–3126.
8. Baran, P. S.; Richter, J. M. *J. Am. Chem. Soc.* **2004**, *126*, 7450–7451.
9. Nicholas, K. M.; Pettit, R. *J. Organomet. Chem.* **1972**, *44*, C21–C24.
10. Green, J. R. *Curr. Org. Chem.* **2001**, *5*, 809–826.
11. Teobald, B. J. *Tetrahedron* **2002**, *58*, 4133–4170.
12. Nakagawa, M.; Hino, T.; Ma, J. *Heterocycles* **1990**, *30*, 451.
13. Isaji, H.; Nakazaki, A.; Isobe, M.; Nishikawa, T. *Chem. Lett.* **2011**, *40*, 1079–1081.
14. Babler, J. H.; Coghlan, M. J. *Synth. Commun.* **1976**, *6*, 469–474.
15. Dauben, W. G.; Michno, D. M. *J. Org. Chem.* **1977**, *42*, 682–685.
16. Hyde, A.; Buchwald, S. *Angew. Chem. Int. Ed.* **2007**, *47*, 177–180.
17. Hyde, A. M.; Buchwald, S. L. *Org. Lett.* **2009**, *11*, 2663–2666.
18. Varseev, G. N.; Maier, M. E. *Org. Lett.* **2005**, *7*, 3881.
19. Terao, Y.; Satoh, T.; Miura, M.; Nomura, M. *Tetrahedron Lett.* **1998**, *39*, 6203–6206.
20. Horning, E. C. *J. Org. Chem.* **1945**, *10*, 263–266.
21. Baran, P. S.; Maimone, T. J.; Richter, J. M. *Nature* **2007**, *446*, 404–408.
22. Meyer, K. H.; Schuster, K. *Chem. Ber.* **1922**, *55*, 819.
23. G., M. G.; Stephen, B.; Todd, M.; I., H. K.; Joana, C. *Angew. Chem. Int. Ed.* **1998**, *37*, 161–164.
24. Schreiber, S. L.; Sammakia, T.; Crowe, W. E. *J. Am. Chem. Soc.* **1986**, *108*, 3128–3130.
25. Ni Runyan,; Mitsuda Naoto,; Kashiwagi Takeru,; Igawa Kazunobu,; Tomooka Katsuhiko, *Angew. Chem. Int. Ed.* **2014**, *54*, 1190–1194.
26. Hosokawa, S.; Isobe, M. *Tetrahedron Lett.* **1998**, *39*, 2609–2612.
27. Ambrosi, A.; Denmark, S. E. *Angew. Chem. Int. Ed.* **2016**, *55*, 12164–12189.
28. Stuart, J. G.; Nicholas, K. M. *Synthesis* **1989**, *6*, 454–455.
29. Nagata, W.; Yoshioka, M. *Tetrahedron Lett.* **1966**, *7*, 1913–1918.
30. Samson, M.; Vandewalle, M. *Synth. Commun.* **1978**, *8*, 231–239.

4.a NMR Spectra Relevant to Chapter 4



4.31

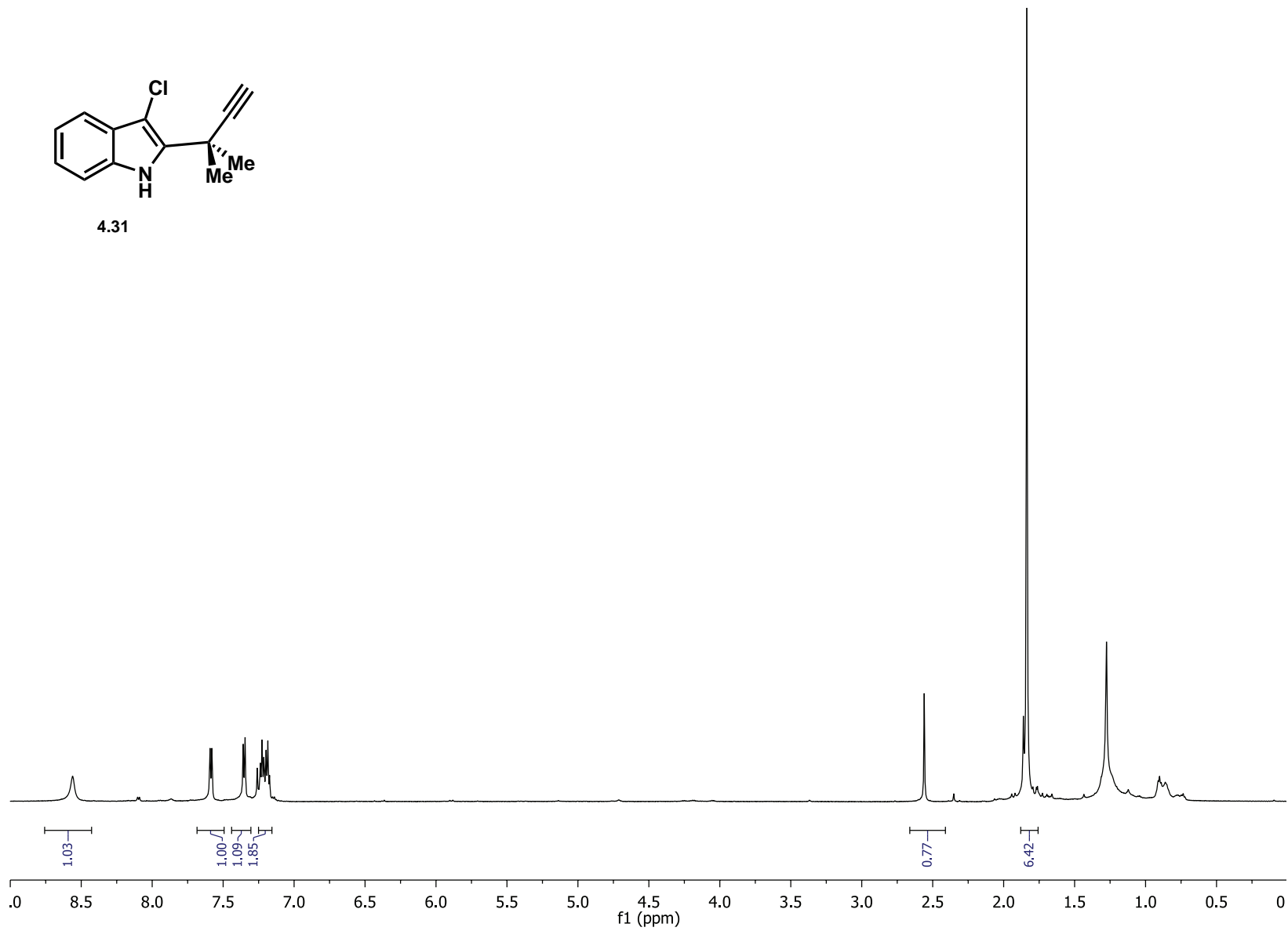
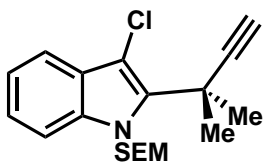


Figure 4.1: ¹H NMR of 4.31 in CDCl₃



4.78

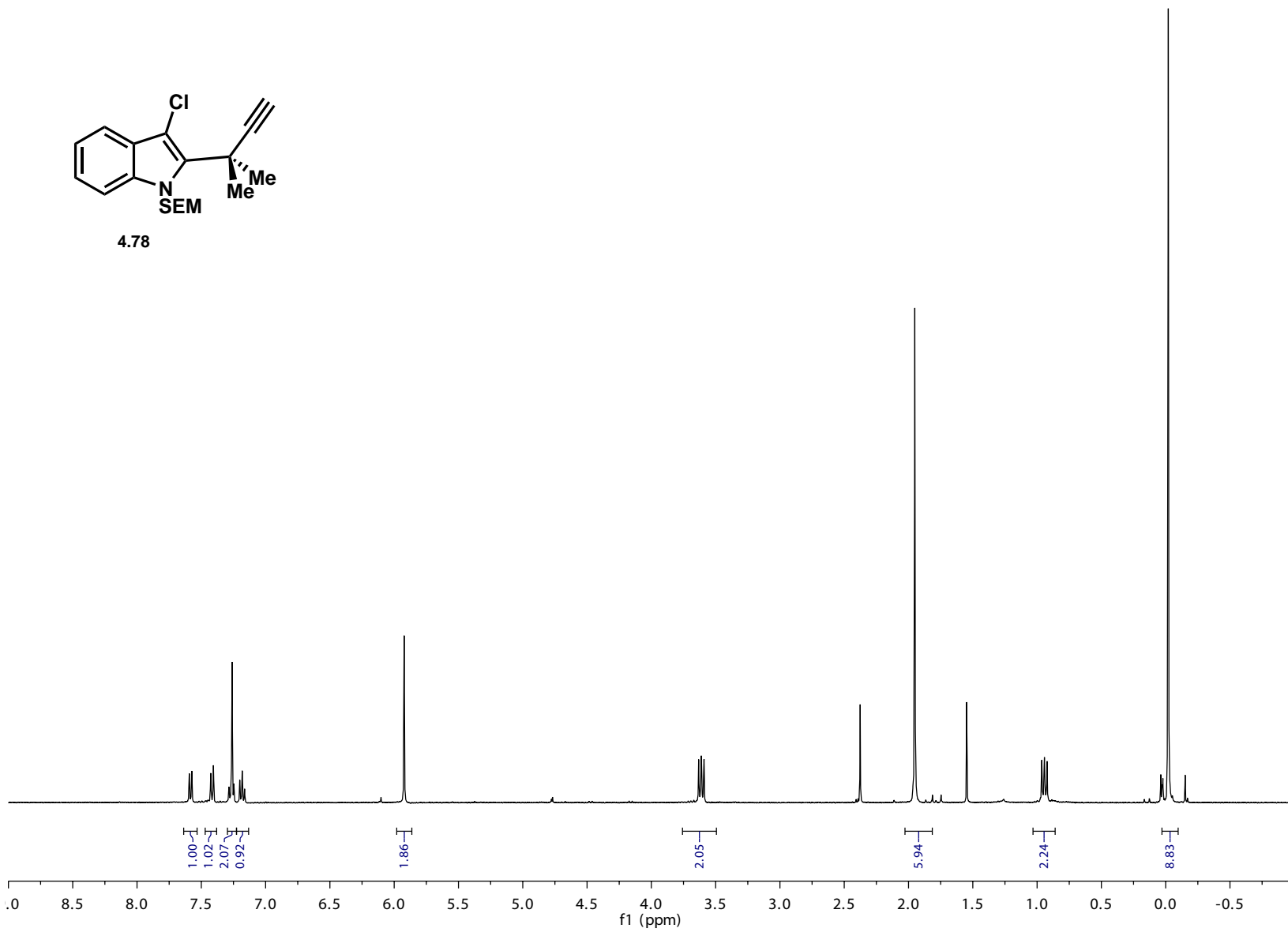


Figure 4.2: ¹H NMR of 4.78 in CDCl₃

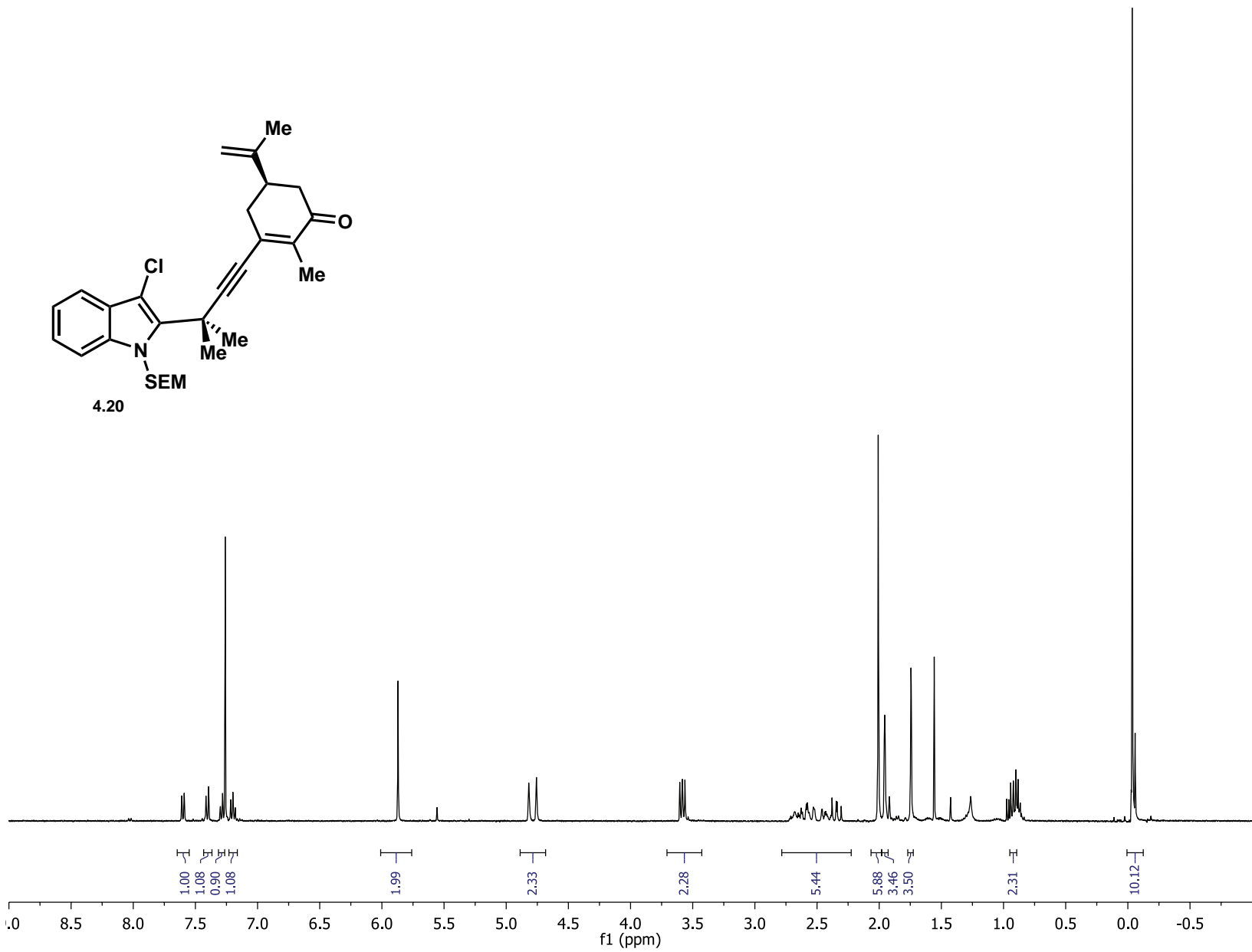


Figure 4.3: ¹H NMR of 4.20 in CDCl₃

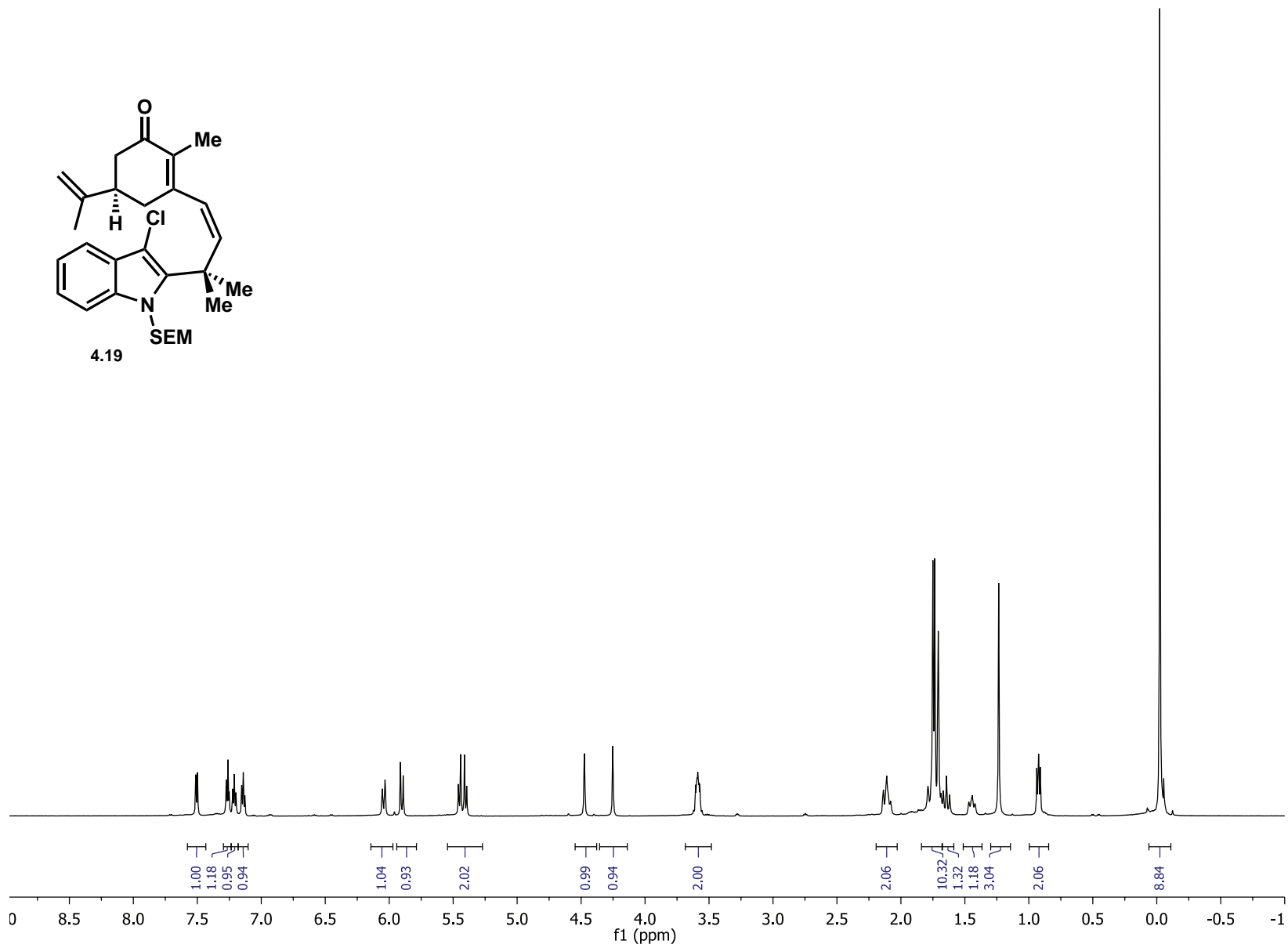
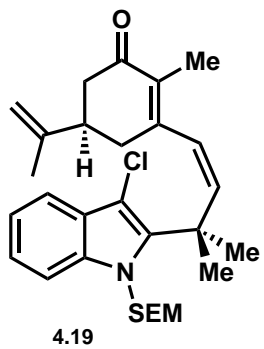


Figure 4.4: ¹H NMR of 4.19 in CDCl₃

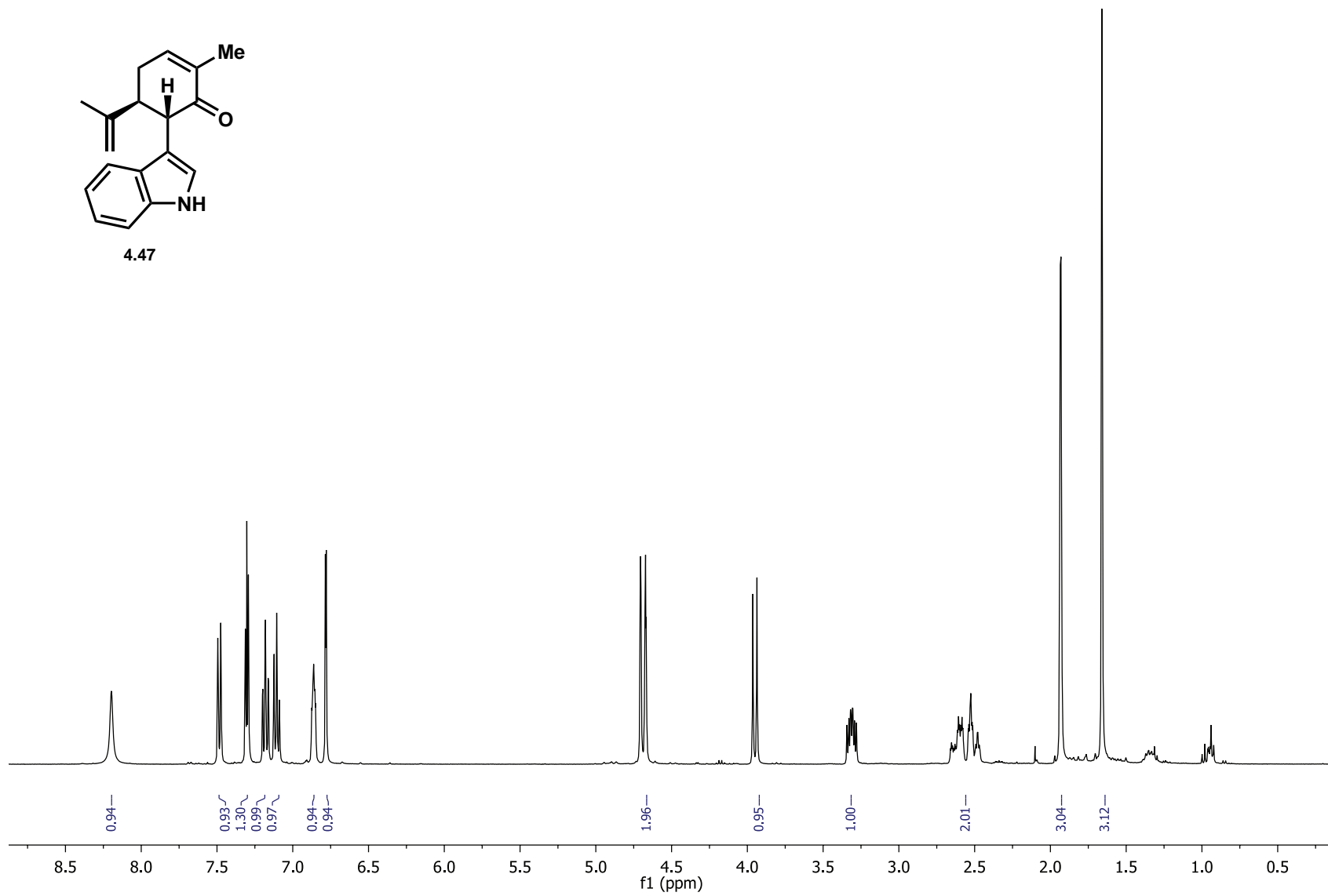
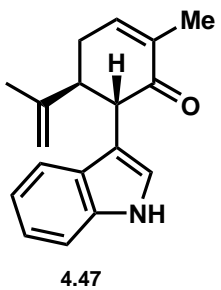


Figure 4.5: ¹H NMR of 4.47 in CDCl₃

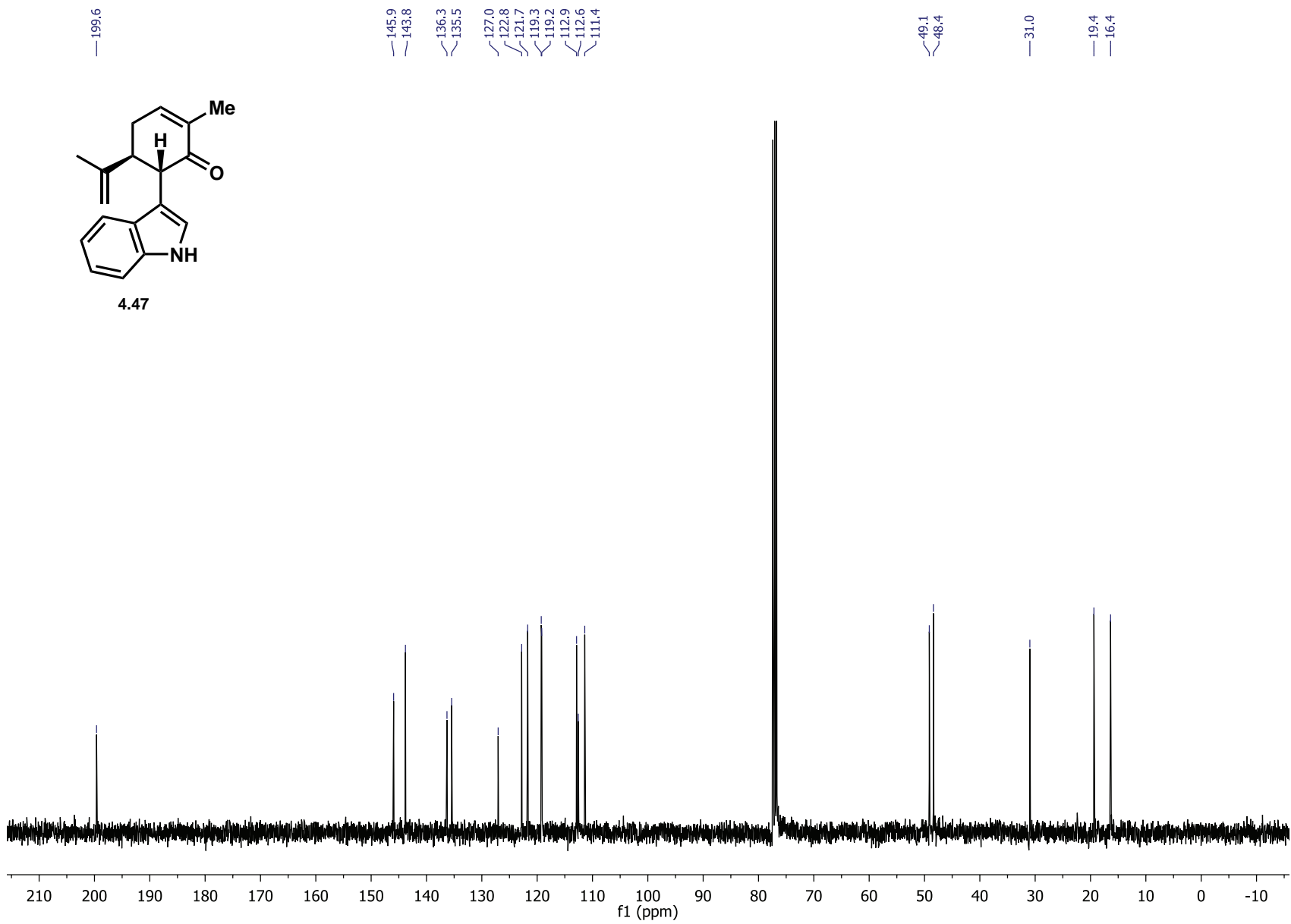


Figure 4.6: ^{13}C NMR of 4.47 in CDCl_3

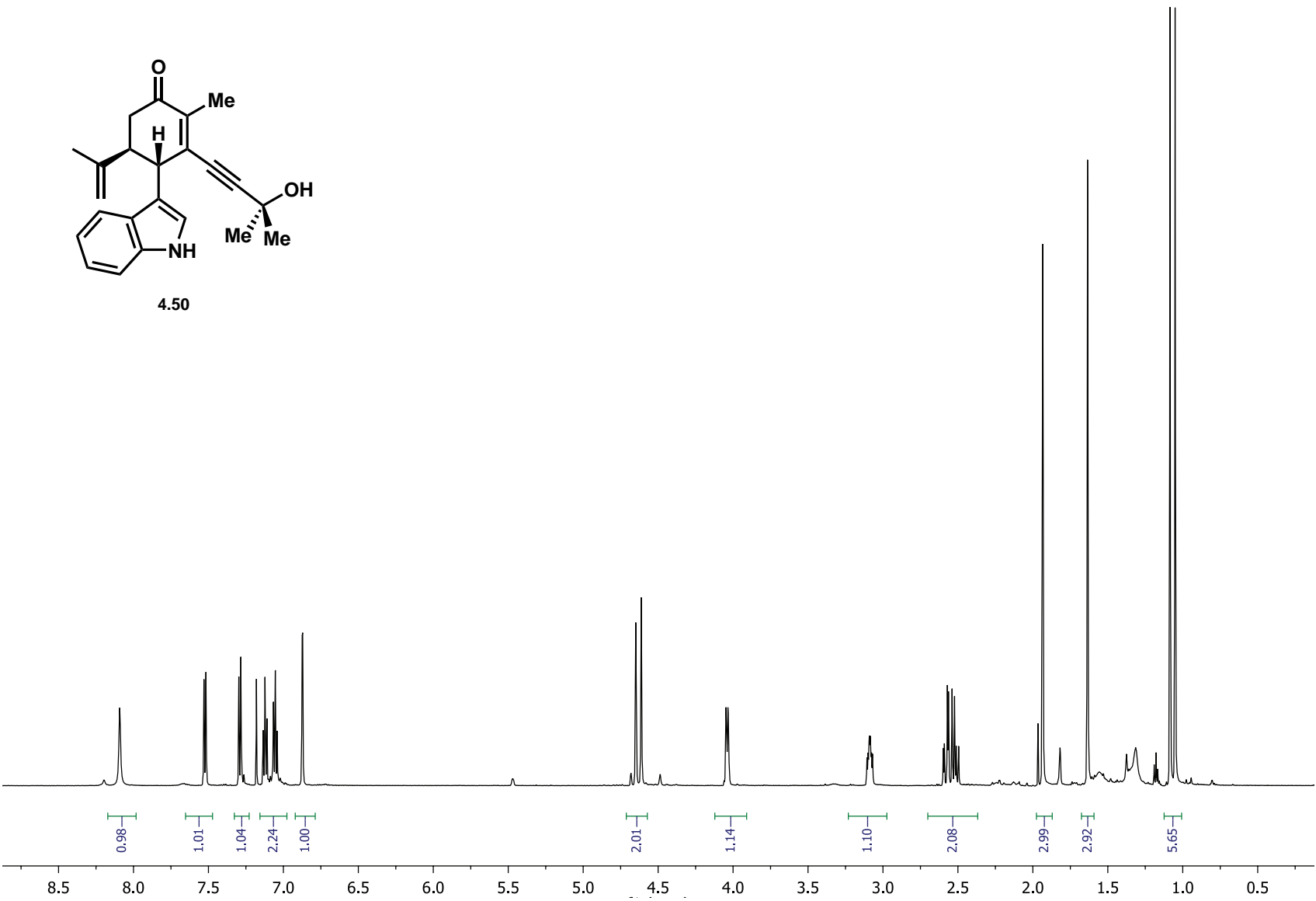


Figure 4.7: ¹H NMR of 4.50 in CDCl₃

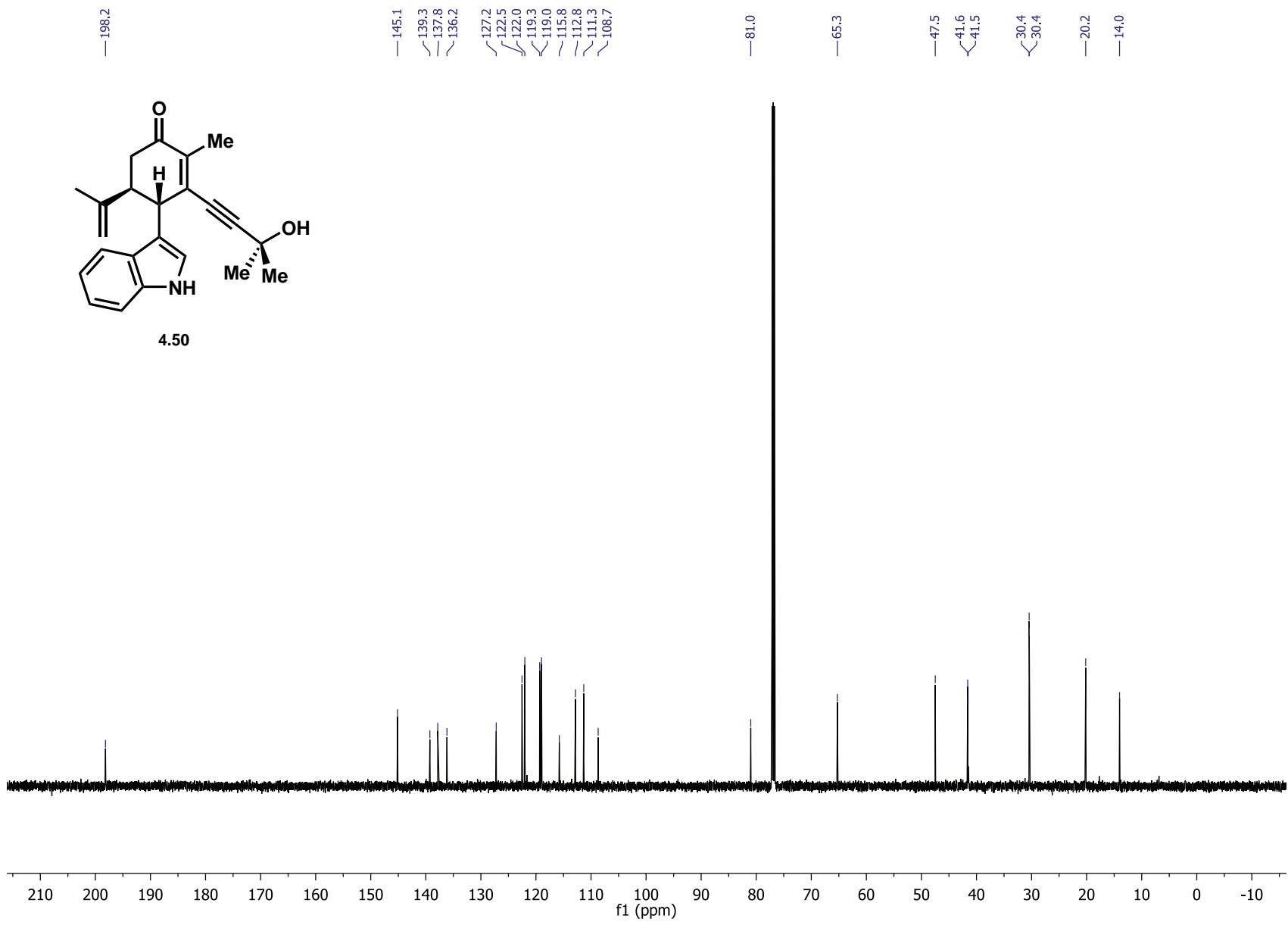


Figure 4.8: ^{13}C NMR of 4.50 in CDCl_3

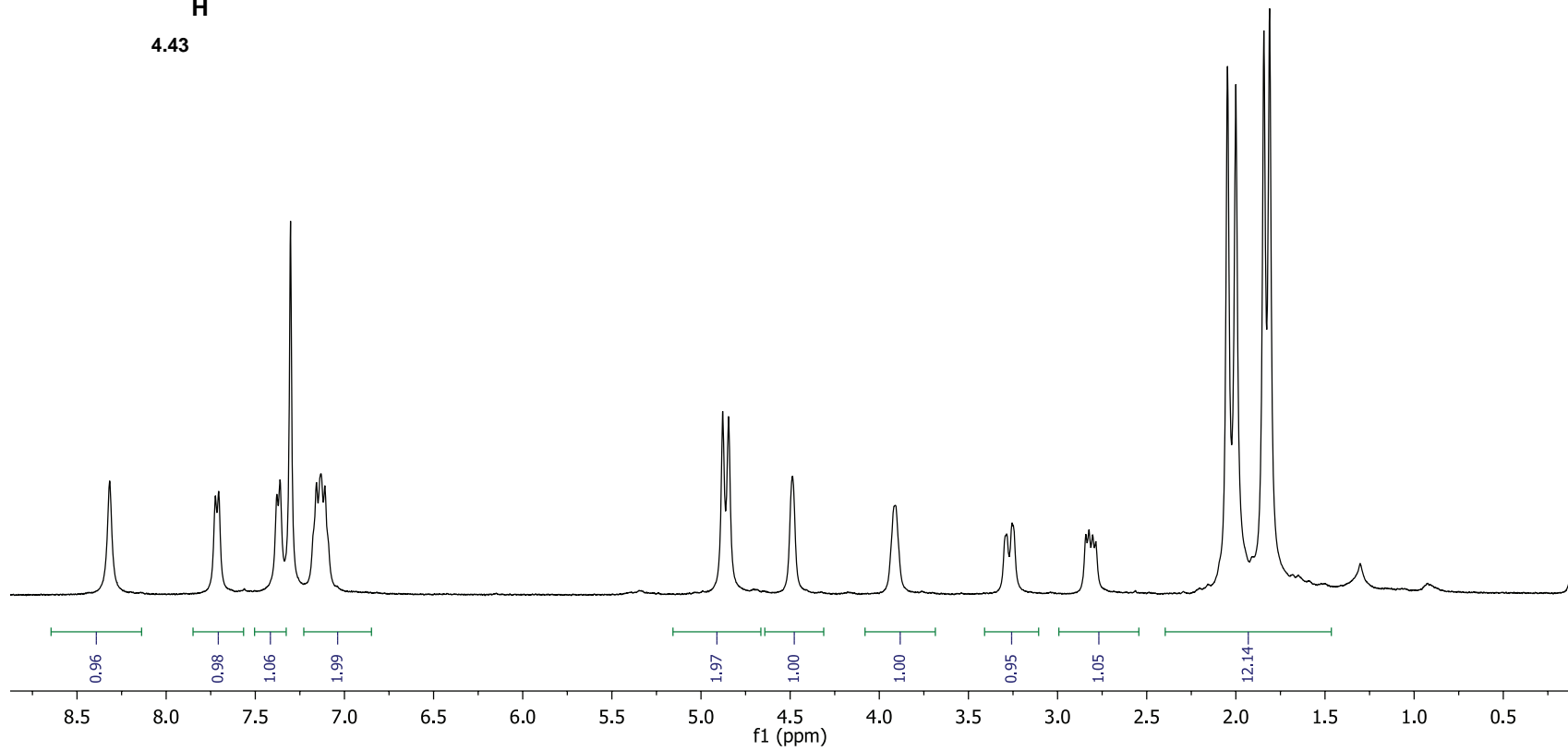
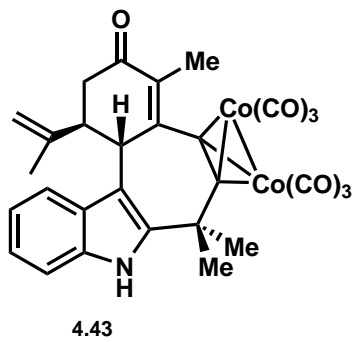


Figure 4.9: ¹H NMR of 4.43 in CDCl₃

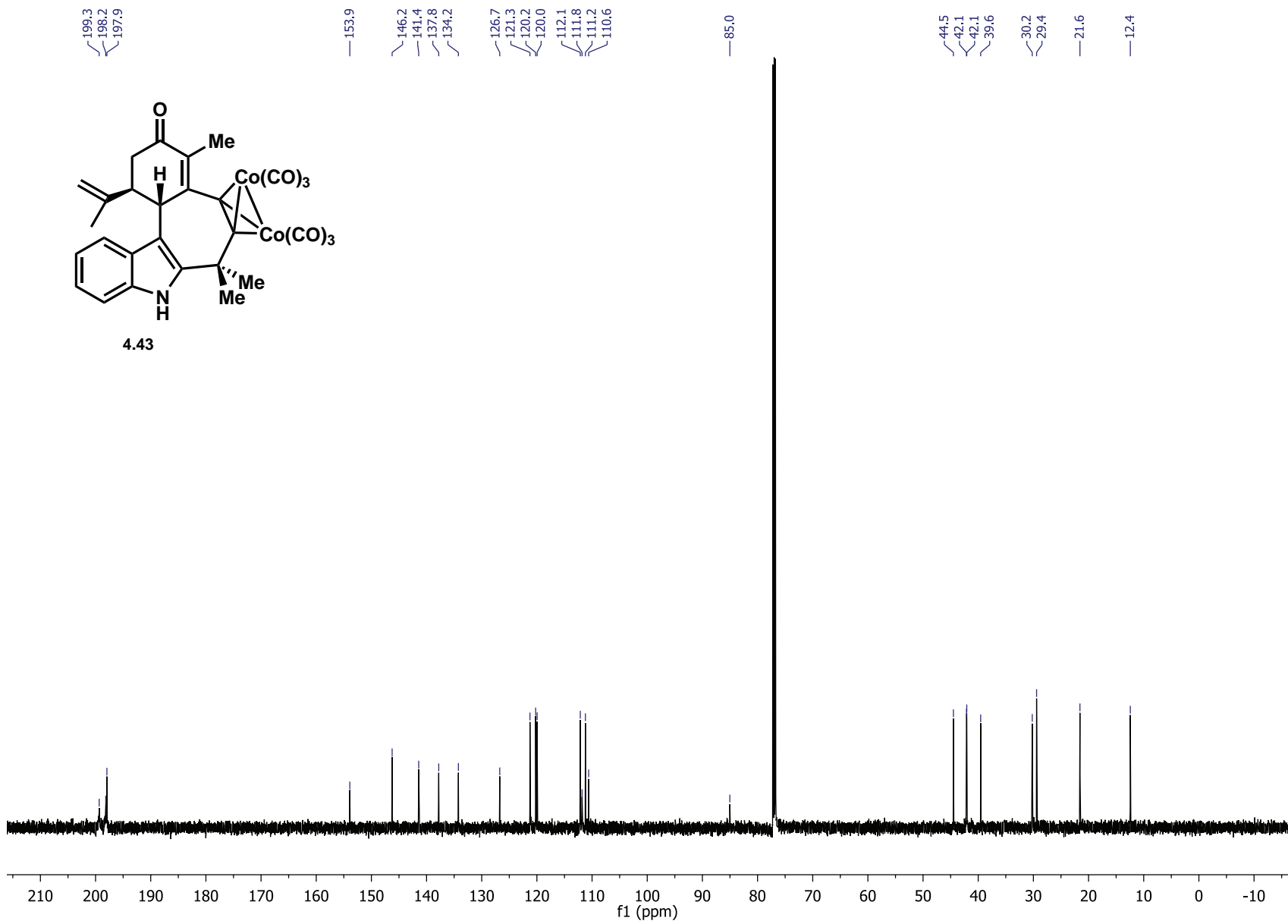


Figure 4.10: ^{13}C NMR of 4.43 in CDCl_3

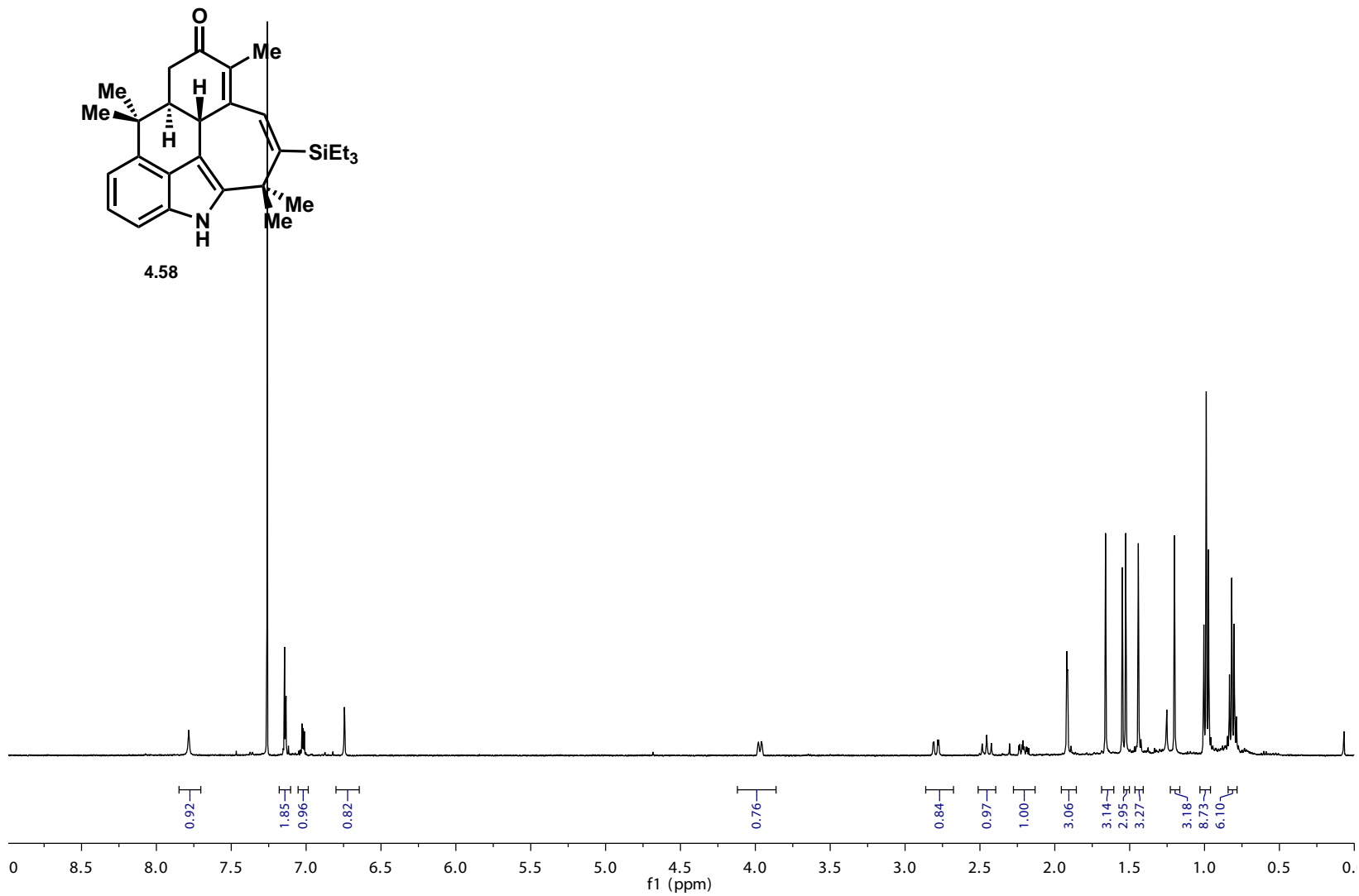
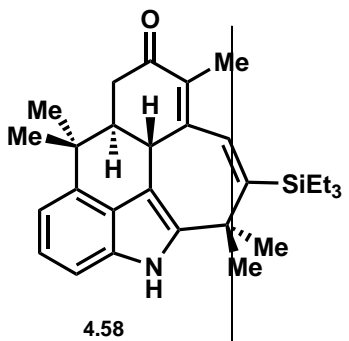


Figure 4.11: ¹H NMR of 4.58 in CDCl₃

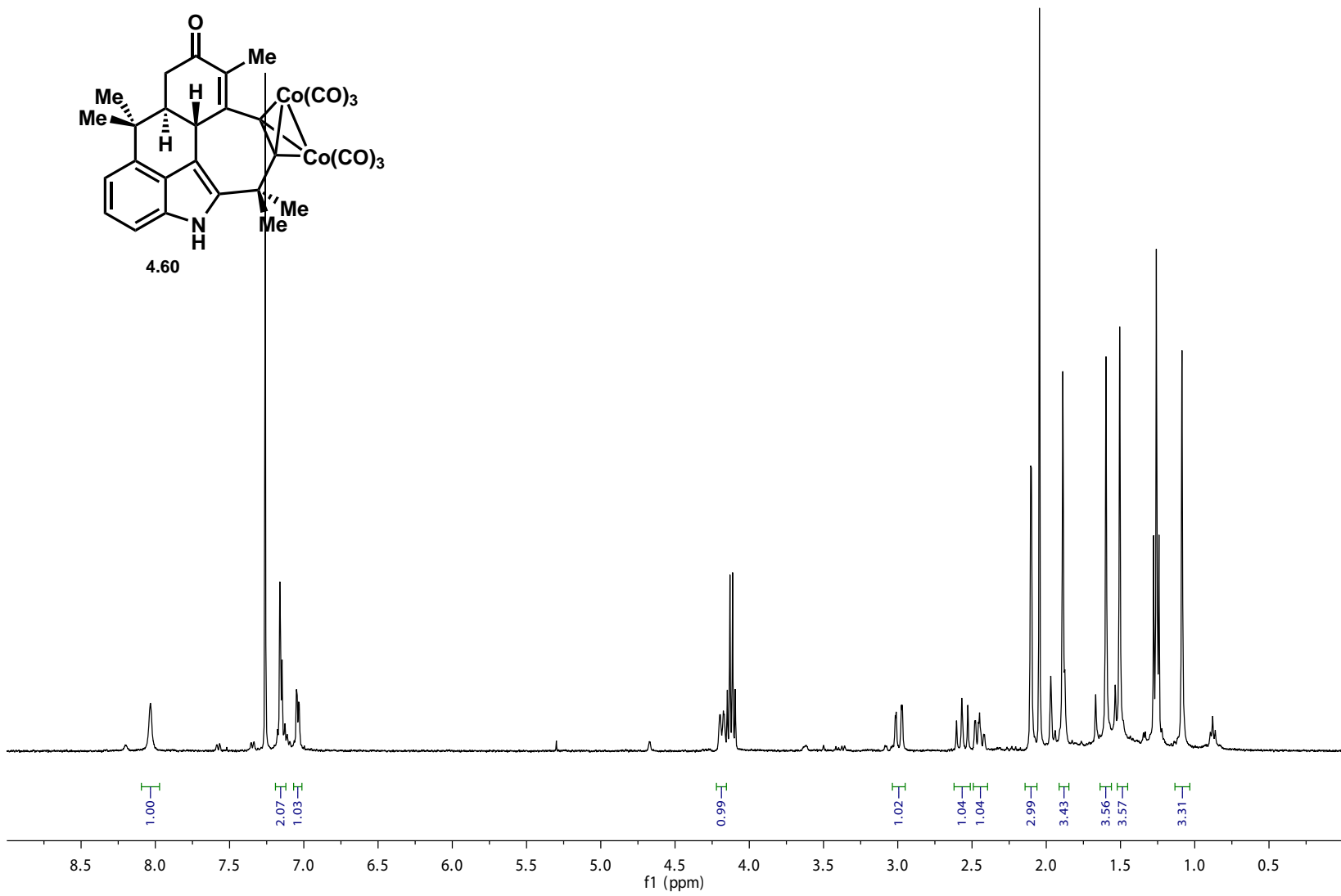


Figure 4.12: ¹H NMR of 4.60 in CDCl₃

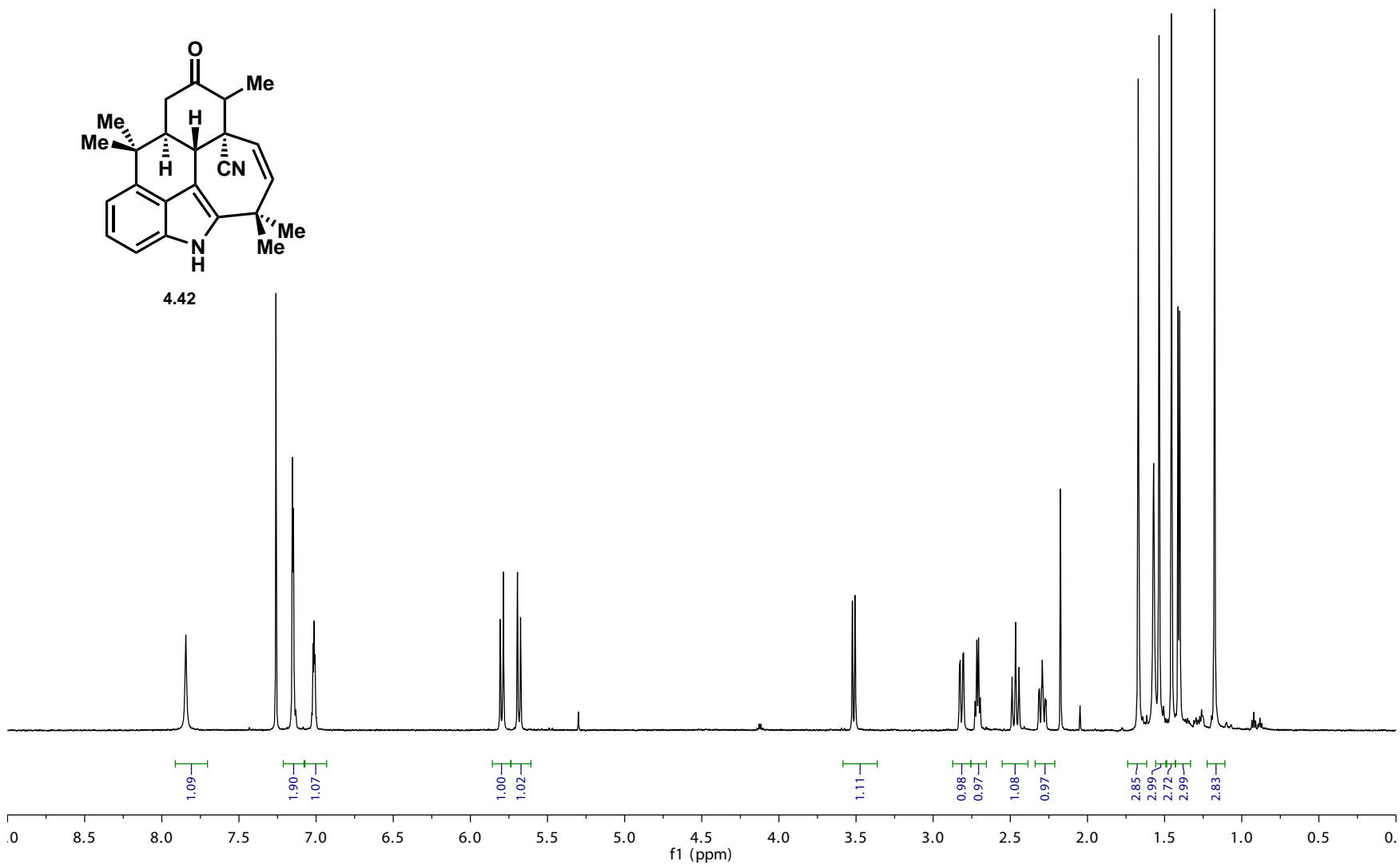
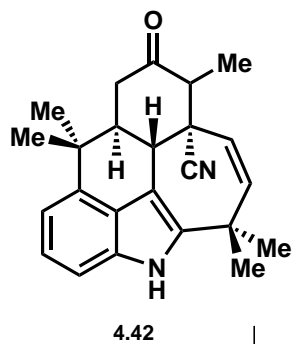


Figure 4.13: $^1\text{H NMR}$ of 4.42 in CDCl_3

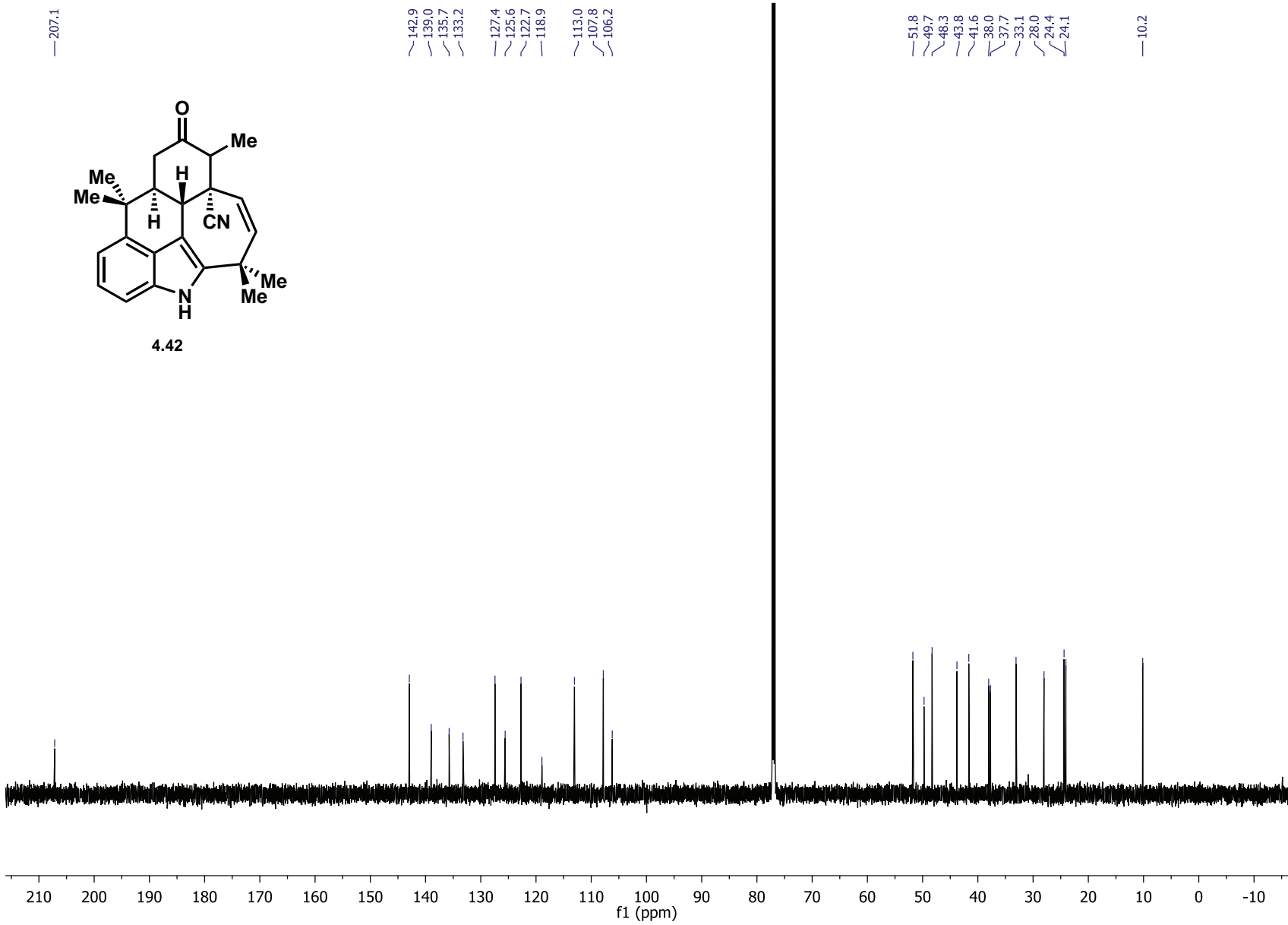


Figure 4.14: ^{13}C NMR of 4.42 in CDCl_3

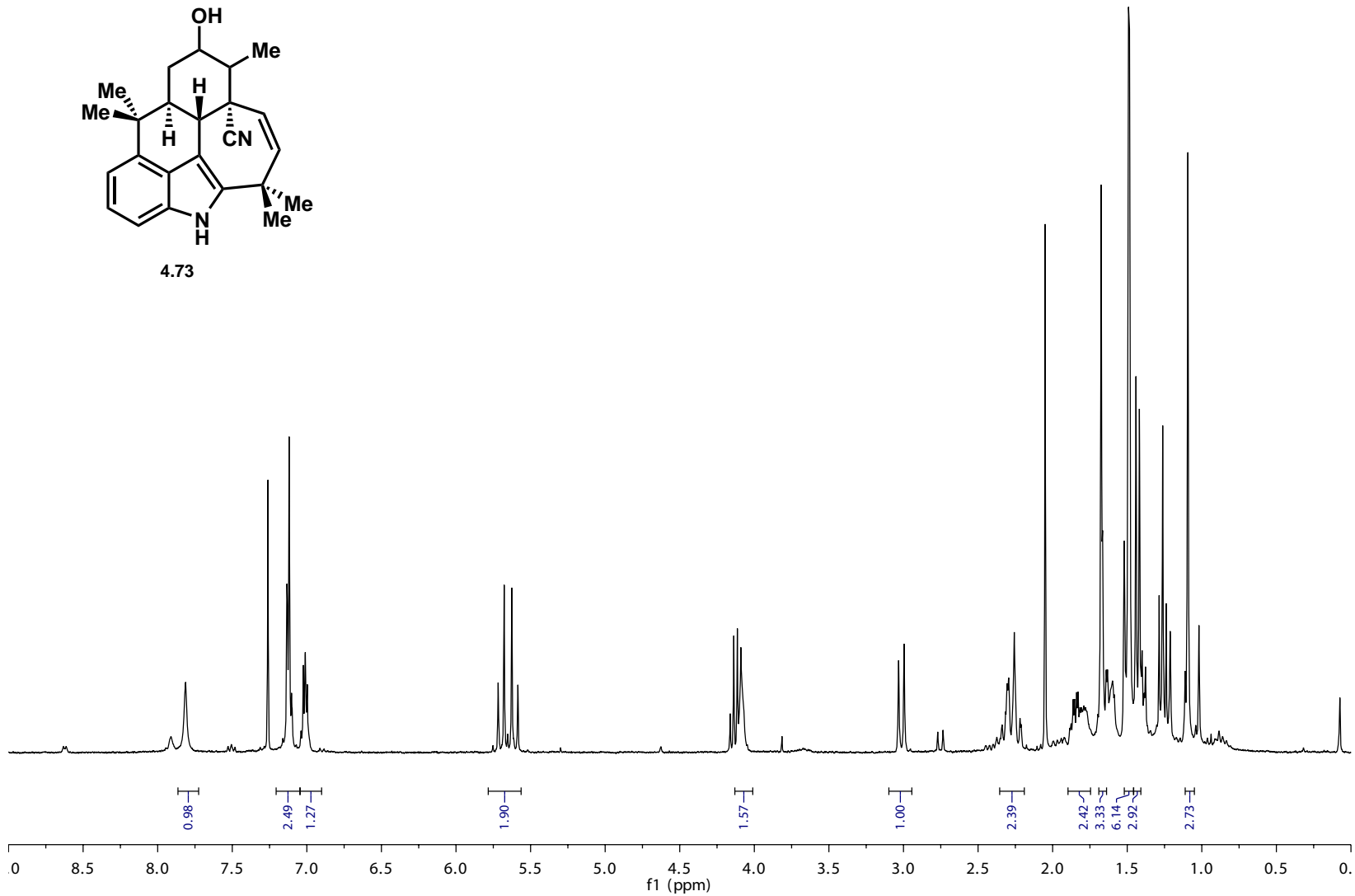
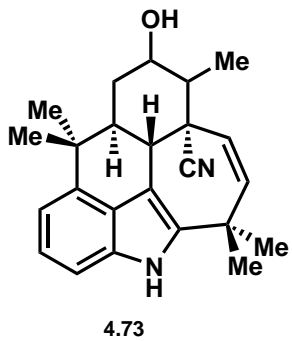


Figure 4.15: ¹H NMR of 4.73 in CDCl₃

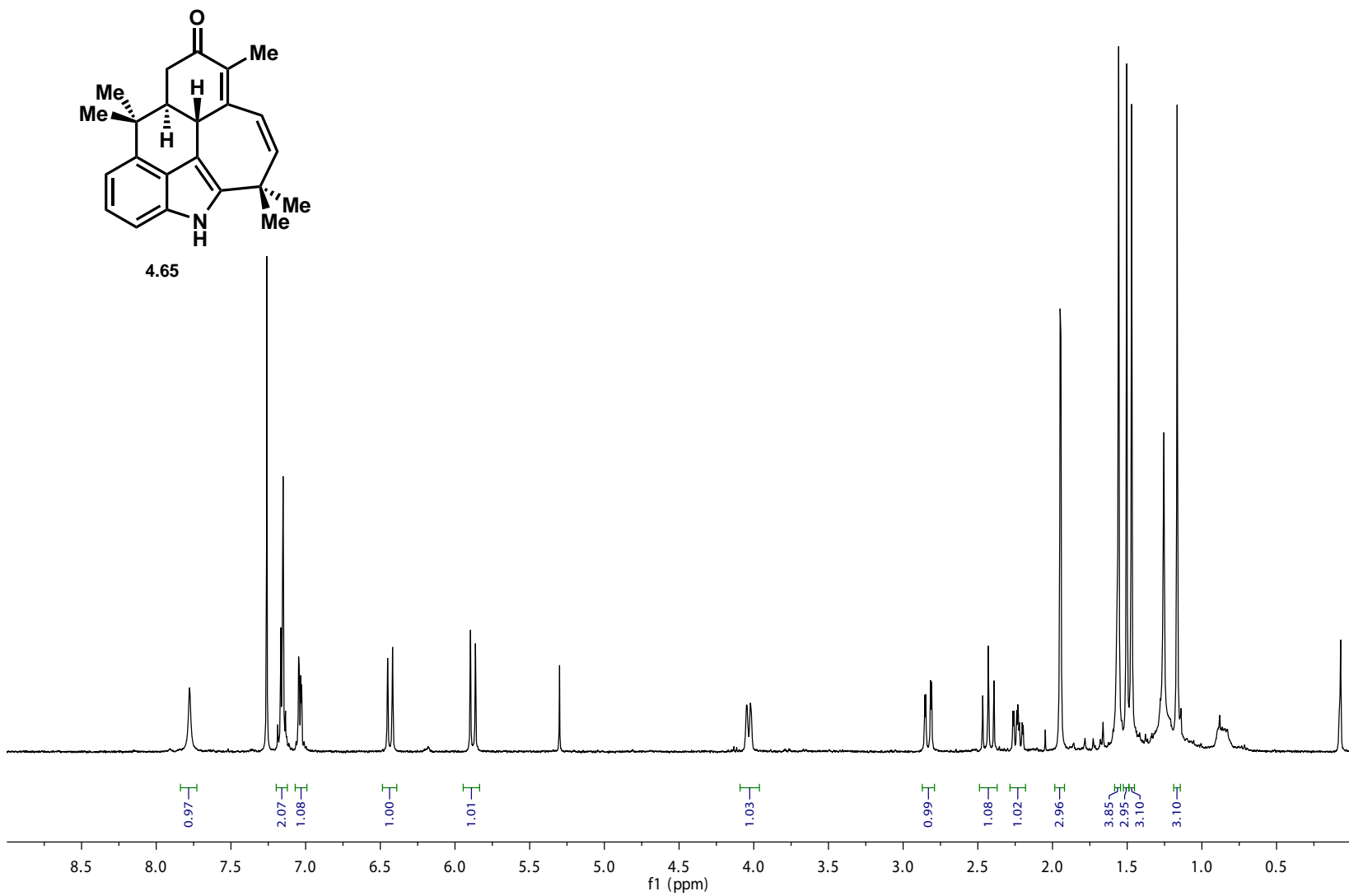


Figure 4.16: ¹H NMR of 4.65 in CDCl₃

4.b X-ray Crystallographic Data Relevant to Chapter 4

X-ray Crystallography Data

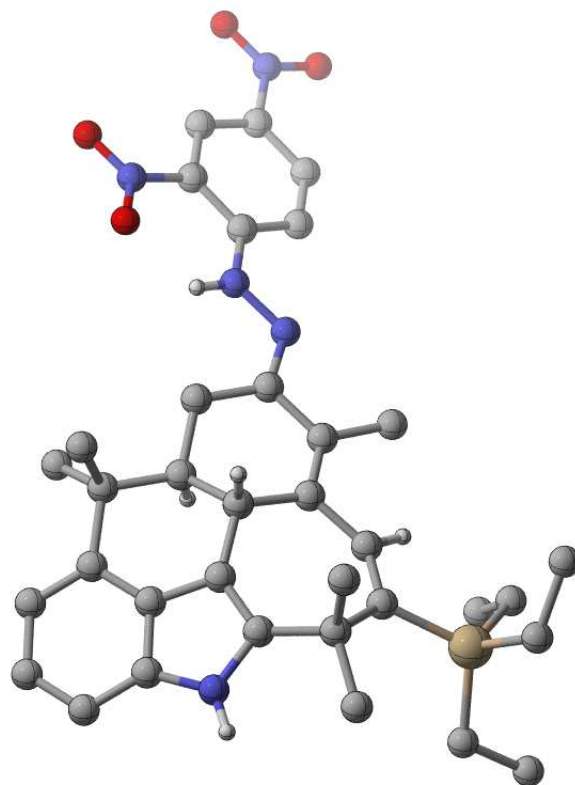


Figure 4.17: X-ray crystal structure of **4.62** (sarpong127)

A brown block 0.080 x 0.050 x 0.030 mm in size was mounted on a Cryoloop with Paratone oil. Data were collected in a nitrogen gas stream at 100(2) K using and scans. Crystal-to-detector distance was 50 mm and exposure time was 30 seconds per frame using a scan width of 1.0°. Data collection was 100.0% complete to 25.000° in θ . A total of 95677 reflections were collected covering the indices, $-21 \leq h \leq 21$, $-14 \leq k \leq 14$, $-22 \leq l \leq 22$. 13121 reflections were found to be symmetry independent, with an R_{int} of 0.1122. Indexing and unit cell refinement indicated a primitive, monoclinic lattice. The space group was found to be P 21 (No. 4). The data were integrated using the Bruker SAINT software program and scaled using the SADABS software program. Solution by iterative methods (SHELXT-2014) produced a complete heavy-atom phasing model consistent with the proposed structure. All non-hydrogen atoms were refined anisotropically by full-matrix least-squares (SHELXL-2014). All hydrogen atoms were placed using a riding model. Their positions were constrained relative to their parent atom using the appropriate HFIX command in SHELXL-2014. Absolute stereochemistry was unambiguously determined to be *R* at C16 and C51, and *S* at C15 and C50, respectively.

Table 4.1: Crystal data and structure refinement for **4.62**.

X-ray ID	sarpong127	
Sample/notebook ID	REJV-020	
Empirical formula	C76 H98 N10 O8 Si2	
Formula weight	1335.82	
Temperature	100(2) K	
Wavelength	0.71073 Å	
Crystal system	Monoclinic	
Space group	P 21	
Unit cell dimensions	a = 17.8360(12) Å b = 12.1097(8) Å c = 18.4418(13) Å	a = 90°. b = 117.0360(10)°. g = 90°.
Volume	3547.9(4) Å ³	
Z	2	
Density (calculated)	1.250 Mg/m ³	
Absorption coefficient	0.113 mm ⁻¹	
F(000)	1432	
Crystal size	0.080 x 0.050 x 0.030 mm ³	
Theta range for data collection	1.240 to 25.477°.	
Index ranges	-21<=h<=21, -14<=k<=14, -22<=l<=22	
Reflections collected	95677	
Independent reflections	13121 [R(int) = 0.1122]	
Completeness to theta = 25.000°	100.00%	
Absorption correction	Semi-empirical from equivalents	
Max. and min. transmission	0.928 and 0.747	
Refinement method	Full-matrix least-squares on F ²	
Data / restraints / parameters	13121 / 1 / 881	
Goodness-of-fit on F ²	1.065	
Final R indices [I>2sigma(I)]	R1 = 0.0645, wR2 = 0.1419	
R indices (all data)	R1 = 0.0962, wR2 = 0.1586	
Absolute structure parameter	-0.03(8)	
Extinction coefficient	n/a	
Largest diff. peak and hole	0.566 and -0.259 e.Å ⁻³	

Table 4.2: Atomic coordinates ($\times 10^4$) and equivalent isotropic displacement parameters ($\text{\AA}^2 \times 10^3$) for sarpong127. $U(\text{eq})$ is defined as one third of the trace of the orthogonalized U^{ij} tensor.

	x	y	z	U(eq)
C(1)	4579(3)	1463(5)	5253(3)	23(1)
C(2)	3768(3)	1212(5)	5323(4)	24(1)
C(3)	3174(4)	412(5)	4894(4)	32(2)
C(4)	2414(4)	362(5)	4947(4)	35(2)
C(5)	2217(4)	1082(5)	5409(4)	30(1)
C(6)	2808(3)	1883(5)	5841(3)	22(1)
C(7)	3571(3)	3340(5)	6581(3)	20(1)
C(8)	3746(3)	4400(5)	7067(3)	22(1)
C(9)	4627(3)	4339(4)	7791(3)	18(1)
C(10)	5326(3)	4012(4)	7727(3)	19(1)
C(11)	5523(3)	3597(4)	7085(3)	19(1)
C(12)	6356(3)	3609(5)	7247(3)	22(1)
C(13)	6606(3)	3127(4)	6661(3)	20(1)
C(14)	5998(3)	2468(5)	5957(4)	23(1)
C(15)	5211(3)	2110(5)	6029(3)	20(1)
C(16)	4860(3)	3143(4)	6277(3)	18(1)
C(17)	4040(3)	2845(5)	6263(3)	17(1)
C(18)	3577(3)	1931(4)	5801(3)	18(1)
C(19)	4327(4)	2128(6)	4474(4)	32(2)
C(20)	4998(4)	388(5)	5187(4)	31(2)
C(21)	3743(4)	5372(5)	6524(4)	31(1)
C(22)	3042(3)	4602(5)	7309(4)	28(1)
C(23)	4196(4)	4281(6)	9293(4)	38(2)
C(24)	4519(5)	4610(8)	10186(4)	62(2)
C(25)	4721(4)	6453(6)	8764(5)	42(2)
C(26)	5380(5)	7046(7)	8583(6)	61(2)
C(27)	5983(4)	4662(6)	9588(4)	33(2)
C(28)	6246(4)	3478(6)	9879(4)	45(2)
C(29)	7024(3)	4164(6)	7983(4)	34(2)
C(30)	8398(3)	2866(5)	6343(3)	20(1)
C(31)	8632(3)	2602(4)	5724(3)	22(1)
C(32)	9469(3)	2580(5)	5878(3)	24(1)
C(33)	10078(3)	2832(5)	6641(3)	23(1)
C(34)	9880(3)	3095(5)	7267(4)	25(1)
C(35)	9049(3)	3123(5)	7115(3)	24(1)
C(36)	1786(3)	4281(5)	3613(3)	22(1)
C(37)	1066(3)	4527(4)	3831(3)	21(1)
C(38)	1055(4)	4336(5)	4563(3)	27(1)
C(39)	316(4)	4499(5)	4643(4)	30(1)

Table 4.2: Atomic coordinates ($\times 10^4$) and equivalent isotropic displacement parameters ($\text{\AA}^2 \times 10^3$) for sarpong127. $U(\text{eq})$ is defined as one third of the trace of the orthogonalized U^{ij} tensor.

	x	y	z	U(eq)
C(40)	-429(3)	4825(5)	4003(3)	27(1)
C(41)	-420(3)	5027(5)	3265(3)	21(1)
C(42)	-689(3)	5404(5)	1962(3)	22(1)
C(43)	-1200(3)	5665(5)	1070(3)	23(1)
C(44)	-778(3)	6585(5)	816(3)	20(1)
C(45)	64(3)	6619(5)	1033(3)	21(1)
C(46)	814(3)	5970(5)	1540(3)	19(1)
C(47)	1535(3)	6199(5)	1467(3)	21(1)
C(48)	2314(3)	5609(5)	1964(3)	21(1)
C(49)	2360(3)	4830(5)	2615(3)	22(1)
C(50)	1692(3)	5043(5)	2888(3)	21(1)
C(51)	828(3)	5063(5)	2123(3)	21(1)
C(52)	152(3)	5148(4)	2378(3)	20(1)
C(53)	325(3)	4898(5)	3191(3)	21(1)
C(54)	1733(4)	3054(5)	3385(4)	29(1)
C(55)	2638(3)	4505(5)	4350(3)	29(1)
C(56)	-1244(4)	4629(5)	573(3)	27(1)
C(57)	-2102(3)	5966(5)	905(4)	27(1)
C(58)	-2034(4)	8600(5)	508(4)	32(2)
C(59)	-2372(4)	9683(6)	50(4)	46(2)
C(60)	-2156(4)	7200(6)	-935(4)	37(2)
C(61)	-1738(4)	6756(6)	-1439(4)	39(2)
C(62)	-700(4)	8732(5)	-80(4)	30(1)
C(63)	-143(4)	9508(5)	615(4)	36(2)
C(64)	1545(4)	7016(5)	852(4)	32(2)
C(65)	4388(3)	5309(5)	2236(3)	23(1)
C(66)	5095(4)	4619(5)	2650(3)	29(1)
C(67)	5867(4)	4844(6)	2654(3)	32(2)
C(68)	5914(4)	5748(6)	2226(4)	33(2)
C(69)	5241(4)	6454(5)	1830(4)	31(2)
C(70)	4495(4)	6237(5)	1837(4)	28(1)
C(71)	9089(6)	1082(8)	3274(6)	73(3)
C(72)	9921(4)	1004(7)	3305(4)	46(2)
C(73)	9846(6)	1096(7)	2454(6)	70(3)
C(74)	9303(7)	2042(9)	1934(6)	85(3)
C(75)	8415(6)	2003(8)	1886(5)	64(2)
C(76)	8527(5)	2049(7)	2767(5)	60(2)
N(1)	2822(3)	2749(4)	6328(3)	23(1)
N(2)	7381(3)	3293(4)	6789(3)	23(1)

Table 4.2: Atomic coordinates ($\times 10^4$) and equivalent isotropic displacement parameters ($\text{\AA}^2 \times 10^3$) for sarpong127. $U(\text{eq})$ is defined as one third of the trace of the orthogonalized U^{ij} tensor.

	x	y	z	U(eq)
N(3)	7579(3)	2884(4)	6209(3)	21(1)
N(4)	8014(3)	2351(4)	4900(3)	33(1)
N(5)	10955(3)	2829(4)	6803(3)	25(1)
N(6)	-1029(3)	5342(4)	2508(3)	22(1)
N(7)	2955(3)	5781(4)	1812(3)	23(1)
N(8)	3640(3)	5112(4)	2244(3)	25(1)
N(9)	5054(3)	3647(5)	3079(3)	44(2)
N(10)	6714(3)	5968(6)	2193(4)	42(2)
O(1)	7263(2)	2287(4)	4743(3)	35(1)
O(2)	8242(3)	2208(6)	4381(3)	65(2)
O(3)	11119(2)	2603(4)	6238(3)	37(1)
O(4)	11494(2)	3069(4)	7490(3)	35(1)
O(5)	4360(3)	3348(5)	3020(3)	59(2)
O(6)	5708(3)	3133(5)	3488(3)	65(2)
O(7)	7291(3)	5328(5)	2543(3)	53(1)
O(8)	6732(3)	6763(5)	1792(4)	56(2)
Si(1)	4849(1)	4908(1)	8831(1)	27(1)
Si(2)	-1418(1)	7746(1)	101(1)	26(1)

Table 4.3: Bond lengths [\AA] for sarpong127.

C(1)-C(19)	1.525(8)	C(8)-C(22)-H(22B)	109.5
C(1)-C(20)	1.534(8)	H(22A)-C(22)-H(22B)	109.5
C(1)-C(2)	1.539(7)	C(8)-C(22)-H(22C)	109.5
C(1)-C(15)	1.570(8)	H(22A)-C(22)-H(22C)	109.5
C(2)-C(18)	1.387(8)	H(22B)-C(22)-H(22C)	109.5
C(2)-C(3)	1.388(8)	C(24)-C(23)-Si(1)	111.9(5)
C(3)-C(4)	1.405(8)	C(24)-C(23)-H(23A)	109.2
C(3)-H(3)	0.95	Si(1)-C(23)-H(23A)	109.2
C(4)-C(5)	1.372(8)	C(24)-C(23)-H(23B)	109.2
C(4)-H(4)	0.95	Si(1)-C(23)-H(23B)	109.2
C(5)-C(6)	1.386(8)	H(23A)-C(23)-H(23B)	107.9
C(5)-H(5)	0.95	C(23)-C(24)-H(24A)	109.5
C(6)-N(1)	1.374(7)	C(23)-C(24)-H(24B)	109.5
C(6)-C(18)	1.407(7)	H(24A)-C(24)-H(24B)	109.5
C(7)-C(17)	1.358(7)	C(23)-C(24)-H(24C)	109.5
C(7)-N(1)	1.396(7)	H(24A)-C(24)-H(24C)	109.5
C(7)-C(8)	1.515(8)	H(24B)-C(24)-H(24C)	109.5

C(8)-C(22)	1.532(7)	C(26)-C(25)-Si(1)	113.4(5)
C(8)-C(9)	1.532(7)	C(26)-C(25)-H(25A)	108.9
C(8)-C(21)	1.543(8)	Si(1)-C(25)-H(25A)	108.9
C(9)-C(10)	1.363(7)	C(26)-C(25)-H(25B)	108.9
C(9)-Si(1)	1.903(5)	Si(1)-C(25)-H(25B)	108.9
C(10)-C(11)	1.468(7)	H(25A)-C(25)-H(25B)	107.7
C(10)-H(10)	0.95	C(25)-C(26)-H(26A)	109.5
C(11)-C(12)	1.375(7)	C(25)-C(26)-H(26B)	109.5
C(11)-C(16)	1.523(8)	H(26A)-C(26)-H(26B)	109.5
C(12)-C(13)	1.464(8)	C(25)-C(26)-H(26C)	109.5
C(12)-C(29)	1.497(8)	H(26A)-C(26)-H(26C)	109.5
C(13)-N(2)	1.308(7)	H(26B)-C(26)-H(26C)	109.5
C(13)-C(14)	1.490(8)	C(28)-C(27)-Si(1)	117.5(5)
C(14)-C(15)	1.532(7)	C(28)-C(27)-H(27A)	107.9
C(14)-H(14A)	0.99	Si(1)-C(27)-H(27A)	107.9
C(14)-H(14B)	0.99	C(28)-C(27)-H(27B)	107.9
C(15)-C(16)	1.558(7)	Si(1)-C(27)-H(27B)	107.9
C(15)-H(15)	1	H(27A)-C(27)-H(27B)	107.2
C(16)-C(17)	1.496(7)	C(27)-C(28)-H(28A)	109.5
C(16)-H(16)	1	C(27)-C(28)-H(28B)	109.5
C(17)-C(18)	1.412(8)	H(28A)-C(28)-H(28B)	109.5
C(19)-H(19A)	0.98	C(27)-C(28)-H(28C)	109.5
C(19)-H(19B)	0.98	H(28A)-C(28)-H(28C)	109.5
C(19)-H(19C)	0.98	H(28B)-C(28)-H(28C)	109.5
C(20)-H(20A)	0.98	C(12)-C(29)-H(29A)	109.5
C(20)-H(20B)	0.98	C(12)-C(29)-H(29B)	109.5
C(20)-H(20C)	0.98	H(29A)-C(29)-H(29B)	109.5
C(21)-H(21A)	0.98	C(12)-C(29)-H(29C)	109.5
C(21)-H(21B)	0.98	H(29A)-C(29)-H(29C)	109.5
C(21)-H(21C)	0.98	H(29B)-C(29)-H(29C)	109.5
C(22)-H(22A)	0.98	N(3)-C(30)-C(35)	120.2(5)
C(22)-H(22B)	0.98	N(3)-C(30)-C(31)	122.7(5)
C(22)-H(22C)	0.98	C(35)-C(30)-C(31)	117.2(5)
C(23)-C(24)	1.529(9)	C(32)-C(31)-C(30)	121.5(5)
C(23)-Si(1)	1.886(6)	C(32)-C(31)-N(4)	116.5(5)
C(23)-H(23A)	0.99	C(30)-C(31)-N(4)	121.9(5)
C(23)-H(23B)	0.99	C(33)-C(32)-C(31)	118.9(5)
C(24)-H(24A)	0.98	C(33)-C(32)-H(32)	120.5
C(24)-H(24B)	0.98	C(31)-C(32)-H(32)	120.5
C(24)-H(24C)	0.98	C(32)-C(33)-C(34)	121.6(5)
C(25)-C(26)	1.538(10)	C(32)-C(33)-N(5)	119.2(5)
C(25)-Si(1)	1.883(7)	C(34)-C(33)-N(5)	119.2(5)
C(25)-H(25A)	0.99	C(35)-C(34)-C(33)	119.6(5)
C(25)-H(25B)	0.99	C(35)-C(34)-H(34)	120.2
C(26)-H(26A)	0.98	C(33)-C(34)-H(34)	120.2

C(26)-H(26B)	0.98	C(34)-C(35)-C(30)	121.1(5)
C(26)-H(26C)	0.98	C(34)-C(35)-H(35)	119.4
C(27)-C(28)	1.528(10)	C(30)-C(35)-H(35)	119.4
C(27)-Si(1)	1.888(6)	C(55)-C(36)-C(54)	109.0(5)
C(27)-H(27A)	0.99	C(55)-C(36)-C(37)	110.0(4)
C(27)-H(27B)	0.99	C(54)-C(36)-C(37)	107.6(5)
C(28)-H(28A)	0.98	C(55)-C(36)-C(50)	109.3(4)
C(28)-H(28B)	0.98	C(54)-C(36)-C(50)	111.6(5)
C(28)-H(28C)	0.98	C(37)-C(36)-C(50)	109.3(4)
C(29)-H(29A)	0.98	C(38)-C(37)-C(53)	117.1(5)
C(29)-H(29B)	0.98	C(38)-C(37)-C(36)	127.5(5)
C(29)-H(29C)	0.98	C(53)-C(37)-C(36)	115.2(5)
C(30)-N(3)	1.367(6)	C(37)-C(38)-C(39)	120.7(5)
C(30)-C(35)	1.404(8)	C(37)-C(38)-H(38)	119.6
C(30)-C(31)	1.419(7)	C(39)-C(38)-H(38)	119.6
C(31)-C(32)	1.387(7)	C(40)-C(39)-C(38)	122.4(5)
C(31)-N(4)	1.447(7)	C(40)-C(39)-H(39)	118.8
C(32)-C(33)	1.366(8)	C(38)-C(39)-H(39)	118.8
C(32)-H(32)	0.95	C(39)-C(40)-C(41)	117.1(5)
C(33)-C(34)	1.389(8)	C(39)-C(40)-H(40)	121.4
C(33)-N(5)	1.453(7)	C(41)-C(40)-H(40)	121.4
C(34)-C(35)	1.378(7)	N(6)-C(41)-C(40)	133.4(5)
C(34)-H(34)	0.95	N(6)-C(41)-C(53)	106.1(4)
C(35)-H(35)	0.95	C(40)-C(41)-C(53)	120.4(5)
C(36)-C(55)	1.534(8)	C(52)-C(42)-N(6)	107.9(5)
C(36)-C(54)	1.536(8)	C(52)-C(42)-C(43)	128.4(5)
C(36)-C(37)	1.540(7)	N(6)-C(42)-C(43)	123.6(5)
C(36)-C(50)	1.568(8)	C(42)-C(43)-C(44)	110.4(4)
C(37)-C(38)	1.377(8)	C(42)-C(43)-C(56)	108.7(5)
C(37)-C(53)	1.387(8)	C(44)-C(43)-C(56)	108.1(4)
C(38)-C(39)	1.407(8)	C(42)-C(43)-C(57)	109.0(4)
C(38)-H(38)	0.95	C(44)-C(43)-C(57)	112.5(5)
C(39)-C(40)	1.374(8)	C(56)-C(43)-C(57)	108.1(4)
C(39)-H(39)	0.95	C(45)-C(44)-C(43)	124.1(5)
C(40)-C(41)	1.389(8)	C(45)-C(44)-Si(2)	114.2(4)
C(40)-H(40)	0.95	C(43)-C(44)-Si(2)	121.6(4)
C(41)-N(6)	1.377(7)	C(44)-C(45)-C(46)	137.1(5)
C(41)-C(53)	1.405(7)	C(44)-C(45)-H(45)	111.4
C(42)-C(52)	1.374(7)	C(46)-C(45)-H(45)	111.4
C(42)-N(6)	1.394(7)	C(47)-C(46)-C(45)	116.8(5)
C(42)-C(43)	1.508(8)	C(47)-C(46)-C(51)	119.7(5)
C(43)-C(44)	1.531(8)	C(45)-C(46)-C(51)	123.6(4)
C(43)-C(56)	1.535(8)	C(46)-C(47)-C(48)	120.3(5)
C(43)-C(57)	1.539(7)	C(46)-C(47)-C(64)	122.3(5)
C(44)-C(45)	1.368(7)	C(48)-C(47)-C(64)	117.4(5)

C(44)-Si(2)	1.911(6)	N(7)-C(48)-C(47)	117.5(5)
C(45)-C(46)	1.465(7)	N(7)-C(48)-C(49)	122.3(5)
C(45)-H(45)	0.95	C(47)-C(48)-C(49)	120.2(4)
C(46)-C(47)	1.381(7)	C(48)-C(49)-C(50)	113.2(5)
C(46)-C(51)	1.528(8)	C(48)-C(49)-H(49A)	108.9
C(47)-C(48)	1.456(8)	C(50)-C(49)-H(49A)	108.9
C(47)-C(64)	1.511(8)	C(48)-C(49)-H(49B)	108.9
C(48)-N(7)	1.313(6)	C(50)-C(49)-H(49B)	108.9
C(48)-C(49)	1.499(8)	H(49A)-C(49)-H(49B)	107.7
C(49)-C(50)	1.512(7)	C(49)-C(50)-C(51)	107.9(4)
C(49)-H(49A)	0.99	C(49)-C(50)-C(36)	112.8(4)
C(49)-H(49B)	0.99	C(51)-C(50)-C(36)	117.6(4)
C(50)-C(51)	1.547(7)	C(49)-C(50)-H(50)	105.9
C(50)-H(50)	1	C(51)-C(50)-H(50)	105.9
C(51)-C(52)	1.484(7)	C(36)-C(50)-H(50)	105.9
C(51)-H(51)	1	C(52)-C(51)-C(46)	114.7(4)
C(52)-C(53)	1.420(8)	C(52)-C(51)-C(50)	109.1(4)
C(54)-H(54A)	0.98	C(46)-C(51)-C(50)	110.1(4)
C(54)-H(54B)	0.98	C(52)-C(51)-H(51)	107.6
C(54)-H(54C)	0.98	C(46)-C(51)-H(51)	107.6
C(55)-H(55A)	0.98	C(50)-C(51)-H(51)	107.6
C(55)-H(55B)	0.98	C(42)-C(52)-C(53)	107.2(5)
C(55)-H(55C)	0.98	C(42)-C(52)-C(51)	132.6(5)
C(56)-H(56A)	0.98	C(53)-C(52)-C(51)	120.2(5)
C(56)-H(56B)	0.98	C(37)-C(53)-C(41)	122.1(5)
C(56)-H(56C)	0.98	C(37)-C(53)-C(52)	129.3(5)
C(57)-H(57A)	0.98	C(41)-C(53)-C(52)	108.5(5)
C(57)-H(57B)	0.98	C(36)-C(54)-H(54A)	109.5
C(57)-H(57C)	0.98	C(36)-C(54)-H(54B)	109.5
C(58)-C(59)	1.528(9)	H(54A)-C(54)-H(54B)	109.5
C(58)-Si(2)	1.894(6)	C(36)-C(54)-H(54C)	109.5
C(58)-H(58A)	0.99	H(54A)-C(54)-H(54C)	109.5
C(58)-H(58B)	0.99	H(54B)-C(54)-H(54C)	109.5
C(59)-H(59A)	0.98	C(36)-C(55)-H(55A)	109.5
C(59)-H(59B)	0.98	C(36)-C(55)-H(55B)	109.5
C(59)-H(59C)	0.98	H(55A)-C(55)-H(55B)	109.5
C(60)-C(61)	1.530(9)	C(36)-C(55)-H(55C)	109.5
C(60)-Si(2)	1.880(7)	H(55A)-C(55)-H(55C)	109.5
C(60)-H(60A)	0.99	H(55B)-C(55)-H(55C)	109.5
C(60)-H(60B)	0.99	C(43)-C(56)-H(56A)	109.5
C(61)-H(61A)	0.98	C(43)-C(56)-H(56B)	109.5
C(61)-H(61B)	0.98	H(56A)-C(56)-H(56B)	109.5
C(61)-H(61C)	0.98	C(43)-C(56)-H(56C)	109.5
C(62)-C(63)	1.534(9)	H(56A)-C(56)-H(56C)	109.5
C(62)-Si(2)	1.887(6)	H(56B)-C(56)-H(56C)	109.5

C(62)-H(62A)	0.99	C(43)-C(57)-H(57A)	109.5
C(62)-H(62B)	0.99	C(43)-C(57)-H(57B)	109.5
C(63)-H(63A)	0.98	H(57A)-C(57)-H(57B)	109.5
C(63)-H(63B)	0.98	C(43)-C(57)-H(57C)	109.5
C(63)-H(63C)	0.98	H(57A)-C(57)-H(57C)	109.5
C(64)-H(64A)	0.98	H(57B)-C(57)-H(57C)	109.5
C(64)-H(64B)	0.98	C(59)-C(58)-Si(2)	113.8(4)
C(64)-H(64C)	0.98	C(59)-C(58)-H(58A)	108.8
C(65)-N(8)	1.364(7)	Si(2)-C(58)-H(58A)	108.8
C(65)-C(70)	1.402(8)	C(59)-C(58)-H(58B)	108.8
C(65)-C(66)	1.412(8)	Si(2)-C(58)-H(58B)	108.8
C(66)-C(67)	1.401(8)	H(58A)-C(58)-H(58B)	107.7
C(66)-N(9)	1.438(8)	C(58)-C(59)-H(59A)	109.5
C(67)-C(68)	1.375(9)	C(58)-C(59)-H(59B)	109.5
C(67)-H(67)	0.95	H(59A)-C(59)-H(59B)	109.5
C(68)-C(69)	1.381(9)	C(58)-C(59)-H(59C)	109.5
C(68)-N(10)	1.478(8)	H(59A)-C(59)-H(59C)	109.5
C(69)-C(70)	1.363(8)	H(59B)-C(59)-H(59C)	109.5
C(69)-H(69)	0.95	C(61)-C(60)-Si(2)	115.5(4)
C(70)-H(70)	0.95	C(61)-C(60)-H(60A)	108.4
C(71)-C(72)	1.462(11)	Si(2)-C(60)-H(60A)	108.4
C(71)-C(76)	1.548(12)	C(61)-C(60)-H(60B)	108.4
C(71)-H(71A)	0.99	Si(2)-C(60)-H(60B)	108.4
C(71)-H(71B)	0.99	H(60A)-C(60)-H(60B)	107.5
C(72)-C(73)	1.516(11)	C(60)-C(61)-H(61A)	109.5
C(72)-H(72A)	0.99	C(60)-C(61)-H(61B)	109.5
C(72)-H(72B)	0.99	H(61A)-C(61)-H(61B)	109.5
C(73)-C(74)	1.524(13)	C(60)-C(61)-H(61C)	109.5
C(73)-H(73A)	0.99	H(61A)-C(61)-H(61C)	109.5
C(73)-H(73B)	0.99	H(61B)-C(61)-H(61C)	109.5
C(74)-C(75)	1.545(13)	C(63)-C(62)-Si(2)	118.3(4)
C(74)-H(74A)	0.99	C(63)-C(62)-H(62A)	107.7
C(74)-H(74B)	0.99	Si(2)-C(62)-H(62A)	107.7
C(75)-C(76)	1.546(11)	C(63)-C(62)-H(62B)	107.7
C(75)-H(75A)	0.99	Si(2)-C(62)-H(62B)	107.7
C(75)-H(75B)	0.99	H(62A)-C(62)-H(62B)	107.1
C(76)-H(76A)	0.99	C(62)-C(63)-H(63A)	109.5
C(76)-H(76B)	0.99	C(62)-C(63)-H(63B)	109.5
N(1)-H(1)	0.88	H(63A)-C(63)-H(63B)	109.5
N(2)-N(3)	1.363(6)	C(62)-C(63)-H(63C)	109.5
N(3)-H(3A)	0.88	H(63A)-C(63)-H(63C)	109.5
N(4)-O(2)	1.211(6)	H(63B)-C(63)-H(63C)	109.5
N(4)-O(1)	1.238(6)	C(47)-C(64)-H(64A)	109.5
N(5)-O(4)	1.228(6)	C(47)-C(64)-H(64B)	109.5
N(5)-O(3)	1.233(6)	H(64A)-C(64)-H(64B)	109.5

N(6)-H(6)	0.88	C(47)-C(64)-H(64C)	109.5
N(7)-N(8)	1.377(6)	H(64A)-C(64)-H(64C)	109.5
N(8)-H(8)	0.88	H(64B)-C(64)-H(64C)	109.5
N(9)-O(6)	1.231(7)	N(8)-C(65)-C(70)	120.8(5)
N(9)-O(5)	1.246(7)	N(8)-C(65)-C(66)	121.9(5)
N(10)-O(7)	1.213(7)	C(70)-C(65)-C(66)	117.3(5)
N(10)-O(8)	1.224(8)	C(67)-C(66)-C(65)	121.4(6)
C(19)-C(1)-C(20)	108.6(5)	C(67)-C(66)-N(9)	116.9(5)
C(19)-C(1)-C(2)	107.3(5)	C(65)-C(66)-N(9)	121.8(5)
C(20)-C(1)-C(2)	110.5(5)	C(68)-C(67)-C(66)	118.0(6)
C(19)-C(1)-C(15)	112.1(5)	C(68)-C(67)-H(67)	121
C(20)-C(1)-C(15)	108.8(5)	C(66)-C(67)-H(67)	121
C(2)-C(1)-C(15)	109.6(4)	C(67)-C(68)-C(69)	122.0(5)
C(18)-C(2)-C(3)	117.1(5)	C(67)-C(68)-N(10)	118.6(6)
C(18)-C(2)-C(1)	116.2(5)	C(69)-C(68)-N(10)	119.3(6)
C(3)-C(2)-C(1)	126.4(5)	C(70)-C(69)-C(68)	119.6(6)
C(2)-C(3)-C(4)	120.1(5)	C(70)-C(69)-H(69)	120.2
C(2)-C(3)-H(3)	119.9	C(68)-C(69)-H(69)	120.2
C(4)-C(3)-H(3)	119.9	C(69)-C(70)-C(65)	121.7(6)
C(5)-C(4)-C(3)	122.9(6)	C(69)-C(70)-H(70)	119.1
C(5)-C(4)-H(4)	118.5	C(65)-C(70)-H(70)	119.1
C(3)-C(4)-H(4)	118.5	C(72)-C(71)-C(76)	116.1(7)
C(4)-C(5)-C(6)	117.3(5)	C(72)-C(71)-H(71A)	108.3
C(4)-C(5)-H(5)	121.3	C(76)-C(71)-H(71A)	108.3
C(6)-C(5)-H(5)	121.3	C(72)-C(71)-H(71B)	108.3
N(1)-C(6)-C(5)	133.8(5)	C(76)-C(71)-H(71B)	108.3
N(1)-C(6)-C(18)	105.8(5)	H(71A)-C(71)-H(71B)	107.4
C(5)-C(6)-C(18)	120.3(5)	C(71)-C(72)-C(73)	110.1(7)
C(17)-C(7)-N(1)	108.2(5)	C(71)-C(72)-H(72A)	109.6
C(17)-C(7)-C(8)	128.9(5)	C(73)-C(72)-H(72A)	109.6
N(1)-C(7)-C(8)	122.7(5)	C(71)-C(72)-H(72B)	109.6
C(7)-C(8)-C(22)	109.4(4)	C(73)-C(72)-H(72B)	109.6
C(7)-C(8)-C(9)	109.2(4)	H(72A)-C(72)-H(72B)	108.2
C(22)-C(8)-C(9)	113.9(4)	C(72)-C(73)-C(74)	116.0(7)
C(7)-C(8)-C(21)	108.8(4)	C(72)-C(73)-H(73A)	108.3
C(22)-C(8)-C(21)	107.8(5)	C(74)-C(73)-H(73A)	108.3
C(9)-C(8)-C(21)	107.6(4)	C(72)-C(73)-H(73B)	108.3
C(10)-C(9)-C(8)	123.7(5)	C(74)-C(73)-H(73B)	108.3
C(10)-C(9)-Si(1)	114.4(4)	H(73A)-C(73)-H(73B)	107.4
C(8)-C(9)-Si(1)	121.4(4)	C(73)-C(74)-C(75)	110.8(8)
C(9)-C(10)-C(11)	137.1(5)	C(73)-C(74)-H(74A)	109.5
C(9)-C(10)-H(10)	111.4	C(75)-C(74)-H(74A)	109.5
C(11)-C(10)-H(10)	111.4	C(73)-C(74)-H(74B)	109.5
C(12)-C(11)-C(10)	116.9(5)	C(75)-C(74)-H(74B)	109.5
C(12)-C(11)-C(16)	119.9(5)	H(74A)-C(74)-H(74B)	108.1

C(10)-C(11)-C(16)	123.2(4)	C(74)-C(75)-C(76)	107.4(7)
C(11)-C(12)-C(13)	119.8(5)	C(74)-C(75)-H(75A)	110.2
C(11)-C(12)-C(29)	122.5(5)	C(76)-C(75)-H(75A)	110.2
C(13)-C(12)-C(29)	117.6(5)	C(74)-C(75)-H(75B)	110.2
N(2)-C(13)-C(12)	117.2(5)	C(76)-C(75)-H(75B)	110.2
N(2)-C(13)-C(14)	121.9(5)	H(75A)-C(75)-H(75B)	108.5
C(12)-C(13)-C(14)	120.8(4)	C(75)-C(76)-C(71)	110.3(7)
C(13)-C(14)-C(15)	114.1(4)	C(75)-C(76)-H(76A)	109.6
C(13)-C(14)-H(14A)	108.7	C(71)-C(76)-H(76A)	109.6
C(15)-C(14)-H(14A)	108.7	C(75)-C(76)-H(76B)	109.6
C(13)-C(14)-H(14B)	108.7	C(71)-C(76)-H(76B)	109.6
C(15)-C(14)-H(14B)	108.7	H(76A)-C(76)-H(76B)	108.1
H(14A)-C(14)-H(14B)	107.6	C(6)-N(1)-C(7)	109.9(4)
C(14)-C(15)-C(16)	107.8(4)	C(6)-N(1)-H(1)	125
C(14)-C(15)-C(1)	111.7(4)	C(7)-N(1)-H(1)	125
C(16)-C(15)-C(1)	116.8(4)	C(13)-N(2)-N(3)	115.7(5)
C(14)-C(15)-H(15)	106.7	N(2)-N(3)-C(30)	120.1(4)
C(16)-C(15)-H(15)	106.7	N(2)-N(3)-H(3A)	120
C(1)-C(15)-H(15)	106.7	C(30)-N(3)-H(3A)	120
C(17)-C(16)-C(11)	115.0(4)	O(2)-N(4)-O(1)	121.6(5)
C(17)-C(16)-C(15)	108.8(4)	O(2)-N(4)-C(31)	119.3(5)
C(11)-C(16)-C(15)	109.9(4)	O(1)-N(4)-C(31)	119.1(5)
C(17)-C(16)-H(16)	107.6	O(4)-N(5)-O(3)	123.2(4)
C(11)-C(16)-H(16)	107.6	O(4)-N(5)-C(33)	118.5(5)
C(15)-C(16)-H(16)	107.6	O(3)-N(5)-C(33)	118.3(5)
C(7)-C(17)-C(18)	107.5(4)	C(41)-N(6)-C(42)	110.2(4)
C(7)-C(17)-C(16)	132.4(5)	C(41)-N(6)-H(6)	124.9
C(18)-C(17)-C(16)	119.9(4)	C(42)-N(6)-H(6)	124.9
C(2)-C(18)-C(6)	122.3(5)	C(48)-N(7)-N(8)	114.4(5)
C(2)-C(18)-C(17)	129.0(5)	C(65)-N(8)-N(7)	120.4(5)
C(6)-C(18)-C(17)	108.5(5)	C(65)-N(8)-H(8)	119.8
C(1)-C(19)-H(19A)	109.5	N(7)-N(8)-H(8)	119.8
C(1)-C(19)-H(19B)	109.5	O(6)-N(9)-O(5)	122.3(6)
H(19A)-C(19)-H(19B)	109.5	O(6)-N(9)-C(66)	118.7(5)
C(1)-C(19)-H(19C)	109.5	O(5)-N(9)-C(66)	119.1(5)
H(19A)-C(19)-H(19C)	109.5	O(7)-N(10)-O(8)	125.1(6)
H(19B)-C(19)-H(19C)	109.5	O(7)-N(10)-C(68)	117.6(6)
C(1)-C(20)-H(20A)	109.5	O(8)-N(10)-C(68)	117.2(6)
C(1)-C(20)-H(20B)	109.5	C(25)-Si(1)-C(23)	110.4(3)
H(20A)-C(20)-H(20B)	109.5	C(25)-Si(1)-C(27)	105.2(3)
C(1)-C(20)-H(20C)	109.5	C(23)-Si(1)-C(27)	106.1(3)
H(20A)-C(20)-H(20C)	109.5	C(25)-Si(1)-C(9)	109.3(3)
H(20B)-C(20)-H(20C)	109.5	C(23)-Si(1)-C(9)	115.0(3)
C(8)-C(21)-H(21A)	109.5	C(27)-Si(1)-C(9)	110.5(2)
C(8)-C(21)-H(21B)	109.5	C(60)-Si(2)-C(62)	105.1(3)

H(21A)-C(21)-H(21B)	109.5	C(60)-Si(2)-C(58)	109.2(3)
C(8)-C(21)-H(21C)	109.5	C(62)-Si(2)-C(58)	106.7(3)
H(21A)-C(21)-H(21C)	109.5	C(60)-Si(2)-C(44)	111.4(3)
H(21B)-C(21)-H(21C)	109.5	C(62)-Si(2)-C(44)	110.3(3)
C(8)-C(22)-H(22A)	109.5	C(58)-Si(2)-C(44)	113.6(3)

Symmetry transformations used to generate equivalent atoms:

Table 4.4: Anisotropic displacement parameters ($\text{\AA}^2 \times 10^3$) for sarpong127. The anisotropic displacement factor exponent takes the form: $-2\pi^2 [h^2 a^{*2} U^{11} + \dots + 2 h k a^* b^* U^{12}]$

	U^{11}	U^{22}	U^{33}	U^{23}	U^{13}	U^{12}
C(1)	19(3)	26(3)	29(3)	-6(3)	16(3)	-1(2)
C(2)	18(3)	25(3)	31(3)	-2(3)	14(3)	-1(2)
C(3)	29(3)	27(3)	48(4)	-14(3)	25(3)	-7(3)
C(4)	26(3)	29(3)	50(4)	-15(3)	19(3)	-14(3)
C(5)	20(3)	33(4)	43(4)	-2(3)	20(3)	-5(3)
C(6)	16(3)	29(3)	24(3)	2(3)	11(3)	2(2)
C(7)	15(3)	26(3)	16(3)	4(2)	5(2)	1(2)
C(8)	15(3)	29(3)	21(3)	-2(3)	7(2)	1(2)
C(9)	15(3)	17(3)	20(3)	-1(2)	8(2)	-2(2)
C(10)	13(3)	23(3)	20(3)	-1(2)	5(2)	-4(2)
C(11)	17(3)	18(3)	24(3)	5(2)	11(3)	2(2)
C(12)	16(3)	25(3)	27(3)	-1(3)	11(3)	-1(2)
C(13)	11(3)	24(3)	27(3)	8(3)	10(2)	5(2)
C(14)	19(3)	23(3)	33(3)	1(3)	17(3)	1(2)
C(15)	19(3)	20(3)	25(3)	4(2)	13(3)	2(2)
C(16)	15(3)	19(3)	21(3)	3(2)	10(2)	2(2)
C(17)	14(3)	23(3)	17(3)	4(2)	9(2)	3(2)
C(18)	16(3)	19(3)	20(3)	4(2)	8(2)	1(2)
C(19)	21(3)	46(4)	30(3)	-2(3)	13(3)	-8(3)
C(20)	22(3)	28(3)	45(4)	-13(3)	17(3)	-3(3)
C(21)	30(3)	27(3)	28(3)	-1(3)	7(3)	5(3)
C(22)	18(3)	34(4)	31(3)	-11(3)	10(3)	2(3)
C(23)	28(3)	62(5)	26(3)	-1(3)	15(3)	1(3)
C(24)	52(5)	100(7)	43(4)	-4(5)	30(4)	0(5)
C(25)	34(4)	43(4)	44(4)	-13(3)	14(3)	2(3)
C(26)	62(5)	38(5)	90(6)	-6(5)	39(5)	-9(4)
C(27)	23(3)	47(4)	24(3)	-10(3)	6(3)	0(3)
C(28)	36(4)	59(5)	32(4)	5(4)	8(3)	4(4)
C(29)	13(3)	48(4)	41(4)	-7(3)	13(3)	-4(3)
C(30)	15(3)	19(3)	26(3)	5(3)	9(2)	2(2)
C(31)	16(3)	21(3)	27(3)	2(3)	9(3)	2(2)
C(32)	20(3)	27(3)	30(3)	2(3)	17(3)	1(2)

Table 4.4: Anisotropic displacement parameters ($\text{\AA}^2 \times 10^3$) for sarpong127. The anisotropic displacement factor exponent takes the form: $-2\pi^2 [h^2 a^{*2} U^{11} + \dots + 2 h k a^* b^* U^{12}]$

	U ¹¹	U ²²	U ³³	U ²³	U ¹³	U ¹²
C(33)	14(3)	29(3)	29(3)	8(3)	13(3)	4(3)
C(34)	11(3)	29(3)	31(3)	4(3)	6(3)	3(2)
C(35)	22(3)	29(3)	27(3)	6(3)	15(3)	4(3)
C(36)	16(3)	29(3)	22(3)	1(3)	9(2)	-2(2)
C(37)	16(3)	21(3)	25(3)	-4(2)	8(3)	0(2)
C(38)	22(3)	34(4)	23(3)	4(3)	10(3)	3(3)
C(39)	32(3)	37(4)	26(3)	1(3)	16(3)	3(3)
C(40)	21(3)	34(3)	31(3)	1(3)	17(3)	1(3)
C(41)	15(3)	23(3)	26(3)	0(3)	10(3)	1(2)
C(42)	17(3)	20(3)	30(3)	-1(3)	13(3)	-4(2)
C(43)	14(3)	28(3)	25(3)	1(3)	7(2)	-3(2)
C(44)	15(3)	23(3)	22(3)	-2(2)	8(2)	0(2)
C(45)	22(3)	20(3)	23(3)	-2(2)	12(3)	-1(2)
C(46)	16(3)	23(3)	13(3)	-2(2)	3(2)	-1(2)
C(47)	17(3)	23(3)	23(3)	-4(2)	9(3)	-4(2)
C(48)	17(3)	20(3)	25(3)	-5(2)	10(2)	-3(2)
C(49)	13(3)	25(3)	26(3)	-1(3)	7(2)	0(2)
C(50)	14(3)	26(3)	24(3)	-1(3)	9(2)	1(2)
C(51)	16(3)	25(3)	23(3)	-1(3)	9(2)	-1(2)
C(52)	16(3)	17(3)	26(3)	-1(2)	9(2)	-1(2)
C(53)	22(3)	17(3)	26(3)	1(2)	12(3)	-1(2)
C(54)	28(3)	28(3)	32(3)	2(3)	15(3)	3(3)
C(55)	24(3)	35(4)	28(3)	3(3)	11(3)	2(3)
C(56)	23(3)	32(4)	26(3)	-2(3)	11(3)	-7(3)
C(57)	15(3)	37(4)	28(3)	6(3)	9(3)	0(3)
C(58)	22(3)	45(4)	34(4)	7(3)	16(3)	4(3)
C(59)	36(4)	55(5)	56(5)	17(4)	29(4)	17(3)
C(60)	24(3)	52(4)	33(4)	12(3)	12(3)	0(3)
C(61)	39(4)	45(4)	30(4)	6(3)	14(3)	-5(3)
C(62)	26(3)	31(4)	33(4)	13(3)	14(3)	4(3)
C(63)	35(4)	32(4)	46(4)	3(3)	23(3)	0(3)
C(64)	16(3)	40(4)	46(4)	10(3)	18(3)	1(3)
C(65)	15(3)	31(3)	22(3)	-8(3)	9(2)	0(2)
C(66)	23(3)	40(4)	24(3)	-2(3)	11(3)	4(3)
C(67)	20(3)	46(4)	24(3)	-6(3)	6(3)	9(3)
C(68)	20(3)	47(4)	35(4)	-13(3)	17(3)	-4(3)
C(69)	24(3)	30(4)	44(4)	-11(3)	19(3)	-8(3)
C(70)	22(3)	29(3)	39(4)	-7(3)	17(3)	1(3)
C(71)	90(7)	68(6)	71(6)	5(5)	44(6)	5(5)

Table 4.4: Anisotropic displacement parameters ($\text{\AA}^2 \times 10^3$) for sarpong127. The anisotropic displacement factor exponent takes the form: $-2\pi^2 [h^2 a^{*2} U^{11} + \dots + 2 h k a^* b^* U^{12}]$

	U ¹¹	U ²²	U ³³	U ²³	U ¹³	U ¹²
C(72)	32(4)	61(5)	46(4)	-14(4)	20(4)	-3(4)
C(73)	82(6)	44(5)	95(7)	-3(5)	50(6)	-3(5)
C(74)	129(10)	69(7)	70(6)	2(6)	56(7)	-10(6)
C(75)	78(6)	64(6)	47(5)	19(4)	26(5)	16(5)
C(76)	57(5)	57(5)	68(6)	8(5)	31(5)	2(4)
N(1)	11(2)	33(3)	26(2)	-3(2)	10(2)	0(2)
N(2)	17(2)	23(3)	29(3)	0(2)	12(2)	1(2)
N(3)	12(2)	26(3)	27(3)	-1(2)	11(2)	-1(2)
N(4)	23(3)	43(3)	35(3)	-10(3)	14(3)	-3(2)
N(5)	17(2)	30(3)	31(3)	8(2)	12(2)	4(2)
N(6)	14(2)	30(3)	27(3)	1(2)	13(2)	2(2)
N(7)	13(2)	28(3)	27(3)	-4(2)	9(2)	0(2)
N(8)	13(2)	34(3)	27(3)	2(2)	10(2)	2(2)
N(9)	32(3)	65(4)	41(3)	21(3)	22(3)	25(3)
N(10)	26(3)	59(4)	45(4)	-21(3)	21(3)	-7(3)
O(1)	14(2)	45(3)	42(3)	-13(2)	11(2)	-2(2)
O(2)	31(3)	132(5)	34(3)	-27(3)	16(2)	-9(3)
O(3)	23(2)	55(3)	41(3)	3(2)	22(2)	3(2)
O(4)	15(2)	51(3)	36(3)	2(2)	9(2)	-2(2)
O(5)	43(3)	72(4)	80(4)	41(3)	44(3)	24(3)
O(6)	43(3)	78(4)	74(4)	34(3)	26(3)	31(3)
O(7)	23(2)	81(4)	57(3)	-3(3)	19(2)	6(3)
O(8)	44(3)	56(4)	91(4)	-8(3)	51(3)	-13(3)
Si(1)	18(1)	39(1)	24(1)	-8(1)	9(1)	0(1)
Si(2)	17(1)	34(1)	27(1)	7(1)	9(1)	2(1)

Table 4.5: Hydrogen coordinates ($\times 10^4$) and isotropic displacement parameters ($\text{\AA}^2 \times 10^3$) for sarpong127.

	x	y	z	U(eq)
H(3)	3282	-103	4564	38
H(4)	2018	-197	4651	42
H(5)	1696	1035	5431	36
H(10)	5818	4069	8234	23
H(14A)	6288	1800	5901	28
H(14B)	5822	2911	5454	28
H(15)	5402	1581	6495	24
H(16)	4744	3724	5854	21

Table 4.5: Hydrogen coordinates ($\times 10^4$) and isotropic displacement parameters ($\text{\AA}^2 \times 10^3$) for sarpong127.

	x	y	z	U(eq)
H(19A)	4818	2228	4376	48
H(19B)	4113	2852	4531	48
H(19C)	3887	1732	4014	48
H(20A)	4593	-51	4730	46
H(20B)	5184	-34	5693	46
H(20C)	5485	562	5095	46
H(21A)	4189	5264	6361	46
H(21B)	3840	6065	6828	46
H(21C)	3196	5404	6038	46
H(22A)	2500	4638	6818	42
H(22B)	3144	5301	7607	42
H(22C)	3031	3997	7656	42
H(23A)	3605	4525	8981	45
H(23B)	4208	3466	9254	45
H(24A)	5107	4377	10496	92
H(24B)	4176	4250	10408	92
H(24C)	4481	5413	10225	92
H(25A)	4152	6636	8331	50
H(25B)	4763	6734	9286	50
H(26A)	5943	6917	9031	92
H(26B)	5262	7840	8527	92
H(26C)	5354	6758	8075	92
H(27A)	6341	4928	9341	40
H(27B)	6112	5127	10072	40
H(28A)	5878	3181	10097	68
H(28B)	6830	3471	10305	68
H(28C)	6196	3021	9420	68
H(29A)	6849	4921	8018	51
H(29B)	7551	4180	7940	51
H(29C)	7108	3754	8472	51
H(32)	9616	2394	5458	28
H(34)	10314	3255	7796	30
H(35)	8914	3319	7541	29
H(38)	1553	4091	5018	32
H(39)	331	4380	5159	37
H(40)	-928	4910	4062	32
H(45)	198	7227	787	25
H(49A)	2921	4895	3091	26
H(49B)	2299	4064	2408	26

Table 4.5: Hydrogen coordinates ($\times 10^4$) and isotropic displacement parameters ($\text{\AA}^2 \times 10^3$) for sarpong127.

	x	y	z	U(eq)
H(50)	1790	5814	3107	26
H(51)	757	4340	1837	25
H(54A)	2200	2865	3266	43
H(54B)	1197	2910	2904	43
H(54C)	1768	2603	3841	43
H(55A)	3093	4326	4211	44
H(55B)	2692	4045	4809	44
H(55C)	2675	5286	4502	44
H(56A)	-673	4413	679	41
H(56B)	-1579	4787	-8	41
H(56C)	-1506	4026	731	41
H(57A)	-2351	5346	1061	40
H(57B)	-2442	6123	324	40
H(57C)	-2088	6620	1223	40
H(58A)	-2513	8155	477	39
H(58B)	-1666	8768	1088	39
H(59A)	-1902	10129	75	69
H(59B)	-2669	10090	301	69
H(59C)	-2761	9524	-520	69
H(60A)	-2496	6601	-867	45
H(60B)	-2548	7800	-1246	45
H(61A)	-1375	7329	-1488	58
H(61B)	-2172	6550	-1982	58
H(61C)	-1398	6107	-1168	58
H(62A)	-327	8289	-232	36
H(62B)	-1054	9195	-556	36
H(63A)	-483	9861	843	54
H(63B)	99	10075	405	54
H(63C)	311	9082	1041	54
H(64A)	1124	6800	305	48
H(64B)	2105	7021	874	48
H(64C)	1414	7755	979	48
H(67)	6343	4387	2945	38
H(69)	5299	7088	1556	37
H(70)	4035	6726	1565	34
H(71A)	9165	1150	3838	88
H(71B)	8785	382	3049	88
H(72A)	10184	288	3549	55
H(72B)	10287	1603	3651	55

Table 4.5: Hydrogen coordinates ($\times 10^4$) and isotropic displacement parameters ($\text{\AA}^2 \times 10^3$) for sarpong127.

	x	y	z	U(eq)
H(73A)	9612	394	2164	84
H(73B)	10418	1179	2501	84
H(74A)	9255	1989	1379	103
H(74B)	9575	2755	2172	103
H(75A)	8123	1315	1615	77
H(75B)	8076	2640	1568	77
H(76A)	7970	2002	2760	72
H(76B)	8789	2760	3021	72
H(1)	2419	2908	6461	27
H(3A)	7179	2631	5748	25
H(6)	-1557	5484	2386	27
H(8)	3593	4555	2528	30

Chapter 5

Chapter 5 : Late-Stage Strategies for the Synthesis of Pentacyclic Ambiguine Natural Products

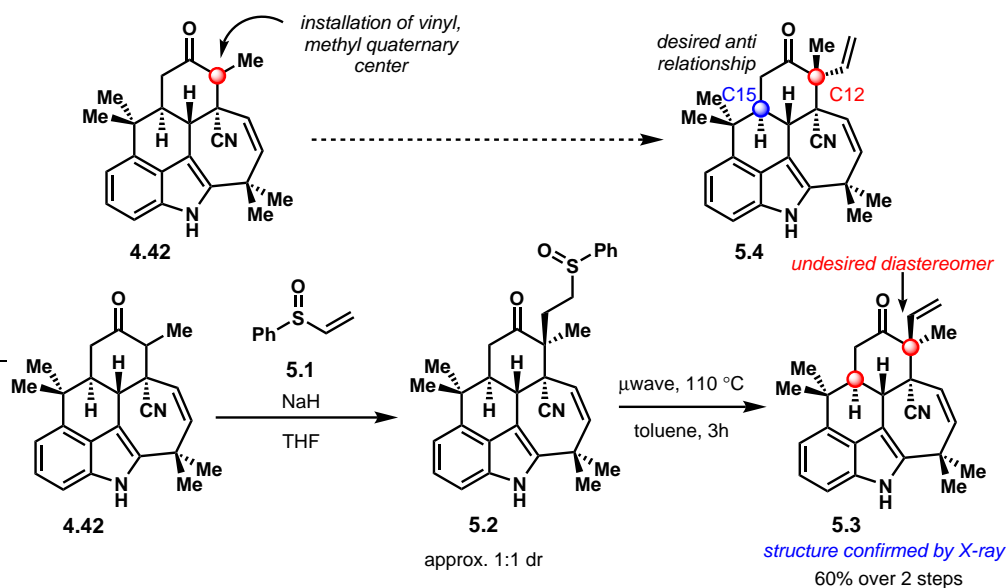
5.1 Installation of the C12 Quaternary Center

A robust route has been developed to access ketone **4.42** as a key intermediate in the synthesis toward the pentacyclic ambiguines (Chapter 4). The next challenge at hand was to install the C12 quaternary center with the desired *anti* relative stereochemistry from **4.42**. Access to **4.42** on gram-scale allowed for vast exploration of various methodologies to install this C12 quaternary center.

Given the complex pentacyclic framework of ketone intermediate **4.42** compared to that of carvone, there was an opportunity to achieve an epimeric mixture at C12 through a simple α -alkylation of **4.42**. To execute this plan, alkylation conditions were explored and it was found that treatment of **4.42** with sodium hydride and vinyl phenyl sulfoxide (**5.1**) furnished sulfoxide intermediate **5.2** as a mixture of diastereomers (Scheme 5.1).¹ Subsequent microwave heating of **5.2** induced sulfoxide extrusion and produced the C12 vinylated compound **5.3**. Unfortunately, as confirmed through X-ray crystallographic analysis, this alkylation reaction proceeded with complete selectivity to give the diastereomer containing the *syn* relative stereochemistry between the C12 and C15 positions. Although this result was undesired, it presented the opportunity to utilize more interesting methodologies to access the desired diastereomer (**5.4**) containing the *anti* relative stereochemistry.

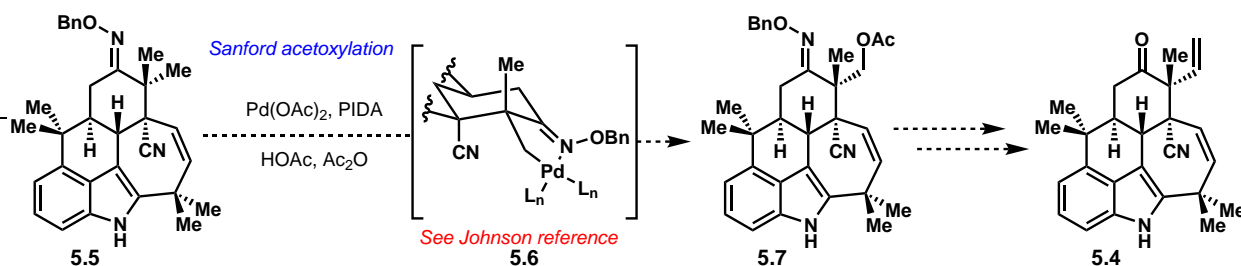
Employing C–H functionalization methodology to access the desired diastereomer at C12 was extremely attractive given the number of strategies available to functionalize a substituent α to a ketone group. We envisioned transforming the ketone moiety into a directing group for C–H functionalization, such as an oxime ether functionality² or a silyl ether group.³ The methodology that seemed the most promising for this transformation was the Sanford acetoxylation protocol developed in 2004 for the C–H oxygenation of unactivated sp^3 bonds.

As shown in the proposed sequence (Scheme 5.2), execution of this plan required access to the geminally dimethylated oxime ether **5.5**. Subsequently, a directed C–H acetoxylation to the α -disposed methyl group could occur through the proposed 5-membered palladacycle intermedi-



Scheme 5.1: Simple α -alkylation using vinyl phenyl sulfoxide (**5.1**) followed by sulfoxide extrusion generated compound **5.3** bearing the undesired *syn* relative stereochemistry between C12 and C15.

ate **5.6**. In 2015, the Johnson group proposed a similar 5-membered palladacycle intermediate, suggesting that, in our case, the desired α -disposed methyl group would be functionalized.⁴ From acetoxyated product **5.7**, further transformation of the acetoxy moiety to the corresponding vinyl group would furnish **5.4** containing the desired *anti* relative stereochemistry. With this plan in mind, our first goal was to synthesize *gem*-dimethyl compound **5.5**.

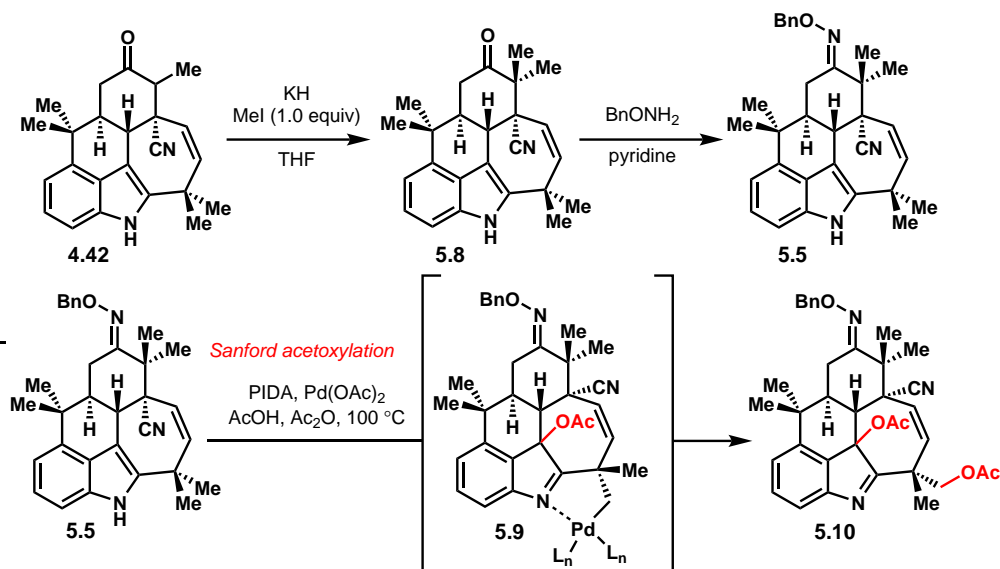


Scheme 5.2: The proposed plan for formation of acetoxyated compound **5.7** using C–H functionalization methodology developed by Sanford and coworkers in 2004.²

As illustrated in Scheme 5.3, thermodynamic deprotonation of **4.42** with potassium hydride followed by a quench with MeI installed the *gem*-dimethyl substituent at C12 of **5.8**. However, extreme care had to be taken with the number of equivalents of MeI used in this reaction. Quenching with more than 1.0 equivalent of MeI resulted in methylation of the indole nitrogen in addition to α -methylation. Nevertheless, with access to **5.8**, a straightforward condensation could be enacted using benzyloxyamine in pyridine to form oxime ether **5.5**. With **5.5** in hand, the stage was set to attempt the key C–H acetoxylation reaction.

However, submitting oxime ether **5.5** to the standard Sanford acetoxylation conditions resulted

in unexpected reactivity. Instead of the desired C–H functionalization, C3-acetoxylation of the indole occurred to produce compound **5.9**. The resulting imine could then direct a C–H acetoxylation event, presumably through palladacycle intermediate **5.9**, to the α -disposed methyl group on the bottom half of the molecule, ultimately generating bis-acetoxyated compound **5.10**. Unfortunately, the observed reactivity is not useful in the forward synthesis. However, a C–H functionalization of this type could be employed to make natural product derivatives of late-stage intermediates. While protection of the indole nitrogen could prevent this undesired reactivity, we wanted to avoid unnecessary protecting group manipulations and instead decided to focus on alternative C12 functionalization strategies.

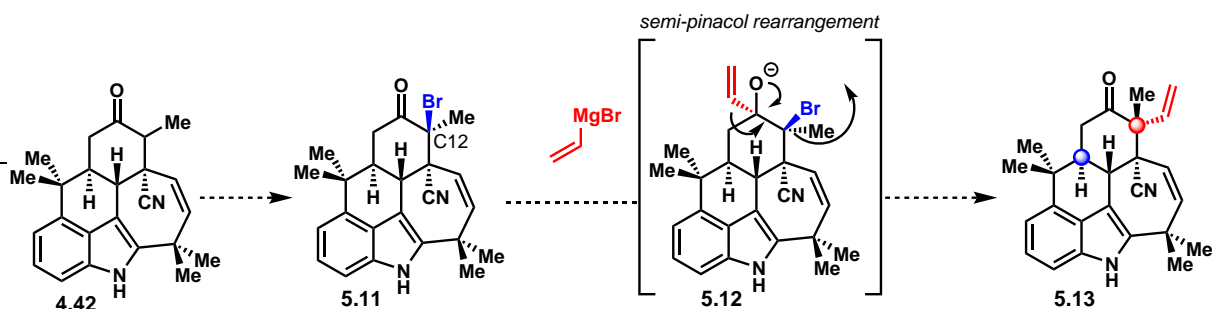


Scheme 5.3: Synthesis of benzyloxime ether **5.5** through methylation and subsequent oxime formation. Submission of compound **5.5** to the standard Sanford acetoxylation conditions produced the undesired compound **5.10**.

We also envisioned installing the C12 quaternary center using a semi-pinacol approach as illustrated in Scheme 5.4. Upon 1,2-addition of a vinyl nucleophile to the ketone group in **5.11**, a spontaneous semi-pinacol rearrangement (see **5.12**) could occur to form **5.13**. This approach relies on a stereoselective β -bromination of **4.42** to produce **5.11** bearing an α -disposed bromine atom at C12.

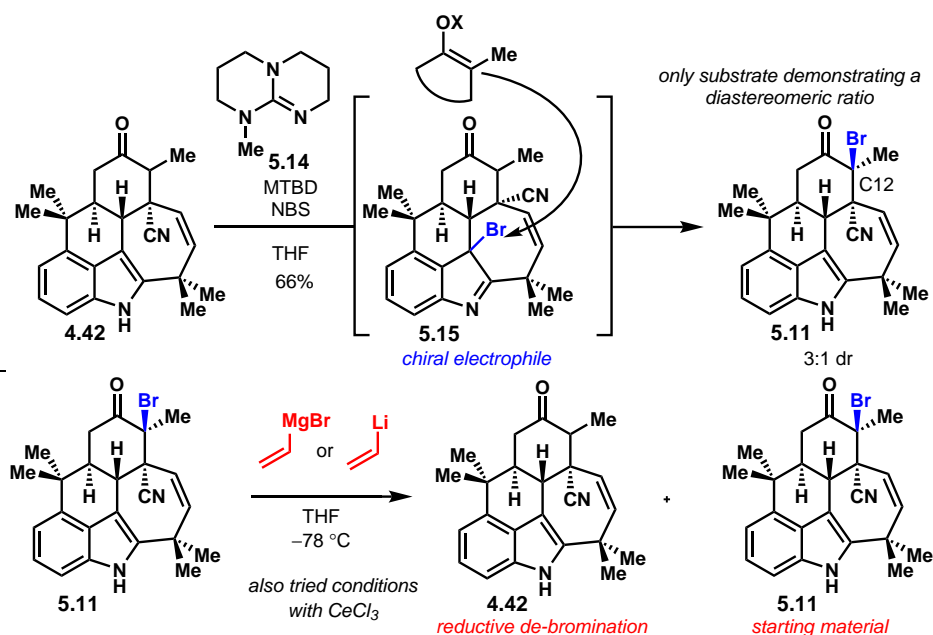
Indeed, α -bromo ketone (**5.11**) was successfully accessed using NBS and guanidine base MTBD (**5.14**) as shown in Scheme 5.5. Interestingly, **5.11** was generated as a mixture of diastereomers in a 3:1 ratio at C12. This is the only example of diastereoselective reactivity at C12 and therefore, a more complex reaction mechanism was proposed for the α -deprotonation/bromination event. Initially, the indole could undergo C3-bromination to generate compound **5.15**. This species (**5.15**) could then serve as a chiral, electrophilic bromine source leading to a scenario in which there are matched and mismatched bromination pathways. Ultimately, the more favorable bromination pathway occurs from the β -face generating the observed product (**5.11**) in a 3:1 diastereomeric ratio.

Despite this unselective α -bromination reaction, various vinyl nucleophilic sources were explored for the 1,2-addition into the ketone group of **5.11**. Unfortunately, 1,2-addition was never



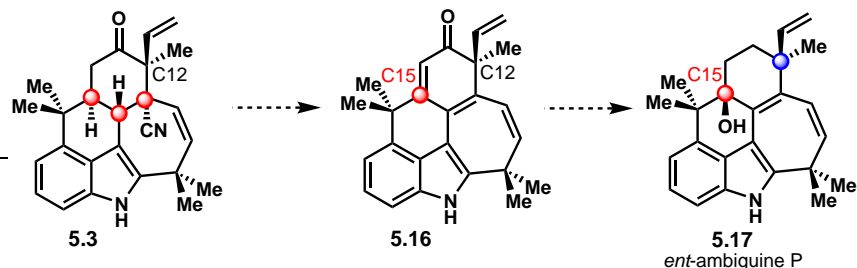
Scheme 5.4: A proposed synthesis of compound **5.13** using a semi-pinacol approach starting from α -bromo ketone **5.11**.

observed when utilizing both vinylmagnesium bromide and vinyllithium in combination with various additives such as CeCl_3 . Evidently, the major pathway was a reductive debromination event that regenerated the ketone starting material **4.42** from the previous step. Having observed no sign of a productive semi-pinacol rearrangement, other strategies were explored for installing the desired C12 quaternary center.



Scheme 5.5: A 3:1 diastereomeric ratio was observed in the α -bromination reaction of **4.42** generating **5.11**. Attempts at 1,2-addition of a vinyl nucleophile into the ketone group of **5.11** were unsuccessful leading only to the reductive debromination product **4.42**.

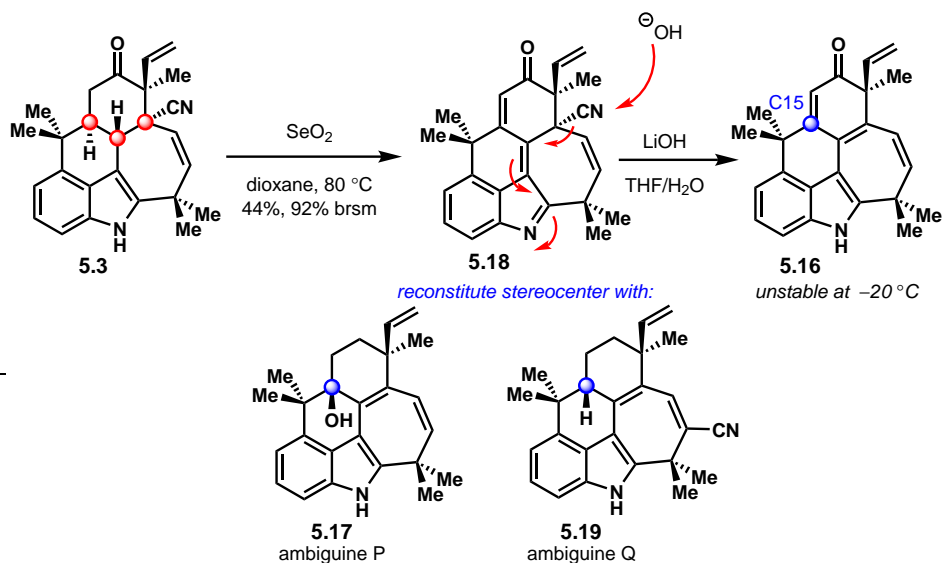
The next plan illustrated in (Scheme 5.6) took advantage of undesired diastereomer **5.3**, which already bears the C12 quaternary center, albeit with the undesired *syn* relative stereochemistry with respect to C15. Following ablation of all other stereocenters in the molecule besides C12, the C15 position of **5.16** could potentially be functionalized with a higher degree of stereocontrol. The enantiomer of ambiguine P (**5.17**) could be accessed following the stereoselective installation of the C15 hydroxyl group.



Scheme 5.6: Beginning with the undesired diastereomer (**5.3**), all stereocenters besides C12 could be ablated to produce **5.16**. *ent*-ambiguine P (**5.17**) may be accessed through a stereoselective functionalization of the C15 position of **5.16**.

With the help of visiting scholar, Laura Lang, along with Dr. Shota Sawano, we set out to synthesize intermediate **5.16**. Remarkably, a route was developed to access **5.16** through an oxidation of undesired diastereomer **5.3** using excess SeO_2 at elevated temperature to provide the highly conjugated $\alpha, \beta, \gamma, \delta$ -unsaturated ketone **5.18**. Although the yield for this oxidation was only 44%, starting material was recovered that could be resubjected to the reaction conditions to acquire enough of **5.18** for further study.

Eventually, we discovered that the cyano-group of **5.18** was readily eliminated in the presence of lithium hydroxide to give **5.16**. Although we were not anticipating this type of reactivity, loss of the cyano-group leads to the rearomatization of indole and forms a homoaromatic 7-membered ring, making the overall transformation thermodynamically favorable. With access to **5.16**, the next challenge was to functionalize at C15 in a stereospecific manner.

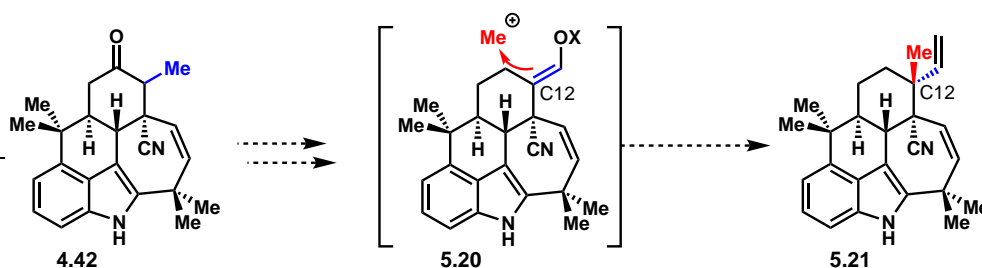


Scheme 5.7: Stereocenter ablation was successful at all other positions besides C12 through a SeO_2 oxidation followed by nitrile elimination with lithium hydroxide to give **5.16**. Attempts to functionalize the highly conjugated compound **5.16** were unsuccessful.

In order to access *ent*-ambiguine P (**5.17**), nucleophilic epoxidation conditions were explored. Alternatively, the conjugate reduction of **5.16** was also investigated to access *ent*-ambiguine Q

(**5.19**). Unfortunately, all attempts at functionalizing compound **5.16** resulted in an intractable mixture of compounds or decomposition. It was also found that storing compound **5.16** at -20°C in the freezer for prolonged periods of time resulted in the addition of water in an unselective manner. The highly conjugated intermediate **5.16** was too unstable for further functionalization and efforts were diverted to other options.

One such idea, was the conversion of the C12 methyl group into an enolate intermediate such as **5.20** (Scheme 5.8). This type of species could undergo methylation from the desired β -face of the molecule—analogue to the previous α -alkylation of **4.42** (Scheme 5.1). The aldehyde at C12 would be transformed into the desired vinyl group through an olefination reaction to generate **5.21** containing the desired *anti* relative stereochemistry. This approach is attractive as it takes advantage of the inherent diastereoselectivity of the α -alkylation at C12 to install the requisite vinyl group.



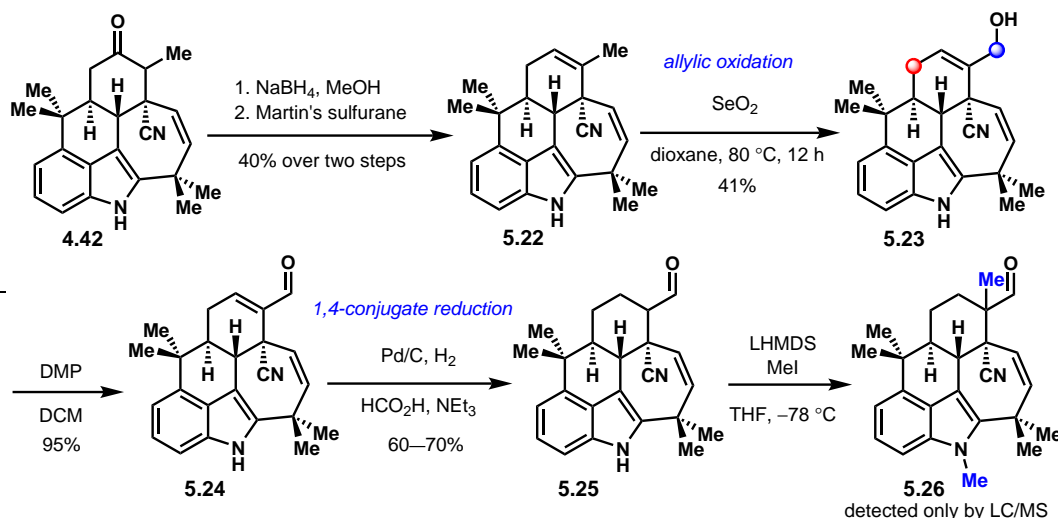
Scheme 5.8: The α -alkylation of enolate intermediate **5.20** takes advantage of the inherent stereoselectivity in this step producing compound **5.21** containing the desired *anti* relative stereochemistry.

Starting with **4.42** (Scheme 5.9), a hydride reduction of the ketone group was performed using NaBH_4 , followed by elimination using Martin's sulfurane to furnish **5.22**.⁵ We were pleased to find this elimination generated exclusively the trisubstituted alkene (**5.22**) as opposed to the disubstituted isomeric product which is also possible from this elimination. From alkene intermediate **5.22**, an allylic oxidation using SeO_2 was employed that preferentially oxidized at the least hindered primary position to produce **5.23**. However, over-oxidized side products were also observed, contributing to the low yield of 41% for this step.

Taking **5.23** forward, oxidation of the primary hydroxyl with DMP generated the α , β -unsaturated aldehyde **5.24** in excellent yield. We examined a variety of methodologies for conjugate reduction of **5.24** including L-selectride, Stryker's reduction,⁶ and Hantzsch ester reduction,⁷ but ultimately found productive conditions for this transformation reported by Heck and coworkers in 1978.⁸ Specifically, reduction of **5.24** with Pd/C and H_2 gas in the presence of formic acid and triethylamine, successfully produced aldehyde **5.25** in good yields.

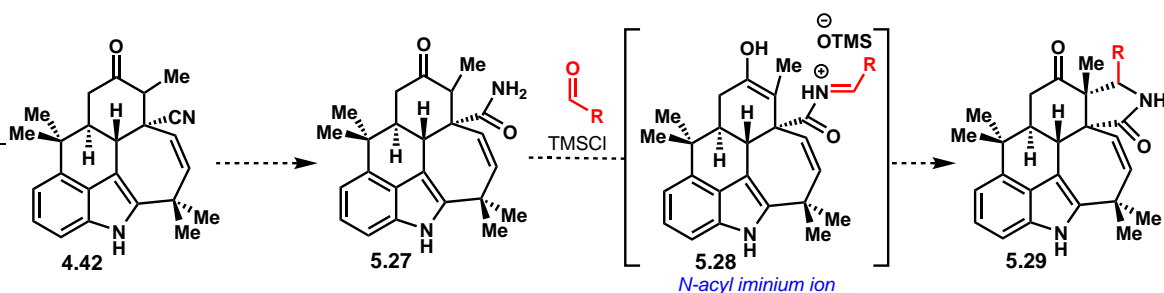
With access to substrate **5.25**, the methylation at C12 could be investigated. Unfortunately, due to limited amounts of material at this stage, we were only able to conduct a few preliminary attempts. Treatment of **5.25** with MeI and LHMDS at low temperature generated trace amounts of product that was detected only by LC/MS analysis. Mass spectrometry indicated that methylation had occurred at two positions in the molecule, likely at the C12 position, in addition to methylation of the indole nitrogen. Unfortunately, the structure of **5.26** could not be confirmed through more extensive analysis. Due to the low-yielding and cumbersome route required to access intermediate

aldehyde **5.25**, our efforts were devoted to more concise and reliable methods for C12 C–C bond construction.



Scheme 5.9: Aldehyde species **5.25** was successfully synthesized, however, low yields resulted in limited quantities of **5.25** and the structure of product **5.26** could not be confirmed.

The final method that was explored for installation of the C12 quaternary center, involved a directed C–C bond construction using amide intermediate **5.27** (Scheme 5.10). This idea was conceived with the help of a visiting student, Marco Hartmann, who proposed using *N*-acyl iminium ion chemistry to generate **5.28** as a precursor to cyclic lactam **5.29**.^{9,10} The proposed amide intermediate (**5.27**) could be accessed through nitrile hydration of **4.42**.

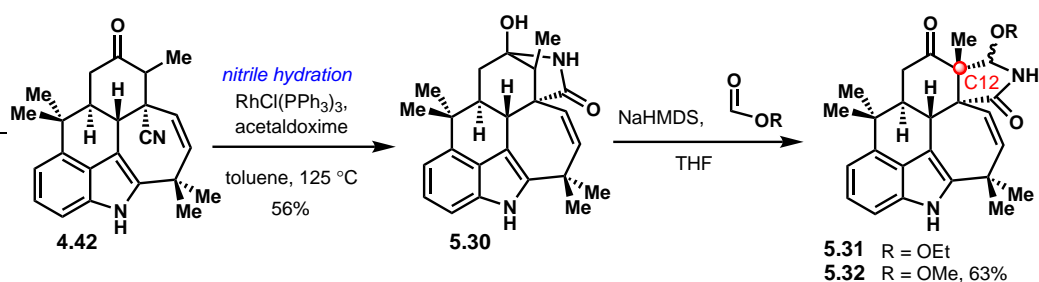


Scheme 5.10: An approach developed for the installation of the C12 quaternary center using α -disposed amide compound **5.27** to direct C–C bond construction. Crucial to this proposal is the use of *N*-acyl iminium ion chemistry to generate **5.29** through proposed precursor **5.28**.

Methodologies to hydrate the nitrile unit of **4.42** were explored. First, hydration was attempted employing the Ghaffar–Parkins platinum catalyst providing the desired product (**5.27**) in low yield and over prolonged reaction times.^{11,12} In pursuit of a higher-yielding and faster nitrile hydration, we adopted conditions developed by Chang and coworkers in 2009, in which they described a Rh(I)-catalyzed water-free nitrile hydration of aryl and aliphatic nitriles.¹³ Therefore, submitting nitrile **4.42** to the reported conditions using acetaldoxime as the hydration source, produced **5.30** in

56% yield. We were surprised to find that the resulting amide (**5.27**) cyclizes spontaneously onto the ketone group forming **5.30** (Scheme 5.11) as the final product.

With **5.30** in hand, we attempted to conduct an *N*-acyl iminium ion C–C bond construction under acidic conditions as proposed in Scheme 5.10 with intermediate **5.28**. However, it became clear that acidic conditions were not compatible with substrate **5.30** and all attempts at forming *N*-acyl iminium ion **5.28** resulted in decomposition of the starting material. Although acidic conditions were not productive, we predicted that **5.30** may be base-tolerant. As a result, the desired cyclization was attempted using NaHMDS in the presence of ethyl or methyl formate, which remarkably generated the desired cyclic hemiaminal products (**5.31** and **5.32**) as illustrated in Scheme 5.11. Each of these products (**5.31** and **5.32**) were formed as a mixture of diastereomers at the hemiaminal position. However, these mixtures were inconsequential as the hemi-aminal epimers would eventually be replaced by the requisite vinyl group present in the natural products.



Scheme 5.11: Rh(I)-catalyzed nitrile hydration of **4.42** generated hemiaminal species **5.30**. Subsequent C–C bond construction was successful under basic conditions in the presence of methyl and ethyl formate to generate the cyclic hemiaminal derivatives **5.31** and **5.32**.

In order to confirm that the newly constructed C12 C–C bond was in fact formed from the desired α -face, compound **5.31** was characterized unambiguously using X-ray crystallography as is shown in Figure 5.1. Compound **5.31** represents the first compound in which the C12 C–C bond has been forged from the desired α -face. However, moving forward in the synthesis, the next challenge would be to convert the cyclic hemiaminal functionality of **5.32** into the vinyl group. In pursuit of this challenge, **5.32** was taken forward as it was more easily manipulated than **5.31**.

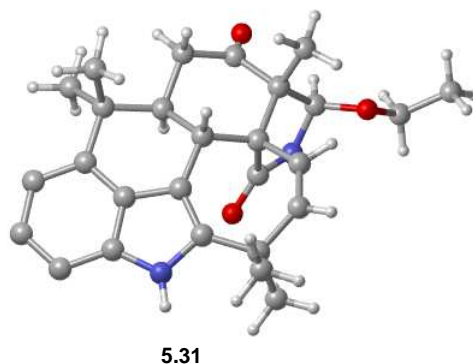
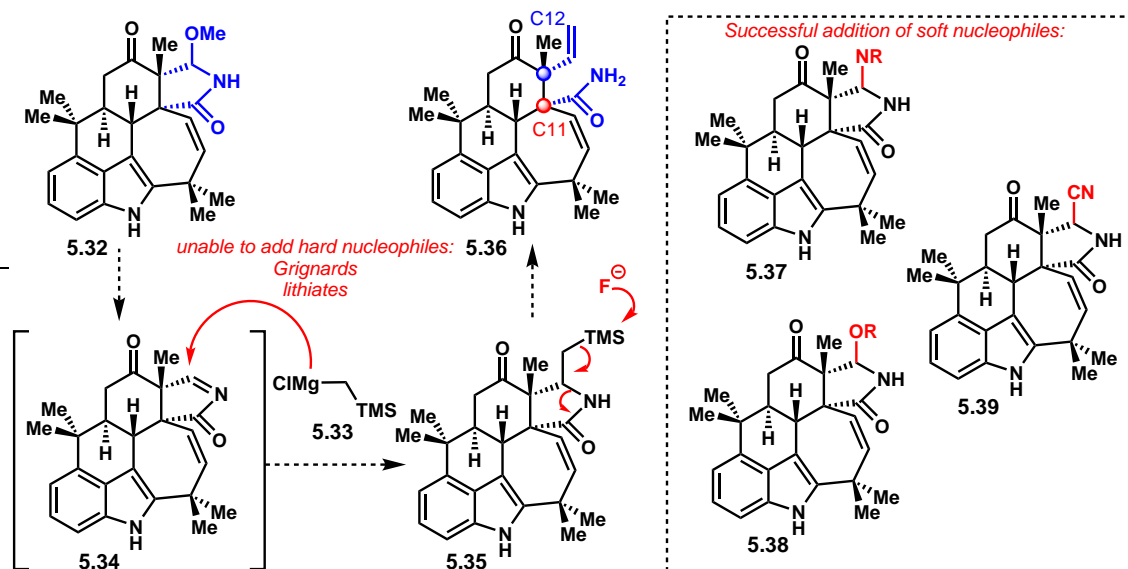


Figure 5.1: Crystal structure of the major diastereomer of compound **5.31**.

5.2 Late-Stage Manipulations to Install the Vinyl Group and the Isonitrile Functionality

Having installed the desired C–C bond at C12 through synthesis of the hexacyclic hemiaminal species **5.32**, we envisioned that nucleophilic functionalization of the hemiaminal position would install the vinyl group. As shown in Scheme 5.12, an ideal strategy involved the addition of Grignard reagent **5.33** to the *N*-acyl imine (**5.34**) generated from **5.32** to give lactam **5.35**. Upon treatment of **5.35** with a fluoride source, a ring opening event would take place to form **5.36**, revealing the desired C12 vinyl group in addition to forming the amide functionality at C11. Despite examining a variety of conditions, replacement of the hemiaminal methoxy group with a TMS-methyl equivalent proved unsuccessful. The addition of hard nucleophiles to *N*-acyl iminium ions is well-precedented in the literature, however, typically the nitrogen atom is protected prior to this substitution.^{9,10} Protection of the hemiaminal nitrogen in **5.32** was challenging and often resulted in decomposition of the starting material.

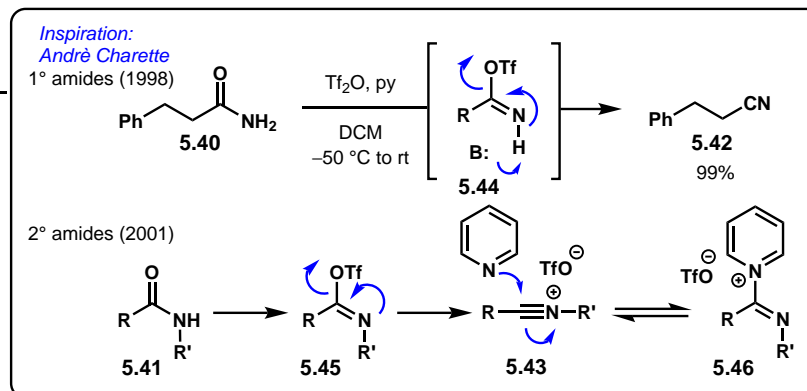
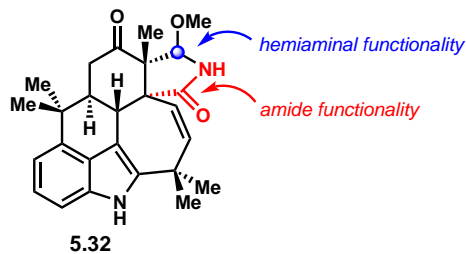
Substitution of hemiaminal **5.32** with softer nucleophiles such as amines (**5.37**), alcohols (**5.38**), and cyanide (**5.39**) was robust. Unfortunately, none of these compounds proved useful in the forward synthesis.



Scheme 5.12: The addition of hard nucleophiles such as **5.33** to the hemiaminal position of **5.34** was unsuccessful. Addition of softer nucleophiles such as amines, alcohols, and cyanide was productive.

As shown in Scheme 5.13, there are two functionalities that can be manipulated in **5.32**: the hemiaminal position (highlighted in blue) and the amide portion (highlighted in red). Having limited success with functionalization at the hemiaminal position, manipulation of the amide portion was investigated next. With this in mind, we were inspired by the work of Charette and coworkers who reported the dehydration of primary (**5.40**) and secondary amides (**5.41**) to the corresponding primary nitriles (**5.42**) and nitrilium ions (**5.43**), respectively using triflic anhydride and pyridine.

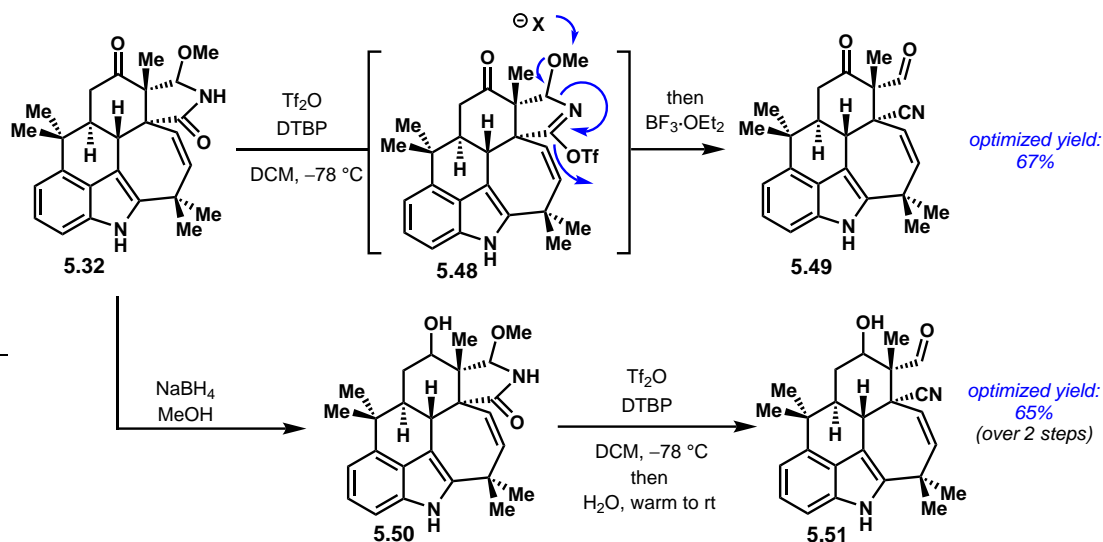
A similar methodology to that of Charette's was applied to the secondary amide functionality



Scheme 5.13: Charette’s work involving the dehydration of primary and secondary amides to generate the primary nitrile **5.42** and nitrilium ion **5.43** respectively. This work inspired derivatization of **5.32** in the synthesis toward pentacyclic ambigines.

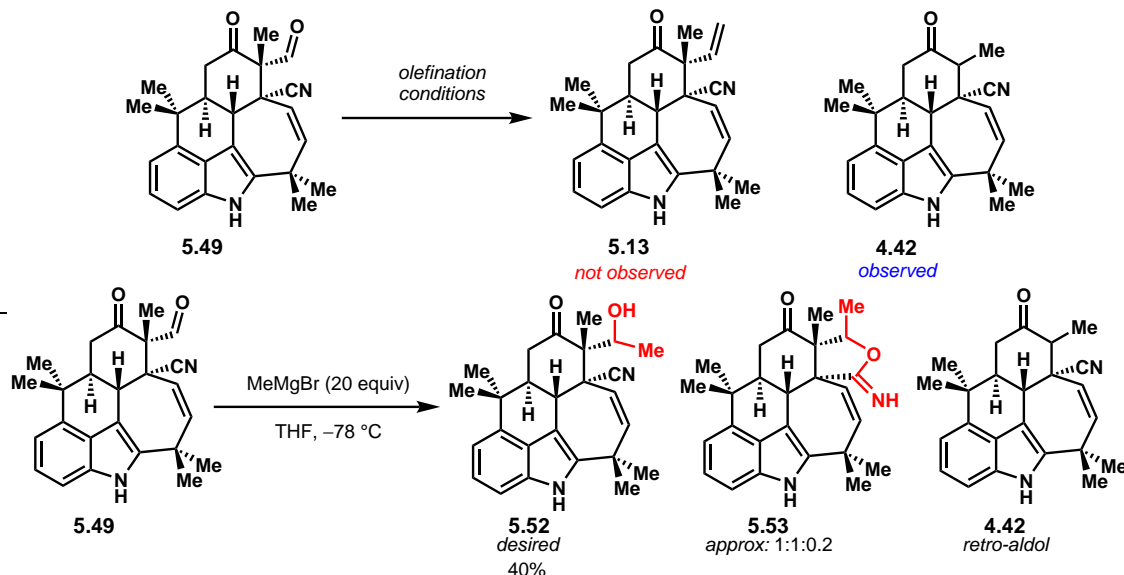
present in **5.32** as shown in Scheme 5.14. We envisioned that upon triflation of **5.47** to generate **5.48**, a dehydrative ring-opening could take place to access β -keto aldehyde product **5.49**. While initial attempts at this transformation worked poorly, it was found that cooling to $-78\text{ }^\circ\text{C}$ before the addition of triflic anhydride was crucial for the formation of **5.48**. The addition of $\text{BF}_3\cdot\text{OEt}_2$ at $-78\text{ }^\circ\text{C}$ was also necessary for the dehydrative ring-opening to take place, increasing the yield to 67% of the desired product **5.49**.

Additionally, this hemiaminal fragmentation reaction was optimized for alcohol substrate **5.50**. The analogous sequence proceeded equally well with **5.50**, providing a 65% yield of **5.51** over 2 steps. However, we found that this reaction (**5.50** to **5.51**) had to be quenched with water at $-78\text{ }^\circ\text{C}$, presumably forming triflic acid, which subsequently promoted the dehydrative ring-opening upon warming to room temperature forming **5.51**. Notably, despite its success in the reaction of **5.32**, the addition of $\text{BF}_3\cdot\text{OEt}_2$ led to decomposition of **5.50**. Having access to both advanced aldehydes **5.49** and **5.51**, we initially chose to proceed from β -keto aldehyde **5.49** in the forward sense.



Scheme 5.14: The dehydrative ring-opening of triflate intermediate **5.48** that generated β -ketoaldehyde **5.49** in an optimized 67% yield. This reaction worked equally well with alcohol derivative **5.50** to generate β -hydroxy aldehyde (**5.51**) in an optimized 65% yield over the two steps.

The next goal in the synthesis was to install the C12 vinyl group using the newly installed aldehyde in substrate **5.49**. It was quickly apparent that a simple olefination was going to be quite challenging, as the favored pathway under most olefination conditions was a retro-aldol reaction that formed nitrile ketone **4.42** (Scheme 5.15). Screening common olefination procedures such as the Wittig, Tebbe,¹⁴ Petasis,¹⁵ Peterson,¹⁶ and Julia-Kocienski¹⁷ olefinations led exclusively to retro-aldol product **4.42**. Even more exotic conditions such as the Takai-Lombardo,^{18,19} and the Lebel²⁰ olefinations all generated retro-aldol product **4.42** with no sign of olefinated product **5.13**. In fact, the only set of conditions that provided productive results was the addition of MeMgBr to aldehyde **5.49** at $-78\text{ }^\circ\text{C}$, providing secondary alcohol **5.52** in a low 40% yield. It is likely that low temperature reaction conditions prevented the retro-aldol product (**4.42**) from forming. Nevertheless, side product formation was still observed in this reaction with the isolation of **5.53** along with small amounts of **4.42**.



Scheme 5.15: All attempts at direct olefination of β -ketoaldehyde species **5.49** resulted in the retro-aldol product **4.42**. The only productive reaction resulted from the addition of MeMgBr to the aldehyde producing secondary alcohol **5.52** along with side products **5.53** and **4.42**.

Extensive optimization of the Grignard addition was required to improve the overall yield and to prevent formation of undesired side products. While the conversion of **5.49** to **5.52** could not be increased, despite using 20 equivalents of Grignard reagent, the formation of side products was prevented through manipulation of the Schlenk equilibrium. Addition of 40 equivalents of 1,4-dioxane resulted in a crude reaction mixture containing exclusively product (**5.52**) and starting material (**5.49**) (Scheme 5.16). It is well-known that treatment of Grignard reagents with 1,4-dioxane shifts the Schlenk equilibrium all the way to the right of the equation, precipitating out MgBr₂ and forming R₂Mg (Figure 5.2). With substrate **5.49**, Me₂Mg provided a clean reaction leading to a 35% yield of desired product **5.52** with no formation of side products.

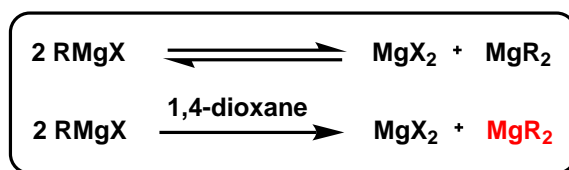


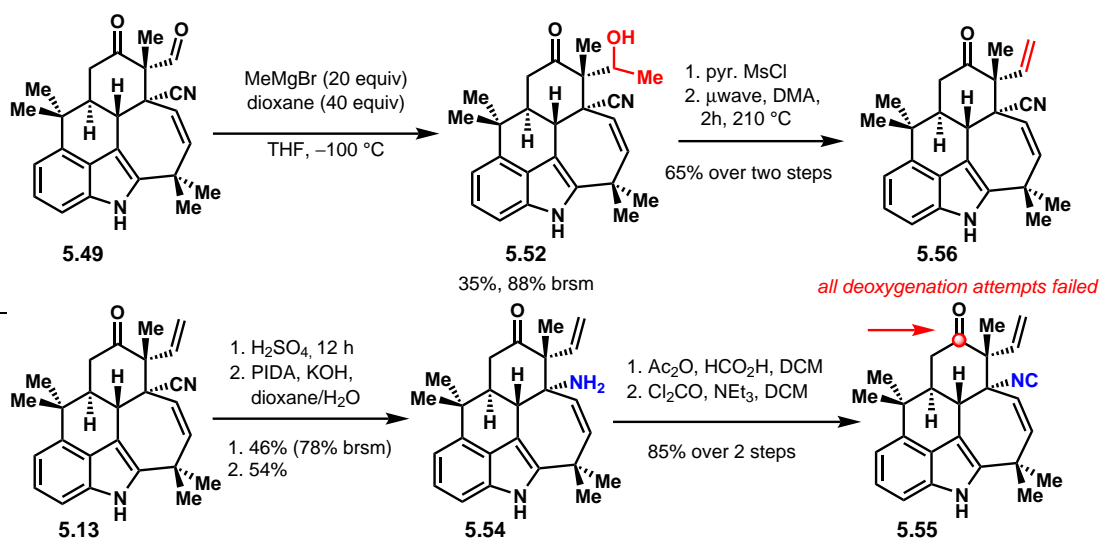
Figure 5.2: The Schlenk equilibrium of RMgX

Starting material (**5.49**) was recycled through this Grignard addition multiple times to generate enough desired product (**5.52**) for further functionalization. The C12 vinyl group was installed through a straightforward elimination sequence starting with the mesylation of alcohol **5.52** and subsequent mesylate elimination by microwave heating at 210 °C to afford compound **5.13**.

With installation of the C12 vinyl group successfully achieved, the focus of the synthesis was then placed on the transformation of the nitrile group of **5.13** into the isonitrile functionality present in the natural product through a Hofmann rearrangement protocol. Hydration of nitrile **5.13** with aqueous sulfuric acid generated the corresponding amide in 46% yield. Subsequent exposure to

aqueous potassium hydroxide and PIDA promoted the desired Hofmann rearrangement generating amine **5.54** in 54% yield.²¹ Finally, a straightforward formylation/dehydration sequence was employed to access isonitrile product **5.55** in 85% yield over two steps.

At this stage, the ketone group of **5.55** had to be transformed into the methylene group in order to access the natural product ambiguine L (**3.17**). Unfortunately, Wölff-Kishner and Barton-McCombie deoxygenation protocols resulted in the formation of undesired side products with no sign of the desired deoxygenated compound. Based on literature precedent by the Rawal group, it is likely that the C12 vinyl group engages ionic or radical intermediates formed in the deoxygenation pathways, generating an intractable mixture of side products.²² Due to limited quantities of material, none of these side products could be isolated and characterized. On the basis of these observations, we decided to implement this deoxygenation at an earlier stage in the synthesis.

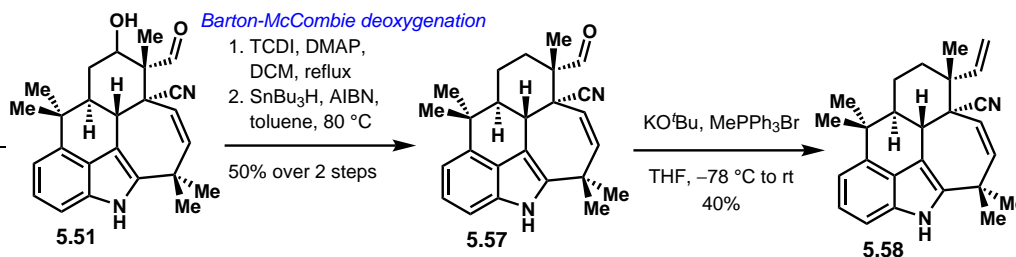


Scheme 5.16: The C12 vinyl group was successfully installed producing compound **5.13**. The isonitrile containing compound (**5.55**) was generated through a 4-step sequence involving a Hofmann rearrangement. All attempts to deoxygenate **5.55** failed at this stage.

5.3 Synthesis of Ambiguine P

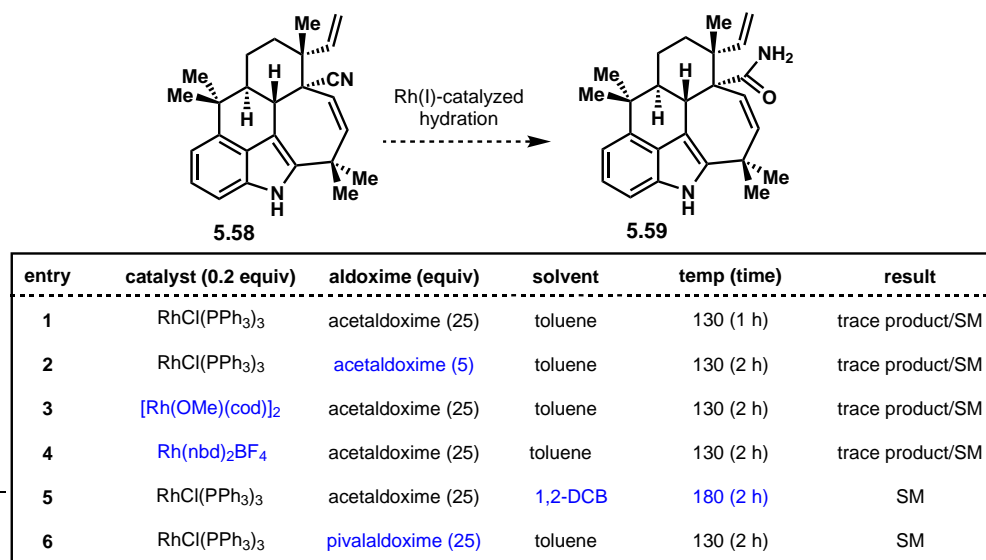
Hypothesizing that the C12 vinyl group was interfering in the deoxygenation of **5.55**, this reaction was explored using the β -hydroxy aldehyde compound **5.51**. Importantly, **5.51** does not contain the C12 vinyl group, and as such, previously observed side product formation and decomposition should no longer pose an issue. As shown in Scheme 5.17, using TCDI to form a thiocarbamate intermediate of **5.51** and subsequent treatment with tributyltin hydride and AIBN generated the reduced compound **5.57** in 50% yield over two steps. Intermediate **5.57** was no longer plagued by retro-aldol reactivity and therefore we envisioned a Wittig olefination would provide the desired C12 vinylated compound **5.58**. Although the desired olefinated product **5.58** was isolated, it was generated in a low 40% yield. It was unclear, at this time, where the other 60% of material went in the course of the reaction and therefore future optimization of this reaction

would be required. Nevertheless, **5.58** was carried forward through the synthesis using the same hydration/Hofmann sequence as with the previous substrate (**5.13**, Scheme 5.16).



Scheme 5.17: A Barton-McCombie deoxygenation was successful on alcohol **5.51** to produce **5.57**. A Wittig olefination proceeded in surprisingly low-yield to generate compound **5.58**.

However, the cyano group of compound **5.58** proved incredibly challenging to hydrate. Many varieties of acidic or basic hydration conditions were explored, but unfortunately no sign of the desired amide (**5.59**) was found in these attempts. The only set of conditions that produced trace amounts of **5.59** was the Chang group's Rh(I)-catalyzed nitrile hydration method that had been used earlier in the synthesis.¹³ An optimization of these conditions was attempted to improve the yield. In the original report, Chang presented some modifications with which to improve the conversion of more challenging hydration substrates. It was suggested that 5 equivalents of acetaldoxime was optimal in many of their reported cases. Therefore, as shown in entry 2 of Scheme 5.18, reducing the number of equivalents to 5 from the original 25 (entry 1) produced only trace product with no improvement in yield.



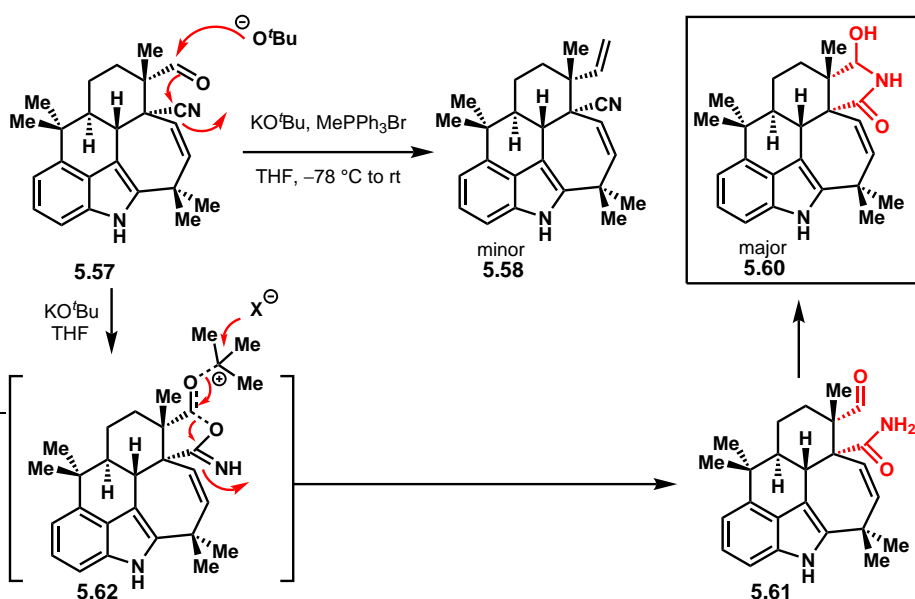
Scheme 5.18: Nitrile hydration of **5.58** was not observed under standard acidic or basic conditions. Attempts to improve the yield of the Rh(I)-catalyzed nitrile hydration were unsuccessful.

We also explored other Rh(I) catalysts including cationic [Rh(OMe)(cod)]₂ (entry 3) and Rh(nbd)₂BF₄ (entry 4). However, these catalysts also only provided trace product. Heating the reaction mixture

to a higher temperature of 180 °C did not improve conversion (entry 5). Finally, using pivalal-doxime, a more sterically hindered aldoxime, to prevent the competing hydration of *tert*-butyl nitrile, also led to no conversion (entry 6).

Having exhausted all foreseeable options for nitrile hydration of **5.58**, the focus was shifted to optimizing the low-yielding Wittig reaction as shown in Scheme 5.17. Indeed, with further exploration into the Wittig reaction, the major product of this olefination was identified not as our desired vinyl compound **5.58**, but rather hemiaminal product **5.60**. This compound (**5.60**) is extremely polar and was easily overlooked in the initial olefination attempts. Remarkably, in the overall transformation from **5.57** to **5.60**, the nitrile has been hydrated to the corresponding amide. While compound **5.61** is not useful for the forward synthesis, this transformation was quite intriguing to us given the previous challenges associated with the nitrile hydration of **5.60**.

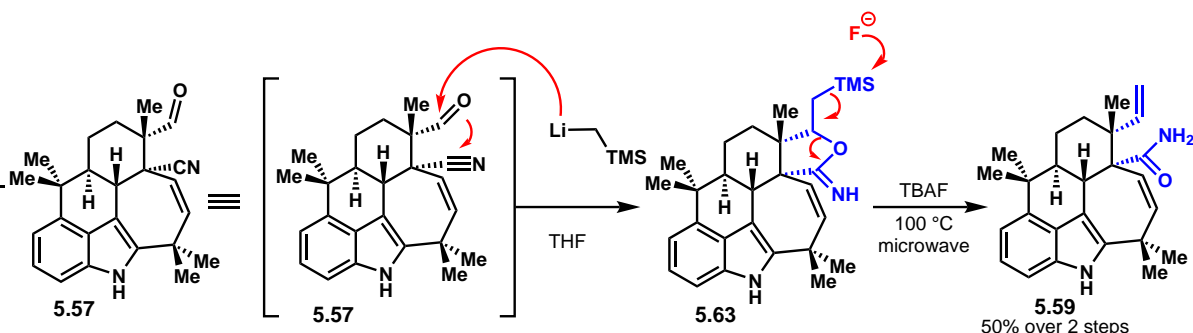
Mechanistically, the formation of **5.61** could begin with the addition of *tert*-butoxide into the aldehyde group of **5.57** (Scheme 5.19). The resulting alkoxide could then attack the pendant nitrile group thus forming intermediate **5.62**. Through a stepwise pathway, the *tert*-butyl cation could be attacked by a nucleophilic species to promote the subsequent ring-opening of **5.62** thus forming compound **5.61**. Immediate cyclization of the amide functionality onto the aldehyde group of **5.61** would form the observed hemiaminal product **5.60**.



Scheme 5.19: Discovery of an unexpected nitrile hydration side reaction in the Wittig olefination of **5.57**. The hemiaminal product **5.60** likely forms through initial attack by *tert*-butoxide into the aldehyde of **5.57** and subsequent alkoxide addition into the pendant nitrile.

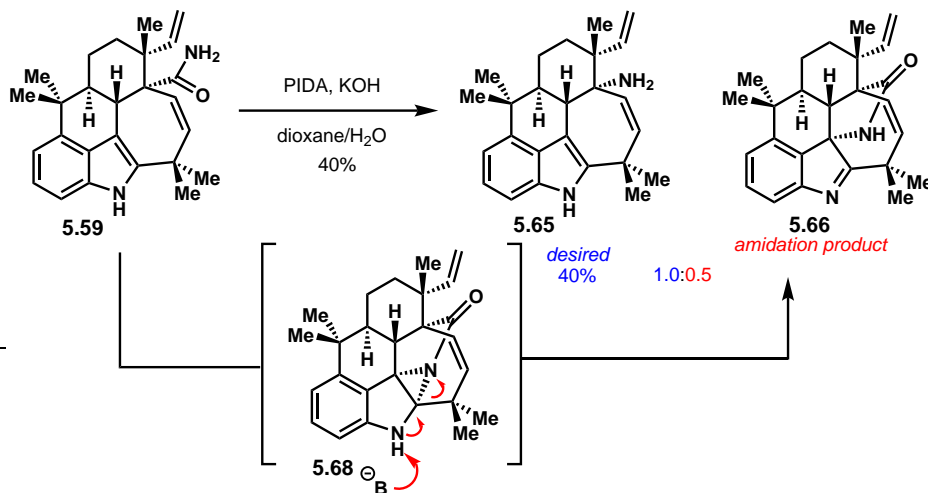
This overall transformation could be used to our advantage by employing the nucleophile TMSCH₂Li instead of *tert*-butoxide in an interrupted Peterson olefination strategy (Scheme 5.20). In this case, formation of acetimidate intermediate **5.63** was possible through the treatment of **5.57** with TMSCH₂Li in one step. Treating **5.63** with TBAF (1 M in THF) at 100 °C in the microwave provided desired amide compound **5.59** in 50% yield over 2 steps. This unanticipated process is remarkable as it achieved the successful nitrile hydration of **5.57** while also installing the requisite C12 vinyl group. To the best of our knowledge, this type of transformation has only been applied

to one other total synthesis by Ciufolini and coworkers in 2015.²³ Such a transformation could be applied more broadly as a methodology for installing amide functional groups with adjacent vinyl units, however, further studies in this realm have not been conducted.



Scheme 5.20: Treatment of aldehyde **5.57** with TMSCH_2Li leads to the formation of acetimidate intermediate **5.63**. Ring-opening using TBAF generates the desired amide containing molecule **5.59**.

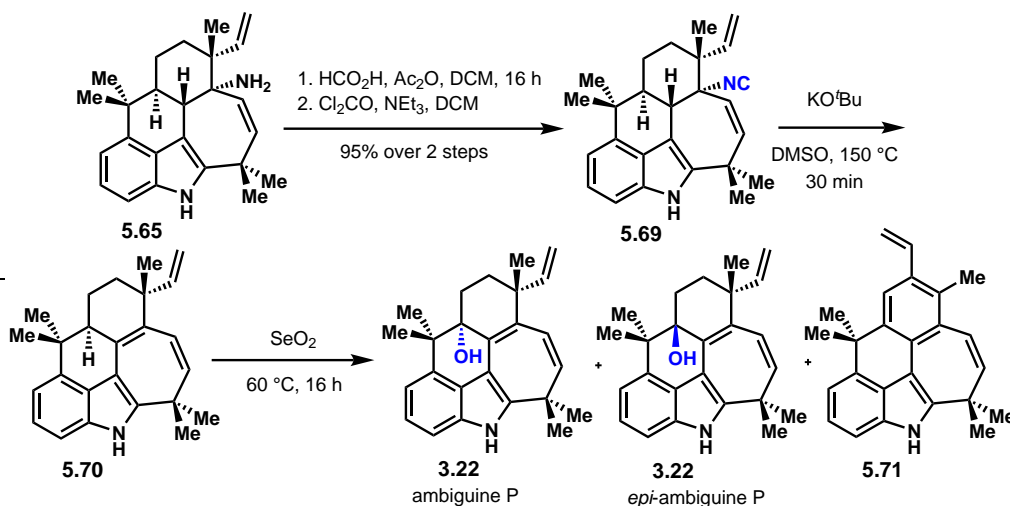
With access to compound **5.59** where the amide and C12 vinyl group are installed, the synthesis moved forward with the Hofmann rearrangement that had already been conducted on previous substrates. In this case, the same hypervalent iodine-mediated conditions were used and formation of amine product **5.65** was confirmed. However, **5.65** was produced in a low 40% yield (Scheme 5.21) along with side product **5.66**. Presumably, amidation product **5.67** was formed via competing aziridination of the indole C2–C3 bond followed by ring-opening of intermediate **5.68**. Despite optimization attempts by exploring other conditions such as I_2 , $\text{Pb}(\text{OAc})_4$, NBS, and PIFA, we were not successful in suppressing the undesired pathway leading to **5.66**. In fact, many of these conditions produced exclusively the undesired compound **5.66**.



Scheme 5.21: Treatment of amide **5.59** with hypervalent iodine formed the desired amine (**5.65**) along with the side product **5.66**.

Nevertheless, with amine **5.65** in hand, the analogous formylation/dehydration sequence was performed as with previous substrates to successfully install the isonitrile functionality in com-

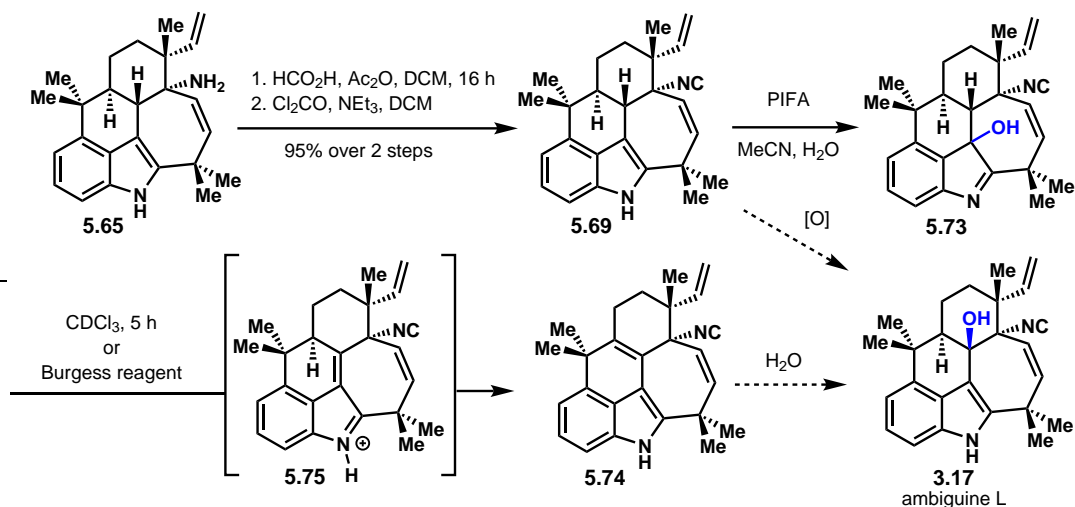
pound **5.69**. While the initial natural product target of this synthesis was ambiguline L (**3.17**), the ultimate goal is to synthesize many members within the pentacyclic ambiguline class of natural products. As such, ambiguline P (**3.22**) was another target within reach at this stage. Indeed, with the help of graduate student Hwisoo Ree, it was found that the isonitrile of **5.69** could be eliminated using KO^tBu to form the homoaromatic 7-membered ring of compound **5.70**. An allylic oxidation was then executed using SeO₂, forming the natural product ambiguline P (**3.22**) as a mixture with its diastereomer, *epi*-ambiguline P (**5.71**). It was also discovered that care must be taken when performing this oxidation step as formation of over-oxidized compound **5.72** (where vinyl group migration has also occurred) was observed when large amounts of SeO₂ were used at temperatures higher than 45 °C.



Scheme 5.22: Elimination of the isonitrile in **5.69** followed by allylic oxidation with SeO₂ generated the natural product ambiguline P (**3.22**) along with its diastereomer, *epi*-ambiguline P (**5.71**). Under forcing conditions, the over-oxidized side product **5.72** was observed.

While this synthesis of ambiguline P (**3.22**) represents the first total synthesis of a pentacyclic ambiguline natural product, completion of ambiguline L (**3.17**, Scheme 5.23) is also of importance. We envisioned accessing **3.17** through an oxidation at the pseudo-benzylic position of deoxy ambiguline L (**5.69**). Although a number of different benzylic oxidation conditions have been studied, such as MnO₂, SeO₂, radical-mediated oxidations, as well as metal-mediated C–H hydroxylations, the only reactivity that was observed was the oxidation of the isonitrile to the isocyanate or the C3 oxidation of indole to produce compound **5.73**. Protection of the indole nitrogen could be explored to prevent undesired C3 oxidation, however attempts to protect this position have been challenging, likely due to steric hindrance from the neighboring *gem*-dimethyl substituent.

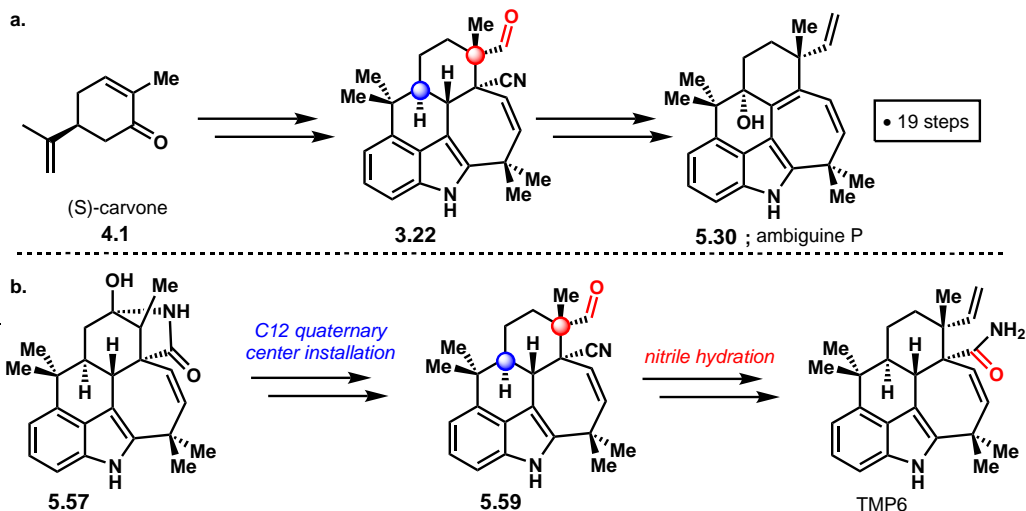
From the C3-hydroxylated compound (**5.73**), it was found that elimination of the hydroxyl group occurred upon standing in CDCl₃ for hours or by employing the Burgess reagent.²⁴ The isomerized compound (**5.74**) was isolated from these reactions, presumably arising through α,β -unsaturated imine intermediate **5.75**. Hydration of the newly formed double-bond in **5.74** was also explored using oxy-mercuration in addition to conditions developed by Mukaiyama²⁵ to access ambiguline L (**3.17**). However, controlling the chemo- and regioselectivity of this desired hydration have not been successful thus far and will likely pose a substantial challenge.



Scheme 5.23: Preliminary pseudo-benzylic oxidations have been studied to access the natural product ambigaine L (**3.17**) from **5.69**. We have also explored initial hydration conditions to access **3.17** from **5.74**.

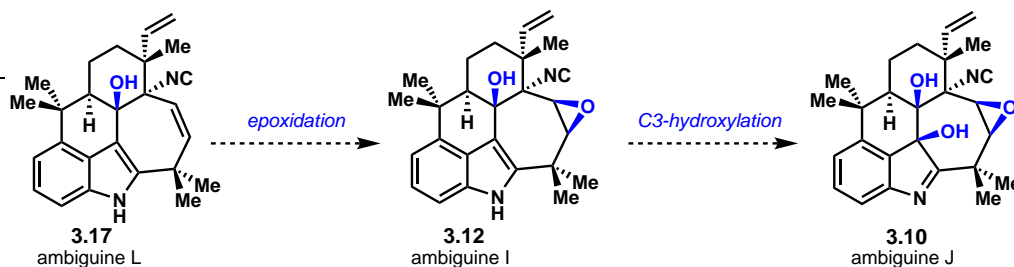
5.4 Conclusion and Outlook

To summarize the accomplishments of this project, as shown in Scheme 5.24, the first total synthesis of a pentacyclic ambigaine natural product, ambigaine P (**3.22**) has been completed in 19 steps from (*S*)-carvone **4.1**. Along this route, new methods were implemented to install the C12 quaternary center with the desired *anti* relative stereochemistry (**5.57**) starting from hemiaminal substrate **5.30**. An otherwise challenging nitrile hydration reaction has been developed using the pendant aldehyde as the oxygen source for the resulting amide compound **5.59**. We believe the development and implementation of these methodologies, which have led to the successful completion of the first total synthesis of ambigaine P (**3.22**), contributes in an impactful way not only to the chemistry of hapalindole alkaloids but also to the synthetic community as a whole.

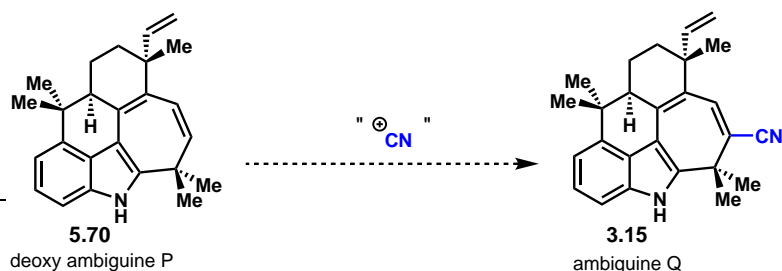


Scheme 5.24: The first total synthesis of a pentacyclic ambiguiene, ambiguiene P (**3.22**) has been developed. Novel methods were employed to install the C12 quaternary center with the *anti* relative stereochemistry in addition to successfully hydrate nitrile **5.57** to access the late-stage intermediate **5.59**.

Having established a robust and scalable route to deoxy ambiguiene L (**5.69**), we envisioned that accessing ambiguiene L (**3.17**) will also allow the synthesis of many other pentacyclic ambiguienes. As shown in Scheme 5.25, a directed epoxidation of ambiguiene L (**3.17**) should generate ambiguiene I (**3.12**). A C3-hydroxylation of ambiguiene I (**3.12**) should then produce the natural product ambiguiene J (**3.10**). We are also interested in developing electrophilic cyanation conditions to transform deoxy ambiguiene P (**5.70**) into the nitrile-containing natural product ambiguiene Q (**3.15**).



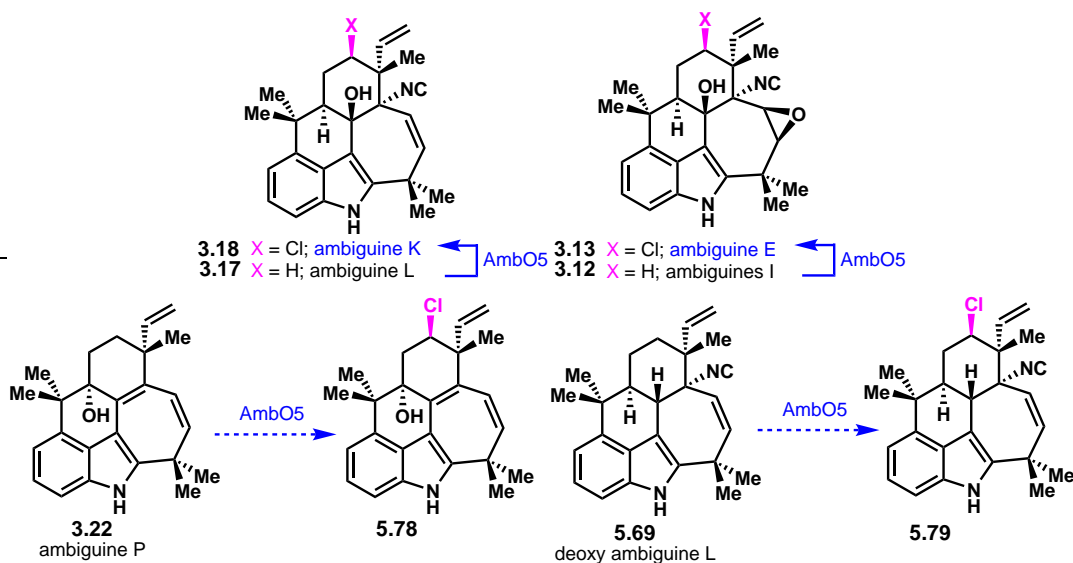
Scheme 5.25: Access to ambiguiene L (**3.17**) should allow the synthesis of other ambiguiene natural products such as ambiguiene I (**3.12**) and ambiguiene J (**3.10**). Ambiguiene Q (**3.15**) could be accessed through an electrophilic cyanation reaction of deoxy-ambiguiene P (**5.76**).



Scheme 5.26: Ambiguine Q (3.15) could be accessed through an electrophilic cyanation reaction of deoxy-ambiguine P (5.76).

While these synthetic studies are ongoing, a collaboration has been established with David Sherman's group at the University of Michigan, which has the expertise to carry out biosynthetic investigations using the late-stage intermediates as shown in Scheme 5.27. As mentioned in Chapter 3, the Liu group in 2016²⁶ has characterized and isolated the late-stage chlorinase AmbO5 and has subsequently carried out late-stage chlorinations on a limited array of pentacyclic ambiguines such as ambiguine L (5.77) and ambiguine I (3.12).

With the capabilities of the Sherman group, we wish to use these enzymes to further explore the promiscuity of these enzymes with unnatural substrates such as deoxy ambiguine L (5.69). Intriguingly, the chlorinated congener of ambiguine P, (5.78) has not yet been isolated from a natural source. The existence of 5.78 could be validated through subsection of 3.22 to the late-stage enzymatic chlorination of AmbO5. In addition, the Sherman group has access to large quantities of the UTEX 1903 strain of *F. ambiguus* and could potentially identify compounds 5.78 and 5.69 as natural products using our synthetic authentic standards.



Scheme 5.27: A collaboration with the Sherman group has begun in which we are using our late-stage intermediates such as ambiguine P (3.22) and deoxy-ambiguine L 3.17 to further examine the promiscuity of the late-stage chlorinase AmbO5.

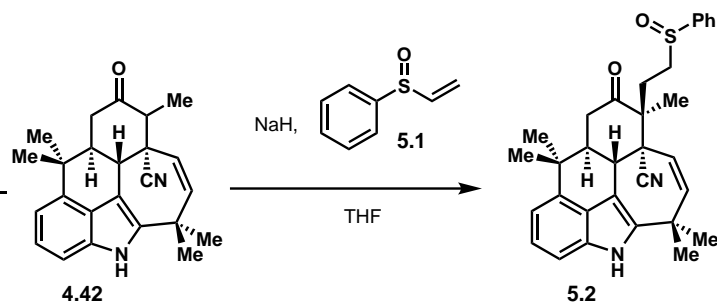
5.5 Experimental Contributors

The work presented in Section 5.1 (Installation of the C12 Quaternary Center) was conducted by Rebecca Johnson (R.J.), Marco Hartmann (M.H.), Laura Lang (L.L.), and Dr. Shota Sawano (S.S.). M.H. contributed to the idea generation for the C12 C–C bond construction via *N*-acyl iminium ion chemistry. L.L. and S.S. contributed to the synthesis of **5.16**. Prof. Richmond Sarpong (R.S.) contributed to the conception of ideas for the installation of the C12 quaternary center. The work discussed in Section 5.2 (Late-Stage Manipulations to Install the Vinyl Group and Isonitrile Functionality) was conducted by R.J. and Hwisoo Ree (H.R.). The work presented in Section 5.3 (Synthesis of Ambiguine P) was conducted by R.J. and H.R. Full characterization is provided for all productive intermediates in the synthesis of ambiguine P (**3.22**) and partial characterization is reported for a selection of other compounds. All data is reported in Section 5.6 (Experimental Methods and Procedures).

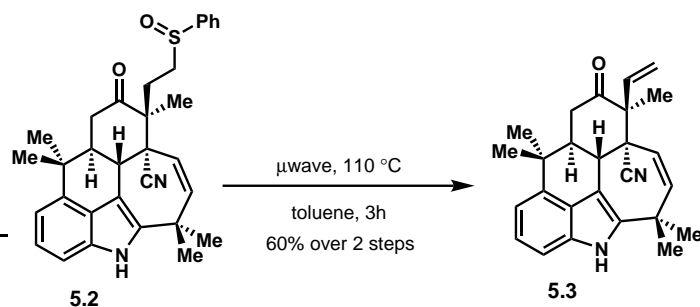
5.6 Materials and Methods

Unless stated otherwise, reactions were performed in oven-dried glassware sealed with rubber septa under a nitrogen atmosphere and were stirred with Teflon®-coated magnetic stir bars. Liquid reagents and solvents were transferred by syringe using standard Schlenk techniques. Tetrahydrofuran (THF), toluene, acetonitrile (MeCN), methanol (MeOH), NEt_3 were dried by passage over a column of activated alumina; Dichloromethane (DCM) was distilled over calcium hydride. All other solvents and reagents were used as received unless otherwise noted. Where stated, solutions were degassed using three cycles of freeze/pump/thaw (freezing the solution contained within a Schlenk flask in liquid nitrogen, opening the flask to vacuum for 5 min, then allowing the solution to thaw under vacuum). Thin layer chromatography was performed using SiliCycle silica gel 60 F-254 precoated plates (0.25 mm) and visualized by UV irradiation, anisaldehyde, cerium ammonium molybdenate (CAM), potassium permanganate, or iodine stain. Optical rotation was recorded on a Perkin Elmer Polarimeter 241 at the D line (1.0 dm path length), $c = \text{mg/mL}$, in CHCl_3 unless otherwise stated. ^1H and ^{13}C -NMR experiments were performed on Bruker spectrometers operating at 300, 400, 500 or 600 MHz for ^1H and 75, 100, 125, or 150 MHz for ^{13}C experiments. Chemical shifts (δ) are reported in ppm relative to the residual solvent signal (CDCl_3 $\delta = 7.26$ for ^1H NMR and $\delta = 77.16$ for ^{13}C NMR; Data are reported as follows: chemical shift (multiplicity, coupling constants where applicable, number of hydrogens). Abbreviations are as follows: s (singlet), d (doublet), t (triplet), q (quartet), dd (doublet of doublet), dt (doublet of triplet), ddq (doublet of doublets of quartets), m (multiplet), bs (broad singlet). IR spectra were recorded on a Bruker ALPHA Platinum ATR FT-IR spectrometer. Low and high-resolution mass spectral data were obtained from the University of California, Berkeley Mass Spectral Facility, on a VG 70-Se Micromass spectrometer for FAB, and a VG Prospec Micromass spectrometer for EI. Purifications were performed with a Yamazen® automatic purification system and gradients were determined by inputting R_f values and using a Yamazen® generated conditions.

5.7 Experimental Methods and Procedures

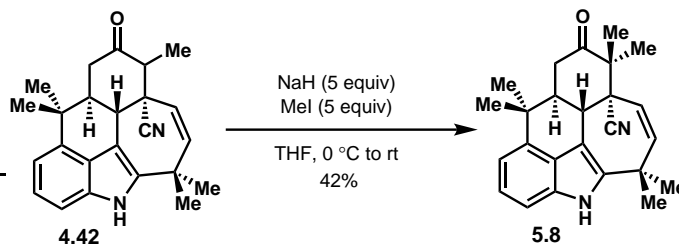


Sulfoxide (5.2): To a 100 mL round-bottomed flask was added **4.42** (270 mg, 0.75 mmol, 1.0 equiv), phenyl vinyl sulfoxide (**5.1**) (0.20 mL, 1.5 mmol, 2.0 equiv), and THF (20 mL) under a positive pressure of N₂. This solution was cooled to 0 °C in an ice bath, and then NaH (60% dispersion in mineral oil, 120 mg, 3.0 mmol, 5.0 equiv) was added all at once by quickly removing and refitting the rubber septum. The ice bath was removed, and the reaction mixture was allowed to stir for 1 h at room temperature. At this time, water (5 mL) was added carefully to the reaction mixture at 0 °C and the reaction mixture was allowed to warm to room temperature. Upon warming to room temperature, the aqueous layer was extracted with ethyl acetate (3 x 10 mL) and the combined organic layers were washed with water (10 mL) followed by brine (10 mL), dried over magnesium sulfate, and concentrated *in vacuo*. The crude reaction mixture was subjected to the next reaction without purification.

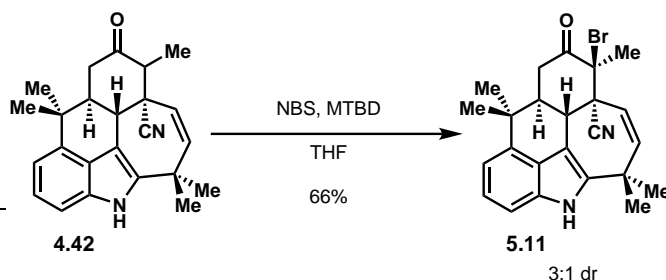


Syn-ketone (5.3): The resulting crude compound (**5.2**) was dissolved in toluene (20 mL), and transferred to a 10 – 20 mL microwave vial. This solution was heated to 140 °C, and stirred for 4 h at this temperature. The reaction mixture was cooled down to room temperature and concentrated *in vacuo*. The product was purified by SiO₂ gel column chromatography eluting with 1:1 DCM:toluene to give the orange solid, which was recrystallized from DCM and hexanes to afford the desired product **5.3** as a single diastereomer in 58% yield (168 mg, 58%). ¹H NMR (600 MHz, CDCl₃) δ 7.83 (br s, 1H), 7.17 - 7.13 (m, 2H), 7.03 - 6.99 (m, 1H), 6.30 (dd, *J* = 17.2, 10.7 Hz, 1H), 5.81 (d, *J* = 12.4, 1H), 5.62 (d, *J* = 12.4 Hz, 1H), 5.47 (d, *J* = 10.8 Hz, 1H), 5.35 (d, *J* = 17.2 Hz, 1H), 3.74 (d, *J* = 11.3 Hz, 1H), 2.75 (dd, *J* = 13.7, 13.7 Hz, 1H), 2.69 (dd, *J* = 13.6, 4.0 Hz, 1H), 2.35 (ddd, *J* = 14.3, 11.3, 4.0 Hz, 1H), 1.64 (s, 3H), 1.58 (s, 3H), 1.52 (s, 3H), 1.45 (s, 3H), 1.19 (s, 3H). ¹³C NMR (150 MHz, CDCl₃) δ 206.9, 143.7, 139.3, 136.2, 136.0, 133.5, 126.0, 124.2, 122.9, 120.6, 119.7, 113.1, 108.0, 106.3, 57.9, 51.8, 48.1, 39.9, 38.6, 38.4, 37.9, 33.1, 28.1, 24.6, 24.3, 18.5. IR (ATR) 3355, 2966, 2237, 1713, 1469, 1328, 928, 773 cm⁻¹. HRMS (ESI):

Exact mass calc'd for $C_{26}H_{28}ON_2K [M+K]^+$, 423.1833. Found 423.1840. $[\alpha]_D -63.8$ (c 5.0×10^{-3} , $CHCl_3$)

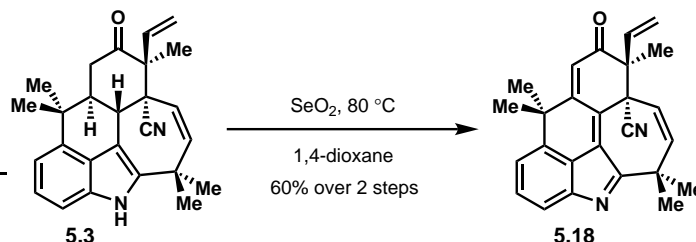


Gem-dimethyl ketone (5.8): To a 25 mL round-bottomed flask were added **4.42** (54 mg, 0.15 mmol, 1.0 equiv), MeI (47 μ L, 0.75 mmol, 5.0 equiv), and THF (0.025 M, 6 mL) under a positive pressure of N_2 . The reaction mixture was cooled down to 0 $^\circ$ C in an ice bath and then NaH (60% dispersion in mineral oil, 30 mg, 0.75 mmol, 5.0 equiv) was added all at once by quickly removing and refitting the rubber septum. The solution was warmed to room temperature and allowed to stir for 11 h at this temperature. At this time, water (5 mL) was added carefully to quench the reaction. The aqueous layer was then extracted with ethyl acetate (3 x 5 mL) and the combined organic layers were washed with water (10 mL) followed by brine (10 mL), and dried over magnesium sulfate. The solution was concentrated *in vacuo*, and then purified by SiO_2 gel column chromatography eluting with 7:1 hexanes:ethyl acetate to give the desired compound **5.8** in 42% yield (23.2 mg, 0.062 mmol). 1H NMR (600 MHz, $CDCl_3$) δ 7.83 (br s, 1H), 7.17 - 7.11 (m, 2H), 7.04 - 6.98 (m, 1H), 5.83 (d, $J = 12.5$ Hz, 1H), 5.68 (d, $J = 11.4$ Hz, 1H), 3.68 (d, $J = 9.5$ Hz, 1H), 2.76 (dd, $J = 13.9, 13.9$ Hz, 1H), 2.67 (dd, $J = 13.7, 4.1$ Hz, 1H), 2.33 (ddd, $J = 14.0, 11.3, 4.1$ Hz, 1H), 1.64 (s, 3H), 1.52 (s, 3H), 1.45 (s, 3H), 1.42 (s, 3H), 1.38 (s, 3H), 1.20 (s, 3H). ^{13}C NMR (150 MHz, $CDCl_3$) 210.7, 143.9, 139.3, 135.9, 133.5, 126.0, 123.3, 122.8, 120.0, 113.1, 107.9, 106.3, 51.2, 51.0, 47.8, 39.0, 38.3, 37.9, 37.4, 33.1, 28.2, 24.5, 24.3, 21.8, 20.4. IR (ATR) 3380, 2964, 2925, 2365, 1702, 1449, 1331, 905, 772, 722 cm^{-1} . 1H NMR (600 MHz, $CDCl_3$) δ 7.83 (br s, 1H), 7.17 - 7.11 (m, 2H), 7.04 - 6.98 (m, 1H), 5.83 (d, $J = 12.5$ Hz, 1H), 5.68 (d, $J = 11.4$ Hz, 1H), 3.68 (d, $J = 9.5$ Hz, 1H), 2.76 (dd, $J = 13.9, 13.9$ Hz, 1H), 2.67 (dd, $J = 13.7, 4.1$ Hz, 1H), 2.33 (ddd, $J = 14.0, 11.3, 4.1$ Hz, 1H), 1.64 (s, 3H), 1.52 (s, 3H), 1.45 (s, 3H), 1.42 (s, 3H), 1.38 (s, 3H), 1.20 (s, 3H). ^{13}C NMR (150 MHz, $CDCl_3$) 210.7, 143.9, 139.3, 135.9, 133.5, 126.0, 123.3, 122.8, 120.0, 113.1, 107.9, 106.3, 51.2, 51.0, 47.8, 39.0, 38.3, 37.9, 37.4, 33.1, 28.2, 24.5, 24.3, 21.8, 20.4. IR (ATR) 3380, 2964, 2925, 2365, 1702, 1449, 1331, 905, 772, 722 cm^{-1} . **HRMS** (EI): Exact mass calc'd for $C_{25}H_{28}N_2O [M]^+$, 372.2202. Found 372.2206. $[\alpha]_D -54.8$ (c 10.4×10^{-3} , $CHCl_3$)

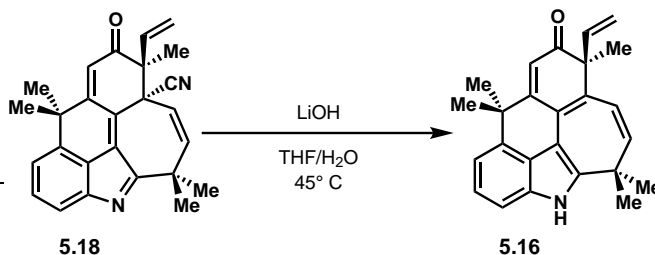


α -Bromoketone (5.11): The ketone starting material (**4.42**) (0.03 mmol, 10 mg, 1 equiv) was dissolved in THF (0.1 M, 0.3 mL) in a round-bottomed flask. NBS (0.06 mmol, 10 mg, 2 equiv) was added to the solution followed by MTBD (0.08 mmol, 10 μ L, 3 equiv) and the reaction mixture was allowed to stir at room temperature for 30 min. The reaction mixture was quenched with sodium bicarbonate (sat. aq.) and the aqueous layer was extracted with ethyl acetate (3 x 10 mL). The combined organic layers were washed with brine (30 mL) and dried over sodium sulfate. The crude mixture was concentrated *in vacuo* and purified via SiO_2 gel column chromatography on a

Yamazen® automatic purification system. The bromoketone (**5.11**) was isolated as a white solid and as a mixture of diastereomers in a 3:1 ratio (8 mg, 66%). ¹H NMR (600 MHz, CDCl₃) δ 7.83 (s, 1H), 7.16 (d, *J* = 4.0 Hz, 2H), 7.01 (t, *J* = 4.0 Hz, 1H), 5.97 - 5.85 (m, 2H), 3.88 (dd, *J* = 20.6, 11.3 Hz, 1H), 3.59 - 3.44 (m, 1H), 2.77 (td, *J* = 13.0, 11.9, 3.9 Hz, 1H), 2.36 - 2.20 (m, 1H), 2.09 (s, 3H), 1.64 (s, 3H), 1.54 (s, 3H), 1.44 (s, 3H), 1.21 (s, 3H).

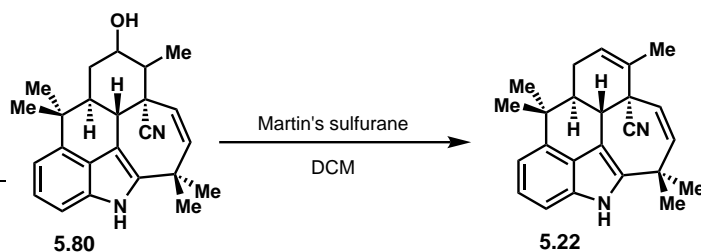


Conjugated enone (5.18): To a 25 mL schlenk flask was added **5.3** (120 mg, 0.30 mmol, 1.0 equiv), SeO₂ (68 mg, 0.61 mmol, 2.0 equiv), and 1,4-dioxane (0.1 M, 3 mL). The resulting solution was stirred at 80 °C for 24 h. After cooling to room temperature, the reaction mixture was concentrated *in vacuo*, and purified by SiO₂ gel column chromatography (DCM only) to provide the desired compound **5.18** in 41% yield (47 mg, 0.12 mmol) with the recovery of the starting material **5.3** in 35% yield (41 mg, 0.11 mmol). If this recovered material (**5.3**) was resubjected to the identical reaction conditions, **5.18** was obtained in 34% yield (14 mg, 0.036 mmol) with the recovery of the starting material **5.3** in 37% yield (15 mg, 0.039 mmol). The combined total yield of product **5.18** was 53% and **5.18** was isolated as an off-white solid. ¹H NMR (500 MHz, CDCl₃) δ 7.41 - 7.36 (m, 2H), 7.21 - 7.16 (m, 1H), 6.56 (s, 1H), 6.02 (d, *J* = 13.0 Hz, 1H), 5.72 (dd, *J* = 17.1, 10.7 Hz, 1H), 5.60 (d, *J* = 12.9 Hz, 1H), 5.21 (d, *J* = 10.5 Hz, 1H), 5.20 (d, *J* = 16.8 Hz, 1H), 1.69 (s, 6H), 1.62 (s, 6H), 1.54 (s, 3H). ¹³C NMR (125 MHz, CDCl₃) δ 194.8, 173.8, 162.7, 151.0, 143.0, 139.9, 137.0, 134.5, 132.0, 131.7, 128.1, 125.1, 121.3, 120.6, 120.1, 118.6, 118.0, 58.0, 49.8, 41.9, 41.3, 32.0, 31.4, 29.5, 28.9, 16.6. IR (ATIR) 2963, 2922, 2365, 1670, 1503, 1364, 1269, 1233, 1116, 945, 805, 781 cm⁻¹. HRMS (ESI): Exact mass calc'd for C₂₆H₂₅ON₂ [M+H]⁺, 381.1961. Found 381.1956. [α]_D +137.7 (c 5.3 x 10⁻³, CHCl₃)

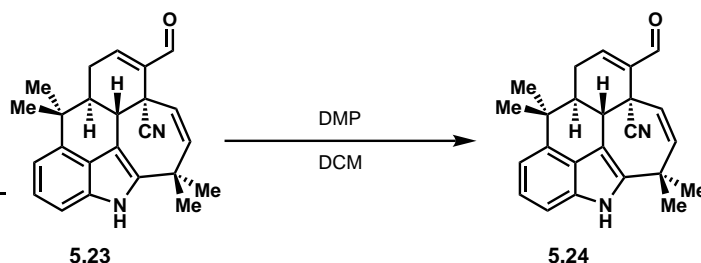


Conjugated pentacycle (5.16): To a 4 mL vial was added **5.18** (5.7 mg, 0.015 mmol, 1.0 equiv), LiOH (3.6 mg, 1.5 mmol, 10 equiv), THF (0.30 mL), and distilled H₂O (37.5 μL). The resulting solution was stirred at 50 °C for 22 h. After cooling to room temperature, it was extracted with ethyl acetate (3 x 5 mL), washed with water (5 mL) and brine (5 mL), and dried over magnesium sulfate. The resulting solution was concentrated *in vacuo* to give crude **5.16** which was used in the subsequent reaction without purification because **5.16** is not stable enough to isolate by SiO₂ gel column chromatography. ¹H NMR (400 MHz, CDCl₃) δ 8.04 (s, 1H), 7.26 - 7.19 (m, 2H),

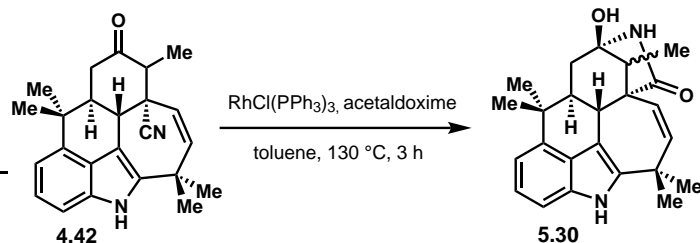
7.13 (dd, $J = 6.7, 1.4$ Hz, 1H), 6.42 (s, 1H), 6.12 (d, $J = 11.7$ Hz, 1H), 5.80 (dd, $J = 17.2, 10.3$ Hz, 1H), 5.51 (d, $J = 11.7$ Hz, 1H), 5.26 - 5.13 (m, 2H), 2.15 - 1.97 (m, 1H), 1.69 (s, 3H), 1.64 (s, 3H), 1.55 (s, 3H), 1.54 (s, 3H), 1.20 (s, 3H).



Trisubstituted alkene (5.22): A flame-dried 4 mL vial was brought into the glovebox and charged with Martin's sulfurane (0.070 mmol, 47 mg, 5.0 equiv). The vial was sealed and brought out of the glovebox and a septum was fitted over the opening of the vial. The alcohol (**5.80**) (0.014 mmol, 5.0 mg, 1.0 equiv) was added to the vial as a solution in DCM (0.1 M, 0.1 mL). The reaction mixture was allowed to stir for 20 min at room temperature at which time the crude mixture was concentrated *in vacuo*. The crude product (**5.22**) was purified using SiO₂ gel preparatory thin-layer chromatography eluting with a mixture of 2:1 hexanes:ethyl acetate. The major UV-active band was scraped off, crushed, and filtered using ethyl acetate to yield the desired product (**5.22**). ¹H NMR (500 MHz, CDCl₃) δ 7.80 (s, 1H), 7.17 - 7.08 (m, 2H), 6.99 (dd, $J = 5.8, 2.2$ Hz, 1H), 5.85 (d, $J = 12.0$ Hz, 1H), 5.82 (dt, $J = 5.9, 1.8$ Hz, 1H), 5.71 (d, $J = 12.0$ Hz, 1H), 3.20 (d, $J = 11.3$ Hz, 1H), 2.36 (dddd, $J = 17.6, 6.2, 4.8, 1.7$ Hz, 1H), 2.23 - 2.12 (m, 1H), 2.09 - 2.00 (m, 1H), 1.97 (dt, $J = 2.7, 1.4$ Hz, 3H), 1.70 (s, 3H), 1.51 (s, 3H), 1.46 (s, 3H), 1.09 (s, 3H).



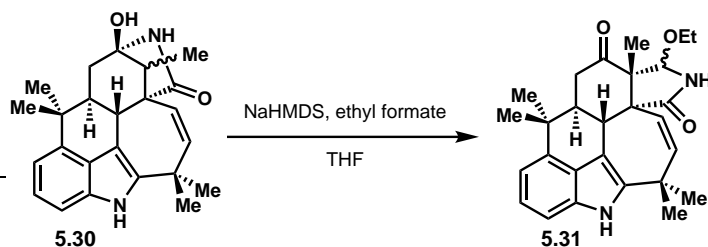
α,β -Unsaturated aldehyde (5.24): To a solution of **5.23** (0.003 mmol, 1 mg, 1 equiv) in DCM (0.1 M, 0.1 mL) was added DMP (0.004 mmol, 2 mg, 2 equiv). The mixture was allowed to stir for 1 h at which time it was quenched with sodium bicarbonate (sat. aq.) (1 mL) followed by sodium thiosulfate (sat. aq.) (1 mL). The resulting reaction mixture was allowed to stir vigorously for 5 min. The layers were separated and the aqueous layer was extracted with ethyl acetate (3 x 10 mL). The combined organic layers were washed with brine (30 mL), dried over sodium sulfate and concentrated *in vacuo* to yield the crude product (**5.24**). The crude product was purified via SiO₂ column chromatography eluting with 2:1 hexanes:ethyl acetate to yield pure **5.24**. ¹H NMR (500 MHz, C₆D₆) δ 9.12 (s, 1H), 7.32 (t, $J = 7.7$ Hz, 1H), 7.09 (d, $J = 7.3$ Hz, 1H), 7.05 (d, $J = 8.1$ Hz, 1H), 7.01 (s, 1H), 6.01 (dd, $J = 5.7, 2.2$ Hz, 1H), 5.83 (d, $J = 12.0$ Hz, 1H), 5.39 (d, $J = 12.0$ Hz, 1H), 2.94 (d, $J = 11.3$ Hz, 1H), 2.00 (td, $J = 11.5, 4.7$ Hz, 1H), 1.81 (dt, $J = 19.9, 5.2$ Hz, 1H), 1.68 - 1.59 (m, 1H), 1.54 (s, 3H), 1.21 (s, 3H), 1.07 (s, 3H), 0.87 (s, 3H).



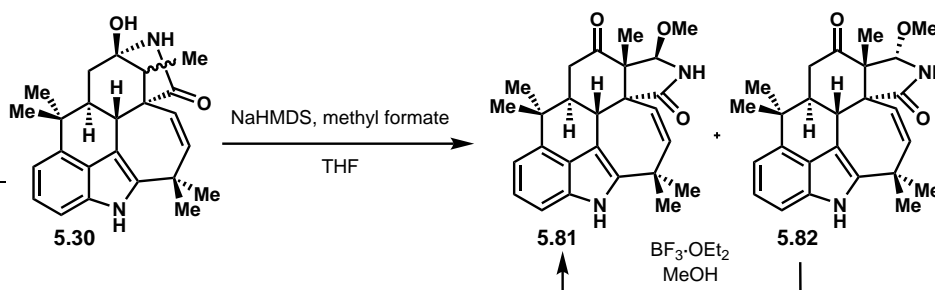
Amide amination (5.30): Ketone **4.42** (2.5 mmol, 890 mg, 1.0 equiv) was added to a 25-mL round bottomed flask. Toluene (1.2 mL, 0.5 M) was added followed by acetaldoxime (freeze-pump-thawed, 3.8 mL, 23 mmol, 25 equiv) via syringe. Wilkinson's catalyst, $\text{RhCl}(\text{PPh}_3)_3$ (0.25 mmol, 230 mg, 0.10 equiv), was added to the mixture and a reflux condenser flushed with N_2 , was placed on the flask and sealed with a septum with a N_2 inlet. The reaction mixture was placed in a 130 °C oil bath and refluxed for 2.5 h at this temperature. After 2.5 h, the reaction flask was taken out of the oil bath and allowed to cool down to room temperature. The mixture was quenched with water (10 mL) and diluted with ethyl acetate (20 mL). The aqueous layer was extracted with ethyl acetate (3 x 20 mL) and the combined organic layers were washed with brine (20 mL) and dried over sodium sulfate. The crude mixture was concentrated *in vacuo* and purified via SiO_2 gel column chromatography on a Yamazen® automatic purification system using a gradient of 50% hexanes/ethyl acetate to 5% hexanes/ethyl acetate. The product was isolated as a slightly orange foam or glassy solid (530 mg, 56%). *Both diastereomers are typically collected at once along with triphenylphosphine oxide that is difficult to remove but does not affect the efficiency of the subsequent steps.*

Diastereomer of lower polarity: $^1\text{H NMR}$ (400 MHz, CD_3OD) δ 7.02 (dt, $J = 8.1, 2.1$ Hz, 1H), 6.96 (tt, $J = 7.9, 2.1$ Hz, 1H), 6.84 (dt, $J = 7.3, 2.0$ Hz, 1H), 5.72 (dt, $J = 13.2, 2.1$ Hz, 1H), 5.58 (dt, $J = 13.3, 2.0$ Hz, 1H), 3.21 (dt, $J = 11.1, 2.0$ Hz, 1H), 2.21 - 2.07 (m, 2H), 1.94 - 1.73 (m, 2H), 1.72 - 1.60 (m, 3H), 1.51 - 1.42 (m, 3H), 1.42 - 1.33 (m, 3H), 1.20 (dt, $J = 7.0, 2.0$ Hz, 3H), 1.16 - 1.06 (m, 3H). $^{13}\text{C NMR}$ (101 MHz, CD_3OD) δ 176.5, 144.1, 141.4, 138.0, 135.4, 127.1, 123.1, 122.3, 112.3, 108.4, 107.2, 87.8, 59.1, 55.0, 49.8, 42.8, 39.8, 38.0, 37.7, 32.9, 31.1, 25.3, 25.2, 10.4. **IR** (ATIR) 3287, 2963, 2927, 1693, 1660, 1450, 1362, 1306, 1263, 1121, 1053, 1022, 735. **HRMS** (ESI): Exact mass calc'd for $\text{C}_{24}\text{H}_{28}\text{O}_2\text{N}_2\text{Na}$ $[\text{M}+\text{Na}]^+$, 399.2043. Found 399.2049. $[\alpha]_{\text{D}} -83.3$ (MeOH).

Diastereomer of higher polarity: $^1\text{H NMR}$ (400 MHz, CD_3OD) δ 9.98 (s, 1H), 7.02 (d, $J = 7.9$ Hz, 1H), 6.95 (t, $J = 7.6$ Hz, 1H), 6.87 - 6.73 (m, 1H), 5.75 (d, $J = 12.9$ Hz, 1H), 5.23 (d, $J = 12.9$ Hz, 1H), 2.25 (q, $J = 7.1$ Hz, 1H), 1.87 (d, $J = 11.8$ Hz, 2H), 1.75 (td, $J = 11.4, 6.6$ Hz, 1H), 1.66 (s, 3H), 1.45 (s, 3H), 1.41 (s, 3H), 1.18 (s, 3H), 1.14 (d, $J = 7.1$ Hz, 3H). **IR** (ATIR) 3353, 2964, 2871, 2487, 1693, 1448, 1384, 1288, 1207, 746. $[\alpha]_{\text{D}} -26.7$ (MeOH).



Ethoxy hemiaminal (5.31): Compound **5.30** (0.027 mmol, 11 mg, 1.0 equiv) was dissolved in THF (0.1 M, 0.3 mL) in a round-bottomed flask. To the solution was added NaHMDS (2.0 M in THF, 0.68 mmol, 340 μ L, 25 equiv) at room temperature via syringe. After 10 min, ethyl formate (0.53 mmol, 43 μ L, 20 equiv) was added via syringe and the reaction mixture was allowed to stir for 30 min at room temperature. The reaction mixture was quenched with ammonium chloride (sat. aq.) (50 mL) and the aqueous layer was extracted with ethyl acetate (3 x 5 mL). The combined organic layers were washed with brine (10 mL) and dried over sodium sulfate. The crude mixture was concentrated *in vacuo* and purified via SiO₂ gel column chromatography on a Yamazen® automatic purification system. The pure **5.31** eluted separately as two diastereomers. Major diastereomer (6 mg, 51%): ¹H NMR (400 MHz, CDCl₃) δ 7.74 (s, 1H), 7.18 - 7.01 (m, 2H), 6.95 (d, *J* = 6.8 Hz, 1H), 6.22 - 5.90 (m, 2H), 5.60 (d, *J* = 13.0 Hz, 1H), 5.30 (s, 1H), 3.72 - 3.39 (m, 3H), 2.81 - 2.49 (m, 2H), 2.19 - 1.85 (m, 1H), 1.48 (s, 3H), 1.46 (s, 3H), 1.45 (s, 3H), 1.42 (s, 3H), 1.29 - 1.22 (m, 3H), 1.10 (s, 3H).

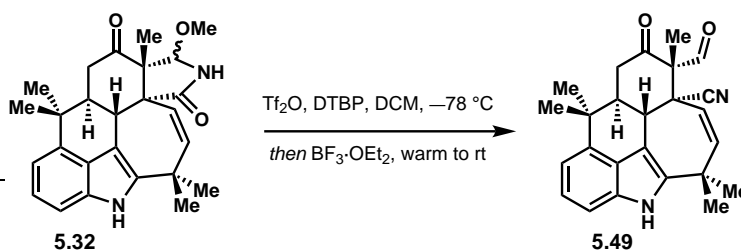


Methoxy hemiaminal (5.81 and 5.82): Compound **5.30** (0.44 mmol, 170 mg, 1.0 equiv) was dissolved in THF (0.1 M, 5 mL) in a round-bottomed flask. To the solution was added NaHMDS (2.0 M in THF, 2.2 mmol, 1.1 mL, 5.0 equiv) at room temperature. After 10 min, methyl formate (22 mmol, 1.4 mL, 50 equiv) was added via syringe and the reaction mixture was allowed to stir for 10 min at room temperature. The reaction mixture was quenched with ammonium chloride (sat. aq.) (20 mL) and the aqueous layer was extracted with ethyl acetate (3 x 20 mL). The combined organic layers were washed with brine (50 mL) and dried over sodium sulfate. The crude mixture was concentrated *in vacuo* and purified via SiO₂ gel column chromatography eluting compound **5.32** as two diastereomers. Major diastereomer of lower polarity (75 mg, 41%). ¹H NMR (400 MHz, (CD₃)₂CO) δ 9.79 (s, 1H), 7.82 (s, 1H), 7.04 (d, *J* = 8.0 Hz, 1H), 6.97 (t, *J* = 7.6 Hz, 1H), 6.88 (d, *J* = 7.2 Hz, 1H), 6.10 (d, *J* = 13.1 Hz, 1H), 5.60 (d, *J* = 13.1 Hz, 1H), 5.15 (s, 1H), 3.66 (d, *J* = 11.1 Hz, 1H), 3.38 (s, 3H), 2.82 (dd, *J* = 33.9, 13.8 Hz, 4H), 2.59 (dd, *J* = 14.1, 3.0 Hz, 1H), 1.99 - 1.78 (m, 1H), 1.45 (s, 3H), 1.41 (s, 3H), 1.08 (s, 3H). ¹³C NMR (101 MHz, (CD₃)₂CO) δ 211.4, 175.4, 141.2, 139.4, 136.9, 134.9, 127.8, 127.4, 122.0, 112.3, 108.3, 105.8, 87.2, 60.6, 56.3, 55.4, 46.3, 40.2, 39.4, 38.3, 38.0, 32.9, 28.9, 25.3, 24.6, 15.1. IR (ATIR) 3401, 3365, 2964, 2931, 1708, 1452, 1364, 1086, 1052, 735. HRMS (ESI): Exact mass calc'd for C₂₆H₃₁O₃N₂ [M+H]⁺, 419.2329. Found 419.2336. [α]_D -20.8 ((CH₃)₂CO).

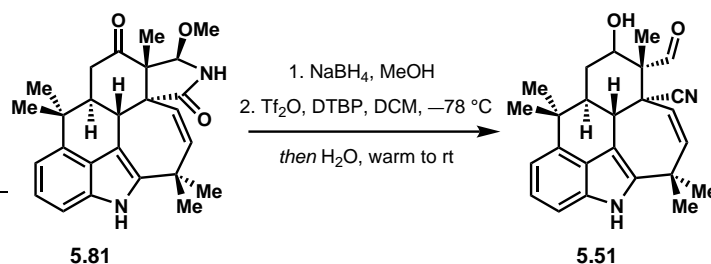
Minor diastereomer of higher polarity (28 mg, 15%) ¹H NMR (600 MHz, (CD₃)₂CO) δ 9.74 (s, 1H), 7.86 (s, 1H), 7.02 (dt, *J* = 7.9, 0.8 Hz, 1H), 6.98 (dd, *J* = 8.0, 7.1 Hz, 1H), 6.88 (dd, *J* = 7.2, 0.8 Hz, 1H), 5.63 (q, *J* = 13.2 Hz, 2H), 4.91 (s, 1H), 3.38 (dd, *J* = 1.7, 0.5 Hz, 3H), 3.08 - 2.92 (m, 2H), 2.51 (dd, *J* = 15.1, 3.3 Hz, 1H), 1.54 (s, 3H), 1.46 (s, 3H), 1.45 (s, 3H), 1.37 (s, 3H), 0.99 (s, 3H). ¹³C NMR (151 MHz, (CD₃)₂CO) δ 209.0, 175.1, 175.0, 141.6, 140.3, 137.2, 135.1,

134.9, 127.0, 125.1, 122.4, 113.1, 113.1, 108.3, 108.2, 107.5, 93.5, 93.4, 61.1, 61.0, 59.4, 59.4, 57.8, 57.8, 45.3, 39.8, 39.5, 39.5, 39.2, 37.6, 32.0, 25.2, 24.5, 16.8. The observation of extra peaks in the ^{13}C spectrum is consistent with slow exchange of rotameric isomers. **IR** (ATIR) 3400, 3260, 2962, 2930, 1703, 1472, 1450, 1106, 1084, 741. $[\alpha]_{\text{D}} -111.8$

The minor diastereomer was dissolved in MeOH (0.05 M, 3 mL) in a round-bottomed flask and $\text{BF}_3 \cdot \text{OEt}_2$ (1.6 mmol, 0.19 mL, 10 equiv) was added via syringe at room temperature. After stirring for 3 h at room temperature the reaction mixture was quenched with sodium bicarbonate (sat. aq.) (30 mL) and the aqueous layer was extracted with ethyl acetate (3 x 20 mL). The combined organic layers were washed with brine (50 mL) and dried over sodium sulfate. The crude mixture was concentrated *in vacuo* and purified via SiO_2 gel column chromatography on a Yamazen® automatic purification system. The major diastereomer **5.83** was isolated as an off-white solid (43 mg, 66%).



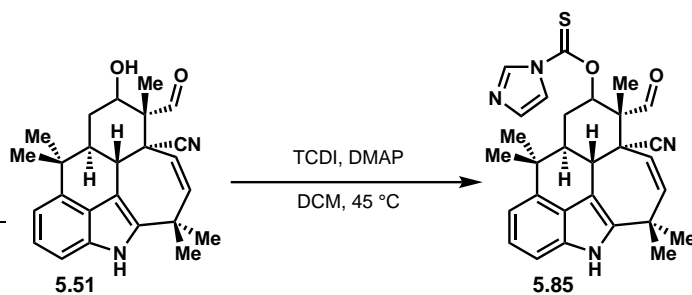
β -Keto aldehyde (5.49): The methyl hemiaminal compound **5.32** (0.024 mmol, 10 mg, 1.0 equiv) was dissolved in DCM (0.010 M, 2.4 mL) in a round-bottomed flask. To this mixture, DTBP (0.036 mmol, 8.1 μL , 1.5 equiv) was added via syringe. The reaction mixture was cooled to -78°C and Tf_2O (0.12 mmol, 20 μL , 5.0 equiv) was added via syringe. After stirring at -78°C for 2.5 h, $\text{BF}_3 \cdot \text{OEt}_2$ (0.24 mmol, 0.30 mL, 10 equiv) was added and the reaction mixture was allowed to warm fully to room temperature. To the reaction mixture was added sodium bicarbonate (sat. aq.) (10 mL) and the aqueous layer was extracted with ethyl acetate (3 x 20 mL). The combined organic layers were washed with brine (60 mL) and dried over sodium sulfate. The crude mixture was concentrated *in vacuo* and purified via SiO_2 gel column chromatography on a Yamazen® automatic purification system. The pure aldehyde **5.49** was isolated as a white solid (6.2 mg, 67%). $^1\text{H NMR}$ (500 MHz, CDCl_3) δ 10.09 (s, 1H), 7.88 (s, 1H), 7.23 - 7.13 (m, 2H), 7.04 (dd, $J = 4.6, 3.5$ Hz, 1H), 5.80 (d, $J = 12.4$ Hz, 1H), 5.25 (d, $J = 12.3$ Hz, 1H), 3.70 (d, $J = 11.3$ Hz, 1H), 2.84 - 2.63 (m, 2H), 2.55 (td, $J = 11.3, 6.8$ Hz, 1H), 1.62 (s, 3H), 1.53 (s, 3H), 1.51 (s, 3H), 1.48 (s, 3H), 1.22 (s, 3H).



β -Hydroxy aldehyde (5.51): The methyl hemiaminal **5.81** (0.470 mmol, 197 mg, 1.00 equiv) was dissolved in MeOH (0.05 M, 9 mL) in a round-bottomed flask and NaBH_4 (2.4 mmol, 89 mg,

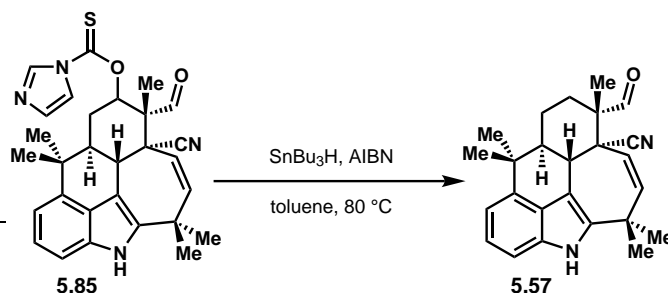
5.0 equiv) was added all at once. After 1 h the mixture was quenched with H₂O (20 mL) and the aqueous layer was extracted with ethyl acetate (3 x 20 mL). The combined organic layers were washed with brine (100 mL) and dried over sodium sulfate. The crude mixture was concentrated *in vacuo* and isolated as an off-white solid. The crude product was taken forward in the next step without further purification.

To the round-bottomed flask containing the crude alcohol (**5.51**) (0.48 mmol, 1.0 equiv) was added DCM (0.005 M, 95 mL). The starting material does not fully dissolve and results in an off-white suspension. To this mixture, DTBP (0.71 mmol, 0.16 mL, 1.5 equiv) was added via syringe and the reaction mixture was cooled to $-78\text{ }^{\circ}\text{C}$. Tf₂O (2.4 mmol, 0.40 mL, 5.0 equiv) was added via syringe and the mixture was allowed to stir at $-78\text{ }^{\circ}\text{C}$ for 2.5 h at which time the reaction mixture was quenched with water (100 mL) at $-78\text{ }^{\circ}\text{C}$. After stirring at $-78\text{ }^{\circ}\text{C}$ for 30 seconds, the flask was removed from the $-78\text{ }^{\circ}\text{C}$ bath and allowed to warm fully to room temperature. To the reaction mixture was added sodium bicarbonate (sat. aq.) (100 mL) and the aqueous layer was extracted with ethyl acetate (3 x 100 mL). The combined organic layers were washed with brine (300 mL) and dried over sodium sulfate. The crude mixture was concentrated *in vacuo* and purified via SiO₂ gel column chromatography on a Yamazen® automatic purification system. The pure aldehyde **5.84** was isolated as a white solid (116 mg, 63%). ¹H NMR (700 MHz, CDCl₃) δ 10.00 (s, 1H), 7.81 (s, 1H), 7.15 (d, *J* = 5.5 Hz, 2H), 7.02 (dd, *J* = 5.6, 2.5 Hz, 1H), 5.75 (d, *J* = 12.3 Hz, 1H), 5.50 (d, *J* = 12.3 Hz, 1H), 4.59 (dd, *J* = 11.6, 4.5 Hz, 1H), 3.28 (d, *J* = 11.4 Hz, 1H), 2.21 (dt, *J* = 12.7, 4.1 Hz, 1H), 2.16 - 2.08 (m, 1H), 1.68 (q, *J* = 12.5 Hz, 1H), 1.61 (s, 3H), 1.51 (s, 3H), 1.48 (s, 3H), 1.33 (s, 3H), 1.15 (s, 3H). ¹³C NMR (176 MHz, CDCl₃) δ 204.1, 144.0, 140.0, 135.7, 133.6, 126.0, 122.9, 122.8, 119.8, 113.0, 107.9, 105.7, 69.1, 56.1, 46.1, 45.4, 38.7, 38.2, 37.5, 32.9, 29.3, 28.1, 24.9, 24.6, 8.5. IR (ATIR) 3408, 2966, 2930, 2867, 1727, 1471, 1450, 1333, 1084, 753. HRMS (ESI): Exact mass calc'd for C₂₅H₂₉O₂N₂ [M+H]⁺, 389.2224. Found 389.2229. [α]_D -165 .

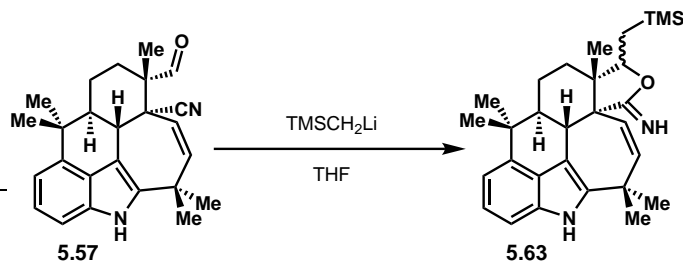


Thiocarbamate (5.85): The compound **5.51** (0.28 mmol, 110 mg, 1.0 equiv) was added as a solution in DCM (0.1 M, 3 mL) to a flame-dried microwave vial. The solvent was removed by passing a heavy stream of N₂ over the solution. DMAP (0.08 mmol, 10 mg, 1 equiv) was added and the vial was subsequently sealed. A needle inlet of N₂ was placed in the septum and the vial was evacuated and backfilled with N₂ three times. The vial was brought into the glovebox, opened, and charged with TCDI (0.33 mmol, 61 mg, 1.0 equiv). The vial was resealed, brought out of the glovebox and DCM (0.1 M, 3 mL) was added. The reaction vessel was then placed in a preheated 45 °C oil bath and allowed to stir for 14 h. Once the vial had cooled to room temperature, the reaction mixture was concentrated *in vacuo* and immediately subjected to SiO₂ gel column chromatography on a Yamazen® automatic purification system. The pure thiocarbamate **5.85** was isolated as a white solid (97 mg, 70%) along with starting material (7.2 mg, 77% brsm). ¹H NMR

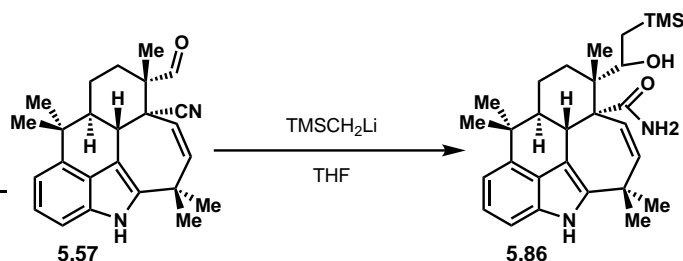
(700 MHz, $(\text{CD}_3)_2\text{CO}$) δ 10.13 (s, 1H), 10.03 (s, 1H), 8.35 (s, 1H), 7.73 (d, $J = 1.5$ Hz, 1H), 7.11 (d, $J = 8.0$ Hz, 1H), 7.06 (t, $J = 7.6$ Hz, 1H), 7.05 - 7.02 (m, 1H), 6.99 (d, $J = 7.2$ Hz, 1H), 6.47 (dd, $J = 11.5, 4.6$ Hz, 1H), 5.93 (d, $J = 12.3$ Hz, 1H), 5.57 (d, $J = 12.3$ Hz, 1H), 3.57 (d, $J = 11.1$ Hz, 1H), 2.85 - 2.77 (m, 2H), 2.77 - 2.67 (m, 1H), 2.18 (ddd, $J = 13.9, 11.1, 3.1$ Hz, 1H), 2.14 - 2.09 (m, 1H), 1.65 (s, 3H), 1.64 (s, 3H), 1.55 (s, 3H), 1.53 (s, 3H), 1.19 (s, 3H). ^{13}C NMR (176 MHz, $(\text{CD}_3)_2\text{CO}$) δ 201.9, 184.3, 145.5, 140.1, 137.6, 137.2, 135.0, 131.9, 126.5, 123.1, 122.5, 119.9, 119.1, 113.0, 108.9, 105.2, 81.8, 56.2, 47.4, 47.0, 39.6, 39.1, 38.3, 32.5, 27.8, 25.5, 25.1, 24.8, 10.5. IR (ATIR) 3370, 2966, 2934, 1789, 1731, 1470, 1388, 1330, 1286, 1229. HRMS (ESI): Exact mass calc'd for $\text{C}_{29}\text{H}_{31}\text{O}_2\text{N}_4\text{S}$ $[\text{M}+\text{H}]^+$, 499.2162. Found 499.2152. $[\alpha]_{\text{D}} -73$ ($(\text{CH}_3)_2\text{CO}$).



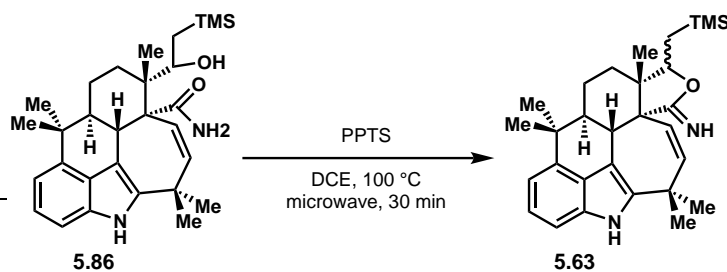
Deoxygenated aldehyde (5.57): Thiocarbamate **5.85** (0.036 mmol, 18 mg, 1.0 equiv) was added as a solid to a flame-dried microwave vial. AIBN (0.015 mmol, 2.4 mg, 0.40 equiv) was added and the vial was sealed. A N_2 inlet was placed in the septum and the flask was evacuated and backfilled with N_2 three times. Toluene (0.03 M, 1.2 mL) was added via syringe, followed by SnBu_3H (0.072 mmol, 19 μL , 2.0 equiv) and the reaction vessel was placed in a preheated 80°C oil bath. After 20 min the reaction mixture was allowed to cool to room temperature and the contents were concentrated *in vacuo*. The crude reaction mixture was immediately subjected to SiO_2 gel column chromatography on a Yamazen@automatic purification system. The pure deoxygenated aldehyde **5.57** was isolated as a white solid (10 mg, 77%). It is important to obtain this compound without any tin residues and a second purification is often necessary. ^1H NMR (700 MHz, CDCl_3) δ 9.88 (s, 1H), 7.83 (s, 1H), 7.17 - 7.11 (m, 2H), 7.01 (dd, $J = 6.4, 1.7$ Hz, 1H), 5.71 (d, $J = 12.5$ Hz, 1H), 5.38 (d, $J = 12.3$ Hz, 1H), 3.31 (d, $J = 11.0$ Hz, 1H), 2.26 - 2.19 (m, 1H), 2.10 - 2.00 (m, 2H), 1.72 - 1.64 (m, 1H), 1.62 (s, 3H), 1.64 - 1.58 (m, 1H), 1.50 (s, 3H), 1.47 (s, 3H), 1.34 (s, 3H), 1.14 (s, 3H). ^{13}C NMR (176 MHz, CDCl_3) δ 204.01, 143.73, 140.39, 135.65, 133.56, 126.01, 124.09, 122.69, 120.31, 112.80, 107.72, 106.47, 51.54, 47.55, 45.45, 38.65, 38.54, 37.44, 32.84, 29.59, 28.17, 24.95, 24.55, 19.51, 14.15. HRMS (ESI): Exact mass calc'd for $\text{C}_{25}\text{H}_{29}\text{ON}_2$ $[\text{M}+\text{H}]^+$, 373.2274. Found 373.2278. $[\alpha]_{\text{D}} -73.5$.



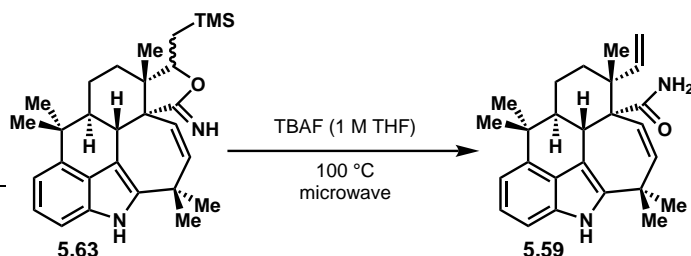
Acetimide (5.63): Aldehyde **5.57** (0.013 mmol, 5.0 mg, 1.0 equiv) was dissolved in THF in a round-bottomed flask. To the solution was added $\text{TMSCH}_2\text{MeLi}$ (1.0 M in pentane, 0.067 mmol, 67 μL , 5.0 equiv). The reaction mixture was allowed to stir at room temperature for 2 h at which time it was quenched with the addition of H_2O (5 mL). The aqueous layer was extracted with ethyl acetate (3 x 10 mL). The combined organic layers were washed with brine (30 mL) and dried over sodium sulfate. The crude mixture was concentrated *in vacuo* and used immediately in the next reaction without further purification.



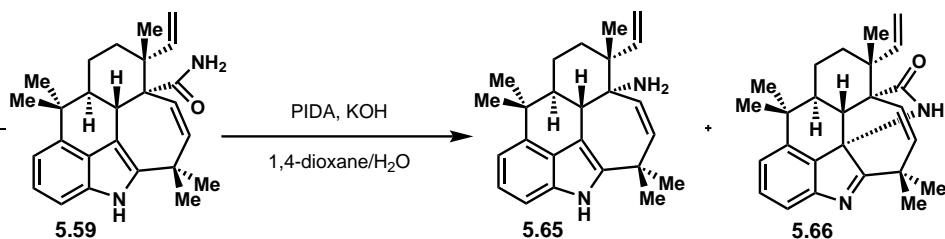
Secondary alcohol (5.86): To a solution of **5.57** (mmol, mg, equiv) in THF (M, mL) was added TMSCH_2Li (1.0 M solution in pentane, mmol, mL, equiv). The solution was allowed to stir for 15 min at which time it was quenched with the addition of ammonium chloride (sat. aq.) (mL). The aqueous layer was extracted with ethyl acetate (3x mL) and the combined organic layers were washed with brine (mL), dried over sodium sulfate, and concentrated *in vacuo* to yield a yellow crude foam which was immediately subjected to the next reaction without further purification.



Acetimide (5.63): The crude mixture containing **5.86** was added to a microwave vial as a solution in DCE (M, mL). PPTS (mmol, mg, equiv) was added and the vial was sealed. The vial was heated to 100 °C in the microwave for 30 min. Once cooled, the solution was poured into H_2O and the aqueous layer was extracted with DCM (3x mL). The combined organic layers were washed with brine (mL), dried over sodium sulfate, and concentrated *in vacuo* to yield the crude mixture of **5.63** as a yellow oil. The crude product was immediately subjected to the next reaction without further purification.



Amide (5.59): The crude reaction mixture containing **5.63** was added as a solution in DCM (1 mL) to a microwave vial. The solvent was removed by passing a heavy stream of N₂ over the solution until only solid remained. The vial was sealed and TBAF (1 M THF, 3 mL) was added via syringe. The brown-yellow solution was then heated to 100 °C in the microwave for 45 min. Upon cooling to room temperature, the reaction mixture was diluted with ethyl acetate (5 mL) and washed with H₂O (10 mL). The aqueous layer was extracted with ethyl acetate (3 x 10 mL) and the combined organic layers were washed with brine (30 mL), dried over sodium sulfate and concentrated *in vacuo* to yield the crude reaction mixture. The crude product was purified via SiO₂ gel column chromatography on a Yamazen® automatic purification system. Pure amide **5.59** was isolated as a glassy, off-white solid (2.8 mg, 49%). ¹H NMR (700 MHz, CDCl₃) δ 7.70 (s, 1H), 7.10 - 7.01 (m, 2H), 7.00 - 6.89 (m, 1H), 6.16 (s, 1H), 5.97 (dd, *J* = 17.4, 10.8 Hz, 1H), 5.83 (d, *J* = 13.1 Hz, 1H), 5.23 (s, 1H), 5.16 (dd, *J* = 17.4, 1.5 Hz, 1H), 5.11 (dd, *J* = 10.8, 1.6 Hz, 1H), 3.36 (d, *J* = 11.3 Hz, 1H), 3.12 (ddd, *J* = 12.6, 11.2, 3.7 Hz, 1H), 2.52 (td, *J* = 13.5, 4.3 Hz, 1H), 2.17 (s, 3H), 1.93 (dq, *J* = 13.1, 3.8 Hz, 1H), 1.62 (qd, *J* = 13.4, 4.2 Hz, 1H), 1.49 (s, 3H), 1.48 (s, 3H), 1.35 (dt, *J* = 13.2, 3.5 Hz, 1H), 1.32 (s, 3H), 1.30 (s, 3H), 1.00 (s, 3H). ¹³C NMR (176 MHz, CDCl₃) δ 175.2, 146.2, 141.9, 140.2, 134.9, 133.8, 131.3, 126.7, 122.2, 113.3, 112.2, 109.2, 107.2, 60.6, 56.4, 43.5, 43.2, 38.9, 38.8, 37.3, 34.5, 33.8, 27.8, 24.3, 21.2, 19.3. IR (ATIR) 3361, 3310, 3185, 2992, 1589, 1561, 1463, 1435. [α]_D -137.



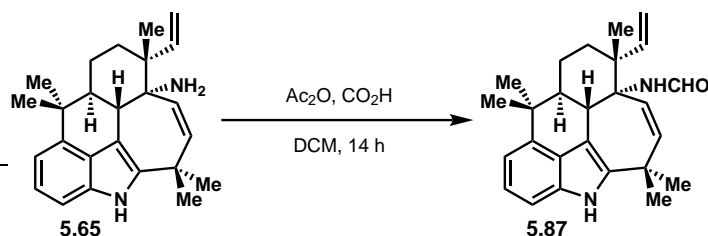
Vinyl amine (5.65) and amidation side product (5.66): Amide compound **5.59** (0.083 mmol, 32 mg, 1.0 equiv) was dissolved in 1,4-dioxane (0.05 M, 2 mL) and H₂O (0.05 M, 2 mL) was added. To this solution was added crushed KOH (2.9 mmol, 160 mg, 35 equiv) and the suspension was allowed to stir for 5 min at room temperature. At this time, PIDA (0.099 mmol, 32 mg, 1.2 equiv) was added and the solution turned light yellow. The suspension was allowed to stir at room temperature for 14 h at which time it was quenched with sodium bicarbonate (sat. aq.) (10 mL) and sodium thiosulfate (sat. aq.) (10 mL). After stirring for 5 min at room temperature the mixture was diluted with ethyl acetate (30 mL) and the aqueous layer was extracted with ethyl acetate (3 x 20 mL). The combined organic layers were washed with brine (100 mL), dried over sodium sulfate, and concentrated *in vacuo* to yield the crude reaction mixture. The crude product was purified using SiO₂ gel preparatory thin-layer chromatography eluting with a mixture of 10% acetone/DCM/NH₄OH. The two major bands were scraped off, crushed, and filtered using ethyl acetate to yield the desired product **5.65** (14 mg, 49%) as well as the amidation side product **5.66**.

Amine product (**5.65**):

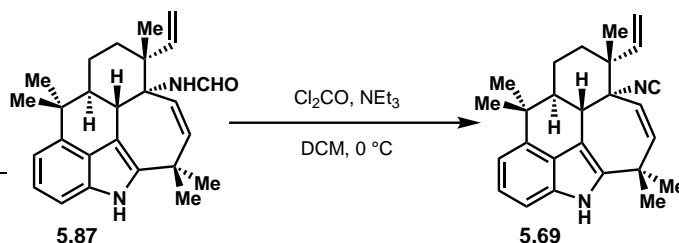
¹H NMR (700 MHz, CD₃OD) δ 7.06 (d, *J* = 7.9 Hz, 1H), 6.99 (dd, *J* = 7.6 Hz, 1H), 6.87 (d, *J* = 7.2 Hz, 1H), 6.20 (dd, *J* = 17.6, 11.0 Hz, 1H), 5.93 (d, *J* = 13.1 Hz, 1H), 5.42 (d, *J* = 13.0 Hz, 1H), 5.21 - 5.13 (m, 2H), 3.41 (d, *J* = 11.4 Hz, 1H), 2.11 - 2.05 (m, 1H), 1.93 - 1.86 (m, 2H), 1.70 - 1.64 (m, 1H), 1.51 (s, 3H), 1.45 (s, 3H), 1.41 (s, 3H), 1.38 - 1.35 (m, 1H), 1.29 (s, 3H), 1.06 (s, 3H). ¹³C NMR (176 MHz, CD₃OD) δ 146.5, 142.0, 139.5, 137.1, 135.8, 134.9, 127.8, 122.8,

114.2, 112.4, 108.3, 107.1, 59.6, 46.3, 44.3, 41.1, 39.5, 38.0, 34.1, 32.9, 30.1, 25.1, 25.0, 22.3, 20.2. **IR** (ATIR) 3500, 2963, 2926, 2854, 1467, 1449, 914, 744. **HRMS** (ESI): Exact mass calc'd for $C_{25}H_{33}N_2$ $[M+H]^+$, 361.2638. Found 361.2643. $[\alpha]_D -73.5$ (MeOH).

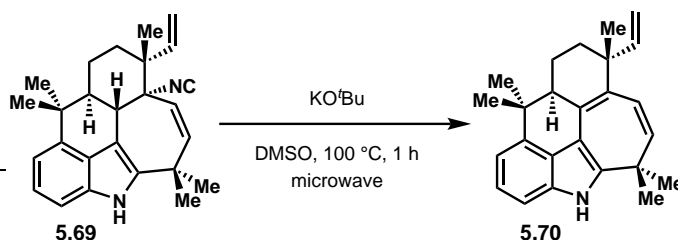
Amidation side product (**5.66**): **1H NMR** (700 MHz, $CDCl_3$) δ 7.35 (t, $J = 7.7$ Hz, 1H), 7.27 (m, 1H), 7.14 (d, $J = 7.9$ Hz, 1H), 7.07 (dd, $J = 17.7, 10.9$ Hz, 1H), 5.62 (d, $J = 13.3$ Hz, 1H), 5.45 (d, $J = 13.3$ Hz, 1H), 5.27 - 5.19 (m, 2H), 5.15 (dd, $J = 17.6, 1.5$ Hz, 1H), 2.35 (dd, $J = 11.0, 1.6$ Hz, 1H), 2.26 (ddd, $J = 13.8, 10.9, 3.1$ Hz, 1H), 1.91 (td, $J = 13.4, 3.7$ Hz, 1H), 1.84 (dq, $J = 13.4, 3.4$ Hz, 1H), 1.56 (m, 1H), 1.54 (s, 3H), 1.50 (dd, $J = 13.1, 3.2$ Hz, 1H), 1.46 (d, $J = 2.8$ Hz, 6H), 1.13 (s, 3H), 0.94 (s, 3H). **^{13}C NMR** δ 192.9, 178.0, 155.5, 146.9, 144.6, 138.4, 131.5, 130.8, 128.1, 122.9, 117.3, 113.4, 70.0, 55.8, 47.6, 43.3, 42.6, 41.5, 38.1, 37.2, 31.7, 31.5, 27.3, 26.3, 20.3, 20.2. **IR** (ATIR) 3223, 2966, 2927, 2854, 1697. **HRMS** (ESI): Exact mass calc'd for $C_{26}H_{31}ON_2$ $[M+H]^+$, 387.2431. Found 387.2437. $[\alpha]_D -244$ (DCM).



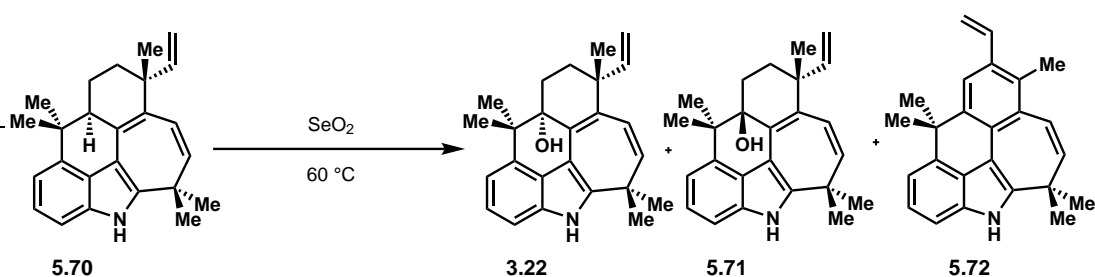
Formamide (5.87): To a round-bottomed flask was added DCM (1 mL) followed by Ac_2O (0.59 mmol, 56 μ L, 18 equiv) and formic acid (0.66 mmol, 25 μ L, 20 equiv). This solution was allowed to stir for 1 h at room temperature, at which time a solution of amine **5.65** (0.033 mmol, 12 mg, 1.0) in DCM (0.1 M, 1 mL) was added. After stirring at room temperature for 14 h, the solution was quenched with sodium bicarbonate (10 mL) and diluted with DCM (10 mL). The aqueous layer was extracted with DCM (3 x 10 mL) and the combined organic layers were washed with brine (50 mL), dried over sodium sulfate, and concentrated *in vacuo* to yield the crude formamide **5.87**. The crude product was purified using SiO_2 gel preparatory thin-layer chromatography eluting with a mixture of 2:1 hexanes:ethyl acetate. The major UV-active band was scraped off, crushed, and filtered using ethyl acetate to yield the desired product as a white solid (13 mg, 99%). **1H NMR** (600 MHz, $CDCl_3$) δ 8.08 (d, $J = 11.1$ Hz, 1H), 7.95 (s, 1H), 7.18 - 7.04 (m, 2H), 6.97 (dd, $J = 5.7, 2.6$ Hz, 1H), 5.96 (dd, $J = 17.6, 11.0$ Hz, 1H), 5.89 (d, $J = 12.9$ Hz, 1H), 5.82 (d, $J = 11.7$ Hz, 1H), 5.60 (d, $J = 12.6$ Hz, 1H), 5.27 (d, $J = 10.8$ Hz, 1H), 5.23 (d, $J = 17.5$ Hz, 1H), 3.49 (d, $J = 10.1$ Hz, 1H), 1.96 - 1.85 (m, 1H), 1.85 - 1.75 (m, 1H), 1.73 - 1.61 (m, 2H), 1.51 - 1.45 (m, 1H), 1.47 (s, 3H), 1.40 (s, 3H), 1.38 (s, 3H), 1.33 (s, 3H), 1.11 (s, 3H). **^{13}C NMR** (176 MHz, $CDCl_3$) δ 166.5, 143.7, 141.5, 140.5, 135.8, 133.6, 129.0, 126.8, 122.3, 116.1, 112.4, 107.6, 106.0, 60.9, 45.5, 44.3, 39.6, 38.2, 37.5, 33.2, 33.0, 28.1, 24.6, 24.5, 20.6, 19.8. **IR** (ATIR) 3297, 2965, 2926, 2868, 1669, 1453, 1337, 761, 739. **HRMS** (ESI): Exact mass calc'd for $C_{26}H_{32}ON_2Na$ $[M+Na]^+$, 411.2407. Found 411.2399. $[\alpha]_D -423$.



Isonitrile (5.69): The crude formamide **5.87** (0.02 mmol, 6 mg, 1 equiv) was dissolved in DCM (0.02 M, 1 mL) and the reaction mixture was cooled to 0 °C. NEt₃ (0.03 mmol, 40 μL, 20 equiv) was added followed by phosgene (20% in toluene, 0.08 mmol, 40 μL, 5 equiv). After stirring for 10 min at 0 °C the reaction mixture was quenched with sodium bicarbonate (5 mL) and diluted with DCM (5 mL). The aqueous layer was extracted with DCM (3 x 10 mL) and the combined organic layers were washed with brine (20 mL), dried over sodium sulfate, and concentrated *in vacuo* to yield the crude isonitrile **5.69**. The crude product was purified using SiO₂ gel preparatory thin-layer chromatography eluting with a mixture of 2:1 hexanes:ethyl acetate. The major UV-active band was scraped off, crushed, and filtered using ethyl acetate to yield the pure product as an off-white solid (5 mg, 84%). ¹H NMR (700 MHz, CDCl₃) δ 7.73 (s, 1H), 7.16 - 7.10 (m, 2H), 7.01 - 6.98 (m, 1H), 6.23 (dd, *J* = 17.5, 10.9 Hz, 1H), 5.67 (d, *J* = 12.6 Hz, 1H), 5.61 (d, *J* = 12.6 Hz, 1H), 5.28 (d, *J* = 10.9 Hz, 1H), 5.24 (d, *J* = 17.5 Hz, 1H), 3.37 (dt, *J* = 11.1, 3.3 Hz, 1H), 2.09 - 2.03 (m, 1H), 2.02 - 1.97 (m, 1H), 1.93 - 1.88 (m, 1H), 1.68 - 1.62 (m, 1H), 1.59 (s, 3H), 1.47 (s, 3H), 1.46 (s, 3H), 1.29 (s, 3H), 1.25 - 1.20 (m, 1H), 1.14 (s, 3H). ¹³C NMR (176 MHz, CDCl₃) δ 156.2, 143.8, 142.4, 140.9, 135.2, 133.6, 127.0, 126.6, 122.3, 115.2, 112.5, 107.5, 106.6, 67.6, 45.9, 43.2, 39.4, 38.3, 37.3, 33.7, 32.9, 27.9, 25.1, 24.6, 20.6, 17.7. HRMS (ESI): Exact mass calc'd for C₂₅H₃₀N₂ [M-HNC+H]⁺, 344.2373. Found 344.2372. [α]_D -141.

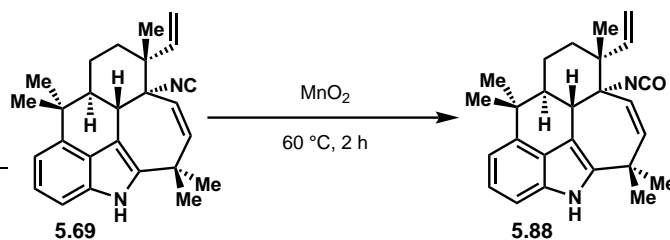


Deoxy-ambiguine P (5.70): Isonitrile compound **5.69** (0.009 mmol, 3 mg, 1 equiv) was dissolved in DMSO (0.02 M, 0.4 mL) and added to a microwave vial already charged with KOtBu (0.09 mmol, 10 mg, 10 equiv). The vial was sealed and heated to 150 °C for 30 min in the microwave. Upon cooling to room temperature, the reaction mixture was then diluted with ethyl acetate (10 mL) and washed with H₂O (3 x 20 mL). The aqueous layer was extracted with ethyl acetate (2 x 20 mL) and the combined organic layers were washed with brine (40 mL), dried over sodium sulfate and concentrated *in vacuo* to yield the crude deoxy ambiguine P (**5.70**). The crude product was purified using SiO₂ gel preparatory thin-layer chromatography eluting with a mixture of 2:1 hexanes:ethyl acetate. The major UV-active band was scraped off, crushed, and filtered using ethyl acetate to yield the pure product as an off-white solid (2.9 mg, 98%). ¹H NMR (700 MHz, CDCl₃) δ 7.81 (s, 1H), 7.18 - 7.12 (m, 2H), 7.03 (dd, *J* = 5.3, 2.6 Hz, 1H), 5.93 (dd, *J* = 11.4, 1.0 Hz, 1H), 5.86 (dd, *J* = 17.5, 10.6 Hz, 1H), 5.34 (dd, *J* = 11.4, 1.0 Hz, 1H), 5.09 (dd, *J* = 17.5, 1.5 Hz, 1H), 5.03 (dd, *J* = 10.6, 1.4 Hz, 1H), 2.89 (dd, *J* = 11.2, 7.0 Hz, 1H), 2.00 - 1.96 (m, 1H), 1.95 - 1.89 (m, 1H), 1.74 - 1.69 (m, 1H), 1.67 - 1.63 (m, 1H), 1.65 (s, 3H), 1.54 (s, 3H), 1.41 (s, 3H), 1.00 (s, 3H). ¹³C NMR (176 MHz, CDCl₃) δ 149.17, 140.77, 138.11, 134.82, 132.90, 130.13, 129.45, 128.19, 125.48, 122.74, 113.37, 110.95, 110.27, 108.10, 46.66, 40.32, 39.58, 36.76, 35.34, 26.86, 25.69, 24.99, 23.72, 23.64, 19.77. HRMS (ESI): Exact mass calc'd for C₂₅H₃₀N₂ [M+H]⁺, 344.2373. Found 344.2372. [α]_D -15.5 (DCM).



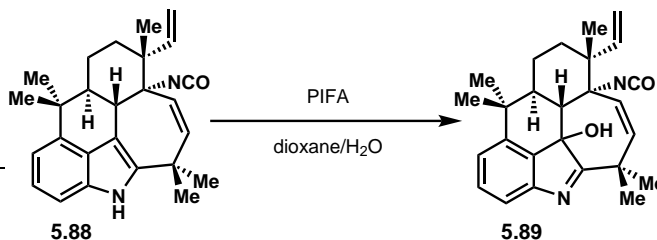
Ambiguine P (3.22): Deoxy ambiguine P **5.70** (0.007 mmol, 2 mg, 1 equiv) was dissolved in 1,4-dioxane (0.01 M, 0.4 mL) and SeO₂ (0.02 mmol, 2 mg, 3 equiv) was added. The 4-mL vial was placed in a pre-heated aluminum heating block at 45 °C and allowed to stir for 30 min at this temperature at which time more SeO₂ (0.009 mmol, 1 mg, 2 equiv) was added. After stirring for 45 min at 45 °C, the vial was removed from the aluminum heating block and allowed to cool to room temperature. The crude mixture was filtered through a Celite® plug and the mixture was concentrated *in vacuo*. The crude product (**3.22**) was purified using SiO₂ gel preparatory thin-layer chromatography eluting with a mixture of 2:1 hexanes:ethyl acetate. The major UV-active band was scraped off, crushed, and filtered using ethyl acetate to yield ambiguine P (**3.22**) as a mixture with its diastereomer, *epi*-ambiguine P (**5.71**) as a yellow oil (1 mg, 47%). Starting material (**5.70**) (1 mg, 50%) was also isolated from this mixture. ¹H NMR (700 MHz, CD₃OD) δ 7.16 (dd, *J* = 8.0, 5.7 Hz, 1H), 7.07 (t, *J* = 7.6 Hz, 1H), 6.96 (dd, *J* = 7.2, 4.2 Hz, 1H), 5.93 (d, *J* = 11.5 Hz, 1H), 5.91 - 5.87 (m, 1H), 5.40 (d, *J* = 11.4 Hz, 1H), 5.11 (dd, *J* = 10.6, 1.9 Hz, 1H), 4.93 (dd, *J* = 17.5, 1.7 Hz, 1H), 2.15 (td, *J* = 13.9, 3.1 Hz, 1H), 1.96 (td, *J* = 13.9, 2.7 Hz, 1H), 1.79 (dt, *J* = 13.5, 3.3 Hz, 1H), 1.68 (s, 3H), 1.60 (dt, *J* = 12.8, 3.4 Hz, 1H), 1.53 (s, 3H), 1.23 (s, 3H), 1.02 (s, 3H), 1.00 (s, 3H). ¹³C NMR (176 MHz, CD₃OD) δ 146.9, 142.1, 139.2, 134.7, 133.9, 133.5, 133.2, 128.6, 123.5, 114.9, 114.6, 109.6, 77.2, 45.9, 42.5, 36.7, 34.1, 34.0, 29.2, 28.9, 27.8, 27.1, 26.4, 18.6. HRMS (ESI): Exact mass calc'd for C₂₅H₂₈ON [M+H]⁺, 358.2176. Found 358.2173. All spectroscopic data matches that for the natural product (**3.22**) as reported by Orjala *et. al.*²⁷

Aromatized product (5.72): ¹H NMR (700 MHz, CD₃OD) δ 7.61 (s, 1H), 7.18 - 7.07 (m, 3H), 7.02 (dd, *J* = 6.9, 1.0 Hz, 1H), 6.64 (d, *J* = 12.5 Hz, 1H), 5.65 (d, *J* = 12.5 Hz, 1H), 5.59 (dd, *J* = 17.3, 1.6 Hz, 1H), 5.27 (dd, *J* = 10.9, 1.5 Hz, 1H), 2.37 (s, 3H), 1.66 (s, 6H), 1.48 (s, 6H).



Isoyanate (5.88): The isonitrile compound **5.69** (0.003 mmol, 1 mg, 1.0 equiv) was dissolved in chloroform (0.01 M, 0.3 mL, dried over 4 Å molecular sieves). Activated MnO₂ (0.14 mmol, 12 mg, 51 equiv) was added to the 4-mL vial and the reaction mixture was placed in a pre-heated aluminum heating block at 65 °C. After 2 h, the reaction mixture was cooled to room temperature and filtered through a Celite® plug, eluting with ethyl acetate to yield the crude isocyanate (**5.88**) very cleanly.

$^1\text{H NMR}$ (500 MHz, CDCl_3) δ 7.76 (s, 1H), 7.19 - 7.09 (m, 2H), 7.02 - 6.92 (m, 1H), 6.16 (dd, $J = 17.6, 11.0$ Hz, 1H), 5.80 (d, $J = 12.8$ Hz, 1H), 5.51 (d, $J = 12.8$ Hz, 1H), 5.25 - 5.15 (m, 2H), 3.42 (d, $J = 10.9$ Hz, 1H), 2.06 - 1.91 (m, 2H), 1.91 - 1.84 (m, 1H), 1.64 (ddd, $J = 13.3, 10.2, 3.8$ Hz, 2H), 1.55 (s, 3H), 1.47 (s, 3H), 1.41 (s, 3H), 1.26 (s, 3H), 1.11 (s, 3H).



C3-oxidized isocyanate(5.89): The isocyanate (**5.88**) was dissolved in MeCN (0.01 M, 0.1 mL) and H_2O (0.01 M, 0.1 mL) was added. PIFA (0.002 mmol, 0.8 mg, 1.5 equiv) was added to this solution and the reaction mixture was allowed to stir for 30 min at room temperature. The reaction mixture was quenched with the addition of sodium bicarbonate (sat. aq.) (5 mL). After stirring for 5 min, the layers were separated and the aqueous layer was extracted with ethyl acetate (3 x 10 mL). The combined organic layers were washed with brine (30 mL), dried over sodium sulfate and concentrated *in vacuo* to yield the crude reaction mixture containing **5.89**. The crude product was clean and used crude in subsequent reactions.

$^1\text{H NMR}$ (700 MHz, CDCl_3) δ 7.36 - 7.28 (m, 2H), 7.11 (d, $J = 7.2$ Hz, 1H), 6.05 (dd, $J = 17.4, 11.0$ Hz, 1H), 5.97 (d, $J = 12.2$ Hz, 1H), 5.73 (d, $J = 12.2$ Hz, 1H), 5.24 (d, $J = 11.0$ Hz, 1H), 5.18 (d, $J = 17.4$ Hz, 1H), 2.87 (d, $J = 11.9$ Hz, 1H), 1.76 (dd, $J = 13.2, 4.3$ Hz, 1H), 1.72 - 1.65 (m, 1H), 1.64 (t, $J = 7.7$ Hz, 1H), 1.62 (s, 3H), 1.58 (s, 3H), 1.50 (t, $J = 11.1$ Hz, 1H), 1.45 (s, 3H), 1.32 (s, 3H), 1.31 (s, 3H), 1.20 - 1.14 (m, 1H).

5.8 References

- Hamlin, A. M.; Lapointe, D.; Owens, K.; Sarpong, R. *J. Org. Chem.* **2014**, *79*, 6783–6800.
- Desai, L. V.; Hull, K. L.; Sanford, M. S. *J. Am. Chem. Soc.* **2004**, *126*, 9542–9543.
- Simmons, E. M.; Hartwig, J. F. *Nature* **2012**, *483*, 70–73.
- Sharpe, R. J.; Johnson, J. S. *J. Am. Chem. Soc.* **2015**, *137*, 4968–4971.
- Arhart, R. J.; Martin, J. C. *J. Am. Chem. Soc.* **1972**, *94*, 5003–5010.
- Mahoney, W. S.; Brestensky, D. M.; Stryker, J. M. *J. Am. Chem. Soc.* **1988**, *110*, 291–293.
- Woon, Y. J.; T., H. F. M.; Benjamin, L. *Angew. Chem. Int. Ed.* **2004**, *43*, 6660–6662.
- Cortese, N. A.; Heck, R. F. *J. Org. Chem.* **1978**, *43*, 3985–3987.
- Maryanoff, B. E.; Zhang, H.-C.; Cohen, J. H.; Turchi, I. J.; Maryanoff, C. A. *Chem. Rev.* **2004**, *104*, 1431–1628.
- Vinogradov, M. G.; Turova, O. V.; Zlotin, S. G. *Russ. Chem. Rev.* **2017**, *86*, 1–17.
- Ghaffar, T.; Parkins, A. W. *Tetrahedron Lett.* **1995**, *36*, 8657–8660.
- Ghaffar, T.; Parkins, A. W. *J. Mol. Catal. A: Chem.* **2000**, *160*, 249–261.
- Lee, J.; Kim, M.; Chang, S.; Lee, H.-Y. *Org. Lett.* **2009**, *11*, 5598–5601.
- Tebbe, F. N.; Parshall, G. W.; Reddy, G. S. *J. Am. Chem. Soc.* **1978**, *100*, 3611–3613.
- Petasis, N. A.; Bzowej, E. I. *J. Am. Chem. Soc.* **1990**, *112*, 6392–6394.

16. Peterson, D. J. *J. Org. Chem.* **1968**, *33*, 780–784.
17. Blakemore, P. R.; Cole, W. J.; Kocieński, P. J.; Morley, A. *Synlett* **1998**, *1998*, 26–28.
18. Takai, K.; Hotta, Y.; Oshima, K.; Nozaki, H. *Tetrahedron Lett.* **1978**, *19*, 2417–2420.
19. Takai, S.; Ploypradith, P.; Hamajima, A.; Kira, K.; Isobe, M. *Synlett* **2002**, *2002*, 588–592.
20. Lebel, H.; Paquet, V. *J. Am. Chem. Soc.* **2004**, *126*, 320–328.
21. Marth, C. J.; Gallego, G. M.; Lee, J. C.; Lebold, T. P.; Kulyk, S.; Kou, K. G. M.; Qin, J.; Lilien, R.; Sarpong, R. *Nature* **2015**, *528*, 493–498.
22. Bhat, V.; Rawal, V. H. *Chem. Commun.* **2011**, *47*, 9705.
23. Xu, S.; Ciufolini, M. A. *Org. Lett.* **2015**, *17*, 2424–2427.
24. Atkins, G. M.; Burgess, E. M. *J. Am. Chem. Soc.* **1968**, *90*, 4744–4745.
25. Isayama, S.; Mukaiyama, T. *Chem. Lett.* **1989**, *18*, 1071–1074.
26. L., H. M.; Qin, Z.; Kuljira, I.; Xinyu, L. *Angew. Chem. Int. Ed.* **2016**, *55*, 5780–5784.
27. Mo, S.; Kronic, A.; Santarsiero, B. D.; Franzblau, S. G.; Orjala, J. *Phytochemistry* **2010**, *71*, 2116–2123.

5.a NMR Spectra Relevant to Chapter 5

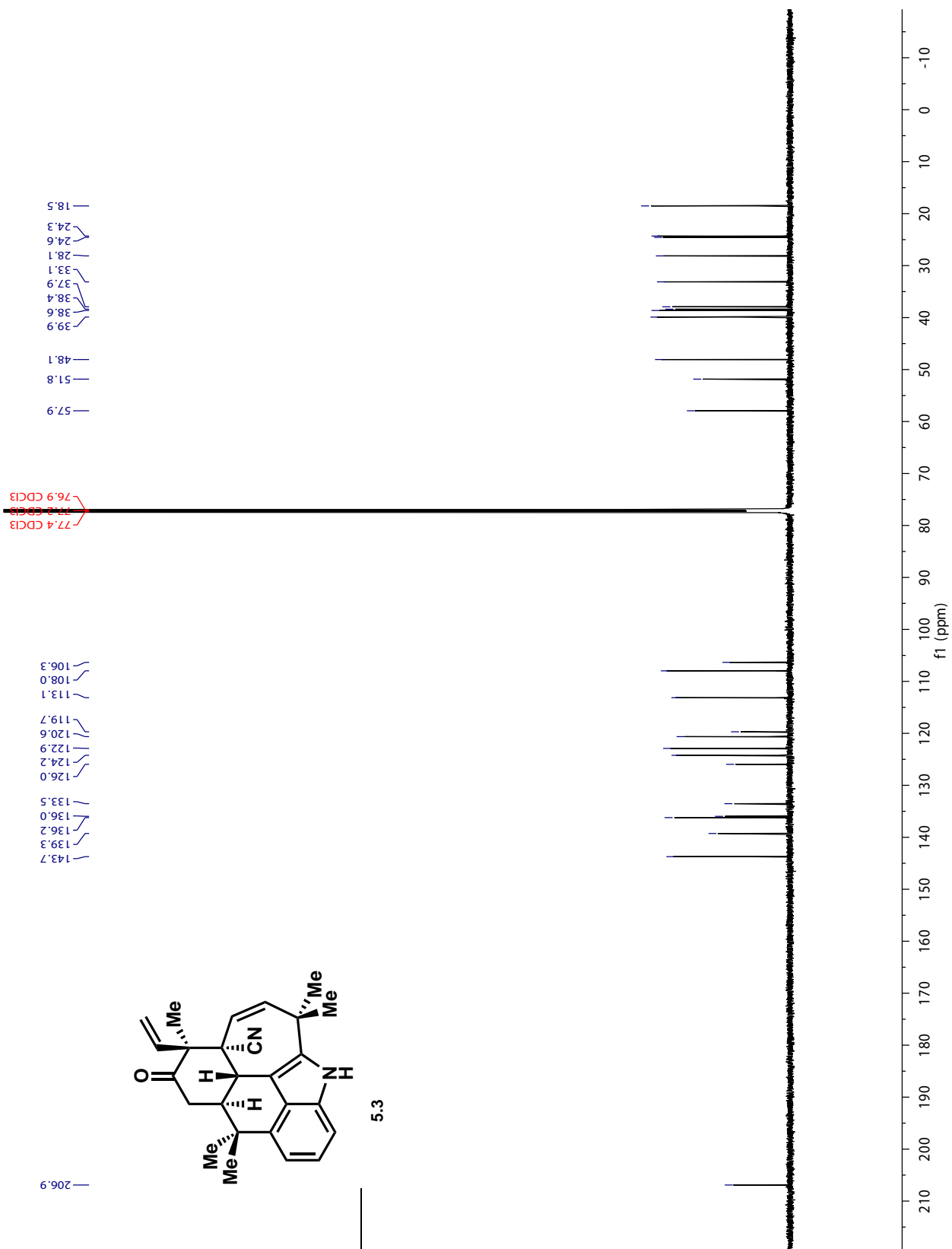


Figure 5.4: ^{13}C NMR of **5.3** in CDCl_3

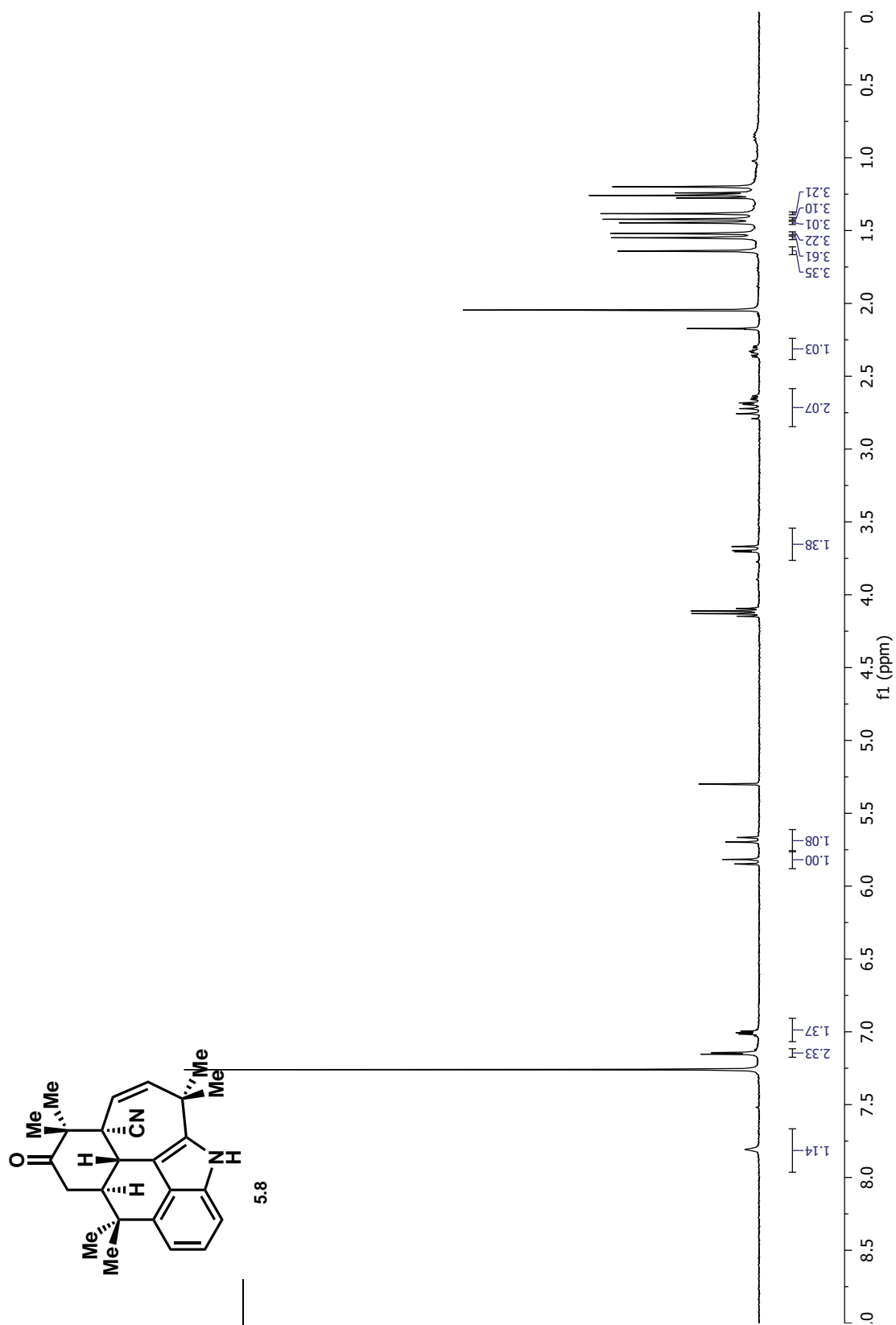


Figure 5.5: ^1H NMR of **5.8** in CDCl_3

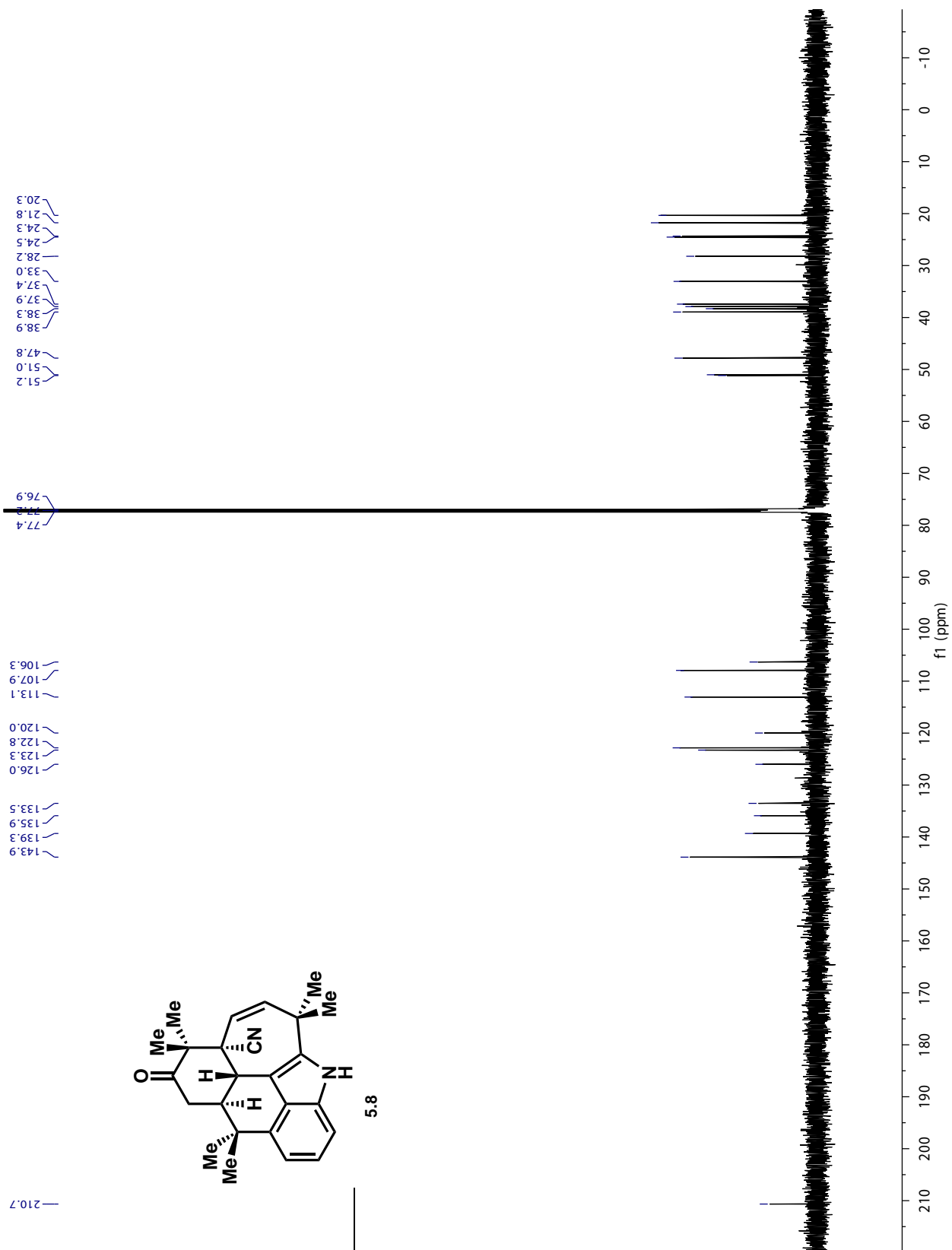


Figure 5.6: ^{13}C NMR of 5.8 in CDCl_3

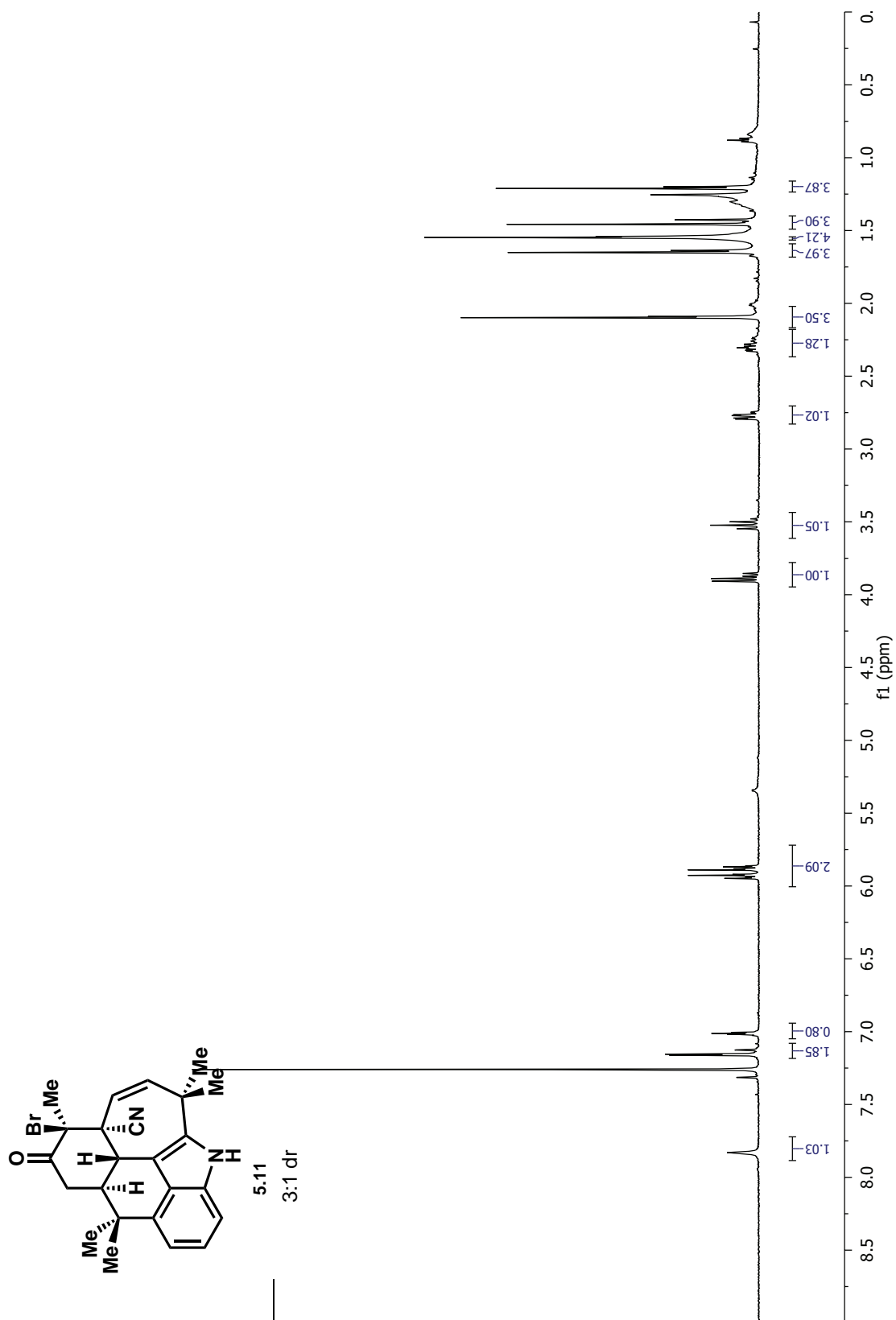


Figure 5.7: ^1H NMR of 5.11 in CDCl_3

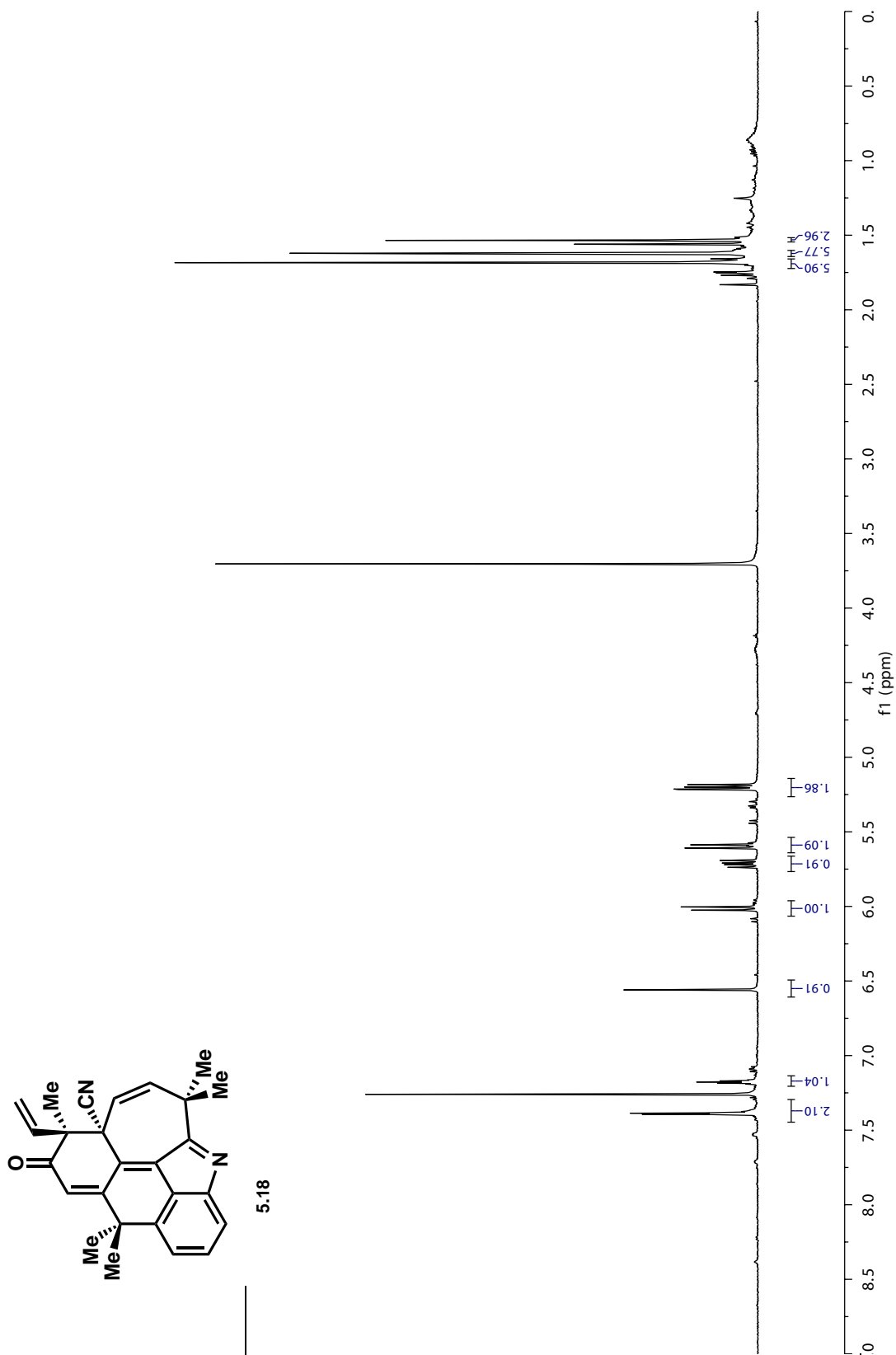


Figure 5.8: ¹H NMR of 5.18 in CDCl₃

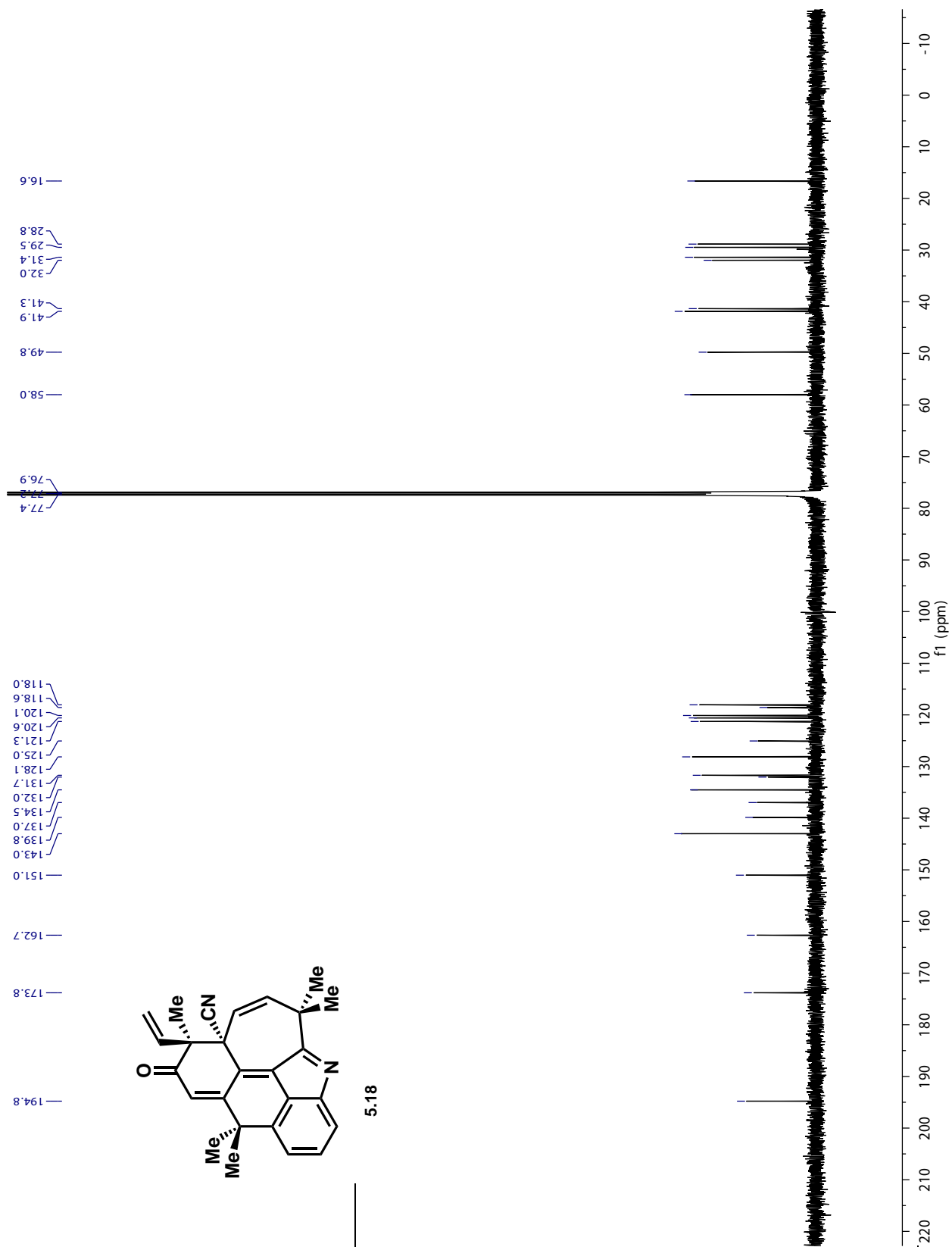


Figure 5.9: ¹³C NMR of 5.18 in CDCl₃

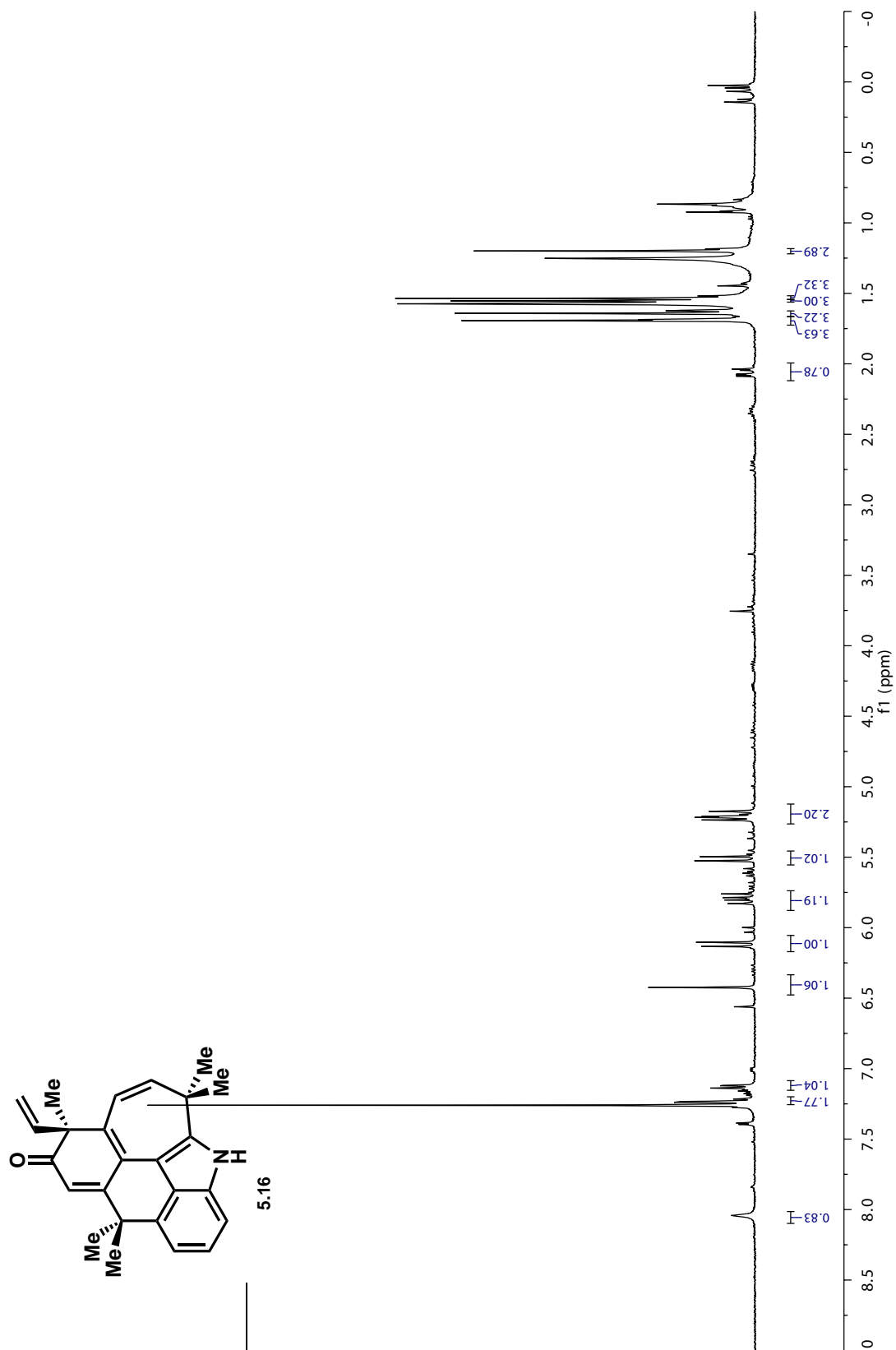


Figure 5.10: ^1H NMR of 5.16 in CDCl₃

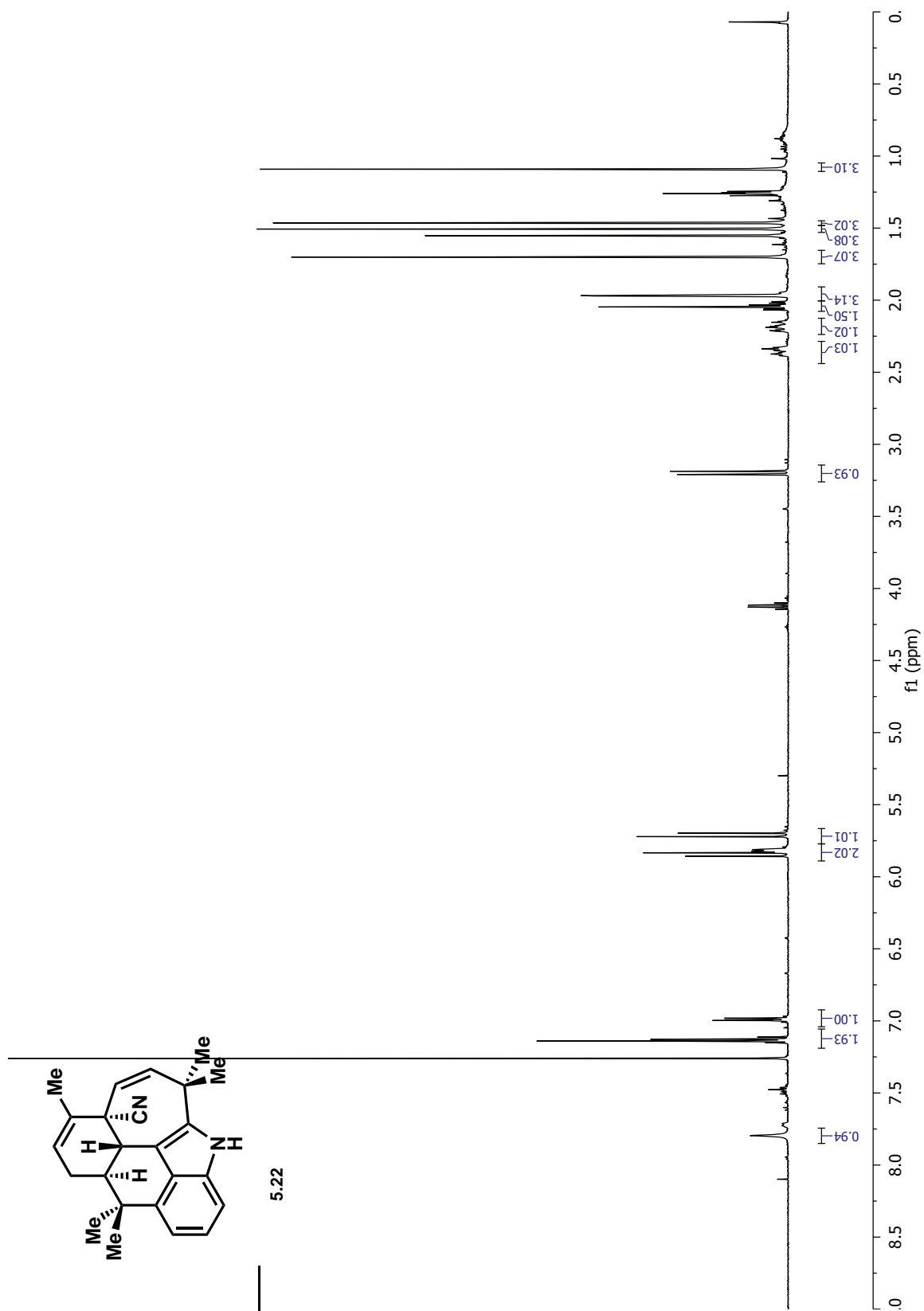


Figure 5.11: ¹H NMR of 5.22 in CDCl₃

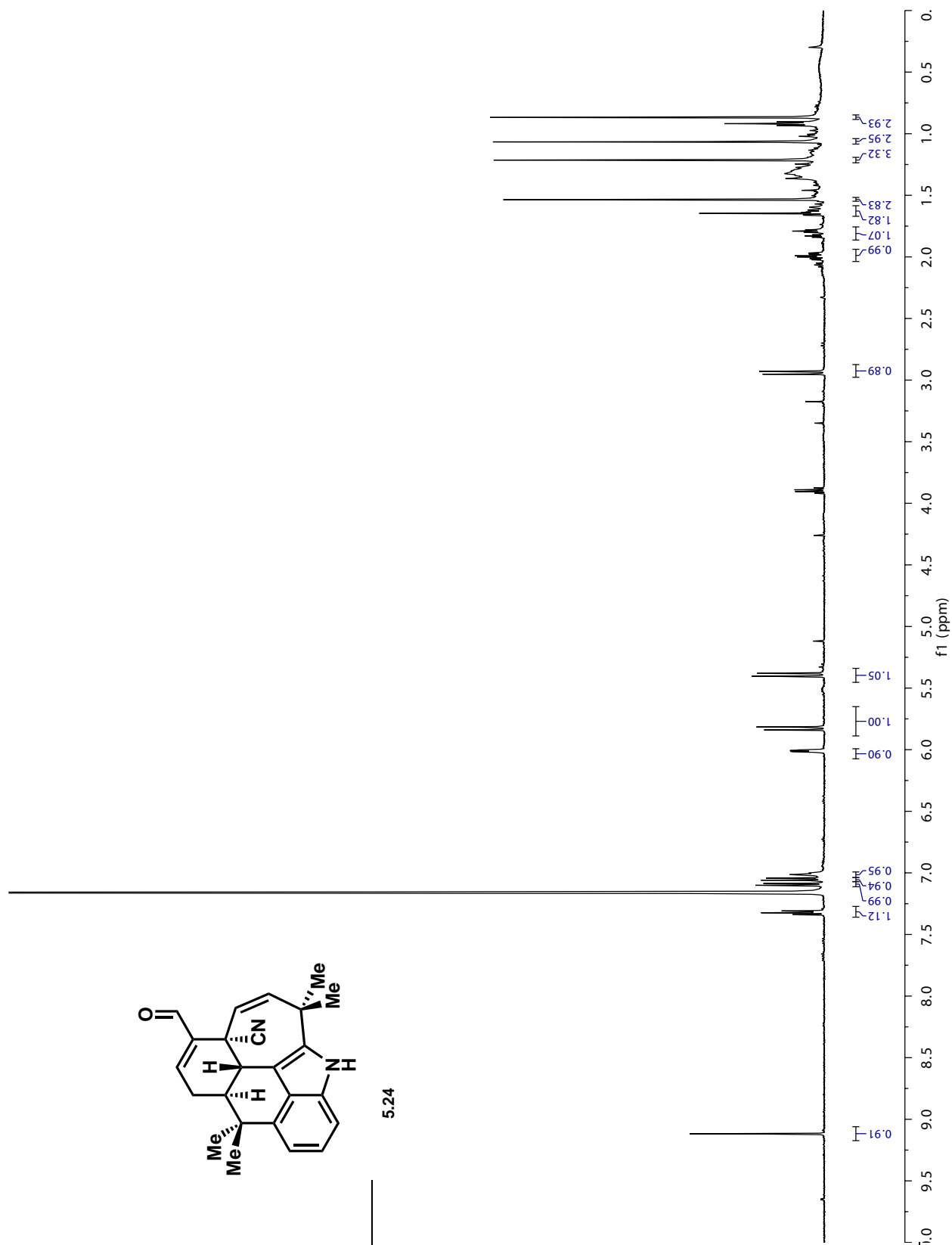


Figure 5.12: ¹H NMR of 5.24 in C₆D₆

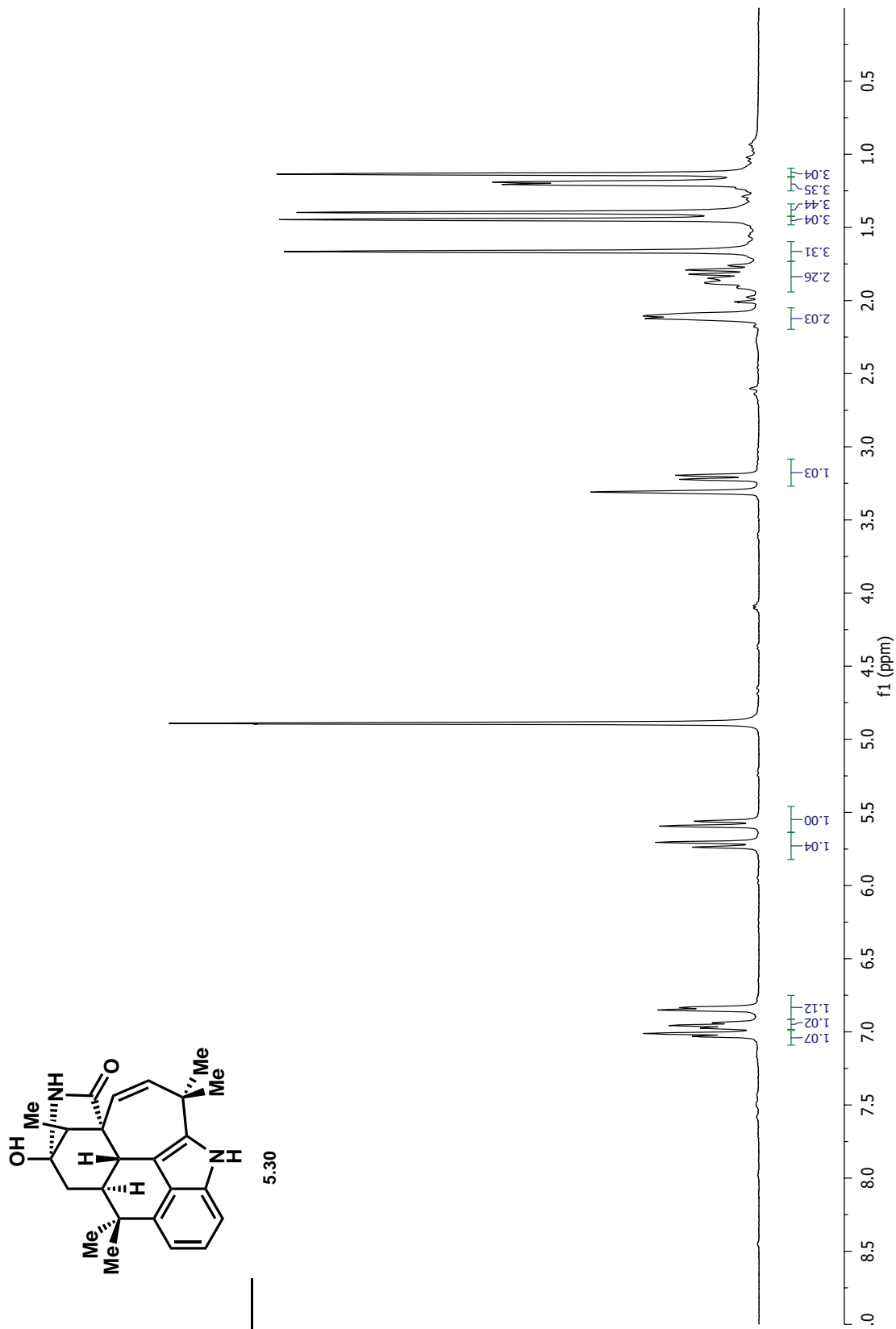


Figure 5.13: ^1H NMR of 5.30 in CD_3OD

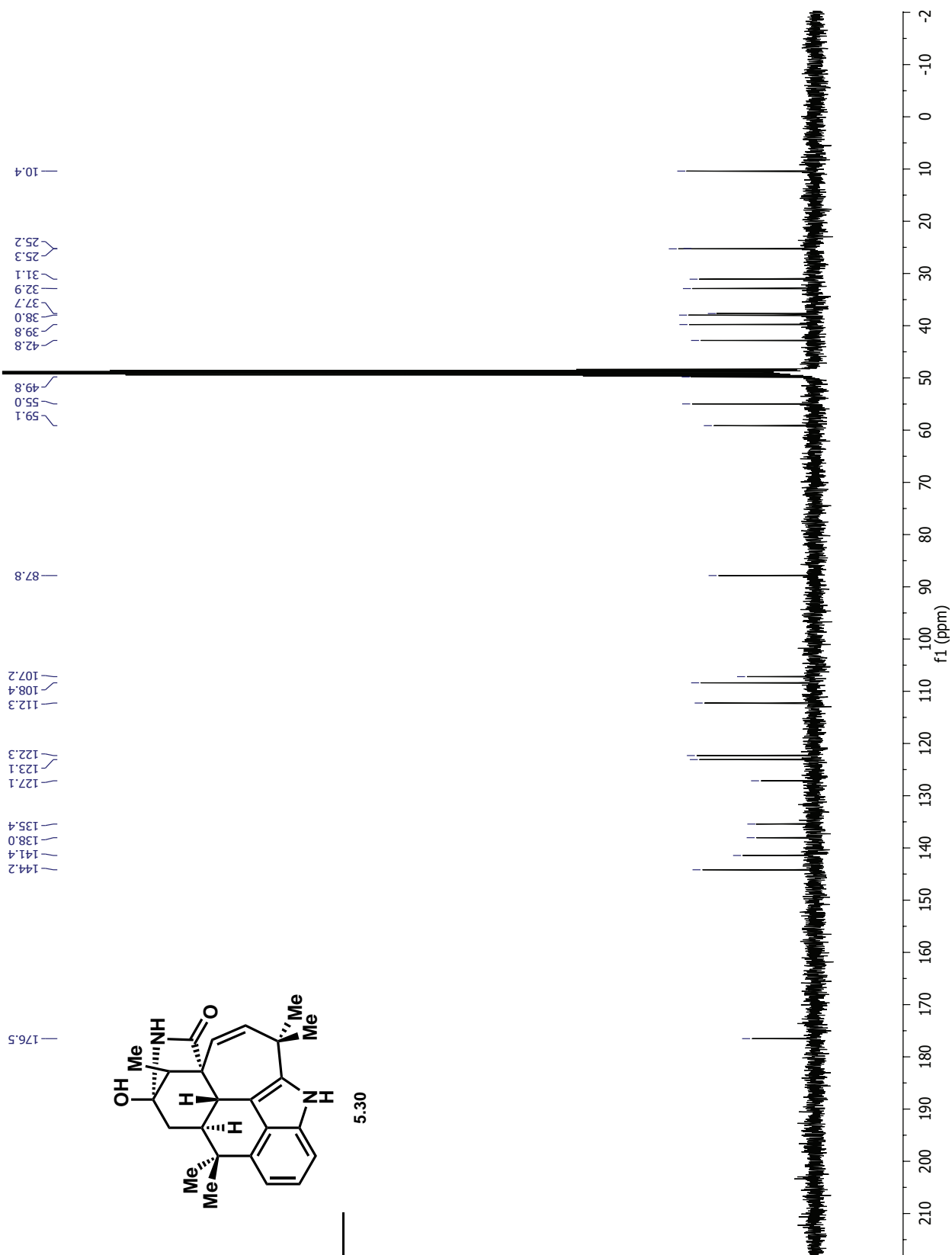


Figure 5.14: ^{13}C NMR of 5.30 in CD_3OD

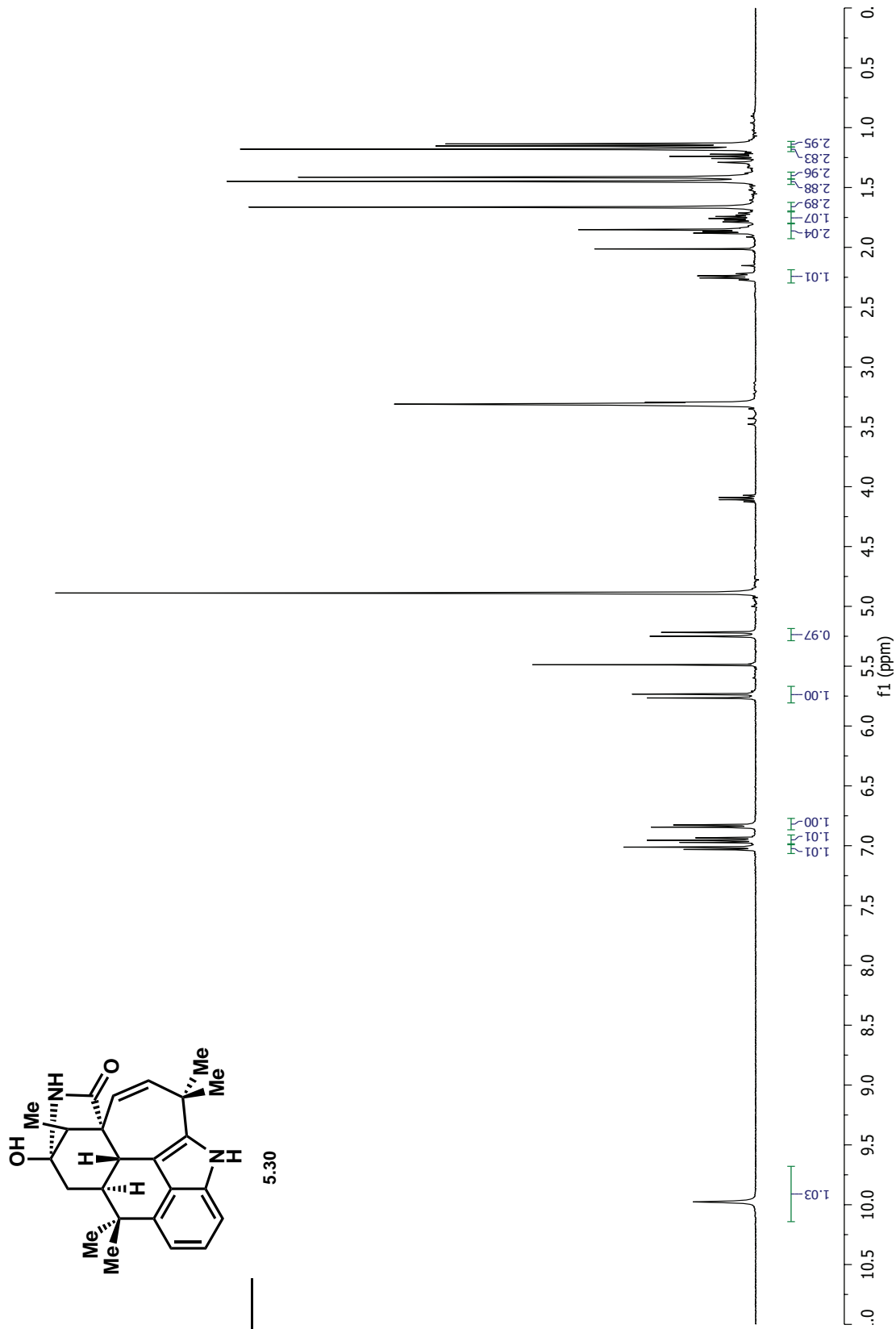


Figure 5.15: ¹H NMR of 5.30 in CD₃OD

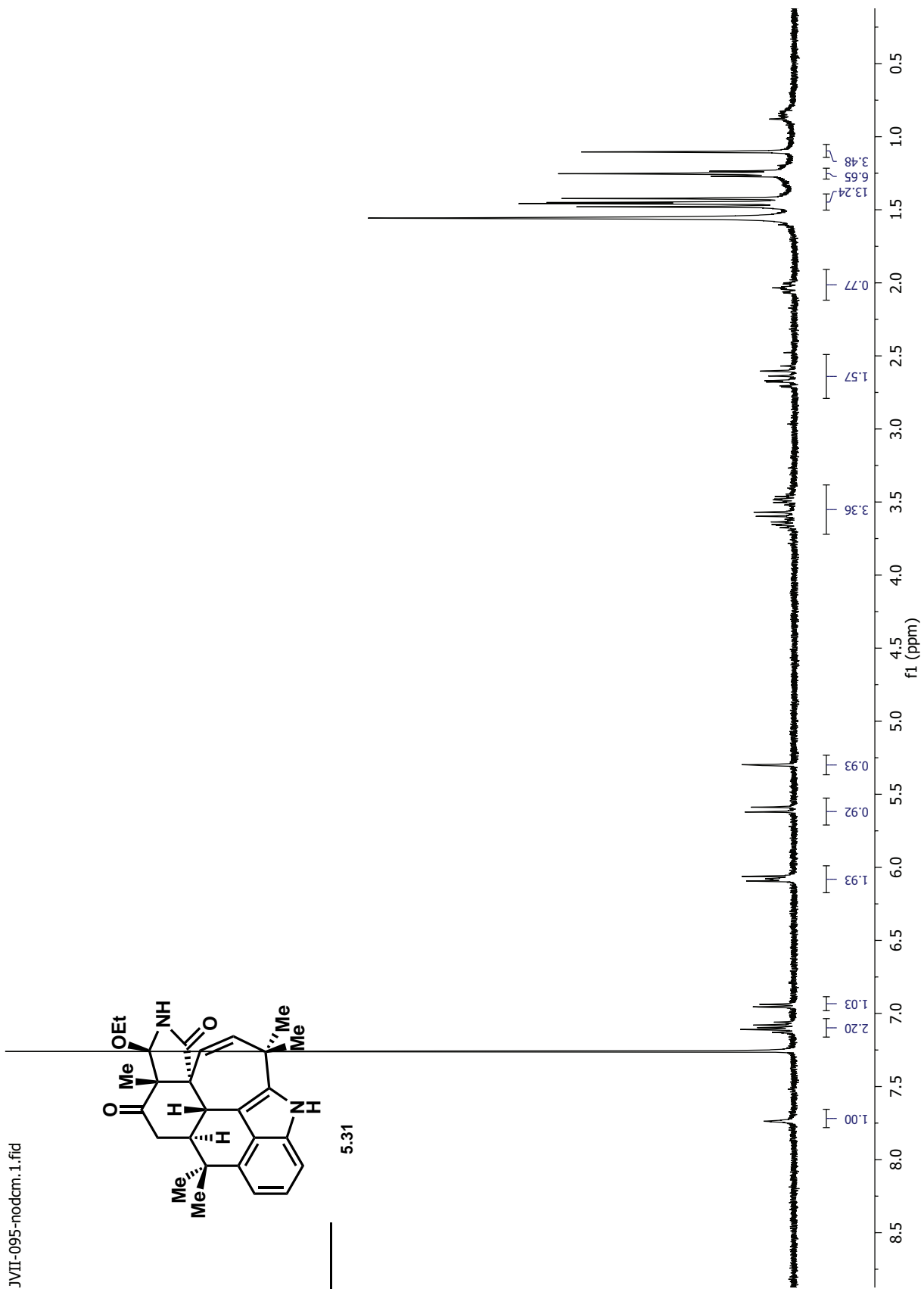


Figure 5.16: ^1H NMR of 5.31 in CDCl_3

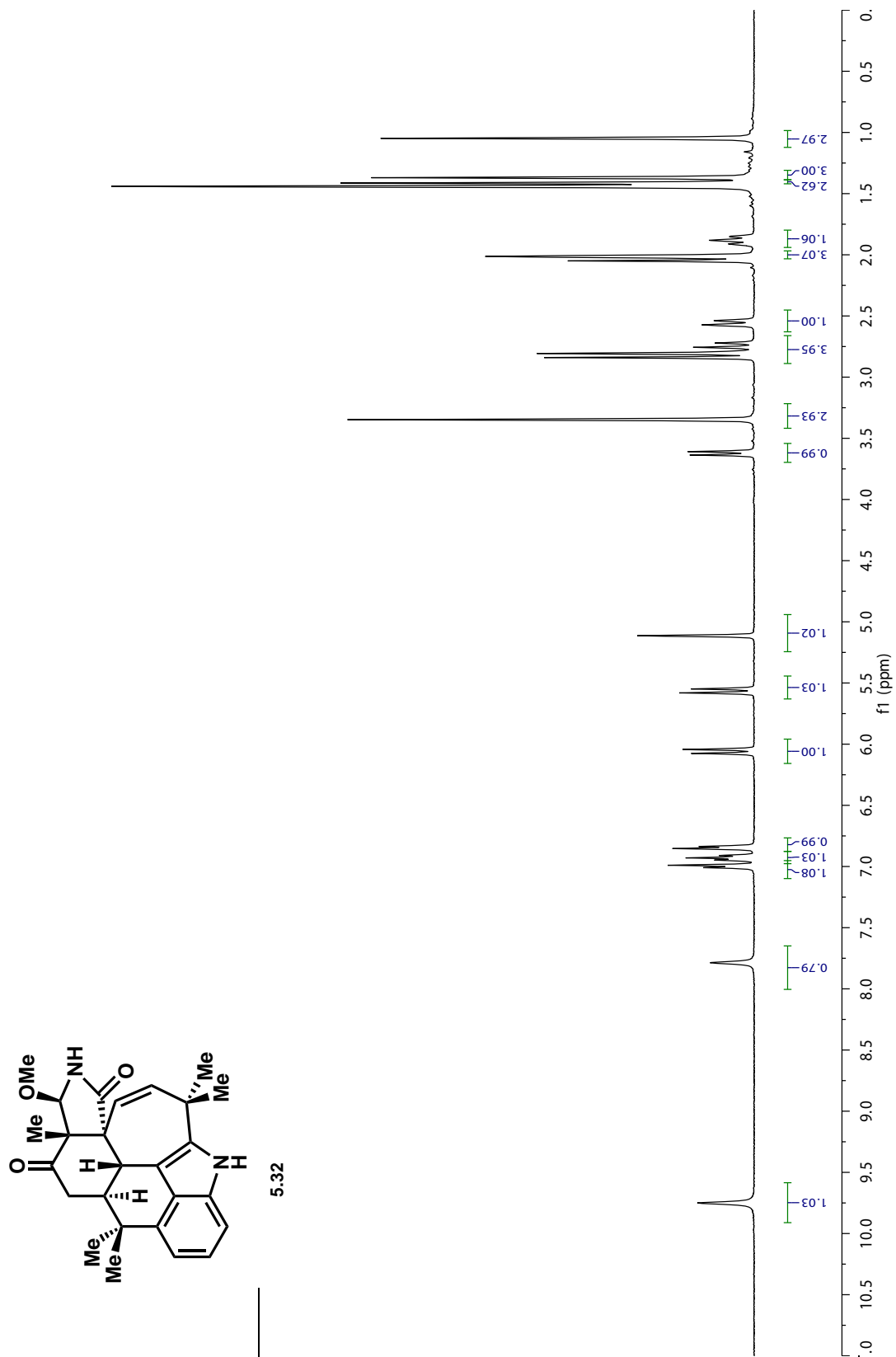


Figure 5.17: ^1H NMR of 5.32 in $(\text{CD}_3)_2\text{CO}$

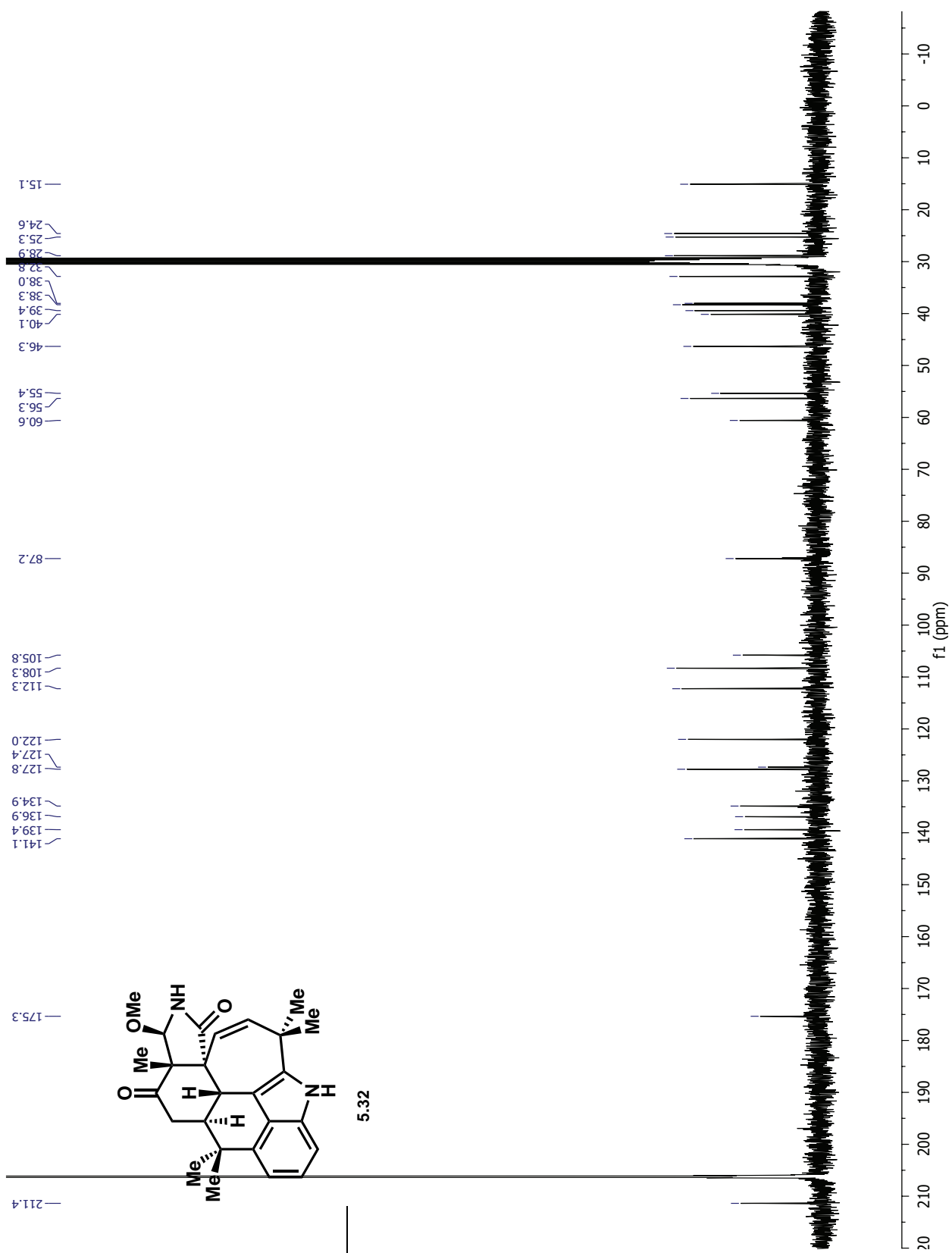


Figure 5.18: ^{13}C NMR of 5.32 in $(\text{CD}_3)_2\text{CO}$

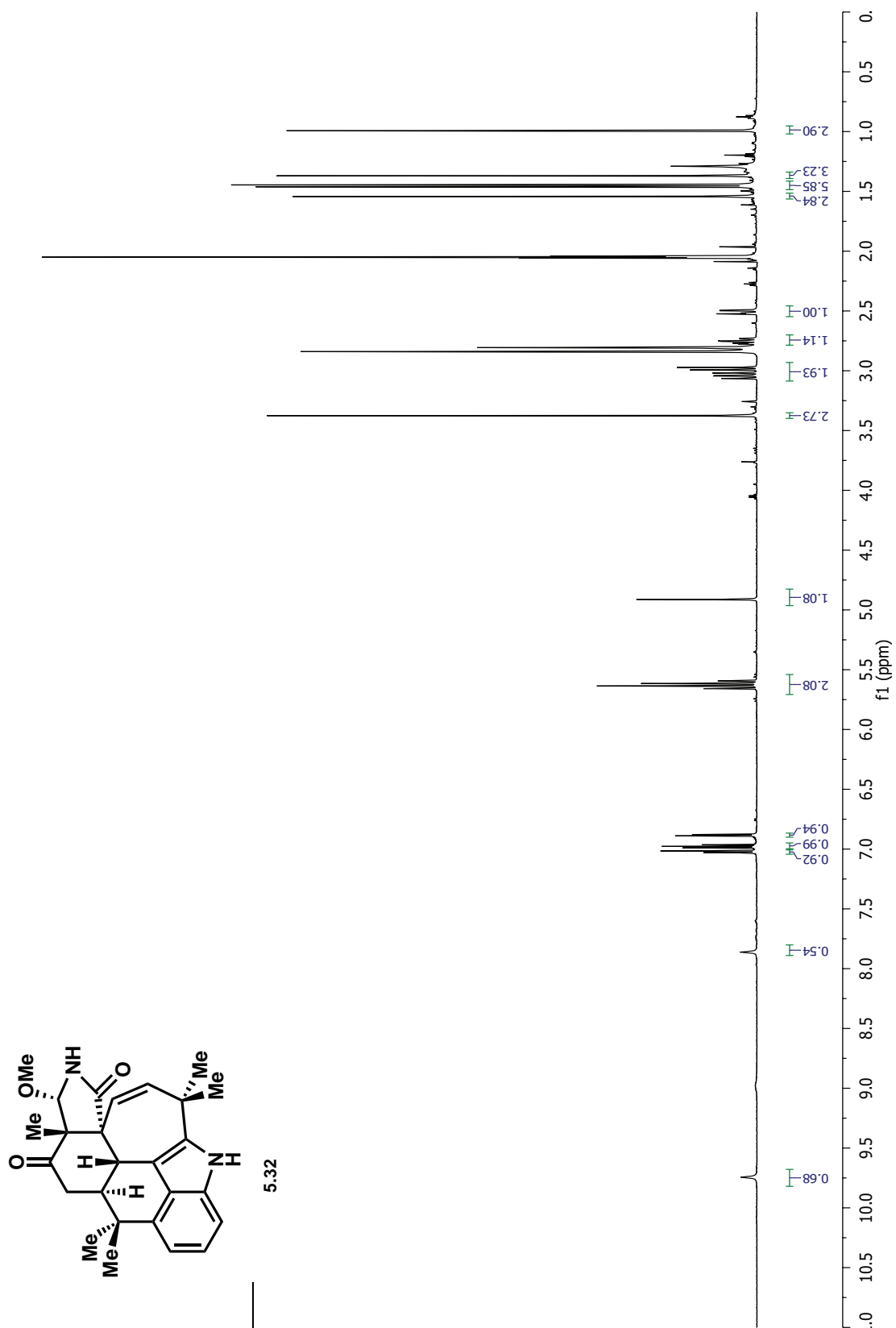


Figure 5.19: ^1H NMR of 5.32 in $(\text{CD}_3)_2\text{CO}$

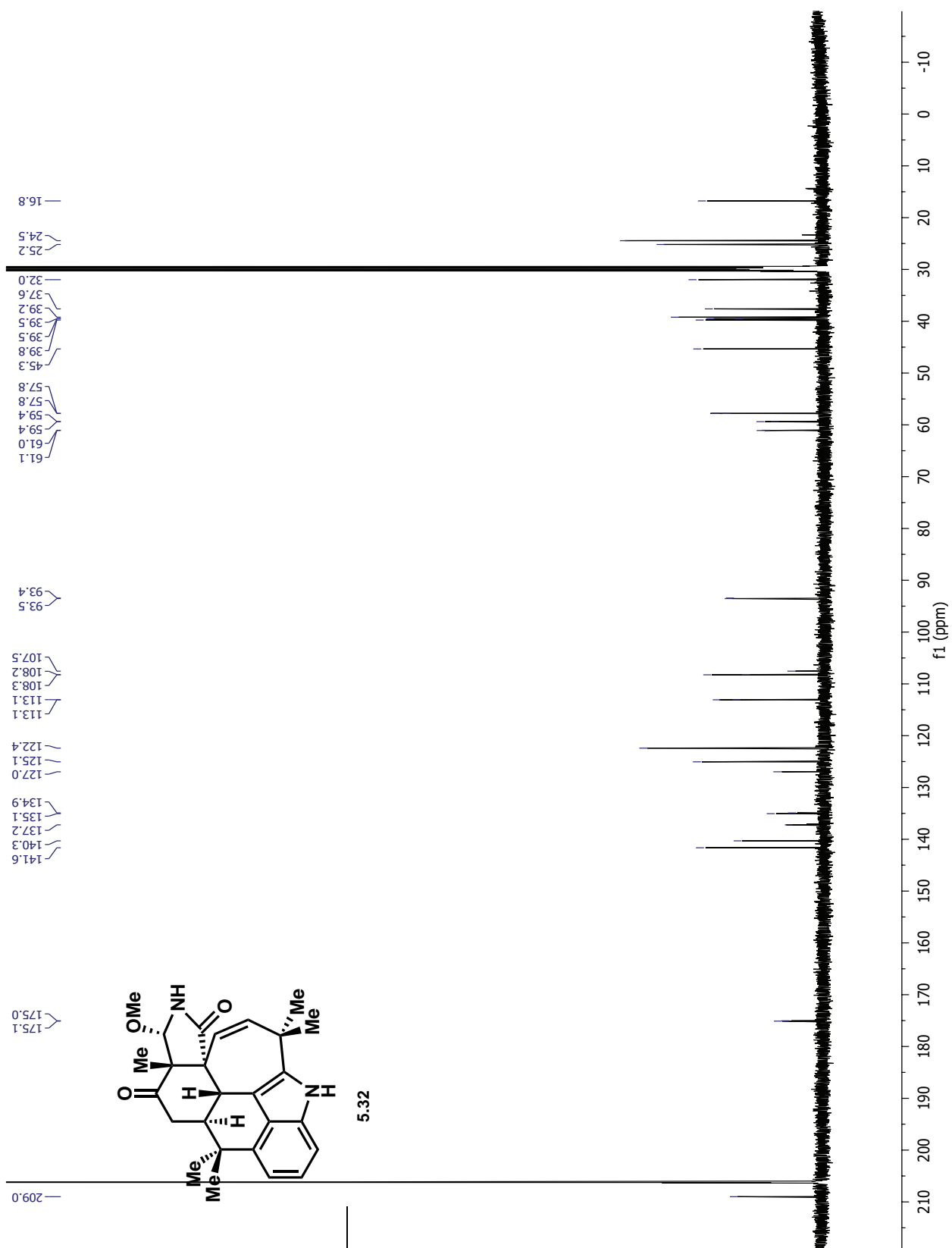


Figure 5.20: ¹³C NMR of 5.32 in (CD₃)₂CO

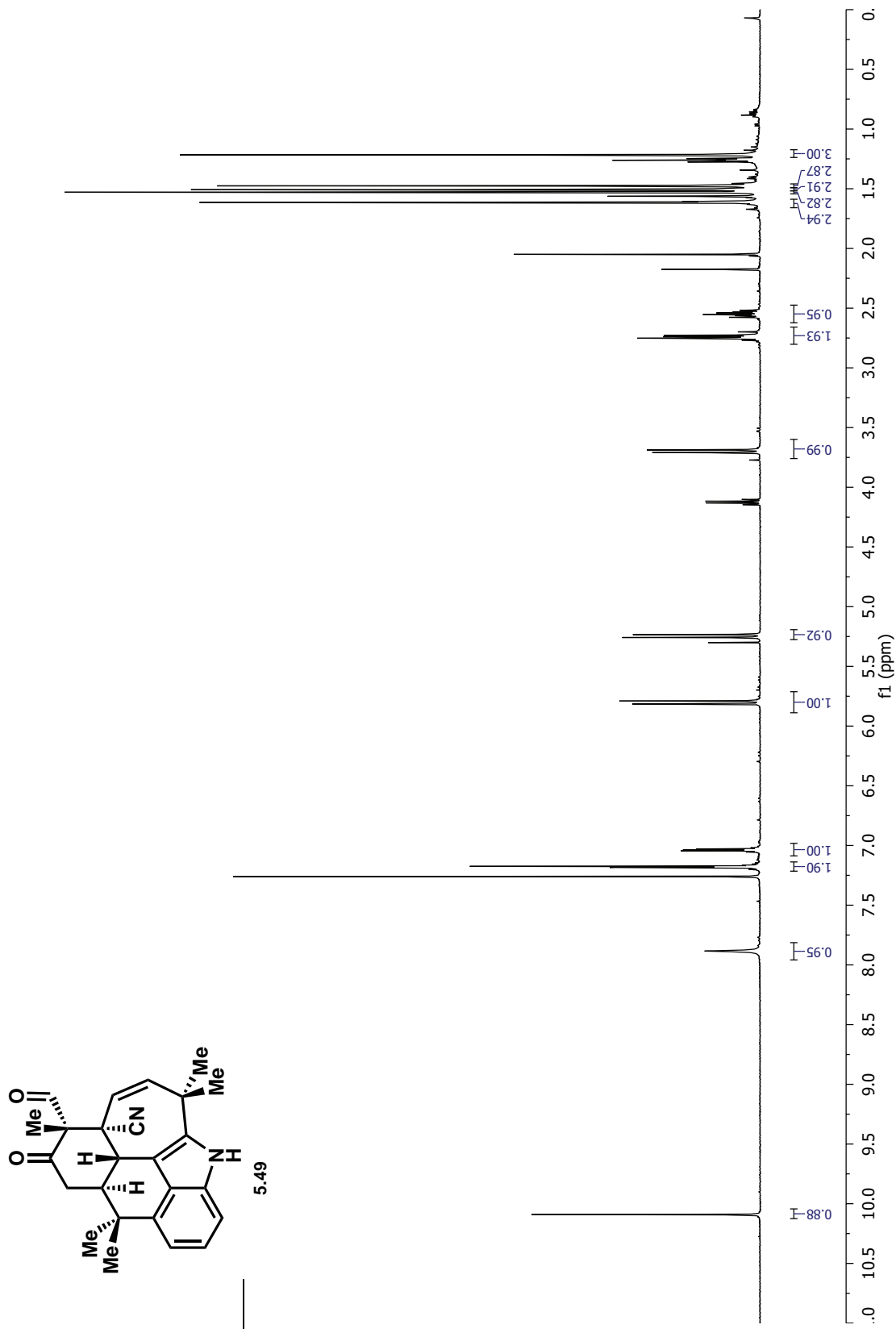


Figure 5.21: ^1H NMR of **5.49** in CDCl_3

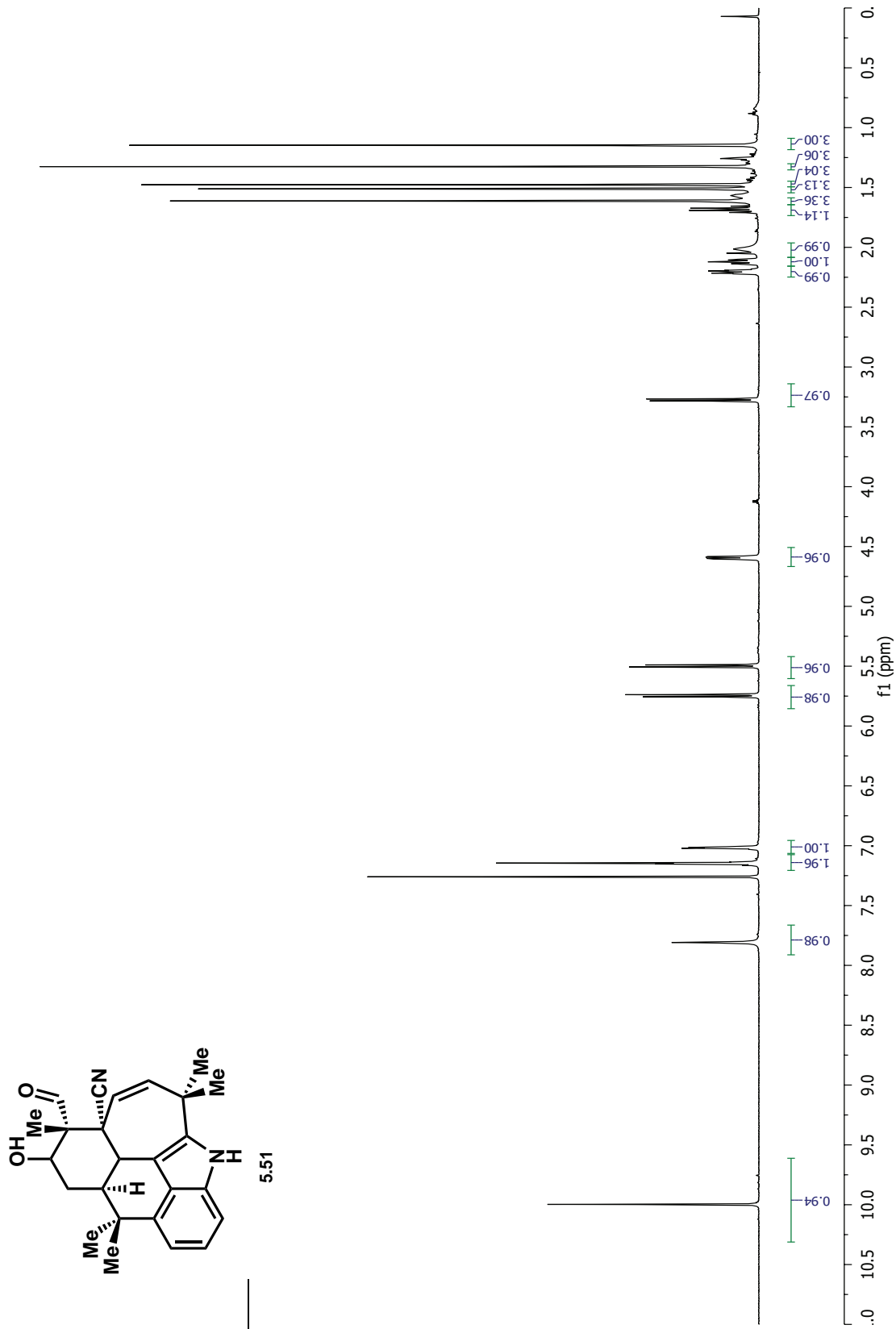


Figure 5.22: ¹H NMR of 5.51 in CDCl₃

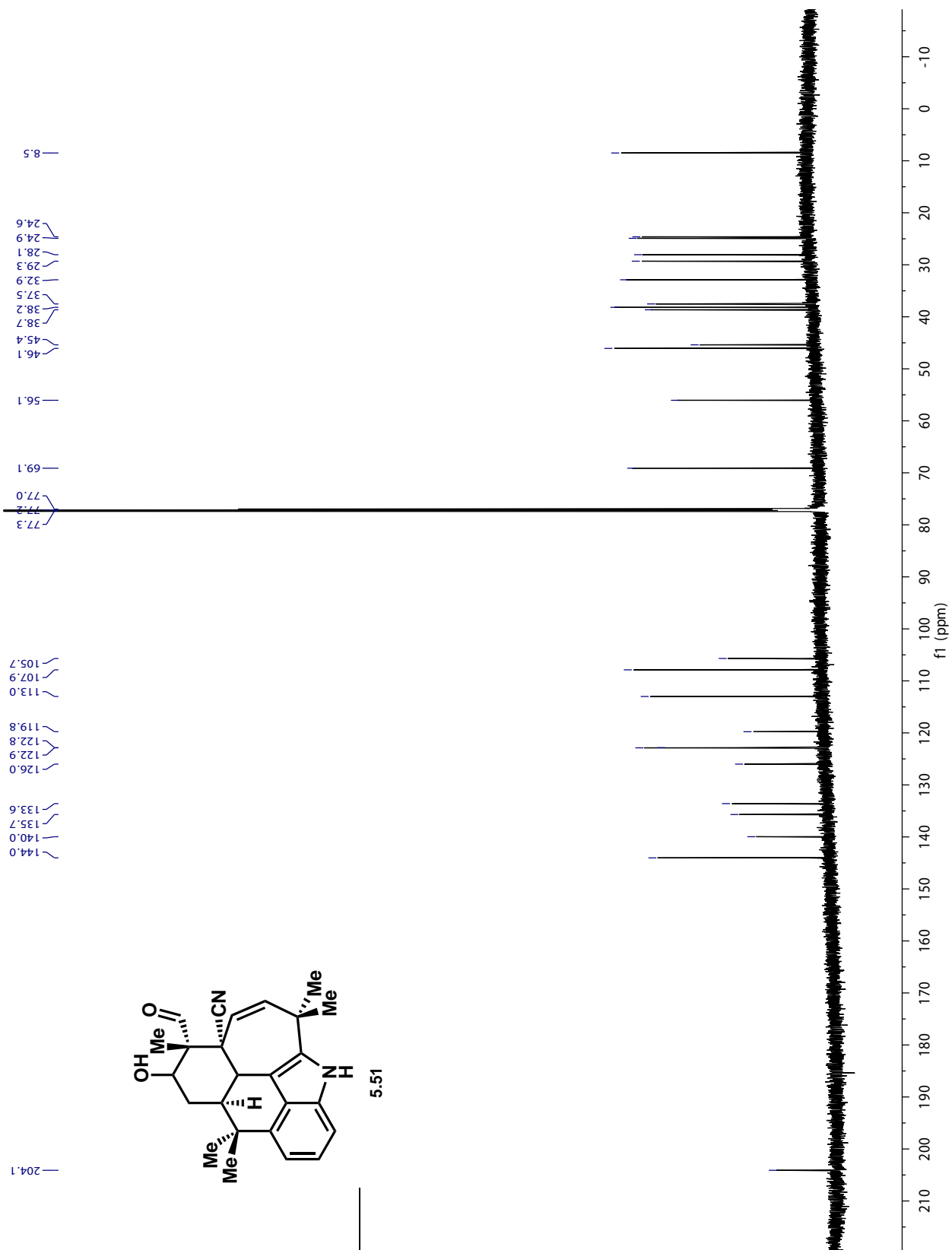


Figure 5.23: ^{13}C NMR of 5.51 in CDCl_3

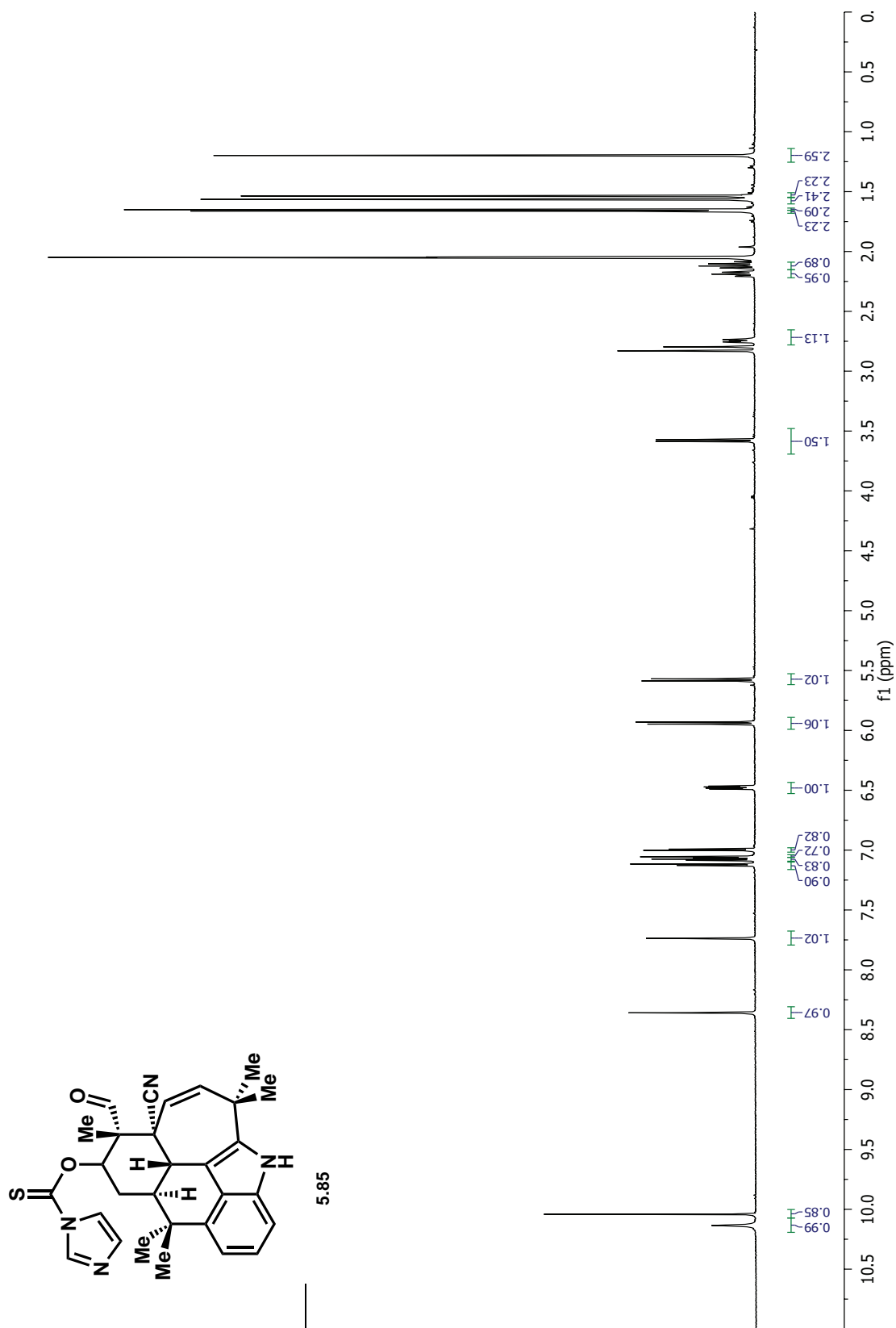


Figure 5.24: ^1H NMR of 5.85 in $(\text{CD}_3)_2\text{CO}$

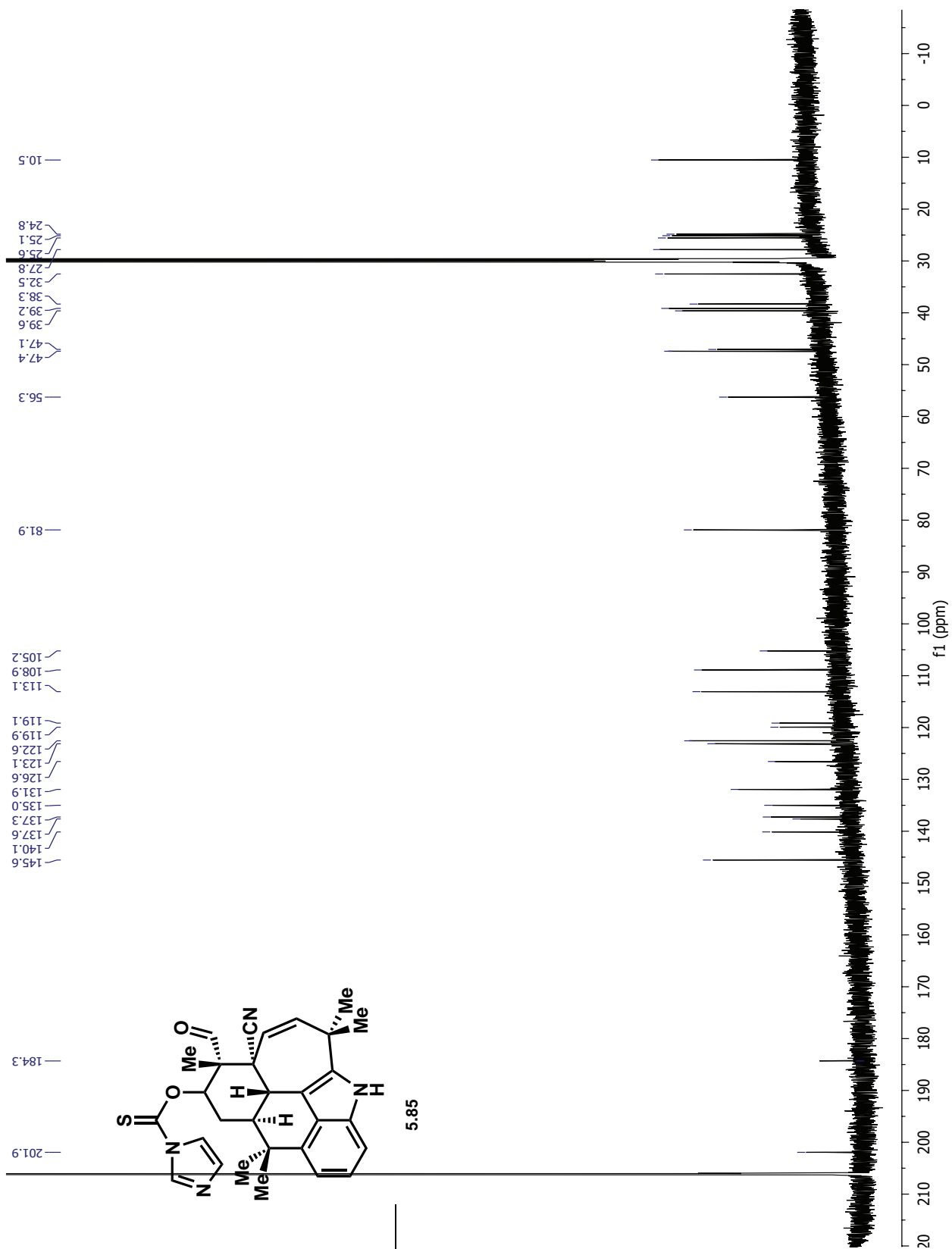


Figure 5.25: ^{13}C NMR of **5.85** in $(\text{CD}_3)_2\text{CO}$

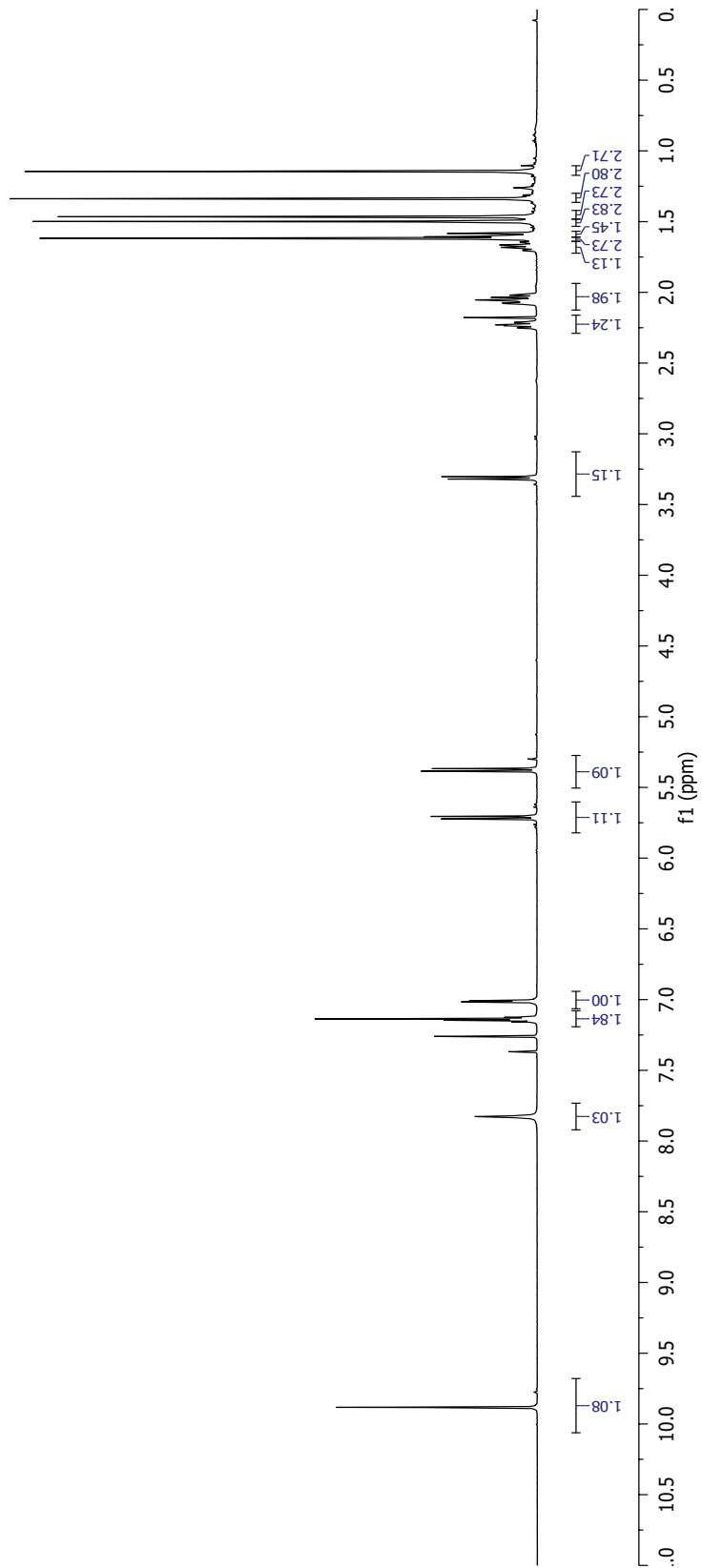
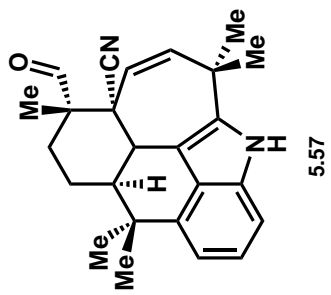


Figure 5.26: ^1H NMR of 5.57 in CDCl_3

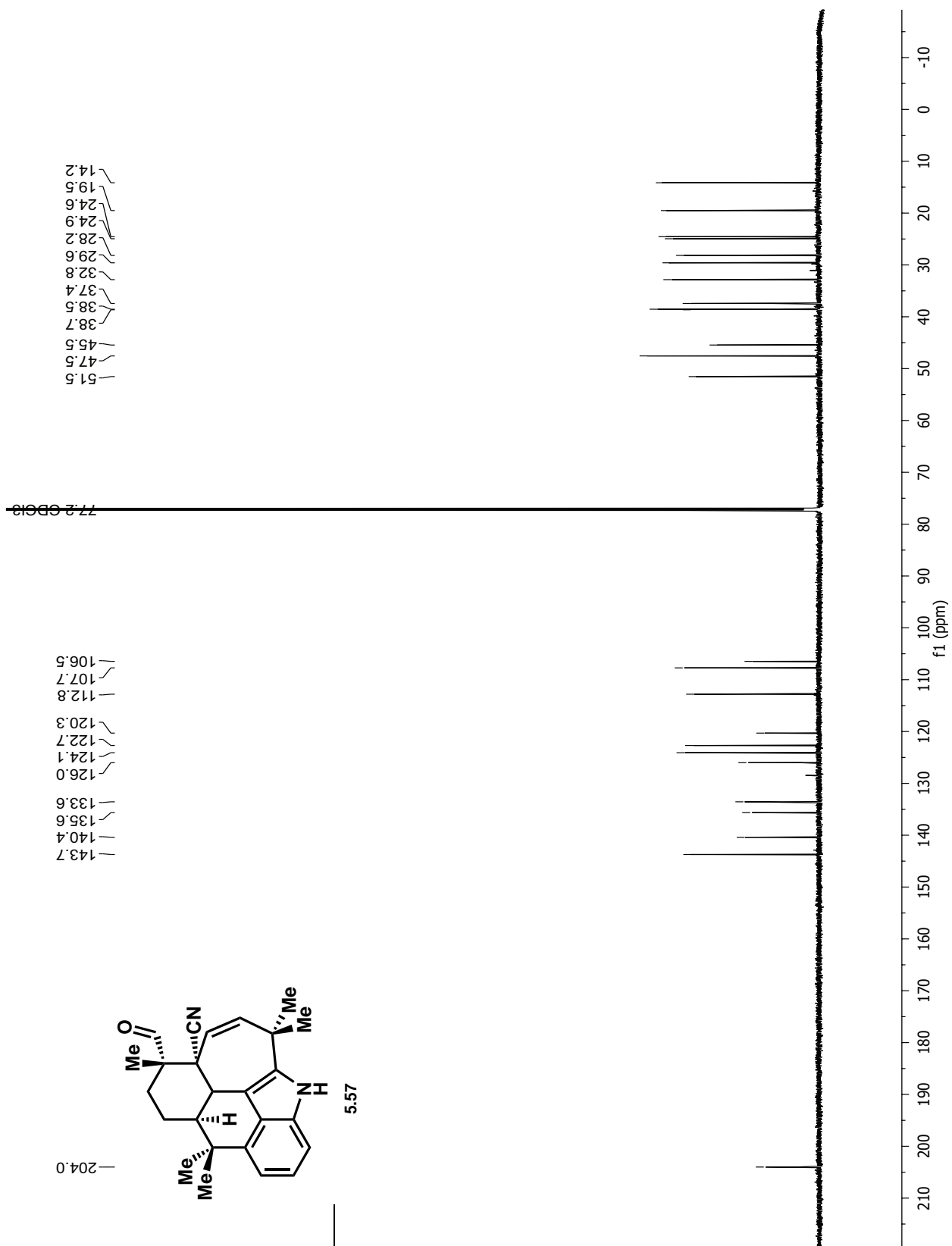


Figure 5.27: ^{13}C NMR of 5.57 in CDCl_3

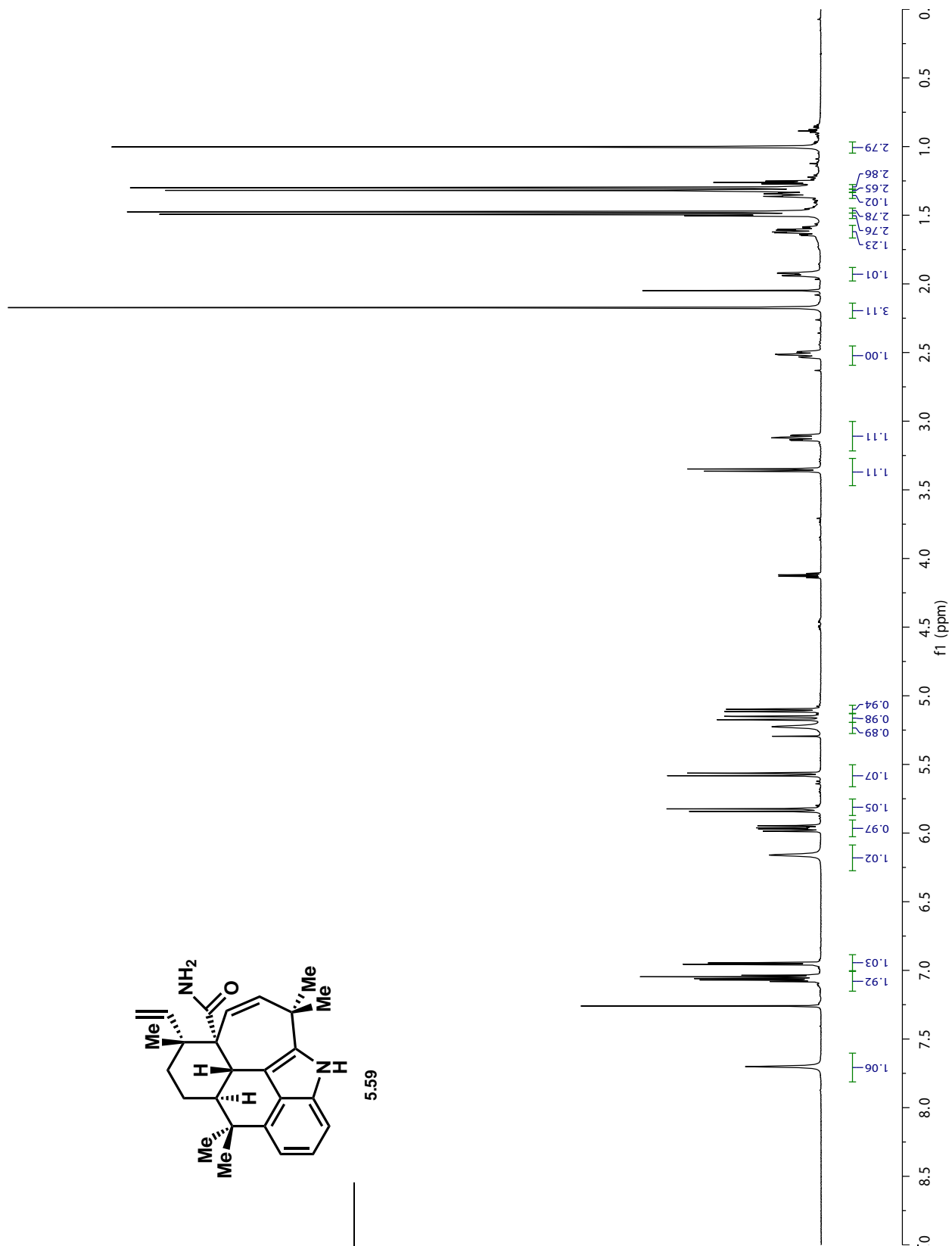


Figure 5.28: ¹H NMR of 5.59 in CDCl₃

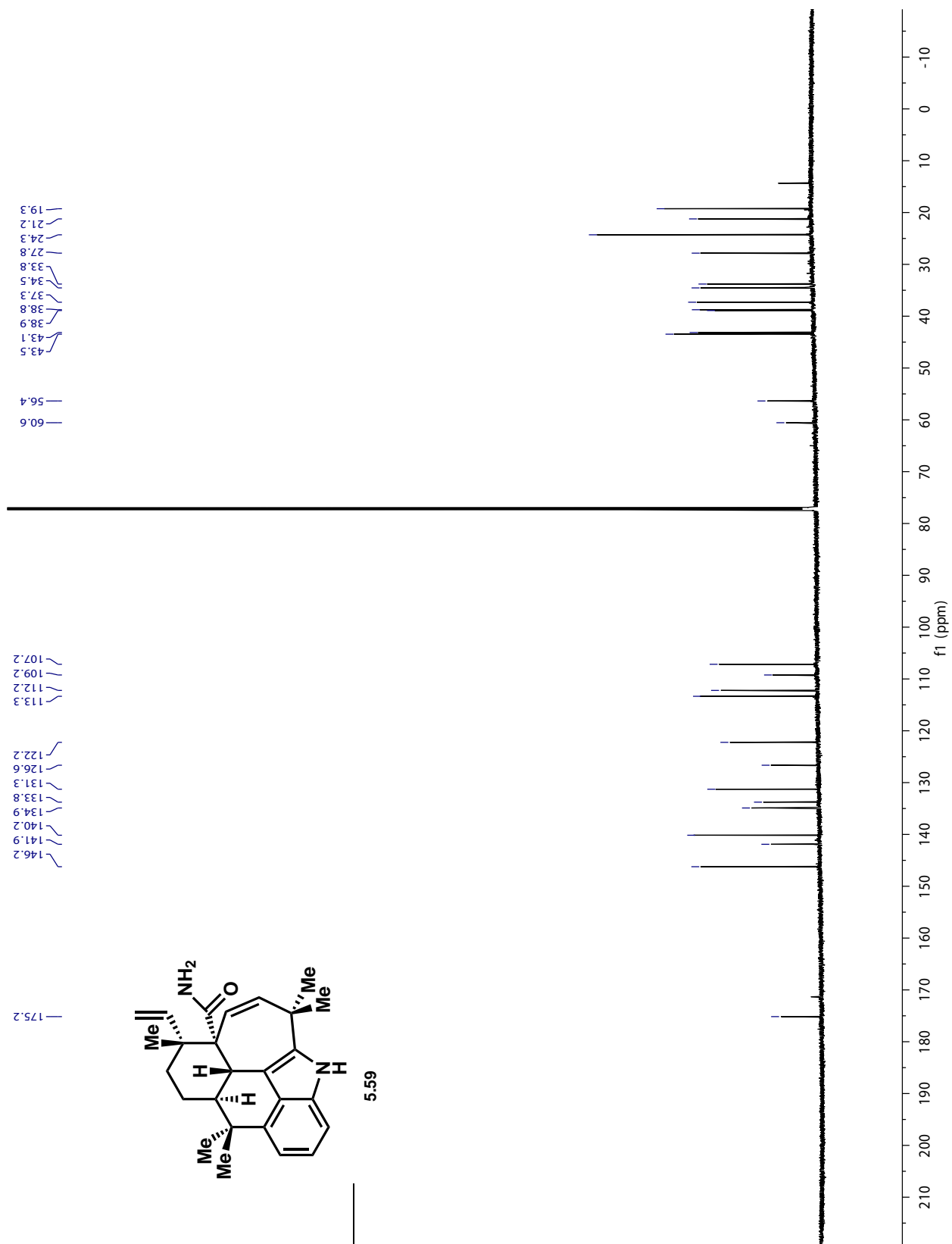


Figure 5.29: ^{13}C NMR of 5.59 in CDCl_3

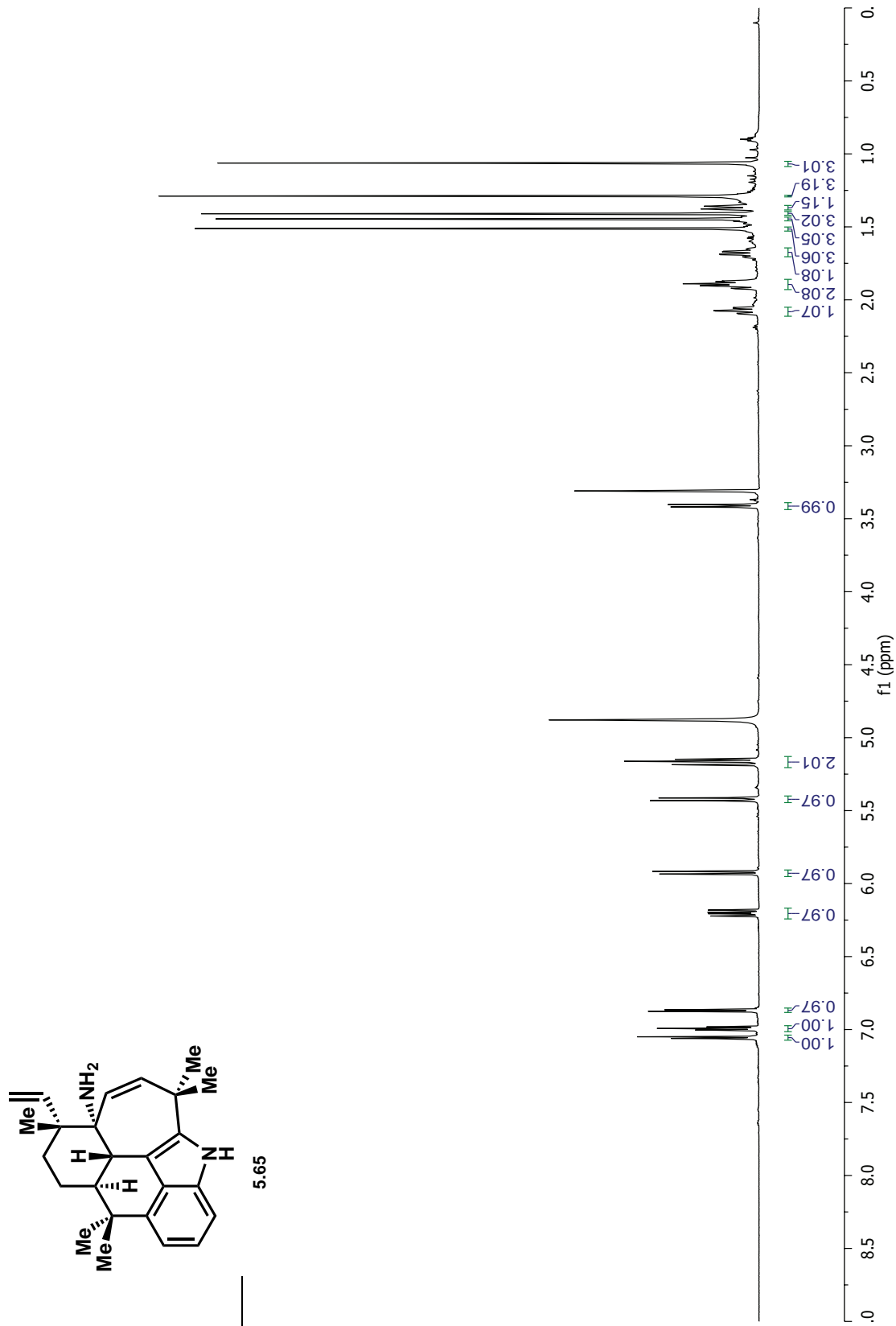


Figure 5.30: ¹H NMR of 5.65 in CD₃OD

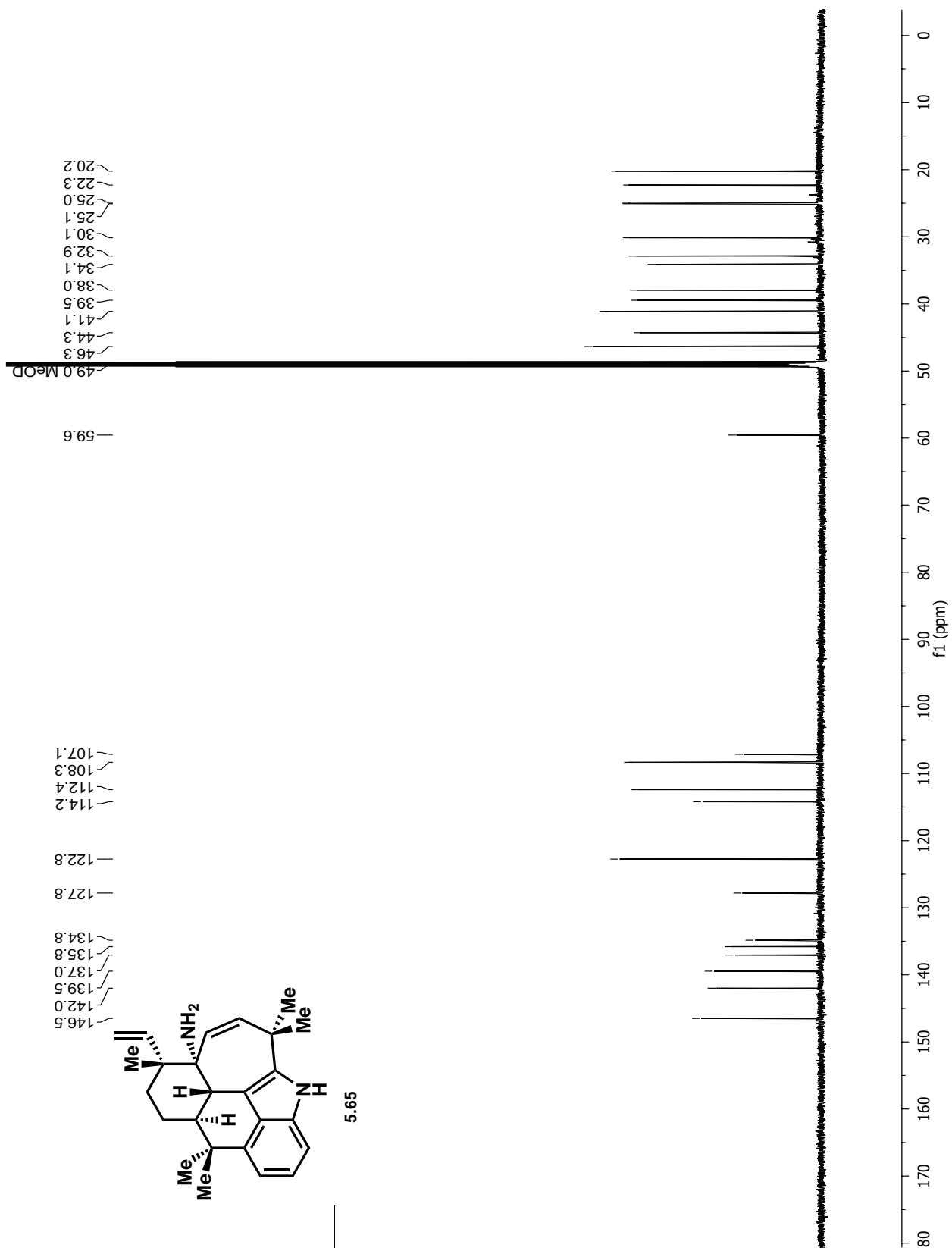


Figure 5.31: ^1H NMR of 5.65 in CD_3OD

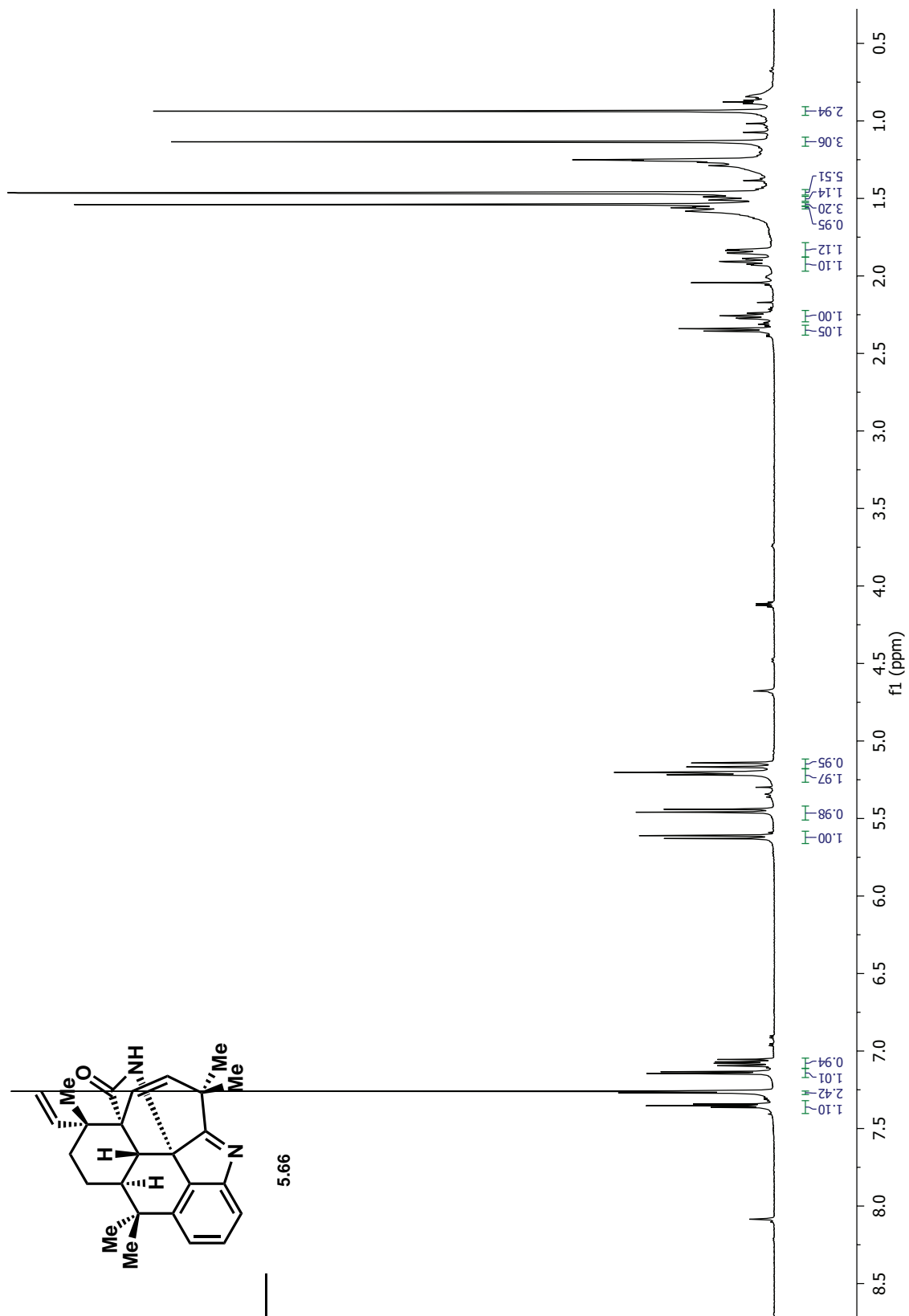


Figure 5.32: ^1H NMR of 5.66 in CDCl_3

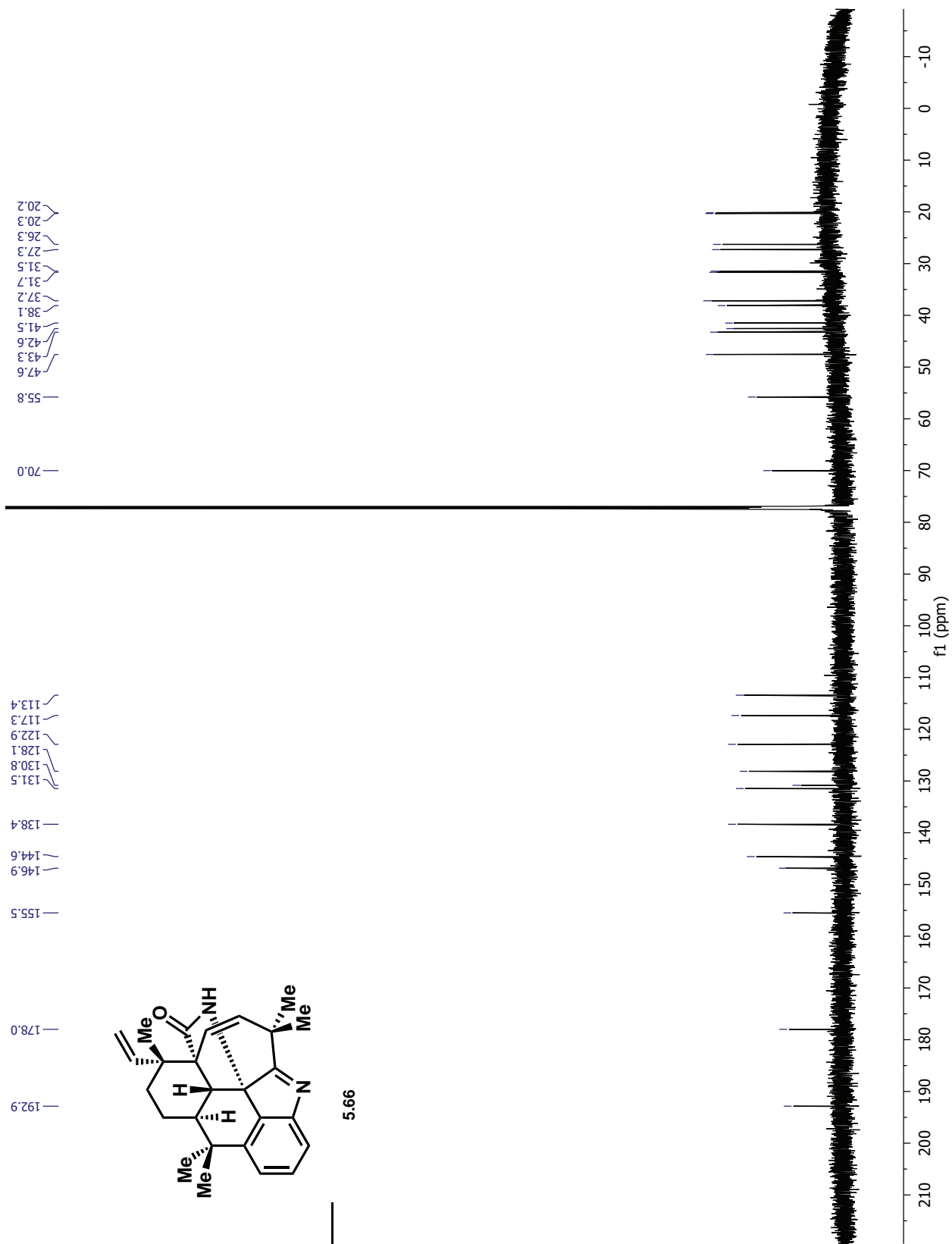


Figure 5.33: ^{13}C NMR of 5.66 in CDCl_3

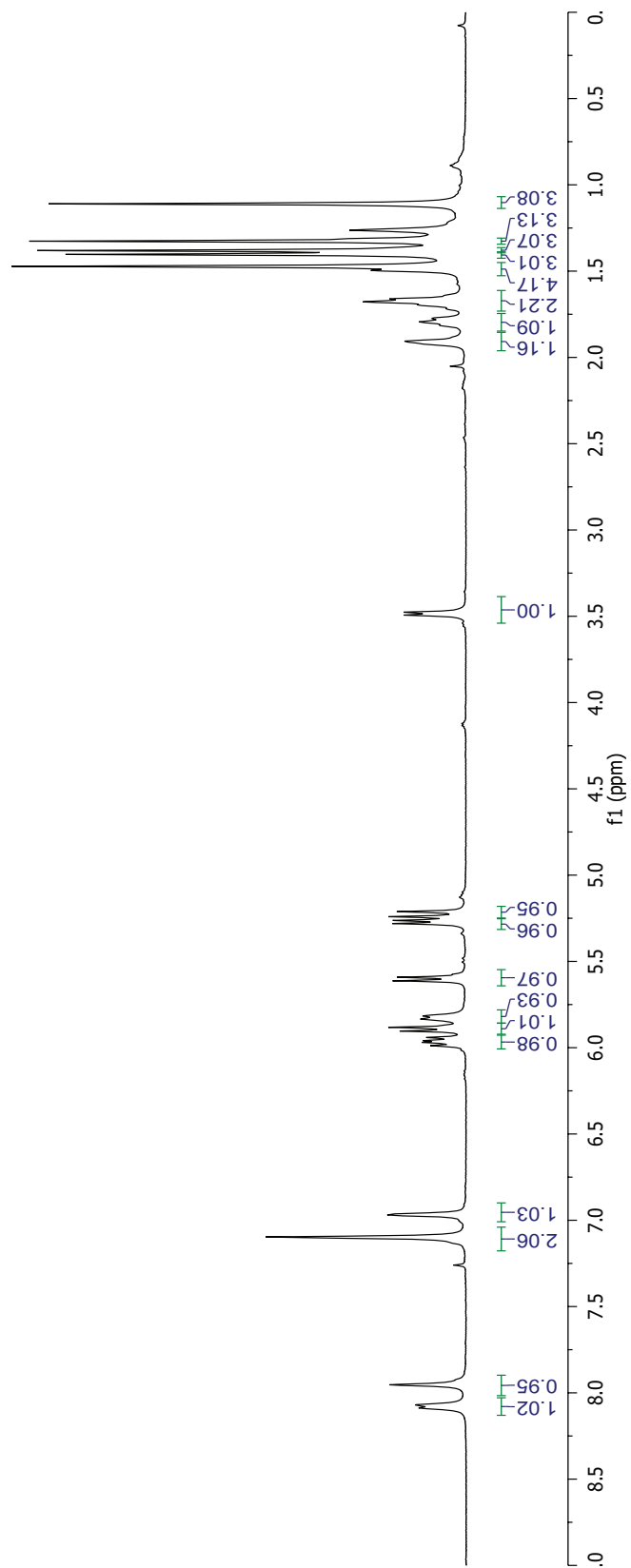
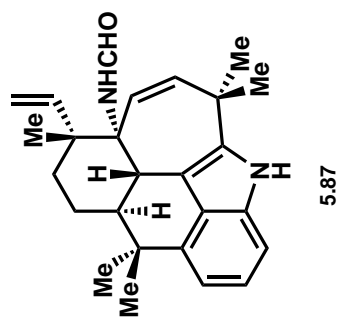


Figure 5.34: ^1H NMR of 5.87 in CDCl_3

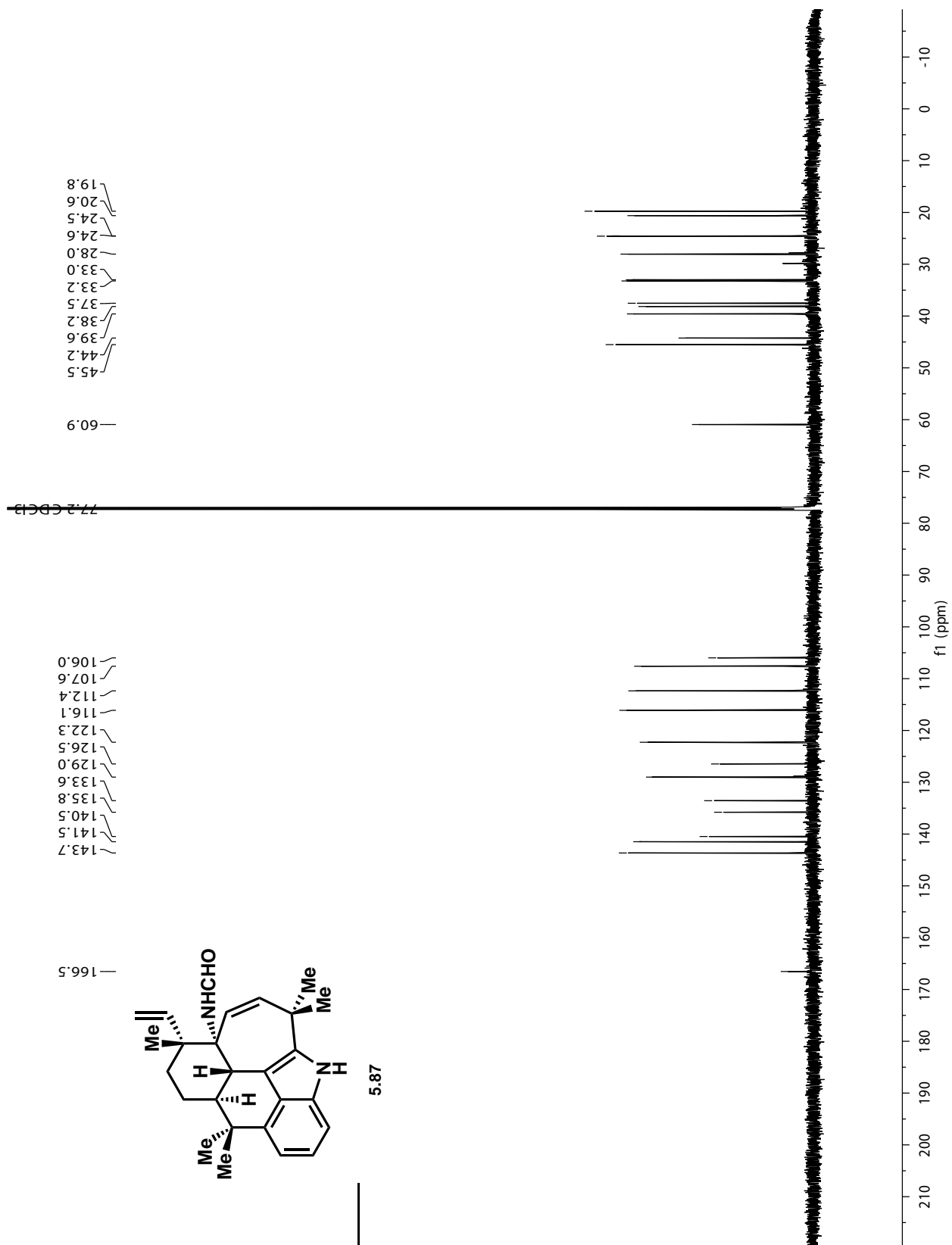


Figure 5.35: ^{13}C NMR of **5.87** in CDCl_3

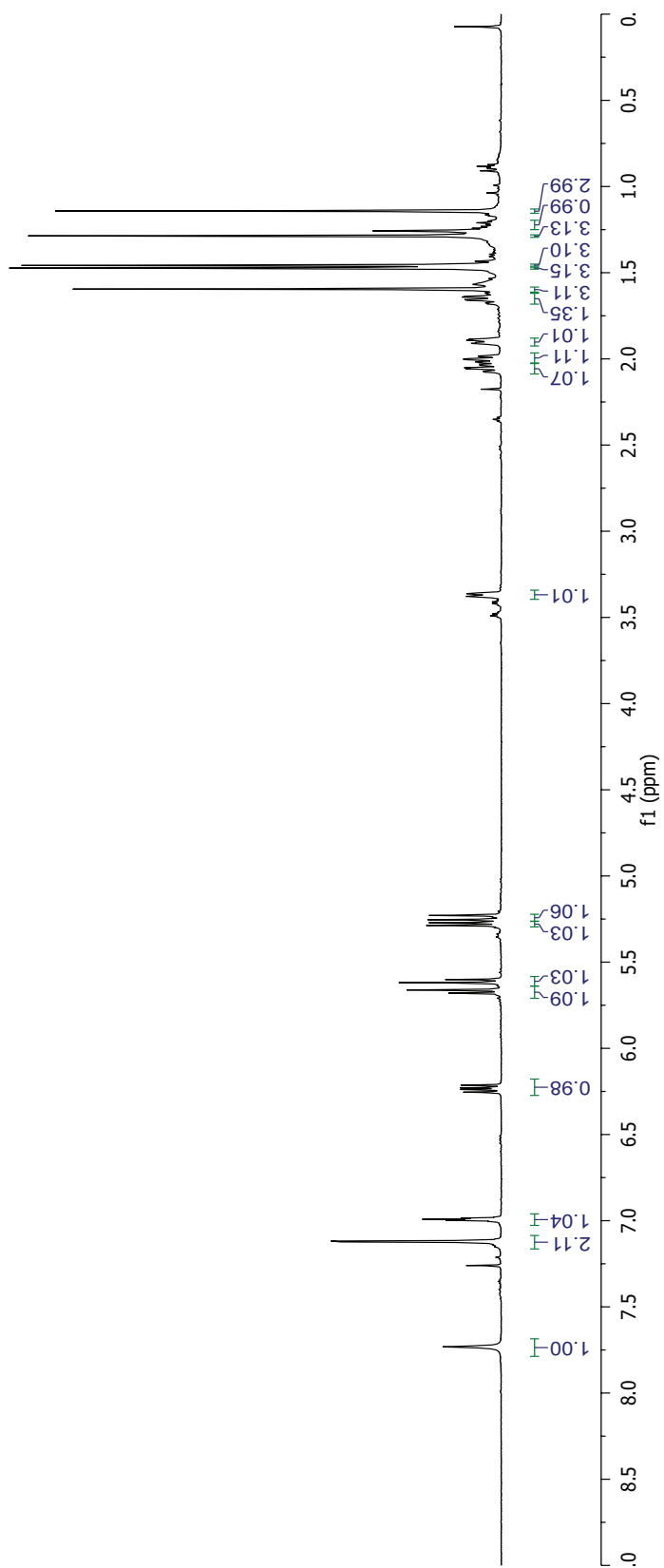
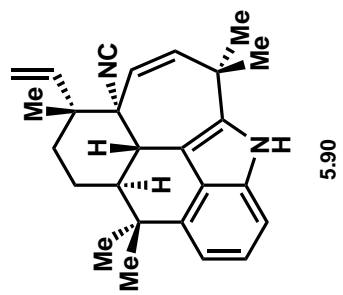


Figure 5.36: ^1H NMR of **5.90** in CDCl_3

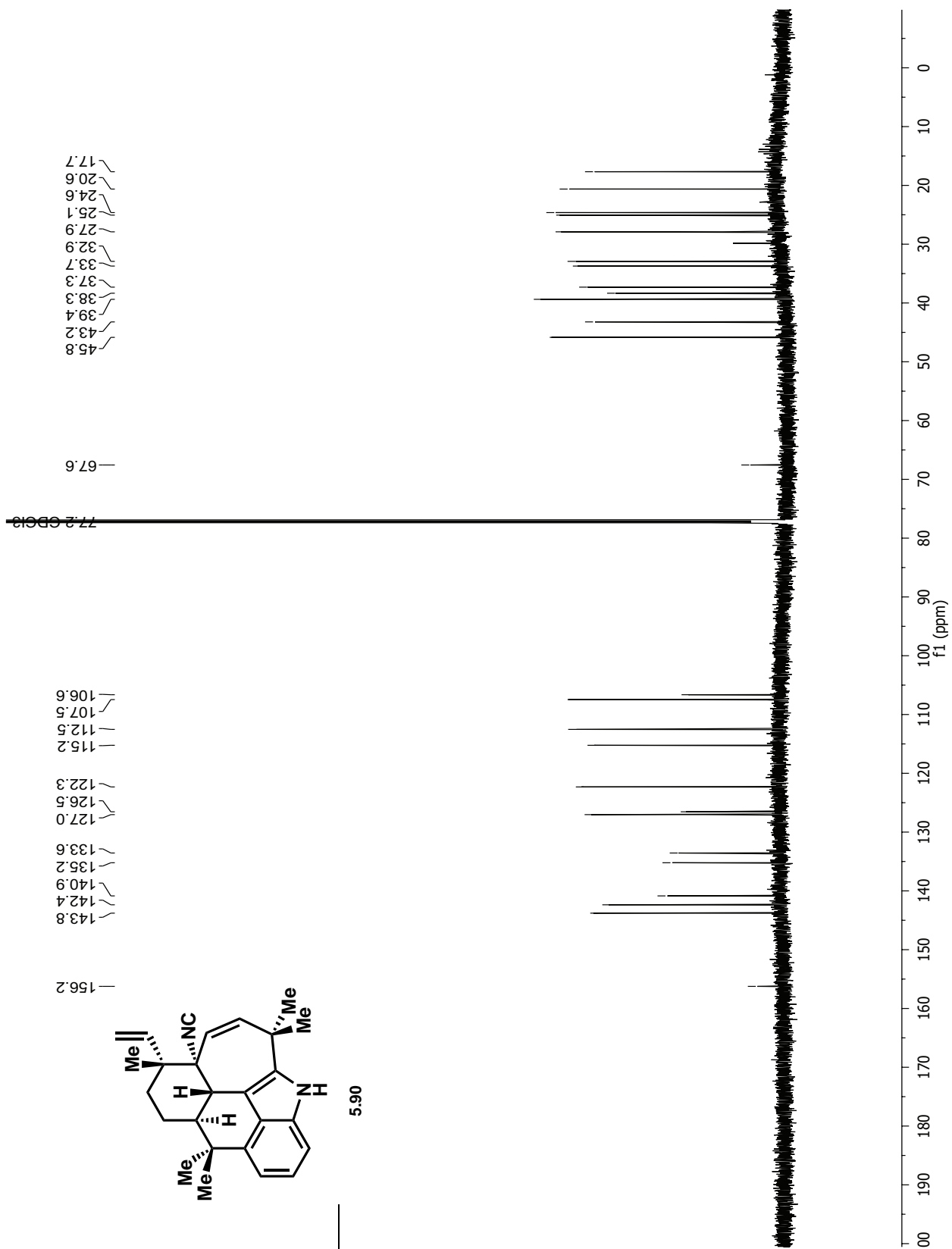


Figure 5.37: ^{13}C NMR of 5.90 in CDCl_3

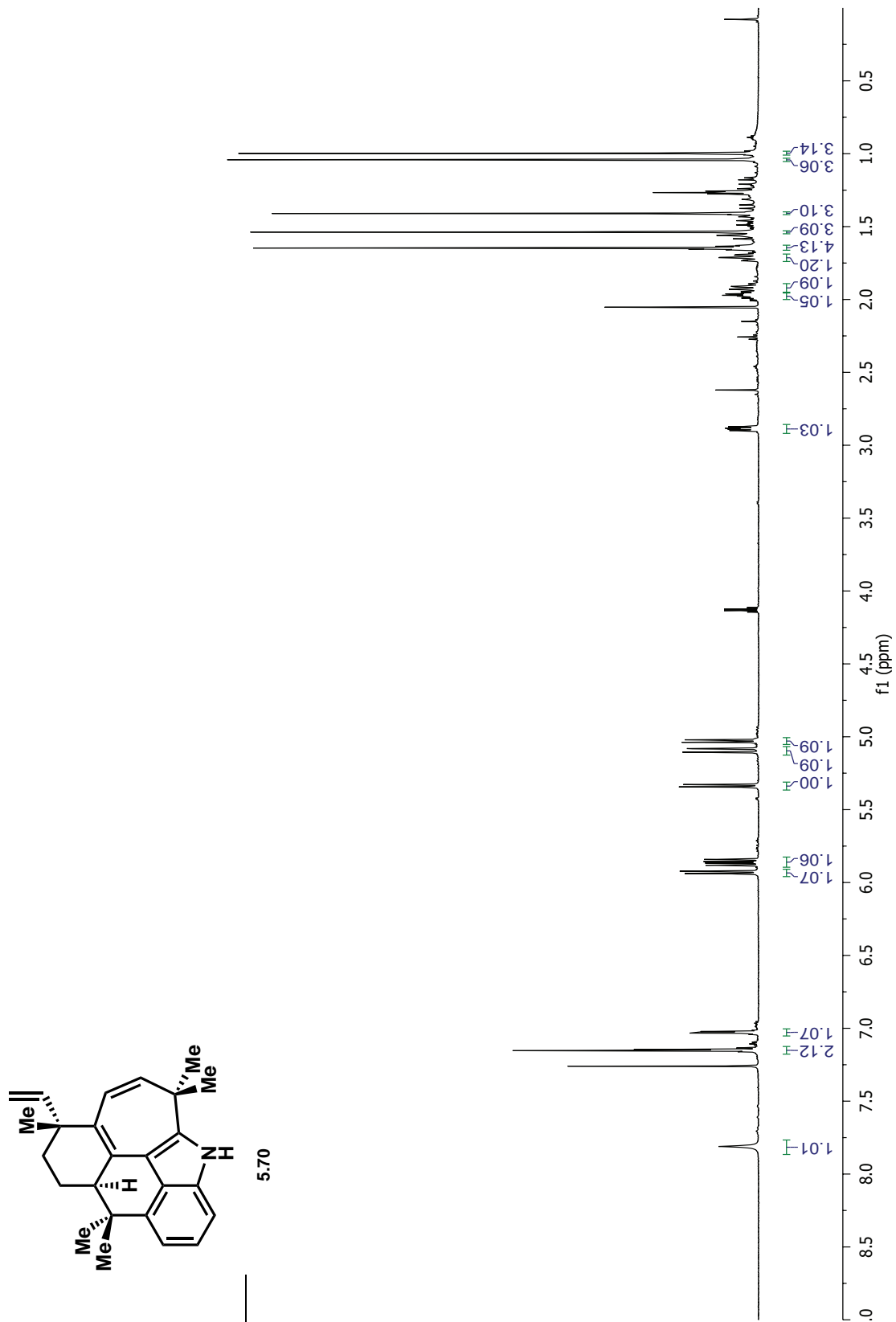


Figure 5.38: ^1H NMR of **5.70** in CDCl_3

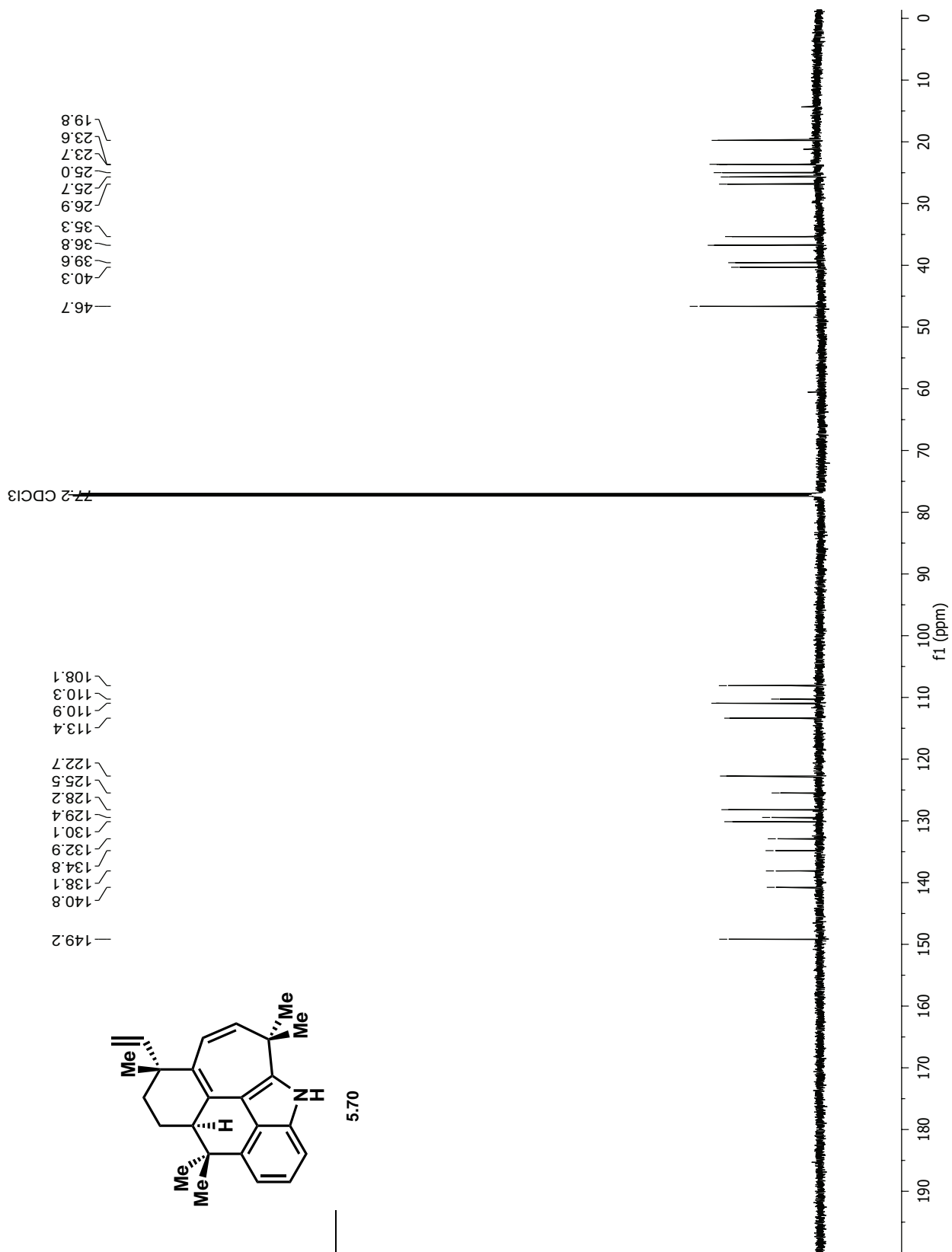


Figure 5.39: ^{13}C NMR of **5.70** in CDCl_3

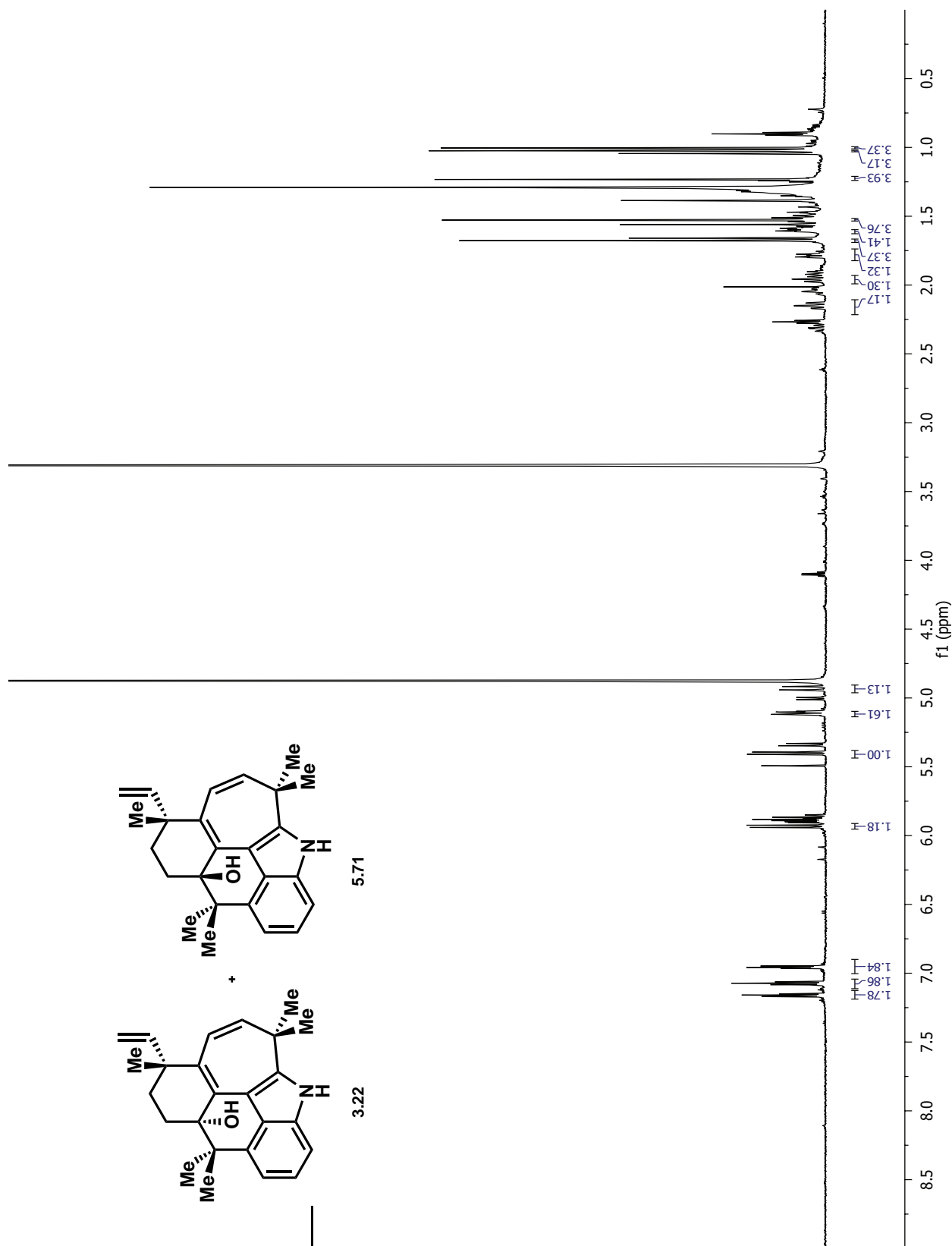


Figure 5.40: ^1H NMR of a mixture of **3.22** and **5.71** in CD_3OD

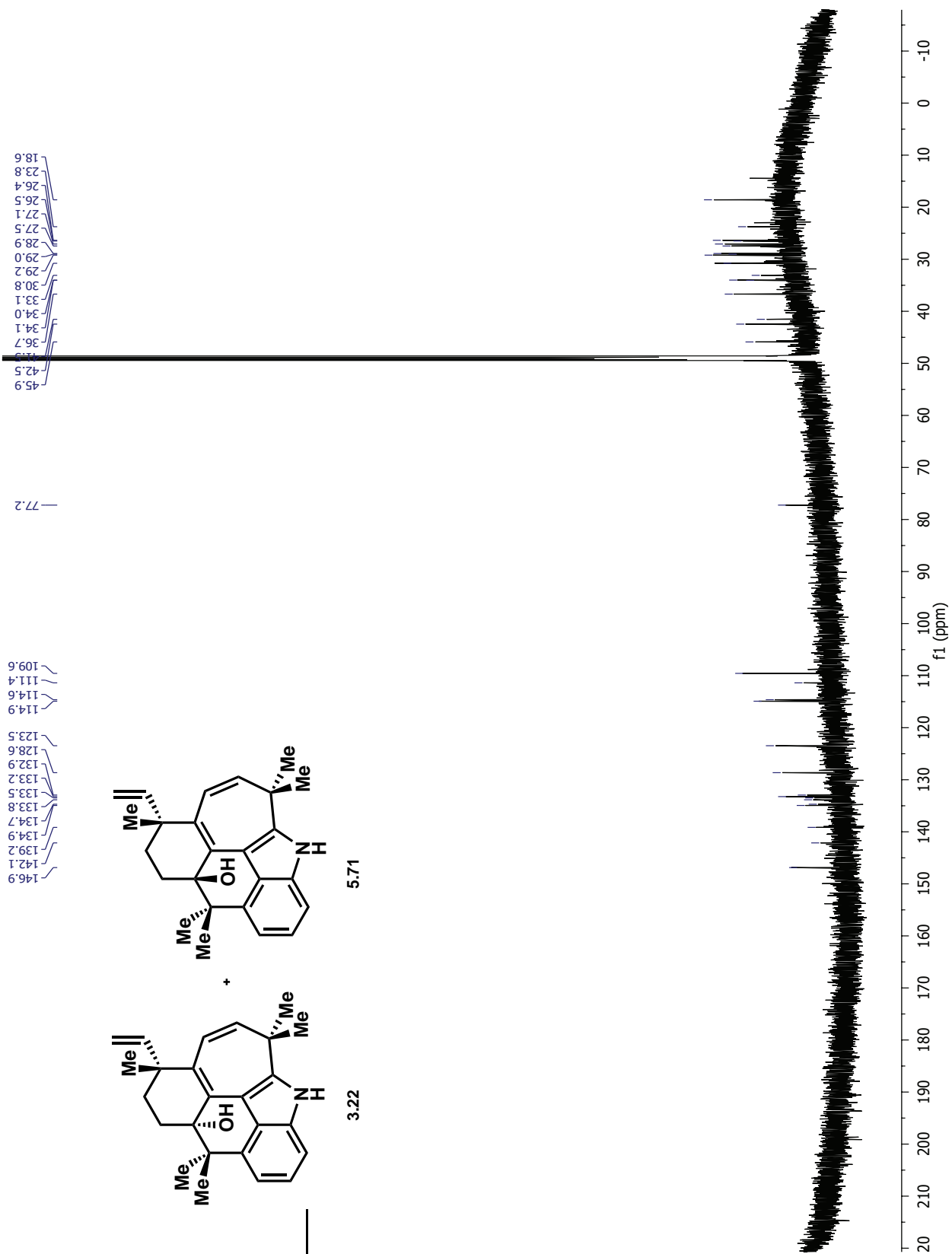


Figure 5.41: ^{13}C NMR of a mixture of **3.22** and **5.71** in CD_3OD

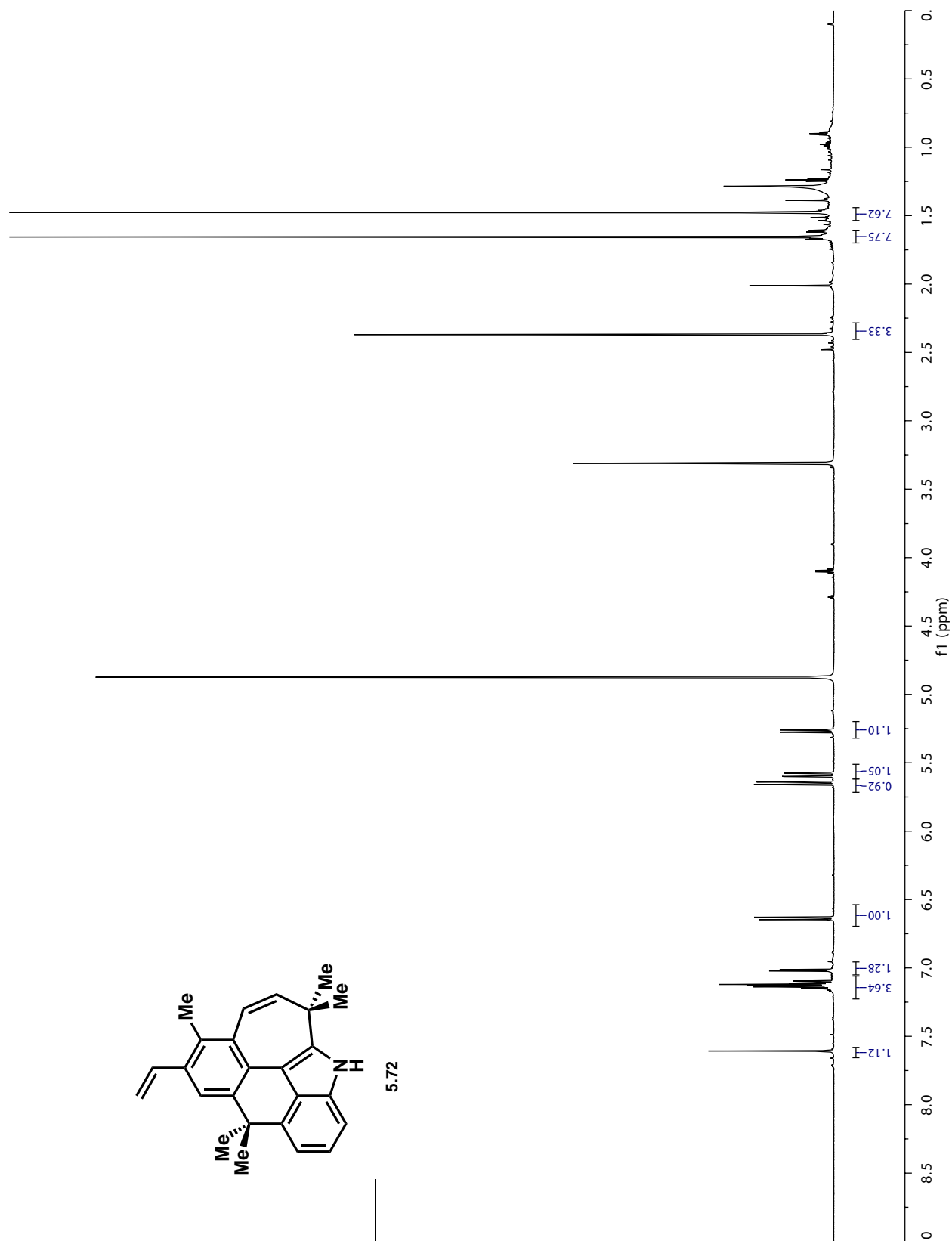


Figure 5.42: ¹H NMR of 5.72 in CD₃OD

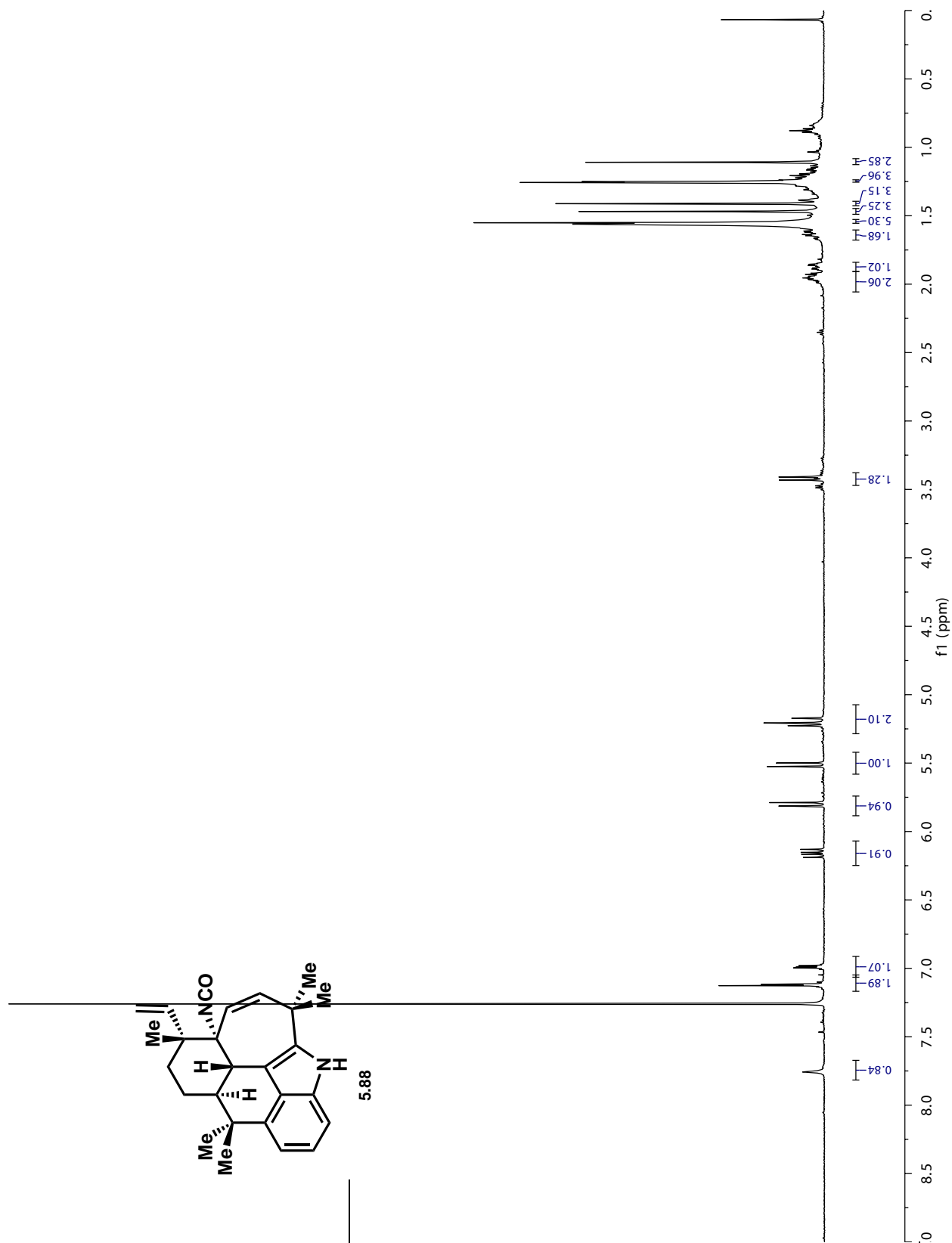


Figure 5.43: ^1H NMR of **5.88** in CDCl_3

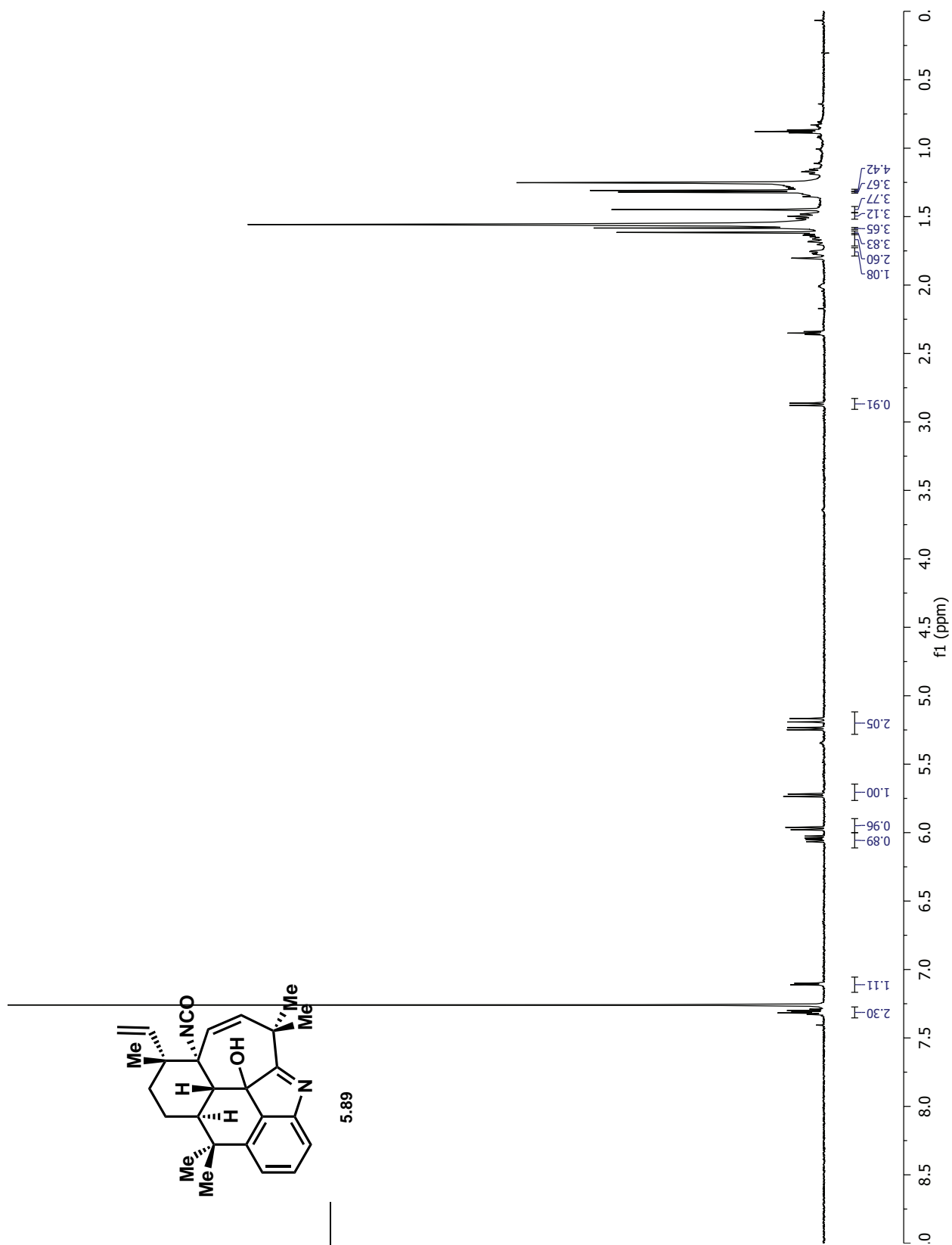


Figure 5.44: ^1H NMR of **5.89** in CDCl_3

5.b X-ray Crystallographic Data Relevant to Chapter 5

X-ray Crystallography Data

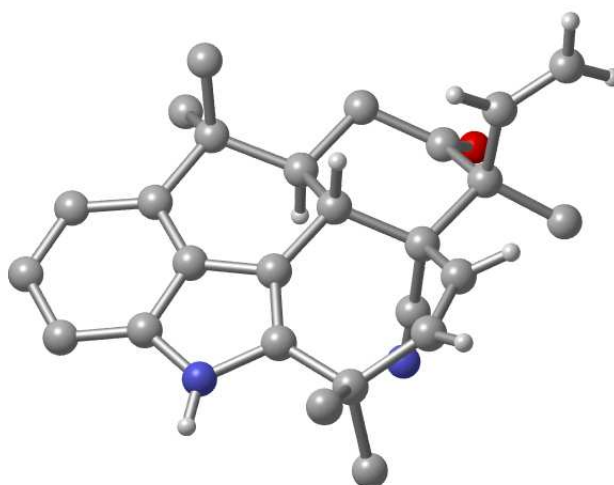


Figure 5.45: X-ray crystal structure of **4.42** (sarpong135)

A colorless needle 0.060 x 0.020 x 0.020 mm in size was mounted on a Cryoloop with Paratone oil. Data were collected in a nitrogen gas stream at 100(2) K using and scans. Crystal-to-detector distance was 60 mm and exposure time was 20 seconds per frame using a scan width of 2.0°. Data collection was 99.7% complete to 67.000° in θ . A total of 30752 reflections were collected covering the indices, $-11 \leq h \leq 10$, $-15 \leq k \leq 15$, $-21 \leq l \leq 21$. 3856 reflections were found to be symmetry independent, with an R_{int} of 0.0559. Indexing and unit cell refinement indicated a primitive, orthorhombic lattice. The space group was found to be P 21 21 21 (No. 19). The data were integrated using the Bruker SAINT software program and scaled using the SADABS software program. Solution by iterative methods (SHELXT-2014) produced a complete heavy-atom phasing model consistent with the proposed structure. All non-hydrogen atoms were refined anisotropically by full-matrix least-squares (SHELXL-2014). All hydrogen atoms were placed using a riding model. Their positions were constrained relative to their parent atom using the appropriate HFIX command in SHELXL-2014. Absolute stereochemistry was unambiguously determined to be *R* at C1 and *S* at C2, C5 and C18, respectively.

Table 5.1: Crystal data and structure refinement for **4.42**.

X-ray ID	sarpong135	
Sample/notebook ID	MLH-B1-115	
Empirical formula	C ₂₆ H ₂₈ N ₂ O	
Formula weight	384.5	
Temperature	100(2) K	
Wavelength	1.54178 Å	
Crystal system	Orthorhombic	
Space group	P 21 21 21	
Unit cell dimensions	a = 9.2170(3) Å b = 12.9842(4) Å c = 17.6732(6) Å	a = 90°. b = 90°. g = 90°.
Volume	2115.05(12) Å ³	
Z	4	
Density (calculated)	1.208 Mg/m ³	
Absorption coefficient	0.568 mm ⁻¹	
F(000)	824	
Crystal size	0.060 x 0.020 x 0.020 mm ³	
Theta range for data collection	4.225 to 68.345°.	
Index ranges	-11<=h<=10, -15<=k<=15, -21<=l<=21	
Reflections collected	30752	
Independent reflections	3856 [R(int) = 0.0559]	
Completeness to theta = 67.000°	99.70%	
Absorption correction	Semi-empirical from equivalents	
Max. and min. transmission	0.929 and 0.809	
Refinement method	Full-matrix least-squares on F ²	
Data / restraints / parameters	3856 / 0 / 267	
Goodness-of-fit on F ²	1.027	
Final R indices [I>2sigma(I)]	R1 = 0.0402, wR2 = 0.1002	
R indices (all data)	R1 = 0.0460, wR2 = 0.1044	
Absolute structure parameter	0.00(17)	
Extinction coefficient	n/a	
Largest diff. peak and hole	0.706 and -0.161 e.Å ⁻³	

Table 5.2: Atomic coordinates ($\times 10^4$) and equivalent isotropic displacement parameters ($\text{\AA}^2 \times 10^3$) for sarpong135. $U(\text{eq})$ is defined as one third of the trace of the orthogonalized U^{ij} tensor.

	x	y	z	U(eq)
C(1)	6365(3)	5390(2)	4145(2)	26(1)
C(2)	7261(3)	6419(2)	4006(2)	28(1)
C(3)	8779(3)	6098(2)	3729(2)	31(1)
C(4)	8813(3)	5400(2)	3054(2)	34(1)
C(5)	8003(3)	4392(2)	3216(2)	26(1)
C(6)	8158(3)	3597(2)	2553(2)	29(1)
C(7)	7337(3)	2622(2)	2764(1)	26(1)
C(8)	7577(3)	1644(2)	2483(2)	31(1)
C(9)	6756(3)	804(2)	2734(2)	34(1)
C(10)	5665(3)	904(2)	3270(2)	33(1)
C(11)	5380(3)	1894(2)	3532(2)	28(1)
C(12)	6201(3)	2732(2)	3278(1)	25(1)
C(13)	5667(3)	3642(2)	3633(1)	24(1)
C(14)	4544(3)	3346(2)	4094(2)	29(1)
C(15)	3544(3)	3933(2)	4615(2)	34(1)
C(16)	3691(3)	5083(2)	4525(2)	36(1)
C(17)	4804(3)	5679(2)	4344(2)	31(1)
C(18)	6419(3)	4637(2)	3458(1)	24(1)
C(19)	7052(3)	4845(2)	4786(2)	27(1)
C(20)	7416(3)	7054(2)	4731(2)	36(1)
C(21)	6545(3)	7024(2)	3368(2)	35(1)
C(22)	6538(4)	8021(3)	3290(2)	51(1)
C(23)	7536(4)	4012(2)	1812(2)	41(1)
C(24)	9770(3)	3338(3)	2439(2)	44(1)
C(25)	1951(3)	3651(3)	4424(2)	46(1)
C(26)	3836(4)	3629(3)	5447(2)	43(1)
N(1)	4384(2)	2283(2)	4032(1)	30(1)
N(2)	7626(3)	4404(2)	5260(1)	35(1)
O(1)	9871(2)	6387(2)	4044(1)	41(1)

Table 5.3: Bond lengths [\AA] for sarpong135.

C(1)-C(19)	1.478(4)	C(7)-C(6)-C(23)	108.5(2)
C(1)-C(17)	1.528(4)	C(7)-C(6)-C(24)	109.4(2)
C(1)-C(18)	1.560(4)	C(23)-C(6)-C(24)	109.1(3)
C(1)-C(2)	1.590(4)	C(7)-C(6)-C(5)	108.6(2)
C(2)-C(21)	1.524(4)	C(23)-C(6)-C(5)	111.9(2)
C(2)-C(20)	1.530(4)	C(24)-C(6)-C(5)	109.3(2)

C(2)-C(3)	1.540(4)	C(8)-C(7)-C(12)	116.7(2)
C(3)-O(1)	1.210(4)	C(8)-C(7)-C(6)	126.6(2)
C(3)-C(4)	1.498(4)	C(12)-C(7)-C(6)	116.7(2)
C(4)-C(5)	1.533(4)	C(7)-C(8)-C(9)	121.1(3)
C(4)-H(4A)	0.99	C(7)-C(8)-H(8)	119.5
C(4)-H(4B)	0.99	C(9)-C(8)-H(8)	119.5
C(5)-C(18)	1.555(4)	C(10)-C(9)-C(8)	122.3(3)
C(5)-C(6)	1.568(4)	C(10)-C(9)-H(9)	118.8
C(5)-H(5)	1	C(8)-C(9)-H(9)	118.8
C(6)-C(7)	1.521(4)	C(9)-C(10)-C(11)	116.8(3)
C(6)-C(23)	1.528(4)	C(9)-C(10)-H(10)	121.6
C(6)-C(24)	1.536(4)	C(11)-C(10)-H(10)	121.6
C(7)-C(8)	1.381(4)	N(1)-C(11)-C(10)	132.9(3)
C(7)-C(12)	1.393(4)	N(1)-C(11)-C(12)	106.4(2)
C(8)-C(9)	1.399(4)	C(10)-C(11)-C(12)	120.6(3)
C(8)-H(8)	0.95	C(7)-C(12)-C(11)	122.4(2)
C(9)-C(10)	1.389(4)	C(7)-C(12)-C(13)	129.2(2)
C(9)-H(9)	0.95	C(11)-C(12)-C(13)	108.4(2)
C(10)-C(11)	1.391(4)	C(14)-C(13)-C(12)	106.9(2)
C(10)-H(10)	0.95	C(14)-C(13)-C(18)	135.4(3)
C(11)-N(1)	1.371(4)	C(12)-C(13)-C(18)	117.6(2)
C(11)-C(12)	1.399(4)	C(13)-C(14)-N(1)	108.1(2)
C(12)-C(13)	1.425(4)	C(13)-C(14)-C(15)	133.0(3)
C(13)-C(14)	1.372(4)	N(1)-C(14)-C(15)	119.0(2)
C(13)-C(18)	1.499(4)	C(16)-C(15)-C(14)	112.4(2)
C(14)-N(1)	1.393(4)	C(16)-C(15)-C(26)	109.7(3)
C(14)-C(15)	1.508(4)	C(14)-C(15)-C(26)	110.2(2)
C(15)-C(16)	1.508(4)	C(16)-C(15)-C(25)	107.2(3)
C(15)-C(26)	1.545(4)	C(14)-C(15)-C(25)	109.1(3)
C(15)-C(25)	1.551(4)	C(26)-C(15)-C(25)	108.1(3)
C(16)-C(17)	1.324(4)	C(17)-C(16)-C(15)	132.4(3)
C(16)-H(16)	0.95	C(17)-C(16)-H(16)	113.8
C(17)-H(17)	0.95	C(15)-C(16)-H(16)	113.8
C(18)-H(18)	1	C(16)-C(17)-C(1)	129.9(3)
C(19)-N(2)	1.144(4)	C(16)-C(17)-H(17)	115.1
C(20)-H(20A)	0.98	C(1)-C(17)-H(17)	115.1
C(20)-H(20B)	0.98	C(13)-C(18)-C(5)	108.3(2)
C(20)-H(20C)	0.98	C(13)-C(18)-C(1)	111.4(2)
C(21)-C(22)	1.302(4)	C(5)-C(18)-C(1)	111.9(2)
C(21)-H(21)	0.95	C(13)-C(18)-H(18)	108.4
C(22)-H(22A)	0.95	C(5)-C(18)-H(18)	108.4
C(22)-H(22B)	0.95	C(1)-C(18)-H(18)	108.4
C(23)-H(23A)	0.98	N(2)-C(19)-C(1)	176.9(3)
C(23)-H(23B)	0.98	C(2)-C(20)-H(20A)	109.5
C(23)-H(23C)	0.98	C(2)-C(20)-H(20B)	109.5

C(24)-H(24A)	0.98	H(20A)-C(20)-H(20B)	109.5
C(24)-H(24B)	0.98	C(2)-C(20)-H(20C)	109.5
C(24)-H(24C)	0.98	H(20A)-C(20)-H(20C)	109.5
C(25)-H(25A)	0.98	H(20B)-C(20)-H(20C)	109.5
C(25)-H(25B)	0.98	C(22)-C(21)-C(2)	126.4(3)
C(25)-H(25C)	0.98	C(22)-C(21)-H(21)	116.8
C(26)-H(26A)	0.98	C(2)-C(21)-H(21)	116.8
C(26)-H(26B)	0.98	C(21)-C(22)-H(22A)	120
C(26)-H(26C)	0.98	C(21)-C(22)-H(22B)	120
N(1)-H(1)	0.88	H(22A)-C(22)-H(22B)	120
C(19)-C(1)-C(17)	110.2(2)	C(6)-C(23)-H(23A)	109.5
C(19)-C(1)-C(18)	106.5(2)	C(6)-C(23)-H(23B)	109.5
C(17)-C(1)-C(18)	111.3(2)	H(23A)-C(23)-H(23B)	109.5
C(19)-C(1)-C(2)	107.4(2)	C(6)-C(23)-H(23C)	109.5
C(17)-C(1)-C(2)	108.5(2)	H(23A)-C(23)-H(23C)	109.5
C(18)-C(1)-C(2)	112.9(2)	H(23B)-C(23)-H(23C)	109.5
C(21)-C(2)-C(20)	112.4(2)	C(6)-C(24)-H(24A)	109.5
C(21)-C(2)-C(3)	107.3(2)	C(6)-C(24)-H(24B)	109.5
C(20)-C(2)-C(3)	109.1(2)	H(24A)-C(24)-H(24B)	109.5
C(21)-C(2)-C(1)	108.8(2)	C(6)-C(24)-H(24C)	109.5
C(20)-C(2)-C(1)	111.8(2)	H(24A)-C(24)-H(24C)	109.5
C(3)-C(2)-C(1)	107.1(2)	H(24B)-C(24)-H(24C)	109.5
O(1)-C(3)-C(4)	122.5(3)	C(15)-C(25)-H(25A)	109.5
O(1)-C(3)-C(2)	121.7(2)	C(15)-C(25)-H(25B)	109.5
C(4)-C(3)-C(2)	115.9(2)	H(25A)-C(25)-H(25B)	109.5
C(3)-C(4)-C(5)	110.9(2)	C(15)-C(25)-H(25C)	109.5
C(3)-C(4)-H(4A)	109.5	H(25A)-C(25)-H(25C)	109.5
C(5)-C(4)-H(4A)	109.5	H(25B)-C(25)-H(25C)	109.5
C(3)-C(4)-H(4B)	109.5	C(15)-C(26)-H(26A)	109.5
C(5)-C(4)-H(4B)	109.5	C(15)-C(26)-H(26B)	109.5
H(4A)-C(4)-H(4B)	108	H(26A)-C(26)-H(26B)	109.5
C(4)-C(5)-C(18)	109.5(2)	C(15)-C(26)-H(26C)	109.5
C(4)-C(5)-C(6)	112.3(2)	H(26A)-C(26)-H(26C)	109.5
C(18)-C(5)-C(6)	115.2(2)	H(26B)-C(26)-H(26C)	109.5
C(4)-C(5)-H(5)	106.4	C(11)-N(1)-C(14)	110.2(2)
C(18)-C(5)-H(5)	106.4	C(11)-N(1)-H(1)	124.9
C(6)-C(5)-H(5)	106.4	C(14)-N(1)-H(1)	124.9

Symmetry transformations used to generate equivalent atoms:

Table 5.4: Anisotropic displacement parameters ($\text{\AA}^2 \times 10^3$) for sarpong135. The anisotropic displacement factor exponent takes the form: $-2\pi^2 [h^2 a^{*2} U^{11} + \dots + 2 h k a^* b^* U^{12}]$

	U^{11}	U^{22}	U^{33}	U^{23}	U^{13}	U^{12}
C(1)	31(1)	25(1)	21(1)	1(1)	2(1)	0(1)
C(2)	39(2)	23(1)	23(1)	1(1)	0(1)	-1(1)
C(3)	38(2)	28(2)	27(1)	6(1)	3(1)	-6(1)
C(4)	36(2)	34(2)	34(2)	0(1)	9(1)	-6(1)
C(5)	28(1)	27(1)	22(1)	1(1)	3(1)	-1(1)
C(6)	31(1)	32(1)	23(1)	-1(1)	3(1)	2(1)
C(7)	26(1)	30(1)	22(1)	-2(1)	-6(1)	1(1)
C(8)	31(1)	34(2)	28(1)	-4(1)	-3(1)	5(1)
C(9)	38(2)	29(2)	35(2)	-6(1)	-10(1)	3(1)
C(10)	36(2)	29(1)	33(2)	1(1)	-12(1)	-5(1)
C(11)	30(1)	32(2)	23(1)	1(1)	-7(1)	-3(1)
C(12)	28(1)	26(1)	21(1)	0(1)	-5(1)	0(1)
C(13)	26(1)	25(1)	21(1)	1(1)	-1(1)	1(1)
C(14)	30(1)	32(2)	25(1)	1(1)	-2(1)	-2(1)
C(15)	29(1)	40(2)	33(2)	2(1)	6(1)	-3(1)
C(16)	34(2)	42(2)	30(2)	-4(1)	5(1)	6(1)
C(17)	35(2)	31(2)	28(1)	-1(1)	3(1)	6(1)
C(18)	29(1)	24(1)	19(1)	2(1)	0(1)	0(1)
C(19)	34(2)	28(1)	20(1)	-3(1)	5(1)	-2(1)
C(20)	45(2)	33(2)	29(1)	-2(1)	-1(1)	-3(1)
C(21)	45(2)	28(2)	32(2)	3(1)	-5(1)	-5(1)
C(22)	57(2)	36(2)	59(2)	8(2)	-21(2)	2(2)
C(23)	63(2)	38(2)	22(1)	1(1)	2(2)	1(2)
C(24)	33(2)	42(2)	56(2)	-16(2)	11(2)	-3(1)
C(25)	31(2)	52(2)	55(2)	-3(2)	7(2)	-4(2)
C(26)	44(2)	53(2)	32(2)	6(2)	13(1)	-2(2)
N(1)	31(1)	31(1)	29(1)	6(1)	2(1)	-8(1)
N(2)	45(1)	35(1)	25(1)	1(1)	-1(1)	5(1)
O(1)	39(1)	44(1)	40(1)	-2(1)	0(1)	-10(1)

Table 5.5: Hydrogen coordinates ($\times 10^4$) and isotropic displacement parameters ($\text{\AA}^2 \times 10^3$) for sarpong135.

	x	y	z	U(eq)
H(4A)	9833	5245	2920	41
H(4B)	8359	5752	2617	41
H(5)	8486	4076	3666	31
H(8)	8311	1541	2113	37

Table 5.5: Hydrogen coordinates ($\times 10^4$) and isotropic displacement parameters ($\text{\AA}^2 \times 10^3$) for sarpong135.

	x	y	z	U(eq)
H(9)	6953	142	2529	41
H(10)	5139	325	3450	39
H(16)	2817	5451	4616	43
H(17)	4601	6397	4337	37
H(18)	5911	4970	3021	29
H(20A)	8004	7667	4627	54
H(20B)	7891	6636	5121	54
H(20C)	6454	7264	4908	54
H(21)	6055	6636	2991	42
H(22A)	7012	8444	3652	61
H(22B)	6058	8326	2870	61
H(23A)	7649	3493	1414	61
H(23B)	8056	4640	1668	61
H(23C)	6504	4169	1880	61
H(24A)	10166	3047	2906	65
H(24B)	10302	3967	2308	65
H(24C)	9869	2836	2028	65
H(25A)	1295	4034	4759	70
H(25B)	1804	2910	4498	70
H(25C)	1745	3831	3897	70
H(26A)	4845	3789	5576	64
H(26B)	3664	2889	5512	64
H(26C)	3183	4016	5780	64
H(1)	3737	1914	4278	36

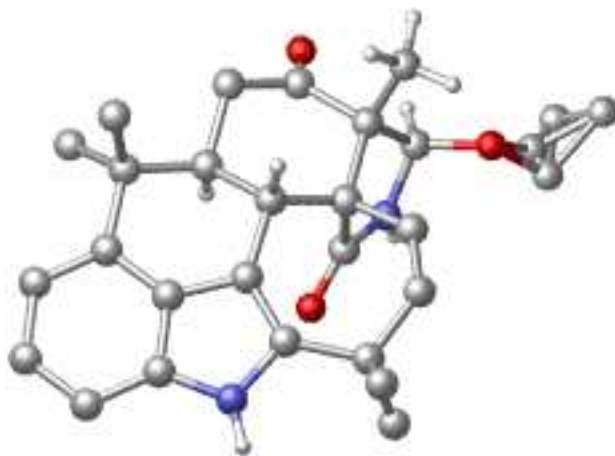


Figure 5.46: X-ray crystal structure of **5.31** (sarpong139)

A colorless prism 0.060 x 0.040 x 0.040 mm in size was mounted on a Cryoloop with Paratone oil. Data were collected in a nitrogen gas stream at 100(2) K using and scans. Crystal-to-detector distance was 60 mm and exposure time was 1 seconds per frame using a scan width of 2.0°. Data collection was 99.8% complete to 67.000° in θ . A total of 32645 reflections were collected covering the indices, $-12 \leq h \leq 12$, $-14 \leq k \leq 14$, $-19 \leq l \leq 23$. 4327 reflections were found to be symmetry independent, with an R_{int} of 0.0288. Indexing and unit cell refinement indicated a primitive, orthorhombic lattice. The space group was found to be P 21 21 21 (No. 19). The data were integrated using the Bruker SAINT software program and scaled using the SADABS software program. Solution by iterative methods (SHELXT-2014) produced a complete heavy-atom phasing model consistent with the proposed structure. All non-hydrogen atoms were refined anisotropically by full-matrix least-squares (SHELXL-2016). All hydrogen atoms were placed using a riding model. Their positions were constrained relative to their parent atom using the appropriate HFIX command in SHELXL-2016. Absolute stereochemistry was unambiguously determined to be *R* at C1, C15, and C17, and *S* at C4 and C18, respectively.

Table 5.6: Crystal data and structure refinement for **4.42**.

X-ray ID	sarpong139	
Sample/notebook ID	REJVII-095	
Empirical formula	C ₂₇ H ₃₂ N ₂ O ₃	
Formula weight	432.54	
Temperature	100(2) K	
Wavelength	1.54178 Å	
Crystal system	Orthorhombic	
Space group	P 21 21 21	
Unit cell dimensions	a = 10.4403(4) Å b = 11.7226(5) Å c = 19.3375(8) Å	a = 90°. b = 90°. g = 90°.
Volume	2366.67(17) Å ³	
Z	4	
Density (calculated)	1.214 Mg/m ³	
Absorption coefficient	0.626 mm ⁻¹	
F(000)	928	
Crystal size	0.060 x 0.040 x 0.040 mm ³	
Theta range for data collection	4.410 to 68.350°.	
Index ranges	-12<=h<=12, -14<=k<=14, -19<=l<=23	
Reflections collected	32645	
Independent reflections	4327 [R(int) = 0.0288]	
Completeness to theta = 67.000°	99.80%	
Absorption correction	Semi-empirical from equivalents	
Max. and min. transmission	0.929 and 0.874	
Refinement method	Full-matrix least-squares on F ²	
Data / restraints / parameters	4327 / 0 / 315	
Goodness-of-fit on F ²	1.048	
Final R indices [I>2sigma(I)]	R1 = 0.0279, wR2 = 0.0720	
R indices (all data)	R1 = 0.0289, wR2 = 0.0728	
Absolute structure parameter	0.04(5)	
Extinction coefficient	n/a	
Largest diff. peak and hole	0.169 and -0.150 e.Å ⁻³	

Table 5.7: Atomic coordinates ($\times 10^4$) and equivalent isotropic displacement parameters ($\text{\AA}^2 \times 10^3$) for sarpong139. $U(\text{eq})$ is defined as one third of the trace of the orthogonalized U^{ij} tensor.

	x	y	z	U(eq)
C(1)	4416(2)	4585(1)	4026(1)	22(1)
C(2)	3738(2)	5077(2)	4663(1)	24(1)
C(3)	4395(2)	6016(2)	5047(1)	25(1)
C(4)	5745(2)	5636(1)	5264(1)	20(1)
C(5)	6340(2)	6509(2)	5787(1)	22(1)
C(6)	7724(2)	6182(1)	5934(1)	21(1)
C(7)	8438(2)	6479(2)	6512(1)	25(1)
C(8)	9739(2)	6164(2)	6572(1)	26(1)
C(9)	10367(2)	5549(2)	6068(1)	24(1)
C(10)	9652(2)	5248(1)	5485(1)	20(1)
C(11)	8891(1)	4629(2)	4454(1)	20(1)
C(12)	9026(2)	4052(2)	3766(1)	24(1)
C(13)	7819(2)	4097(2)	3336(1)	25(1)
C(14)	6582(2)	4228(2)	3482(1)	23(1)
C(15)	5892(2)	4417(1)	4165(1)	20(1)
C(16)	5882(2)	3256(1)	4545(1)	22(1)
C(17)	3916(2)	3354(2)	3934(1)	26(1)
C(18)	6514(1)	5394(1)	4592(1)	18(1)
C(19)	7895(2)	5175(1)	4773(1)	19(1)
C(20)	8362(2)	5569(1)	5421(1)	19(1)
C(21)	4067(2)	5388(2)	3429(1)	25(1)
C(22)	6319(2)	7729(2)	5493(1)	28(1)
C(23)	5560(2)	6487(2)	6460(1)	31(1)
C(24)	10106(2)	4640(2)	3356(1)	34(1)
C(25)	9362(2)	2774(2)	3857(1)	35(1)
C(26)	3180(5)	1984(4)	3166(3)	36(1)
C(27)	2619(4)	1982(3)	2463(2)	48(1)
C(26A)	3714(9)	1868(6)	2994(4)	26(2)
C(27A)	2303(7)	1670(6)	3083(5)	50(3)
N(1)	9952(1)	4652(1)	4895(1)	20(1)
N(2)	4790(1)	2715(1)	4361(1)	27(1)
O(1)	2684(1)	4746(1)	4837(1)	34(1)
O(2)	6697(1)	2881(1)	4934(1)	27(1)
O(3)	3937(1)	3035(1)	3231(1)	36(1)

Table 5.8: Bond lengths [\AA] for sarpong139.

C(1)-C(2)	1.533(2)	C(7)-C(8)-H(8)	118.8
-----------	----------	----------------	-------

C(1)-C(21)	1.533(2)	C(8)-C(9)-C(10)	116.64(16)
C(1)-C(17)	1.544(2)	C(8)-C(9)-H(9)	121.7
C(1)-C(15)	1.577(2)	C(10)-C(9)-H(9)	121.7
C(2)-O(1)	1.214(2)	N(1)-C(10)-C(9)	132.59(15)
C(2)-C(3)	1.495(3)	N(1)-C(10)-C(20)	106.38(14)
C(3)-C(4)	1.537(2)	C(9)-C(10)-C(20)	121.04(16)
C(3)-H(3A)	0.99	C(19)-C(11)-N(1)	108.54(14)
C(3)-H(3B)	0.99	C(19)-C(11)-C(12)	133.09(15)
C(4)-C(18)	1.554(2)	N(1)-C(11)-C(12)	118.37(14)
C(4)-C(5)	1.567(2)	C(11)-C(12)-C(13)	113.19(14)
C(4)-H(4)	1	C(11)-C(12)-C(24)	108.87(14)
C(5)-C(6)	1.522(2)	C(13)-C(12)-C(24)	108.19(15)
C(5)-C(23)	1.535(2)	C(11)-C(12)-C(25)	110.86(15)
C(5)-C(22)	1.539(2)	C(13)-C(12)-C(25)	106.62(15)
C(6)-C(7)	1.388(2)	C(24)-C(12)-C(25)	109.00(16)
C(6)-C(20)	1.394(2)	C(14)-C(13)-C(12)	134.17(17)
C(7)-C(8)	1.413(3)	C(14)-C(13)-H(13)	112.9
C(7)-H(7)	0.95	C(12)-C(13)-H(13)	112.9
C(8)-C(9)	1.378(3)	C(13)-C(14)-C(15)	131.35(16)
C(8)-H(8)	0.95	C(13)-C(14)-H(14)	114.3
C(9)-C(10)	1.398(2)	C(15)-C(14)-H(14)	114.3
C(9)-H(9)	0.95	C(14)-C(15)-C(16)	106.68(14)
C(10)-N(1)	1.374(2)	C(14)-C(15)-C(18)	111.82(13)
C(10)-C(20)	1.403(2)	C(16)-C(15)-C(18)	113.55(13)
C(11)-C(19)	1.368(2)	C(14)-C(15)-C(1)	109.44(13)
C(11)-N(1)	1.398(2)	C(16)-C(15)-C(1)	100.58(12)
C(11)-C(12)	1.500(2)	C(18)-C(15)-C(1)	114.01(13)
C(12)-C(13)	1.511(2)	O(2)-C(16)-N(2)	125.56(16)
C(12)-C(24)	1.541(2)	O(2)-C(16)-C(15)	127.31(15)
C(12)-C(25)	1.549(3)	N(2)-C(16)-C(15)	107.13(14)
C(13)-C(14)	1.331(2)	O(3)-C(17)-N(2)	113.85(15)
C(13)-H(13)	0.95	O(3)-C(17)-C(1)	110.69(14)
C(14)-C(15)	1.521(2)	N(2)-C(17)-C(1)	101.88(13)
C(14)-H(14)	0.95	O(3)-C(17)-H(17)	110
C(15)-C(16)	1.547(2)	N(2)-C(17)-H(17)	110
C(15)-C(18)	1.554(2)	C(1)-C(17)-H(17)	110
C(16)-O(2)	1.218(2)	C(19)-C(18)-C(15)	113.42(13)
C(16)-N(2)	1.352(2)	C(19)-C(18)-C(4)	109.32(13)
C(17)-O(3)	1.410(2)	C(15)-C(18)-C(4)	111.33(13)
C(17)-N(2)	1.441(2)	C(19)-C(18)-H(18)	107.5
C(17)-H(17)	1	C(15)-C(18)-H(18)	107.5
C(18)-C(19)	1.506(2)	C(4)-C(18)-H(18)	107.5
C(18)-H(18)	1	C(11)-C(19)-C(20)	106.81(14)
C(19)-C(20)	1.422(2)	C(11)-C(19)-C(18)	134.63(15)
C(21)-H(21A)	0.98	C(20)-C(19)-C(18)	118.55(14)

C(21)-H(21B)	0.98	C(6)-C(20)-C(10)	122.29(16)
C(21)-H(21C)	0.98	C(6)-C(20)-C(19)	129.09(15)
C(22)-H(22A)	0.98	C(10)-C(20)-C(19)	108.62(15)
C(22)-H(22B)	0.98	C(1)-C(21)-H(21A)	109.5
C(22)-H(22C)	0.98	C(1)-C(21)-H(21B)	109.5
C(23)-H(23A)	0.98	H(21A)-C(21)-H(21B)	109.5
C(23)-H(23B)	0.98	C(1)-C(21)-H(21C)	109.5
C(23)-H(23C)	0.98	H(21A)-C(21)-H(21C)	109.5
C(24)-H(24A)	0.98	H(21B)-C(21)-H(21C)	109.5
C(24)-H(24B)	0.98	C(5)-C(22)-H(22A)	109.5
C(24)-H(24C)	0.98	C(5)-C(22)-H(22B)	109.5
C(25)-H(25A)	0.98	H(22A)-C(22)-H(22B)	109.5
C(25)-H(25B)	0.98	C(5)-C(22)-H(22C)	109.5
C(25)-H(25C)	0.98	H(22A)-C(22)-H(22C)	109.5
C(26)-O(3)	1.470(4)	H(22B)-C(22)-H(22C)	109.5
C(26)-C(27)	1.481(6)	C(5)-C(23)-H(23A)	109.5
C(26)-H(26A)	0.99	C(5)-C(23)-H(23B)	109.5
C(26)-H(26B)	0.99	H(23A)-C(23)-H(23B)	109.5
C(27)-H(27A)	0.98	C(5)-C(23)-H(23C)	109.5
C(27)-H(27B)	0.98	H(23A)-C(23)-H(23C)	109.5
C(27)-H(27C)	0.98	H(23B)-C(23)-H(23C)	109.5
C(26A)-O(3)	1.462(8)	C(12)-C(24)-H(24A)	109.5
C(26A)-C(27A)	1.501(11)	C(12)-C(24)-H(24B)	109.5
C(26A)-H(26C)	0.99	H(24A)-C(24)-H(24B)	109.5
C(26A)-H(26D)	0.99	C(12)-C(24)-H(24C)	109.5
C(27A)-H(27D)	0.98	H(24A)-C(24)-H(24C)	109.5
C(27A)-H(27E)	0.98	H(24B)-C(24)-H(24C)	109.5
C(27A)-H(27F)	0.98	C(12)-C(25)-H(25A)	109.5
N(1)-H(1)	0.88	C(12)-C(25)-H(25B)	109.5
N(2)-H(2)	0.88	H(25A)-C(25)-H(25B)	109.5
C(2)-C(1)-C(21)	105.31(14)	C(12)-C(25)-H(25C)	109.5
C(2)-C(1)-C(17)	106.74(14)	H(25A)-C(25)-H(25C)	109.5
C(21)-C(1)-C(17)	113.97(14)	H(25B)-C(25)-H(25C)	109.5
C(2)-C(1)-C(15)	111.18(14)	O(3)-C(26)-C(27)	107.0(3)
C(21)-C(1)-C(15)	115.91(13)	O(3)-C(26)-H(26A)	110.3
C(17)-C(1)-C(15)	103.51(13)	C(27)-C(26)-H(26A)	110.3
O(1)-C(2)-C(3)	120.92(17)	O(3)-C(26)-H(26B)	110.3
O(1)-C(2)-C(1)	121.38(17)	C(27)-C(26)-H(26B)	110.3
C(3)-C(2)-C(1)	117.66(14)	H(26A)-C(26)-H(26B)	108.6
C(2)-C(3)-C(4)	110.10(14)	C(26)-C(27)-H(27A)	109.5
C(2)-C(3)-H(3A)	109.6	C(26)-C(27)-H(27B)	109.5
C(4)-C(3)-H(3A)	109.6	H(27A)-C(27)-H(27B)	109.5
C(2)-C(3)-H(3B)	109.6	C(26)-C(27)-H(27C)	109.5
C(4)-C(3)-H(3B)	109.6	H(27A)-C(27)-H(27C)	109.5
H(3A)-C(3)-H(3B)	108.2	H(27B)-C(27)-H(27C)	109.5

C(3)-C(4)-C(18)	107.29(13)	O(3)-C(26A)-C(27A)	105.4(6)
C(3)-C(4)-C(5)	110.51(13)	O(3)-C(26A)-H(26C)	110.7
C(18)-C(4)-C(5)	117.05(13)	C(27A)-C(26A)-H(26C)	110.7
C(3)-C(4)-H(4)	107.2	O(3)-C(26A)-H(26D)	110.7
C(18)-C(4)-H(4)	107.2	C(27A)-C(26A)-H(26D)	110.7
C(5)-C(4)-H(4)	107.2	H(26C)-C(26A)-H(26D)	108.8
C(6)-C(5)-C(23)	109.97(14)	C(26A)-C(27A)-H(27D)	109.5
C(6)-C(5)-C(22)	108.47(14)	C(26A)-C(27A)-H(27E)	109.5
C(23)-C(5)-C(22)	108.78(15)	H(27D)-C(27A)-H(27E)	109.5
C(6)-C(5)-C(4)	109.34(14)	C(26A)-C(27A)-H(27F)	109.5
C(23)-C(5)-C(4)	109.03(14)	H(27D)-C(27A)-H(27F)	109.5
C(22)-C(5)-C(4)	111.24(14)	H(27E)-C(27A)-H(27F)	109.5
C(7)-C(6)-C(20)	116.47(16)	C(10)-N(1)-C(11)	109.61(13)
C(7)-C(6)-C(5)	126.61(16)	C(10)-N(1)-H(1)	125.2
C(20)-C(6)-C(5)	116.83(15)	C(11)-N(1)-H(1)	125.2
C(6)-C(7)-C(8)	121.12(17)	C(16)-N(2)-C(17)	116.11(14)
C(6)-C(7)-H(7)	119.4	C(16)-N(2)-H(2)	121.9
C(8)-C(7)-H(7)	119.4	C(17)-N(2)-H(2)	121.9
C(9)-C(8)-C(7)	122.42(17)	C(17)-O(3)-C(26A)	123.2(3)
C(9)-C(8)-H(8)	118.8	C(17)-O(3)-C(26)	107.2(2)

Symmetry transformations used to generate equivalent atoms:

Table 5.9: Anisotropic displacement parameters ($\text{\AA}^2 \times 10^3$) for sarpong139. The anisotropic displacement factor exponent takes the form: $-2\pi^2 [h^2 a^{*2} U^{11} + \dots + 2 h k a^* b^* U^{12}]$

	U ¹¹	U ²²	U ³³	U ²³	U ¹³	U ¹²
C(1)	15(1)	22(1)	29(1)	4(1)	-4(1)	-2(1)
C(2)	15(1)	25(1)	33(1)	8(1)	-1(1)	2(1)
C(3)	17(1)	30(1)	29(1)	-1(1)	2(1)	3(1)
C(4)	16(1)	21(1)	23(1)	2(1)	2(1)	-1(1)
C(5)	22(1)	23(1)	20(1)	0(1)	2(1)	1(1)
C(6)	22(1)	20(1)	22(1)	4(1)	2(1)	-4(1)
C(7)	27(1)	26(1)	21(1)	0(1)	3(1)	-5(1)
C(8)	27(1)	30(1)	21(1)	3(1)	-5(1)	-9(1)
C(9)	18(1)	28(1)	25(1)	4(1)	-2(1)	-5(1)
C(10)	18(1)	20(1)	23(1)	4(1)	-1(1)	-3(1)
C(11)	14(1)	24(1)	22(1)	2(1)	-2(1)	-3(1)
C(12)	17(1)	33(1)	24(1)	-4(1)	-1(1)	1(1)
C(13)	24(1)	29(1)	21(1)	-4(1)	-1(1)	0(1)
C(14)	22(1)	24(1)	22(1)	-2(1)	-5(1)	-1(1)
C(15)	15(1)	22(1)	24(1)	2(1)	-3(1)	0(1)
C(16)	20(1)	21(1)	25(1)	-1(1)	1(1)	1(1)
C(17)	21(1)	23(1)	35(1)	4(1)	-6(1)	-4(1)

Table 5.9: Anisotropic displacement parameters ($\text{\AA}^2 \times 10^3$) for sarpong139. The anisotropic displacement factor exponent takes the form: $-2\pi^2 [h^2 a^{*2} U^{11} + \dots + 2 h k a^* b^* U^{12}]$

	U^{11}	U^{22}	U^{33}	U^{23}	U^{13}	U^{12}
C(18)	15(1)	20(1)	20(1)	2(1)	0(1)	0(1)
C(19)	16(1)	20(1)	20(1)	3(1)	-1(1)	-2(1)
C(20)	17(1)	20(1)	21(1)	3(1)	1(1)	-3(1)
C(21)	19(1)	24(1)	32(1)	5(1)	-5(1)	0(1)
C(22)	28(1)	22(1)	33(1)	-2(1)	-3(1)	0(1)
C(23)	25(1)	44(1)	25(1)	-2(1)	4(1)	1(1)
C(24)	22(1)	56(1)	24(1)	-6(1)	2(1)	-4(1)
C(25)	31(1)	38(1)	35(1)	-11(1)	-5(1)	10(1)
C(26)	31(3)	28(2)	48(3)	-6(2)	-5(2)	-8(2)
C(27)	49(2)	44(2)	50(2)	-14(2)	-11(2)	-15(2)
C(26A)	25(4)	22(3)	31(4)	-2(3)	1(3)	1(3)
C(27A)	34(4)	45(4)	71(6)	-32(4)	9(3)	-14(3)
N(1)	12(1)	24(1)	24(1)	0(1)	-1(1)	0(1)
N(2)	26(1)	19(1)	36(1)	5(1)	-7(1)	-4(1)
O(1)	16(1)	35(1)	50(1)	6(1)	5(1)	-1(1)
O(2)	23(1)	25(1)	32(1)	4(1)	-5(1)	4(1)
O(3)	44(1)	24(1)	38(1)	-1(1)	-18(1)	-8(1)

Table 5.10: Hydrogen coordinates ($\times 10^4$) and isotropic displacement parameters ($\text{\AA}^2 \times 10^3$) for sarpong139.

	x	y	z	U(eq)
H(3A)	3890	6219	5462	30
H(3B)	4455	6700	4748	30
H(4)	5653	4893	5514	24
H(7)	8045	6901	6874	30
H(8)	10198	6383	6975	32
H(9)	11242	5341	6115	28
H(13)	7978	4014	2855	30
H(14)	6033	4197	3091	27
H(17)	3025	3290	4121	31
H(18)	6484	6101	4303	22
H(21A)	3133	5457	3398	38
H(21B)	4403	5078	2995	38
H(21C)	4442	6141	3513	38
H(22A)	6773	8243	5808	42
H(22B)	5429	7983	5442	42
H(22C)	6740	7737	5040	42

Table 5.10: Hydrogen coordinates ($\times 10^4$) and isotropic displacement parameters ($\text{\AA}^2 \times 10^3$) for sarpong139.

	x	y	z	U(eq)
H(23A)	5559	5712	6650	47
H(23B)	4678	6725	6364	47
H(23C)	5946	7011	6796	47
H(24A)	9894	5447	3289	51
H(24B)	10200	4269	2904	51
H(24C)	10912	4576	3613	51
H(25A)	10186	2705	4096	52
H(25B)	9419	2409	3403	52
H(25C)	8694	2400	4132	52
H(26A)	2494	1967	3520	43
H(26B)	3734	1307	3232	43
H(27A)	3308	2020	2119	71
H(27B)	2055	2644	2410	71
H(27C)	2124	1281	2395	71
H(26C)	4213	1319	3274	32
H(26D)	3963	1783	2503	32
H(27D)	2111	1557	3575	75
H(27E)	2048	989	2823	75
H(27F)	1829	2333	2911	75
H(1)	10698	4333	4808	24
H(2)	4623	2013	4495	32